Defining a role for xanthine oxidoreductase in promoting the healing of chronic ulcers

Bennett, Emily Jane

Award date:
2006

Awarding institution:
University of Bath

Defining a role for Xanthine oxidoreductase in promoting the healing of chronic ulcers

Emily Jane Bennett

A thesis submitted for the degree of Doctor of Philosophy

University of Bath

School for Health

October 2006

Supervisors

Professor M. Horrocks
Dr C. R. Stevens

Copyright

ProQuest LLC
789 East Eisenhower Parkway
P.O. Box 1346
Ann Arbor, MI 48106-1346

Dedication

To my family, especially Mum, Dad and Andrew

Acknowledgements

I would like to thank:

Dr Cliff Stevens and Prof Michael Horrocks for guidance throughout my PhD and for proof reading which allowed this thesis to come together

Dr Tulin Bodamyali for her valuable help and advice, and supporting me in the initial stages of my PhD

Dr Pauline Wood, Dr Mark Enright, Prof David Thomas in providing me with advice and materials for this PhD

Abstract

Chronic ulcers are a major healthcare problem characterised by ineffectual healing and infection. Xanthine oxidoreductase (XOR, EC 1.1.3.22), incorporated into a dressing or graft may provide enhanced healing and antibacterial activity. XOR is a complex molybdoflavoprotein with broad substrate specificity, and in aerobic conditions, generates superoxide ($O_2^{\bullet-}$) and hydrogen peroxide (H_2O_2) through purine catabolism. Low levels of these species from XOR are known to enhance the proliferation of many mammalian cells including human dermal fibroblasts, essential for the healing process (Murrell *et al*, 1990).

XOR also generates nitric oxide ($^{\bullet}NO$) from physiological levels of nitrite, optimally at low pH in anoxic conditions (cf the conditions prevailing in a chronic ulcer). Nitric oxide contributes to healing in general by increasing perfusion, stimulating angiogenesis and killing bacteria. Chronic wounds are known to harbour a range of anaerobic and facultative bacteria, many of which are detrimental to wound healing. It has been shown that the simultaneous generation of $O_2^{\bullet-}$ and $^{\bullet}NO$ by XOR in low oxygen, results in the rapid production of peroxynitrite ($ONOO^-$), a very much more potent bactericidal species than $O_2^{\bullet-}$, $^{\bullet}NO$ or H_2O_2.

Experiments were performed to characterise the effects of XOR activities on factors pertinent to healing to test the hypothesis that XOR incorporated into a dressing or dermograft will facilitate ulcer healing. Superoxide generation by xanthine oxidase (XO) was characterised, and shown to vary in biological media commonly used for the growth of either fibroblasts or bacteria in the laboratory setting. In support of existing research, superoxide generation by XO in low oxygen (1%) was reduced when compared with air. Nevertheless, peroxynitrite generation was also observed in low oxygen (1%).

This thesis supports previous research showing that XO enhances the proliferation of adult human dermal fibroblasts (HDF) using standard culture conditions in air. In the presence of 21% oxygen (air), high levels of XO (10-50mU ml^{-1}) were shown to be cytotoxic to adult fibroblasts whereas lower levels appeared to increase DNA synthesis suggesting enhanced proliferation (1mUml^{-1}). This thesis also extends these findings showing a similar effect on neonatal HDF. The novel findings in this thesis are that at low oxygen tension (pO_2 below 5%) the growth of adult HDF is not adversely affected in the presence of high XO concentrations (5-50mU ml^{-1} XO); in fact, HDF appear to show some evidence of enhanced proliferation under these conditions. Bacterial strains relevant to the chronic wound responded differentially to XO but showed growth inhibition at 10 and 50mU ml^{-1} XO. Overall, these findings suggest that an XO-incorporating graft or dressing may deliver both proliferative and antimicrobial effects in a hypoxic ulcer setting.

Contents

i. List of Figures vi

ii. List of Tables x

iii. Abbreviations xi

CHAPTER 1 1

1 INTRODUCTION: THE BIOLOGY OF THE SKIN 1

1.1 The epidermal layer 2
1.1.1 Stratum basale (SB) 2
1.1.2 Stratum spinosum (SS) 3
1.1.3 Stratum granulosum (SG) 3
1.1.4 Stratum corneum (SC) 3

1.2 The Dermal-Epidermal Basement Membrane (BM) 3

1.3 The Dermal Layer 4
1.3.1 Fibroblasts 6

1.4 Biology of successful wound healing 7
1.4.1 Haemostasis 7
1.4.2 Inflammation 8
1.4.3 Proliferation 9
1.4.4 Remodelling 11

CHAPTER 2 12

2 INTRODUCTION: IMPAIRED HEALING OF CHRONIC WOUNDS 12

2.1 Pathogenesis of chronic wounds 12
2.1.1 Decubitus (stasis) ulcers 12
2.1.2 Vascular ulcers 12
2.1.3 Diabetic ulcers 14

2.2 Chronic wound environment and the factors involved in impaired healing 15
2.2.1 Hypoxia/ ischaemia 16
2.2.2 Chronic inflammation 17
2.2.3 Excessive proteinase production in the chronic wound 18
2.2.3.1 Imbalance between MMPs and their inhibitors 18
2.2.4 Degradation of the matrix components 20
2.2.5 Reduced levels of active growth factors 21
2.2.6 Role of inflammatory networks 22
2.2.7 Cellular senescence and inhibition of cell proliferation 23
2.2.8 The microbiology of chronic ulcers 24
2.2.8.1 Bacterial colonisation and infection 24
2.2.8.2 Bacteria and impaired healing 25
2.2.8.3 Antibiotic resistance and chronic wounds 28
2.2.8.4 Measures to counteract resistance 30

2.3 Existing approaches and associated problems for chronic wound treatment 32
2.3.1 Basic care 32
2.3.2 Dressings 33
2.3.3 Topical treatments 33
2.3.4 Skin Grafts 35

2.3.4.1 Autologous skin grafts 35
2.3.4.2 Bioengineered skin equivalents 35
2.3.5 Current advances for acceleration of healing 37
2.3.6 The burden of chronic wounds 39

CHAPTER 3 40

3 INTRODUCTION: AN ALTERNATIVE APPROACH FOR PROMOTING THE HEALING OF CHRONIC WOUNDS 40

3.1 RONS involved in cellular and physiological processes 40
3.1.1 The major types of RONS and their generating systems in living organisms. 40
3.1.1.1 Reactive oxygen and nitrogen species classification and nomenclature. 41
3.1.1.2 Physiological ROS generating systems 42
3.1.1.3 Physiological RNS generating systems 42
3.1.2 The role of RONS in physiological systems 43
3.1.2.1 ROS and cell proliferation 43
3.1.2.1.1 Regulation of cell division in mammals 44
3.1.2.1.2 Mechanism of action 44
3.1.2.2 Nitric oxide in wound healing 46
3.1.2.2.1 Modes of action of nitric oxide in wound healing 47
3.1.2.3 The damaging effects of RONS with emphasis on their antibacterial role 49

3.2 Xanthine Oxidoreductase (XOR) 52
3.2.1 Distribution and activity of XOR with particular reference to the skin 53
3.2.2 Enzyme structure 53
3.2.2.1 Molybdopterin cofactor centre 54
3.2.2.2 FAD centre 54
3.2.2.3 Iron-sulphur centre 55
3.2.3 Superoxide generation by XOR 55
3.2.4 Nitric oxide generation by XOR 56
3.2.5 Peroxynitrite generation by XOR 57
3.2.5.1 Roles for the XOR-catalysed generation of RONS 58

3.3 Aims and objectives 60

CHAPTER 4 61

4 ASSESSMENT OF XOR ACTIVITY BY DETECTION OF ITS PRODUCTS 61

4.1 Introduction 61
4.1.1 XOR generated species 61
4.1.2 Measurement of reactive species 63
4.1.3 Use of the oxygen controlled cabinet 64
4.1.4 Chapter aims 65

4.2 Materials and Methods 66
4.2.1 Enzyme Characterisation 66
4.2.1.1 Protein determination using the Bio-Rad assay 66
4.2.1.1.1 Materials 66
4.2.1.1.2 Protocol 66
4.2.1.2 Protein determination using the Bio-Rad *DC* protein assay 66
4.2.1.2.1 Materials 67
4.2.1.2.2 Protocol 67
4.2.1.3 Comparison of Oxidase and dehydrogenase activity by the pterin assay 67
4.2.1.3.1 Materials 68
4.2.1.3.2 Protocol 68
4.2.2 Development of methods for the measurement of XO activity in cell growth medium 70
4.2.2.1 Cytochrome *c* assay for superoxide generation by XO 70
4.2.2.1.1 Materials 70

4.2.2.1.2 Protocol 71
4.2.2.1.2.1 Calculation of superoxide generation 72
4.2.2.2 Oxidation of Dihydrorhodamine for peroxynitrite generation by XO 73
4.2.2.2.1 Materials 74
4.2.2.2.2 Protocol 75
4.2.3 Statistical analysis 75

4.3 Results 75
4.3.1 Enzyme characterisation 75
4.3.1.1 Protein determination using the Bio-Rad assay 75
4.3.1.2 Protein determination using the Bio-Rad *DC* protein assay 76
4.3.1.3 Comparison of oxidase and dehydrogenase activity by the pterin assay 78
4.3.2 Development of methods for the measurement of XO activity cell growth medium 78
4.3.2.1 Cytochrome *c* assay for superoxide generation by XO 78
4.3.2.1.1 Superoxide generation by XO in air in PBS 78
4.3.2.1.2 Superoxide generation by XO in PBS in 1% O_2 102
4.3.2.1.3 Superoxide generation by XO in bacterial culture medium in air 107
4.3.2.1.4 Superoxide generation by XO in bacterial culture medium in 1% oxygen 113
4.3.2.1.5 Superoxide generation by XO in fibroblast culture medium in air 119
4.3.2.1.6 Superoxide generation by XO fibroblast culture medium in 1% oxygen 125
4.3.2.2 Oxidation of dihydrorhodamine for peroxynitrite generation by XO 128
4.3.2.2.1 Oxidation of dihydrorhodamine by SIN-1 128
4.3.2.2.2 Oxidation of Dihydrorhodamine by XO 132

4.4 Discussion 137
4.4.1 Enzyme characterisation 137
4.4.2 Development of methods for the measurement of XO activity in cell growth medium 138
4.4.2.1 Cytochrome *c* assay for superoxide generation by XO 138
4.4.2.2 Oxidation of dihydrorhodamine for peroxynitrite generation by XO 145
4.4.3 Chapter summary 147

CHAPTER 5 148

5 EFFECTS OF XO-GENERATED PRODUCTS ON HUMAN DERMAL FIBROBLASTS 148

5.1 Introduction 148
5.1.1 Chapter aims 149

5.2 Materials and Methods 149
5.2.1 Cell culture 149
5.2.1.1 Origin of primary human dermal fibroblasts (HDF) 149
5.2.1.2 Maintenance, passage and subculture of dermal fibroblasts 149
5.2.1.2.1 Materials 149
5.2.1.2.2 Protocol 150
5.2.1.3 Cryopreservation and revival of cells for cell stocks 150
5.2.1.3.1 Materials 150
5.2.1.3.2 Protocol 150
5.2.1.4 Manually observed cell counts and assessment of viability using trypan blue 151
5.2.1.4.1 Materials 151
5.2.1.4.2 Protocol 151
5.2.2 Characterisation of HDF 152
5.2.2.1 Immunocytochemistry 152
5.2.2.1.1 Materials 152
5.2.2.1.2 Protocol 153
5.2.3 Effects of H_2O_2 and XO on the viability of HDF 153
5.2.3.1 Colourimetric methylthiazolyldiphenyl-tetrazolium bromide (MTT) reduction assay 153
5.2.3.1.1 Materials 154
5.2.3.1.2 Protocol 154
5.2.4 Effects of XO on the DNA synthesis and proliferation of HDF 155
5.2.4.1 Bromodeoxyuridine assay using chamber slides for cell counts 155
5.2.4.1.1 Materials 155

5.2.4.1.2 Protocol 155
5.2.4.2 Bromodeoxyuridine assay using an ELISA system in a range of oxygen tensions 157
5.2.4.2.1 Materials 157
5.2.4.2.2 Protocol 157
5.2.5 Statistical analysis 158

5.3 Results 158
5.3.1 Characterisation of human dermal fibroblasts 158
5.3.1.1 Immunocytochemistry 158
5.3.2 Effects of H_2O_2 and XO on the viability of human dermal fibroblasts 161
5.3.2.1 Dissociation of dermal fibroblast cultures for seeding 161
5.3.2.2 Effects of XO on the viability of nHDF in air 162
5.3.2.3 Effects of H_2O_2 on the viability and proliferation of nHDF 167
5.3.2.4 Effects of XO on the viability of human dermal fibroblasts in a range of oxygen tensions 175
5.3.3 Effects of XO on the DNA synthesis and proliferation of HDF 182
5.3.3.1 Bromodeoxyuridine assay using chamber slides for cell counts 182
5.3.3.2 Bromodeoxyuridine assay using an ELISA system in a range of oxygen tensions 189

5.4 Discussion 193
5.4.1 Characterisation of human dermal fibroblasts 194
5.4.2 Effects of XO on the viability of human dermal fibroblasts 194
5.4.3 Effects of XO on the proliferation of HDF 199
5.4.4 Chapter summary 200

CHAPTER 6 201

6 EFFECTS OF XO-GENERATED PRODUCTS ON BACTERIA RELEVANT TO THE CHRONIC WOUND 201

6.1 Introduction 201
6.1.1 Facultative anaerobes and chronic wound infection 201
6.1.1.1 Gram positive bacteria *S. aureus* and *S. faecalis* 201
6.1.1.2 Gram-negative bacteria *P. mirabilis, P. aeruginosa and E.coli* 202
6.1.2 XOR and bacterial killing 204
6.1.3 Bacterial survival and antioxidant mechanisms 204
6.1.4 Chapter aim 206

6.2 Principles, methods and materials 206
6.2.1 Culture of bacterial strains 206
6.2.1.1 Materials 206
6.2.1.2 Protocol 208
6.2.2 Chemically generated oxidants, XO and reduced Oxygen on bacterial growth 208
6.2.2.1 Peroxynitrite generation 209
6.2.2.1.1 Materials 209
6.2.2.1.2 Protocol 209
6.2.2.2 The effect of H_2O_2 and $ONOO^-$ and XO on bacterial growth 210
6.2.2.2.1 Materials 210
6.2.2.2.2 Protocol 210
6.2.2.3 The effect of reduced oxygen on bacterial growth 211
6.2.2.3.1 Materials 211
6.2.2.3.2 Protocol 211
6.2.2.4 Mean growth rate constant and generation time 211
6.2.3 Effect of H_2O_2 and XO on bacterial viability in air 212
6.2.3.1 Assessment of viability using disk inhibition assays 212
6.2.3.1.1 Materials 212
6.2.3.1.2 Protocol 212
6.2.4 Effect of XO on bacterial viability in variable oxygen 213
6.2.4.1 Assessment of viable cells by colony counts 213
6.2.4.1.1 Materials 213
6.2.4.1.2 Protocol 213
6.2.5 Statistical analysis 214

6.3 Results **214**
6.3.1 Effect of H_2O_2 and $ONOO^-$ on the growth of *S. aureus* disease Isolates 214
6.3.1.1 Growth curves of *S. aureus* strains 214
6.3.1.2 Effects of H_2O_2 on the growth of *S. aureus* strains 216
6.3.1.3 Effects of $ONOO^-$ on the growth of *S. aureus* strains 221
6.3.2 Effect of H_2O_2 and XO on the growth of bacterial species relevant to the chronic wound 222
6.3.2.1 Growth curves of *S. faecalis, E. coli, S. aureus, P. aeruginosa* 222
6.3.2.2 Correlation of absorbance versus viable cell counts. 223
6.3.2.3 Treatment of *S. aureus* and *S. faecalis* with H_2O_2 226
6.3.2.4 Treatment of *S. faecalis* with SIN-1 227
6.3.2.5 Treatment of *E. coli* with XO in air (cuvette method) 229
6.3.2.6 Treatment of bacterial species with XO in air (96-well plate method) 230
6.3.3 Effects of H_2O_2 and XO on the viability of bacteria in air 240
6.3.3.1 Disk inhibition assays 241
6.3.3.1.1 Treatment of S. aureus with H_2O_2 241
6.3.3.1.2 Treatment of S. aureus with XO 243
6.3.4 Effects of XO on the viability of bacteria in varying oxygen concentrations 245
6.3.4.1 Growth of *E. coli* and *S. aureus* in air (21%) and 2% oxygen. 245
6.3.4.2 Treatment of bacteria with XO in variable oxygen for 1 and 3 hours 246

6.4 Discussion **252**
6.4.1 The effect of H_2O_2 and $ONOO^-$ on the growth of *S. aureus* disease isolates 252
6.4.2 Effect of H_2O_2, SIN-1 and XO on the growth of bacterial species relevant to the chronic wound 254
6.4.3 Effect of H_2O_2 and XO on the viability of bacterial species relevant to the chronic wound .. 257
6.4.4 Effect of XO on the viability of bacteria relevant to the chronic wound in variable oxygen . 257
6.4.5 Chapter summary 258

CHAPTER 7 ..... **259**

7 GENERAL DISCUSSION-A POTENTIAL ROLE FOR XO IN THE HEALING OF CHRONIC WOUNDS **259**

7.1 Future work **265**

8 APPENDIX **267**

8.1 Fibroblast culture **267**
8.1.1 Fibroblast growth Medium 267
8.1.2 Trypsin/EDTA 268

8.2 Bacterial Growth medium **268**
8.2.1 Luria Broth (LB) 268
8.2.2 LB agar plates 268
8.2.3 Soft agar overlay (0.4%) 268

9 REFERENCES **269**

i. List of Figures

FIGURE 1.1 BASIC DIAGRAM TO SHOW THE THREE LAYERS OF THE SKIN AND VARIOUS ASSOCIATED STRUCTURES. 1
FIGURE 1.2 DETAILED SCHEMATIC OF THE BASEMENT MEMBRANE ZONE AT THE DERMO-EPIDERMAL JUNCTION 4
FIGURE 1.3 A SUMMARY OF THE CYTOKINE SUPPLY FOR WOUND HEALING 9
FIGURE 1.4 A SUMMARY OF THE WOUND HEALING PROCESS. 11
FIGURE 2.1 VENOUS STASIS ULCER 14
FIGURE 2.2 DIABETIC FOOT ULCER 15
FIGURE 2.3 PROPOSED PATHWAY FOR ACTIVATION OF PRO-MMP2 IN HUMAN DERMAL FIBROBLASTS. 20
FIGURE 2.4THE FIBRINOLYTIC PATHWAY. 21
FIGURE 2.5 IMPAIRED WOUND HEALING RESPONSES BY *PEPTOSTREPTOCOCCUS* SPP. AND THEIR METABOLITES. 28
FIGURE 2.6 SUMMARY OF IMPAIRED HEALING IN CHRONIC WOUNDS. 31
FIGURE 2.7 TREATMENT OF A CHRONIC NONHEALING WOUND. 32
FIGURE 2.8DERMAGRAFT- NEONATAL FIBROBLASTS CULTURED ON A POLYGLACTIN MESH. 37
FIGURE 2.9APLIGRAF- A BILAYERED SKIN EQUIVALENT. 37
FIGURE 3.1PATHWAYS OF REACTIVE OXYGEN SPECIES (ROS) PRODUCTION AND CLEARANCE IN BIOLOGICAL SYSTEMS. 42
FIGURE 3.2. REACTIVE OXYGEN SPECIES CONTROL OVER GENE EXPRESSION. 45
FIGURE 3.3 A SUMMARY OF THE ROLES OF $^{\bullet}NO$ IN WOUND HEALING 49
FIGURE 3.4THE PHYSIOLOGICAL EFFECTS OF $^{\bullet}NO$ AND $ONOO^{-}$ GENERATION. 52
FIGURE 3.5 XOR-CATALYSED SUPEROXIDE GENERATION. 55
FIGURE 3.6XOR-CATALYSED SUPEROXIDE GENERATION. 56
FIGURE 3.7 A SCHEMATIC DIAGRAM SHOWING XOR-CATALYSED REDUCTION OF NITRATES AND NITRITES. 57
FIGURE 3.8 XOR-CATALYSED PEROXYNITRITE GENERATION. 58
FIGURE 4.1 OXYGEN CONTROLLED CABINET 65
FIGURE 4.2 XOR CATALYSED GENERATION OF IXP FROM THE PTERIN SUBSTRATE. 68
FIGURE 4.3 A TYPICAL TRACE FROM THE TIME-SCAN XOR ASSAY. 69
FIGURE 4.4 XOR CATALYSED GENERATION OF SUPEROXIDE AND REDUCTION OF CYTOCHROME *C*. 72
FIGURE 4.5 XO-CATALYSED OXIDATION OF DIHYDRORHODAMINE TO RHODAMINE 74
FIGURE 4.6FENTON REACTION. 74
FIGURE 4.7STANDARD CURVE FOR PROTEIN DETERMINATION OF XO USING THE BIO-RAD ASSAY. 76
FIGURE 4.8 STANDARD CURVE FOR PROTEIN DETERMINATION OF XO USING THE BIO-RAD *DC* ASSAY. 77
FIGURE 4.9 STANDARD CURVE FOR PROTEIN DETERMINATION OF XO2 USING THE BIO-RAD *DC* ASSAY. 77
FIGURE 4.10 MEASUREMENT OF XO AND XDH ACTIVITY IN COMMERCIALLY AVAILABLE XO (BIOZYME). 78
FIGURE 4.11 INITIAL RATE OF XO-CATALYSED SUPEROXIDE GENERATION BY XO IN PBS IN AIR 79
FIGURE 4.12 INITIAL RATE OF SUPEROXIDE GENERATION BY XO AT VARYING SOD CONCENTRATIONS. 79
FIGURE 4.13 INITIAL RATE OF SUPEROXIDE GENERATION BY XO AT VARYING SOD CONCENTRATIONS. 80
FIGURE 4.14 COMPARISON OF THE RATE OF SUPEROXIDE GENERATION BY XO IN A CUVETTE AND 96-WELL PLATE. 81
FIGURE 4.15TIMECOURSE OF SUPEROXIDE GENERATION AT A RANGE OF CONCENTRATIONS OF XO IN A 96-WELL PLATE. 82
FIGURE 4.16 RATE OF SUPEROXIDE GENERATION AT A RANGE OF CONCENTRATIONS OF XO IN A 96-WELL PLATE 82
FIGURE 4.17 RATE OF SUPEROXIDE GENERATION AT A RANGE OF XO CONCENTRATIONS IN A CUVETTE. 83
FIGURE 4.18 COMPARISON OF SUPEROXIDE GENERATION BY XO IN A 96-WELL PLATE AND A CUVETTE. 83

FIGURE 4.19 COMPARISON OF THE 96-WELL PLATE AND CUVETTE METHODS AT A RANGE OF XO CONCENTRATIONS 84
FIGURE 4.20 COMPARISON OF THE RATE OF SUPEROXIDE GENERATION IN A 96-WELL PLATE DATA WITH AND WITHOUT SHAKING 85
FIGURE 4.21 COMPARISON OF THE RATE OF CYTOCHROME *C* REDUCTION IN A STIRRED AND UNSTIRRED CUVETTE AT VARYING XO CONCENTRATIONS 85
FIGURE 4.22 CALCULATION OF THE EXPECTED SUPEROXIDE GENERATION RATE 86
FIGURE 4.23 INITIAL RATES OF SUPEROXIDE GENERATION BY XO WITH HYPOXANTHINE. 87
FIGURE 4.24 INHIBITION OF XO-GENERATED SUPEROXIDE BY SOD 87
FIGURE 4.25 INITIAL RATES OF SUPEROXIDE GENERATION AT 0 TO 10MU ML^{-1} XO. 88
FIGURE 4.26 INITIAL RATES OF SUPEROXIDE GENERATION BY XO WITH VARYING HYPOXANTHINE. 89
FIGURE 4.27 INITIAL RATES OF SUPEROXIDE GENERATION BY XO WITH AND WITHOUT HEPES BUFFER. 89
FIGURE 4.28 COMPARISON OF OLD AND NEW BATCH OF XO. 90
FIGURE 4.29 COMPARISON OF CYTOCHROME *C* REDUCTION BY XO IN A CUVETTE OR A 96-WELL PLATE. 91
FIGURE 4.30 COMPARISON OF CYTOCHROME *C* REDUCTION IN 96-WELL PLATE AND CUVETTE. 91
FIGURE 4.31. COMPARISON OF THE INITIAL RATES OF SUPEROXIDE GENERATION BY FOUR BATCHES OF XO. 92
FIGURE 4.32 TIMECOURSE OF CYTOCHROME *C* REDUCTION BY XO AT 50MU ML^{-1}. 93
FIGURE 4.33. CYTOCHROME *C* REDUCTION AND SUPEROXIDE GENERATION BY 50MU ML^{-1} XO 93
FIGURE 4.34 EFFECT OF VARYING CONCENTRATIONS OF SOD ON SUPEROXIDE GENERATION BY XO IN PBS 95
FIGURE 4.35 EFFECT OF VARYING CONCENTRATIONS OF CATALASE ON SUPEROXIDE GENERATION BY XO IN PBS. 95
FIGURE 4.36 EFFECT OF ALLOPURINOL ON THE REDUCTION OF CYTOCHROME *C* BY XO IN PBS. 96
FIGURE 4.37 TIMECOURSE OF CYTOCHROME *C* REDUCTION IN PBS BY XO IN AIR. 98
FIGURE 4.38 TIMECOURSE OF CYTOCHROME *C* REDUCTION IN PBS BY XO AT 21% WITH SOD. 99
FIGURE 4.39 TIMECOURSE OF CYTOCHROME *C* REDUCTION IN PBS BY XO IN 21% O_2 WITH CATALASE 100
FIGURE 4.40 TIMECOURSE OF CYTOCHROME *C* REDUCTION IN PBS BY XO AT 21% O_2 WITH SOD AND CATALASE. 101
FIGURE 4.41 INITIAL RATES OF SUPEROXIDE GENERATION IN PBS BY XO AT 21% O_2 WITH CATALASE AND SOD. 102
FIGURE 4.42TIMECOURSE OF CYTOCHROME *C* REDUCTION IN PBS BY XO IN 1% OXYGEN 103
FIGURE 4.43 TIMECOURSE OF CYTOCHROME *C* REDUCTION IN PBS BY XO IN 1% OXYGEN WITH SOD. 104
FIGURE 4.44 TIMECOURSE OF CYTOCHROME *C* REDUCTION IN PBS BY XO IN 1% OXYGEN WITH CATALASE. 105
FIGURE 4.45 REDUCTION OF CYTOCHROME *C* BY XO AT 1% O_2 IN PBS 106
FIGURE 4.46 INITIAL RATES OF SUPEROXIDE GENERATION BY XO IN PBS AT 1% O_2 WITH CATALASE AND SOD. 107
FIGURE 4.47 TIMECOURSE OF THE REDUCTION OF CYTOCHROME *C* BY BACTERIAL CULTURE MEDIUM IN AIR. 107
FIGURE 4.48 TIMECOURSE OF THE REDUCTION OF CYTOCHROME *C* BY XO IN LB 108
FIGURE 4.49 TIMECOURSE OF CYTOCHROME *C* REDUCTION BY XO IN AIR IN LB. 109
FIGURE 4.50 TIMECOURSE OF CYTOCHROME *C* REDUCTION BY XO IN AIR IN LB WITH SOD. 110
FIGURE 4.51 TIMECOURSE OF CYTOCHROME *C* REDUCTION BY XO IN AIR IN LB WITH CATALASE 111
FIGURE 4.52 TIMECOURSE OF CYTOCHROME *C* REDUCTION BY XO IN AIR IN LB WITH CATALASE AND SOD. 112
FIGURE 4.53 INITIAL RATES OF SUPEROXIDE GENERATION BY XO IN BACTERIAL CULTURE MEDIUM AT 21% O_2. 113
FIGURE 4.54TIMECOURSE OF CYTOCHROME *C* REDUCTION BY BACTERIAL CULTURE MEDIUM IN 1% OXYGEN 113
FIGURE 4.55 TIMECOURSE OF CYTOCHROME *C* REDUCTION BY XO IN 1% OXYGEN. 114
FIGURE 4.56 TIMECOURSE OF THE REDUCTION OF CYTOCHROME *C* BY XO IN LB AT 1% O_2 115

FIGURE 4.57 TIMECOURSE OF THE REDUCTION OF CYTOCHROME *C* BY XO IN LB AT 1% O_2 WITH SOD 116
FIGURE 4.58 TIMECOURSE OF THE REDUCTION OF CYTOCHROME *C* BY XO IN LB AT 1% O_2 WITH CATALASE 117
FIGURE 4.59 TIMECOURSE OF THE REDUCTION OF CYTOCHROME *C* BY XO IN LB AT 1% OXYGEN. 118
FIGURE 4.60 INITIAL RATES OF SUPEROXIDE GENERATION BY XO IN LB AT 1% OXYGEN. 119
FIGURE 4.61 RATE OF CYTOCHROME *C* REDUCTION BY FIBROBLAST GROWTH MEDIUM.. 120
FIGURE 4.62 REDUCTION OF CYTOCHROME *C* BY FIBROBLAST GROWTH MEDIUM. 120
FIGURE 4.63 REDUCTION OF CYTOCHROME *C* BY VARYING COMPONENTS OF FIBROBLAST CULTURE MEDIUM. 121
FIGURE 4.64 REDUCTION OF CYTOCHROME *C* BY STERILE FILTERED AND UNFILTERED MEDIUM..... 121
FIGURE 4.65 REDUCTION OF CYTOCHROME *C* BY XO IN DMEM. 122
FIGURE 4.66 REDUCTION IN XO ACTIVITY IN FIBROBLAST GROWTH MEDIUM..... 122
FIGURE 4.67 INITIAL RATES OF CYTOCHROME *C* REDUCTION BY XO IN FIBROBLAST MEDIUM WITH VARYING FCS CONCENTRATION. 123
FIGURE 4.68 THE SOD-INHIBITABLE RATES OF SUPEROXIDE GENERATION BY XO. 124
FIGURE 4.69 TIMECOURSE OF CYTOCHROME *C* REDUCTION IN FIBROBLAST MEDIUM BY XO IN 1% OXYGEN 126
FIGURE 4.70 TIMECOURSE OF CYTOCHROME *C* REDUCTION IN FIBROBLAST MEDIUM BY XO IN 1% OXYGEN WITH SOD..... 126
FIGURE 4.71 TIMECOURSE OF CYTOCHROME *C* REDUCTION IN FIBROBLAST MEDIUM BY XO IN 1% OXYGEN WITH CATALASE 127
FIGURE 4.72 TIMECOURSE OF CYTOCHROME *C* REDUCTION IN FIBROBLAST MEDIUM BY XO IN 1% OXYGEN WITH CATALASE AND SOD 127
FIGURE 4.73 INITIAL RATES OF SUPEROXIDE GENERATION BY XO IN FIBROBLAST MEDIUM AT 1% OXYGEN WITH CATALASE AND SOD. 128
FIGURE 4.74 OXIDATION OF DHR USING A 2ML OR A 3ML REACTION VOLUME IN A 3ML CUVETTE. 129
FIGURE 4.75 WAVELENGTH SCAN OF THE OXIDATION OF DHR..... 130
FIGURE 4.76 OXIDATION OF DHR AT VARYING CONCENTRATIONS OF SIN-1..... 131
FIGURE 4.77 PEROXYNITRITE GENERATION AT VARYING CONCENTRATIONS OF SIN-1. 132
FIGURE 4.78 TIMECOURSE OF THE OXIDATION OF DHR BY XO WITH DPI..... 133
FIGURE 4.79 OXIDATION OF DHR BY XO IN AIR..... 134
FIGURE 4.80 OXIDATION OF DHR IN AIR AND 2% OXYGEN. 134
FIGURE 4.81 OXIDATION OF DHR IN AIR..... 135
FIGURE 4.82 OXIDATION OF DHR IN AIR..... 136
FIGURE 4.83 OXIDATION OF DHR BY URIC ACID. 137
FIGURE 5.1 IMPROVED NEUBAUER HAEMOCYTOMETER FOR CELL COUNTING. 152
FIGURE 5.2 BRDU INCORPORATION AND VISUALISATION. 156
FIGURE 5.3 NEONATAL HUMAN DERMAL FIBROBLASTS STAINED WITH FIBROBLAST MARKER 159
FIGURE 5.4 NEONATAL HUMAN DERMAL FIBROBLASTS STAINED WITH FIBROBLAST MARKER 159
FIGURE 5.5 NEONATAL HUMAN DERMAL SKIN FIBROBLASTS STAINED WITH FIBROBLAST MARKER 160
FIGURE 5.6 NEONATAL HUMAN DERMAL SKIN FIBROBLASTS STAINED WITH FIBROBLAST MARKER 160
FIGURE 5.7 NEGATIVE ANTIBODY CONTROL. 161
FIGURE 5.8 CLUMPS OF CELLS AFTER DETACHMENT FROM CULTURE PLASTIC USING CELL DISSOCIATION SOLUTION..... 162
FIGURE 5.9 CELL NUMBER VERSUS ABSORBANCE USING THE MTT ASSAY..... 163
FIGURE 5.10 VIABILITY OF NEONATAL HUMAN DERMAL FIBROBLASTS AT VARYING XO CONCENTRATIONS. 163
FIGURE 5.11VIABILITY OF NEONATAL HUMAN DERMAL FIBROBLASTS AT VARYING XO CONCENTRATIONS. 164
FIGURE 5.12 EFFECT OF SEEDING DENSITY ON THE VIABILITY OF NHDF EXPOSED TO XO. 165
FIGURE 5.13 THE EFFECT OF CHANGING CONCENTRATIONS OF XO ON NHDF VIABILITY.. 166
FIGURE 5.14 THE EFFECT OF CHANGING CONCENTRATIONS OF XO ON NHDF VIABILITY.. 167
FIGURE 5.15 GROWTH OF NHDF AT VARYING CONCENTRATIONS OF FCS..... 168
FIGURE 5.16 GROWTH OF NHDF AT VARYING CONCENTRATIONS OF FCS..... 169
FIGURE 5.17 THE EFFECT OF H_2O_2 ON THE VIABILITY OF NHDF..... 170
FIGURE 5.18 TREATMENT OF NHDF WITH H_2O_2 FOR 72 HOURS..... 170

FIGURE 5.19 TREATMENT OF NHDF WITH H_2O_2 171
FIGURE 5.20 TREATMENT OF CELLS WITH H_2O_2 WITH AND WITHOUT HEPES BUFFER FOR 24, 48 AND 72 HOURS. 172
FIGURE 5.21 TREATMENT OF NHDF WITH XO 173
FIGURE 5.22 THE EFFECT OF BFGF ON NHDF 174
FIGURE 5.23 SENSITIVITY AND KINETICS OF THE MTT ASSAY AT 21% OXYGEN. 175
FIGURE 5.24 TREATMENT OF AHDF WITH XO AT 0% OXYGEN. 176
FIGURE 5.25 TREATMENT OF AHDF WITH XO FOR 3 HOURS IN 1, 2, 5, AND 21% O_2 177
FIGURE 5.26 TREATMENT OF AHDF WITH XO FOR 3 HOURS IN 1, 2, 5, AND 21% O_2 177
FIGURE 5.27 TREATMENT OF AHDF WITH XO FOR 24 HOURS IN 1, 2, 5, AND 21% O_2 178
FIGURE 5.28 TREATMENT OF AHDF WITH XO FOR 24 HOURS IN 1, 2, 5, AND 21% O_2 178
FIGURE 5.29 TREATMENT OF AHDF WITH XO FOR 24 HOURS AT 21% O_2 180
FIGURE 5.30 TREATMENT OF AHDF WITH XO FOR 72 HOURS IN 1, 2, 5, AND 21% O_2 181
FIGURE 5.31 TREATMENT OF AHDF WITH XO FOR 72 HOURS IN 1, 2, 5, AND 21% O_2 181
FIGURE 5.32 BRDU LABELLED NHDF (SUBSTRATE ONLY CONTROL). 183
FIGURE 5.33 BRDU LABELLED NHDF (SUBSTRATE ONLY CONTROL). 183
FIGURE 5.34 BRDU LABELLED NHDF (SUBSTRATE ONLY CONTROL). 184
FIGURE 5.35 BRDU LABELLED NHDF TREATED WITH XO (0.001MU ML^{-1}). 184
FIGURE 5.36COUNT OF BRDU POSITIVE CELLS AFTER TREATMENT WITH XO. 185
FIGURE 5.37 BRDU LABELLED NHDF WITH (4 HOUR BRDU INCUBATION). 186
FIGURE 5.38 BRDU LABELLED NHDF WITH (4 HOUR INCUBATION). 186
FIGURE 5.39 BRDU LABELLED NHDF (4 HOUR INCUBATION) 187
FIGURE 5.40 BRDU INCORPORATION FOR THE ASSESSMENT OF NHDF GROWTH. 188
FIGURE 5.41 GROWTH CURVE OF THE BRDU INCORPORATION OF NHDF OVER 32 HOURS. 188
FIGURE 5.42 SENSITIVITY AND KINETICS OF THE CELL PROLIFERATION ELISA IN 21% OXYGEN. 189
FIGURE 5.43 SENSITIVITY AND KINETICS OF THE CELL PROLIFERATION ELISA IN 0% OXYGEN. 190
FIGURE 5.44TREATMENT OF AHDF WITH XO IN 0% OXYGEN. 190
FIGURE 5.45 TREATMENT OF AHDF WITH XO FOR 72 HOURS IN 1, 2 5 AND 21% OXYGEN.... 192
FIGURE 5.46 TREATMENT OF AHDF WITH XO FOR 72 HOURS IN 2, 5 AND 21% OXYGEN..... 193
FIGURE 6.1 AGAR PLATE LAYOUT FOR COLONY COUNTS. 214
FIGURE 6.2 GROWTH CURVES OF *S. AUREUS* (ISOLATE MU 3) AT VARYING CONCENTRATIONS. 215
FIGURE 6.3GROWTH CURVES OF *S. AUREUS* (ISOLATE MU 50) AT VARYING CONCENTRATIONS. 215
FIGURE 6.4 GROWTH CURVES OF *S. AUREUS* (ISOLATE 117) AT VARYING CONCENTRATIONS. 215
FIGURE 6.5 GROWTH CURVES OF *S. AUREUS* (ISOLATE N317) AT VARYING CONCENTRATIONS. 216
FIGURE 6.6 GROWTH CURVES OF *S. AUREUS* (ISOLATE MU 3) TREATED WITH H_2O_2 217
FIGURE 6.7 GROWTH CURVES OF *S. AUREUS* (ISOLATE MU 50) TREATED WITH H_2O_2 217
FIGURE 6.8 GROWTH CURVES OF *S. AUREUS* (ISOLATE 117) TREATED WITH H_2O_2 217
FIGURE 6.9 GROWTH CURVES OF *S. AUREUS* (ISOLATE N315) TREATED WITH H_2O_2 218
FIGURE 6.10 MAXIMAL GROWTH RATES OF *S. AUREUS* ISOLATES TREATED WITH H_2O_2 218
FIGURE 6.11 GROWTH CURVES OF *S. AUREUS* (ISOLATE 13) TREATED WITH H_2O_2 219
FIGURE 6.12 GROWTH CURVES OF *S. AUREUS* (ISOLATE 357) TREATED WITH H_2O_2 219
FIGURE 6.13 GROWTH CURVES OF *S. AUREUS* (ISOLATE 197) TREATED WITH H_2O_2 219
FIGURE 6.14 GROWTH CURVES OF *S. AUREUS* (ISOLATE 283) TREATED WITH H_2O_2 220
FIGURE 6.15 GROWTH CURVES OF *S. AUREUS* (ISOLATE 301) TREATED WITH H_2O_2 220
FIGURE 6.16 GROWTH CURVES OF *S. AUREUS* (ISOLATE 13) TREATED WITH H_2O_2 220
FIGURE 6.17 GROWTH RATES OF *S. AUREUS* STRAINS AFTER TREATMENT WITH H_2O_2 221
FIGURE 6.18 GROWTH CURVES OF FOUR FACULTATIVE ANAEROBES WITH VARYING CELL CONCENTRATION 223
FIGURE6.19 CORRELATION OF ABS_{595NM} VERSUS CELLS ML^{-1} OF *S. AUREUS*, *P. MIRABILIS*, *S. FAECALIS*, *E. COLI* 224
FIGURE 6.20 CORRELATION OF ABSORBANCE AGAINST VIABLE COUNT. 225
FIGURE 6.21 LINEAR RELATIONSHIP BETWEEN ABS_{595NM} AND CELLS ML^{-1} BEFORE STATIONARY PHASE IS REACHED. 225
FIGURE 6.22 TREATMENT OF *S. AUREUS* WITH H_2O_2 226
FIGURE 6.23 TREATMENT OF *S. FAECALIS* WITH H_2O_2. 227
FIGURE 6.24 OXIDATION OF DHR WITH SIN-1 IN PBS AND LB WITH AND WITHOUT DTPA.. 228
FIGURE 6.25 TREATMENT OF *S. FAECALIS* WITH $ONOO^-$ 228
FIGURE 6.26 GROWTH CURVES OF *E. COLI* TREATED WITH XO IN AIR. 229

FIGURE 6.27 TREATMENT OF *S. AUREUS* WITH XO IN AIR (CONTROLS). 231
FIGURE 6.28 TREATMENT OF *S. AUREUS* WITH XO IN AIR. 232
FIGURE 6.29TREATMENT OF *S. FAECALIS* WITH XO IN AIR (CONTROLS). 233
FIGURE 6.30 TREATMENT OF *S. FAECALIS* WITH XO IN AIR 234
FIGURE 6.31TREATMENT OF *E. COLI* WITH XO IN AIR (CONTROLS). 235
FIGURE 6.32 TREATMENT OF *E. COLI* WITH XO IN AIR. 236
FIGURE 6.33 TREATMENT OF *P. AERUGINOSA* WITH XO IN AIR (CONTROLS). 237
FIGURE 6.34 TREATMENT OF *P. AERUGINOSA* WITH XO IN AIR. 238
FIGURE 6.35 TREATMENT OF *P. MIRABILIS* WITH XO IN AIR (CONTROLS) 239
FIGURE 6.36. TREATMENT OF *P. MIRABILIS* WITH XO IN AIR. 240
FIGURE 6.37 INHIBITION OF THE GROWTH OF *S. AUREUS* USING H_2O_2. 242
FIGURE 6.38 TREATMENT OF *S. AUREUS* WITH XO IN AIR 244
FIGURE 6.39 TREATMENT OF *S. AUREUS* WITH XO IN AIR 245
FIGURE 6.40 GROWTH CURVES OF *E. COLI* AND *S. AUREUS* IN 21 % AND 2 % OXYGEN. 246
FIGURE 6.41 TREATMENT OF *S. AUREUS* WITH XO IN VARIABLE OXYGEN. 248
FIGURE 6.42TREATMENT OF *S. FAECALIS* WITH XO IN VARIABLE OXYGEN 249
FIGURE 6.43TREATMENT OF *P. MIRABILIS* WITH XO IN VARIABLE OXYGEN. 250
FIGURE 6.44 TREATMENT OF *E. COLI* WITH XO IN VARIABLE OXYGEN. 251
FIGURE 7.1THE PROPOSED MODEL OF XO-RELEASE FROM A DERMAL GRAFT OR DRESSING FOR ENHANCED HEALING IN A CHRONIC ULCER 264

ii. List of tables

TABLE 1.1CLASSIFICATION OF MATRIX METALLOPROTEINASES 10
TABLE 2.1THE MICROBIOLOGY OF INFECTED AND NONINFECTED LEG ULCERS. 26
TABLE 2.2GROWTH FACTORS, WOUND HEALING AND THEIR USE IN CHRONIC ULCER TREATMENT. 34
TABLE 2.3 CURRENTLY AVAILABLE SKIN SUBSTITUTES USED IN THE TREATMENT OF CHRONIC WOUNDS. 36
TABLE 3.1NOMENCLATURE OF REACTIVE SPECIES ENZYME REACTIONS 41
TABLE 4.1 PLASMA CONCENTRATIONS OF RELEVANT SUBSTANCES (MILLAR, 1999) 62
TABLE 4.2 INITIAL RATES OF SUPEROXIDE GENERATION AT 0 TO 10MU ML^{-1} OF XO 88
TABLE 4.3ABSORBANCE VALUES AT 500NM AND 490NM AND PERCENTAGE CHANGE IN ABSORBANCE 130
TABLE 6.1 SEVERE DISEASE *S. AUREUS* ISOLATES. 207
TABLE 6.2 RATE OF BACTERIAL GROWTH (LOG2 A595NM MIN^{-1}) OF FOUR *S. AUREUS* STRAINS. 216
TABLE 6.3 DOUBLING TIMES OF BACTERIAL GROWTH (MINUTES) OF FOUR *S. AUREUS* STRAINS. 216
TABLE 6.4 SENSITIVITY OF *S. AUREUS* TO H_20_2. 243
TABLE 8.1DULBECCO'S MODIFIED EAGLE'S MEDIUM WITH AND WITHOUT THE ADDITION OF PHENOL RED 267

iii. Abbreviations

Abs	Absorbance
ADP	Adenosine diphosphate
ANOVA	Analysis of variance
AP	Alkaline phosphatase
ATP	Adenosine triphosphate
bFGF	Basic fibroblast growth factor
BM	Basement membrane
BrdU	Bromodeoxyuridine
BSA	Bovine serum albumin
°C	Degrees celsius
CAT	Catalase
CFU	Colony forming units
CG	Cathepsin G
CO_2	Carbon dioxide
cGMP	Cyclic guanosine monophosphate
cGMP-PDE	Cyclic guanosine monophosphate-phosphodiesterase
DAB	3,3'-diaminobenzidine
EDTA	Ethylenediaminetetraacetic acid
DHR	Dihydrorhodamine
DMEM	Dulbecco's modified Eagle's medium
DMSO	Dimethyl Sulphoxide
DNA	Deoxyribonucleic acid
DTPA	Diethylenetriaminepentaacetic acid
DPI	Diphenyliodonium Chloride
EC	Endothelial cell
ECM	Extracellular matrix
EGF	Epidermal growth factor
EGF-R	Endothelial growth factor receptor
ELISA	Enzyme-linked Immunosorbant assay
EPR	Electron spin resonance
ERKs	Extracelluar signal Regulated Kinases
FAD	Flavin adenine dinucleotide
FCS	Foetal calf serum
FGF	Fibroblast growth factor
bFGF	Basic fibrobast growth factor
GAG	Glycosaminoglycan
GC	Guanylate cyclase
GPAC	Gram-positive anaerobic cocci
GSH	Glutathione
GSSH	Glutathione disulphide
GTP	Guanylate triphosphate
h	Hours
H_2O	Water
H_2O_2	Hydrogen Peroxide
HB-EGF	Heparin-binding EGF-like growth factor
HCL	Hydrochloric acid
HDF	Human dermal fibroblast
aHDF	Adult human dermal fibroblast
nHDF	Neonatal human dermal fibroblast
HEPES	N-(2-hydroxyethyl)-piperazine-N'-2-ethanesulfonic acid
HGF	Hepatocyte growth factor
HIF-1	Hypoxia inducible factor-1
HIV	Human Immunodeficiency virus
HLE	Human leukocyte elastase

HOONO	Peroxynitrous acid
HSPG	Heparin sulphate proteoglycan
HUVEC	Human umbilical vein endothelial cell
HMW	High molecular weight
HPF	Hydroxylphenyl fluorescein
ICAM	Intercellular adhesion molecule
IGF-1	Insulin growth factor-1
IgG	Immunoglobulin G
IL	Interleukin
IFN	Interferon
IXP	Isoxanthopterin
JNKs	c-jun N-terminal Kinases
KGF	Keratinocyte growth factor
KHG	Keratahyalin granules
K_m	Michealis constant
LB	Luria Bertani Broth
LFA-1	Leukocyte function-associated antigen
LG	L-Glutamine
M	Fibroblast growth medium
MAPKs	Mitogen-activated kinases
MB	Methylene blue
mg	Milligrams
min	Minute
ml	Milliletre
mm	Millimetre
mmHg	Millimeters of mercury
MMPs	Matrix metalloproteinases
MO	Molybdopterin cofactor
MSSA	Meticillin sensitive *Staphylococcus aureus*
MT-MMP	Membrane type matrix metalloproteinase
MRSA	Meticillin-resistant *Staphyloccus aureus*
MTT	Methylthiazolyldiphenyl-tetrazolium bromide
NAD^+	Nicotinamide adenine dinucleotide
NADH	Nicotinamide adenine dinucleotide (Reduced)
$NADP^+$	Nicotinamide adenine dinucleotide phosphate
NADPH	Nicotinamide adenine dinucleotide phosphate (Reduced)
NaOH	Sodium hydroxide
NE	No enzyme
NEP	Neural endopeptidase
NF-κB	Nuclear Factor kappa B
NHS	National health service
HRP	Horse radish peroxidase
$^{\bullet}NO$	Nitric Oxide
NO^+	Nitrosyl cation
NO^-	Nitroxyl anion
NO_2^-	Nitrite
NO_3^-	Nitrate
NOS	Nitric oxide synthase
eNOS	Endothelial nitric oxide synthase
iNOS	Inducuble nitric oxide synthase
NS	No substrate
O_2	Molecular oxygen
$O_2^{\bullet -}$	Superoxide
$^{\bullet}OH$	Hydroxyl radical
$ONOO^-$	Peroxynitrite
$dONOO^-$	Decomposed peroxynitrite
PARS	Poly(ADP-ribose) synthetase
PBS	Phosphate buffered saline

PDGF	Platelet derived growth factor
PEI	Polethyleneimine
PKC	Protein kinase c
PO_2	Partial pressure of oxygen
PS	Penicillin/Streptomycin
PVA	Polyvinyl alcohol
mRNA	Messenger ribonucleic acid
RNS	Reactive nitrogen species
ROS	Reactive oxygen Species
ROIs	Reactive oxygen intermediates
RONS	Reactive oxygen and nitrogen species
Rpm	Revolutions per minute
SAPKs	Stress activating protein kinase
SC	Stratum corneum
SCFA	Short chain fatty acid
SOD	Superoxide dismutase
SB	Stratum basale
SD	Standard Deviation
SEM	Standard error of the mean
SG	Stratum granulosum
SIN-1	3-Morpholinosydononimine
Spp	Species
SS	Stratum spinosum
STAT	Signal transducers and activators of transcription
TAF	Thrombin activatible fibrinolysis inhibitor
TGF-β	Transforming growth factor-β
TIMPs	Tissue inhibitors of metalloproteinases
TMB	3,3'5,5'-tetramethylbenzidine
TNF-α	Tumour necrosis factor α
TSB	Tryptone-Soya Broth
TSP-1	Thrombospondin-1
uPA	Urokinase-type plasminogen activator
U	Units
UTIs	Urinary tract infections
VLA	Very late activation antigen
VCAM	Vascular cell adhesion molecule
VEGF	Vascular endothelial growth factor
VRSA	Vancomycin-resistant *Staphylococcus aureus*
XDH	Xanthine dehydrogenase
XO	Xanthine oxidase
XOR	Xanthine oxidoreductase
µl	Microlitre
µm	Mircrometre
µm	Micromolar

CHAPTER 1

1 Introduction: The Biology of the Skin

The skin is the largest organ in the body, and is composed of three layers: a stratified epithelium (epidermis), an underlying connective tissue stroma (dermis) separated by a basement membrane and subcutaneous (or fatty) tissue (Figure 1.1).

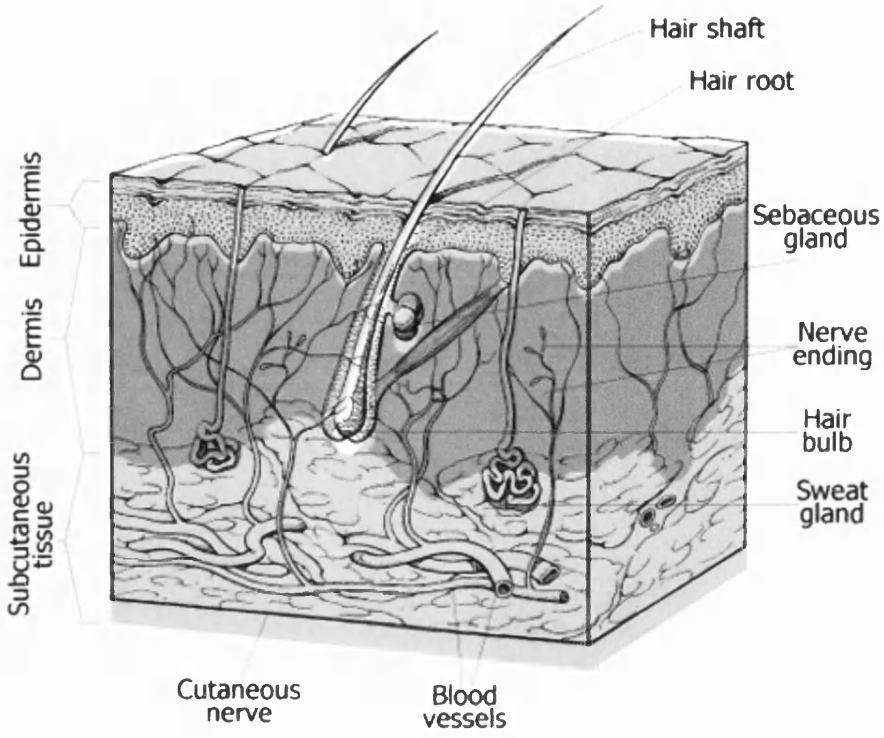

Figure 1.1 Basic diagram to show the three layers of the skin and various associated structures.

American Medical Association Current Procedural Terminology, Revised 1998 edition. http://www.ama-assn.org/ama/pub/category/7176.html

The skin is often described as a bilayer organ which refers to the epidermal and dermal layers. The average thickness of the bilayer is 1-2 mm being considerably thinner in infants and the elderly especially the dermis which is underdeveloped in infants and atrophic in the elderly. These layers possess many specific properties that are essential for survival some of which are listed below;

Epidermis

- protection from desiccation
- protection from bacterial entry
- protection from toxins
- preventing excess fluid loss

- neurosensory
- social-interactive

Dermis

- Protection from trauma due to elasticity and durability properties
- Fluid balance and thermoregulation through regulation of skin blood flow
- Growth factors and cytokines for epidermal replication and dermal repair

1.1 The epidermal layer

The epidermis is a stratified squamous epithelium mostly ~100-150μm thick, although its thickness is greater (0.8-1.4mm) on the palm and sole (Gawkrodger, 1992). The main function of this outer layer of skin is to act as a protective barrier. Around 95% of the epidermis is made up of cells known as keratinocytes (which produce keratin), and the rest are melanocytes, Langerhans cells, and Merkel cells (Mechanoreceptors) (Menon, 2002). The epidermis can be divided into four layers that represent stages of maturation of keratinocytes.

- Stratum basale
- Stratum spinosum
- Stratum granulosum
- Stratum corneum

1.1.1 Stratum basale (SB)

The SB adjacent to the dermis, is the innermost layer of the epidermis and is mainly composed of a single layer of columnar basal cells. The SB also consists of epidermal stem cells which transiently amplify cells to renew the epidermis (Menon, 2002). These cells are mainly keratinocytes which contain keratin filaments (tonofibrilaments) which are attached to the dermal-epidermal basement membrane by hemidesmosomes (Figure 1.2). Two keratins, K14 and K5, are expressed in the basal cells (Menon, 2002). Melanocytes make up 5-10% of the basal cell population. These cells synthesise melanin and transfer it via dendritic processes to neighbouring keratinocytes. Melanocytes, being of neural crest origin, are most numerous on the face and other exposed sites. Merkel cells are occasionally found in the SB and appear to be associated with terminal filaments of cutaneous nerves, having a possible role in sensation. Neuropeptide granules, neurofilaments and keratin can be found in the cytoplasm of merkel cells (Gawkrodger, 1992).

1.1.2 Stratum spinosum (SS)

Daughter basal cells migrate upwards to form this layer of polyhedral cells. Adjacent cells are interconnected by an abundance of desmosomes giving its cells a characteristically spiny appearance at light microscope level. Langerhans cells are found mostly in this layer; these are dendritic, immunologically active cells. An increase in keratin filaments is noticeable in this layer. Keratin tonofibrils form a supportive mesh in the cytoplasm of these cells. Keratins 1 and 10 are the biochemical markers for this layer (Menon, 2002). Lipid-enriched lamellar bodies, also known as Odland bodies, keratinosomes and membrane-coating granules, begin to appear in the SS which supply the extracellular domains with specialised lipid components. Lamellar bodies are 0.2 to 0.5μm in diameter (Menon, 2002).

1.1.3 Stratum granulosum (SG)

Compared with the basal layer and in the uppermost layers of the SS, the cells begin to elongate and flatten. Cells become flattened and lose their nuclei in the granular cell layer. Keratohyalin (KHG) granules characterise the SG, and are present in the cytoplasm together with membrane-coating granules (which expel their lipid contents into the intercellular spaces) (Gawkrodger, 1992).

1.1.4 Stratum corneum (SC)

The stratum corneum is the outermost layer of the epidermis. Terminally differentiated keratinocytes can be found in this layer which is comprised of overlapping polyhedral cornified cells with no nuclei (corneocytes). In the SC, cells adhere to each other using lipid glue giving a brick-and-mortar organisation, and in human skin it usually consists of 18 to 21 layers of cells (Menon, 2002). The corneocyte cell envelope is broadened, and the cytoplasm is replaced by keratin tonofibrils in a matrix formed from the keratohyalin granules (Gawkrodger, 1992).

1.2 The Dermal-Epidermal Basement Membrane (BM)

Basement membranes are collections of extracellular matrix (ECM) molecules organised in specific patterns which separate epithelium, endothelium, nerve and muscle from neighbouring connective tissue stroma (Timpl, 1989). The dermal-epidermal basement membrane (BM) forms an extensive interface between the dermis and the epidermis, and is one of the largest epithelio-mesenchymal junctions in the body. The basement membrane maintains tissue architecture, provides anchorage of adjacent cells,

functions as a selective barrier to migrating or invading cells, and facilitates diffusion or temporary storage of macromolecules. It is permeable to oxygen and allows nutrients to pass from the dermis into the epidermis. Transmission electron microscopy has shown that the BM consists of a lamina lucida, underlying epithelial or endothelial plasma membranes, and a lamina densa which is located between the lamina lucida and underlying stroma (Figure 1.2).

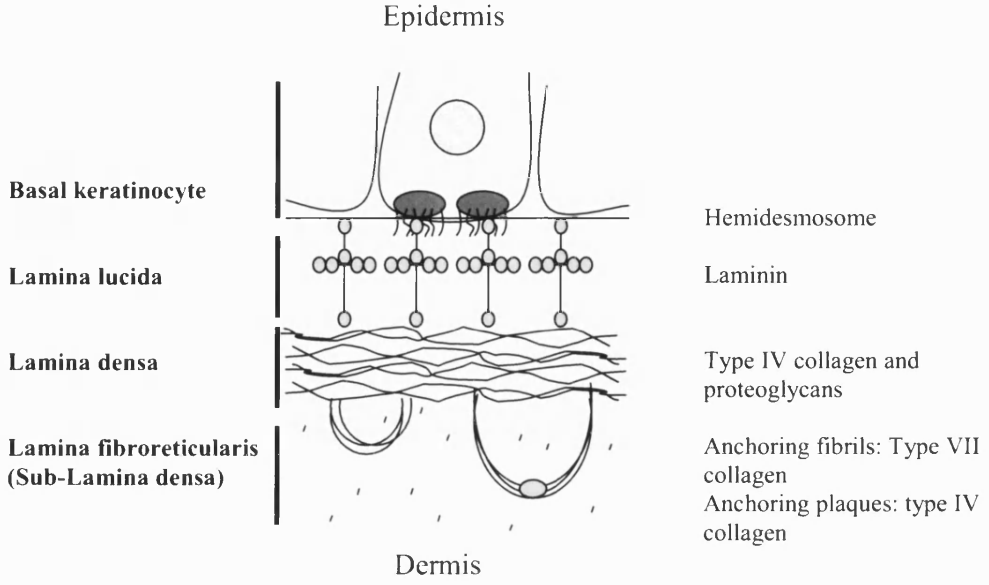

Figure 1.2 Detailed schematic of the basement membrane zone at the dermo-epidermal junction

Studies of the dermal-epidermal BM suggest that both epithelial tissues and differentiated fibroblasts in the dermal layer produce BM components and assist in BM assembly. Dermal fibroblasts were shown to synthesise and deposit type IV collagen, type VII collagen, and laminin in a linear manner into the BM zone. Whereas, foetal bovine keratinocytes were found to synthesise and deposit type IV collagen, type VII collagen, laminin, K-laminin, kalanin, and BM associated heparin sulphate proteoglycan (HSPG) (Marinkovich *et al*, 1993). The BM is rich in the adhesive proteins, laminin and fibronectin which help cells to attach to the appropriate part of the ECM. Laminin promotes the attachment of epithelial cells to the basal lamina, whereas fibronectin anchors the epidermal cells from above and the dermal cells from below.

1.3 The Dermal Layer

The dermal layer is defined as a dynamic and thick layer of connective tissue matrix that is in constant turnover. This layer contains specialised structures, and is found immediately below and intimately connected with the epidermis. It varies in thickness,

being thin (0.6mm) on the eyelids and thicker (3mm or more) on the back, palms and soles. The dermis is divided into a thin upper layer known as the papillary dermis that lies beneath the epidermis. The papillary dermis contains anchoring epidermal rete pegs and is composed of loosely interwoven collagen. The papillary dermis is the most biologically active part of the dermis producing proteins that provide direction for epidermal replication. The upper dermis also contains the highest blood flow. Coarser and horizontally running bundles of collagen are found in the deeper and thicker reticular dermis. Collagen fibres make up 70% of the dermis and impart a toughness and strength to the structure. Elastin fibres are loosely arranged in all directions in the dermis and provide elasticity to the skin. They are numerous near hair follicles and sweat glands, and less so in the papillary dermis. The ground substance or matrix of the dermis is made up of complex polysaccharide, a protein complex known as glycosaminoglycan or GAG component, as well as hyaluronic acid. The matrix is semi fluid which allows movement of dermal structures, cell and connective tissue orientation, nutrient diffusion to the cells, scaffolding for cell migration, viscosity and hydration. In the dermis, chondroitin sulphate is the main GAG, along with dermatan sulphate and hyaluronic acid. GAGs often exist as high molecular weight polymers with a protein core. These structures are known as proteoglycans.

The dermis also contains dermal dendrocytes (dendritic cells with a probable immune function), mast cells, macrophages and lymphocytes, platelets and endothelial cells. However, the primary cell type is the fibroblast which synthesises ECM proteins collagen and elastin, other connective tissue and matrix or ground substance. Fibroblasts produce the key adhesion proteins used to attach epidermal cells to the BM and are used for epidermal cell migration and proliferation. For example, fibronectin is a key fibroblast derived signal protein that is important in cutaneous healing and has numerous roles in the orchestration of wound healing (Grinnell, 1984).

Collagen synthesised by fibroblasts, is the major structural protein of the dermis. The main amino acids in collagen are glycine, proline and hydroxyproline. There are over eight types of collagen, at least five of which are found in skin:

- Type I- found in the reticular dermis (Predominant matrix protein of dermis, besides structure; provides a contact orientation for dividing and migrating epithelial cells)
- Type III-found in the papillary dermis
- Types IV and VII- found in the basement membrane structures
- Type VIII-found in endothelial cells

Tropocollagen is formed from three polypeptide chains which are coiled around each other in a triple helix. Assembled collagen fibrils are 100nm wide, with cross-striations visible with electron microscopy every 6nm. Ehlers-Danlos syndrome is characterised by aberrant collagen production and can result in hyperextensible skin, easy bruising and 'cigarette paper' scars, to mention but a few of the clinical manifestations (Byers *et al*, 1981; Byers, 1989).

1.3.1 Fibroblasts

As mentioned previously, fibroblasts are the main cell type within the dermis. Under electron microscopy, the developing fibroblast has an abundant cytoplasm, with a well developed endoplasmic reticulum and prominent ribosomes, suggesting active protein synthesis.

Numerous factors control fibroblast activity, in particular cytokines, such as transforming growth factor β (TGF-β) which appears to play an important role in fibrotic disorders such as scleroderma, in which there is up regulation in the production of extracellular matrix precursor molecules for types I and type III collagen. Much work has been aimed at controlling the physiological effects of this molecule (Leroy *et al*, 1990).

Fibroblasts adhere to proteins, which they secrete, including several forms of collagen (types I, III, IV and VI), fibronectin and laminin, which allows the fibroblasts to be suspended in the ECM of the ground substance (Mauch and Kreig, 1990). The ground substance itself appears to be important in the control of fibroblast growth. Laminin fragments induce growth via a specific receptor, and this has been linked to the growth associated with wound damage or tissue remodelling, as these fragments become exposed (Mauch and Krieg, 1990). Fibronectin and collagens I, II and III (and their fragments) have also been shown to be chemotactic to human dermal fibroblasts. This could be important in wound healing, in that collagen degradation during tissue injury releases peptides from the matrix, recruiting fibroblasts to the area for repair (Mauch and Kreig, 1990). Some of these migrating fibroblasts do not only produce the ground substance, but can also differentiate into myofibroblasts, which express α-(smooth muscle) actin. Myofibroblasts can form very tight fibronexus junctions with the neighbouring fibronectin in the granulation tissue of the damaged area and are involved in wound contraction (Grinnell, 1994).

1.4 Biology of successful wound healing

Wound healing is a complex process of many overlapping phases. It involves a complex interaction between a variety of ECM components, cell types and soluble mediators, which is coordinated by a wide array of cytokines and growth factors. Nevertheless, despite its complexity, wound healing can be loosely divided into 4 interrelated phases (Figure 1.4);

- Haemostasis
- Inflammation
- Proliferation
- Remodelling

1.4.1 Haemostasis

The process of skin wound healing begins at the moment of injury, whether it is intentional, such as a surgical incision, or unintentional, as in trauma. Damage to blood vessels initiates a haemostatic cascade of blood clotting, platelet aggregation and degranulation. A blood clot, or thrombus, fills the defect in the skin and seals the wound, providing protection against bacterial infection and fluid loss (Mast and Schultz, 1996). Thrombus formation occurs via an interaction between endothelial cells, platelets trapped in a fibrin meshwork and coagulation factors (Grinnell, 1984). Platelets are important, not only in recognising and occluding the defect, but also in promoting blood coagulation and in secreting growth factors for fibroblasts and perhaps other cells implicated in the wound healing process. Growth factors released from platelets and other injured cells, rapidly diffuse from the wound into the surrounding tissues and blood system (Figure 1.3). Trapped cells within the clot, predominantly platelets, trigger an inflammatory response by the release of vasodilators and chemoattractants and activation of the complement cascade.

Injuries that damage the microvasculature result in localised low oxygen tension (hypoxia) in the wound (Niinikoski *et al*, 1972). Hypoxia inducible factor-1 (HIF-1) has been identified as a transcription factor that is induced by hypoxia and is known to be important in triggering the transcription of growth factors such as TGF-β1, platelet derived growth factor (PDGF), endothelin-1, fibroblast growth factor (FGF-2), vascular endothelial growth factor (VEGF) and hepatocyte growth factor (HGF) (Kourembanas *et al*, 1991; Falanga *et al*, 1991a; Helfman and Falanga, 1993; Onimaru, *et al*, 2002; Brogi *et al*, 1994; D'Arcangelo *et al*, 2000). These factors support healing by stimulating angiogenesis, fibroblast proliferation and collagen synthesis (Falanga *et al*, 1993; Falanga

and Kirsner, 1993). Angiogenesis is vital for the delivery of oxygen, nutrients and growth factors necessary to initiate wound healing. These cellular and tissue responses occur in response to hypoxia for effective repair and re-establishment of tissue homeostasis.

1.4.2 Inflammation

The early stages of inflammation are characterised by neutrophils invading the wound almost immediately, following formation of the blood clot. The role of these cells is to continue to produce proinflammatory cytokines, such as tumour necrosis factor-α (TNF-α) and interleukins. Neutrophils are also important in controlling infection by removal of bacteria by phagocytosis, and by removal of other foreign material such as damaged ECM, by the release of enzymes (elastase and collagenase). This early protease activity is important in the debridement of the wound, although, in the absence of infection, neutrophils do not seem necessary for the normal healing of wounds. After approximately 24 hours neutrophils reduce in number and macrophages predominate. Circulating monocytes are chemotactically drawn into the wound, by TGF-β or fragments of fibronectin and become activated macrophages. Macrophages secrete pro-inflammatory cytokines and engulf and destroy bacteria. Interest has also focused on the role of macrophages in coordinating the transition from inflammation to proliferation through the release of soluble mediators, which include PDGF, TNF-α, TGF-β, insulin growth factor 1 (IGF-1) (Figure 1.3). Cytokines interleukin (IL)-4 and interferon-gamma (IFN-γ) differentially modulate VEGF release, from normal human keratinocytes and fibroblasts. Under normal circumstances, neutrophils disappear from the wound after about 3 days and the inflammatory phase begins to decline. Macrophages continue to secrete growth factors that stimulate migration of fibroblasts, epithelial cells, and vascular endothelial cells into the wound, in preparation for the next phase of repair.

Many wound related cells including both neutrophils and macrophages also possess specialised enzymes that can reduce molecular oxygen to produce reactive oxygen species (ROS). These ROS include H_2O_2 and $O_2^{\bullet-}$ which disinfect the wound, and at low concentrations act as signalling molecules to support wound healing. Lactate accumulation is a common characteristic of wounds in which glycolysis, occurs both aerobically and anaerobically, contributing to its production. In a study carried out by Wagner *et al* (2004) increased proliferation of cultured fibroblasts by exogenous lactate was mediated by intracellular oxidant production. Hydroxyl radicals have also been shown to stimulate lymphocyte proliferation (Novogrodsky *et al*, 1982).

1.4.3 Proliferation

The fibrin clot, which is formed in the inflammatory phase, is used as a provisional matrix by fibroblasts that specifically recognise fibrin and are able to migrate into the wound bed. Fibroblasts begin to proliferate and the cellularity of the wound increases. Furthermore, fibroblasts are the key cells involved in the production of ECM. They are known to produce collagen, tenascin, fibronectin, and proteoglycans (such as hyaluronic acid). Production of ECM is seen clinically as the formation of granulation tissue. This repair phase often lasts several weeks (Mast and Schultz, 1996). As the number of macrophages in the wound decrease, other cells in the wound such as fibroblasts, keratinocytes and endothelial cells, begin to synthesise and secrete a range of growth factors (Figure 1.3). These growth factors continue to stimulate proliferation, ECM protein synthesis and angiogenesis.

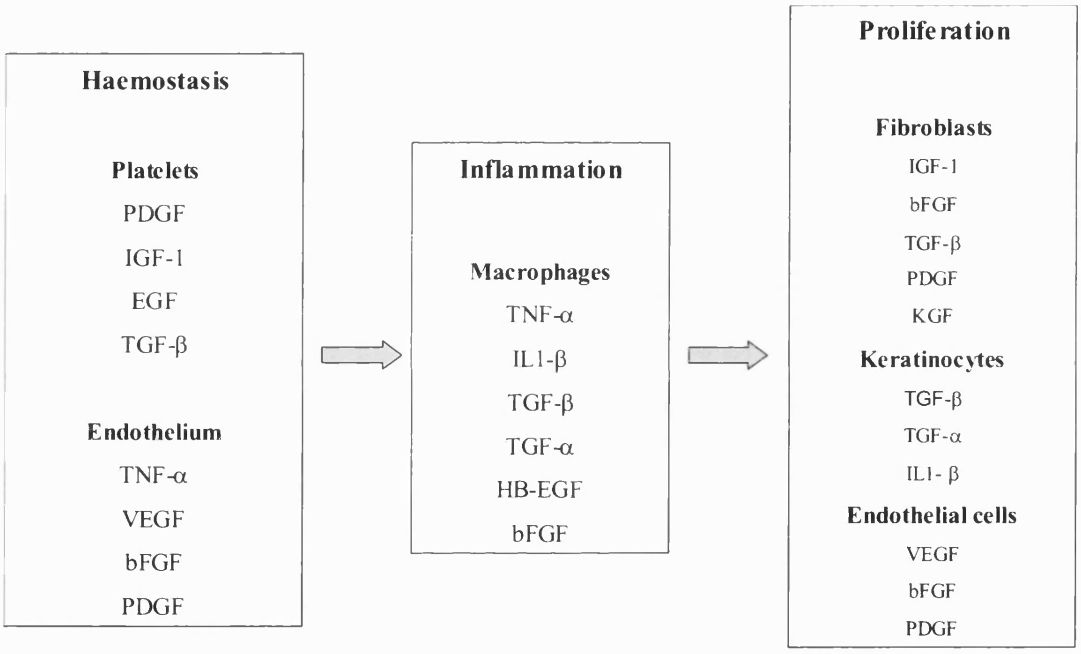

Figure 1.3 A summary of the cytokine supply for wound healing

Whilst new matrix is synthesised, the existing matrix in and around the wound margin is degraded by proteinases such as matrix metalloproteinases (MMPs) and serine proteinases (plasmin). Proteinases are enzymes that cleave peptide bonds in the central regions of polypeptides and are classified into groups due to mechanisms of catalytic activity, namely; serine, metallo-, cysteine and aspartic proteinases. Serine and metalloproteinases are also termed 'neutral proteinases' as their activity is optimal at a neutral pH. These proteinases play an important role in ECM degradation and are both calcium, and zinc dependent. MMPs are of particular research interest (Table 1.1), and are well known for their proteolytic activity. They exist as single chain proenzymes that are

secreted as latent zymogens requiring activation for proteolytic activity. In the wound healing process MMPs play an important role in the regulation of cellular migration and ECM remodelling following injury (Tomasek *et al*, 1997; Shi *et al*, 1999). Fibroblast MMP production has in fact been shown to be increased in tissues that exhibit increased rates of healing, for example foetal fibroblasts (Gould *et al*, 1997). MMPs have also been shown to be necessary in the epithelial resurfacing of cutaneous wounds (Agren, 1999a). MMPs are regulated by specific tissue inhibitors (TIMPs) which are believed to be important in healing by preventing excessive tissue degradation.

Some keratinocytes at the wound edge proliferate, whilst others undergo transformation to enable phagocytosis of debris and migration across the wound bed. Keratinocyte migration and wound contraction results in re-epithelialisation and wound closure. Inhibition of keratinocyte growth factor (KGF) receptor signalling has been shown to reduce the proliferation rate of epidermal keratinocytes at the wound edge, resulting in substantially delayed reepithelialisation of the wound (Werner *et al*, 1994).

Subgroup	Name	Other names	MMP Number	Substrate
Collagenases	Collagenase 1	Interstitial collagenase (Fibroblast-type collagenase)	MMP-1	Collagen types I, II, III, VI, X, gelatins, proteoglycans
	Collagenase 2	Neutrophil collagenase (PMN-type collagenase)	MMP-8	See MMP-1
	Collagenase 3	Rat interstitial collagenase	MMP-13	Gelatins, collagen types IV, V, X, XI, elastin, fibronectin, proteoglycans
Gelatinases	Gelatinase A	72 KDa gelatinase Type IV collagenase	MMP-2	Gelatins, collagen types IV, V, elastin, proteoglycans
	Gelatinase B	92 KDa type IV collagenase	MMP-9	Gelatin, Collagen types II, IV, V, IX, X,
Stromelysins	Stromelysin 1	Transin, proteoglycanase, CAP	MMP-3	Proteoglycans, fibronectin, laminin, elastin
	Stromelysin 2	Transin 2	MMP-10	See MMP-3
	Stromelysin 3	Furin motif	MMP-11	Gelatin, fibronectin, proteoglycan
Membrane-type MMPs	Matrilysin	Pump-1	MMP-7	See MMP-11
	Metalloproteinase	Metalloelastase, Macrophage elastase	MMP-12	Elastin
	MT-MMP-1 MT-MMP-2		MMP-14 MMP-15	Collagen type IV, gelatin

Table 1.1Classification of matrix metalloproteinases

A number of MMPs have been isolated and characterised, and are known to share common features that allow their classification as a family (Woessner and Nagase, 2000). The MMP family can be divided into 4 main subgroups, mainly based on their substrate preferences. These members include collagenases,

gelatinases, matrilysins, stromelysins and membrane-type matrix metalloproteases. MMPs are known to function at a neutral pH, contain zinc at their active site and require calcium for stability.

1.4.4 Remodelling

Once closure is achieved, remodelling of the scar occurs, over months or years, with a reduction of both cell content and blood flow in scar tissue. TGF-β has been implicated as a mediator of excessive ECM deposition in scar tissue and in fibrosis.

Figure 4.1 summarises the normal wound healing processes that lead to the resolution and successful closure of a wound.

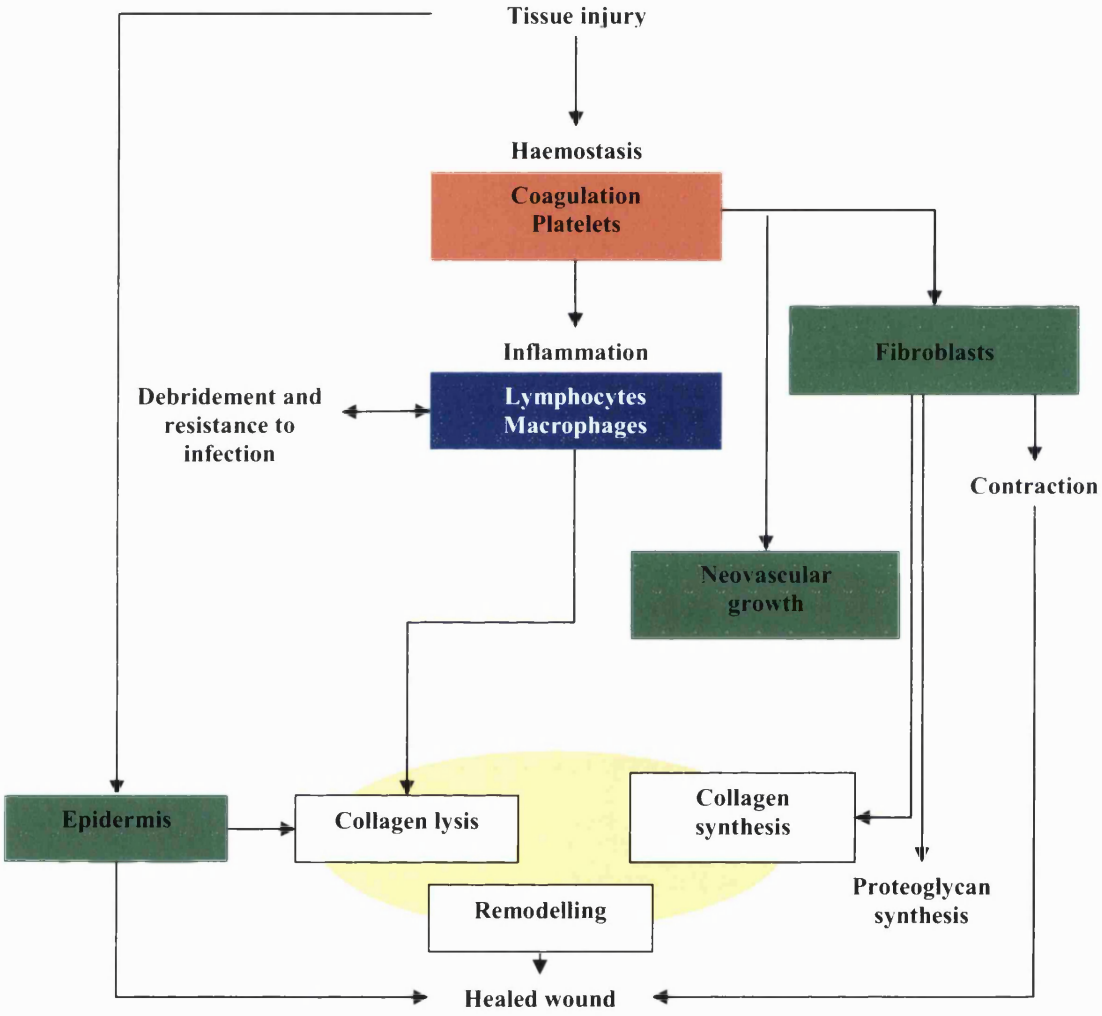

Figure 1.4 A summary of the wound healing process.

Wound healing can be divided into haemostasis (Orange), inflammation (Blue), cell proliferation (Green) and tissue remodelling (Yellow). Immediately after injury, platelets and coagulation factors result in thrombus formation. Platelets and other damaged cells secrete inflammatory mediators triggering an inflammatory response. Lymphocytes and macrophages act to control infection and debride the wound, and they also secrete growth factors to stimulate migration of wound-related cells into the wound. New collagen matrix is synthesised by fibroblasts and old matrix degraded by MMPs (Harding *et al*, 2002). Migration of keratinocytes and fibroblasts across the wound, results in contraction and wound closure.

CHAPTER 2

2 Introduction: Impaired healing of chronic wounds

A wound is considered chronic or non-healing if it does not heal in an orderly or timely sequence, or if the healing process does not result in structural integrity (Robson, 1997). Furthermore, wounds that heal improperly may not possess the necessary mechanical integrity to remain healed. In 1997, Tallman defined chronic wounds as those that do not appear to follow the normal healing process in less than 4 weeks.

2.1 Pathogenesis of chronic wounds

The term chronic wound covers a wide range of disease states that exist in three principal forms, decubitus (stasis) ulcers, vascular ulcers and diabetic ulcers. An ulcer can be defined as an area of skin loss extending through the epidermis into the dermis.

2.1.1 Decubitus (stasis) ulcers

Decubitus ulcers are a result of impaired capillary flow, reducing vascular or nutrient supply to the skin. The bony sites of the body are most prone to ulceration where the forces of compression can reach as much as 2600mmHg (Lindan *et al*, 1965). Both the degree of pressure and the duration have been found to be important in necrosis (Falanga, 1993c). It is thought that the application of an external force may cause interstitial pressure to rise and exceed the 12mmHg present in the venous capillary limb. This results in an increase in total tissue pressure, increased capillary filtration, oedema (an excessive accumulation of serous fluid in the extracellular spaces of tissue), and cell autolysis. Lymphatic channels are occluded, resulting in further oedema and autolysis (Reuler and Cooney, 1981). Fibrinolysis (the breakdown of fibrin in blood clots), is also altered following ischaemia, which may be due to endothelial cell damage and epidermal injury. Fibrin thrombi are a common feature of decubitus ulcers.

2.1.2 Vascular ulcers

Ulceration due to vascular causes is multifactorial and can be a result of both arterial and venous disease. Arterial disease is caused by hypertension (abnormally high blood pressure) and either progressive atherosclerosis (fatty deposits on the inner lining of the arterial wall) or by arterial embolisation (blockage) of the peripheral vessels. These

factors lead to ischaemia of the skin and arterial (or ischaemic) ulceration (Falanga, 1993a).

Venous disease is a result of chronic venous insufficiency, and the resulting venous hypertension results in the formation of venous ulcers (Falanga, 1993a). However, not all patients with venous disease develop active skin ulcerations. Venous insufficiency develops because of inadequate calf muscle pump action after the onset of, primary (with no obvious underlying aetiology) or secondary (as seen after deep venous thrombosis), valvular incompetence. When these valves become incompetent, the backflow of venous blood causes venous congestion and hypertension. Two hypotheses have been proposed to explain venous ulceration, once venous hypertension develops. The first states that distension of the capillary beds occurs because of increased stasis. This leads to leakage of fibrinogen into the surrounding dermis. Over time, a fibrinous pericapillary cuff is formed, impeding the delivery of oxygen and other nutrients or growth factors to the affected tissue (Falanga *et al*, 1987; Falanga *et al*, 1992b). It has been shown that the transcutaneous oxygen pressure of the skin surrounding a venous ulcer is decreased, suggesting that there are forces obstructing the normal vascularity of the area. The resulting hypoxic injury leads to fibrosis and then ulceration. The other hypothesis suggests that the endothelium is damaged by increased venous pressure and leukocyte activation. Proteolytic enzymes and free radicals are released, escape through the leaky vessel walls, and damage the surrounding tissue, leading to injury and ulceration. Haemoglobin, from the red blood cells, also leaks into the extravascular space, causing the brownish discoloration commonly noted. The typical venous ulcer is shallow and appears near the bony projections of the ankle joint, in combination with an oedematous and indurated leg. These ulcers may also present with a weeping discharge from the leg. Vascular ulcers are distinct with regard to their location, appearance, bleeding, and associated pain.

Figure 2.1 Venous Stasis Ulcer

2.1.3 Diabetic ulcers

The diabetic ulcer is characterised by neuropathy, ischaemia, and infection. The clinical result of neuropathy is due to the biomechanical properties of the foot being altered due to failure of motor nerves. This sensory impairment causes what is known as 'Insensate foot' and leads to the breakdown of skin after prolonged pressure or trauma and the occurrence of ulcers over bony prominences. Autonomic nerve failure also causes a decrease in sweating and blood flow, resulting in dry and easily damaged skin which is more sensitive to the effects of pressure (Falanga, 1993c).

The overwhelming factor that causes ischaemia in diabetic patients is atherosclerosis, which typically involves the distal arteries. The prevalence of peripheral vascular disease in diabetic patients is estimated to be 45% after 20 years of disease. Furthermore, in comparison with the general population, patients with diabetes mellitus are at a 4- to 6-fold increased risk of the development of atherosclerotic macro-vascular disease (Kannel, 1985; Keen and Jarret, 1979). Therefore, these patients have a substantially increased risk of amputation due to peripheral vascular disease (Most and Sinnock, 1983). Infection also plays a large part in the perpetuation of ulcerations and is aided by the well known negative effects of diabetes on neutrophil function (Falanga, 1993c).

Figure 2.2 Diabetic Foot Ulcer

2.2 Chronic wound environment and the factors involved in impaired healing

Chronic wounds possess features that are specific to the wound type and the individual. However, many factors related to wound chronicity have been identified, and are common to various wound types. As a result, the treatment of chronic wounds has been targeted to common factors by similar therapeutic methods. Normal wound healing is a tightly regulated balance of new tissue formation and the destructive mechanisms required to remove damaged tissue. Within this complex environment there are many stages that precisely control the biological processes required to achieve normal wound repair. A variety of factors have been identified that are believed to play a role in the impaired healing of chronic wounds. These include hypoxia/ischaemia, reactive oxygen species, imbalances in cytokine levels and proteolytic enzymes/inhibitors, excessive fibrin deposition, failure of reepithelialisation, prolonged/impaired inflammation, a defective wound matrix, infection, and cell senescence and are covered in more detail this section. Systemic factors are also important, such as advanced age, malnutrition, and disease.

2.2.1 Hypoxia/ ischaemia

Whatever their initial cause, chronic wounds usually result from a lack of oxygen and nutrients to the tissues involved. Although hypoxia is to some degree a result of normal tissue injury, and may even stimulate normal repair, chronic ischaemia is clearly a pathological condition that inhibits normal healing. Prolonged hypoxia or ischaemia is a common characteristic of the chronic wounds, and is implicated in their development, perpetuation and aberrant healing.

When a cell is deprived of oxygen, it switches to anaerobic metabolic pathways. This produces less adenosine triphosphate (ATP) energy for normal cellular activities, and causes an increase in lactic acid. If oxygen deprivation is short term, as in normal healing, the cell can function relatively normally until oxygen levels are restored. If hypoxia is prolonged or severe, as in chronic wounds, the cell will become ischaemic. A build up of lactic acid in the cell lowers intra-cellular pH. This denatures the cellular proteins and they become unable to perform their normal functions. In particular, the proteins in the cell membrane denature and the membrane begins to leak. The cell and its internal organelles swell and start to rupture resulting in leakage of cytosolic enzymes into the circulation. The cell releases inflammatory mediators, such as prostaglandins causing pain and inflammation to the area. At this stage, the cell can still recover if the oxygen supply is restored. Further stress and continued hypoxia however, leads to necrosis or cell death (McCord, 1985).

Low oxygen tension is well established in chronic wounds (Falanga *et al*, 1987; Falanga, 1991b; Falanga *et al*, 1992b; Moosa *et al*, 1987; Falanga *et al* 1994), particularly in venous ulceration and ulcers due to atherosclerosis and diabetes (Pecoraro *et al,* 1991a; Pecoraro, 1991b). Mean values as low as 13mmHg have been quoted for venous ulcers in comparison to mean reference values of 75mmHg (Falanga *et al*, 1992b). Low pH has also been measured by Dissemond *et al* (2003) who measured pH values ranging from 5.45 to 8.65 in 39 patients with chronic wounds of varying origins. Furthermore, over a period of 12 months, individual values varied up to 1.73 units, showing pH to be a dynamic factor. In low oxygen tension, human-derived fibroblast cultures synthesise larger amounts of TGF-β1, and the proliferative activity of dermal fibroblasts is enhanced (Falanga *et al*, 1991a; Falanga and Kirsner, 1993). TGF-β is a potent growth factor that stimulates the production of collagen types I, II, III, IV, V,VII, elastin and fibronectin. Studies by Uitto *et al* (1974) have also shown that oxygen is required for procollagen hydroxylation. These results suggest that the ischaemia in chronic wounds may lead to the synthesis of a less stable procollagen, or to fibres with decreased strength. However, even with the possibility

of impaired collagen synthesis, it is also believed that hypoxia may account for the fibrotic response seen in many chronic wounds (e.g lipodermatosclerosis of venous ulceration). This fibrotic tissue may then interfere with normal tissue repair. This suggests that, optimal oxygen concentrations may be required to allow appropriate cellular repair and synthesis of appropriate amounts and quality of matrix material.

As briefly mentioned in section 1.4.2 ROS generation is important in reducing infection and cellular signalling to support the wound healing processes. These ROS are generated by an enzyme known as Nicotinamide adenine dinucluotide phosphate (NADPH) oxidase which is associated with many wound related cells and defects in this enzyme and low wound pO_2 are associated with impaired healing in humans (Gordillo and Sen, 2003). The concentration of O_2 necessary to achieve half maximal ROS production (the K_m) is in the range of 45 to 80mmHg, with maximal ROS production seen at >300mmHg (Allen *et al*, 1997). Therefore, it is likely that the ischaemic environment of the chronic ulcer would compromise the function of these enzymes.

2.2.2 Chronic inflammation

Whatever the cause of chronic wounds, one of the hallmarks is the presence of chronic inflammation (Agren *et al*, 2000). Although, the importance of local inflammation in the healing process of acute wounds is well established, excessive or prolonged inflammation may delay healing and increase scar potential. An inflammatory response in the wound environment may be caused by complement degradation products; polymorphonuclear leukocyte products; oxygen free radicals; enzymes e.g proteinases and microbial products. Infection ischaemia, necrotic or damaged tissue, or foreign matter can prolong inflammation in the chronic wound environment. Neutrophils and macrophages are phagocytic cells that secrete TNF-α, IL-1 and IL-8 during the inflammatory response. TNF-α initiates the proinflammatory cascade and promotes IL-1β synthesis. Studies have shown the TNF-α and IL-1β were increased in chronic wounds when compared with acute wound fluid (Mast and Schultz, 1996). Tumour necrosis factor-α and IL-1β are implicated in the upregulation of adhesion molecules such as ICAM-1 and VCAM. ICAM-1 and VCAM have been shown to be upregulated in venous ulcers allowing the migration of inflammatory cells into the wound. Weyl *et al* (1996) demonstrated perivascular accumulation of ICAM-1 and VCAM ligands, LFA-1 and VLA-4-positive inflammatory cells in leg ulcers.

2.2.3 Excessive proteinase production in the chronic wound

Imbalance of proteinases in the chronic wound environment appears to be responsible for the continuous breakdown of the newly formed ECM. Excessive proteinase activity in the chronic wound is probably due to prolonged inflammation, and the ongoing recruitment and activation of inflammatory cells, such as neutrophils and macrophages, which are attracted to the wound site by inflammatory cytokines. Excessive proteinase activity is therefore thought to contribute to tissue injury by overwhelming their inhibitors and binding to their substrates.

Fluid derived from chronic wounds has been shown to contain several leukocyte proteinases including serine proteinases, human leukocyte elastase (HLE), cathepsin G (CG), and urokinase-type plasminogen activator (uPA), and MMPs (Yager *et al*, 1997; Stacey *et al*, 1993). Excessive, inappropriate or prolonged activities of these leukocyte-derived proteinases are thought to play a role in the chronic ulcer environment (Barrick *et al*, 1999). Neutrophils and macrophages also secrete large amounts of elastase, which may cause constant degradation of granulation tissue that is crucial for cell migration and wound repair (Heiden *et al*, 1996; Herrick *et al*, 1997). Elastase activity is 10- 40-fold increased in chronic wounds when compared with acute wounds (Rao *et al*, 1995). Inhibitor inactivation may also contribute to the presence of active proteinases in chronic wounds, as inactivated α_1-proteinase inhibitor and α_2-macroglobulin which are responsible for the inactivation of thrombin and plasmin respectively, have been detected in chronic wound fluid (Yager *et al*, 1997; Rao *et al*, 1995).

2.2.3.1 Imbalance between MMPs and their inhibitors

Much of the research on impaired healing in chronic wounds has focused on imbalances in MMPs and their inhibitors (TIMPS) and their role in the disruption of ECM remodelling. Numerous studies have shown increased in MMP activity in fluid taken from chronic leg ulcers, in particular, increases in gelatinase and collagenase activity has been reported (Wysoki *et al*, 1993; Bullen *et al*, 1995; Weckroth *et al*, 1996). Furthermore, in fluid derived from pressure ulcers, levels of gelatinases MMP-2 and MMP-9 were found to be elevated more than 10-fold and 25-fold respectively, and increased levels of both total and active collagenase were measured (Yager *et al*, 1996). Collagenases have the unique ability to degrade the major structural ECM proteins in the dermis, namely the triple helical type I and type II collagens at Gly^{775}-Leu(lle)^{776}. After this initial and specific cleavage, ¾ and ¼ cleavage products are formed, and collagen is spontaneously denatured (helix to coil transition) to gelatine (Miller *et al*, 1976). Gelatin is further

degraded by a multitude of enzymes, in particular by gelatinases of types MMP-2 and -9 (Murphy *et al*, 1985).

Fibroblasts derived from unwounded skin from diabetics have shown elevated production of MMP-2 and pro-MMP-3 when compared with their non-diabetic counterparts (Wall *et al*, 2003). This may contribute to the increased risk of non-healing foot ulceration in diabetics. The growth of patient matched and chronic wound fibroblasts in three-dimensional collagen lattice systems showed the ability of chronic wound fibroblasts to reorganise the ECM was impaired. These studies described significantly decreased levels of MMP-2 and MMP-1 and an increased production of tissue inhibitors metalloproteinase-1 and -2 by chronic wound fibroblasts. (Cook *et al*, 2000). This result contrasts with numerous studies that report an increase in MMP activity and a decrease in TIMP activity; however, this suggests that it is an imbalance that is important in the disruption of ECM reorganisation. Furthermore, studies of normal human dermal fibroblasts in three-dimensional culture, indicates that hypoxia increases MMP-1 synthesis which is not restored by reoxygenation (Kan *et al*, 2003). Studies also indicate that a slower rate of proliferation, a greater collagenase activity and expression of collagenase mRNA by aging fibroblasts could be some of the main reasons for attenuation of wound healing in elderly patients (Khorramizadeh *et al*, 1999).

As well as chronic ulcer fluid, and chronic ulcer fibroblasts, studies on tissue biopsies taken from the ulcer bed have been used to determine proteinase activity, as it is thought wound fluid may not give an accurate impression of tissue levels of proteinases (Ashcroft *et al*, 1997). MMP levels recorded in chronic wound fluid are due to the activities of a variety of cell types such as inflammatory cells, keratinocytes as well as fibroblasts. Therefore, it is thought that local production and activation of MMPs in the tissue may give a clearer understanding of the impaired healing of chronic wounds. Studies using type II diabetic mice show that in the early stages of wound healing, protein levels of pro-MMP-2 and -9 are significantly reduced within wound tissue as well as the levels of active MMP-3 within the fluid. However, when human diabetic chronic wound fluid is compared with acute wound fluid, increased MMP-2 and reduced MMP-9 is detected. These differences may be due to the difference between tissue and wound fluid (Wall S. J *et al*, 2002). Excessive MMP-1 and MMP-2 activity has been observed in skin biopsies taken at the earlier stages of chronic venous insufficiency, (Herouy *et al*, 1998).

Decreased levels of active TIMPs, which inhibit MMPs preventing excessive ECM degradation, has also been reported in chronic wound fluid (Bullen *et al*, 1995, Yager *et al*, 1996). Studies have also shown that TIMPs, appear to to be complex-bound and inactivated (Bullen *et al*, 1995; Wysocki *et al*, 1993). Biopsies taken from chronic wounds

have also been found to be characterised by a decrease in TIMP-1 (Vaalamo *et al*, 1996). TIMPs-1 and -2 are responsible for the inhibition of collagenases, MMPs-1 and -2 respectively (Howard *et al*, 1991). As well as TIMPs, plasminogen activator and growth factors such as PDGF and TGF-β (Cullen *et al*, 1997; O'Kane and Ferguson, 1997) are known to regulate MMP activity within the wound. MMP production is also stimulated by inflammatory cytokines, such as IL-1, TNF-α and ECM proteins. For example, studies carried out by Han *et al* (2000), show the activation of pro-MMP-2 in dermal fibroblasts by TNF-α, and collagen. This suggests that the prolonged inflammation that is characteristic of chronic wounds may result in excessive MMP-2 production from fibroblasts present in the wound resulting in enhanced ECM degradation (Figure 2.3).

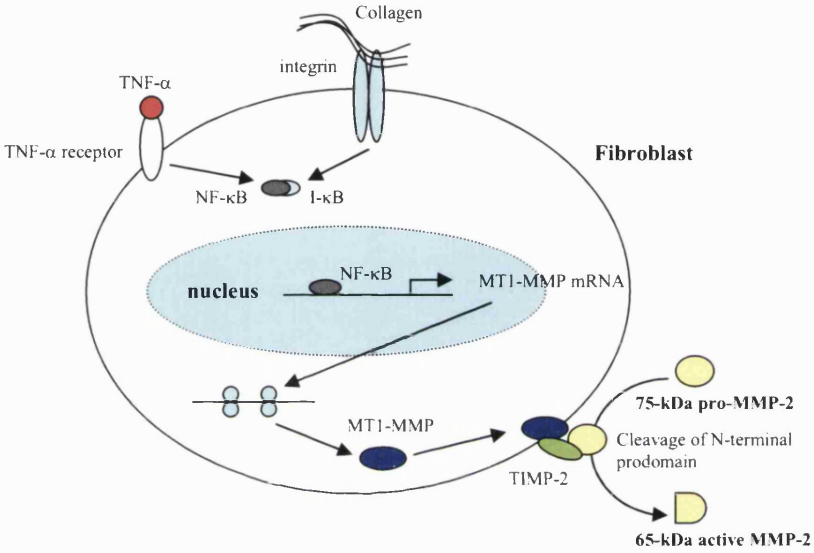

Figure 2.3 Proposed pathway for activation of pro-MMP2 in human dermal fibroblasts.

Activation of pro-MMP2 by TNF-α and collagen, resulting in NF-κB mediated induction of MT1-MMP (Membrane type metalloproteinase) (Han *et al*, 2000).

2.2.4 Degradation of the matrix components

Studies have shown that chronic wound fibroblasts synthesise comparable amounts of ECM as normal fibroblasts; suggesting that the defective wound matrix within chronic wounds is likely to be due to alterations in protease activity (Hasan *et al*, 1997). However, this contrasts with some studies by Herrick *et al* (1996) who reported a reduction in collagen production but similar amounts of fibronectin. However, this study used fibroblasts taken from venous ulcers and site-age matched individuals as controls, rather than fibroblasts from the patients themselves, as in the previously mentioned study. This difference might account for the variation in the observed outcome. The initial wound matrix contains glycosaminoglycans and fibronectin. Fibronectin is an adhesive glycoprotein that promotes cell adhesion, migration, differentiation and proliferation of

macrophages and fibroblasts (Grinnell, 1984). Fibronectin appears to be particularly susceptible to proteolysis (Wysocki and Grinnell, 1990). Extensively degraded adhesion proteins such as vitronectin and fibronectin have been described in some chronic wounds (Grinnell *et al*, 1992). Furthermore, diabetic and venous ulcers have been shown to contain decreased levels of fibronectin, and its degraded products (Grinnell and Zhu, 1996; Palolahti *et al*, 1993). Excessive protease activity in wounds may prevent cell adhesion necessary for normal wound closure. Other enzymes and proteases, including urokinase, play an important role in matrix degradation and in facilitating cellular migration. Urokinase enhances the synthesis of plasminogen an inactive protease precursor that is abundant in blood. Plasminogen is cleaved locally by other proteases, called 'plasminogen activators', to yield the active serine protease plasmin. Plasmin has an important role in wound healing and angiogenesis by allowing the cellular migration of microvascular cells through a fibrin matrix and restoring blood flow by helping to break up blood clots (Figure 2.4).

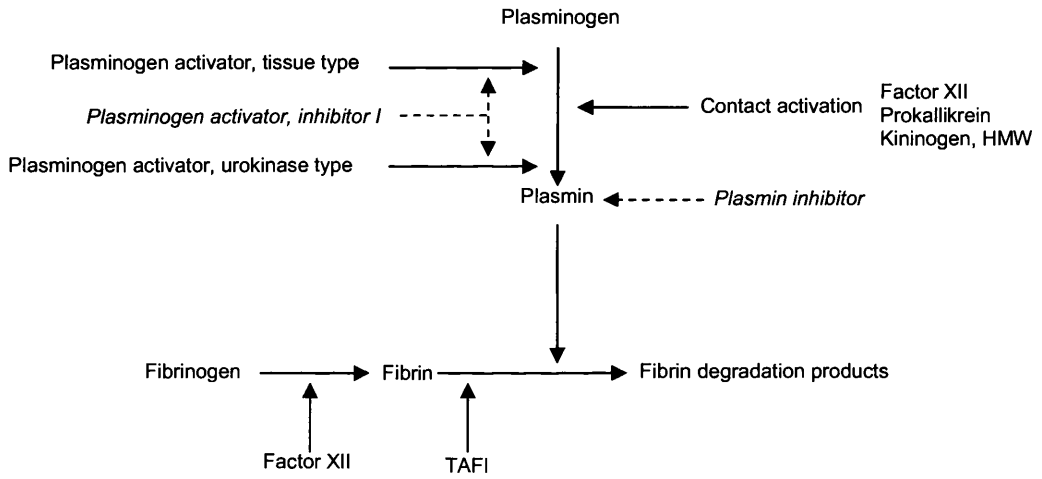

Figure 2.4The fibrinolytic pathway.

Inactive protease plasminogen is cleaved by plasminogen activators, tissue type and urokinase type, and by initiation of the contact phase (intrinsic pathway). This pathway is activated when Factor XII, which activates prokallikrein (inactive form of kallikreins which are serine proteases), and High molecular weight (HMW) kininogen (coagulation protein which acts as a cofactor) are exposed to a negatively-charged surface, or a "foreign" surface, for example collagen, basement membrane, lipopolysaccharide, or non-physiological surfaces such as glass. The active plasmin is then able to cleave fibrin. Fibrinolysis is regulated by inhibitors such as Thrombin activatable fibrinolysis inhibitor (TAFI).

2.2.5 Reduced levels of active growth factors

Growth factors are essential regulatory peptides involved in the cellular activities that take place in wound repair. Chronic wounds show reduced levels of PDGF, Basic fibroblast growth factor (bFGF), epidermal growth factor (EGF), and TGF-β compared with acute wounds (Falanga, 1992; Higley *et al*, 1995). Endothelial growth factor receptor (EGF-R) was also shown to be downregulated in the bed of venous ulcers, and

upregulated in the wound edge (Falanga *et al*, 1995). Keratinocyte growth factor expression in wounded skin of diabetic mice is significantly reduced and delayed, possibly contributing to impaired re-epithelialisation (Werner *et al*, 1994). A hypothesis for the pathogenesis of venous ulceration, suggests that macromolecules leaking into the dermis bind to growth factors or ECM molecules 'trapping' them and making them unavailable to the repair process (Falanga and Eaglestein, 1993). Fibrin persists in chronic wounds because fibrin is capable of forming less readily degradable complexes (Claudy *et al*, 1991). Other molecules bound to fibrin, such as fibronectin may facilitate binding of growth factors, as suggested by the 'trap hypothesis'. This suggests that there is not a lack of growth factors in the chronic wound environment, but that they are bound or inactivated by excessive proteolytic activity (Falanga, 1993b). However, a local lack of growth factors has not been demonstrated in chronic wounds. Expression of PDGF receptor-α and -β chains and VEGF receptors are upregulated in venous ulcers (Peschen *et al*, 1998a). Expression of bFGF (Peschen *et al*, 1998b), TGF-β (Mast and Schultz, 1996) and Insulin-like growth factor-1 (IGF-1) have shown to be increased in chronic wounds.

2.2.6 Role of inflammatory networks

An intact and correctly functioning neurosensory system is essential to the inflammatory response. Evidence does suggest that denervation impairs cutaneous microvascular function in healing (Carr *et al*, 1993). The loss of neuropeptide homeostasis is particularly relevant in diabetic wounds, decubitus ulcers and ulcers developed as a result of spinal cord injury. The inflammatory response is mediated by cutaneous sensory nerves by the release of neuropeptides, such as substance P, which stimulates the proinflammatory responses of keratinocytes, fibroblasts and endothelial cells. Neural endopeptidase (NEP) is responsible for the breakdown and thus regulation of substance P, and is found to be upregulated in the skin of diabetic patients and in diabetic ulcer fibroblasts (Antezana *et al*, 2002). Furthermore, NEP enzyme activity in mutant diabetic murine skin significantly exceeds that found in nondiabetic murine skin. The NEP inhibitor thiorpan was also found to improve wound closure kinetics in diabetic mice and appeared to enhance the inflammatory response (Spenny *et al*, 2002). It is therefore thought, that NEP may have an involvement in the disruption of the proinflammatory response and impairment of normal wound healing. Diabetes may also be responsible for a delayed infiltration of inflammatory cells into the wound space, resulting in a lack of cytokines that promote cell growth and wound repair.

2.2.7 Cellular senescence and inhibition of cell proliferation

The Hayflick model of cellular aging was developed with human neonatal fibroblasts. These fibroblasts showed they undergo proliferation and passage 40 to 60 times until they were no longer able to replicate, and it is this point that is referred to as cellular senescence (Hayflick and Moorhead, 1961). Chronic ulcers appear to contain a large number of fibroblasts that are arrested because of senescence, and accumulation of these cells within the tissues is though to mediate impaired dermal healing. It has been suggested that prolonged inflammation, delayed wound closure and extended exposure to chronic wound fluid affects cellular activity in the wound bed resulting in non-proliferative senescent cellular phenotype (Mulder and Vande Berg, 2002).

Fibroblast senescence, decreased population-doubling, and proliferation of chronic wound fibroblasts has been extensively covered in the literature (Stanley *et al*, 1997, Mendez *et al*, 1998; Vande Berg *et al*, 1998; Agren *et al*, 1999b). Studies by Bucalo *et al* (1993) have shown that venous ulcer fluid inhibits the proliferation of human dermal fibroblasts. Furthermore, dermal fibroblasts derived from ulcers older than 3 years grow at a slower rate when compared with ulcers that are less than 3 years old, and have a reduced proliferative response to platelet-derived growth factor. It is thought that this decrease in proliferative potential may be due to an increasing percentage of senescent fibroblasts (Agren *et al*, 1999b). Cells have also been shown to become less responsive to growth factors as they reach higher passage numbers. This is thought to be due to decreased receptors, lowered binding affinities of growth factor receptors and decreased efficiency of internalisation of the growth factor receptor complex (Reenstra *et al*, 1993). Venous ulcer fibroblasts taken from different patients have shown differing responses to growth factors (Stanley *et al*, 1997). Therefore replicative senescence in wound fibroblasts and reduction in proliferation provides a possible reason for the failure of wounds to respond to treatment (Mendez *et al*, 1998; Vande Berg *et al*, 1998).

However, these findings contrast with those of Herrick *et al* (1996) and Cook *et al* (2000). Differences may relate in part to cell culture techniques used, as Vande Berg *et al* (1998), showed that fibroblast senescence varied with biopsy site within the ulcer. Stephens *et al* (2003a) assessed cellular proliferation, senescence, telomere length, and ECM reorganisational ability, and observed that chronic wound fibroblasts demonstrated no evidence of senescence. It is therefore possible, that the distinct phenotype of chronic wound fibroblasts is not simply due to the aging process, mediated through replicative senescence, but instead reflects disease-specific cellular alterations of the fibroblasts themselves.

2.2.8 The microbiology of chronic ulcers

2.2.8.1 Bacterial colonisation and infection

Chronic ulcers occur in individuals and tissues that are prone to bacterial invasion due to local factors such as impaired vascular supply, trauma and systemic factors. Chronic ulcers are commonly contaminated with a variety of endogenous microorganisms, primarily of faecal, oral, and cutaneous origin. Studies have shown that the mean number of bacterial species in leg and foot ulcers ranges from 1.6 to 4.4 (Tentolouris *et al*, 1999; Bowler and Davies, 1999; Kontiainen and Rinne, 1988). The interaction between ulcer and bacteria can be separated into four levels: contamination, colonisation, critical colonisation and infection (Schultz *et al*, 2003). Contamination and colonisation are not thought to impair healing; whereas critical colonisation has been used to describe the stage at which bacteria begin to adversely affect healing in the absence of the typical clinical features of infection. In clinical terms infection is recognised by increased local pain, cellulitis, local abscess, necrotising faciitis, osteomyelitis, bacteraemia, or sepsis. Studies have shown that 86% of ulcers with no clinical signs of infection contained more than one bacterial species (Hansson *et al*, 1995). The progression from wound colonisation to infection depends not only on the bacterial count or the species present, but also on the host immune response, the number of different species present, the virulence of the organisms and synergistic interactions between the different species. There is increasing evidence that bacteria within chronic wounds live within biofilm communities, in which the bacteria are protected from host defences and develop resistance to antibiotic treatment.

Although the polymicrobial nature of many chronic ulcers involves aerobic, facultative and anaerobic microorganisms, (Ademiluyi *et al*, 1988; Daltrey *et al*, 1981; Gilchrist and Reed, 1989; Hansson *et al*, 1995; Bowler and Storr, 1998) delayed wound healing with or without clinical signs of infection has frequently been associated with aerobic or facultative pathogens (Danielsen *et al*, 1996; Eriksson *et al*, 1984; Gilliland *et al*, 1988; Madsen *et al*, 1996; Schraibman, 1990). However, anaerobic bacteria have also been isolated from chronic wounds using stringent anaerobic techniques. In 1999 Bowler and Davies, extensively studied the microbiology of 74 leg ulcers and reported 220 isolates from 44 infected leg ulcers compared with 110 isolates from 30 non-infected leg ulcers (Table 2.1). Statistical analysis also indicated a significantly greater mean number of anaerobic bacteria, particularly *Peptostreptococcus* spp. and *Prevotella* spp., per infected ulcer in comparison with the noninfected ulcer group. Subsequently, research by

Stephens *et al* (2003b) has shown anaerobic organisms to be present in the deep tissues of 14 out of 18 wounds as shown by a comparison of surface wound swabs and punch biopsy methods of isolation. Several of the anaerobic bacteria found in tissue biopsies were not found in tissue swabs implying that the latter do not give an accurate indication of the microflora present in the chronic wound. Furthermore, these ulcers were classified as noninfected with routine diagnostic tests and would not have been identified without the strict isolation and extended incubation techniques used in this study. Chronic ulcers are not only able to support a complex interaction of aerobic and facultative anaerobes, but they are also able to harbour obligate anaerobes, thus confirming the existence of a hypoxic environment.

2.2.8.2 Bacteria and impaired healing

The deep dermal tissues of all chronic wounds harbour microorganisms and the presence of microbes *per se* is not indicative of wound infection. However, the possibility that a critical microbial load might directly affect the healing outcome in both acute and chronic wounds has been considered for several decades, with a direct relationship first being demonstrated by Bendy and Landman (1964). Since then work by Robson (1997) and others has led to the widely-held opinion that non-healing is associated with a bacterial load of more than 10^5 bacteria per gram of tissue.

The precise interaction between microbes in the wounds and impaired healing is unknown. The concept of bacterial synergy which recognises the importance of interspecies interactions has been purported to occur in chronic wounds through studies such as that by Bowler and Davies (1999). They found the growth and pigmentation of some Gram-negative anaerobes to be enhanced by some facultative anaerobes through the provision of an essential, unidentified growth factor. Furthermore, enhanced virulence caused by synergistic interactions between aerobic and anaerobic bacteria in polymicrobial populations has been well documented (Brook, 1988; Brook, 1987; Rotstein *et al*, 1985a and b) and, although this has not been directly related to impaired healing and infection in leg ulcers, the effects in soft tissue infections are well recognised (Kingston and Seal, 1990).

Microbial isolates (aerobic and facultative anaerobes)	Infected leg Ulcers	Noninfected leg ulcers	Microbial isolates (Obligate anaerobes)	Infected leg ulcers	Noninfected leg ulcers
Coagulase-negative staphylococcus	✓	✓	Peptostreptococcus asaccharolyticus	✓	✓
Micrococcus sp.	✓		Peptostreptococcus anaerobius	✓	✓
Staphylococcus aureus	✓	✓	Peptostreptococcus magmus	✓	✓
Streptococcus agalactiae (Grp B)	✓		Peptostreptococcus micros	✓	✓
β-Hemolytic streptococcus (Grp G)	✓	✓	Peptostreptococcus prevotii	✓	✓
Streptococcus spp. (fecal)	✓	✓	Peptostreptococcus tertradius	✓	
Streptococcus spp. (Vridans)	✓	✓	Peptostreptococcus indolicus	✓	✓
Germella morbillorum	✓	✓	Peptostreptococcus sp.		✓
Corynebacterium xerosis	✓		Streptococcus intermedius	✓	✓
Corynebacterium sp.	✓	✓	Clostridium clostridioforme	✓	✓
			Clostridium sporogenes	✓	
Escherichia coli	✓	✓	Eubacterium aerofaciens	✓	
Klebsiella pneumoniae	✓	✓	Lactobacillus acidophilus	✓	
Klebsiella oxytoca	✓	✓	Propionibacterium acnes	✓	
Enterobacter cloacae	✓	✓	Propionibacterium avidum	✓	
Citrobacter freundii	✓		Propionibacterium granulosum		✓
Citrobacter amalonaticus	✓				
Proteus mirabilis	✓	✓	Bacteroides fragilis	✓	
Morganella morganii	✓		Bacteroides ureolyticus	✓	✓
Pseudomonas aeruginosa	✓	✓	Bacteroides distasonis	✓	
Pseudomonas paucimobilis	✓		Bacteroides capillosus		✓
Stentrophomonas maltophilia	✓		Bacteroides thetaiotaomicron		✓
Flavimonas orizihabitans	✓		Prevotella oralis	✓	✓
			Prevotella bivia	✓	✓
Candida albicans	✓		Prevotella buccalis	✓	
Candida parapsilosis	✓		Prevotella sp.	✓	
			Prevotella loescheil	✓	✓
			Prevotella corporis	✓	
			Prevotella melaninogenica		✓
			Porphyromonas asaccharolytica	✓	
			Porphyromonas gingivalis	✓	✓
			Gram-negative pigmenting bacillus	✓	✓
			Fusobacterium necrophorum	✓	
			Veillonella spp.	✓	✓
Number of isolates (n = 24)	24	13	Number of isolates (n = 33)	28	20

Table 2.1The microbiology of infected and noninfected leg ulcers.

Leg ulcers were defined as infected on the basis of clinical signs, and were swab sampled and investigated for aerobic, facultative and anaerobic organisms using stringent isolation and identification techniques (Bowler and Davies, 1999).

With regard to specific pathogens, beta-haemolytic streptococci, (Schraibman, 1990; Robson, 1997), *S. aureus*, Enterobacteriaceae and Pseudomonas species (Trengove *et al*, 1996) have all been implicated as having potentially adverse effects on wound

healing. However, the impact of these species may vary in different settings, e.g, over 60% of arterial and diabetic ulcers colonised with *S. aureus* went on to develop infection compared with only 20% of venous ulcers similarly infected.

Several studies support the idea that bacteria can in fact inhibit the growth of fibroblasts (Henke *et al*, 1998; Letzelter *et al*, 1998). However, studies using bacterial supernatants have only a limited effect (Larjava *et al*, 1987) or even stimulate proliferation (Kilcullen *et al*, 1998). Bacterial endotoxins (e.g. lipopolysaccharide complex associated with the outer cell membrane of Gram-negative bacteria), have been shown to inhibit human cellular migration (Pitaru *et al*, 1987). However, this mode of action does not apply to the Gram-positive *Peptostreptococcus* spp. Interestingly, volatile fatty acids are the principle metabolic component of anaerobic cocci, and have been shown to change the growth and cellular responses of human fibroblasts (Rittenberg and Ehrlich, 1992; Davidson *et al*, 1993; Jeng *et al*, 1999). Cellular wound repopulation may also occur by an indirect mechanism via production and activation of MMPs. Bacteria such as *P. gingivalis*, *P. aeruginosa* and *E. coli* are able to alter MMP-1, -2, -3, -7 and -9 production and activation by epithelial cells (DeCarlo *et al*, 1998). As MMPs are known to be involved in wound repopulation *in vivo* and *in vitro* this is a potential mechanism by which bacterial supernatants are involved in impaired wound closure. Studies also suggest that Gram-positive anaerobic cocci (GPAC) and their metabolites interfere with normal wound healing responses by disruption of inflammation, proliferation and remodelling phases of wound repair (Wall I. B *et al*, 2002). GPAC produce a range of terminal short chain fatty acids (SCFA) including butyrate, acetate, isovalerate, isocaproate, and n-caproate. These SCFA are thought to be responsible for the malodour of infected leg ulcers, hyperlipidemia and impaired healing responses (Figure 2.5). *Peptostreptocci* are known to produce a range of proteolytic enzymes such as collagenases and aminopeptidases which could impair wound healing and prolong inflammation. Studies by Stephens *et al* (2003b), found that *Peptostreptococcus* spp. isolated from chronic venous leg ulcers and their supernatants, significantly reduced keratinocyte and fibroblast proliferation, impaired keratinocyte re-epithelialisation and endothelial cell proliferation, suggesting that these microorganisms may contribute to the delayed re-epithelialisation, impaired ECM reorganisation and angiogenesis in chronic wounds.

Studies by Schmidtchen *et al* (2002) of proteinases of the clinically significant bacterial species *P. aeruginosa, E. faecalis, P. mirabilis* and *S. pyogenes* have shown that they are able to degrade the major human antibacterial peptide LL-37 which has shown antibacterial activity against both gram-negative and gram-positive bacteria (Sorensen *et al*, 2001). This degradation leads to loss of LL-37 binding to bacteria and ultimately

abolished bacterial killing. The study suggests how bacterial pathogens can overcome the innate immune defence systems, giving rise to infections such as chronic ulcers of the skin.

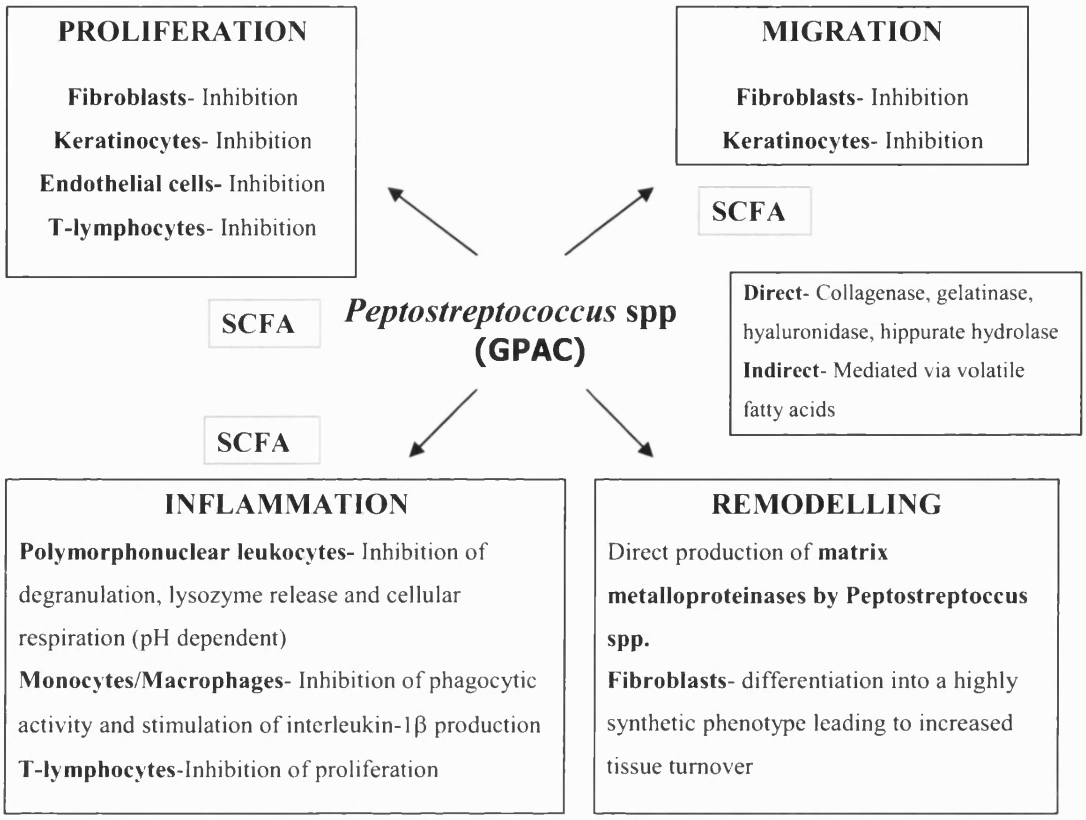

Figure 2.5 Impaired wound healing responses by *Peptostreptococcus* spp. and their metabolites. SCFA = Short chain fatty acids. GPAC = Gram-positive anaerobic cocci. (Wall I. B *et al*, 2002).

2.2.8.3 Antibiotic resistance and chronic wounds

Antibiotics were first isolated in the 1930s and '40s, and were used as a first line of treatment for bacterial infections in a variety of infectious diseases. However, soon after their introduction the first signs of resistance began to emerge (Moellering, 1995). Further antibiotics were developed by modifications of the original penicillin and the generation of other molecules, but resistance has continued to be an ongoing problem (Harrison and Svec, 1998). Hospitals, particularly intensive care units are an important environment for the development and spread of resistant bacteria, due to the use of high doses of antibiotics in conjunction with a high concentration of people, giving an enhanced potential for cross infection (Gold and Moellering, 1996). The molecular basis of resistance relies on four basic mechanisms: Antibiotic modification, blocking antibiotic entry or removal at a rate higher than uptake, alterations to the target rendering the antibiotic less efficient and by the production of an alternative target (Hawkey, 1998). Resistance can be intrinsic or

acquired, and may arise by spontaneous mutation of the genome in the presence or absence of antibiotics to leave a particular bacterium with an advantage over non-mutant types. DNA can also be acquired from resistant bacteria in the form of plasmids. Plasmids are pieces of DNA outside of the host genome that can confer resistance on the recipient that was once sensitive to a particular antibiotic. The overuse of antibiotics forces bacterial evolution by selecting out those individuals that are resistant to the strategy in use.

Systemic antibiotics are generally accepted as being the preferred choice for treating infection in chronic ulcers, provided that ischaemia does not interfere. With an increasing population at risk of developing chronic wounds, antibiotic resistance is an important issue. The polymicrobial nature of chronic wounds is likely to provide an appropriate environment for genetic exchange between bacteria. In fact, the first two cases of vancomycin resistant *S. aureus* (VRSA) in the United States were both isolated from chronic wound patients (Howell-Jones *et al*, 2005). Studies have also found that half of the *S. aureus* isolated from leg ulcers were meticillin resistant *S. aureus* (MRSA) and more than one-third of *P. aeruginosa* isolates to be resistant to ciprofloxacin (Colsky *et al*, 1998). Tentolouris *et al* (1999) found that 40% of *S. aureus* isolated from infected diabetic foot ulcers to be MRSA and had a prevalence of 15% in all ulcer patients. Furthermore, there were significantly more MRSA isolates in patients that had received prior antibiotic therapy, with those that had not. In a follow up study, the prevalence of MRSA in the ulcer patients had almost doubled, (30%) in a three year period. It also appears that populations of wound patients can show wide variation in the level of antibiotic resistance encountered, which may be due to prior antibiotic therapy and the level of contact with healthcare institutions (Howell-Jones *et al*, 2005). Whilst the additional impact of antibiotic-resistant organisms on wound healing is not known, the overall morbidity, mortality and cost associated with infections in hospital patients caused by antibiotic resistant organisms has been shown to be 1.3- to 2-fold higher, than infections caused by antibiotic-sensitive organisms (Cosgrove *et al*, 2003). Due to the proliferation of antibiotic and antiseptic resistant strains of bacteria around the world, attention is increasingly being focused alternative methods of controlling bacterial infection in chronic wounds. Healthcare professionals have already begun to look towards more 'traditional' methods of combating and preventing wound infections such as povidone-iodine (a form of iodine commonly used in skin cleansing), as a means of preventing and treating infection in a range of acute and chronic wounds (Flynn, 2003).

2.2.8.4 Measures to counteract resistance

To overcome bacterial resistance a number of strategies have been introduced. A prime aim is to reduce antibiotic use by increased education on their effectiveness, regulatory measures on their availability, public health surveillance to reduce outbreaks and further research into alternatives (Murray, 1994). The apparent fitness of bacterial strains may also be an area for exploitation by using a particular treatment that may combat resistance. It has been noted that in the absence of antibiotic, some resistant strains of bacteria are not as fit as the wild type, non-resistant strains (Levy, 1994). By the removal of the antibiotic, the resistant strains will be out-competed by the non-resistant strains until the main infectious agents will consist of the antibiotic-sensitive bacteria. The antibiotic can then be reintroduced and the drug regains its efficacy. However, the above set of experimental observations apparently did not take into account the effect of multiple generations and "forced evolution" (Lenski, 1997). Cells which are transfected with a resistance plasmid do not compare well with the wild-type in the absence of the antibiotic to which it now has resistance to. Over time however, the resistant strain begins to evolve a strategy to overcome this short fall and over ~500 generations will compete with the wild-type as effectively without the antibiotic present (Spratt, 1996; Schrag *et al*, 1997).

The reduction in drug usage over time may still mediate an effect in a mixed population with reversions back to the resistant wild type but at a much slower rate than was previously thought. Work by Levin *et al* (1997) using mathematical models of population growth, shows an increased likelihood of reversion only if the sensitive strains have some advantage. This may be in the form of reduced drug concentrations and helped by the relative proportions of sensitive and resistant strains in the population. Therefore, along with the education and surveillance strategies suggested above, alternative treatments are required. With the increasing need for a reduction in the use of antibiotics, other strategies need to be sought. Education and surveillance strategies will work in the medium to long term, but it is what to do in the meantime to combat infection whilst the long-term measures begin to show their effect, that is important.

Figure 2.6 summarises the impaired healing responses that result in prolonged ulceration.

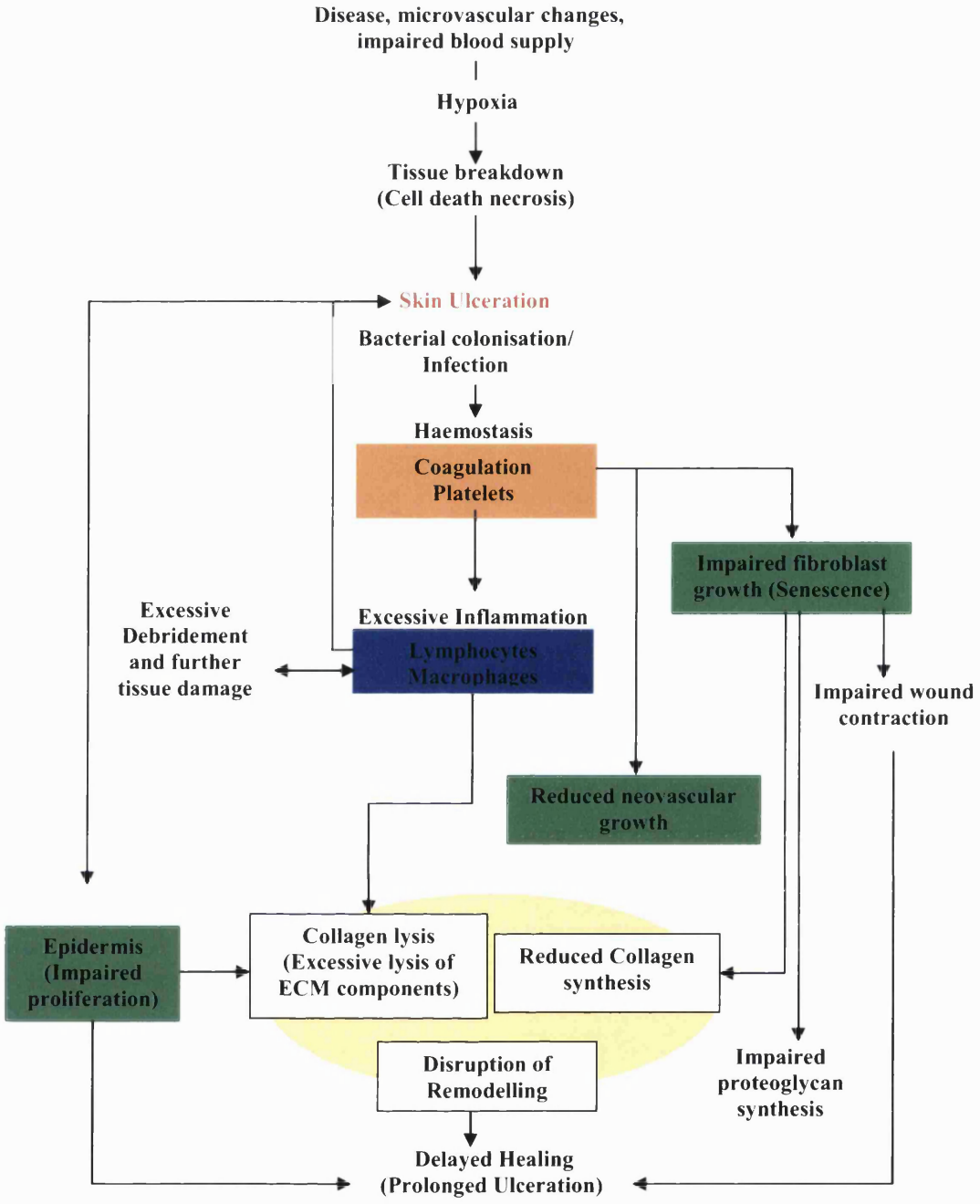

Figure 2.6 Summary of impaired healing in chronic wounds.
Orange=Haemostasis Blue =Chronic Inflammation (Excessive protease activity), Green=Impaired cell proliferation/migration (Degradation of growth factors adhesion proteins due chronic inflammation), Yellow=Impaired Tissue Remodelling (Reduced ECM production and excessive degradation by proteases).

2.3 Existing approaches and associated problems for chronic wound treatment

Many approaches are used in the treatment of chronic wounds, firstly to try and reduce the likelihood of a chronic wound forming, and secondly to attempt to rectify the aberrant healing once a chronic wound has occurred Figure 2.7.

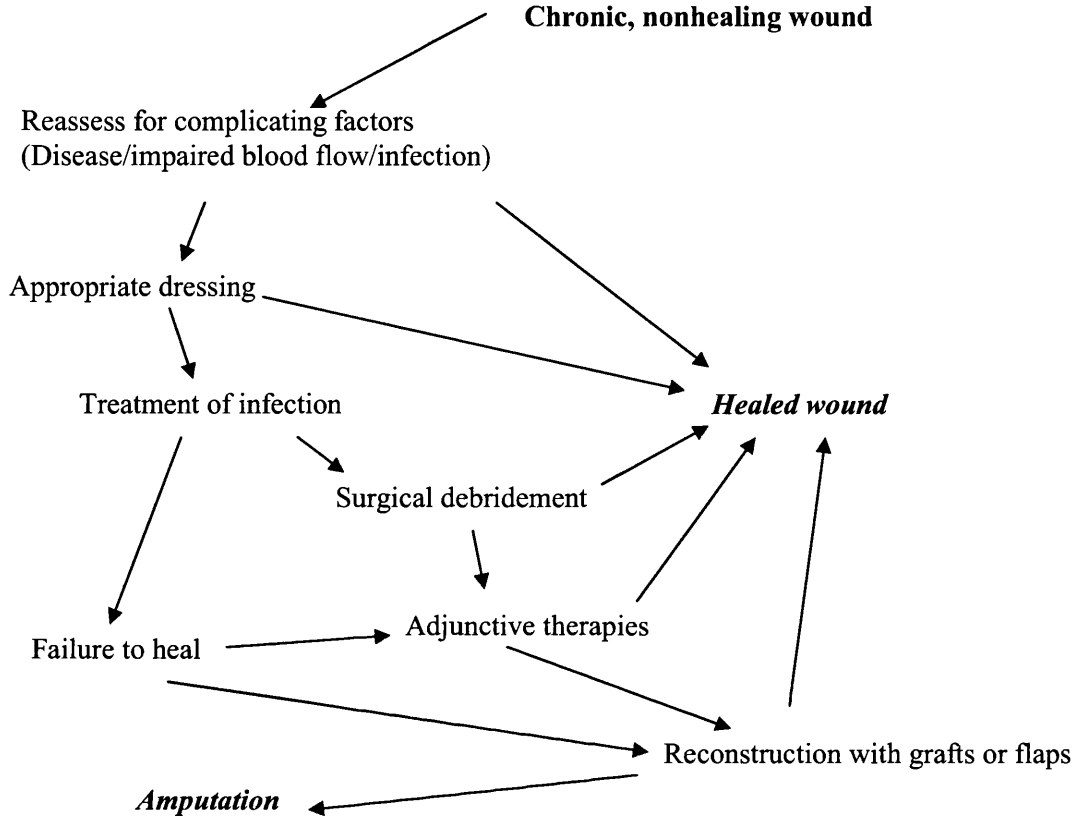

Figure 2.7 Treatment of a chronic nonhealing wound.

The flow chart demonstrates the general process that is followed in order to encourage a chronic wound to heal. Treatment can take from months to years, and in the event that treatment is unsuccessful, amputation is the final outcome.

2.3.1 Basic care

Pressure relief by good nursing care, use of mattresses and cushions is extremely important for patients at risk from pressure ulceration (Colin, 1996). Furthermore, regular debridement of callus, nail care, and pressure offloading footwear are fundamental to the care of foot disease from diabetic neuropathy (Boulton, 1986). Use of compression bandages and stockings are an essential and effective component to managing venous ulceration (Kitahama *et al*, 1982; Falanga, 1993a; Agren *et al*, 2000). The beneficial effects of compression therapy are well documented (Fletcher *et al*, 1997). It is thought that by applying external pressure the leakage of the dilated capillaries is prevented,

oedema removed and the superficial capillary perfusion improved (Fagrell, 1982). There are a variety of bandaging systems some producing up to 70% complete healing in three months (Guest *et al*, 1999), 95% healing in 3 months has even been reported using individualised and optimised compression techniques (Olofsson *et al*, 1996). Furthermore, high compression, bandaging systems appear to produce better short term results than low compression systems (Fletcher *et al*, 1997; Backhouse *et al*, 1987). These basic methods of care should feature in all new treatments (Harding *et al*, 2002).

2.3.2 Dressings

Major focus of chronic wound care in recent years has been the development of dressings that promote a moist environment to assist healing. Winter showed in an animal model that re-epithelialisation of a partial thickness acute wound proceeded 1.5 times more rapidly if the wound was occluded (Winter, 1962). Occlusive dressings have not shown such dramatic effects in clinical studies on patients with chronic wounds, but they may still benefit patients by reducing pain and by improving convenience of use and cost effectiveness. Advances in dressing technology have not yet resulted in the development of materials that correct abnormalities in the healing cascade, with the exception of dressings containing hyaluronic acid, which specifically promotes healing.

2.3.3 Topical treatments

Considerable research has gone into the application of exogenous growth factors in an attempt to stimulate healing. The function of growth factors in the wound setting is to attract various cell types to the wound, stimulate cellular proliferation, promote angiogenesis, and regulate synthesis and degradation of the ECM. However, the success of exogenous growth factor application to chronic wounds for therapeutic purposes has been limited, and is not as effective as when used to treat acute wounds and has also been less impressive than in animal models of wounding (Table 2.2). However, this is unsurprising given the complex nature of wound healing and several reasons have been proposed. For example, a lack of an orderly progression of cytokines and the insufficiency of application of individual growth factors to induce wound healing. 'Bound' endogenous growth factors would also be unable to work in an ordered manner. This idea has also been suggested by the inability of grafted epithelial cell cultures to remain on the cell bed but stimulate wound closure from the wound margin. It is therefore thought, that a skin equivalent graft may produce growth factors in the correct order and amounts. Another possible reason for this difference may be due to the protease-rich nature of chronic wound fluid, resulting

from resident cells and bacteria within the wound. Chronic wound fluid has been shown to decrease the proliferation of fibroblasts, endothelial cells, and keratinocytes, whereas acute wound fluid stimulates their growth (Katz *et al*, 1991).

Growth Factor or cytokine	Effect on wound	Current use
TGF β	Re-epithelialisation	Initial studies in venous ulcers encouraging
	Neovascularisation	
	Increased granulation tissue and collagen	
PDGF	Re-epithelialisation	Licensed for the treatment of neuropathic diabetic foot ulcers
	Neovascularisation	
	Increased granulation tissue and collagen	
FGF	Re-epithelialisation	Biological effects in pressure ulcers
	Neovascularisation of a provisional matrix	No effect on diabetic or venous ulcers to date
IL-1β	Healing of infected wounds	Currently under trial for pressure ulcers
Granulocyte macrophage-colony stimulating factor	Improved healing in acute wounds	Pilot studies in infected diabetic foot ulcers encouraging

Table 2.2Growth factors, wound healing and their use in chronic ulcer treatment.

Growth factors are known to have a range of important functions to encourage normal wound healing. However, the beneficial effects of exogenous growth factor application to chronic wounds for therapeutic purposes has been limited (Harding *et al*, 2002).

So far, only PDGF has been licensed for use in the treatment of uninfected neuropathic diabetic foot ulcers. Research also suggests that it may be of some benefit in the treatment of pressure ulcers and other nondiabetic and non-pressure-related refractory chronic ulcers (Harrison-Balestra *et al*, 2002). Although not yet licensed, granulocyte colony stimulating factor has been evaluated for treating infected foot ulcers in diabetic patients and was associated with more rapid resolution of cellulitis and decreased antibiotic requirements (Gough *et al*, 1997). Furthermore, FGF has been assessed for treating pressure ulcers (Robson *et al*, 1992). Topical application of human recombinant-EGF, to patients with venous ulceration has also been attempted, but failed to significantly enhance re-epithelialisation of venous ulcers (Falanga *et al*, 1992a). In the future, growth factors may be administered sequentially, in combination, or at timed intervals to more closely mimic the normal healing process. The diversity of growth factors and types of chronic wound suggest that these factors have potential as new treatments if patient's individual requirements can be met (Harding *et al*, 2002).

2.3.4 Skin Grafts

Over the past decade, the development of tissue replacements has been a rapidly advancing aspect of wound care and a number of grafts and skin-equivalents are used in the treatment of chronic ulcers.

2.3.4.1 Autologous skin grafts

Venous leg ulcers have been successfully treated by autologous skin grafting (using a patients own skin), using split thickness and pinch skin grafting techniques. For successful management of pressure ulcers, both cutaneous and subcutaneous tissues need to be grafted, particularly over bony prominences. This is best achieved by fasciocutaneous or musculocutaneous flap surgery.

2.3.4.2 Bioengineered skin equivalents

Twenty years ago cultured epidermal autografts, in which a small skin biopsy ($1cm^2$) is harvested and cultured to produce large epidermal sheets, were developed to help treat patients with extensive burns. Unfortunately, these have had only limited success, due to the 3- to 4-week period required to produce sufficient amounts of skin for grafting, which may be too long for burns patients (Langer and Vacanti, 1993), graft fragility, difficulty in application, poor rate of uptake, and the frequent occurrence of infection (Eldad *et al*, 1987). However, the potential benefit of the technology was evident and led to the development of skin equivalents, in which donor tissue with limited immunogenicity is used to construct epidermal, dermal and combined epidermal and dermal grafts. There are now several commercially available products (Table 2.3, Figure 2.8 and 2.9). The relatively low direct cost of tissue replacements has made this wound care option increasingly popular. Bioengineered skin equivalents are absorbed into the wound bed and are thought to improve chronic ulcers, at least in part, by altering the profile of cytokines within the chronic wound. The exact method of action however, is unknown. Recent studies carried out by Martin *et al* (2003) showed that conditioned media from tissue-engineered human fibroblast-derived dermis, contained potent angiogenic factors such as hepatocyte growth factor/scatter factor and IL-8. These findings may explain in part the enhanced healing seen in clinical applications of human fibroblast–derived dermis on chronic wounds. There still remains a need to improve uptake of these grafts by improved angiogenesis and to tackle recurrent infection.

Type of skin substitute	Composition	Current use
Epidermal	Cultured autologous epidermal cells Cultured allogenic epidermal cells	Used for severe burn injuries Used for severe burn injuries
Dermal		
Alloderm	Acellular allogenic human skin/dermal matrix	Approved for treating burns
Integra	Bovine collagen with chondroitin 6-sulphate and dermal fibroblasts	Approved for treating burns
Dermagraft-TC	Non-immunogenic neonatal Fibroblasts on nylon (polygalactin) mesh (Figure 2.8)	Treatment of diabetic foot ulceration (Gentzkow *et al*, 1996) of 6 weeks or longer duration. In clinical trials. Also in trials for use in venous stasis ulcers and decubitus ulcers.
Combined epidermal and dermal		
Apligraft	Bovine collagen Type I matrix, allogenic human fibroblasts, and epidermal cells (human keratinocytes). Both fibroblasts and keratinocytes derived from neonatal foreskin (Figure 2.9).	Licenced for treating diabetic foot ulcers (Veves *et al*, 2001) and venous leg ulcers (Falanga *et al*, 1998)
Composite Cultured Skin	Collagen matrix substrate with fibroblasts and epidermal cells	Trials for venous leg ulcers and diabetic foot ulcers.
OrCel	Absorbable bovine collagen sponge matrix, favourable for host cell migration. Neonatal keratinocytes and fibroblasts, that secrete cytokines normally found in acute wounds.	

Table 2.3 Currently available skin substitutes used in the treatment of chronic wounds.

A range of skin substitutes have been developed with varying compositions many of which have been used in the treatment of chronic wounds. Note. All of these products have been used to treat burns. The table was adapted from Harding *et al* (2002).

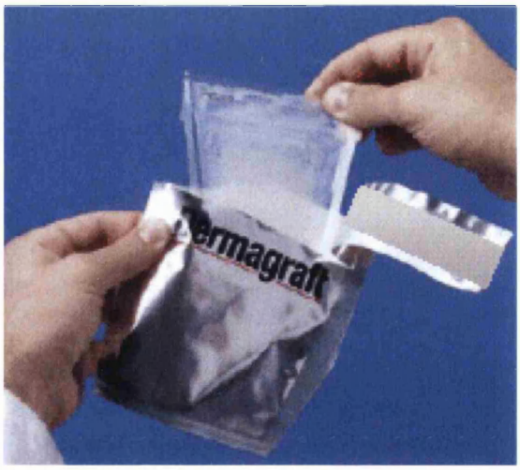

Figure 2.8Dermagraft- Neonatal fibroblasts cultured on a polyglactin mesh.

Dermagraft is stored frozen and warmed in saline bath before application. Edges are trimmed and applied to wound within ulcer boundary (U.S. Department of Health and Human Services, 2001)

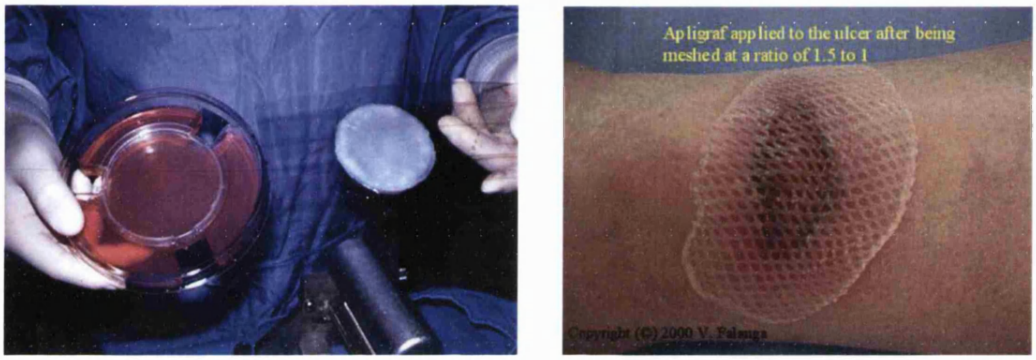

Figure 2.9Apligraf- a bilayered skin equivalent.

Apligraf was developed by Organogenesis and is a cellular, bi-layered skin substitute with an upper epidermal layer and a lower dermal layer. There are no blood vessels, sweat glands, immune cells or melanocytes, however, if the bi-layer is cut, it will heal itself. Apligraf is supplied frozen, and lying on a culture gel (left, Copyright University of Florida, 1998). Small slits are made in it, after which it is trimmed and laid onto the wound surface so that the edges overlap the ulcer edge (right).

2.3.5 Current advances for acceleration of healing

There is a strong theoretical basis to justify the further development and clinical evaluation of proteinase inhibitors as a means of improving the healing of chronic ulcers. A potent, selective inhibitor of MMP-3 has been described by Fray *et al* (2003) for possible progression into clinical trials for the topical treatment of chronic wounds. The progression of gene therapy may also have important benefits, allowing genes important in healing to be delivered directly into a wound. Interest is presently focused on vascular endothelial growth factor (VEGF), a key component in the promotion of angiogenesis (Taub *et al*, 2000). Studies have also shown that PDGF is stabilised by thrombospondin-1 (TSP-1), an ECM protein that enhances the biological effects of PDGF in proliferative tissue repair. It is suggested that the effect of TSP-1 along with its matrix-modulating

activities may have important clinical utility regarding topical growth factor therapy in wound healing, since high proteolytic activity is believed to be partially responsible for limiting the efficacy of this treatment (Krishnaswami *et al*, 2002).

Recent studies carried out by White *et al* (2003) have demonstrated that the human homeobox gene Prx-2 is strongly upregulated in fibroblasts within foetal, but not adult, mesenchymal tissues during healing. This gene was shown to affect a number of foetal fibroblastic responses believed to be important in mediating scarless healing *in vivo*; such as cellular proliferation, ECM reorganisation, and MMP-2 and hyaluronic acid production. It is hoped, that a further understanding of these processes will enable the targeting of specific therapies in wound healing, both to effect scarless healing and to stimulate healing in chronic, nonhealing wounds. Recent developments also include the use of bone-marrow derived stem cells (Badiavas *et al*, 2003) to heal chronic wounds. Furthermore, a potential treatment also lies in the development of skin replacements from embryonic stem cells. However, the ethical implications of using such technology will first have to be addressed.

Hyperbaric oxygen therapy, which involves placing a patient in a chamber filled with pure oxygen at pressures above one atmosphere, has previously shown to improve the oxygenation of tissue and stimulate healing. In addition to wound hyperoxia, increased wound $^{\bullet}NO$ production caused by hyperbaric oxygen therapy also appears important in diabetic wound repair (Boykin, 2000). A systematic review of small studies suggests that hyperbaric oxygen may provide real benefits, for example, there appears to be a reduction in the risk of major amputation diabetic patients (Roeckl-Wiedmann *et al*, 2005). Dressings are also being improved to maximise healing; for example, a novel $^{\bullet}NO$-modified hydrogel has also been developed, by Masters *et al* (2002), to release $^{\bullet}NO$ over a time period of up to 48 hours, to supply the wound with therapeutic levels of $^{\bullet}NO$. Preliminary studies were carried out in a diabetic mouse model of impaired healing, showing similar healing to that observed in control mice. Recent therapeutic strategies have also included the targeting of reactive oxygen species with antioxidants, as it is thought that reactive oxygen species may play a role in the tissue damage due to prolonged inflammatory responses in chronic wounds (Dissemond *et al*, 2002). Studies have also shown that application of honey as a dressing on wounds is beneficial to wound healing, with claims that it reduces inflammation and infection, debrides necrotic tissue, reduces oedema and promotes angiogenesis, granulation and epithelialisation (Molan *et al*, 2001). Maggot (larval) biotherapy seems to be effective for the debridement of chronic wounds and acceleration of healing (Horobin *et al*, 2003). *Lucilia sericata* larval secretion has been shown to modify fibroblast adhesion and spreading across ECM protein surfaces (Horobin *et al*, 2003).

2.3.6 The burden of chronic wounds

Chronic wounds remain a significant clinical problem as they are timeconsuming, expensive and difficult to treat. Complications of lower extremity wounds are the number-one reason for hospitalisation of patients with diabetes and account for 10% of all direct costs related to diabetes care (Harrington *et al*, 2000). As many as 15% of people with diabetes are thought to develop a foot ulcer in their lifetime (Harrington *et al*, 2000), and 15-20% of these diabetic ulcers eventually require a lower extremity amputation (Ramsey *et al*, 1999; Ollendorf *et al*, 1998). Chronic ulcers are associated with morbidity and high treatment costs (Harrington *et al*, 2000; Thomas *et al*, 1996). Venous ulcerations of the lower extremities represent an increasing healthcare problem. It has been estimated that about 0.1% of the population of developed countries have venous leg ulcers and more than 90% are over the age of 60 years (Cornwall *et al*, 1986; Baker *et al*, 1991; Nelzen *et al*, 1994). Studies have calculated the cost of wounds to the NHS to be about £1bn a year (Harding, 2002) and the total annual cost for the treatment of leg ulcers probably amounts to over 400 million pounds in the UK (Ruckley, 1997). Only about half of the patients heal their ulcers in a-five year period and once healed, venous ulcers often recur (Nelzen *et al*, 1994; Nelzen *et al*, 1997; Morrell *et al*, 1998). With an aging population the numbers of people with diabetes and associated chronic ulcers these figures are expected to increase. It is these concerns that have been the driving force behind recent innovations in wound care.

CHAPTER 3

3 Introduction: An alternative approach for promoting the healing of chronic wounds

As previously discussed a number of methods have been used in order to facilitate the correct healing of chronic wounds. Over the last decade skin grafts and improved dressing have become increasingly important in the treatment of chronic wounds and burns, however they also have several limitations that need to be addressed. This project aims to investigate the effects of reactive oxygen and nitrogen species (RONS), particularly those generated by xanthine oxidoreductase (XOR) on wound-related cells with a view to facilitate wound healing. This section reviews how RONS can affect a multitude of cellular and physiological processes many of which are important to the wound healing process and natural antibiotic systems.

3.1 RONS involved in cellular and physiological processes

The study of free-radicals and their generation has continued for many decades and it has long been understood that free radicals have many detrimental effects such as in ageing, reperfusion injury and in certain forms of cancer. Their role in physiology has usually been seen as a pathological one, with the dogma being that radicals were so reactive and unselective that they could not be involved in normal biochemical processes. More recently an increasing body of evidence implicates a whole range of these species in important cellular and physiological processes within healthy organisms including man. These are summarised here.

3.1.1 The major types of RONS and their generating systems in living organisms.

Living organisms contain many systems for both the generation and removal, inhibition and scavenging of reactive oxygen and nitrogen species. A complex balance exists in health, and imbalances can result in disease. Therefore, RONS can be both protective and aetiological as outlined below.

3.1.1.1 Reactive oxygen and nitrogen species classification and nomenclature.

The term ROS includes both oxygen radicals and certain nonradicals that are oxidising agents and/or are easily converted into radicals (HOCl, HOBr, O_3, $ONOO^-$, $^1O_2$, H_2O_2). Therefore, all oxygen radicals are ROS, but not all ROS are oxygen radicals. A summary of the nomenclature of reactive oxygen (ROS) and nitrogen species (RNS) and whether they are classed as radicals or nonradicals is provided in table 3.1.

Free radicals[a]	Nonradicals
Reactive oxygen species (ROS)	
Superoxide, $O_2^{\bullet -}$	Hydrogen peroxide, H_2O_2
Hydroxyl, $^{\bullet}OH$	Hypobromous acid, HOBr[b]
Hydroperoxyl, $HO_2^{\bullet}$	Hypochlorous acid, HOCl[c]
Peroxyl, $RO_2^{\bullet}$	Ozone O_3
Alkoxyl, $RO^{\bullet}$	Singlet oxygen ($O^1{}_2\Delta g$)
Carbonate, $CO_3^{\bullet -}$	Organic peroxides, ROOH
Carbon dioxide, $CO_2^{\bullet -}$	Peroxynitrite, $ONOO^-$[d]
	Peroxynitrous acid, ONOOH[d]
Reactive nitrogen species (RNS)	
Nitric oxide, $^{\bullet}NO$	Nitrous acid, HNO_2
Nitrogen dioxide, $NO_2^{\bullet}$	Nitrosyl cation, NO^+
	Nitroxyl anion, NO^-
	Dinitrogen tetroxide, N_2O_4
	Dinitrogen trioxide, N_2O_3
	Peroxynitrite, $ONOO^-$[d]
	Peroxynitrous acid, ONOOH
	Nitronium (nitryl) cation, $NO2^+$
	Alkyl peroxynitrites, ROONO
	Nitryl (nitronium) chloride, NO_2Cl[e]

Table 3.1Nomenclature of reactive species enzyme reactions

Peroxynitrite and H_2O_2 are frequently erroneously described in the literature as free radicals. RNS is also a collective term including nitric oxide and nitrogen dioxide radicals, as well as nonradicals such as HNO_2 and N_2O_4. 'Reactive' is not always an appropriate term: H_2O_2, $^{\bullet}NO$ and $O_2^{\bullet -}$ react quickly with only a few molecules, whereas $^{\bullet}OH$ reacts quickly with almost everything. $RO_2^{\bullet}$, $RO^{\bullet}$, HOCl, HOBr, $NO_2^{\bullet}$, $ONOO^-$, NO_2^+ and O_3 have intermediate reactivites.

[a]A free radical is any species that contains one or more unpaired electrons, that is, electrons singly occupying anatomic or molecular orbital.

[b]HOBr could also be regarded as a 'reactive bromine species'.

[c]HOCl can also be refered to as a reactive chlorine species.

[d]$ONOO^-$ and ONOOH are often included as ROS.

[e]NO_2Cl is a chlorinating and nitrating species that can be formed by reaction of HOCl with NO_2^-.

(Table modified from Halliwell and Whiteman, 2004).

3.1.1.2 Physiological ROS generating systems

The superoxide anion is formed by the reduction of molecular oxygen and is mediated by enzymes such as Nicotinamide adenine dinucleotide phosphate (NADPH) oxidases, xanthine oxidase or nonenzymatically by redox-reactive compounds such as the semi-ubiquinone compound of the mitochondrial electron transport chain. Superoxide dismutases (SODs) convert $O_2^{\bullet -}$ enzymatically into H_2O_2. In biological tissues $O_2^{\bullet -}$ can also be converted nonenzymatically into H_2O_2 and singlet oxygen. In the presence of reduced transition metals (e.g., ferrous or cuprous ions), H_2O_2 can be converted into the highly reactive hydroxyl radical ($^{\bullet}OH$). Alternatively, H_2O_2 may be converted into water by the enzymes catalase or glutathione peroxidase (Figure 3.1). In animal cells catalase is located in a cell organelle called the peroxisome. Peroxisomes are involved in the oxidation of fatty acids, and the synthesis of cholesterol and bile acids. Hydrogen peroxide is a by product of fatty acid oxidation.

Because $O_2^{\bullet -}$ and $^{\bullet}NO$ are readily converted by enzymes or nonenzymatic chemical reactions into nonradical species such as singlet oxygen, H_2O_2, or $ONOO^-$ i.e., species which can in turn give rise to new radicals, the regulatory effects of these nonradical species have also been included. Most of the regulatory effects are indeed not directly mediated by $O_2^{\bullet -}$ but rather by its reactive oxygen species (ROS) derivatives. Frequently, different reactive species coexist in the reactive environment and make it difficult to identify unequivocally which agent is responsible for a given biological effect.

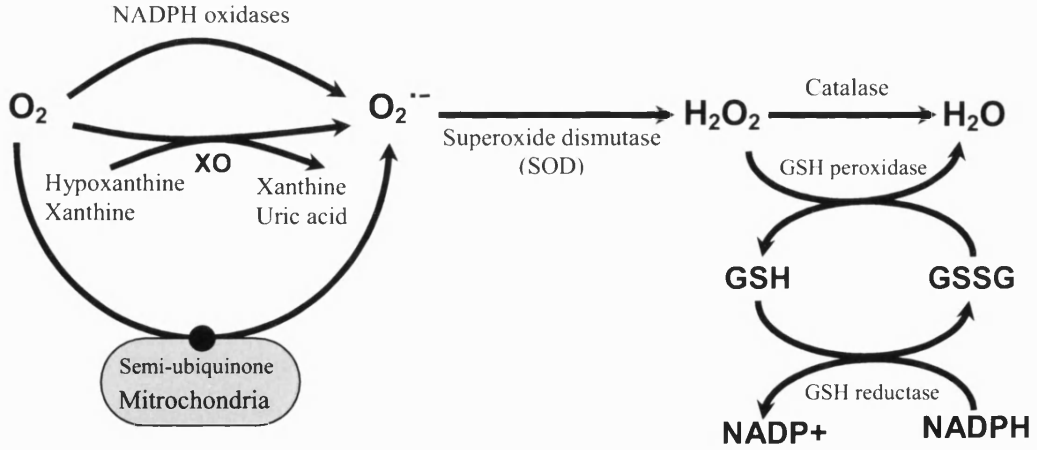

Figure 3.1 Pathways of reactive oxygen species (ROS) production and clearance in biological systems. GSH, glutathione; GSSG glutathione disulfide (adapted from Droge, 2002).

3.1.1.3 Physiological RNS generating systems

It is generally accepted that the physiological source of Nitric oxide ($^{\bullet}NO$) in higher organisms is by the oxidative deamination of L-arginine. This process is catalysed

by Nitric oxide synthase (NOS), a complex enzyme which is dependent on the availability of oxygen for its activity. Nitric oxide is generated by a variety of cell types, including endothelial cells (Palmer *et al*, 1987), hepatocytes (Curran *et al*, 1989), neurons (Garthwaite *et al*, 1988), neutrophils (Schmidt *et al*, 1989) and macrophages (Hibbs *et al*, 1987). Nitric oxide has been shown to be generated by macrophages that have been stimulated by interferon gamma and *E. coli* lipopolysaccharide (Marletta *et al*, 1988). Depending on the microenvironment, $^{\bullet}NO$ can be converted to various other reactive nitrogen species (RNS) such as nitrosyl cation (NO^{+}), nitroxyl anion (NO^{-}) or peroxynitrite ($ONOO^{-}$). Some of the effects may be mediated through the intermediate formation of *S*-nitroso-cysteine or *S*-nitro-glutathione (Droge, 2002).

3.1.2 The role of RONS in physiological systems

As previously stated, RONS are implicated in numerous systems which control physiological mechanisms in the body. Studies suggest that a physiological rate of ROS production activates signalling pathways necessary for cell growth and proliferation while an excessive production of ROS, overmatching the antioxidant capacities of the cell, leads to an oxidative stress that results in metabolic disturbances and cell death. With relevance to this thesis the role of RONS in wound healing with particular emphasis on their role in cellular proliferation and their antibacterial properties will be discussed.

3.1.2.1 ROS and cell proliferation

A range of mechanisms have been proposed whereby $O_2^{\bullet -}$ and H_2O_2, both from exogenous sources or generated celullarly, can influence cell proliferation and possibly function as cellular "messengers" along with the possibility of cellular oxidative stress that may occur if these species are present to excess (Burdon, 1995). A wide variety of normal cell types generate and release $O_2^{\bullet -}$ or H_2O_2 *in vitro* either in response to specific cytokine/growth factor stimulus or constitutively in the case of tumour cells. Expression of NADPH oxidase and low $O_2^{\bullet -}$ generation (approx 0.06 nmol/min per 10^6 cells) by cytokine- or ionophore-stimulated human fibroblasts is known. Studies have also shown that these cells also contain an ectoplasmic enzyme, distinct from NADPH oxidase, which can generate $O_2^{\bullet -}$ (2.10 ± 0.14 nmol/min per 10^6 cells) at levels similar to phorbol ester-stimulated monocytes on exogenous NADH stimulation. These species at submicromolar levels appear to act as intra and intercellular 'messengers' capable of promoting growth responses in culture.

3.1.2.1.1 Regulation of cell division in mammals

Proliferation occurs by cell division, and for this to take place, a cell must double its mass and duplicate all its components (Pardee, 1989; Laskey *et al*, 1989). Most of these processes take place during the period between cell division known as *interphase*. Within interphase there is a specific period during which time DNA is replicated. This is refered to as the S-phase (Laskey *et al*, 1989). Present evidence suggests that the growth regulated biochemical events critical for cell proliferation to occur in the period between mitotic division and the S-phase known as the G_1-*phase*. The G_1/S transition is the boundary prior to DNA replication and is a key regulatory point in the cell division cycle. The cells of an organism divide at very different rates, the major difference being the time they spend in G_1. Cells that are quiescent are essentially arrested in G1 and are often referred to as being in the G_0-*phase*.

3.1.2.1.2 Mechanism of action

ROS are able to elicit signal transduction events, such as protein tyrosine phosphorylation and early gene activation reminiscent of cell stimulation by growth factors (Devary *et al*, 1992). More importantly, "traditional" proliferative signals, such as those delivered by the activation of growth factor receptors and G-proteins of the Ras family, are accompanied by intracellular production of endogenous oxygen species, which are, in turn, necessary for downstream propagation of mitogenic signalling. In fact, ROS and H_2O_2, in particular, have been convincingly shown to operate as key signalling molecules in the cascades triggered by PDGF (Sundaresan *et al*, 1995), EGF (Bae *et al*, 1997), and cytokine and antigen receptors (Pani *et al*, 2000) and to be required for proliferative response to oncogenic Ras (Irani *et al*, 1997).

The mechanisms by which ROS act may involve direct interaction with specific receptors or oxidation of growth signal transduction molecules such as protein kinases, protein phosphatases, transcription factors, or transcription factor inhibitors. It is also possible that H_2O_2 may modulate the redox state and activity of these important signal transduction proteins indirectly through changes in cellular levels of GSH and GSSG. The effects of ROS essentially depend on the overall redox status of the cell that is crucial for the activity of nuclear transcription factors (Xanthoudakis *et al*, 1992), and signaling of proliferation or death (Kamata and Hirata, 1999; McCord, 1985). In mammals, these ambivalent signals are mediated by three subgroups of mitogen-activated kinases (MAPKs): ERKs (extracellular signal regulated kinases), JNKs (c-jun N-terminal Kinases), and p38 MAPKs. The ERK pathway plays a major role in regulating cell growth and differentiation in response to growth factors, cytokines and phorbol esters (Robinson

and Cobb, 1997). JNKs and p38 MAPKs, described as SAPKs (Stress activating Protein Kinase), are involved in stress responses and cell death (Kyriakis and Avruch, 2001). The pro-apoptotic effect of JNK results probably from the inhibition of anti-apoptotic molecules such as Bcl2 and NF-κB (Deng *et al*, 2001; Baichwal and Baeuerle, 1997). In normal cells, persistant ROS production leads to activation of the JNK pathway, and apoptosis, whereas low concentrations or transiently high levels of ROS induce the proliferation of normal cells through activation of the ERK pathway (Nicco *et al*, 2005).

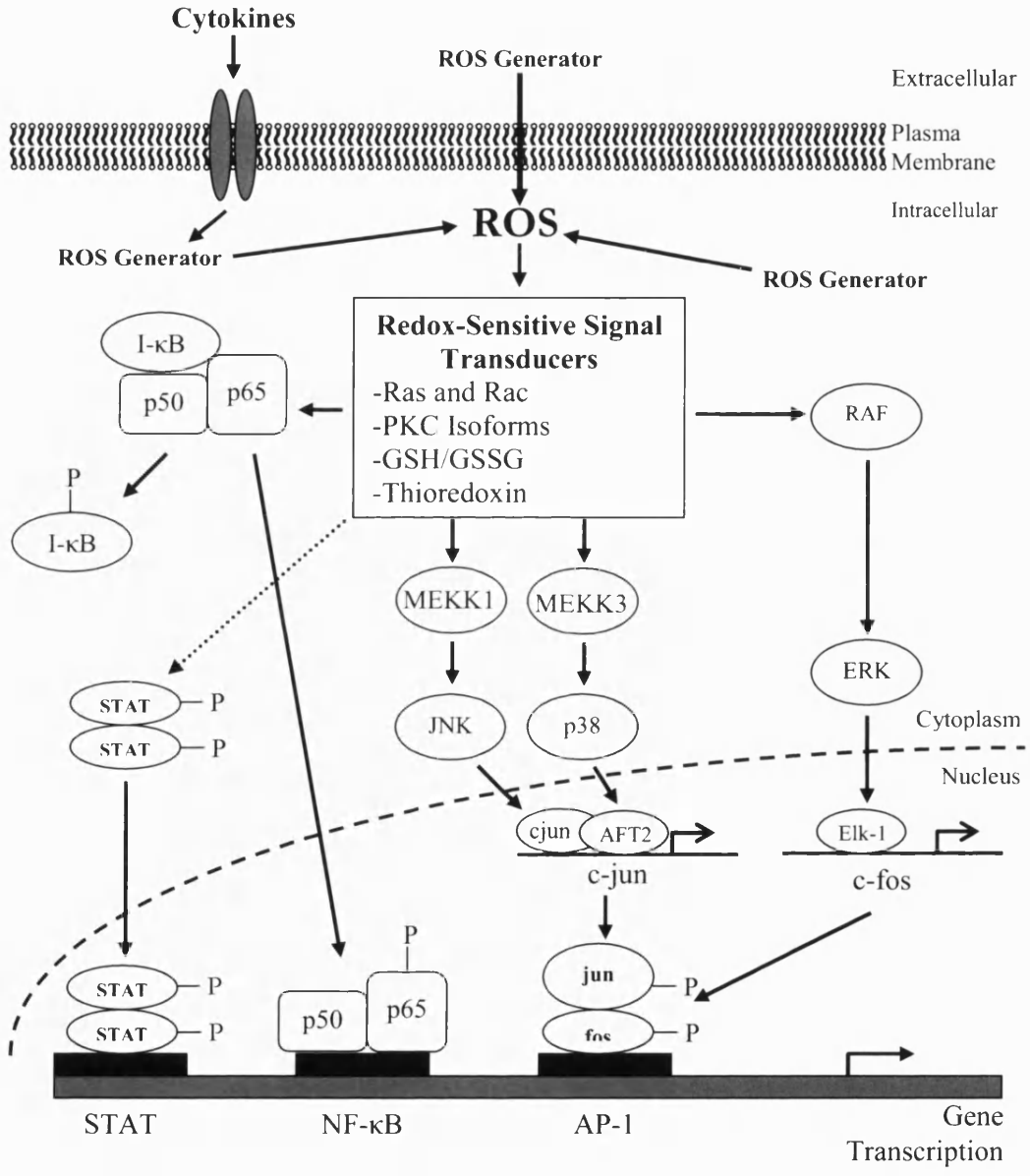

Figure 3.2. Reactive oxygen species control over gene expression.

Intracellular ROS signal changes in gene expression via redox-sensitive signal transducers, a group made up of monomeric G-proteins (Ras and Rac), protein kinase C (PKC), the ratio of GSH and GSSG, and thioredoxin. ROS species promote nuclear translocation and binding of STAT (Signal Transducers and Activators of Transcription) to promoter elements. NF-κB is usually maintained in the cytoplasm in an inactive form by the association of the inhibitory factor I-κB. Upon stimulation I-κB dissociates and active NF-κB translocates to the nucleus. NF-κB activation is modulated by glutathione, thioredoxin and PKC. The

AP-1 transcription factor is composed of a Jun and Fos heterodimer. AP-1 is activated by three MAP Kinase pathways that regulate the transcription of *jun* and *fos*, and phosphorylate these proteins. The three transcription factors STAT, NF-κB, and AP-1 may act independently or cooperatively for the activation transcription of genes. The STAT transcription factor for example, is involved in regulating many aspects of cell growth differentiation and survival (Adapted from Lum and Roebuck, 2001).

3.1.2.2 Nitric oxide in wound healing

Nitric oxide is a small molecule of diverse function and profound importance in biological systems, at low levels •NO is a key signalling molecule in eukaryotes (Robbins and Grisham, 1997). Nitric oxide is well known for mediating the relaxation of smooth muscle in vasodilation, inhibition of platelet aggregation and adhesion and angiogenesis. Evidence clearly implicates •NO in the wound healing process. Several studies have suggested an association between decreased •NO production and delayed wound healing (Stallmeyer *et al*, 1999; Schaffer *et al*, 1997a). Healing is impaired during systemic administration of •NO synthesis inhibitors (Schaffer *et al*, 1996) and in inducible nitric oxide synthase (iNOS) knockout mice. Studies using iNOS knockout mice showed that cutaneous wound closure was delayed after wounding, and that the effect could be reversed by the delivery of the iNOS gene by an adenoviral vector at the wound site (Yamasaki *et al*, 1998). The impaired wound healing common in people with diabetes has also shown to be associated with reduced wound •NO synthesis at the wound site (Schaffer *et al*, 1997b).

As mentioned previously, L-arginine, has been shown to be a unique substrate for •NO synthesis, and is therefore indirectly involved in many regulatory mechanisms relevant to wound healing, such as angiogenesis and cell proliferation (Schwentker *et al*, 2002). Supplemental L-arginine has been shown to improve healing in both animal and human wounds (Barbul *et al*, 1990 and 1985; Seifter *et al*, 1978; Holt *et al*, 1992). Furthermore, data show that the impaired healing of diabetic wounds can be partially corrected by L-arginine supplementation, and that this effect is accompanied by enhanced wound •NO synthesis (Shi *et al*, 2003). Examination of the influence of arginine dietary supplements has also suggested that their beneficial effects are lost in mice without the iNOS gene (Shi *et al*, 2000).

Numerous compounds that spontaneously produce •NO under physiologic conditions (•NO donors) have been identified. The exogenously applied •NO donors mimic the normal biologic functions of endogenous •NO. Several classes of •NO donor exist, including S-nitrosothiols (Butler and Rhodes, 1997) and •NO-nucleophile complexes (NONOates or diazeniumdiolates) (Maragos *et al*, 1991; Keefer *et al*, 2001). For example, exogenous •NO supplementation at the wound site by an •NO donor (molsidomine) is also known to partly reverse impaired healing in diabetes. Additionally, direct generation of

•NO via a chemical reaction between sodium nitrite and ascorbic acid can stimulate vasodilation in healthy skin when applied through a gas permeable membrane. However, the duration of the •NO release and the dose control was limited in this system. Materials that are suitable for prolonged, localised •NO release at the site of a dermal wound are still under development. A polethyleneimine (PEI)-nitric oxide donor that was applied to full-thickness wounds in aged rats did not favourably affect the wound healing process (Bauer *et al*, 1998). Wounds to which PEI or PEI-•NO were applied experienced impaired wound healing when compared to untreated wounds, indicating that PEI itself may contribute to dermal toxicity and failure to enhance wound healing. Sustained delivery of an elevated and prolonged dose of •NO well beyond physiological levels also resulted in increased inflammation in the PEI-•NO treated wounds. Physiologically relevant levels of •NO at the wound site have been shown to have beneficial effects on wound healing. Studies carried out by Masters *et al* (2002) using hydrogel dressings supplemented with low 0.5mM and high 5mM doses of •NO, showed no alteration in fibroblast proliferation, however, *In vitro* studies of fibroblasts in culture with the •NO hydrogels where also shown to have an increased production of ECM. In addition, preliminary studies carried out in a diabetic mouse showed increased thickness of granulation and scar tissue in animals exposed to higher dose •NO suggesting that endothelial cell migration and angiogenesis may be increased. Therefore, rather than accelerating wound closure, •NO in this study appears to improve the quality of the tissue in the healing wound. When considering wounds that do not remain healed, the formation of scar and granulation tissue may play an important role in creating a more mechanically stable wound. Similar findings have been reported in studies examining the effect of growth factors on wound healing in animals such as PDGF-BB (LeGrand, 1998).

3.1.2.2.1 Modes of action of nitric oxide in wound healing

Nitric oxide acts as a cellular messenger and is known to directly regulate the expression and activity of several transcription factors, including NF-κB, which in turn modulate the synthesis and release of multiple wound healing-participating cytokines/proteins. It is thought that •NO functions via multiple mechanisms to improve wound healing including vasodilation, antibacterial activity, increased cell proliferation, migration via up-regulation of growth factors and receptors, and up-regulation of matrix synthesis. The well-known and vasodilatory and antibacterial action of •NO is likely to be important in the process of wound healing, particularly because vasodilation increases blood flow in the microvasculature, thus facilitating the delivery of both nutrients and cells to the site of injury. During the early post injury stages, •NO may act to prevent

infection, thereby also preventing excess inflammation. Nitric oxide is thought to encourage fibroblast and keratinocyte migration via growth factor up-regulation (Frank *et al*, 1999; Reenstra *et al*, 2004). Nitric oxide and cyclic guanosine monophosphate (cGMP) have been shown to promote growth factor induced DNA synthesis in human dermal fibroblasts, suggesting another possible mechanism by which •NO may promote skin wound healing (Dhaunsi and Ozand, 2004). Particularly as similar improvements in wound healing appear to occur following application of either growth factors or •NO and it is thought to be attributed to their interrelated mechanisms of action. For example, a proposed mechanism for impaired healing in diabetic patients is reduced fibroblast proliferation caused by impaired growth factor expression (Reenstra *et al*, 2004). These linked growth factor-•NO mechanisms may also affect other cells important in wound healing such as endothelial cells and keratinocytes, and some studies have suggested that growth of the latter cell type is modulated by •NO in a manner similar to that observed in fibroblasts (Krischel *et al*, 1998, Wetzler *et al*, 2000). Reports of the effects of •NO on keratinocytes are conflicting because inflammatory stimuli have been implicated for induction of •NO production by keratinocytes via iNOS and, conversely, EGF, which promotes the proliferation of keratinocytes, suppresses the production of •NO by an unknown mechanism (Heck *et al*, 1992).

Expression of •NO by macrophages and other cell types has been shown to be important in regulation of their angiogenic activity, specifically by enhancing the expression of VEGF (Xiong *et al*, 1998; Frank *et al*, 1999). Additionally, the importance of •NO in wound angiogenesis has been shown by examining the impaired wound healing in endothelial nitric oxide synthase (eNOS)-deficient mice (Lee *et al*, 1999). *In vitro* endothelial cell sprouting assays showed that eNOS is required for proper endothelial cell migration, proliferation, and differentiation. Furthermore, angiogenesis was significantly reduced *in vivo* in eNOS knockout mice compared to wild-type controls. Inhibition of angiogenesis and inability to provide sufficient nutrients to the wound site are described as primary reasons for the development of chronic wounds (Iocono *et al,* 1998). Angiogenesis is severely impaired in diabetics, contributing to the inability of diabetic ulcers to heal properly.

One of the most significant positive effects attributed to •NO is increased collagen production, which enhances the quality of granulation tissue and can increase wound strength (Witte *et al*, 2000; Thornton *et al*, 1998; Schaffer *et al*, 1997a; Lee *et al*, 1999). Studies have shown that increased •NO synthesis *in vivo*, enhances collagen synthesis by wound fibroblasts, and cells transfected with the iNOS gene, and implanted subcutaneously, result in increased collagen accumulation in rats (Witte *et al*, 2000;

Thornton *et al*, 1998). Conversely, inhibition of •NO synthesis by competitive inhibitors, results in decreased wound mechanical strength and collagen accumulation (Schaffer *et al*, 1997a and 1996). Furthermore, Lee *et al* (1999) observed a 38% decrease in wound tensile strength in mice deficient in eNOS when compared to wild-type controls.

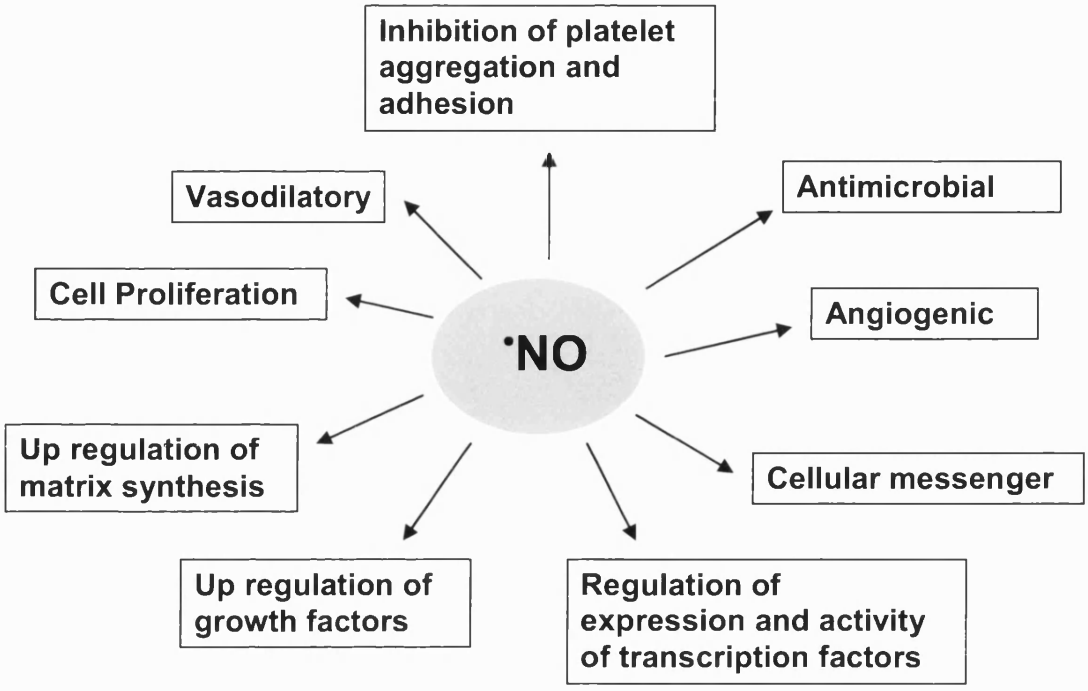

Figure 3.3 A summary of the roles of •NO in wound healing

Nitric oxide has a wide variety of functions which form an essential part of the wound healing processes. Other activities include antimicrobial activities which are covered in the next section.

3.1.2.3 The damaging effects of RONS with emphasis on their antibacterial role

Free radicals have previously been implicated in bacterial cytotoxicity (Akaike *et al*, 1992; Bowdy *et al*, 1990; Pabst *et al*, 1982) and especially in the respiratory burst of macrophages and neutrophils (Morel *et al*, 1991; Miller and Britigan, 1997; Hampton *et al*, 1998). The range and variety spans singlet oxygen and $O_2^{\bullet -}$ from the oxidation of NADPH in the neutrophil membrane to the generation of "bleach" in hypochlorous acid generation by myeloperoxidase in phagosomes within a restricted environment (Byun *et al*, 1999; Saran *et al*, 1999). Inflammatory situations and bacterial infections, which are rich in exuded inflammatory cells, contain a range of free-radical generating systems in the form of activated cells. The macrophage has also been shown to generate oxygen radicals under resting conditions and following phagocytosis (Drath and Karnowsky 1975; Karnowsky *et al*, 1975). Extracellular $O_2^{\bullet -}$ generation is primarily associated with phagocyte defence against disease. In both neutrophils and monocytes this is accomplished by a trans-plasma-membrane enzyme, NADPH oxidase, which oxidises

intracellular NADPH via flavin adenine dinucleotide (FAD) and cytochrome b_{-245} and reduces oxygen on the outer surface to form $O_2^{\bullet-}$. Studies carried out by Takeuchi *et al* (1999) have also shown that H_2O_2 results in oxidative DNA damage and decreased survival of strictly anaerobic *Prevotella. melaninogenica* as found in chronic wounds.

Nitric oxide at elevated concentrations inhibits terminal oxidases (Stevanin *et al*, 2000) and aconitases (Gardner *et al*, 1997) and therefore is also a potent bactericidal agent that may limit the persistence of bacteria in a number of different environments. Long *et al* (1999) demonstrated the mycobacteriocidal actions of exogenous $^{\bullet}NO$ treatment and suggested this as a possible therapy in patients with pulmonary tuberculosis. Intragastric levels of $^{\bullet}NO$ have been measured to be between 10 and 100ppm and this is suggested as having biological effect in the stomach (Weitzeberg and Lundberg, 1998). Acidified nitrite which generates $^{\bullet}NO$ has also been shown to kill various gut pathogens much more efficiently than acid alone (Benjamin *et al*, 1994; Dykhuizen *et al*, 1996). Nitrates are generally excreted in the urine at higher concentrations compared to the low level of measurable nitrites (Green *et al*, 1981). However bacteria that cause urinary tract infections (UTIs) may convert nitrate to nitrite using a nitrate reductase enzyme and the detection of nitrite in the urine has been used for a diagnostic tool for UTIs. Acidification and vitamin C intake have been used as treatment against UTIs (Weitzeberg and Lundberg, 1998).

Reactions and effects that were once attributed to either $^{\bullet}NO$ or $O_2^{\bullet-}$ have had to be reassessed. The evidence comes from the combination of the radicals forming the strong oxidant $ONOO^-$ (Beckman *et al*, 1990; Beckman and Koppernol, 1996). In many pathological conditions (including inflammation, sepsis, and ischemia/ reperfusion), simultaneous cellular production of $O_2^{\bullet-}$ and $^{\bullet}NO$ may occur, from various sources potentially leading to the formation of $ONOO^-$. The biological formation of $ONOO^-$ is mainly due to the diffusion-limited reaction between $^{\bullet}NO$ and $O_2^{\bullet-}$, a reaction that occurs with a second order rate constant of approximately $1 \times 10^{10}\ M^{-1}\ S^{-1}$ (Radi *et al*, 2001). This reaction leads to the modulation of the effect of each individual radical. For example, $O_2^{\bullet-}$ can reduce the effects of $^{\bullet}NO$ by causing the generation of $ONOO^-$ (Rubbo *et al*, 1994). In the same manner the capture of $O_2^{\bullet-}$ by $^{\bullet}NO$ has been suggested as the modification of actions previously described for $O_2^{\bullet-}$ alone (Bautista and Spitzer, 1994; Wink *et al*, 1994).

Peroxynitrite is a potent and versatile oxidant with strong oxidising, nitrating and hydroxylating properties that can inflict damage on a wide range of biological molecules. The peroxynitrite anion has a pKa of 6.8 and is relatively stable under these basic conditions. However $ONOO^-$ is protonated (around 20%) at a physiological pH, and under these conditions, the half-life of the protonated species, peroxynitrous acid, is about 1

second. Peroxynitrous acid decomposes to form potent oxidants with the reactivity of hydroxyl radical and nitrogen dioxide (Beckman *et al*, 1990). Such damage is mediated through the oxidation of sulphydryl compounds, lipids, proteins and DNA, leading to cellular damage and cytotoxity. Reaction with DNA can lead to oxidation and/or nitration of bases to initiate a complex series of transformations involving base damage or strand breaks as well as reactions with the deoxyribose portion of the DNA. Following strand breakage a secondary effect has been suggested involving the activation of the nuclear enzyme poly(ADP-ribose) synthetase (PARS) and apoptosis. Single (not double) strand breakage is an obligatory signal for PARS activation. PARS causes the ADP-ribosylation of a number of important proteins involved in repair including topoisomerase I and II, DNA polymerase α and β and DNA ligase 2. This ribosilation tends to decrease their activity and therefore has an effect on the cell function (Szabo *et al*, 1996). Activation of PARS can also deplete cell energy stores by using up the electron transport substrate, NAD^+, which can then go on to cause acute cell dysfunction. Peroxynitrite can also nitrate tyrosine residues in cellular proteins forming nitro-tyrosine (Beckman and Koppernol, 1996; Radi *et al*, 2001; Brunelli *et al*, 1995).

As a result of these effects on cell function $ONOO^-$ is powerfully cytotoxic, contributing to tissue injury in a variety of human diseases that include atherosclerosis, heart disease and a number of neurodegenerative disorders. In addition, peroxynitrite has also been shown to be formed by macrophages during bacterial engulfment (Ischiropoulos *et al*, 1992) and to function as a powerful bactericidal agent (Zhu *et al*, 1992; Brunelli *et al*, 1995). Peroxynitrite has been found to be toxic to common infective bacteria (Brunelli *et al*, 1995; Millar *et al*, 2002). Studies carried out by Motohashi and Saito (2002) showed that $ONOO^-$, generated gradually from SIN-1, penetrates through the cell membrane of *Salmonella typhimurium*, damages the DNA and induces the SOS response. The SOS response is an inducible DNA repair system that allows bacteria to survive sudden increases in DNA damage. Figure 3.4 outlines the generation and cellular and physiological effects of $^{\bullet}NO$ and $ONOO^-$.

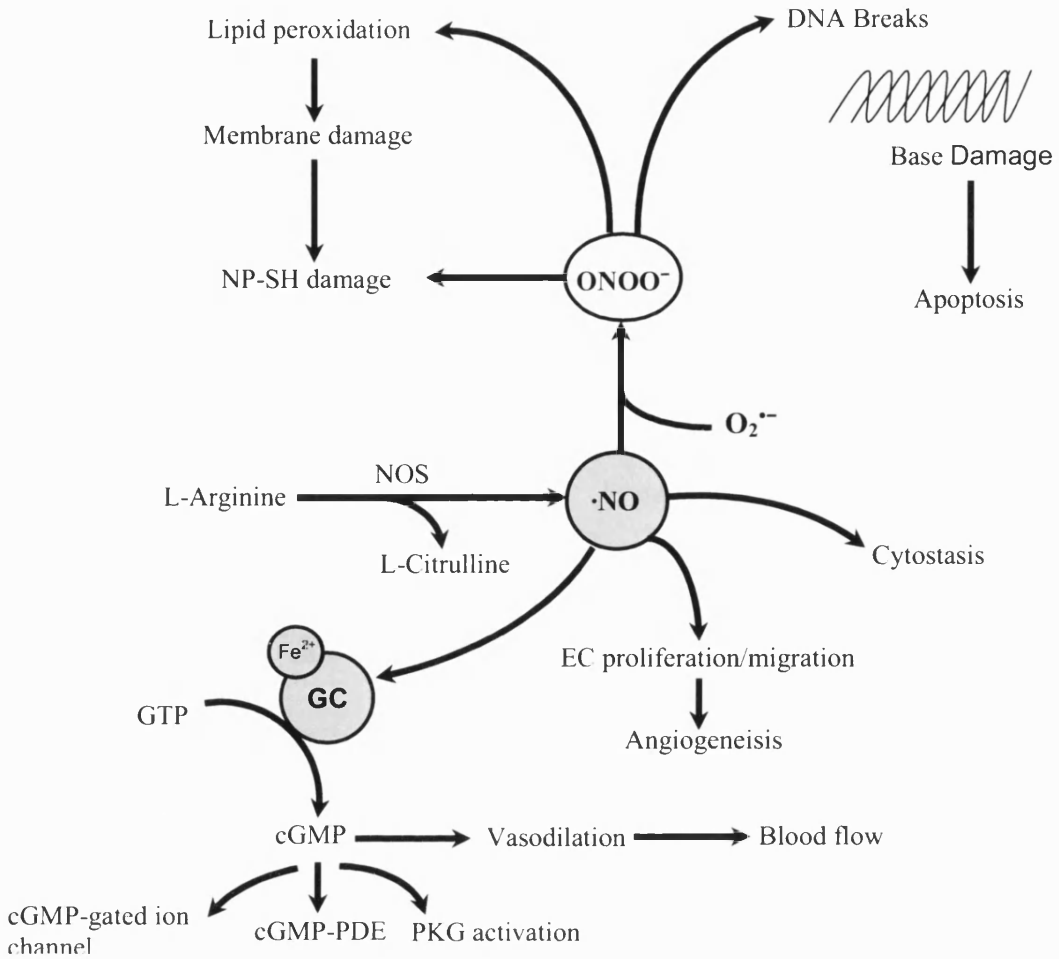

Figure 3.4The physiological effects of 'NO and $ONOO^-$ generation.

Nitric oxide synthase (NOS) converts L-arginine to 'NO which is responsible for a variety of cellular effects which are discussed above. Nitric oxide also binds to the enzyme guanylate cyclase (GC) which results in GC activation. Activated GC cleaves two phosphate groups from the compound Guanylate triphosphate (GTP) to form Cyclic guanosine monophosphate (cGMP) which is used to phosphorylate proteins including the smooth muscle contractile protein called myosin resulting in relaxation and increased blood flow in the vessel exposed to 'NO. Signalling by cGMP is mediated by three cGMP effector molecules, protein kinase G (PKG), cyclic guanosine monophosphate-phosphodiesterase (cGMP-PDE) and cGMP-gated ion channels. cGMP-PDE degrades cGMP. Cyclic guanosine monophosphate is also involved in signal transduction in the nervous system and inhibition of platelet aggregation. Nitric oxide and $O_2^{\bullet-}$ rapidly react to form $ONOO^-$ which can result in a number of damaging cellular effects. NP-SH also stands for non protein thiol damage. For example the damage of glutathione which maintains the intracellular redox state. EC = Endothelial cell.

3.2 Xanthine Oxidoreductase (XOR)

XOR activity was first measured in bovine milk, by Schardinger in 1902, when investigating the hydroxylation of hypoxanthine to xanthine. Research has since shown XOR to belong to a group of proteins known as oxidoreductases. This refers to the redox activity of the enzyme and the fact that the enzyme can function with a range of substrates to yield a range of products over a variety of environmental conditions. The enzyme is a homodimer of 150kDa subunits and exists in two interconvertable forms, xanthine

dehydrogenase (XDH) and xanthine oxidase (XO). XDH preferentially reduces NAD^+, whereas XO does not reduce NAD^+, preferring molecular oxygen. XDH and XO are often cumulatively referred to as Xanthine oxidoreductase (XOR).

3.2.1 Distribution and activity of XOR with particular reference to the skin

XOR has been isolated from a range of species and tissues and shows a diversity of activities to certain substrates. The bovine milk enzyme is the most commonly studied and differs from certain sources of the human enzyme in the rate at which it catalyses purines (Parks and Granger, 1986). These investigators showed that the human heart enzyme had reduced activity towards purines whereas the liver enzyme displayed similar activity to that of bovine milk.

The presence of XOR is variable within different tissues of a specific species and between species. Histochemistry of laboratory rodents in a study carried out by Gossrau *et al* (1990), showed epithelial cells of a wide range of external and internal surface epithelia, including stratified squamous epithelia of skin, to contain highly a effective XOR and SOD system. It was hypothesised that this system may have a general antimicrobial function. Studies have also shown XOR activity to be significantly increased in the distal end of ischaemic skin flaps after 1 hour and that activity remained elevated at 6 hours. Allopurinol also significantly reduced neutrophil concentrations at the distal ends of skin flaps suggesting that XOR activity is associated with an increase in neutrophils. Allopurinol was also found to reduce skin necrosis (Rees *et al*, 1994). The average human plasma activity of XO is reported to be 2.1 ± 0.8 ($x10^{-3}$ U ml^{-1}) (Liu *et al*, 2003).

Furthermore, in a study carried out by Picard-Ami *et al* (1991) activity of XOR was measured after varying intervals of ischaemia and in rats following reperfusion. Control pig and human skin were found to contain minimal enzyme activity, almost 40 times less than that of the rat. In the rat, XOR activity was stable throughout a prolonged period of ischaemia, and a significant decrease in activity was found after 12 hours of reperfusion. In humans XOR activity was unaffected by ischaemia time, and in the pig, it did not increase until 24 hours of ischaemia.

3.2.2 Enzyme structure

Xanthine Oxidoreductase exists as a homodimer containing three redox centres namely the molybdopterin cofactor centre, the FAD centre and the iron-sulphur centre.

3.2.2.1 Molybdopterin cofactor centre

Xanthine oxidase belongs to a group of mononuclear molybdenum enzymes that possess, at their active site, a molybdopterin cofactor (MO) that is essential for activity (Hille, 1996). Molybdenum is incorporated into proteins as the molybdenum cofactor that contains a mononuclear molybdenum atom coordinated to the sulphur atoms of a pterin derivative named molybdopterin. Molybdenum-cofactor-containing enzymes catalyze the transfer of an oxygen atom, ultimately derived from or incorporated into water, to or from a substrate in a two-electron redox reaction (Kisker *et al*, 1997). In 1996 Hille suggested that the reason for the possession of pterin cofactor to be the provision of a method by which electrons can be shuttled away from the molybdenum active site to allow a more rapid turnover and modulation of the molybdenum reduction potential. The molybdopterin cofactor known to be the site at which the purine substrates xanthine and hypoxanthine are oxidised to urate and xanthine respectively in the presence of oxygen as an electron acceptor.

3.2.2.2 FAD centre

Purified XO occurs as a brown solution which is due to the presence of a flavin moiety which is known as flavin adenine dinucleotide (FAD) (Ball, 1939; Corran *et al*, 1939). Flavin is known to be important for enzyme turnover and the generation of $O_2^{\bullet -}$. In the absence of oxygen and any other oxidising substrate the enzyme will gain electrons from hydroxylation of a purine substrate. This enzyme will now not be able to turnover as it is loaded with electrons and cannot return to the oxidised state without passing them on to an acceptor substrate. Oxygen has been shown to accept electrons from the electron rich enzyme with the formation of $O_2^{\bullet -}$. This allows the turnover of the enzyme to carry out further hydroxylations of purine substrates. Oxygen is supposed to bind and receive its electrons from the flavin thus allowing further turnover of the enzyme by utilising a second site removed from the molybdopterin.

The flavin is the apparent site at which NADH will donate electrons and cause the generation of NAD^+. The electron-rich enzyme again in the presence of oxygen will give up its electrons to generate $O_2^{\bullet -}$ radical and allow further turnover of the enzyme. The flavin specific inhibitor Diphenyliodonium (DPI) has been shown to inhibit the oxidation of NADH to NAD^+ by XO and also therefore to inhibit the production of $O_2^{\bullet -}$ radical by the same means of denying the enzyme electrons (Sanders *et al*, 1997).

3.2.2.3 Iron-sulphur centre

Iron is also required for the activity of xanthine oxidation (Richert and Westerfeld, 1954; Palmer *et al*, 1964). Studies by Palmer in 1964, also suggest that the iron is reduced from a ferrous to a ferric state during enzyme turnover. Furthermore, studies carried out by Bray and colleagues (1961), used Electron spin resonance (EPR) techniques to show a paramagnetic signal from resting XO enzyme occurred following those attributable to MO and FAD and therefore suggesting an involvement in electron transport mechanisms that were carried out in this order. Studies carried out by Lowe *et al* (1972) have attributed this iron signal to an iron sulphur moiety (Fe-S).

3.2.3 Superoxide generation by XOR

XOR participates in a range of reactions and is particularly well known for its role in purine metabolism. Figure 3.5 below details the oxidation of hypoxanthine to xanthine and xanthine to uric acid by XOR with the associated cofactors and products. When XOR catalyzes the aerobic oxidation of xanthine, it generates an unstable reduced form of oxygen, the superoxide anion, and it is this radical that directly reduces cytochrome *c* (McCord and Fridovich, 1968).

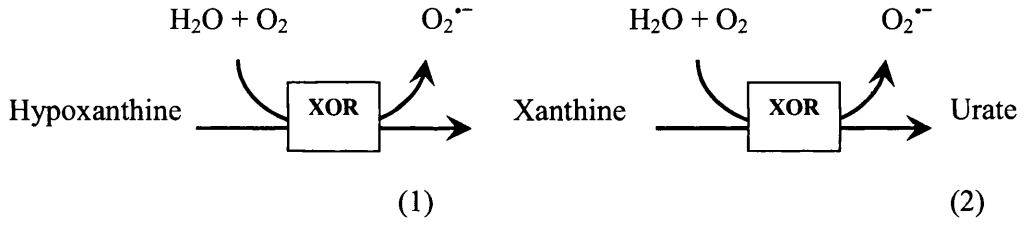

Figure 3.5 XOR-catalysed superoxide generation.

XOR-catalyses the oxidation of the purine substrates hypoxanthine to xanthine (1) and xanthine to urate (2). In the presence of oxygen the electrons donated to XOR from the oxidation of these substrates are used to reduce molecular oxygen resulting in the formation of $O_2^{\bullet-}$.

These reactions can be inhibited by blocking the molybdenum centre of the enzyme with purine analogues such as allopurinol and oxypurinol. This reaction occurs in the presence of oxygen as the electron acceptor and is rate dependent on its concentration (Fridovich and Handler, 1962). The Michaelis constant (K_m) for xanthine and hypoxanthine are ~ 6μM under room air conditions and the K_m for oxygen reduction was 27μM and 800μM for the reduction of cytochrome *c* (Fridovich and Handler, 1962).

The oxidation of NADH to NAD^+ is shown in figure 3.6 with the electron again being given to oxygen to produce $O_2^{\bullet-}$. This reaction is not affected by the molybdenum site inhibitors allopurinol and oxypurinol in the presence of oxygen but is inhibited by

NAD^+ and also by the FAD specific inhibitor diphenyliodonium (DPI) (Sanders *et al*, 1997). The K_m for the oxidation of NADH in both bovine-derived and human milk enzymes was calculated by Sanders *et al* (1997), to be 1.23 and 0.597μM respectively. This reaction was dependent on the availability of oxygen in the absence of any other electron acceptor. The K_m for oxygen utilisation in this system was not been calculated but it was suggested, by Sanders *et al* (1997), that NADH oxidation was linearly increased over the physiological range in the absence of other electron acceptors.

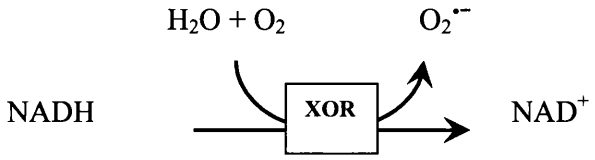

(3)

Figure 3.6XOR-catalysed superoxide generation.

3.2.4 Nitric oxide generation by XOR

In 1997 work carried out by Millar *et al*, provided the first description of the nitrate and nitrite reductase activities of XO with •NO as the end product. Furthermore, under hypoxic conditions and in the presence of NADH or hypoxanthine, XOR is capable of catalysing the reduction of organic and inorganic nitrates and nitrites to •NO (Millar *et al*, 1998).

With conditions occurring during ischaemia, myocardial XO and nitrate levels were determined to generate up to 20μM nitrite within 10-20min that can be further reduced to •NO with rates comparable to those of maximally activated NOS. Thus, XO catalyzed nitrate reduction to nitrite and •NO occurs and can be an important source of •NO production in ischaemic tissues (Li *et al*, 2003). The pH dependence of nitrite and •NO formation also indicate that XO-mediated nitrate reduction occurs via an acid catalysed mechanism. Based on work carried out in our group, it has also been proposed that XO, abundant in milk, serves to sterilise the neonatal gut by way of •NO production (Stevens *et al*, 2000).

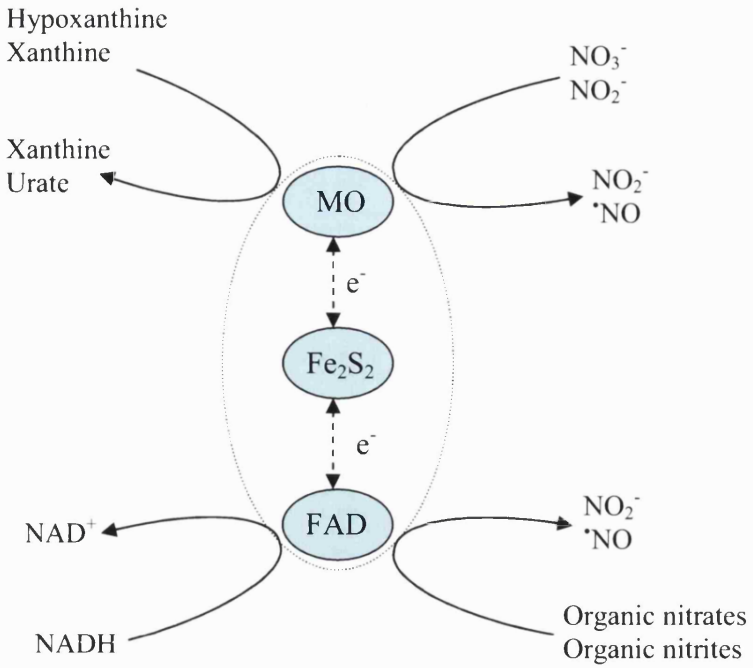

Figure 3.7 A schematic diagram showing XOR-catalysed reduction of nitrates and nitrites.

Under anaerobic conditions, organic nitrates are reduced at the FAD site to inorganic nitrite, which can itself be subsequently further reduced to •NO at the MO site. Organic nitrites are similarly reduced at FAD, in this case directly to •NO. In contrast to organic nitrites but similarly to in organic nitrites, inorganic nitrates are reduced at MO.

3.2.5 Peroxynitrite generation by XOR

It is known, that whatever the origin, •NO and $O_2^{\bullet-}$ react rapidly to form $ONOO^-$ which is a powerful and destructive oxidant (Saran and Bors, 1990). As discussed, XO is capable of producing both •NO and $O_2^{\bullet-}$ simultaneously and it has been shown that $ONOO^-$ can be produced by XO itself (Godber *et al*, 2000b). Superoxide is generated by donation of electrons from the substrates, such as xanthine or NADH, to oxygen. Production of •NO from nitrite reduction by electrons derived from NADH or xanthine. Nitric oxide is produced in the absence of oxygen but as oxygen concentrations increase, the two electrons donated to the enzyme per xanthine can be split to reduce, by one electron reductions, both oxygen and nitrite. Simultaneous generation of •NO and $O_2^{\bullet-}$ leads to the formation of $ONOO^-$ (Figure 3.8).

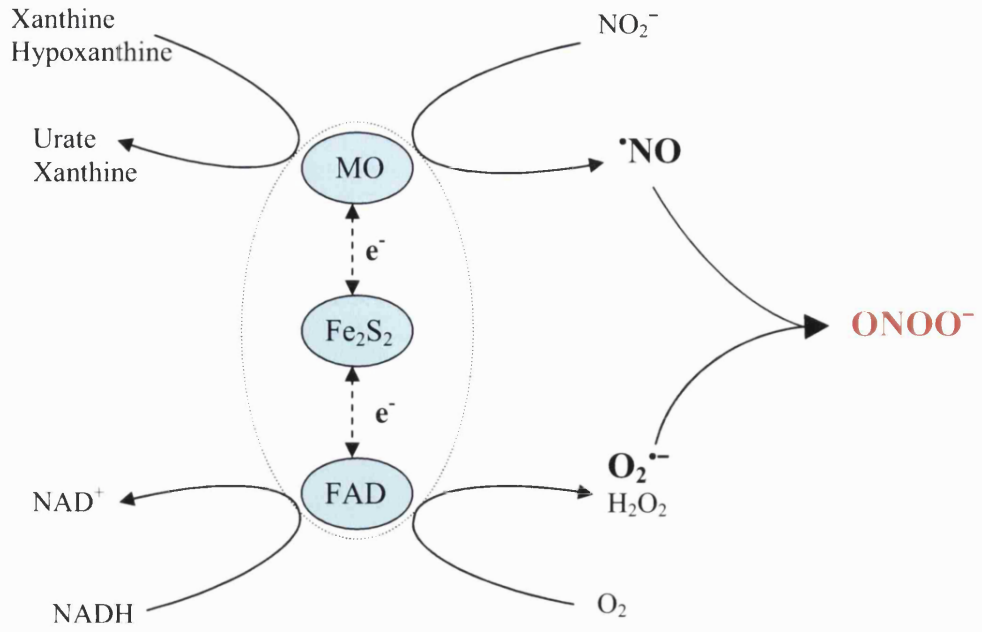

Figure 3.8 XOR-catalysed peroxynitrite generation.

Under hypoxic conditions, XOR can generate •NO; however, if O_2 concentrations rise to around 70 μM/about 50mmHg (Millar unpublished data), pairs of electrons derived from either hypoxanthine, xanthine, or NADH, can be used to reduce nitrite or O_2 (the preferred substrate), therefore generating •NO and $O_2^{\bullet-}$, respectively. •NO and $O_2^{\bullet-}$ can react together forming $ONOO^-$ (Huie and Padmaja, 1993).

3.2.5.1 Roles for the XOR-catalysed generation of RONS

Reactive oxygen species have been long recognised as important mediators of inflammation, injury, and cell death. Xanthine oxidase is traditionally thought to be an important source of free radical-induced cellular injury and is implicated as a key enzyme contributing to ischaemia-reperfusion injury (Parks and Granger, 1998). However, over the last ten years, there has been accumulating evidence of the advantageous biological effects of both ROS and RNS. It is known that XOR has bactericidal properties in the presence of hypoxanthine and is activated in response to bacterial infection *in vivo* (Tubaro *et al*, 1980). In the presence of nitrite, $ONOO^-$ can be generated by XOR alone. This may also explain the presence of XOR in milk with a possible role in sterilisation of the neonatal gut. The enzyme is upregulated by proinflammatory cytokines and is thought to have a defensive role due to its production of ROS. In 1997 Umezawa *et al*, carried out studies in mice, looking at induction of •NO and XOR in response to *Salmonella typhimurium* infection and showed that mortality rates where improved by XOR inhibitors. XOR is also known for its affinity for acidic polysaccarides (Adachi *et al*, 1993), such as occur in many bacterial capsules (Harrison, 2002). The optimal pH for anaerobic XOR-catalysed generation of •NO in the presence of xanthine is pH 6 or less (Godber *et al*, 2000b). XOR-catalysed production of •NO, a prerequisite for $ONOO^-$

generation, was shown to occur at maximal rates of approximately 1μmol min^{-1} mg^{-1}, significant in physiological terms. K_m values for nitrite were, however, in the millimolar range (Godber *et al*, 2000b); levels that would have to be obtained in order to achieve maximal rates. It is known, that at least in anaerobic culture, bacteria can excrete millimolar levels of nitrite (DeMoss and Hsu, 1991). It is possible that by way of nitrite secretion, bacteria might initiate their own destruction (Harrison, 2002). First, the conversion of XDH to the more efficient ROS-generating enzyme form, XO, is stimulated by bacterial lipopolysaccharide structures (Takeyama *et al*, 1996). Further, circulating enzyme may bind to glycosaminoglycans (Adachi *et al*, 1993), which are similar to structural components found on the surface of some bacteria (Roberts, 1996). Therefore, by utilising circulating substrate the enzyme can generate microbicidal RONS in tight proximity to microbes. Indeed, the antimicrobial function of XOR has been demonstrated in milk (Millar *et al*, 2002; Stevens *et al*, 2000; Hancock *et al*, 2002) where it is believed that XOR-generated RONS afford protection to the suckling neonate from diseases, such as gastroenteritis, early post partum. This mechanism also has been shown to be effective in Cape buffalo where an anti-microbial role for circulating XOR in the control of trypanosome infection has been established (Wang *et al*, 2002).

As mentioned previously, NOS is dependent on the availability of oxygen for its activity and thus ineffective in a hypoxic environment, where vasodilatory and antimicrobial properties of $^{\bullet}NO$ would be advantageous. Conversely previous research has shown that XOR is capable of generating $^{\bullet}NO$ at a range of oxygen tensions and as a result may be beneficial in encouraging wound healing in the hypoxic environment of a chronic wound.

3.3 Aims and objectives

As outlined in the introduction, chronic wounds are characterised by hypoxia, providing an ideal environment for the growth of facultative and anaerobic bacteria. Clearly for correct wound healing, treatments are required which are bactericidal but allow dermal fibroblast proliferation. The enzyme XO has special redox properties and is known to facilitate both microbial killing and cell proliferation through the generation of reactive oxygen and nitrogen species. Therefore, in this study, I have addressed the following questions:

1. What specific reactive species are generated by purified XO in a simulated chronic ulcer environment at varying oxygen tensions?
2. Can XO-generated species improve wound healing by enhancing proliferative activity of dermal fibroblasts in a hypoxic ulcer environment?
3. Can XO-generated species also be antimicrobial in the same environment?

Primary investigations involved the measurement of XO-generated species at varying enzyme concentrations using the pterin assay, cytochrome *c* assay and the dihydrorhodamine assay. These experiments were conducted in a variety of biological media, used in the culture of fibroblasts and bacteria, to provide an understanding of the levels of species to which wound-related cells could be exposed in varying conditions *in vivo*, most particularly low oxygen. The effects of these XO-generated species on human dermal fibroblasts (HDF) at a range of oxygen tensions including hypoxia were determined by the measurement of viability and proliferation using the MTT assay, and BrdU incorporation.

Further investigations involved the study of bacterial species relevant to chronic wounds and how these were affected by species generated by XO in appropriate environments. Bacterial viability of facultative strains was assessed by growth curves, diffusion zone assays and viable colony counts.

Overall, the objective of this research was to investigate ways in which exploitation of the special redox properties of XO can provide a novel way to improve the clinical effectiveness of wound dressings and tissue engineered dermal replacements.

CHAPTER 4

4 Assessment of XOR activity by detection of its products

4.1 Introduction

This chapter follows the development of several assays that were used to measure some of the important species generated by XOR. Assays were used to determine levels of species generated by the enzyme in PBS, fibroblast and bacterial culture medium, in air and in hypoxia.

4.1.1 XOR generated species

XOR is a molybdoflavoprotein (Bray *et al*, 1975), existing as a homodimer, each 147 kDa subunit of which contains one molybdenum atom, one FAD and two Fe_2S_2 centres (Bray *et al*, 1975; Hille, 1996). XOR has a wide specificity for reducing substrates, although its conventionally accepted role is in purine catabolism, where it catalyses the oxidation of hypoxanthine to xanthine and xanthine to uric acid. High concentrations are found in mammalian milk and liver, expressed in the vascular endothelium and measured in the circulation (Parks and Granger, 1986; Kayyali *et al*, 2001; Houston *et al*, 1999). In mammals, XOR occurs in two interconvertable forms, xanthine dehydrogenase (XDH, EC 1.1.1.204), which predominates *in vivo*, and xanthine oxidase (XO, EC 1.1.3.22). During ischaemia the purine bases xanthine and hypoxanthine accumulate (Jones *et al*, 1968), and endothelial XDH is converted into reversible and irreversible forms of XO (McKelvey *et al*, 1988; Parks *et al*, 1988). Both forms of the enzyme can reduce molecular oxygen, although only XDH can reduce NAD^+, which is its preferred electron acceptor. Reduction of oxygen leads to $O_2^{\bullet-}$and H_2O_2 generation. The roles for oxygen free radicals in the bactericidal activities of phagocytic cells, and in mediating tissue damage after acute ischaemia are well documented (McCord, 1985). More recently, an increasing body of evidence suggests a role for ROS in signal transduction (Thannickal and Franburg, 2000).

Peroxynitrite can also be produced by the enzyme in the presence of inorganic nitrite, molecular oxygen and a reducing agent. Peroxynitrite generation by the physiologically predominant dehydrogenase form of the enzyme is greater than the oxidase form under aerobic conditions but the oxidase form generates more $ONOO^-$ in hypoxia. These differences can be explained in terms of the production of $^{\bullet}NO$, the

essential precursor of $ONOO^-$ formation in combination with $O_2^{\bullet-}$. Under anaerobic conditions, rates of $^{\bullet}NO$ production in the presence of XO or XDH are comparable. As oxygen levels increase, levels of $^{\bullet}NO$ fall much more rapidly in the case of XO. The reasons for this may be explained in terms of competition between nitrite and molecular oxygen for donated electrons. It is well established that reducing substrates, other than NADH, donate electrons to the molybdenum centre of XOR, while molecular oxygen accepts electrons at the FAD site. Organic nitrite however, accepts electrons directly from the molybdenum site. XO is known to reduce molecular oxygen some six times faster than does XDH, implying the XO will have fewer electrons available for the reduction of nitrite than will XDH; a situation that will be exacerbated as oxygen tensions increase (Sanders, 1997). Peak $ONOO^-$ generation is reported to occur at 7μM oxygen (0.6%) oxygen (Godber *et al*, 2000a). However, Millar 2004 reports that optimal $ONOO^-$ formation occurs at 70μM oxygen (~6% oxygen) with purine substrates in both cases reaching around 25nmol min^{-1} mg^{-1} $ONOO^-$ at their peak. Both studies point to hypoxia but it appears to be at varying intensities.

The physiological dissolved oxygen concentration range of plasma is 120-135μM (10-11 %) on the arterial side to 55-70μM (4.8 - 6.1%) on the venous side (West, 1990). However, in chronic venous ulcers, mean values as low as 13mmHg (1.7% oxygen) have been quoted (Falanga *et al*, 1992b). Plasma nitrite can be generated from nitrate reduction, the reaction of $^{\bullet}NO$ with oxygen and cyt *c* catalysed formation of nitrite from $^{\bullet}NO$ (Torres *et al*, Pearce *et al*, 2002) and ranges from 10 to 50μM in normal adults but can rise to 130μM in patients with sepsis (Evans *et al*, 1993) (See Table 4.1). This suggests that $ONOO^-$ formation from XO can occur under normal physiological concentrations of substrate.

Compound	Plasma Concentration	
	Normal	**Disease**
Xanthine Oxidase	0.2μU ml^{-1}	1.52-200 μU ml^{-1}
Xanthine	0.65μM	21μM
Hypoxanthine	1.43, 1.65μM	18.8, 81.6μM
Nitrite	10 to 50μM	Up to 130μM (Evans *et al*, 1993)

Table 4.1 Plasma concentrations of relevant substances (Millar, 1999)

Inoue *et al* (2002) has shown evidence of 3-nitrotyrosine formation in healthy adults suggesting that normal physiological processes can lead to the formation of $ONOO^-$ in plasma. We have also found that the optimum pH for the production of $^{\bullet}NO$ from XOR under hypoxic conditions is about 5.5. Therefore, ulcers present an environment in which the production of $^{\bullet}NO$ in the presence of XOR would be at or near its peak.

A possible problem exists for a functional $ONOO^-$ forming enzyme utilising xanthine in the form of the reported scavenging activity of the product urate. Scavenging of $ONOO^-$ by uric acid has been suggested to decrease $ONOO^-$ neurotoxicity in diseases such as multiple sclerosis (Hooper *et al*, 1997). However, the reaction of $ONOO^-$ with uric acid has given conflicting results. Skinner *et al* (1998) showed that $ONOO^-$ and uric acid react to give an $^{\bullet}NO$ donor species having downstream effects on vascular relaxation whereas the reaction of $ONOO^-$ with CO_2 was shown to be 920 times faster than $ONOO^-$ with uric acid at physiological CO_2 concentrations (Squadrito *et al*, 2000). The picture is further complicated with $ONOO^-$ permeation of erythrocytes in the presence of CO_2 (Romero *et al*, 1999). The suggestion therefore that the simultaneous formation of uric acid and $ONOO^-$ by XO does not automatically lead to scavenging in physiological environments due to the competing reactions. Further to these observations, using NADH as the donor substrate can lead to the simultaneous reduction of nitrite and oxygen by XO and derive $ONOO^-$ in the complete absence of purines and urate.

4.1.2 Measurement of reactive species

Previous studies carried out by Murrell *et al*, 1990, showed that addition of XOR into cell culture enhanced the proliferation of adult human dermal fibroblasts. Therefore Murrells methodology was used as a starting point for enzyme assays with a view to derive a greater understanding of the potential effects of the enzyme in the presence of high and low oxygen concentration along with substrates at levels similar to physiological levels that may be found in the chronic wound fluid. Murrell used 1mM hypoxanthine, 20mM HEPES buffer with XO 0 - 100mU ml^{-1} in fibroblast growth medium. A similar system formed the basis of the assays in this chapter with some modifications as described below. Nitrite (1mM) was also added to assays (levels previously used by Dr. Millar) to generate $ONOO^-$ at the lower oxygen concentrations, for a possible antimicrobial role for the enzyme.

Superoxide was measured using the cytochrome *c* assay. This method has been used to measure rates of formation of $O_2^{\bullet -}$ by numerous enzymes, whole cells, and vascular tissue (Azzi *et al*, 1975; Landmesser *et al*, 2003; Massey, 1959). There are several precautions which must be taken when using this reaction to detect $O_2^{\bullet -}$. Reduction of cytochrome *c* is not absolutely specific for $O_2^{\bullet -}$. Cellular reductants such as ascorbate and glutathione are capable of reducing cytochrome *c* and may be present in high concentration within tissue extracts, as are cellular reductases that enzymatically mediate cytochrome *c* reduction. Additionally, enzymes such as xanthine oxidase are capable of reducing quinines or redox-active dyes that may also be present and whose reduced forms

are capable of directly reducing cytochrome *c*. It is important therefore to demonstrate specificity of this reaction for $O_2^{\bullet -}$ by the extent of inhibition of cytochrome c reduction by exogenous SOD. Reduced cytochrome *c* can be re-oxidised by cytochrome oxidases, cellular peroxidases, and oxidants, including H_2O_2 and $ONOO^-$ (Thomson *et al*, 1995). These influences cause an apparent decrease in cytochrome *c* reduction therefore underestimating the rate of $O_2^{\bullet -}$ formation. To this effect enzyme inhibitors (10μM CN for cytochrome oxidase) or scavengers of reactive species (100U ml^{-1} catalase for H_2O_2, 10mM urate for $ONOO^-$) can be added to the reaction mixture to avoid this draw back. The applicability of the cytochrome *c* method for *in vivo* detection is limited because it is relatively insensitive and can be interfered with by a variety of endogenous reductants. However, the use of the cytochrome *c* reaction has received "gold standard" status for the detection of $O_2^{\bullet -}$, particularly with *in vitro* assays such as will be described and activated leukocytes.

Dihydrorhodamine, DHR is a probe widely used to detect several reactive species ($^{\bullet}OH$, $ONOO^-$, $NO_2^{\bullet}$, peroxidase-derived species), but is poorly responsive to $O_2^{\bullet -}$, H_2O_2 and $^{\bullet}NO$ (Buxser *et al*, 1999). Although a direct reaction of DHR 123 with H_2O_2 does not occur, it can be catalyzed by haem-containing peroxidases such as HRP (LeBel *et al*, 1992) or other haem compounds, including cytochrome *c* (Royall and Ischiropoulos, 1993).

4.1.3 Use of the oxygen controlled cabinet

Enzyme assays and cellular incubation with XOR were to be carried out, as closely as possible under conditions which prevail in the chronic wound. With regard to oxygen tension, the chronic wound is known to be hypoxic (Section 2.2.1). Mean values as low as 13mmHg which is around 1.7% oxygen have been quoted for venous ulcers (Falanga *et al*, 1992b). Therefore, as air is around 21% oxygen, to mimic the chronic wound environment as closely as possible it was necessary to control the oxygen tension using a sealable hypoxia cabinet (Don Whitley Scientific miniMACS Workstation A03000). This cabinet allowed for the delivery of customised mixtures of three different gases and the manipulation of a large number of reactions at one oxygen concentration. The hypoxia cabinet could also be environmentally controlled including temperature and humidity adjustments. For the purposes of these experiments the cabinet was operated on a single cylinder of mixed gas at the relevant oxygen concentration for the experiment, special mixed gases were supplied by British Oxygen Corporation (BOC) and typically contained 5% CO_2 and 0-5% oxygen balanced nitrogen. Once the relevant cylinder had been attached the cabinet was purged twice using the automatic commissioning sequence that

lasts for 75 minutes and prepares the cabinet for use. At the start of each experiment the percentage of atmospheric oxygen inside the cabinet was confirmed using an oxygen meter (Analox Mini O2DII). The meter was calibrated in air in accordance with the manufacturer's instructions.

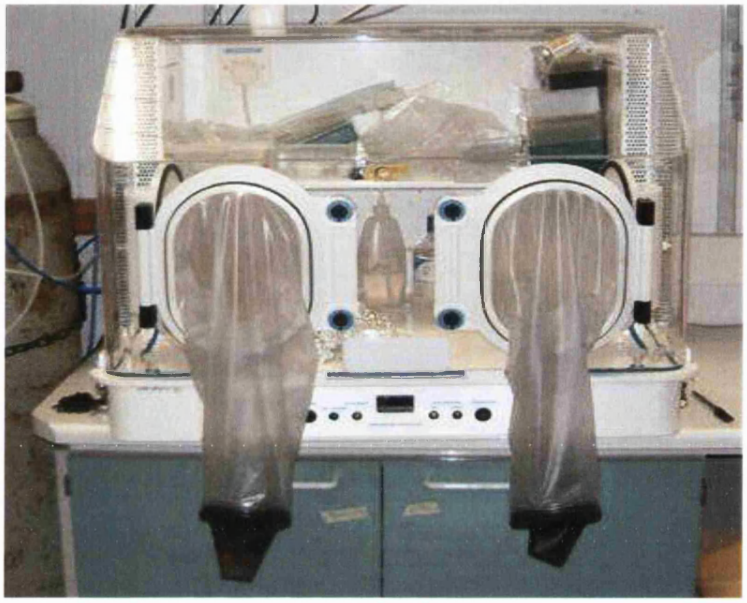

Figure 4.1 Oxygen controlled cabinet

The sleeve door system allows for the manipulation of samples without altering the environment inside the cabinet. Hands are inserted into sleeves and a foot-pedal controlled vacuum is used to remove the air in the sleeves, a second foot-pedal is used to replace the air with the relevant gas from the cylinder which is also supplying the cabinet. This process is repeated 3 times before the doors into the cabinet are opened.

4.1.4 Chapter aims

This chapter aims to develop several assays for the measurement of XO-generated species such as $O_2^{\bullet -}$ and $ONOO^-$. These assays will be used to measure XO-generated species at varying concentrations of substrate and enzyme, in both fibroblast and bacterial growth medium and in variable oxygen in order provide information on the levels of XO-generated species that dermal fibroblasts and bacteria would be exposed to under these culture conditions. These observations will indicate the levels of XO-generated species that could potentially be produced in a chronic ulcer setting.

4.2 Materials and Methods

4.2.1 Enzyme Characterisation

4.2.1.1 Protein determination using the Bio-Rad assay

The protein concentration of a commercial preparation of XO (See above) was assessed using a Bio-Rad protein assay. This technique works on the change in absorbance maximum when Coomassie Brilliant Blue G-250 reacts with peptides, and shifts from 465nm to 595nm. Protein binding results in a brown to blue colour change, the intensity of the blue colouring is dependent on the concentration of protein. The Coomassie blue dye binds to primarily basic and aromatic amino acid residues, especially arginine.

4.2.1.1.1 Materials

Bovine Serum Albumin (BSA), Bio-Rad Reagent, (Bio-Rad, Hertfordshire, UK), 96-well, flat-bottomed tissue culture test plates (Fisher Scientific, Loughborough, UK), Xanthine Oxidase (XO), (From buttermilk XO2B), Suspension in 60% saturated ammonium sulphate solution containing sodium salicylate and EDTA. Lactoperoxidase not detected, (Biozyme Laboratories Ltd, Gwent, UK).

4.2.1.1.2 Protocol

Doubling dilutions of protein standards from 0 to 1.35mg ml^{-1} were added to the wells of a 96-well plate, in triplicate, in a total volume of 10µl of standard per well. 10µl of sample was also added to separate wells in triplicate. All dilutions were made in Milli-Q purified water 200µl of Bio-Rad protein assay reagent working solution was added to all sample wells and incubated at room temperature for 5 minutes to allow colour development. The absorbance across the plate was read at 595nm a multi-well plate reader (Dynex Technologies, MRX TC II). The concentration of protein in test samples was determined with reference to a graph plotted from the absorbance readings of the standard samples.

4.2.1.2 Protein determination using the Bio-Rad *DC* protein assay

The Bio-Rad *DC* protein assay was also used to assess the protein concentration of xanthine oxidase. This is a colourimetric assay that is very similar to the Lowry assay. The assay is based on the reaction of protein with an alkaline copper tartrate solution and Folin reagent. There are two steps that lead to colour development: the reaction between protein and copper in an alkaline medium, and the subsequent reduction of Folin reagent by the

copper-treated protein. Colour development is primarily due to the amino acids tyrosine and tryptophan, and to a lesser extent, cystine, cysteine, and histidine. Proteins affect the reduction of the Folin reagent by the loss of 1, 2, or 3 oxygen atoms, thereby producing one or more of several possible reduced species that have a characteristic blue colour with maximum absorbance at 750nm and minimum absorbance at 405nm.

4.2.1.2.1 Materials

Reagent A (Alkaline copper tartrate solution) and Reagent B (Folin Reagent), Bio-Rad, Hertfordshire, UK, Far UV quartz cuvette (200-2500nm, working volume 3.5ml), Fisher Scientific, Loughborough, UK

4.2.1.2.2 Protocol

A volume of 300µl of the protein standard (doubling dilutions 0 to1.35mg ml^{-1}BSA) or samples diluted in Milli-Q purified water was reacted with 1,200µl Reagent A. A further 4,800µl of Reagent B was also added. The reaction mixtures were then incubated at room temperature (approximately 25°C) for 15 minutes. 2mls of standard solution or sample was added into crystal cuvettes, and readings were taken in triplicate. Absorbance was read at 750nm using the Hitachi U-2010 spectrophotometer.

4.2.1.3 Comparison of Oxidase and dehydrogenase activity by the pterin assay

A sensitive, fluorometric assay for XO and XDH has been developed over several decades (Lowry *et al*, 1949; Haining and Legan, 1967; Markley *et al*, 1973; Beckman *et al*, 1989). This method is based on the use of pterin (2-amino-4-hydroxypteridine) as a substrate for XOR, which is oxidised to the fluorescent compound isoxanthopterin (2-amino-4,7-dihydroxypteridine, IXP). This fluorometric assay is 100-500 times more sensitive than the traditional spectrophotometric assay of urate formation from xanthine and enzyme activity as low as 0.1 pmol min^{-1} ml^{-1} can be measured. The protocol from the Beckman *et al*, 1989 assay will now be described and, in this case, was used to check the relative proportion and specific activity of both XO and XDH in the Biozyme XO. XO activity is assayed in the presence of the pterin substrate alone, using oxygen as an electron acceptor for the reduced enzyme. With the addition of methylene blue, an electron acceptor from the Fe-S clusters of XO and XDH, the combined activity of XO and XDH are assayed (methylene blue is used instead of NAD^+ as an electron acceptor, as NADH fluorescence overlaps with that of IXP). Allopurinol is added to the sample to inhibit XOR activity, thus allowing the calculation of XO- and XDH-specific generation

of IXP [both lactoperoxidase in the presence of H_2O_2 and aldehyde oxidase were shown to catalyse pterin-IXP conversion but were not allopurinol inhibitable (Beckman et al 1989)]. Finally the addition of an IXP internal standard of a known concentration, allows for the correction of any fluorescence quenching and the quantification of IXP production. The XOR catalysed conversion of pterin to IXP and the role of methylene blue and allopurinol are shown in Figure 4.2.

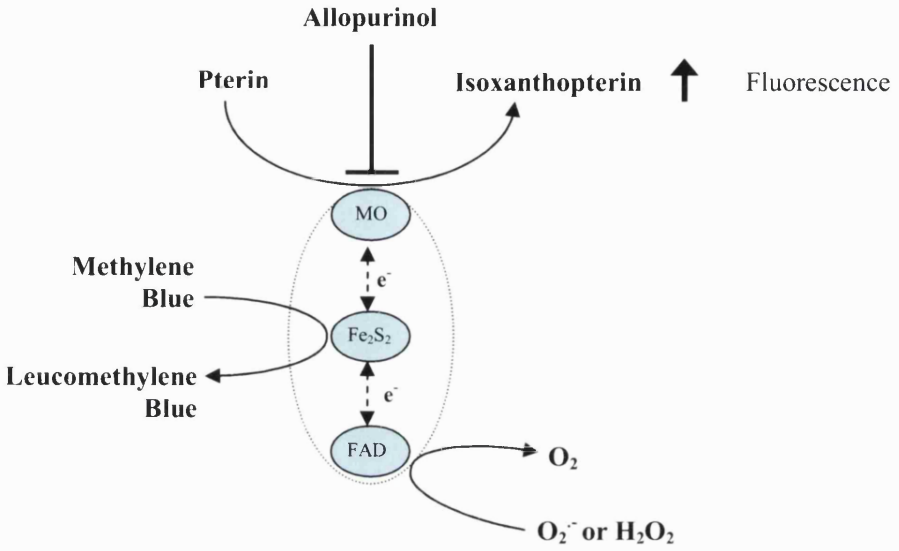

Figure 4.2 XOR catalysed generation of IXP from the pterin substrate.

Electrons donated to XOR during the oxidation of pterin to IXP (leading to increased fluorescence) are accepted by O_2 at the FAD-containing moiety in XO, however in the presence of methylene blue electrons are accepted at the Fe-S cluster-containing moiety of XO and XDH. Allopurinol inhibits the oxidation of pterin at the Mo-containing moiety.

4.2.1.3.1 Materials

Allopurinol, isoxanthopterin (IXP), methylene blue (MB), and pterin (2-amino-4-hydroxypteridine) (Pt) (Sigma Aldrich Company Ltd. Dorset, UK). Quartz crystal cuvettes (Fisher Scientific UK Ltd. Leicestershire, UK). Xanthine oxidase (Biozyme Laboratories. Gwent, UK).

4.2.1.3.2 Protocol

To analyse XO and XDH in the Biozyme enzyme the protocol described in Beckman *et al*, 1989 was followed, except for minor adjustments. In a final volume of 1ml the final concentrations of the reagents used for this assay were as follows; 100ng ml^{-1} XO, 10μM pterin, 10μM methylene blue (MB), 10μM allopurinol (A) and 100nM IXP. Stock concentrations of XO (1ng ml^{-1}), pterin (1mM) and IXP (10μM) were made up on the day of the experiment. 1mM stocks of MB and allopurinol were made up prior to the

experiment and stored at -20°C. The assay was initiated by adding 860µl PBS and a magnetic stirring flea to a quartz-crystal cuvette. The cuvette was placed into a Hitachi F-4500 fluorescence spectrophotometer (set at: excitation wavelength (Ex) 345nm, emission wavelength (Em) 390nm, monochromator Ex slit width 5nm, Em slit width 5nm, and the photomultiplier voltage set at 700V) with stirring set at 50rpm. The run was started immediately after the addition of 100µl of 1ng ml^{-1} XO. All other additions were carried out as shown on the trace below (Figure 4.3). Measurements were carried out for a sufficient time after each addition to the cuvette to enable rate calculations. All incubations were at room temperature.

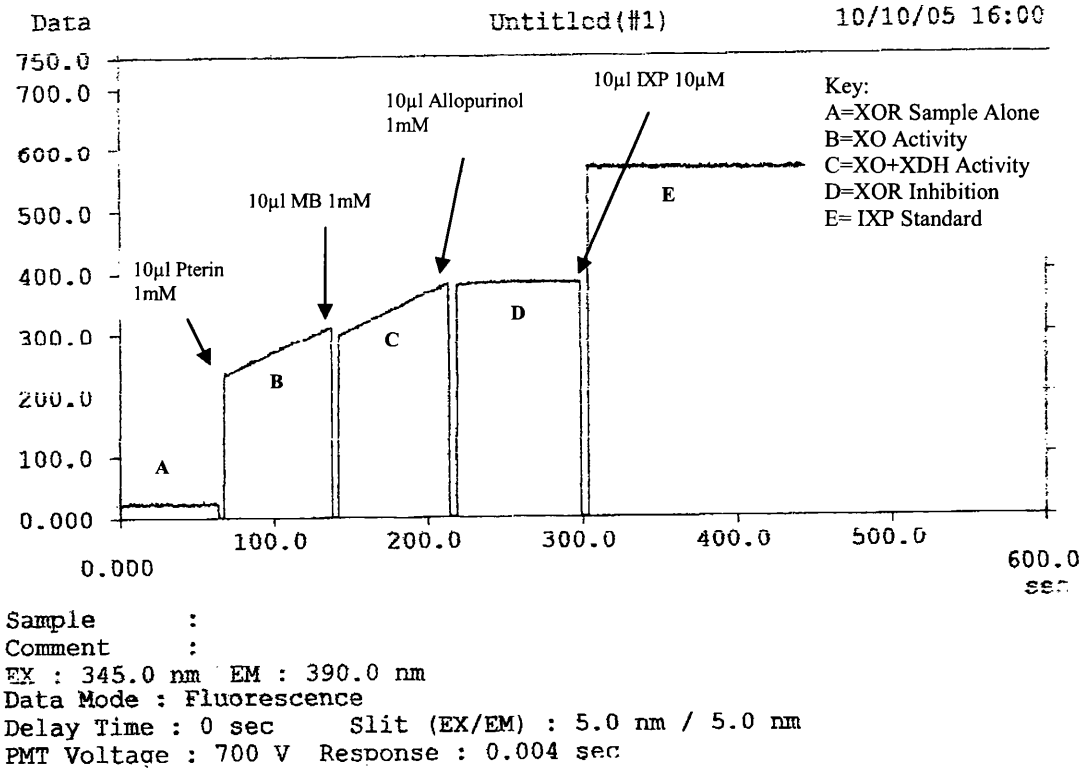

Figure 4.3 A typical trace from the Time-Scan XOR assay.

XO is assayed in the presence of pterin alone (with oxygen as the acceptor substrate), whereas the combined activites of XO and XDH are measured in the presence of methylene blue, which replaces the need of NAD^+ as an electron acceptor for XDH. Following the inhibition of XOR activity using allopurinol, the measurement of the fluorescence change following the addition of a known concentration of IXP (which acts as an internal standard) allows the quantification of IXP generation by XO and XDH. Additions were made to the cuvette at varying time points as indicated by the arrows. The Y axis = Fluorescence Intensity and the X axis = Time (Sec). IXP= isoxanthopterin, MB=Methylene Blue.

From the data recorded the change in fluorescence per unit time was calculated, and using the change in fluorescence readings following the addition of the IXP standard (100mM final concentration) it was possible to calculate[IXP] generated, as shown in equation 1.

$$[\text{IXP}] = \Delta F^{*} \, (IXPc \, / \, F_{IXP})$$

Equation 4.1 Calculation of Isoxanthopterin Generation in XOR Activity Time-Course Assay.

Where ΔF= Change in fluorescence units per unit time, *IXPc* = concentration of IXP standard added, and F_{IXP} = the change in fluorescence units immediately following the addition of the IXP standard.

4.2.2 Development of methods for the measurement of XO activity in cell growth medium

4.2.2.1 Cytochrome *c* assay for superoxide generation by XO

The cytochrome *c* – based method of measuring $O_2^{\bullet-}$ was adapted from the method of McCord and Fridovich (McCord and Fridovich, 1968; McCord and Fridovich, 1969). The reduction of ferricytochrome *c* to ferrocytochrome *c* was followed by spectrophotometer at 550nm to determine $O_2^{\bullet-}$ generation by XOR in the following process:

$$Fe^{3+} \text{ cyt } c + O_2^{\bullet-} \rightarrow Fe^{2+} \text{ cyt } c + O_2$$

In some of the assays SOD and/ or catalase was added to the reaction to try and determine the actual levels of $O_2^{\bullet-}$ being generated. SOD was first discovered in 1969 (McCord and Fridovich, 1969) and catalyses the following antioxidant reaction:

$$2O_2^{\bullet-} + 2H \rightarrow H_2O_2 + O_2$$

SOD converts $O_2^{\bullet-}$ to H_2O_2 and O_2, therefore slowing the rate of cytochrome *c* reduction, and making it possible to determine proportion of cytochrome *c* reduction that is attributable to $O_2^{\bullet-}$ generation. Superoxide dismutase functions to remove $O_2^{\bullet-}$, however in that process the ROS H_2O_2 is generated, which is more stable compared to $O_2^{\bullet-}$. Furthermore, H_2O_2 can also be generated by XOR. Hydrogen peroxide can reoxidise cytochrome *c* so the enzyme catalase was used in some of the assays as it functions in the disposal of H_2O_2 by the following process (Hancock, 1999):

$$2H_2O_2 \rightarrow 2H_2O + O_2$$

4.2.2.1.1 Materials

Hypoxanthine ($C_5H_4N_4O$); xanthine (2,6-dihydroxypurine, $C_5H_4N_4O_2$); cytochrome *c* (From horse heart); disposable spectrophotometer cuvettes (Polystyrene, without stopper), superoxide dismutase (SOD), Sodium nitrite ($NaNO_2$) crystalline (hereafter referred to as "nitrite"); Catalase; Allopurinol; HEPES; 96-well plate seals, Luria-Bertani Broth (see appendix 8.2) (Sigma-Aldrich Co Ltd, Poole, UK). Dulbecco's phosphate buffered saline (PBS), Dulbecco's Modified Eagles Medium (DMEM, without phenol red see appendix 8.1), Penicillin/Streptomycin, L-Glutamine (Gibco, Life Tech,

Paisley, UK). Foetal claf serum (FCS) (GlobePharm Ltd, UK). Sodium hydroxide pellets (NaOH), Hydrochloric acid (HCL) (BDH laboratory supplies, Poole), UK. XO (Biozyme Laboratories, Gwent, UK). 96-well flat-bottomed plates (Fisher Scientific, Loughborough, UK).

4.2.2.1.2 Protocol

Using a final volume of 2 or 3mls, the standard reagents used for these assays were as follows, 20-50μM cytochrome *c*, 1mM Hypoxanthine, PBS, and XO (for specific details see results). All solutions were prepared in PBS and maintained on ice until required with the exception of hypoxanthine which remained at room temperature (approximately 25°C) until use. The reduction of cytochrome *c* was followed using a spectrophotometer (Hitachi U-2010 UK) with a 1cm light path in 3ml plastic cuvettes at 550nm. The spectrophotometer was fitted with a circulating fluid regulator so that the reaction could be maintained at 37°C throughout the experiment. The initial rate of reaction was measured as the linear slope of the absorbance readings. Activity was expressed as nmol $O_2^{\bullet-}$ produced min^{-1} by using the extinction coefficient for reduced cytochrome *c* of 21.1 mM^{-1} cm^{-1}.

Experiments were also carried out for measurement on a 96-well plate reader (DYNEX MRX TC II) with a final volume of 200μl. Final concentrations of all reagents were as described above. For experiments carried out in hypoxia, PBS, DMEM, or Luria-Bertani broth (LB) was placed in the cabinet in vented T75 flasks 24 hours before the experiement. In the case of the DMEM, 1% Penicillin/Streptomycin, 5% FCS and 1% L-Glutamine were added 2 hours before the start of the experiment this is to prevent degradation at 37°C before addition to the cells in the cell culture experiments. All additions to the plates were made in the hypoxia cabinet. Once the additions had been made to the plates they were sealed with clear film and transferred to the plate reader (this step generally took around 3 minutes). The XOR catalysed $O_2^{\bullet-}$ generation and reduction of cytochrome *c* and the role of SOD and catalase are shown in Figure 4.4.

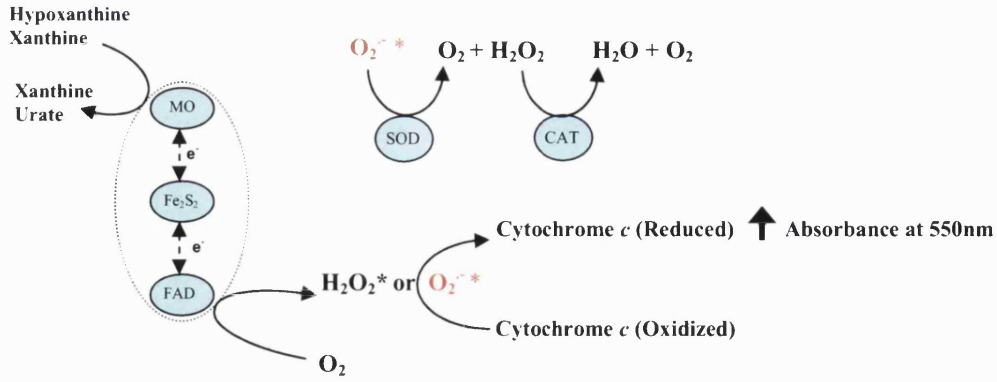

Figure 4.4 XOR Catalysed Generation of Superoxide and Reduction of Cytochrome *c*.

Electrons donated to XOR during the oxidation of hypoxanthine or xanthine to xanthine or urate respectively, are accepted by O_2 at the FAD-containing moiety in XOR forming $O_2^{\bullet-}$ and leading to the reduction of cytochrome *c*. SOD was used to convert $O_2^{\bullet-}$ to H_2O_2 and O_2 to determine the SOD inhibitable portion of the cytochrome *c* reduction. Catalase was used to remove H_2O_2 from the system to prevent the reoxidation of cytochrome *c* by XOR-and SOD-generated H_2O_2.

4.2.2.1.2.1 Calculation of superoxide generation

In order to determine the $O_2^{\bullet-}$ generated by XOR, the extinction coefficient or molar absorbtivity (ε) for cytochrome *c*, 21100 M^{-1} cm^{-1}, was used. Superoxide generation was calculated for the cuvette and the 96-well plate method using the Beer-Lambert Law which is the linear relationship between absorbance and concentration of an absorbing species thus:

$A = \varepsilon bc$

Equation 4.2 Beer-Lambert Law

A =Absorbance, ε =molar absorbtivity (M^{-1} cm^{-1}), b=Pathlength through the sample, c =concentration of the compound in solution.

In the cuvette method, the light from the spectrophotometer is passed through the side of the cuvette which has a 1cm pathlength. In the 96-well plate method, the light from the spectrophotometer is passed through the base of the plate which means that the pathlength is the depth of liquid in the well correlating with the volume used. The Beer-Lambert law allows for the calculation of the absolute $O_2^{\bullet-}$ generation in the two different measuring systems by taking into account the differing pathlengths. A paper published by Smith *et al* (2001) described how the differences in pathlengths can be corrected allowing only a small amount of error to be introduced. This correction was carried out as follows. The 96-well plates used in the lab were manufactured by orange scientific and the product data sheet gave a radius of each well of 0.335cm. Therefore, the base of a well could be calculated as $\pi \times R^2 = 0.352cm^2$. For the 96-well plate assays a final volume of 200µl was

used which has a $0.2cm^3$ area. Therefore, the pathlength was calculated as follows 0.2/0.352 = 0.568 cm and provides a theoretical pathlength that is just over half that of the cuvette. Therefore if the cuvette pathlength is 1cm and the 96-well plate has a pathlength of 0.586, 1cm/0.568cm = 1.760. Therefore the 96-well plate absorbance values must be multiplied by 1.760 to account for the difference in pathlength. Therefore the absolute $O_2^{\bullet -}$ generated in the cuvette and the 96-well plate was calculated as follows:

Cuvette

A / ε (21100 M^{-1} cm^{-1}) = Superoxide M^{-1} cm^{-1}

96 well plate

A / ε (21100 M^{-1} cm^{-1}) x Pathlength (0.568) = Superoxide M^{-1} cm^{-1}

Or

A x 1.760*/ ε (21100 M^{-1} cm^{-1}) = Superoxide M^{-1} cm^{-1}

* Pathlength correction

In order to test this, the spectrophotometer was blanked with a cuvette containing PBS, this cuvette was removed and replaced with a cuvette containing 50μM cytochrome *c* which gave a reading of 0.570 abs_{550nm} (n = 1) a 96-well plate assay was also carried out simultaneously in which the PBS wells were subtracted from the wells containing 50μM cytochrome *c* giving and average value of 0.2927 abs_{550nm} (n = 3). Therefore, in order to test the theoretical pathlength 0.2927 x 1.760 = 0.515 abs_{550nm}. With this correction the 96-well plate measurement is still slightly less than the cuvette measurement a reduction in absorbance of around 9.7 %.

4.2.2.2 Oxidation of Dihydrorhodamine for peroxynitrite generation by XO

Peroxynitrite generation was measured using the oxidation of Dihydrorhodamine (DHR) to rhodamine as described by Kooy *et al* (1994) and Crow (1997). Authentic peroxynitrite causes the oxidation of DHR to rhodamine which has an absorbance peak at 500nm with a high molar extinction coefficient (74500M^{-1} cm^{-1}). This assay was followed spectrophotometrically and was adapted for use in a cuvette or a 96-well plate (Figure 5.2). Assays were carried out using SIN-1 as a positive control for $ONOO^-$ generation at 0-500μM. Measurements of $ONOO^-$ generation by XO using DHR (Figure 4.5) were carried out using 1mM nitrite, 1mM hypoxanthine and 50mU ml^{-1} XO.

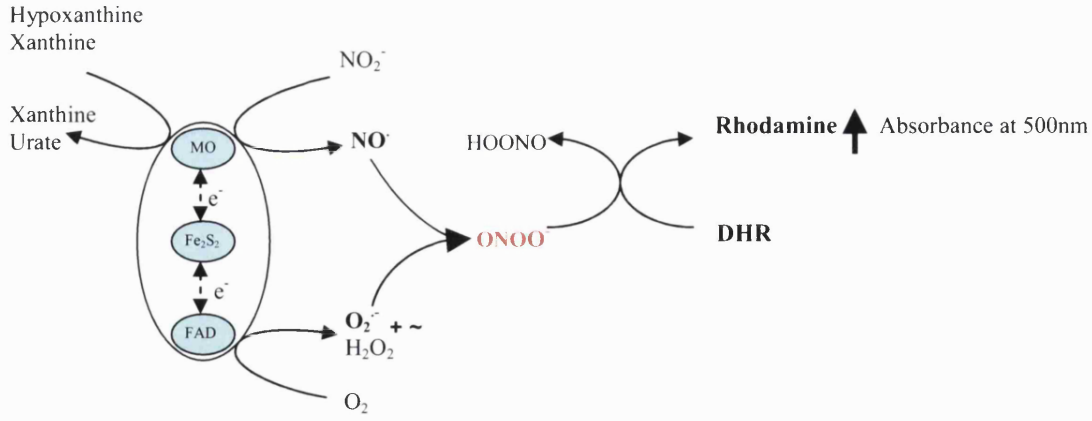

Figure 4.5 XO-catalysed oxidation of dihydrorhodamine to rhodamine

In the presence of oxygen, electrons donated to XO during the oxidation of hypoxanthine accepted by O_2 at the FAD-containing moiety in XOR forming $O_2^{\bullet-}$ and H_2O_2. Under hypoxic conditions, XOR can generate NO•; however, if O_2 concentrations rise to around 70μM/about 50mmHg (Millar unpublished data), pairs of electrons derived from either hypoxanthine, xanthine, or NADH, can be used to reduce nitrite or O_2 (the preferred substrate), therefore generating $^{\bullet}NO$ and $O_2^{\bullet-}$, respectively. $^{\bullet}NO$ and $O_2^{\bullet-}$ can react together forming $ONOO^-$ (Huie *et al*, 1993). HOONO = Peroxynitrous acid.

Some assays were also carried out in the presence the iron chelator Diethylenetriaminepentaacetate (DTPA) (0.1mM) to prevent iron mediated reactions with XO-generated H_2O_2 particularly the Fenton reaction (Figure 4.6). DPI, which blocks the ability of the FAD site to transfer electrons to molecular oxygen, was also used to simulate hypoxia by reducing the production of $O_2^{\bullet-}$ and shifting the balance of competition for electrons to nitrite, effectively increasing $^{\bullet}NO$ production. Thus resulting in $ONOO^-$ generation.

$$Fe^{2+} + H_2O_2 \rightarrow Fe^{3+} + {}^{\bullet}OH + OH^-$$

$$Fe^{3+} + H_2O_2 \rightarrow Fe^{2+} + {}^{\bullet}OOH + H^+$$

Figure 4.6 Fenton reaction.

Iron and H_2O_2 can react together to generate hydroxyl radicals in a reaction that is termed the Fenton reaction.

4.2.2.2.1 Materials

Acetonitrile (methyl cyanide), Sodium nitrite ($NaNO_2$) crystalline, SIN-1 (3-Morpholinosydononimine), Dihydrorhodamine 123, HEPES Buffer (1M) (Sterile filtered Cell culture tested), DTPA (Diethylenetriaminepentaacetic acid) (Sigma-Aldrich, Co. Ltd, Poole, UK), DPI (diphenyliodonium chloride) (ICN Biomedicals Inc, Aurora Ohio, USA).

4.2.2.2.2 Protocol

In experiments on the generation of $ONOO^-$ by XO the following assay procedure was used. Reaction solutions were made up fresh from frozen DHR stock solutions (10mM) to give final concentrations of 0.1mM DHR, 0.1mM DTPA in 2 or 3mls of PBS. This was then placed into a spectrophotometer at 37°C and the absorbance at 500nm was measured over time with a 1cm light path.

This assay was also reduced to a 200µl volume and read on a plate reader (DYNEX MRX TC II) using a 490nm filter (See results figure 4.67 for wavelength scan results at 500nm and 490nm). Reagents were as described above.

4.2.3 Statistical analysis

Statistical analysis of data collected was performed using GraphPad Prism Version 4.00 (GraphPad Software Inc.). Statistical analysis performed was the unpaired t-test for comparisons between independent samples, and a one-way ANOVA statistical test with Dunnett's post test for analysis of variance between XO concentrations.

4.3 Results

4.3.1 Enzyme characterisation

4.3.1.1 Protein determination using the Bio-Rad assay

Each new batch of XO (Biozyme) was assessed for protein content using a Bio-Rad assay. Protein assays were performed in order to determine the concentration of protein in each batch of enzyme. The protein content of the first batch of XO (XO 1) was assessed using the Bio-Rad Protein assay methodology (Figure 4.7). According to the data sheet included with the enzyme, the protein concentration of XO was measured by Biozyme to be at 10.5 mg ml^{-1} using a Lowry assay.

As shown in figure 4.7 the protein concentration of the enzyme was found to be 6.2mg ml^{-1} using the Bio-Rad protein assay, and the protein concentration was considerably lower than was indicated by the data sheet (10.5mg ml^{-1}). Therefore, a second method for the assessment of protein was used to determine the correct measurement.

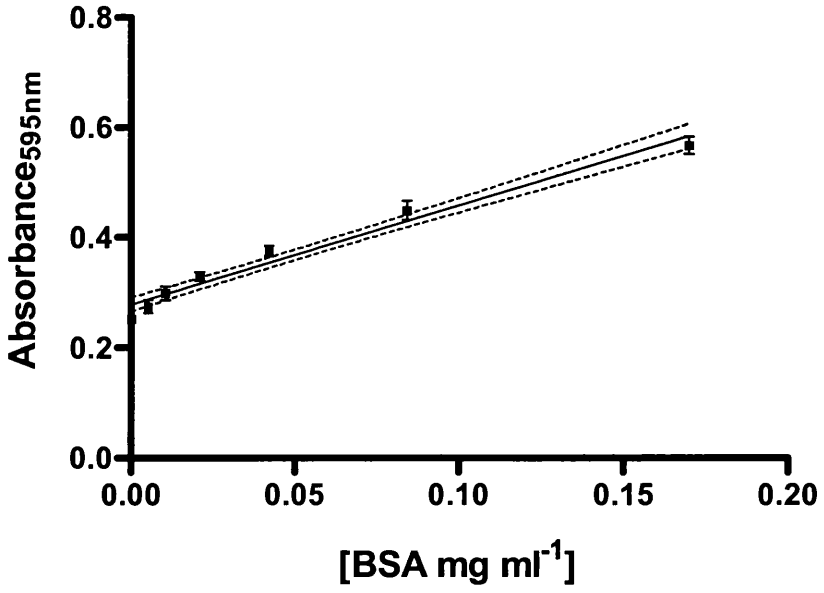

Figure 4.7Standard curve for protein determination of XO using the Bio-Rad assay.

A 1:100 dilution of XO gave an absorbance of 0.39nm and a protein content of 0.062mg ml^{-1} as extrapolated from the graph (See section 4.2.1.1.1 for methodology). The final protein content was 6.2mg ml^{-1} after correction for the dilution factor. $r^2 = 0.96$. Mean ± SD.

4.3.1.2 Protein determination using the Bio-Rad *DC* protein assay

The results shown in figure 4.7 show the protein level to be 6.2mg ml^{-1} using a Bio-Rad assay. In order to determine the true protein concentration of the enzyme a second assay called the Bio-Rad *DC* Protein Assay, which is described as being similar to the Lowry assay was used (Figure 4.8).

The observed protein concentration using the Bio-Rad *DC* assay was determined to be 10.81mg ml^{-1} which is extremely close to the protein concentration shown on the data sheet (10.5mg ml^{-1}). Therefore this value will be considered to reflect the true protein concentration. The Bio-Rad *DC* assay will also used to measure all new batches of xanthine oxidase. The Bio-Rad *DC* assay was used to determine the concentration of a second batch of XO (XO 2) to show that the result was reproducible between batches (Figure 4.9).

The extrapolated protein values from Figure 4.9 indicate that the protein content of XO2 is 10.49 mg ml^{-1} which was extremely close both to the previous batch of enzyme (10.81 mg ml^{-1}) and the data sheet (10.5 mg ml^{-1}).

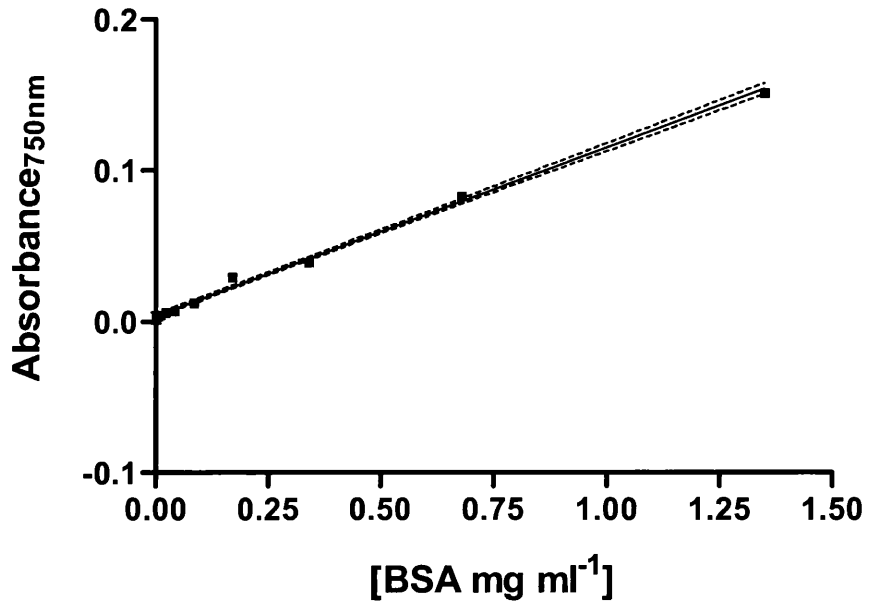

Figure 4.8 Standard curve for protein determination of XO using the Bio-Rad *DC* assay.

A 1:10 and a 1:100 dilution of XO gave absorbances of 0.135nm and 0.015 respectively and a corresponding protein content of 1.182mg ml^{-1} and 0.098mg ml^{-1}, as extrapolated from the graph (see section 4.2.1.1.2). The final protein content was 11.82mg ml^{-1} and 9.8mg ml^{-1} after correction for the dilution factor. The final concentration was taken as an average of the corrected protein concentration values 10.81mg ml^{-1}. r^2 = 0.995. Mean ± SD.

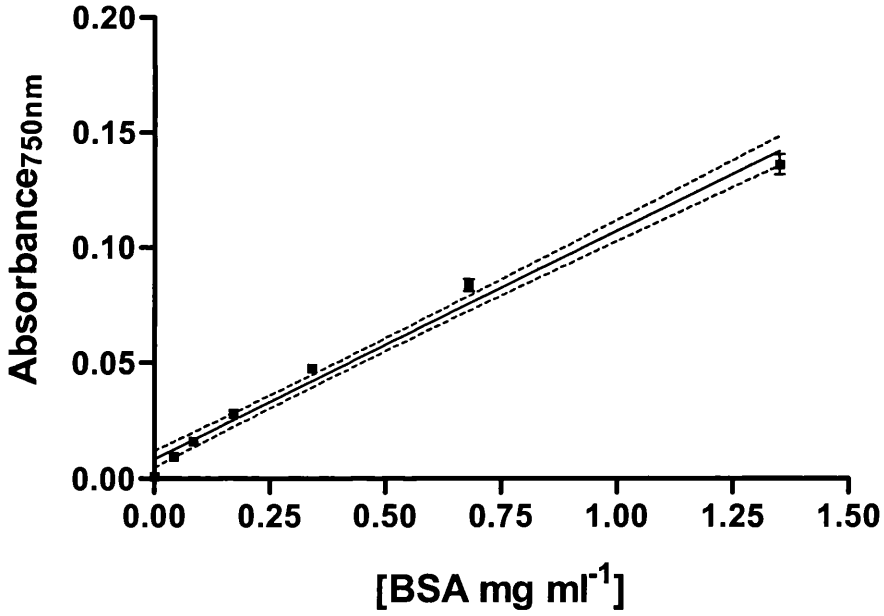

Figure 4.9 Standard curve for protein determination of XO2 using the Bio-Rad *DC* assay.

A 1:10 and a 1:20 dilution of XO gave absorbances of 0.123 nm and 0.055 respectively and a corresponding protein content of 1.160mg ml^{-1} and 0.469mg ml^{-1}, as extrapolated from the graph. Therefore, after correction for the dilution factor, the final protein content was indicated to be 11.6mg ml^{-1} and 9.38mg ml^{-1}. The final concentration was taken as an average of the corrected protein concentration values 10.49mg ml^{-1}. r^2 = 0.984

4.3.1.3 Comparison of oxidase and dehydrogenase activity by the pterin assay

A fluorometric pterin assay was used to determine whether the Biozyme XO contains any of the dehydrogenase form of the enzyme (Figure 4.10). This figure shows that with XO alone IXP is not generated. However, when pterin is added, around 0.5nM IXP is generated per second. The addition of methylene blue does not increase the rate of IXP generation, suggesting that there is no dehydrogenase activity in this commercially available enzyme preparation.

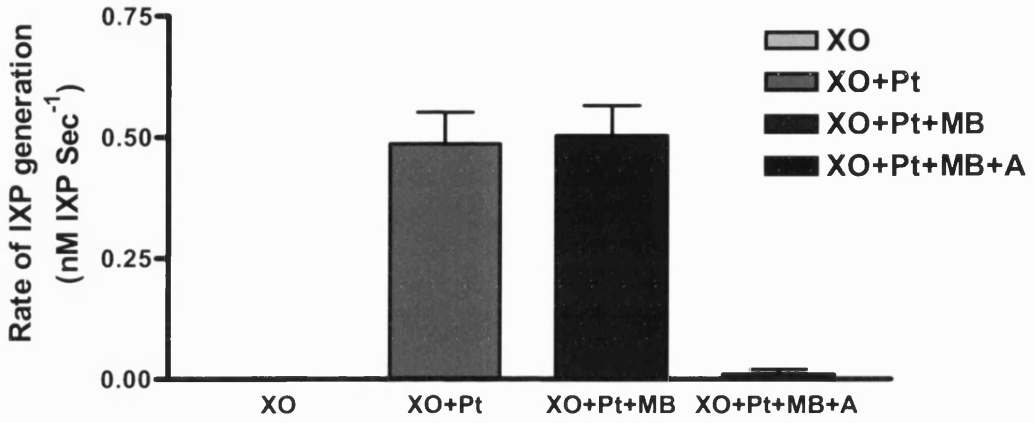

Figure 4.10 Measurement of XO and XDH activity in commercially available XO (Biozyme).

Experiments were carried out using XO (100ng ml^{-1}), Pterin (Pt) (10μM), Methylene Blue (MB) (10μM), Allopurinol (A) (10μM) made up to 1ml in PBS. MEAN ± SD. n = 8.

4.3.2 Development of methods for the measurement of XO activity cell growth medium

4.3.2.1 Cytochrome *c* assay for superoxide generation by XO

4.3.2.1.1 Superoxide generation by XO in air in PBS

Superoxide production by XO in air was initially measured using the cytochrome *c* assay. Cytochrome *c* reduction was rapid at high enzyme concentrations; a measurable rate was observed at 7.7mU ml^{-1} XO which reduced cytochrome *c* at 0.088 Abs550nm min^{-1} and produced around 4nmole min^{-1} ml^{-1} of $O_2^{\bullet -}$ which was SOD inhibitable (Figure 4.11). Xanthine was used as the electron donor substrate for these initial experiments.

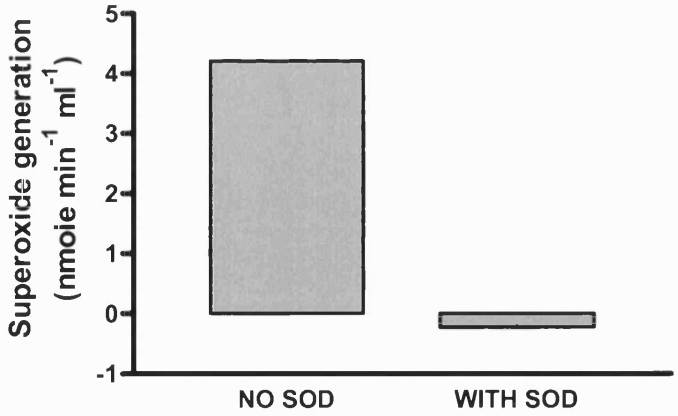

Figure 4.11 Initial rate of XO-catalysed superoxide generation by XO in PBS in air

Experiments were carried out in air using final concentrations of cytochrome *c* (20μM), XO (7.7mU ml^{-1}), xanthine (20μM), SOD (667U ml^{-1}) in a 3ml final volume of PBS at 37°C with stirring. This figure shows the initial rate of $O_2^{\bullet -}$ generation nmole min^{-1} ml^{-1} and was calculated as described in the methods from the raw absorbance data. n = 1.

A wider range of SOD concentrations were then assessed to determine whether a lower concentration could be used for further experiments. The assay was also developed for use in a 96-well plate format to preserve expensive reagents and increase the number of samples that could be assayed at one time. Figure 4.12 shows the rate of $O_2^{\bullet -}$ generation by XO (2mU ml^{-1}) and the inhibition of this rate by SOD. All control experiments of incomplete reaction mixtures gave a zero rate of cytochrome *c* reduction. Superoxide generation by XO (2mU ml^{-1}) was shown to be at around 5nmoles min^{-1} ml^{-1} and a concentration of 3.9U ml^{-1} SOD or above was sufficient to inhibit this rate of $O_2^{\bullet -}$ generation.

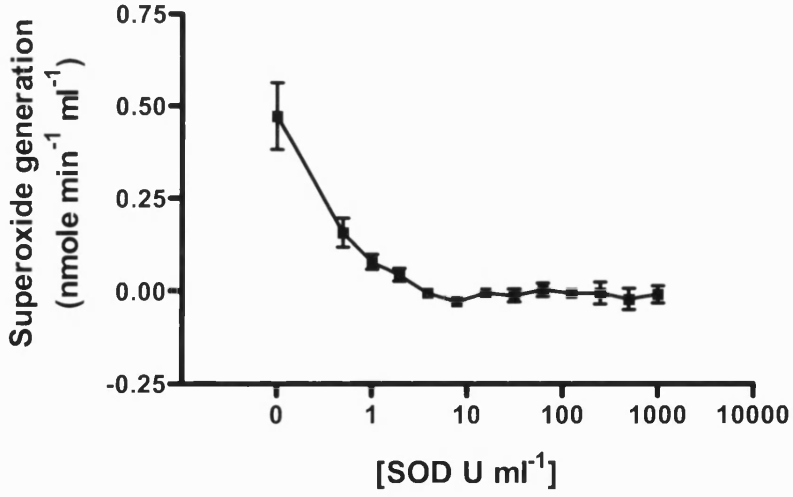

Figure 4.12 Initial rate of superoxide generation by XO at varying SOD concentrations.

Experiment was carried out in air using cytochrome *c* (20μM), XO (2mU ml^{-1}), xanthine (20μM), and SOD (0.5, 1, 1.95, 3.9, 7.8, 15.65, 31.25, 62.5, 125, 250, 500, 1000 U ml^{-1}) in a final volume of 200μl PBS at

37°C. This figure shows the initial rates of superoxide generation (nmole min ml^{-1}) and was calculated as described in the methods from the raw absorbance data. n = 3. Mean ± SD.

The experiment shown in figure 4.12 was repeated using slightly different SOD concentrations to check that the assay was reproducible. The results in Figure 4.13 show a partial inhibition at of $O_2^{\bullet-}$ generation by XO at 0.5U ml^{-1} SOD with complete inhibition at 5U ml^{-1}. Furthermore a concentration of 5U ml^{-1} SOD was similar to 3.9U ml^{-1} SOD which was found to completely inhibit the XO in figure 4.12 showing that the assay was reproducible.

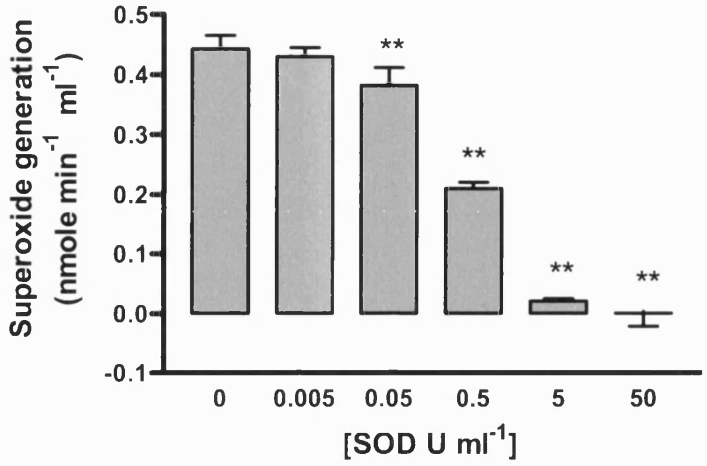

Figure 4.13 Initial rate of superoxide generation by XO at varying SOD concentrations.

Experiment was carried out in air using final concentrations of cytochrome *c* (20μM), XO (2mU ml^{-1}), xanthine (20μm) and SOD (0, 0.005, 0.05, 0.5, 5 and 50U ml^{-1}) in a final volume of 200μl PBS at 37°C. This figure shows the initial rates of superoxide generation (nmole min^{-1} ml^{-1}) calculated from the raw absorbance data as described in the methods. Statistical analysis used was One-way ANOVA with Dunnett's multiple comparisons test using 0 SOD as the control. ** $P < 0.01$.

A comparison was also made between the cuvette method and the 96-well plate method to ensure that the assays were equally sensitive and producing similar reaction profiles for assessment of the levels of $O_2^{\bullet-}$ generation. Figure 4.14 shows that the rate of cytochrome *c* reduction is three times faster in the cuvette method than the 96-well plate method.

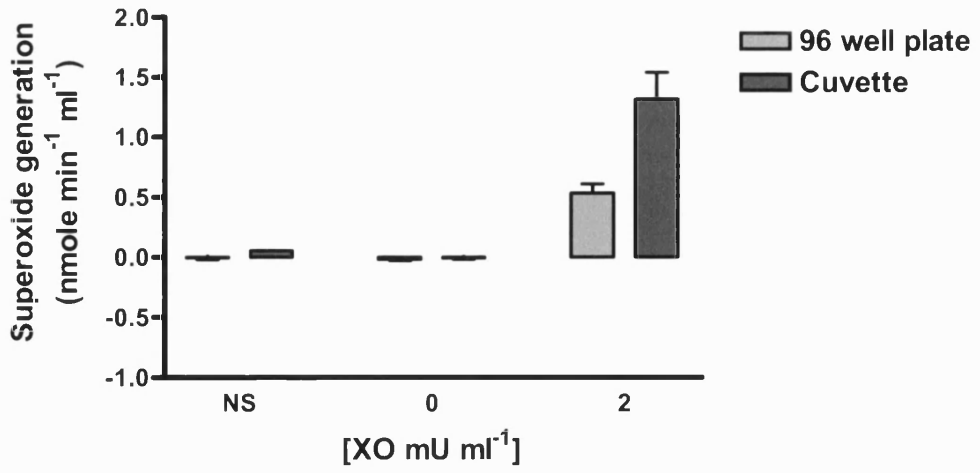

Figure 4.14 Comparison of the rate of superoxide generation by XO in a cuvette and 96-well plate.

Experiment was carried out in air using final concentrations of xanthine (20μM), cytochrome *c* (20μM) and XO (2mU ml^{-1}) in a final volume of 200μl PBS at 37°C. This figure shows the initial rates of superoxide generation (nmole min^{-1} ml^{-1}) and was calculated from the raw absorbance data as described in the methods. The experiment was carried out on two separate occasions. 96-well plate data: All n = 6, except XO n = 9. Cuvette data: PBS + NE n = 2, NS n = 1, XO n = 6. Mean ± SD.

The comparison of the 96-well plate and cuvette method was repeated in Figure 4.15-4.19 with more attention to temperature control. Assay reagents were warmed in a water bath set at 37°C prior to the experiment. A wider range of enzyme concentrations were also used to determine the sensitivity of the assay for $O_2^{\bullet-}$ detection at low XO concentrations. Superoxide generation in the 96-well plate (Figure 4.15 and 4.16) and the cuvette (Figure 4.17) was assessed and comparison of the initial rates of $O_2^{\bullet-}$ generation (Figure 4.18) show that the rate of cytochrome *c* reduction in the cuvette method is at least twice as fast as the 96-well plate method. The assays also indicate that the cytochrome *c* method does not measure $O_2^{\bullet-}$ generation from the enzyme at concentrations below 250μU ml^{-1} XO in either the 96-well plate method or the cuvette method. The comparison of the 96-well plate and cuvette shown in figure 4.18 was also repeated on a separate occasion to determine if the data was reproducible (Figure 4.19).

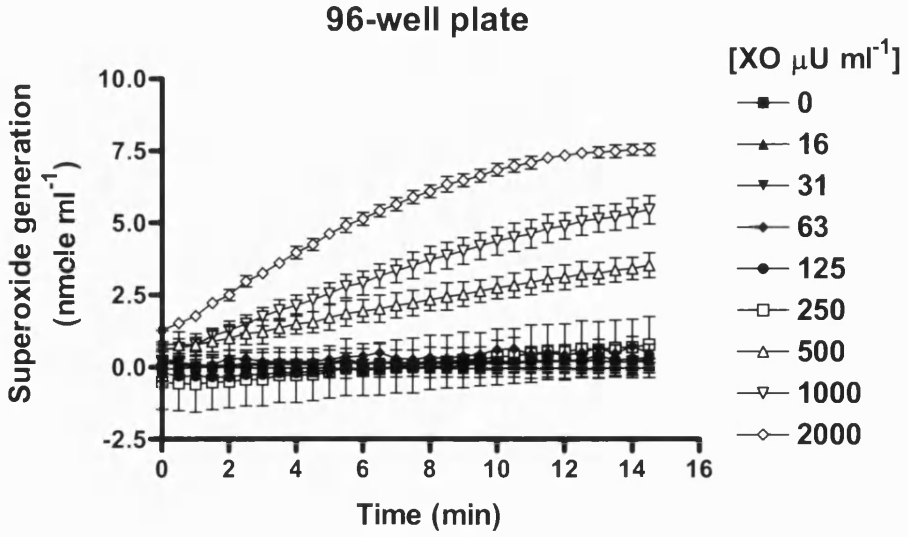

Figure 4.15Timecourse of superoxide generation at a range of concentrations of XO in a 96-well plate.

Experiment was carried out in air using final concentrations of xanthine (20μM), cytochrome *c* (20μM) and XO (0, 16, 31, 63, 125, 250, 500, 1000, 2000μU ml^{-1}) in a final volume of 200μl PBS at 37°C. PBS wells contained 200μl PBS alone. No Substrate (NS) wells contained XO (2000μU ml^{-1}) and cytochrome *c* (20μM) diluted in PBS for a final concentration of 200μl. Absorbance readings were taken every 30 seconds over a 15 minute time period at 550nm. Superoxide generation (nmole ml^{-1}) was calculated using Beer-lambert's equation as described in the methods section using the raw absorbance data. Mean ± SD. n = 3.

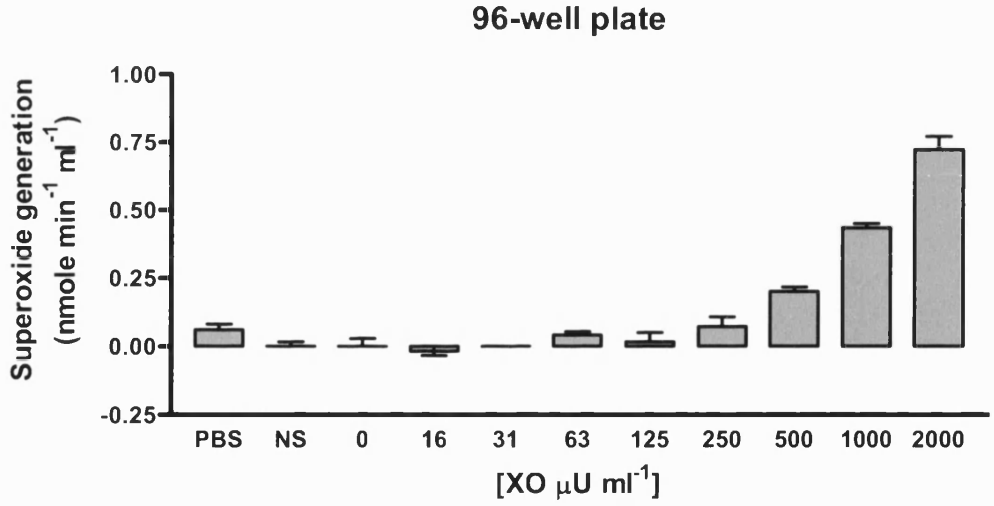

Figure 4.16 Rate of superoxide generation at a range of concentrations of XO in a 96-well plate.

Experiment was carried out in air using final concentrations of xanthine (20μM), cytochrome *c* (20μM) and XO (0, 16, 31, 63, 125, 250, 500, 1000, 2000μU ml^{-1}) in a final volume of 200μl PBS at 37°C. PBS wells contained 200μl PBS alone. No Substrate (NS) wells contained XO (2000μU ml^{-1}) and cytochrome *c* (20μM) diluted in PBS for a final concentration of 200μl. Initial rates of superoxide generation per minute (nmoles min^{-1} ml^{-1}) were calculated from the data shown in figure 4.15. Mean ± SD. n = 3.

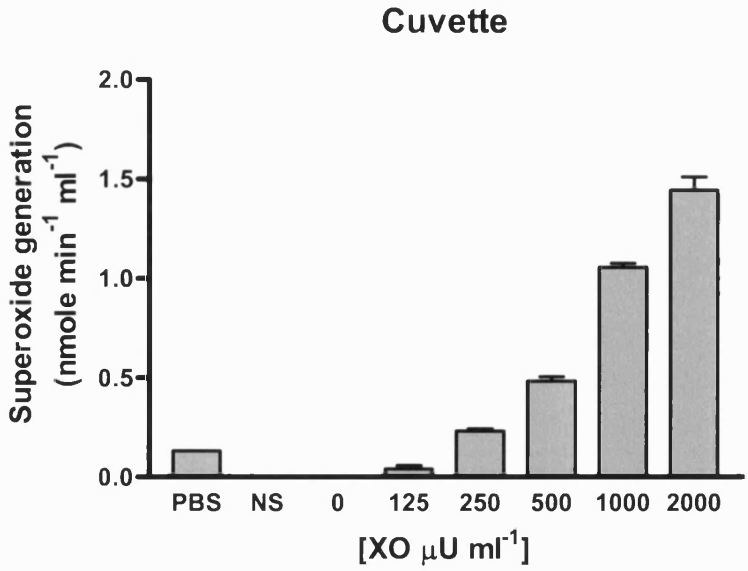

Figure 4.17 Rate of superoxide generation at a range of XO concentrations in a cuvette.

Experiment was carried out in air using final concentrations of xanthine (20μM), cytochrome *c* (20μM) and XO (0, 125, 250, 500, 1000, 2000μU ml^{-1}) in a final volume of 3mls PBS at 37°C. PBS cuvette contained 3ml PBS alone. No Substrate (NS) cuvette contained XO (2000μU ml^{-1}) and cytochrome *c* (20μM) diluted in PBS for a final concentration of 3mls. Rate of change in absorbance per minute (550nm min^{-1}) was calculated from the raw data as shown in the methods. Mean ± SD. n = 3. The initial rate of superoxide generation (nmole min^{-1} ml^{-1}) was calculated from the raw data as shown in the methods.

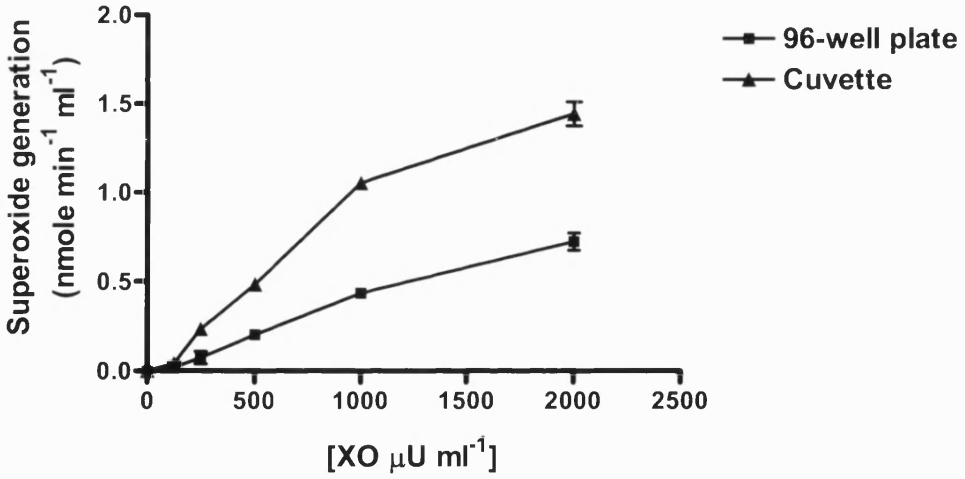

Figure 4.18 Comparison of superoxide generation by XO in a 96-well plate and a cuvette.

Experiment was carried out in air using final concentrations of xanthine (20μM), cytochrome *c* (20μM) and XO (0, 125, 250, 500, 1000, 2000μU ml^{-1}) in a final volume of 200μl PBS (96-well plate) or 3mls PBS (Cuvette) at 37°C. The initial rate of superoxide generation per minute (nmole min^{-1} ml^{-1}) was calculated from the raw data as shown in in the methods. Mean ± SD. n = 3.

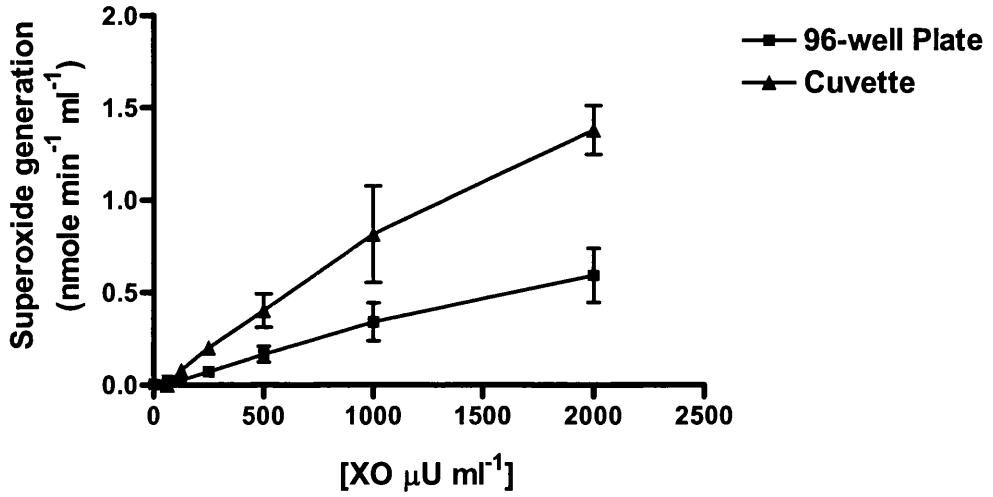

Figure 4.19 Comparison of the 96-well plate and cuvette methods at a range of XO concentrations.

Experiment was carried out in air using final concentrations of xanthine (20μM), cytochrome *c* (20μM) and XO at (0, 16, 31, 63, 125, 250, 500, 1000, 2000μU ml^{-1}) in a final volume of 200μl PBS (96-well plate) or 3mls PBS (Cuvette) at 37°C. The rate of superoxide generation per minute (nmole min^{-1} ml^{-1}) was calculated from the raw data as shown in the methods. Mean ± SD. n = 6.

Further assays were carried out to determine whether shaking of the 96-well plate prior to measurements and stirring of the cuvettes during the experiment significantly changed the reaction rates and could possibly account for the differences seen between the 96-well plate and the cuvette. Cell based assays would also be carried out in a static reaction volume so this assay investigates the effect of a static and agitated reaction volume on the rate of $O_2^{\bullet-}$ generation by XO. The results in figure 4.20 show little difference between the rate of $O_2^{\bullet-}$ production with or without shaking the 96-well plate prior to measurements at varying concentrations of XO. There is also little difference between stirring the cuvettes during the experiments compared with inverting the cuvette prior to the experiments (figure 4.21). Therefore for subsequent experiments 96-well plates will not be shaken for 15 seconds prior to measurements and cuvettes will only be inverted three times before measurements are taken for future experiments. A comparison of Figure 4.20 and 4.21 also shows that there is still considerable difference in the rate of $O_2^{\bullet-}$ generation in the 96-well plate and the cuvette method.

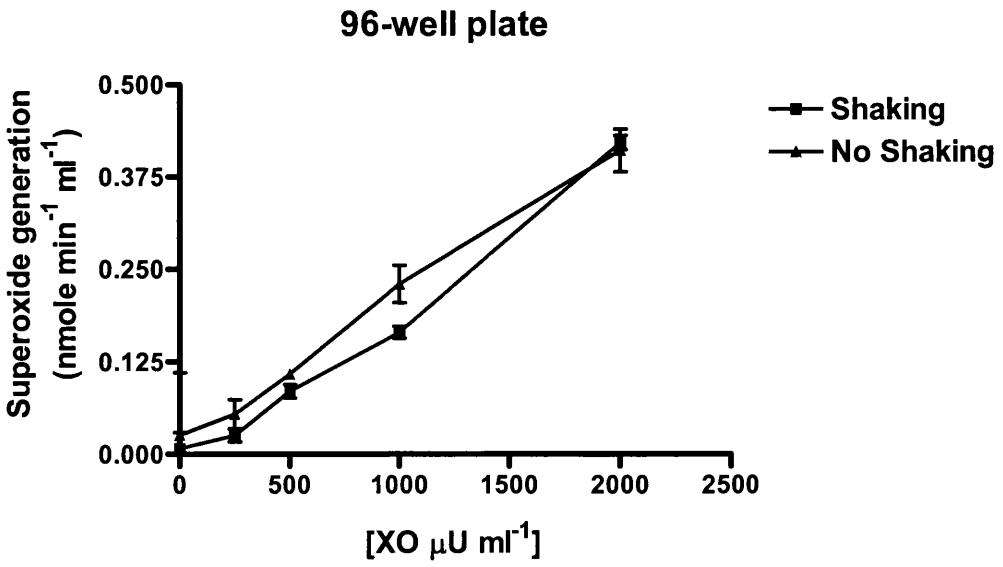

Figure 4.20 Comparison of the rate of superoxide generation in a 96-well plate data with and without shaking

Experiment was carried out in air using final concentrations of cytochrome *c* (20μM), xanthine (20μm) and XO (0, 250, 500, 1000, 2000μU ml^{-1}) in a final volume of 200μl PBS in a 96-well plate at 37°C. The assays were carried out with or without a 15 second shake before measurements began at 550nm. Initial rates of superoxide generation (nmoles min^{-1} ml^{-1}) were calculated from the raw data as described in the methods. n=3. Mean±SD.

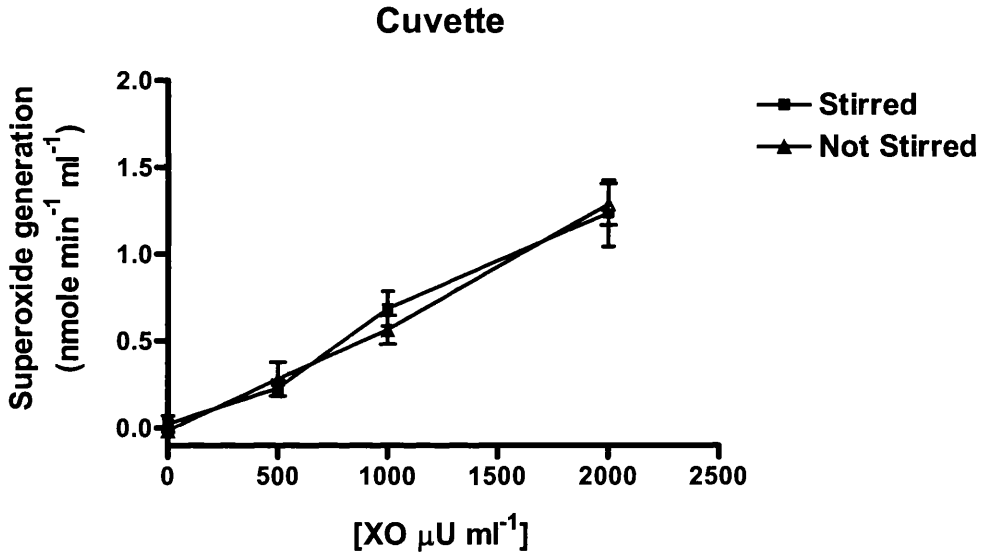

Figure 4.21 Comparison of the rate of cytochrome *c* reduction in a stirred and unstirred cuvette at varying XO concentrations

Experiment was carried out in air using final concentrations of cytochrome *c* (20μM), XO (0, 500, 1000, 2000μU ml^{-1}), xanthine (20μm) in a final volume of 3mls in cuvettes at 37°C. Cuvettes were either stirred with a magnetic flea (Stirred) or inverted three times before measurements (Not stirred) at 550nm. Initial rates of superoxide generation (nmole min^{-1} ml^{-1}) were calculated from the raw data as described in the methods. Assays were carried out on two separate occasions and the n numbers are as follows: XO (0μU ml^{-1}) n=2, XO (500 and 1000μU ml^{-1}) n=6, XO (2000μU ml^{-1}) n=8. Mean±SD.

Due to the slight discrepancy between the rates of $O_2^{\bullet-}$ production in the 96-well plate and the cuvette method the expected rate of $O_2^{\bullet-}$ production was calculated to determine whether the 96-well plate or the cuvette method was closer to the expected rate. Figure 4.22 shows that the expected rate of $O_2^{\bullet-}$ generation is roughly calculated at 4nmoles min^{-1} ml^{-1} assuming all donated electrons produce $O_2^{\bullet-}$. However as H_2O_2 is also generated by the enzyme, it is likely that 2nmoles superoxide min^{-1} ml^{-1} is a closer estimation. The closest rate in the previous assays to this theoretical rate was achieved using the cuvette method which produced around 1.5nmoles superoxide min^{-1} ml^{-1}. At this stage it was decided that further development of the cytochrome *c* assay would be carried out using the cuvette method of measurement.

Xanthine (1000 nmole) x XO (0.002U ml^{-1}) x 2 Superoxide =

4nmoles superoxide min^{-1} ml^{-1}

Figure 4.22 Calculation of the expected superoxide generation rate

The international unit (U) is defined as that amount of enzyme which will convert 1 micromole of substrate to product in 1 minute under defined conditions (generally 25°C or 30°C and the optimum pH). Xanthine provides XO with two electrons therefore in theory two $O_2^{\bullet-}$ can be produced however, it is likely in practice, that as the enzyme also produces H_2O_2 these electrons also go onto produce hydrogen peroxide as well as $O_2^{\bullet-}$. The hypothesised scheme for $O_2^{\bullet-}$and H_2O_2 generation during the re-oxidation of reduced XO with O_2 was confirmed in 1981 (Porras *et al.*, 1981). It was concluded that a fully reduced (six electron reduced) XO monomer could generate two H_2O_2 and two $O_2^{\bullet-}$molecules. Therefore it is likely that 4nmole superoxide min^{-1} ml^{-1} is an overestimation of the actual $O_2^{\bullet-}$ produced it is likely to be roughly half this value at around 2nmole min^{-1} ml^{-1}.

The assays shown below were carried out using substrate and enzyme concentrations based on assays carried out by Murrell *et al* (1990) which showed enhanced proliferation of adult human dermal fibroblasts. Hypoxanthine was used at 1mM as the substrate for XO and XO was used at 1mU ml^{-1} as Murrell showed increased proliferation between 0.001 and 1mU ml^{-1} XO. Cytochrome *c* was also increased to 50μM. The controls for the cytochrome *c* assay were therefore repeated at these concentrations of substrate and enzyme (Figure 4.23). This figure shows that cytochrome *c* is not reduced by hypoxanthine (1mM) alone or in combination with SOD, or by XO (1mU ml^{-1}) alone or in combination with SOD. Cytochrome *c* is only reduced in the presence of hypoxanthine (1mM) and XO (1mU ml^{-1}) which is shown to generate around 0.4nmole min^{-1} ml^{-1} $O_2^{\bullet-}$. SOD at 3.3U ml^{-1} partially inhibits this reaction showing that $O_2^{\bullet-}$ is largely responsible for the reduction of cytochrome *c*. A higher concentration of SOD may be required for complete inhibition of the reduction of cytochrome *c*.

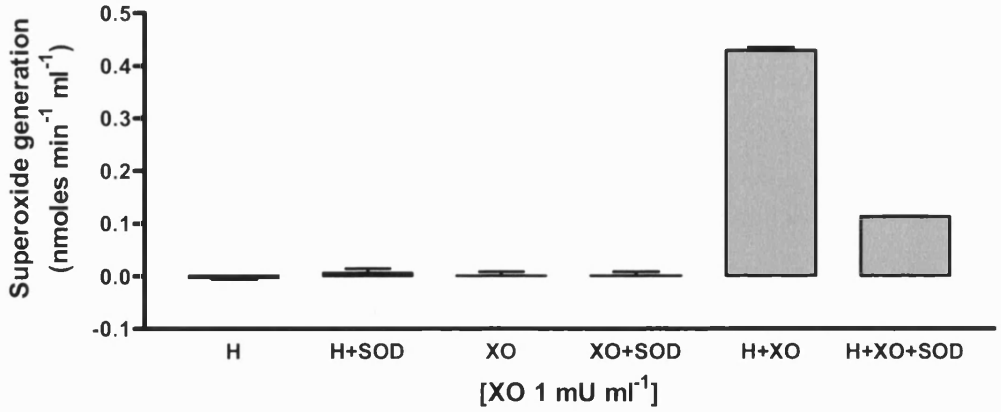

Figure 4.23 Initial rates of superoxide generation by XO with hypoxanthine.

Experiments were carried out in air using final concentrations of cytochrome *c* (50μM), hypoxanthine (H) (1mM), XO (1mU ml^{-1}) and SOD (3.3U ml^{-1}) were diluted in a final volume of 3mls PBS at 37°C. This figure shows the initial rate of superoxide generation (nmole min^{-1} ml^{-1}) and was calculated as described in the methods. Mean ± SD. n = 2.

Murrell's studies with adult human dermal fibroblasts showed visible detachment and detachment from the culture surface of cells treated with 10mU ml^{-1} XO therefore the $O_2^{\bullet-}$ generation by XO at 10mU ml^{-1} was also assessed with a range of SOD concentrations (Figure 4.24). This figure shows that XO (10mU ml^{-1}) produces a rate of $O_2^{\bullet-}$ generation of around 5nmole min^{-1} ml^{-1}, which can be dose dependently inhibited by SOD (Figure 4.24).

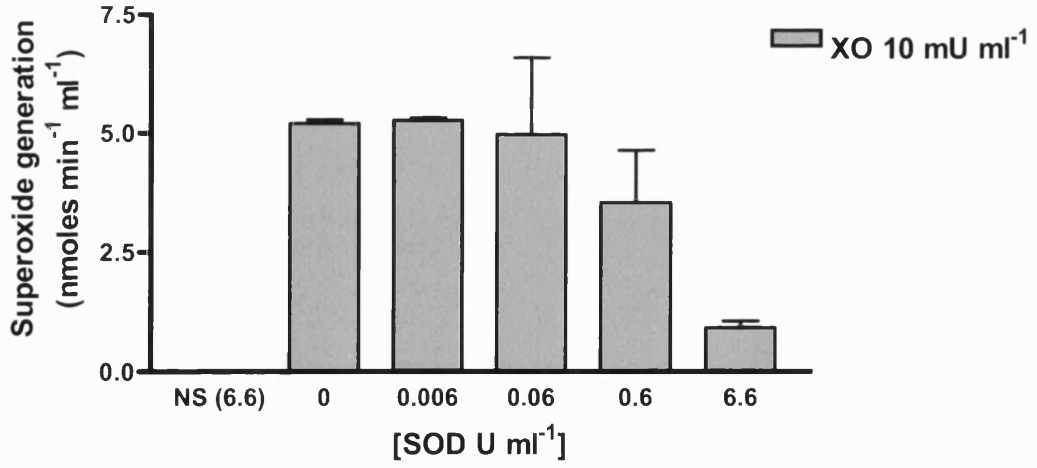

Figure 4.24 Inhibition of XO-generated superoxide by SOD.

Experiment was carried out in air using final concentrations of cytochrome *c* (50μM), XO (10mU ml^{-1}), hypoxanthine (1mM) and SOD (0, 0.006, 0.06, 0.6, 6.6U ml^{-1}) diluted in a final volume of 3mls PBS at 37°C. Initial rates of superoxide (nmoles min^{-1} ml^{-1}) were calculated from the raw data as described in the methods No substrate (NS) = XO (10mU ml^{-1}) and SOD (6.6U ml^{-1}) diluted in 3mls PBS. Mean ± SD. n =2.

The rate of $O_2^{\bullet-}$ generation was assessed at varying XO concentrations which covered a range that would be used in the cell culture experiments. Measurements were made at varying XO concentrations from 0 to 10mU ml^{-1} using hypoxanthine as a substrate. The rate of $O_2^{\bullet-}$ production was shown to increase with increasing concentrations of XO (Figure 4.25 and Table 4.2).

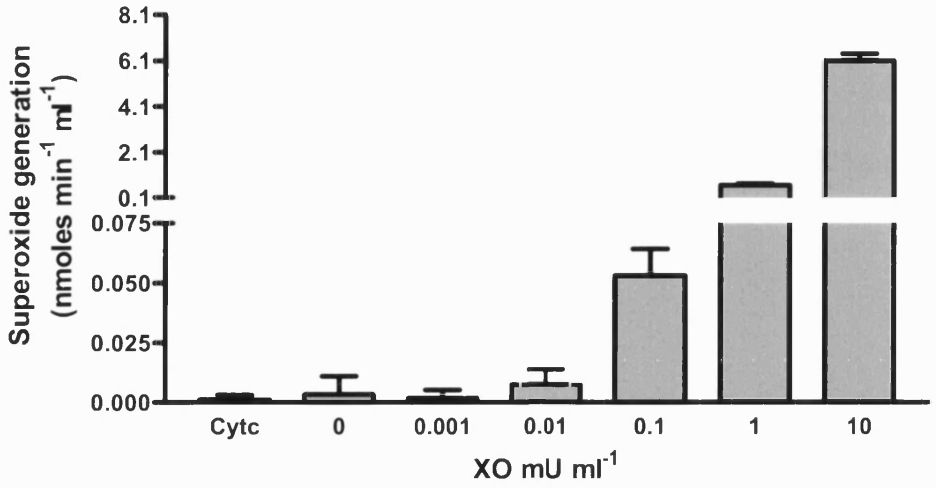

Figure 4.25 Initial rates of superoxide generation at 0 to 10mU ml^{-1} XO.

Experiments were carried out in air using final concentrations of Cytochrome *c* (50μM), XO (0, 0.001, 0.01, 0.1, 1 and 10mU ml^{-1}) and hypoxanthine (1mM) diluted in a final volume of 3mls PBS at 37°C. This graph shows the initial rate of superoxide generation (nmoles min^{-1} ml^{-1}) by XO at 0 to 10mU ml^{-1} XO as calculated from raw absorbance data. All n = 6. Except XO (0.001mU ml^{-1}) n = 3 and (10mU ml^{-1}) XO n = 8. Mean ± SD.

XO mU ml^{-1} X	Superoxide nmol min^{-1} ml^{-1} Y	SD	N
0	0.000	0.008	6
0.001	0.000	0.004	6
0.01	0.009	0.006	6
0.1	0.073	0.011	6
1	0.748	0.066	6
10	6.825	0.302	8

Table 4.2 Initial rates of superoxide generation at 0 to 10mU ml^{-1} of XO

Experiments were also carried out to assess the effect of varying concentrations of hypoxanthine on $O_2^{\bullet-}$ generation by XO (Figure 4.26). Figure 4.26 shows that the rate of $O_2^{\bullet-}$ generation increases with increasing hypoxanthine until around 5μM hypoxanthine. As the substrate concentration continues to increase to 1mM hypoxanthine the rate of $O_2^{\bullet-}$ generation plateaus at a rate of 0.7nmole $O_2^{\bullet-}$ min^{-1} ml^{-1}.

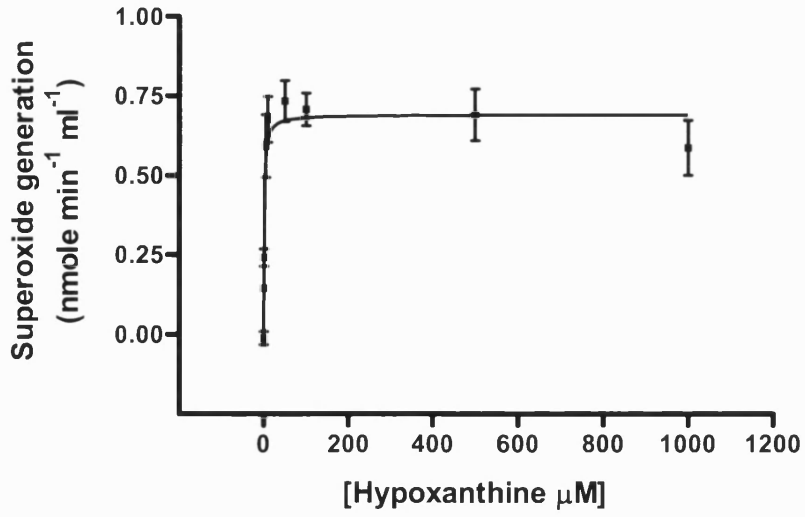

Figure 4.26 Initial rates of superoxide generation by XO with varying hypoxanthine.

Experiments were carried out in air using a final concentration of cytochrome *c* (50μM), XO (1mU ml^{-1}), with hypoxanthine at (0.5, 1, 5, 10, 50, 100, 500, 1000μM) in a final volume of 2mls PBS at 37°C. N numbers are as follows 0.5: n = 3, 1 - 50: n = 6, 100: n = 5, 1000: n = 9. Mean±SD.

The cell culture buffer HEPES (20mM) was routinely used in the cell culture experiments carried out by Murrell *et al*, 1990. However, HEPES has been reported to have scavenging activity (Simpson *et al*, 1988). Therefore, a series of experiments were carried out to determine whether there was any effect on the $O_2^{\bullet -}$ production in the presence and absence of HEPES. Figure 4.27 indicates that there is no significant difference in $O_2^{\bullet -}$ production when HEPES is added to the reaction volume.

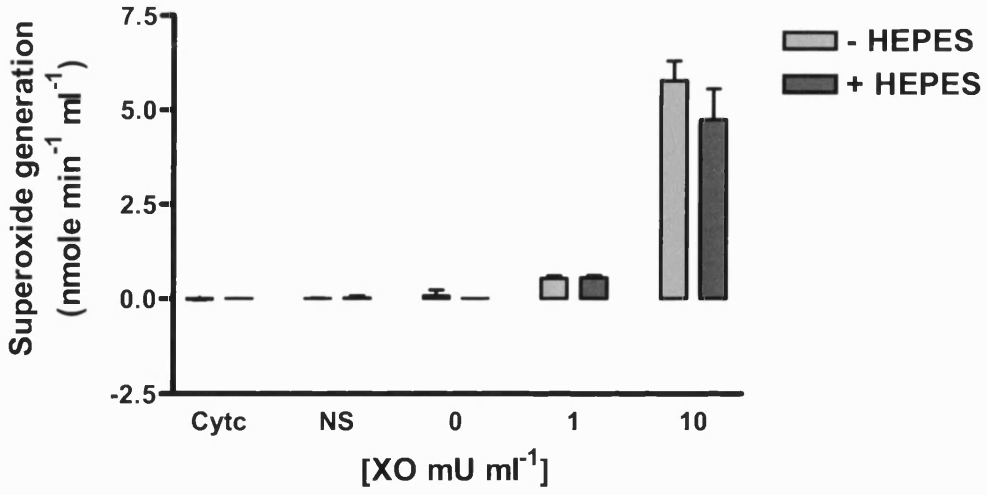

Figure 4.27 Initial rates of superoxide generation by XO with and without HEPES buffer.

Experiments were carried out in air using final concentrations of cytochrome *c* (50μM), XO (1mU ml^{-1}), hypoxanthine (1mM) with (+ HEPES, 20mM) or without HEPES (-HEPES) in a 3mls total volume of PBS at 37°C. Initial rates of superoxide generation (nmole min^{-1} ml^{-1}) were calculated from the raw absorbance data as shown in the methods. These experiments were carried out in triplicate on three separate occasions. Mean±SD The n numbers for this experiment are as follows; - HEPES: NS and NE n = 2, XO (1mU ml^{-1}) n

= 9, XO (10mU ml^{-1}) n = 6. + HEPES: NS and NE, n = 7, XO (1mU ml^{-1}) n = 9, XO (10mU ml^{-1}) n = 3. There is no significant difference between assays carried out with or without HEPES. At XO (1mU ml^{-1}) P = 0.6406 (two-tailed unpaired t test).

New batches of XO enzyme were routinely tested to assess the activity was comparable with the previous batch of enzyme. There is little difference between the old and new batches of enzyme (Figure 4.28).

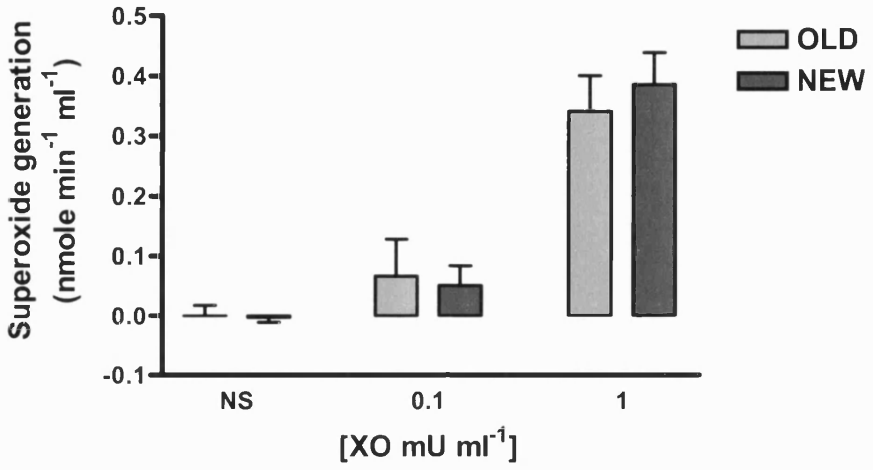

Figure 4.28 Comparison of old and new batch of XO.

Experiments were carried out in air using final concentrations of XO (0.1 and 1mU ml^{-1}), with hypoxanthine (1mM) and HEPES (20mM) in 3mls PBS at 37°C. Initial rates of superoxide generation (nmole min^{-1} ml^{-1}) were calculated from the raw data as described in the methods. These experiments were carried out in triplicate on three different occasions. The n numbers for this experiment are as follows OLD: No substrate (NS) and XO (0.1mU ml^{-1}), n = 8, and for XO (1mU ml^{-1}) n = 9. NEW: Control n = 5, XO (0.1mU ml^{-1}) n = 8, XO (1mU ml^{-1}) n = 9. Mean±SD There is no significant difference between old and new batch of enzyme at either concentration of XO. At XO (1mU ml^{-1}) P value = 0.0697 and at XO (0.1mU ml^{-1}) P value = 0.9923 (two-tailed unpaired t test).

In the previous assays (Figure 4.23-4.28) cytochrome *c* for the assessment of XO-generated $O_2^{\bullet -}$ was carried out in cuvettes rather than 96-well plates due to unexplained differences in the rate of $O_2^{\bullet -}$ generation in the 96-well plate and the cuvette (Figure 4.14-4.21). The nature of the ongoing studies made it important to increase the number of samples that could be tested at one time and experiment that could be easily transferred to hypoxia. Therefore, the cuvette and a 96-well plate method were compared again and it was at this stage that the temperature setting of the 96-well plate reader was carefully considered. It was noted that the heated base plate of the reader was only reaching 32°C when set at 37°C via the software. Therefore the system was recalibrated to achieve an actual temperature at the sample of 37°C. All reagents were warmed in a water bath prior to the experiments and the plate was placed in an incubator between additions. The results of these changes are shown below in figure 4.29-4.30. Figure 4.29A) and B) show the difference in the absorbances values in the 96-well plate and the cuvette method before the

pathlength correction. Figure 4.30A) and B) shows a comparable timecourse of $O_2^{\bullet-}$ generation over a ten minute time period and comparable rates of reduction. Therefore this improved 96-well plate methodology is suitable for determining rates of $O_2^{\bullet-}$ generation and will be developed for $O_2^{\bullet-}$ measurements in hypoxia.

Figure 4.29-4.30

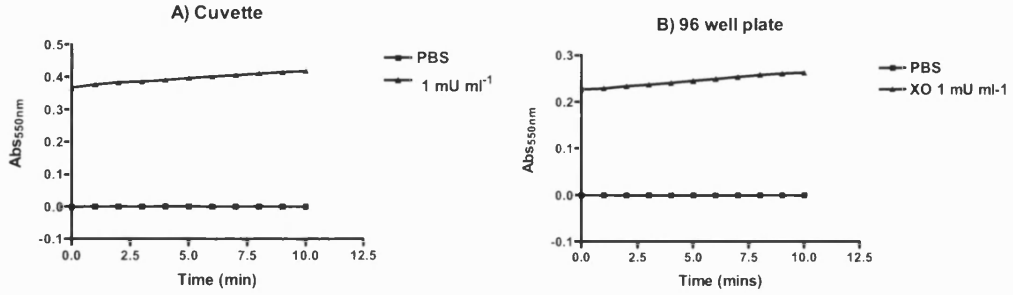

Figure 4.29 Comparison of cytochrome *c* reduction by XO in a cuvette or a 96-well plate.

Experiments were carried out using final concentrations of cytochrome *c* (50μM), hypoxanthine (1mM), XO (1mU ml^{-1}) in a final volume of 200μl PBS at 37°C. Measurements were taken over a 10 minute time period at 550nm. Graph A shows the cuvette method (3ml final volume). Graph B shows the 96-well plate method (200μl final volume).

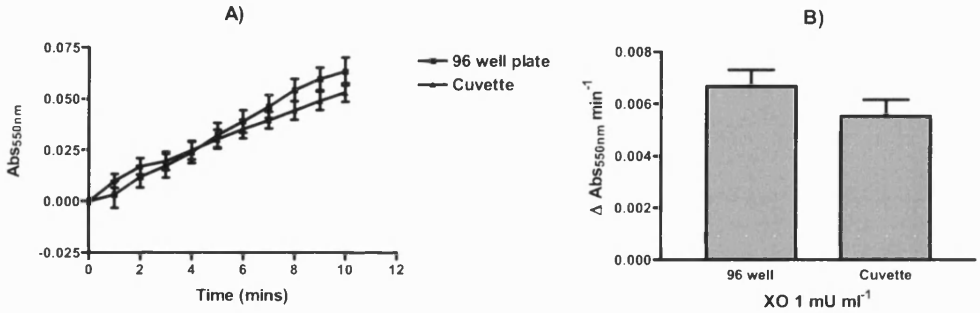

Figure 4.30 Comparison of cytochrome *c* reduction in 96-well plate and cuvette.

Experiments were carried out using final concentrations of hypoxanthine (1mM), cytochrome *c* (50μM), XO (1mU ml^{-1}) at 37°C measurements were taken in air every minute for 10mins. Graph A shows a time course of absorbance values corrected for pathlength and zeroed for comparison. For the 96-well plate data, to correct for pathlength 1.760 was multiplied by the 96-well plate raw absorbance values (Figure 4.30A). For both the 96-well plate and the cuvette values the time 0 absorbance value was subtracted from the rest of the data so that both sets of data began at zero and could be graphed together for comparison (Figure 4.31A). Graph B shows the initial rate of change in absorbance (ΔAbs_{550nm} min^{-1}) of 96-well plate data and cuvette data. Statistical analysis using unpaired t test showed no significant difference ($P>0.05$) $P = 0.088$. $n = 3$.

The $O_2^{\bullet-}$ generating activities of four batches of stock XO were compared in a 96-well plate for future assays and are labelled as A, B, C and D (Figure 4.31). This figure shows that batch A has a reduced rate of $O_2^{\bullet-}$ generation whereas batches B-C appear to have similar activities. Therefore, batch B was used for continuation of the cytochrome *c* assays (Figure 4.32–4.73). Batch B was also used for fibroblast experiments in Chapter 5 and batch C was used for bacterial experiments (Chapter 6).

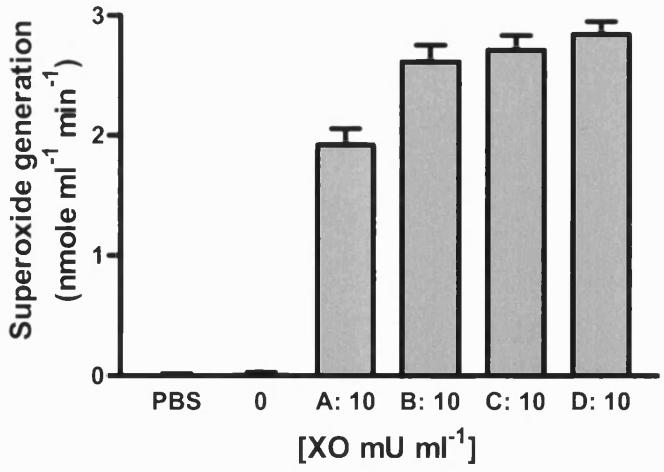

Figure 4.31. Comparison of the initial rates of superoxide generation by four batches of XO.

Experiments were carried out in air using hypoxanthine (1mM) and XO (10mU ml^{-1}) in a final volume of 200µl PBS at 37°C. Cytochrome *c* reduction at 550nm measured in air every minute for a duration of 20mins expressed as the initial rate of superoxide generation (nmole ml^{-1} min^{-1}). Mean ± SD. n = 3.

Xanthine oxidoreductase at 50mU ml^{-1} was also measured in PBS to determine whether cytochrome *c* reduction at this concentration of XO would be measurable with 1mM hypoxanthine as the substrate. Nitrite (1mM) was also included in this experiment as this substrate will be used in the cell based experiments along with 1mM hypoxanthine as a substrate for the generation of $^{\bullet}NO$ and $ONOO^{-}$. Figure 4.32 shows that nitrite and hypoxanthine do not reduce cytochrome *c* either alone or in combination. Cytochrome *c* is not reduced by nitrite and 50mU ml^{-1} XO. However, the reduction of cytochrome *c* by hypoxanthine and 50mU ml^{-1} XO is rapid both with (shown in red in figure 4.32) and with out nitrite (shown in blue in figure 4.32); the graph just catches a peak in absorbance at around 1 minute. The absorbance values then return to baseline levels after around 9 minutes suggesting that the cytochrome *c* has been reduced and then is rapidly re-oxidised. The reaction was also measured over a longer period of time as both fibroblasts and bacteria would be exposed to the enzyme and substrates for a longer duration in culture. This assay also shows that cytochrome c is not reduced in air over a 1 hour time period.

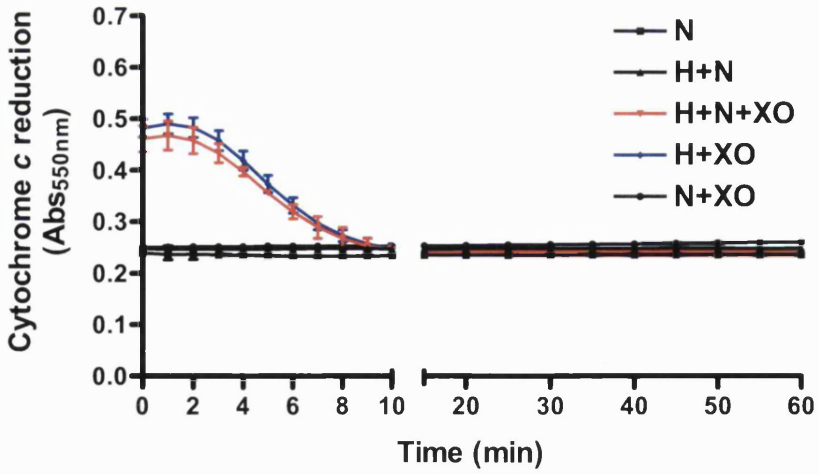

Figure 4.32 Timecourse of cytochrome *c* reduction by XO at 50mU ml^{-1}.

Experiments were carried out in air using final concentrations of cytochrome *c* (50μM), hypoxanthine (1mM) (H), nitrite (1mM) (N) and XO (50mU ml^{-1}) diluted in a final volume of 200μl PBS at 37°C. Measurements were taken in air at 1 minute intervals over a 1 hour time period, however, only selection of time points are shown on the graph for clarity. This experiment shows that neither nitrite alone nor nitrite with XO causes any reduction in cytochrome *c*. n = 3. Mean±SD.

The previous experiment shown in figure 4.32 was repeated with fewer samples so it was possible to add the enzyme to the relevant wells and begin the readings immediately allowing the initial rapid stages of cytochrome *c* reduction to be recorded (Figure 4.33).

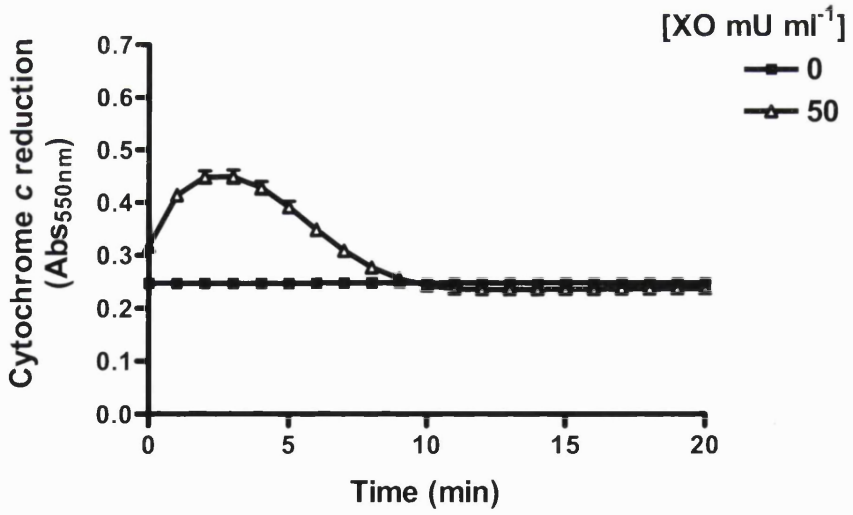

Figure 4.33. Cytochrome *c* reduction and superoxide generation by 50mU ml^{-1} XO.

Experiments were carried out in air using final concentrations of cytochrome *c* (50μM), hypoxanthine (1mM), nitrite (1mM) and XO (50mU ml^{-1}) diluted in a final volume of 200μl PBS at 37°C. Measurements were taken in air at 1 minute intervals over a 20 minute time period. Timecourse of cytochrome *c* reduction at 550nm by XO. n = 3. Mean ± SD.

Experiments were carried out to determine whether the initial reduction of cytochrome *c* shown in figure 4.33 was due to $O_2^{\bullet-}$ generation by XO. Figure 4.34A shows that at 50mU ml^{-1} XO without SOD in PBS has a rapid initial rate of cytochrome *c* reduction followed by a re-oxidation of cytochrome *c* as shown in the previous assays (shown in blue) and addition of increasing concentrations of SOD completely inhibits the reduction of cytochrome *c* with complete inhibition occurring at 50U ml^{-1} SOD (shown in red). Figure 4.34B shows the inhibition of the initial rate of $O_2^{\bullet-}$ generation by XO (50mU ml^{-1}) at concentrations of SOD above 10U ml^{-1} suggesting that the reduction of cytochrome *c* is due to $O_2^{\bullet-}$ generation at 5nmole min^{-1} ml^{-1} (Figure 4.34B). Therefore, this level of SOD will be used in subsequent assays carried out in culture medium to determine the proportion of cytochrome *c* reduction that is due to the presence of $O_2^{\bullet-}$. The assay was also repeated on a separate occasion which supported the findings shown in the figure below.

Figure 4.34 A)

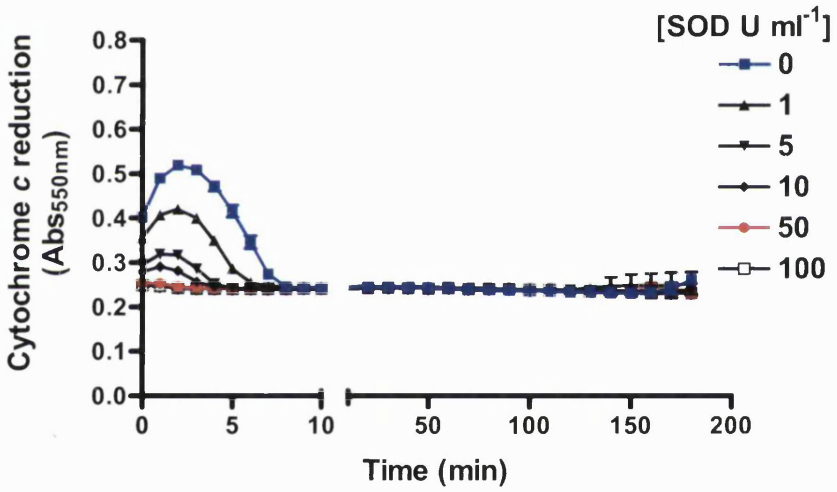

Figure 4.34 B)

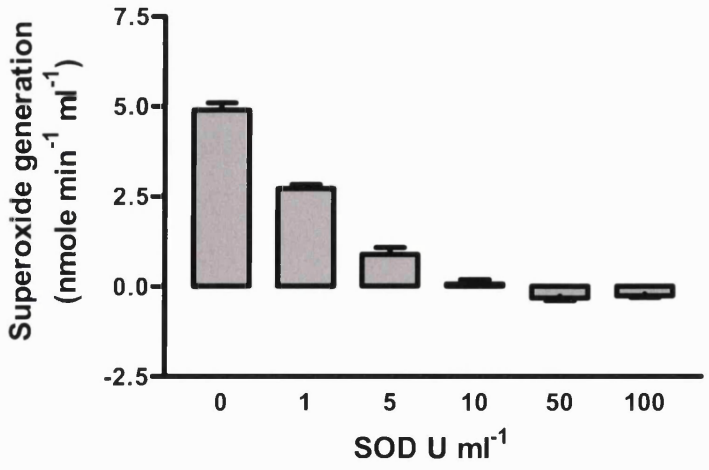

Figure 4.34 Effect of varying concentrations of SOD on superoxide generation by XO in PBS

Experiments were carried out using final concentrations of cytochrome *c* (50μM), hypoxanthine (1mM), nitrite (1mM) and XO (50mU ml^{-1}) and SOD at (1, 5, 10, 50 and 100U ml^{-1}) diluted in a final volume of 200μl PBS at 37°C. Graph A shows the timecourse of the reduction of cytochrome *c*. Measurements were taken in air at 1 minute intervals over a 1 hour time period. Graph B shows the initial rates of superoxide generation (nmole min^{-1} ml^{-1}) calculated as described in the methods using the raw data in figure 4.34A). n = 3. Mean±SD.

The previous assay (figure 4.34) was repeated using catalase instead of SOD to determine whether H_2O_2, which is known to be capable of the re-oxidation of cytochrome *c* was responsible for the re-oxidation effect shown in figures 4.32-4.34. Catalase, which converts H_2O_2 to H_2O and O_2, was used at concentrations between 0-2500U ml^{-1}. Figure 4.35 clearly shows the dose dependent reversal of the re-oxidation of cytochrome *c* by catalase. Compared with the control (which did not contain catalase and is shown in blue in figure 4.35), between 50mU ml^{-1} and 250U ml^{-1} catalase (shown in red in figure 4.35) prevented the re-oxidation of cytochrome *c*, confirming that at high XO concentrations (50mU ml^{-1}) H_2O_2 as well as $O_2^{\bullet-}$ is being generated by XO under these conditions. This assay was also repeated on a separate occasion which supported the findings shown in the figure below (data not shown).

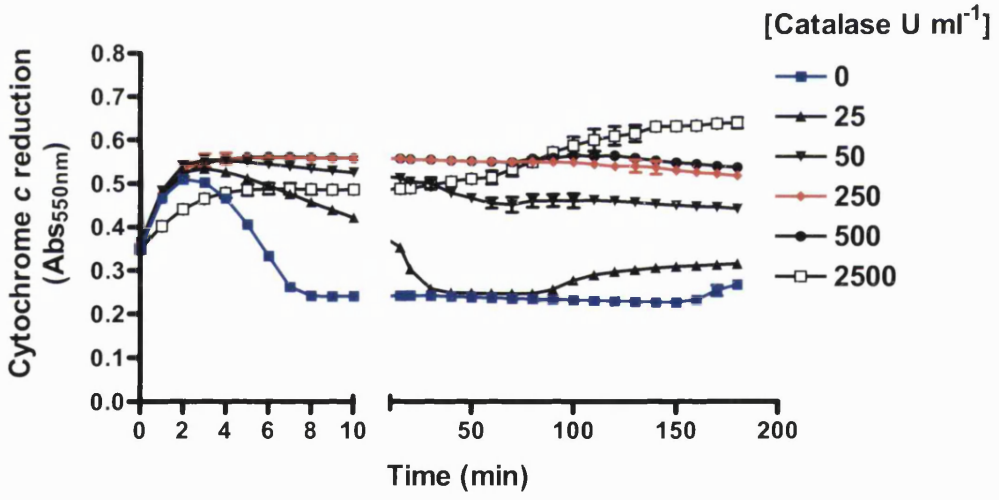

Figure 4.35 Effect of varying concentrations of catalase on superoxide generation by XO in PBS.

Experiments were carried out using final concentrations of cytochrome *c* (50μM), hypoxanthine (1mM), nitrite (1mM), XO (50mU ml^{-1}) and catalase at (25, 50, 250, 500 and 2500 U ml^{-1}) diluted in a final volume of 200μl PBS at 37°C. Measurements were taken in air at 1 minute intervals over a 3 hour time period. n = 3. Mean±SD.

The effect of the XO inhibitor allopurinol on $O_2^{\bullet-}$ generation by XO was assessed to show that the $O_2^{\bullet-}$ generation that was measured in the previous assays was due to XO. Figure 4.36 shows that the reduction of cytochrome *c* by XO (shown in blue) is decreased in the presence of 0.5 and 1mM allopurinol (1mM is shown in red). However, both of

these concentrations appear to inhibit cytochrome *c* reduction to a similar extent. However, these concentrations do not completely inhibit the reduction of cytochrome *c* compared with controls containing only hypoxanthine and nitrite. This is likely to be due to the fact that allopurinol acts as a 'suicide' substrate initially donating electrons to the enzyme before binding tightly and inhibiting any further activity. Allopurinol will also compete for the active site with hypoxanthine. Therefore the low levels of $O_2^{\bullet-}$ that are observed even at high concentrations of allopurinol are likely to have been generated by the enzyme before complete inhibition occurs. This result suggests that $O_2^{\bullet-}$ generation is largely due to XO activity.

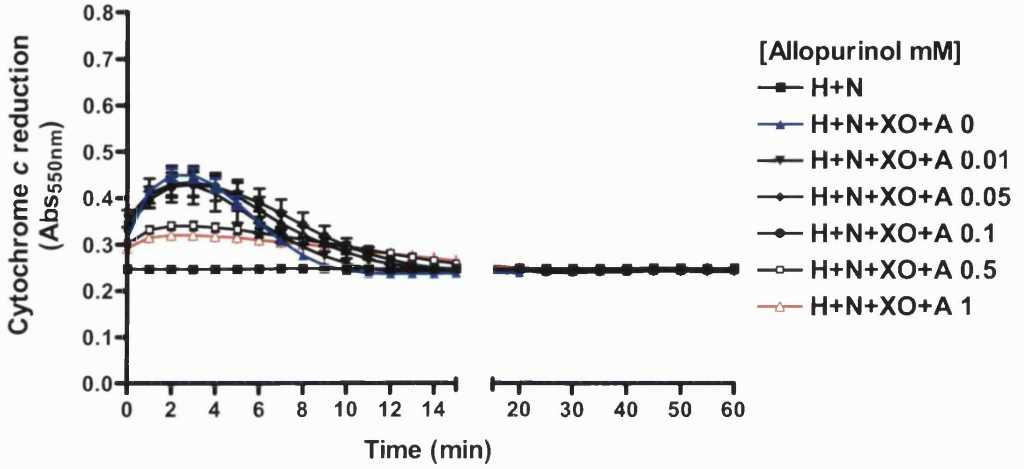

Figure 4.36 Effect of allopurinol on the reduction of cytochrome *c* by XO in PBS.

Experiments were carried out using final concentrations of cytochrome *c* (50μM), hypoxanthine (H) (1mM), nitrite (N) (1mM) and XO (50mU ml^{-1}) and allopurinol (A) at (0.01, 0.05, 0.1, 0.5 and 1U ml^{-1}) diluted in a final volume of 200μl PBS at 37°C. Measurements were taken in air at 1 minute intervals over a 1 hour time period. n = 3. Mean±SD.

Superoxide generation by XO at 1, 10 and 50mU ml^{-1} which are the concentrations to be used in the fibroblast and bacterial experiments were assessed in PBS in air and at 1% O_2. As determined by preliminary experiments shown in figure 4.34-4.35, catalase was included in these assays at 250U ml^{-1} to prevent to re-oxidation of cytochrome *c* by H_2O_2 and a possible underestimation of $O_2^{\bullet-}$, and SOD was used at 50U ml^{-1}. Catalase and SOD were used both individually and in combination to determine the actual $O_2^{\bullet-}$ generation by XO. Figure 4.37A in the absence of SOD and catalase shows that cytochrome *c* reduction by XO (1mU ml^{-1}) in the presence of hypoxanthine and nitrite, cytochrome *c* reduction is gradual (shown in purple). However, with 10 (shown in green) and 50mU ml^{-1} XO both in the presence and absence of nitrite (shown in blue) the cytochrome *c* shows an initial rapid reduction of cytochrome *c* followed by re-oxidation to control levels. Figure 4.37B shows that $O_2^{\bullet-}$ generation by 50mU ml^{-1} XO peaks at around

20nmoles ml^{-1} $O_2^{\bullet-}$ both in the presence and absence of nitrite and (shown in red and blue) and 10mU ml^{-1} XO peaks at 15nmoles ml^{-1} $O_2^{\bullet-}$ (shown in green). A gradual rate of $O_2^{\bullet-}$ generation is observed at 1mU ml^{-1} XO (shown in purple). These rates are completely inhibited by SOD, although, after an hour the cytochrome *c* appears to be slightly reduced (Figure 4.38). Figure 4.39A shows that the addition of catalase prevents the re-oxidation of cytochrome *c* at high XO concentrations over a 3 hour time period. Superoxide generation is also increased compared with figure 4.37B $O_2^{\bullet-}$ generation in the presence of catalase at 50mU ml^{-1} XO peaks at around 30nmoles ml^{-1} $O_2^{\bullet-}$ with hypoxanthine alone (shown in red), and in presence of nitrite although the rate does appear slightly reduced (shown in blue), and 10mU ml^{-1} XO peaks at 15nmoles ml^{-1} $O_2^{\bullet-}$ (shown in green). Addition of a combination of both catalase and SOD to the assay (Figure 4.39) shows a significant reduction in the rate observed in the presence of catalase alone. However, a rate of cytochrome *c* reduction in the presence of 50mU ml^{-1} XO in the presence of hypoxanthine is observed which is reduced when nitrite is also included. Compared with catalase alone the majority of the rate is inhibited suggesting that it is due to $O_2^{\bullet-}$ generation. Figure 4.41 shows that the initial rates of $O_2^{\bullet-}$ generation without SOD and catalase is around 4nmole min^{-1} ml^{-1} with XO and hypoxanthine and slightly lower at 3nmole min^{-1} ml^{-1} with the addition of nitrite. Superoxide generation is slightly increased with the addition of catalase to 6 and 5nmoles min^{-1} ml^{-1} respectively and $O_2^{\bullet-}$ generation is also shown to be inhibited by the addition of SOD.

Figure 4.37-4.41

Figure 4.37 A)

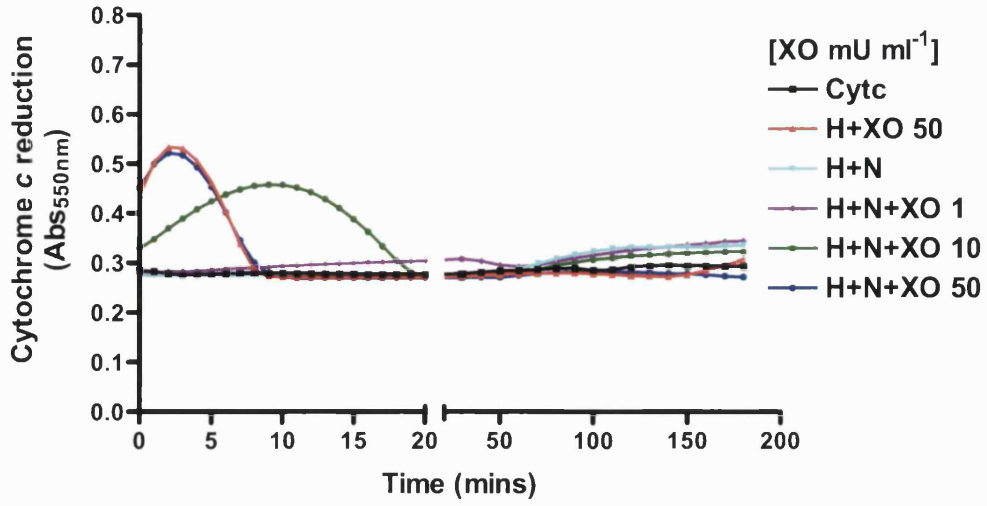

Figure 4.37 B)

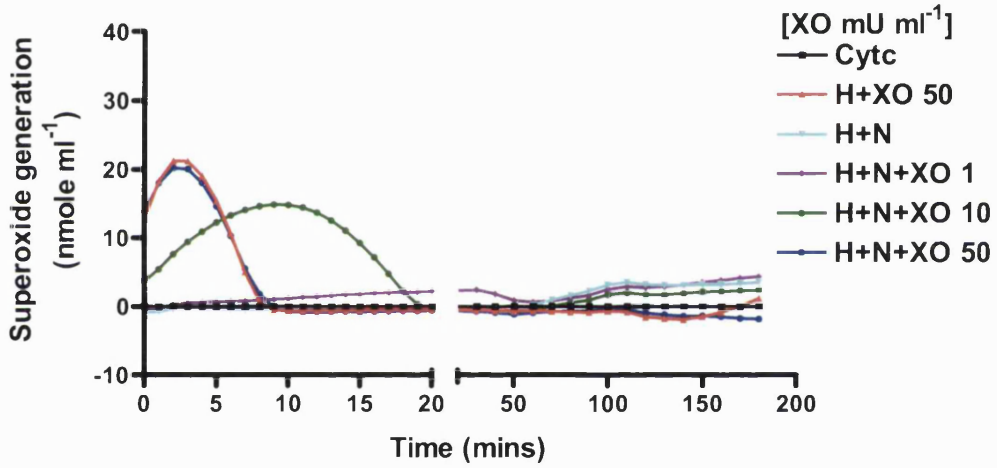

Figure 4.37 Timecourse of cytochrome *c* reduction in PBS by XO in air.

Experiments were carried out in air using final concentrations of cytochrome *c* (50μM), hypoxanthine (H) (1mM), nitrite (N) (1mM) and XO at (1 10 and 50mU ml^{-1}) in a final volume of 200μl PBS at 37°C in a sealed 96-well plate. Graph A shows a timecourse of cytochrome *c* reduction at 550nm over a 3 hour time period. Graph B shows a timecourse of superoxide generation (nmoles ml^{-1}) calculated from the raw data in graph A. Absorbance values of wells containing PBS and cytochrome *c* were subtracted from the data before analysis. n = 4. Mean bars were removed for clarity.

Figure 4.38 A)

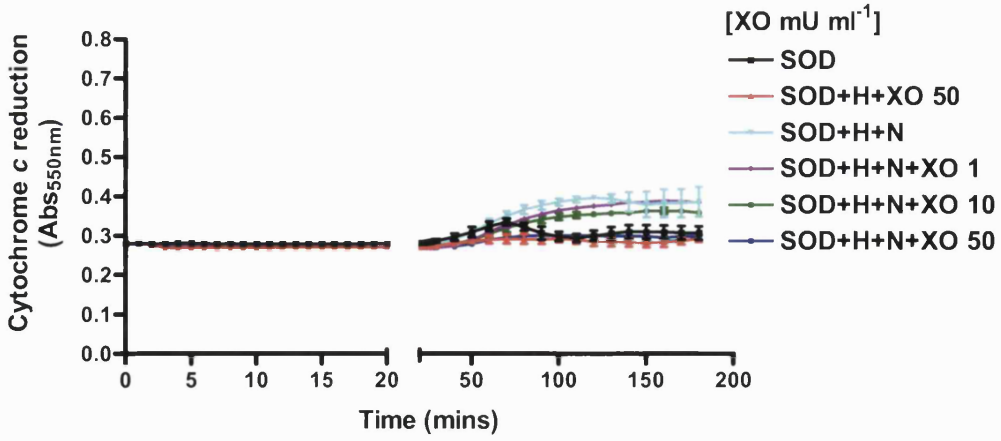

Figure 4.38 B)

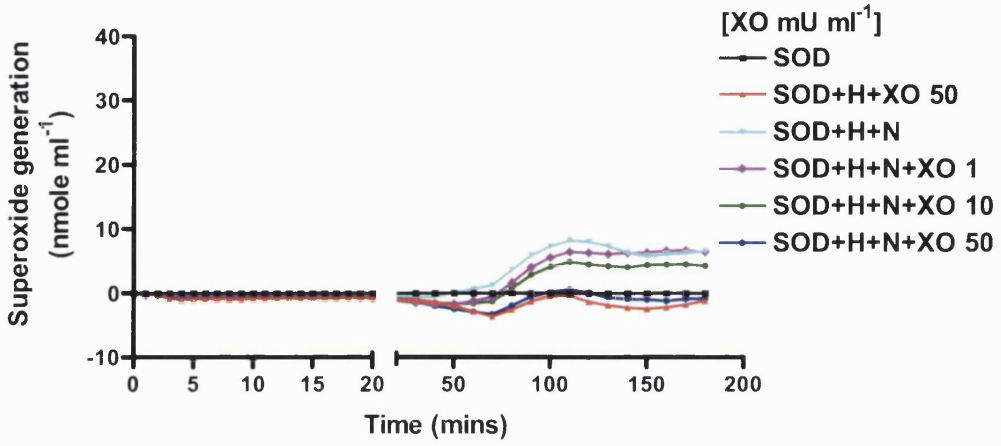

Figure 4.38 Timecourse of cytochrome *c* reduction in PBS by XO at 21% with SOD.

Experiments were carried out in air using final concentrations of cytochrome *c* (50μM), hypoxanthine (H) (1mM), nitrite (N) (1mM), SOD (50U ml^{-1}) and XO at (1, 10 and 50mU ml^{-1}) in a final volume of 200μl PBS at 37°C. Graph A shows a timecourse of cytochrome *c* reduction at 550nm over a 3 hour time period. Graph B shows a timecourse of superoxide generation (nmoles ml^{-1}) calculated from the raw data in graph A. Absorbance values of wells containing PBS and cytochrome *c* were subtracted from the data before analysis. n = 4. Mean bars were removed for clarity.

Figure 4.39 A)

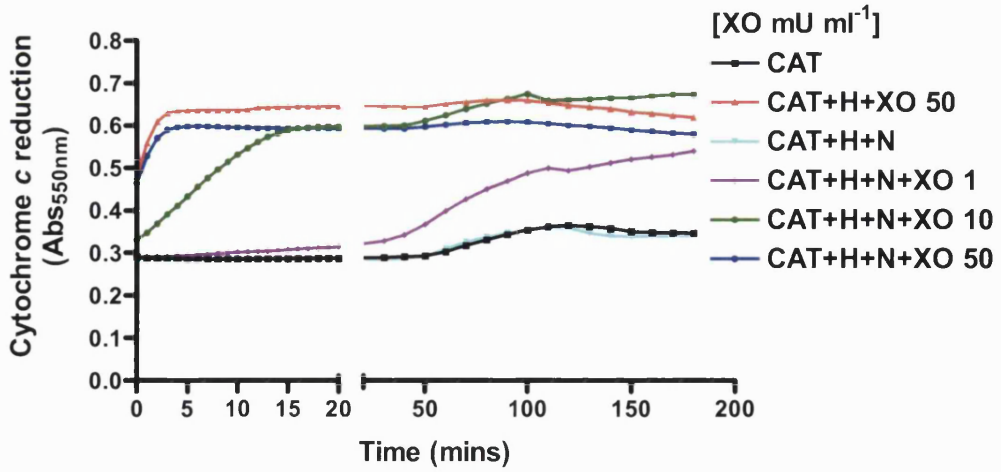

Figure 4.39 B)

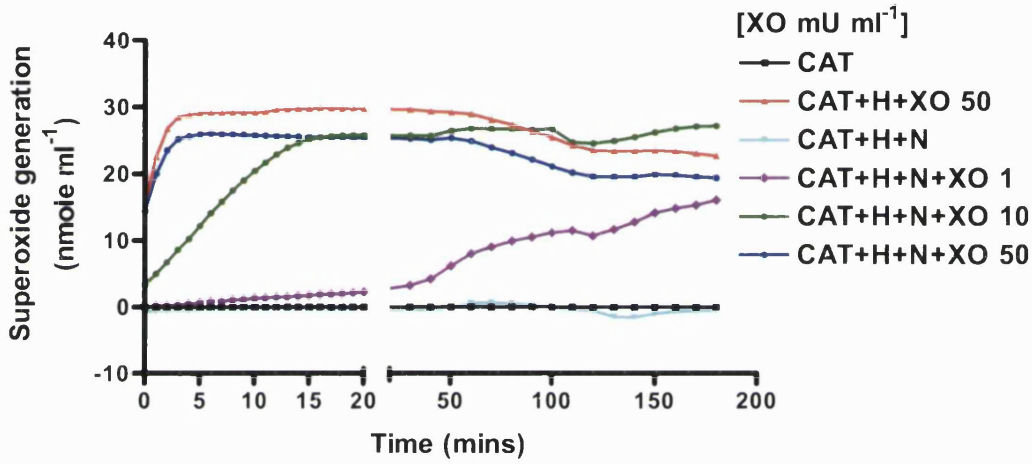

Figure 4.39 Timecourse of cytochrome *c* reduction in PBS by XO in 21% O_2 with catalase.

Experiments were carried out in air using final concentrations of cytochrome *c* (50μM), hypoxanthine (H) (1mM), nitrite (N) (1mM), catalase (CAT) (250U ml^{-1}) and XO at (1, 10 and 50mU ml^{-1}) in a final volume of 200μl PBS at 37°C. Graph A shows a timecourse of cytochrome *c* reduction at 550nm over a 3 hour time period. Graph B shows a timecourse of superoxide generation (nmoles ml^{-1}) calculated from the raw data in graph A. Absorbance values of wells containing PBS and cytochrome *c* were subtracted from the data before analysis. n = 4. Mean bars were removed for clarity.

Figure 4.40 A)

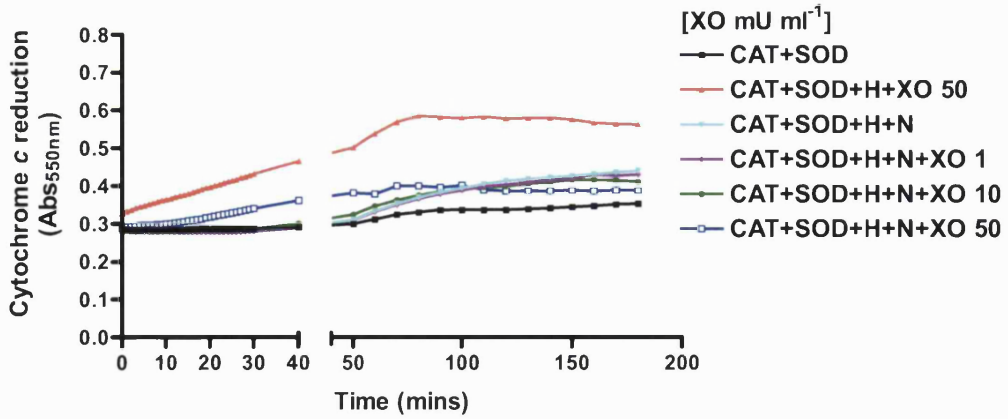

Figure 4.40 B)

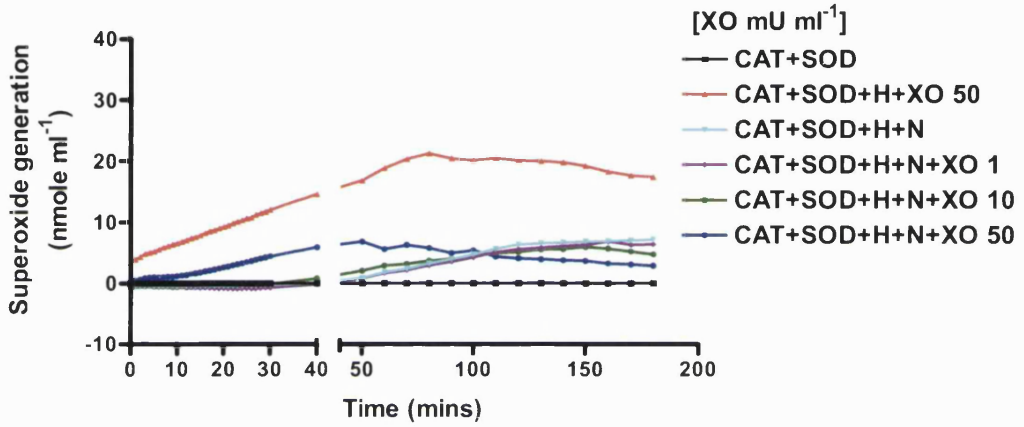

Figure 4.40 Timecourse of cytochrome *c* reduction in PBS by XO at 21% O_2 with SOD and catalase.

Experiments were carried out in air using final concentrations of cytochrome *c* (50μM), hypoxanthine (H) (1mM), nitrite (N) (1mM), catalase (CAT) (250U ml^{-1}), SOD (50U ml^{-1}) and XO at (1 10 and 50mU ml^{-1}) in a final volume of 200μl PBS at 37°C. Graph A shows a timecourse of cytochrome *c* reduction at 550nm over a 3 hour time period. Graph B shows a timecourse of superoxide generation (nmoles ml^{-1}) calculated from the raw data in graph A. Absorbance values of wells containing PBS and cytochrome *c* were subtracted from the data before analysis. n = 4. Mean bars were removed for clarity.

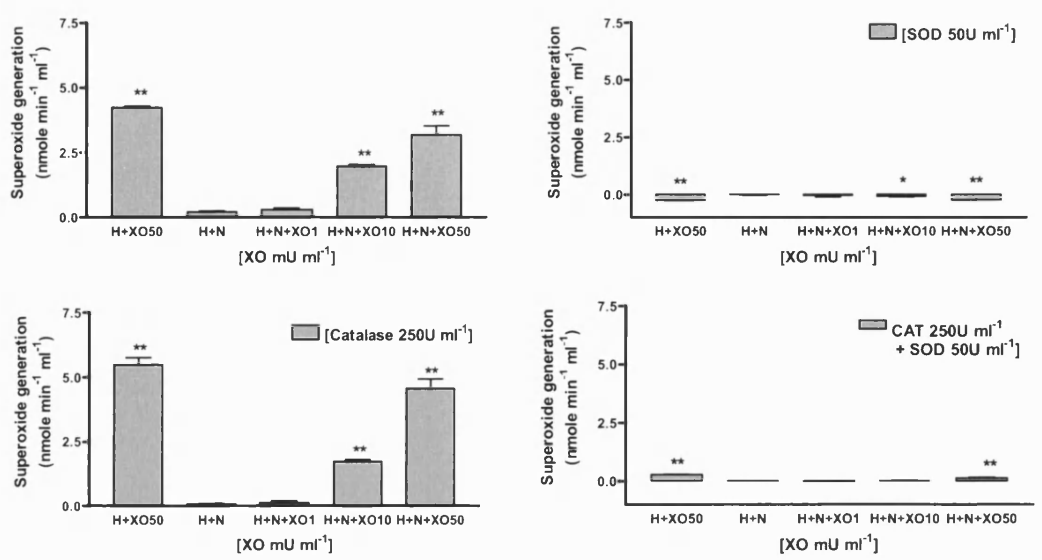

Figure 4.41 Initial rates of superoxide generation in PBS by XO at 21% O_2 with catalase and SOD.

Experiments were carried out in air using final concentrations of cytochrome *c* (50μM), hypoxanthine (H) (1mM), nitrite (N) (1mM), catalase (CAT) (250U ml^{-1}), SOD at (50U ml^{-1}) and XO at (0, 1, 10 and 50mU ml^{-1}) in a final volume of 200μl PBS at 37°C. Initial rates of superoxide generation (nmole $min\ ml^{-1}$) were calculated from the raw data shown in figure 4.37-4.40 n = 4. Mean±SD.

4.3.2.1.2 Superoxide generation by XO in PBS in 1% O_2

Superoxide generation by XO in PBS was repeated in hypoxia (1% oxygen) to mimic the low oxygen environment of the chronic wound, and to compare with the levels of $O_2^{\bullet-}$ generated in 21% O_2 (Figure 4.37-4.41). Compared with the previous assay carried out in air in the absence of SOD and catalase (figure 4.37) at 1% oxygen (figure 4.42) there is little reduction of cytochrome *c* suggesting $O_2^{\bullet-}$ generation is minimal or absent at 1% oxygen. Therefore, the addition of SOD (figure 4.43) had no effect compared with figure 4.42. Interestingly, however, when catalase is added, which breaks H_2O_2 down to H_2O and O_2, cytochrome *c* reduction is observed in the presence of 50mU ml^{-1} XO with hypoxanthine and to a lesser extent when nitrite is also included (figure 4.44). Addition of both catalase and SOD (figure 4.45) produced a result that was almost identical to that seen in figure 4.44 showing cytochrome *c* reduction by XO (50mU ml^{-1}) with hypoxanthine in the presence and absence of nitrite, with a reduced rate of reduction when nitrite was also included. This results suggesting that the observed rates in figure 4.44 are not due to $O_2^{\bullet-}$ generation, or that SOD is inactivated by XO-generated RONS. Overall, however, the rate of $O_2^{\bullet-}$ generation by XO when compared with 21% oxygen (figure 4.41) was found to be decreased in 1% oxygen (figure 6.46).

Figure 4.42-4.45

Figure 4.42A)

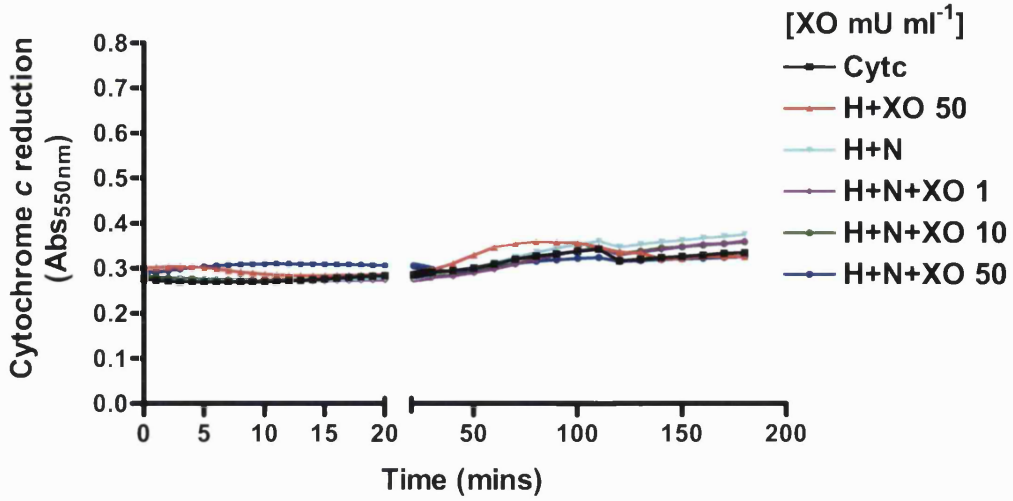

Figure 4.42B)

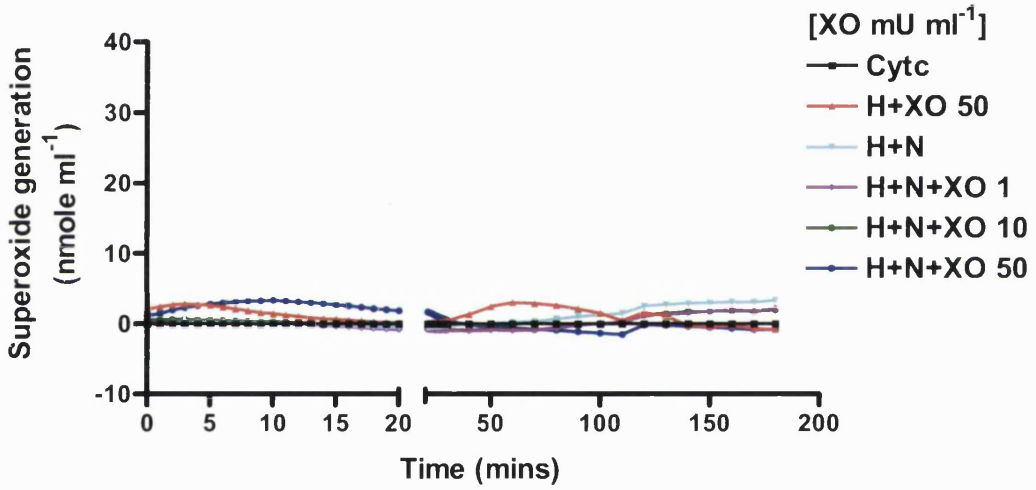

Figure 4.42Timecourse of cytochrome *c* reduction in PBS by XO in 1% oxygen

Experiments were carried out in 1% oxygen using final concentrations of cytochrome *c* (50μM), hypoxanthine (H) (1mM), nitrite (N) (1mM) and XO at (0, 1, 10 and 50mU ml^{-1}) in a final volume of 200μl PBS at 37°C in a sealed 96-well plate. Graph A shows a timecourse of cytochrome *c* reduction at 550nm over a 3 hour time period. Graph B shows a timecourse of superoxide generation (nmoles ml^{-1}) calculated from the raw data in graph A. Absorbance values of wells containing PBS and cytochrome *c* were subtracted from the data before analysis. Experiments were carried out on two separate occasions in quadruplicate therefore n=8. Mean bars were removed for clarity.

Figure 4.43A)

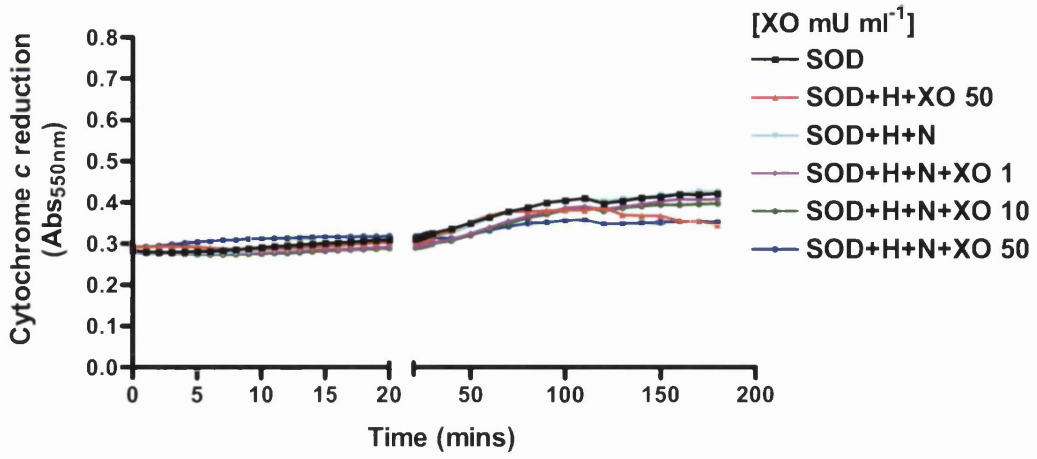

Figure 4.43B)

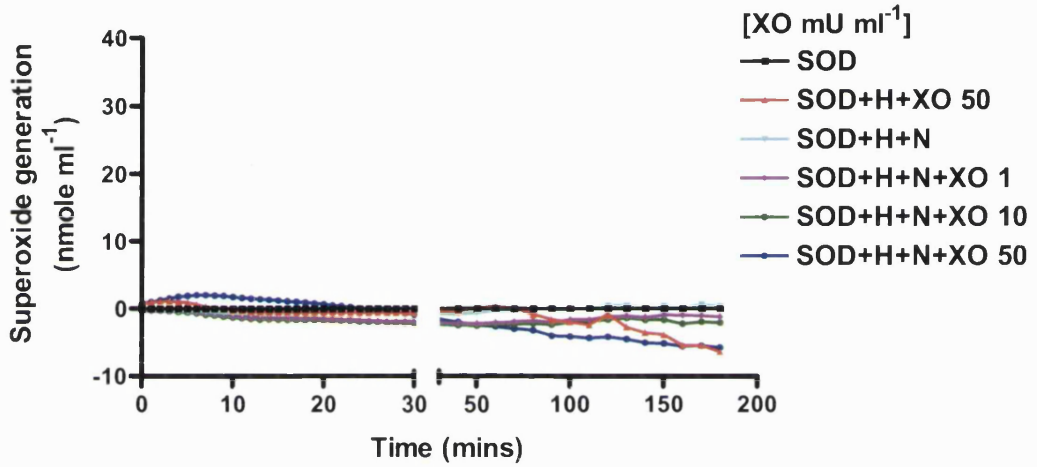

Figure 4.43 Timecourse of cytochrome *c* reduction in PBS by XO in 1% oxygen with SOD.

Experiments were carried out in 1% oxygen using final concentrations of cytochrome *c* (50μM), hypoxanthine (H) (1mM), nitrite (N) (1mM), SOD (50U ml^{-1}) and XO at (0, 1, 10 and 50mU ml^{-1}) in a final volume of 200μl PBS at 37°C in a sealed 96-well plate. Graph A shows a timecourse of cytochrome *c* reduction at 550nm over a 3 hour time period. Graph B shows a timecourse of superoxide generation (nmoles ml^{-1}) calculated from the raw data in graph A. Absorbance values of wells containing PBS and cytochrome *c* were subtracted from the data before analysis. Experiments were carried out on two separate occasions in quadruplicate therefore n=8. Mean bars were removed for clarity.

Figure 4.44A)

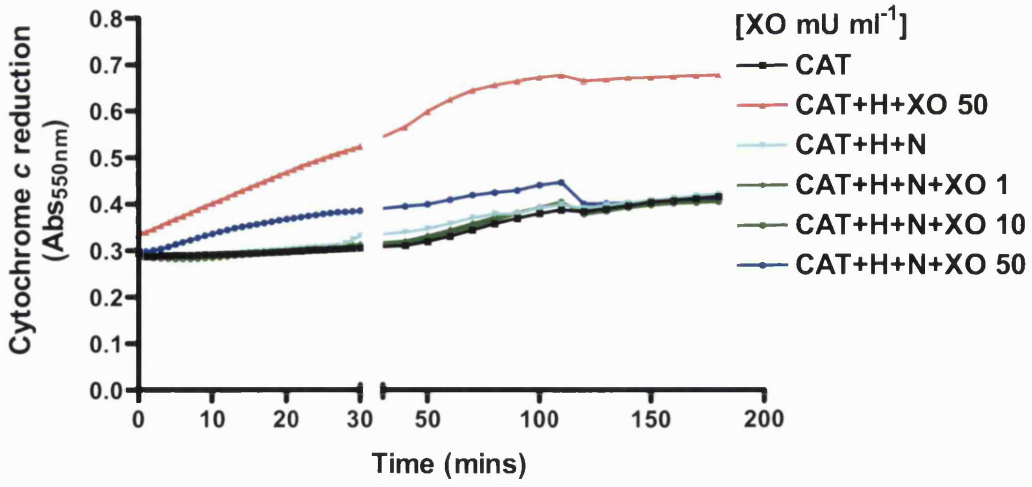

Figure 4.44B)

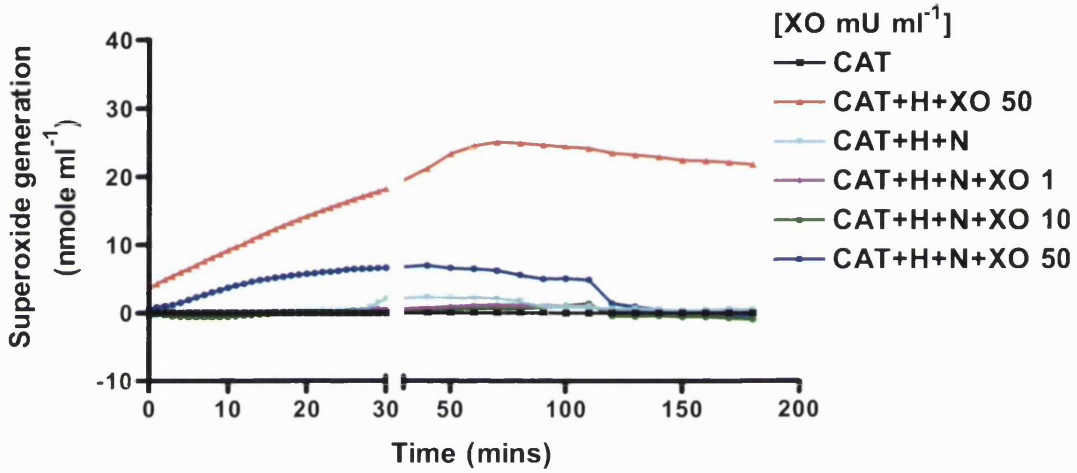

Figure 4.44 Timecourse of cytochrome *c* reduction in PBS by XO in 1% oxygen with catalase.

Experiments were carried out in 1% oxygen using final concentrations of cytochrome *c* (50μM), hypoxanthine (H) (1mM), nitrite (N) (1mM), catalase (CAT) (250U ml^{-1}) and XO at (0, 1, 10 and 50mU ml^{-1}) in a final volume of 200μl PBS at 37°C in a sealed 96-well plate. Graph A shows a timecourse of cytochrome *c* reduction at 550nm over a 3 hour time period. Graph B shows a timecourse of superoxide generation (nmoles ml^{-1}) calculated from the raw data in graph A. Absorbance values of wells containing PBS and cytochrome *c* were subtracted from the data before analysis. Experiments were carried out on two separate occasions in quadruplicate therefore n = 8. Mean bars were removed for clarity.

Figure 4.45A)

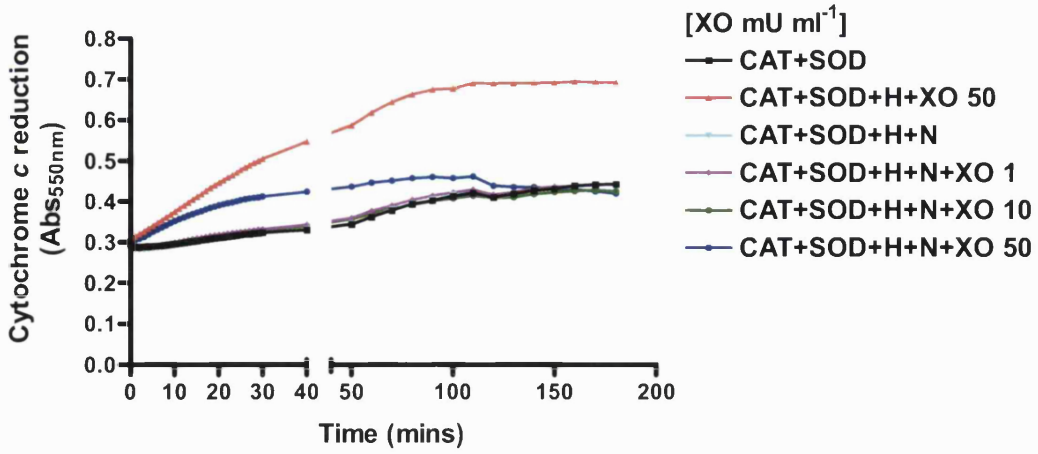

Figure 4.45B)

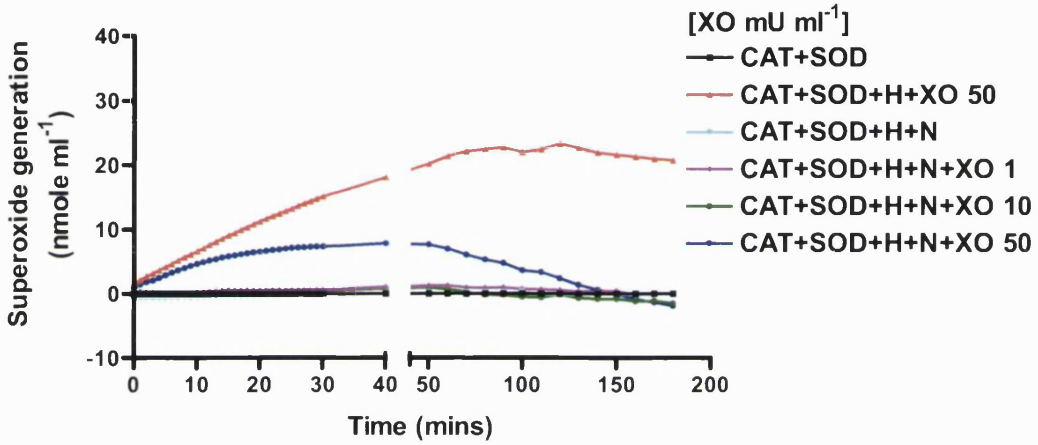

Figure 4.45 Reduction of cytochrome *c* by XO at 1% O_2 in PBS

Experiments were carried out in 1% oxygen using final concentrations of cytochrome *c* (50μM), hypoxanthine (H) (1mM), nitrite (N) (1mM), SOD (50U ml^{-1}), catalase (CAT, 250U ml^{-1}) and XO at (0, 1 10 and 50mU ml^{-1}) in a final volume of 200μl PBS at 37°C in a sealed 96-well plate. Graph A shows a timecourse of cytochrome *c* reduction at 550nm over a 3 hour time period. Graph B shows a timecourse of superoxide generation (nmoles ml^{-1}) calculated from the raw data in graph A. Absorbance values of wells containing PBS and cytochrome *c* were subtracted from the data before analysis. Experiments were carried out on two separate occasions in quadruplicate therefore n = 8. Mean bars were removed for clarity.

Figure 4.46

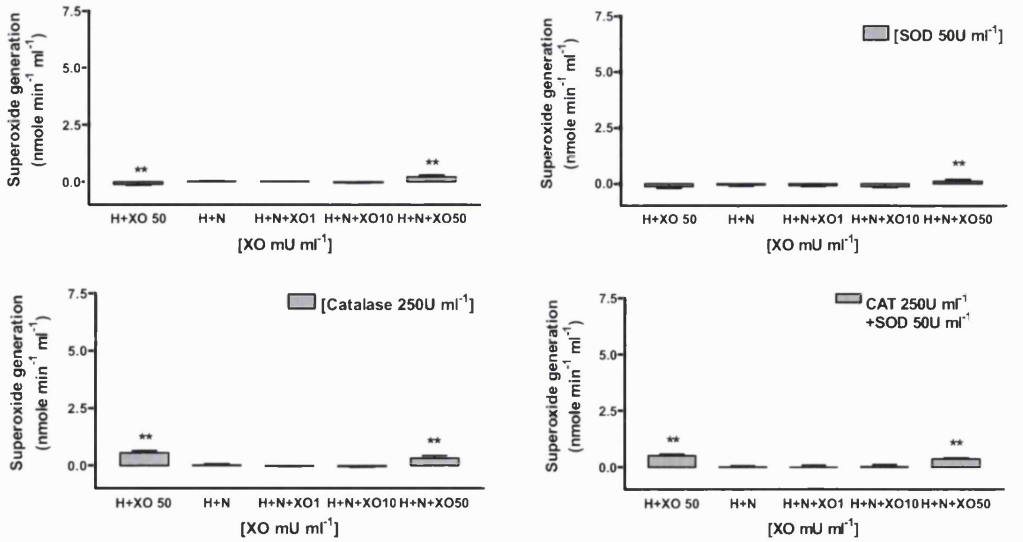

Figure 4.46 Initial rates of superoxide generation by XO in PBS at 1% O_2 with catalase and SOD.

Experiments were carried out in 1% oxygen using final concentrations of cytochrome *c* (50μM), hypoxanthine (H) (1mM), nitrite (N) (1mM), catalase (CAT) (250U ml^{-1}), SOD (50U ml^{-1}) and XO at (0, 1, 10 and 50mU ml^{-1}) in a final volume of 200μl PBS at 37°C. Mean±SD. n=8.

4.3.2.1.3 Superoxide generation by XO in bacterial culture medium in air

Superoxide generation by XO in bacterial culture medium (Luria-Bertani Broth) was also assessed using the cytochrome *c* assay to determine the levels of $O_2^{\bullet -}$ that bacteria would be exposed to in culture. Cytochrome *c* was added to bacterial culture medium and the absorbance followed at 550nm for 3 hours. Luria-Bertani broth (LB) alone was found to reduce cytochrome *c* over time and the addition of catalase and SOD has no effect on this reduction (figure 4.47).

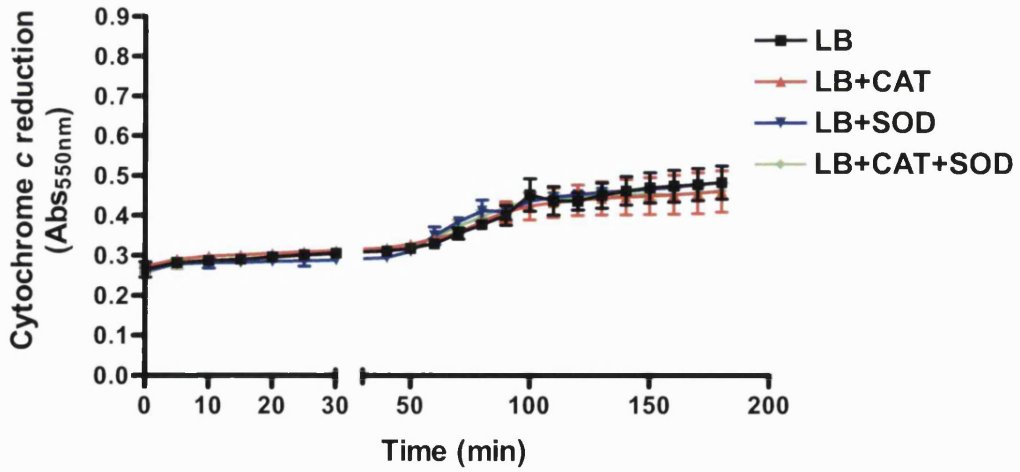

Figure 4.47 Timecourse of the reduction of cytochrome *c* by bacterial culture medium in air.

Experiment was carried out in air using final concentrations of cytochrome *c* (50μM), SOD (50mU ml^{-1}) and catalase (100mU ml^{-1}) diluted in bacterial culture medium (LB) for a 200μl final volume. Reduction of cytochrome *c* was followed at 550nm for 3 hours in a sealed 96-well plate at 37°C. Mean±SD. n = 4.

Cytochrome *c* was reduced by XO (10mU ml^{-1}) alone in LB demonstrating that XO substrates were present in the medium. This reduction was also inhibited by SOD showing the superoxide generation was responsible (Figure 4.48).

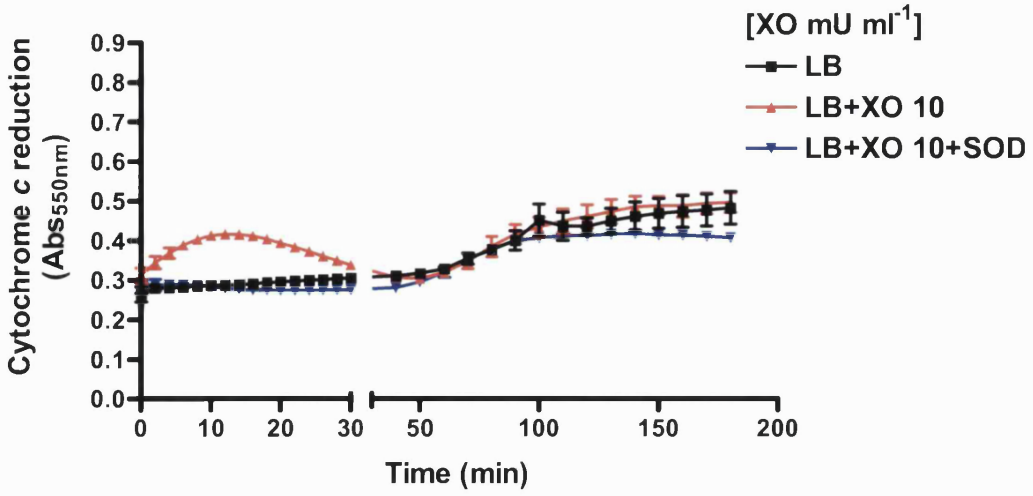

Figure 4.48 Timecourse of the reduction of cytochrome *c* by XO in LB

Experiments were carried out in air using final concentrations of cytochrome *c* (50μM), XO (10mU ml^{-1}) and SOD (50U ml^{-1}) diluted in bacterial culture medium (LB) for a 200μl final volume. Reduction of cytochrome *c* was followed at 550nm for 3 hours in a sealed 96-well plate at 37°C. Mean±SD. n = 4.

The reduction of cytochrome *c* by 10 and 50mU ml^{-1} XO was followed in figure 4.49-4.52. These figures showed similar results to those found in PBS. An initial rapid rate of reduction and re-oxidation of cytochrome *c* in the absence of SOD and catalase was observed in the presence of 50mU ml^{-1} XO with hypoxanthine, in the presence and absence of nitrite. A similar profile was also shown in the presence of 10mU ml^{-1} XO with hypoxanthine and nitrite at slightly reduced rate (Figure 4.49). With the addition of SOD, the reduction of cytochrome *c* is almost entirely prevented (Figure 4.50) suggesting that the observed rates are due to $O_2^{\bullet-}$ generation. Alternatively, addition of catalase prevented the re-oxidation of cytochrome *c* and showed increased $O_2^{\bullet-}$ generation (Figure 4.51). Interestingly, the reduction of cytochrome *c* by XO at 50mU ml^{-1} with hypoxanthine appeared considerably greater in the presence of nitrite (Figure 4.51). Addition of both catalase and SOD (figure 4.52) shows a reduced rate of cytochrome *c* reduction compared with catalase alone. However, the rates at 10 and 50mU ml^{-1} are not completely inhibited by the addition of SOD. Furthermore, in the presence of catalase alone (figure 4.51), it was noted that the rate of reduction at 50mU ml^{-1} XO with hypoxanthine and nitrite was greater than in the absence of nitrite. With the addition of SOD these rates appear to be the same (figure 4.52). Figure 4.53 shows that in LB in air around 2-3 nmoles min^{-1} ml^{-1} of $O_2^{\bullet-}$ are produced by 50mU ml^{-1} XO and around

1.5nmoles min ml^{-1} of $O_2^{\bullet-}$ is produced by 10mU ml^{-1} XO. These levels of $O_2^{\bullet-}$ generation are considerably reduced when compared with $O_2^{\bullet-}$ generation by XO in PBS at 21% O_2, which showed initial rates of generation of 4-6 nmoles $O_2^{\bullet-}$ at 50mU ml^{-1} XO and 2.5 nmoles $O_2^{\bullet-}$ at 10mU ml^{-1} XO (Figure 4.41).

Figure 4.49A)

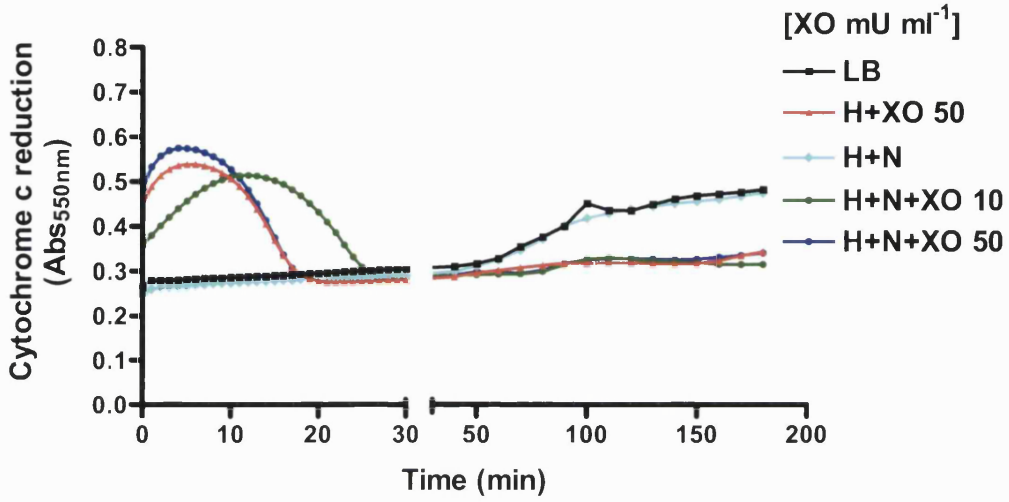

Figure 4.49B)

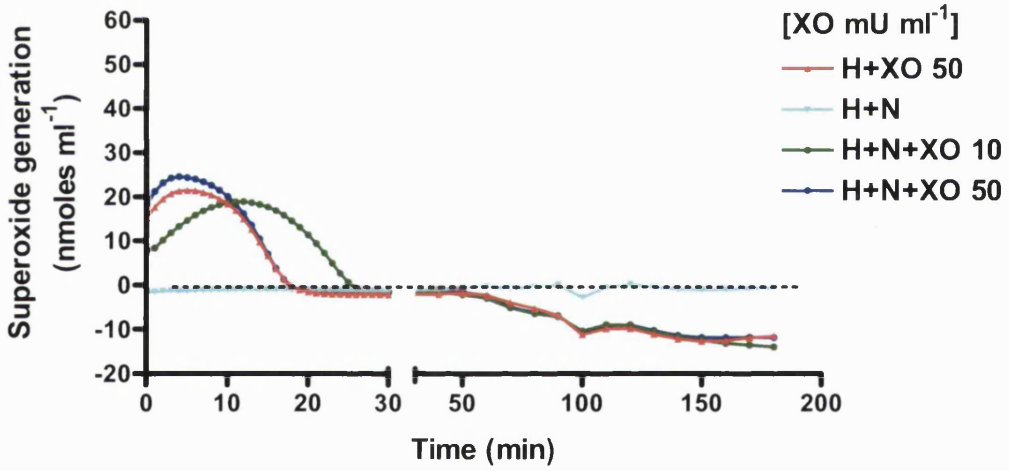

Figure 4.49 Timecourse of cytochrome *c* reduction by XO in air in LB.

Experiments were carried out in air using final concentrations of cytochrome *c* (50μM), hypoxanthine (H) (1mM), nitrite (N) (1mM) and XO (0, 10, 50mU ml^{-1}) diluted in bacterial culture medium (LB) for a 200μl final volume in a sealed 96-well plate at 37°C. Graph A shows a timecourse of cytochrome *c* reduction at 550nm over a 3 hour time period. Graph B shows a timecourse of superoxide generation (nmoles ml^{-1}) calculated from the raw data in graph A. Luria Broth wells were subtracted from the raw data before analysis. n = 4. Mean bars were removed for clarity.

Figure 4.50A)

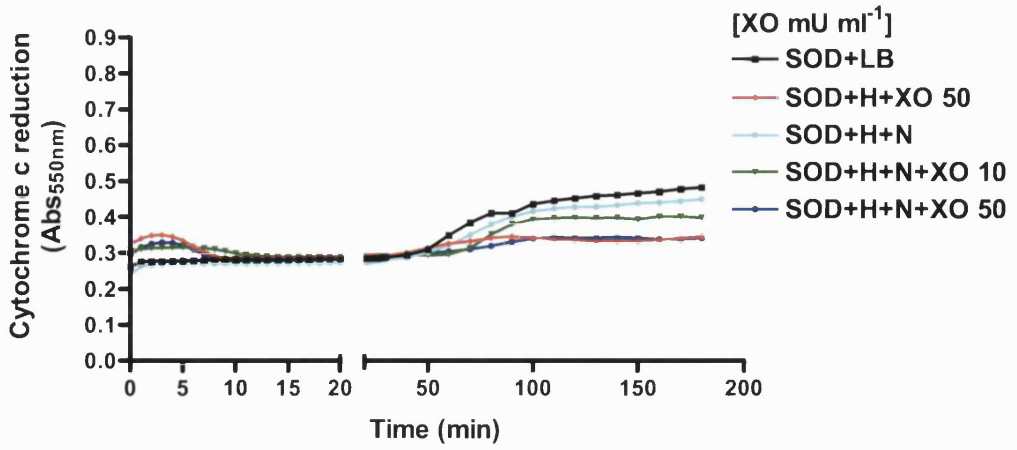

Figure 4.50B)

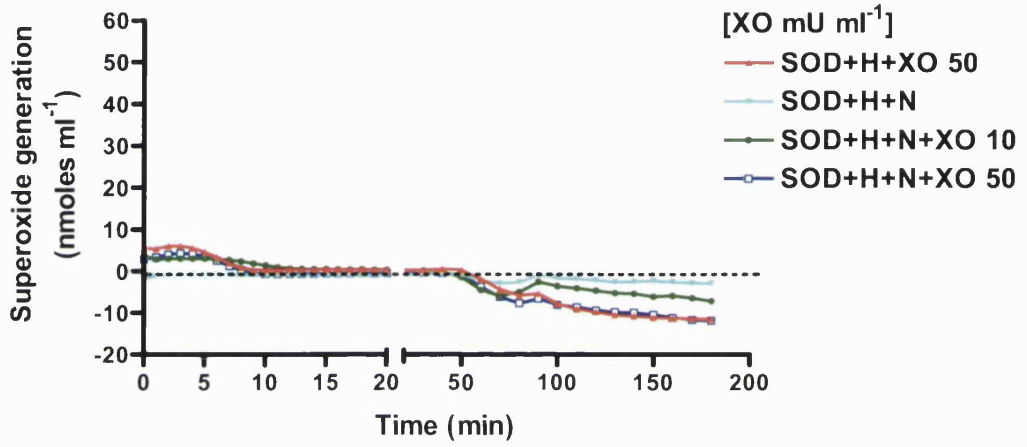

Figure 4.50 Timecourse of cytochrome *c* reduction by XO in air in LB with SOD.

Experiments were carried out in air using final concentrations of cytochrome *c* (50μM), hypoxanthine (H) (1mM), nitrite (N) (1mM), SOD (50U ml^{-1}) and XO (0, 10 and 50mU ml^{-1}) diluted in bacterial culture medium (LB) for a 200μl final volume. Graph A shows a timecourse of cytochrome *c* reduction at 550nm over a 3 hour time period in a sealed 96-well plate at 37°C. Graph B shows a timecourse of superoxide generation (nmoles ml^{-1}) calculated from the raw data in graph A. Luria Broth wells were subtracted from the raw data before analysis. Mean bars were removed for clarity. n = 4.

Figure 4.51A)

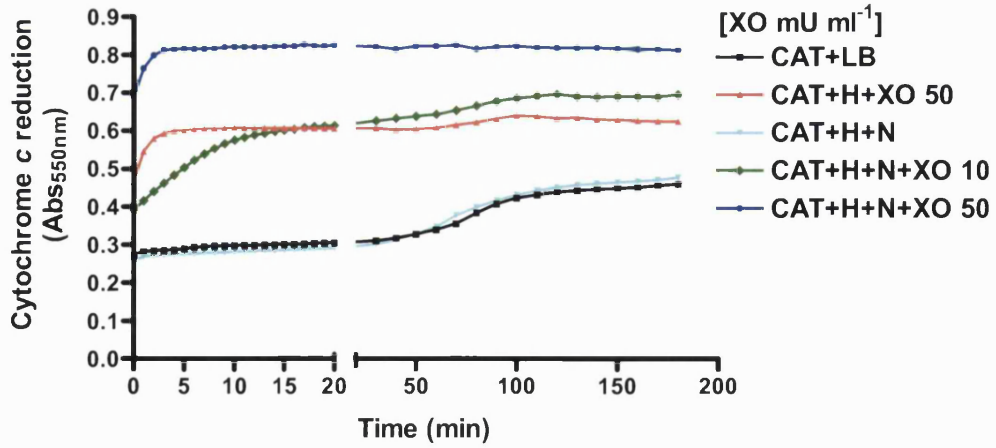

Figure 4.51B)

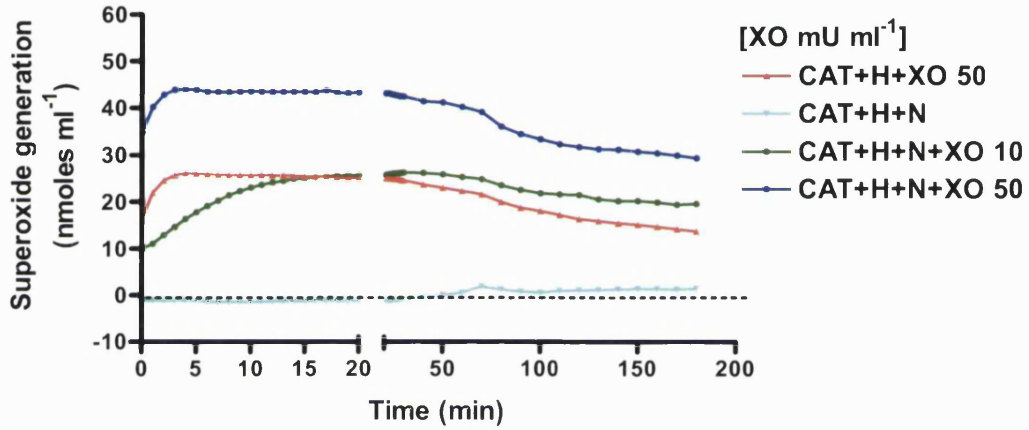

Figure 4.51 Timecourse of cytochrome *c* reduction by XO in air in LB with catalase.

Experiments were carried out in air using final concentrations of cytochrome *c* (50μM), hypoxanthine (H) (1mM), nitrite (N) (1mM), catalase (CAT) (100U ml^{-1}) and XO (0, 10 and 50mU ml^{-1}) diluted in bacterial culture medium (LB) for a 200μl final volume. Graph A shows a timecourse of cytochrome *c* reduction at 550nm over a 3 hour time period in a sealed 96-well plate at 37°C. Graph B shows a timecourse of superoxide generation (nmoles ml^{-1}) calculated from the raw data in graph A. Luria Broth wells were subtracted from the raw data before analysis. Mean bars were removed for clarity. n = 4.

Figure 4.52 A)

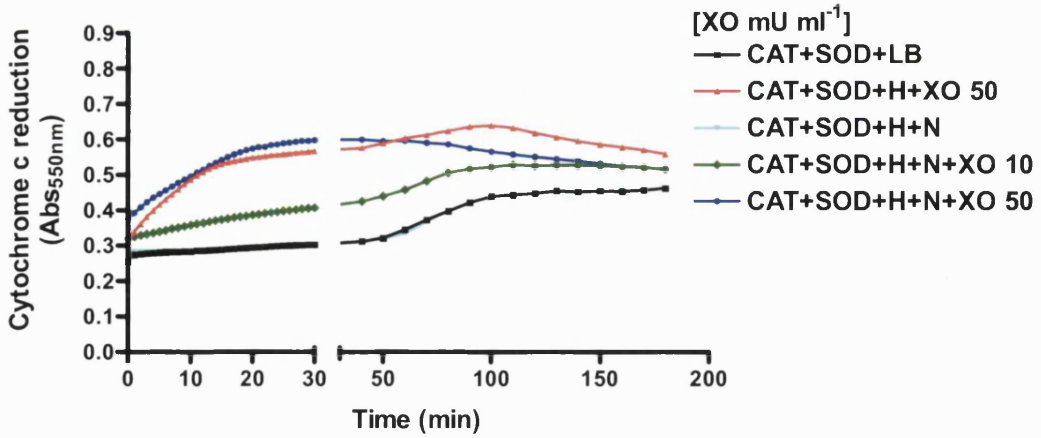

Figure 4.52 B)

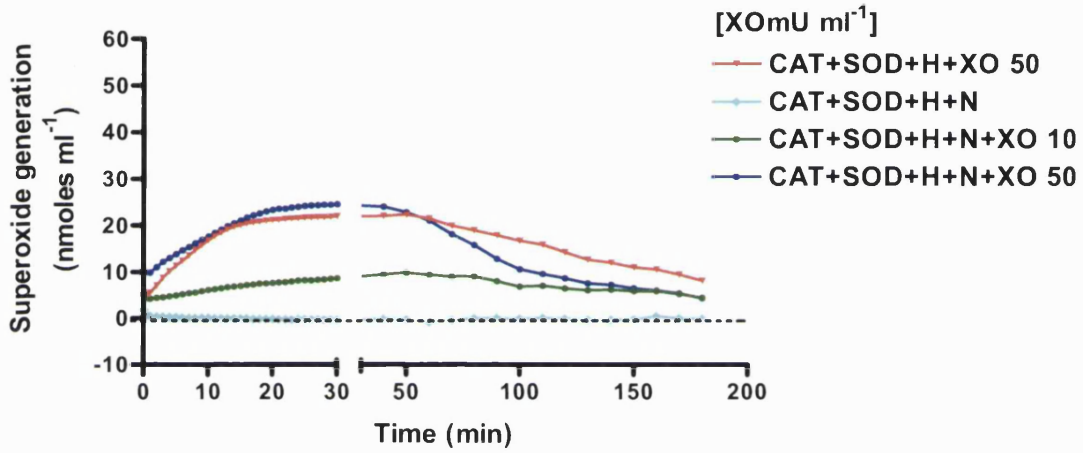

Figure 4.52 Timecourse of cytochrome *c* reduction by XO in air in LB with catalase and SOD.

Experiments were carried out in air using final concentrations of cytochrome *c* (50μM), hypoxanthine (H) (1mM), nitrite (N) (1mM), catalase (CAT) (100U ml^{-1}), SOD (50U ml^{-1}) and (0, 10 and 50mU ml^{-1}) XO diluted in bacterial culture medium (LB) for a 200μl final volume. Graph A shows a timecourse of cytochrome *c* reduction at 550nm over a 3 hour time period in a sealed 96-well plate at 37°C. Graph B shows a timecourse of superoxide generation (nmoles ml^{-1}) calculated from the raw data in graph A. Luria Broth wells were subtracted from the raw data before analysis. Mean bars were removed for clarity. n= 4.

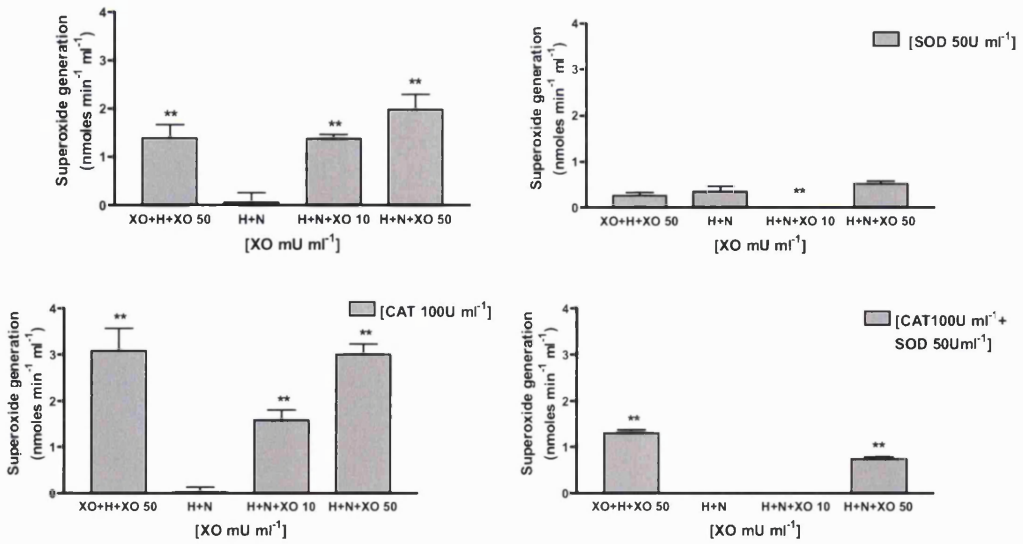

Figure 4.53 Initial rates of superoxide generation by XO in bacterial culture medium at 21% O_2.

This assay was carried out using final concentrations of cytochrome *c* (50μM), nitrite (N) (1mM), hypoxanthine (H) (1mM), SOD (50U ml^{-1}), catalase (CAT) (100U ml^{-1}) and XO at (0, 10, 50mU ml^{-1}) in bacterial culture medium (LB) for a 200μl final volume. The initial rate of superoxide generation was calculated using timecourse assays of superoxide generation (figure 4.49-52B). Statistical analysis used was One-way ANOVA with Dunnett's post test using H+N as the control. Mean±SD. n = 4.

4.3.2.1.4 Superoxide generation by XO in bacterial culture medium in 1% oxygen

The reduction of cytochrome *c* in bacterial culture medium (LB) at 1% oxygen showed a slight rate of reduction comparable to that shown in air. Addition of SOD and catalase had no effect on this rate (figure 4.54).

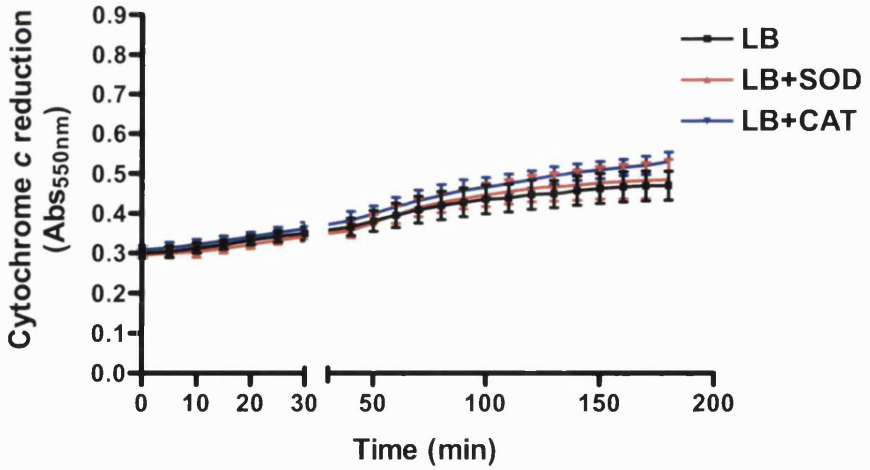

Figure 4.54Timecourse of cytochrome *c* reduction by bacterial culture medium in 1% oxygen.

Experiment was carried out in 1% oxygen using final concentrations of cytochrome *c* (50μM), SOD (50mU ml^{-1}) and catalase (CAT) (100mU ml^{-1}) diluted in bacterial culture medium (LB) for a 200μl final volume. Reduction of cytochrome *c* was followed at 550nm for 3 hours in a sealed 96-well plate at 37°C. Mean±SD. n = 8

Xanthine oxidase (50mU ml^{-1}) in LB without the addition of substrates is capable of the reduction of cytochrome *c* in 1% oxygen (figure 4.55), confirming that there are substrates in the LB that can be utilized by XO. However, this reduction is only slightly inhibited by SOD which suggests that the reduction of cytochrome *c* may be due to other XO-generated products, or that SOD has been inactivated or overwhelmed by XO generated products at 50mU ml^{-1}. As seen in previous assays catalase increases cytochrome *c* reduction suggesting that H_2O_2 is re-oxidising cytochrome *c*.

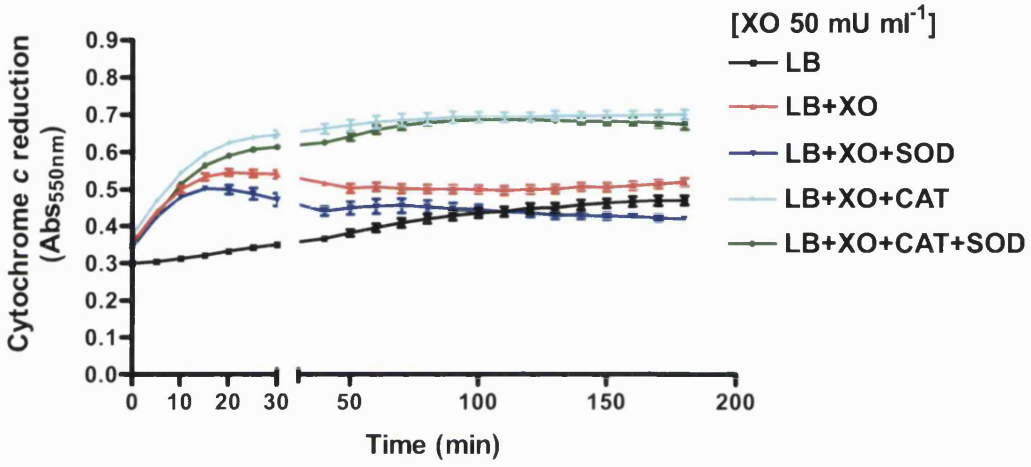

Figure 4.55 Timecourse of cytochrome *c* reduction by XO in 1% oxygen.

Experiment was carried out in 1% oxygen using final concentrations of cytochrome *c* (50µM), SOD (50mU ml^{-1}) and catalase (CAT) (250mU ml^{-1}) and XO (50mU ml^{-1}) diluted in bacterial culture medium (LB) for a 200µl final volume. Reduction of cytochrome *c* was followed at 550nm for 3 hours in a sealed 96-well plate at 37°C. Mean±SD. n = 8.

Assessments of $O_2^{\bullet-}$ generation by XO in 1% oxygen in LB in the absence of both SOD and catalase showed reduced rates of $O_2^{\bullet-}$ generation (figue 4.56) compared with in air (figure 4.49). Xanthine oxidase at 50mU ml^{-1} with hypoxanthine both with and without nitrite showed similar rates of reduction of cytochrome *c*, although reduction was slightly reduced in the presence of nitrite (Figure 4.56). This reduction of cytochrome *c* was not inhibited by SOD (Figure 4.57) which suggests that the reduction of cytochrome *c* in 1% LB is not due to $O_2^{\bullet-}$ generation. Addition of catalase slightly increases cytochrome *c* reduction which suggests that H_2O_2 is partially re-oxidising cytochrome *c* (figure 4.58), and addition of both catalase and SOD in figure 4.59, has no effect on the observed reduction of cytochrome *c*. Figure 4.60 show initial rates of cytochrome c reduction at 1% oxygen however, these rates are not SOD inhibitable so it is possible that they are not due to $O_2^{\bullet-}$ generation. Nevertheless, these rates are reduced when compared with at 21% oxygen in LB (figure 4.53).

Figure 4.56A)

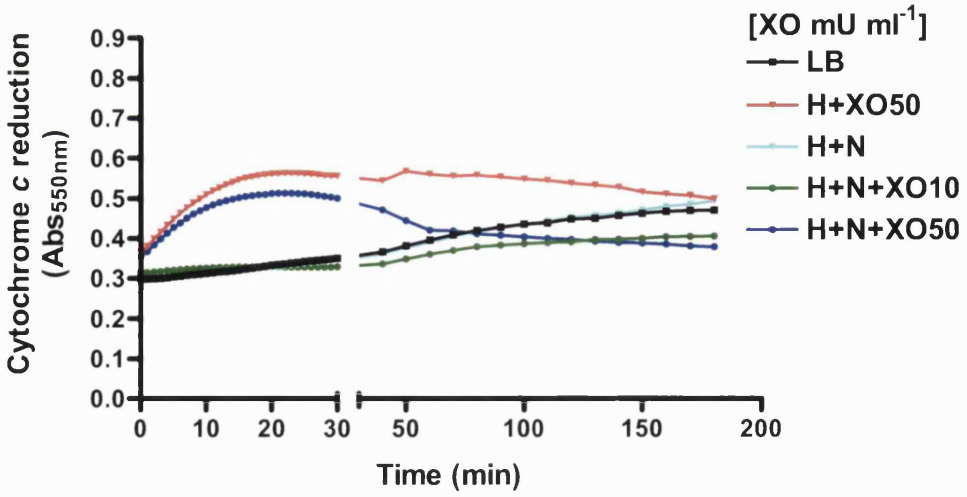

Figure 4.56B)

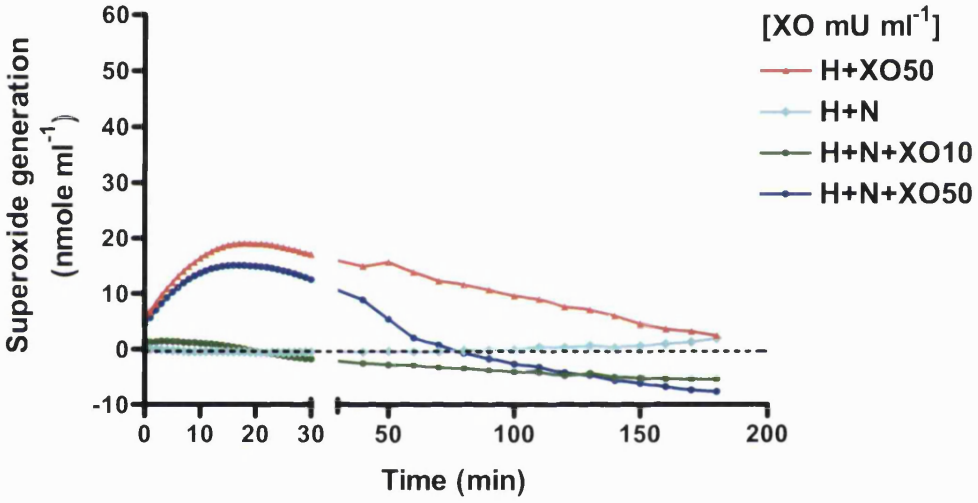

Figure 4.56 Timecourse of the reduction of cytochrome *c* by XO in LB at 1% O_2

Experiment was carried out in 1% oxygen using final concentrations of cytochrome *c* (50μM), nitrite (N) (1mM), hypoxanthine (H) (1mM) and XO at (0, 10 and 50mU ml^{-1}) diluted in bacterial culture medium (LB) for a 200μl final volume. Graph A shows a timecourse of cytochrome *c* reduction at 550nm over a 3 hour time period in a sealed 96-well plate at 37°C. Graph B shows a timecourse of superoxide generation (nmoles ml^{-1}) calculated from the raw data in graph A. LB only wells were subtracted from the raw data before analysis. Mean bars were removed for clarity. n = 8.

Figure 4.57 A)

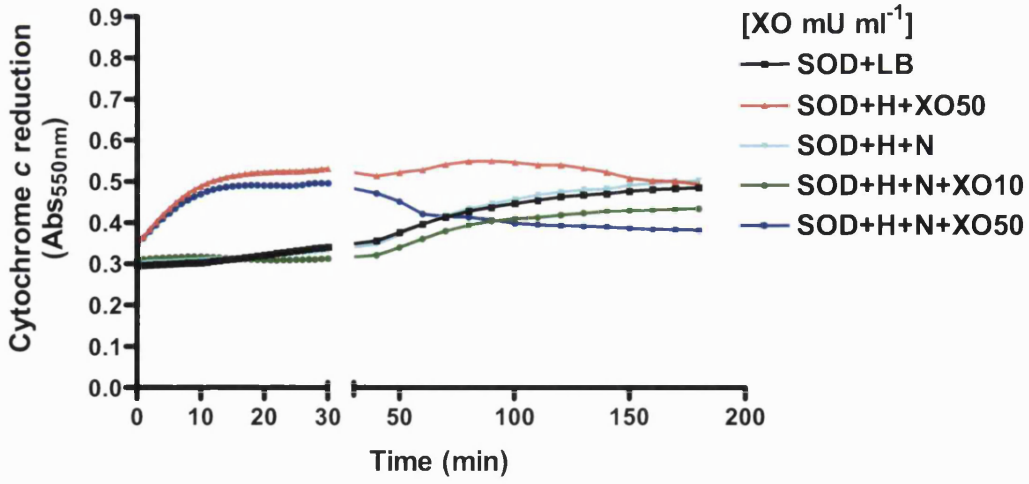

Figure 4.57 B)

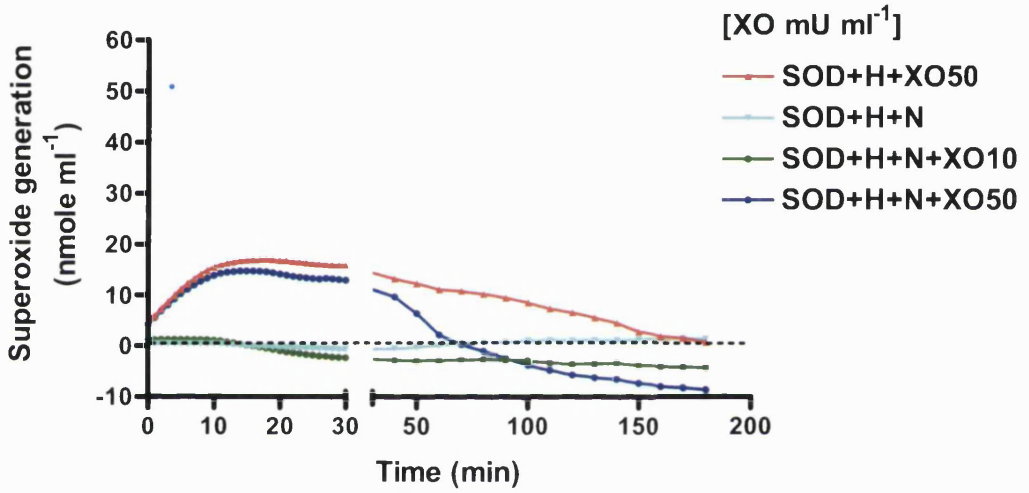

Figure 4.57 Timecourse of the reduction of cytochrome *c* by XO in LB at 1% O_2 with SOD

Experiment was carried out in 1% oxygen using final concentrations of cytochrome *c* (50µM), nitrite (N) (1mM), hypoxanthine (H) (1mM) XO at (0, 10 and 50mU ml^{-1}) and SOD (50U ml^{-1}) diluted in bacterial culture medium (LB) for a 200µl final volume. Graph A shows a timecourse of cytochrome *c* reduction at 550nm over a 3 hour time period in a sealed 96-well plate at 37°C. Graph B shows a timecourse of superoxide generation (nmoles ml^{-1}) calculated from the raw data in graph A as shown in the methods. LB only wells were subtracted from the raw data before analysis. Mean bars were removed for clarity. n = 8.

Figure 4.58 A)

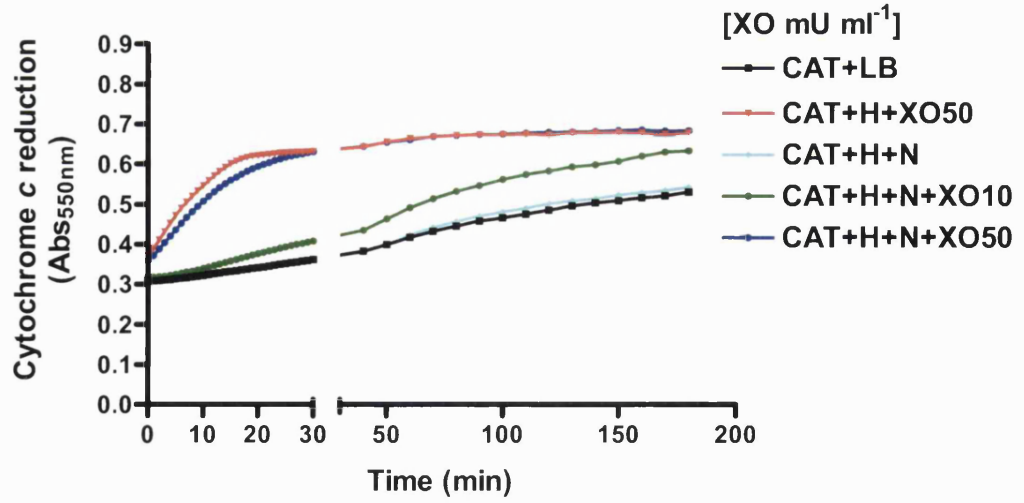

Figure 4.58 B)

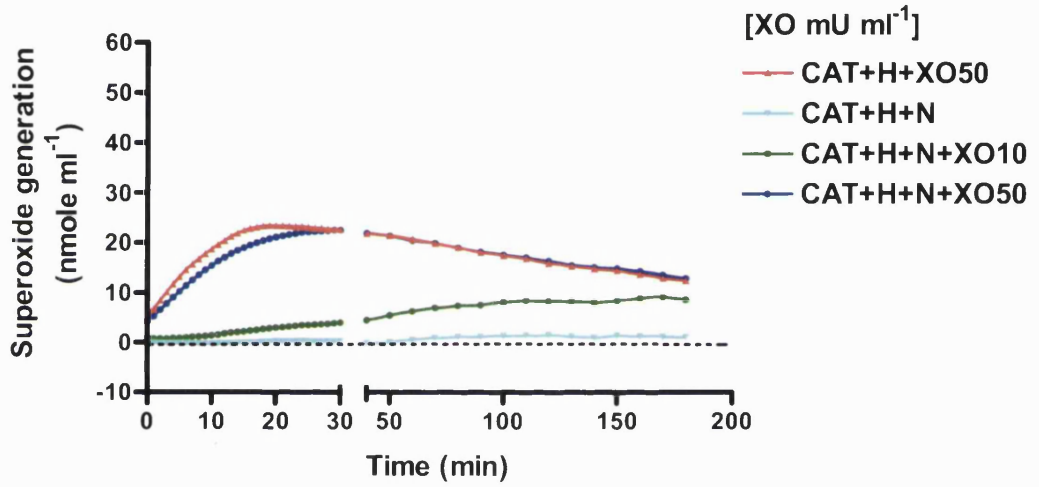

Figure 4.58 Timecourse of the reduction of cytochrome *c* by XO in LB at 1% O_2 with catalase

Experiment was carried out in 1% oxygen using final concentrations of cytochrome *c* (50μM), nitrite (N) (1mM), hypoxanthine (H) (1mM), XO at (0, 10 and 50mU ml^{-1}) and catalase (CAT) (250U ml^{-1}) diluted in bacterial culture medium (LB) for a 200μl final volume. Graph A shows a timecourse of cytochrome *c* reduction at 550nm over a 3 hour time period in a sealed 96-well plate at 37°C. Graph B shows a timecourse of superoxide generation (nmoles ml^{-1}) calculated from the raw data in graph A as shown in the methods. LB only wells were subtracted from the raw data before analysis. Mean bars were removed for clarity. n = 8.

Figure 4.59 A)

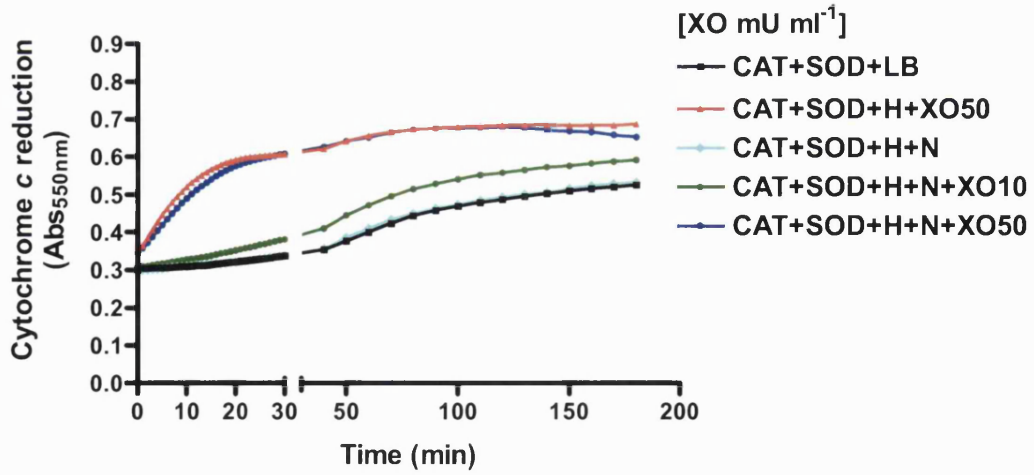

Figure 4.59 B)

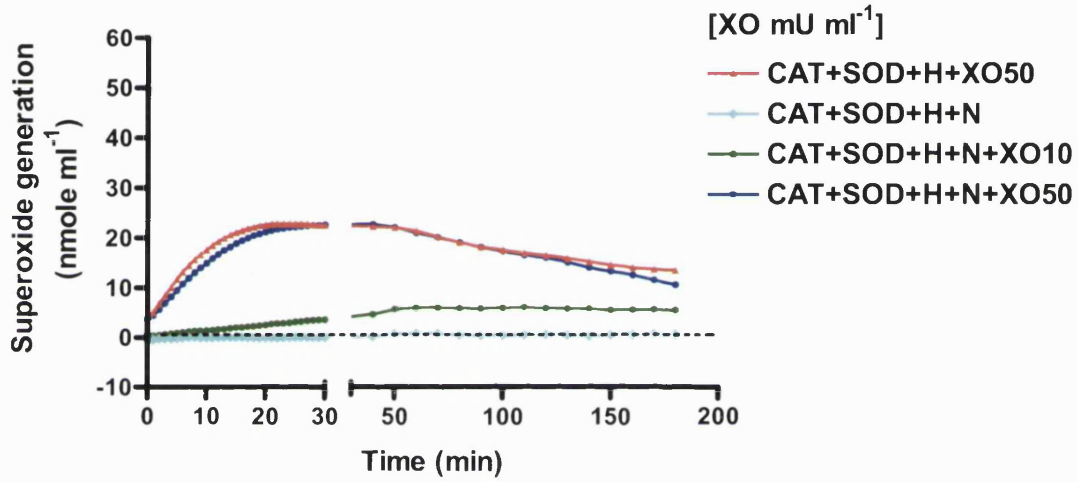

Figure 4.59 Timecourse of the reduction of cytochrome *c* by XO in LB at 1% Oxygen.

Experiment was carried out in 1% oxygen using final concentrations of cytochrome *c* (50μM), nitrite (N) (1mM), hypoxanthine (H) (1mM) XO at (0, 10 and 50mU ml^{-1}), catalase (CAT) (250U ml^{-1}) and SOD (50U ml^{-1}) diluted in bacterial culture medium (LB) for a 200μl final volume. Graph A shows a timecourse of cytochrome *c* reduction at 550nm over a 3 hour time period in a sealed 96-well plate at 37°C. Graph B shows a timecourse of superoxide generation (nmoles ml^{-1}) calculated from the raw data in graph A as shown in the methods. LB only wells were subtracted from the raw data before analysis. Mean bars were removed for clarity. n = 8.

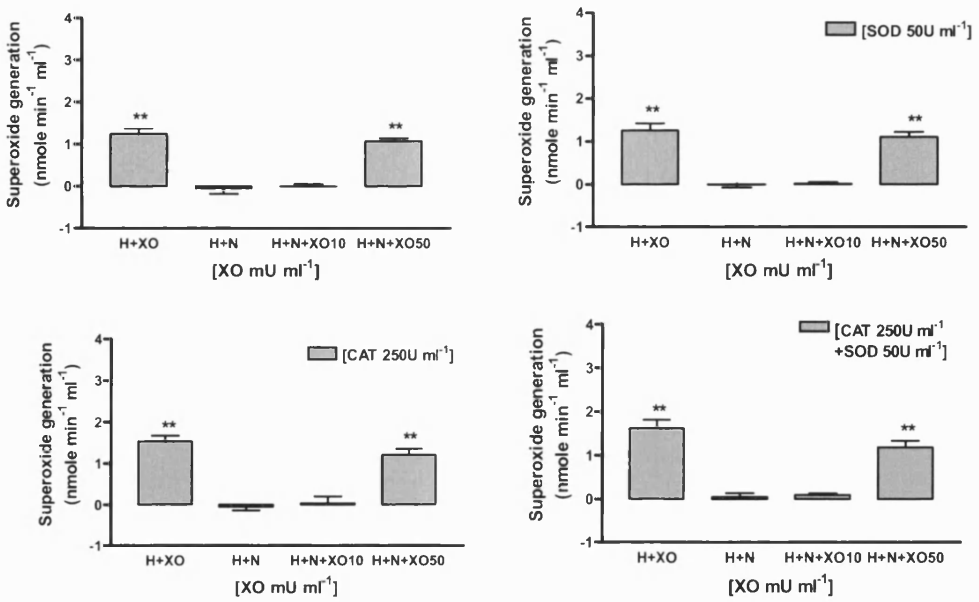

Figure 4.60 Initial rates of superoxide generation by XO in LB at 1% Oxygen.

Experiment was carried out in 1% oxygen using final concentrations of cytochrome *c* (50μM), nitrite (N) (1mM), hypoxanthine (H) (1mM), XO at (0, 10 and 50mU ml^{-1}) catalase (CAT) (250U ml^{-1}) and SOD (50U ml^{-1}) diluted in bacterial culture medium (LB) for a 200μl final volume. Initial rate of superoxide generation (nmole min^{-1} ml^{-1}) was calculated as shown in the methods using the timecourse data shown in figure 4.80-483. Mean±SD. n = 8.

4.3.2.1.5 Superoxide generation by XO in fibroblast culture medium in air

Cytochrome *c* assays were carried out in order to assess $O_2^{\bullet-}$ generation by XO when added to fibroblast culture medium (DMEM without phenol red, containing Penicillin/Streptomycin, L-Glutamine and FCS). Initial experiments in air were carried out in cuvettes to determine the levels of $O_2^{\bullet-}$ generated in conditions as close as possible to those that the dermal fibroblasts will be exposed in culture. Figure 4.61 shows that the fibroblast growth medium (DMEM without phenol red, containing 10% FCS, 1% L-Glutamine, and 1% FCS) reduces cytochrome *c*. Cytochrome *c* was reduced by fibroblast growth medium at a rate of approximately 0.005 Abs_{550nm} min^{-1}.

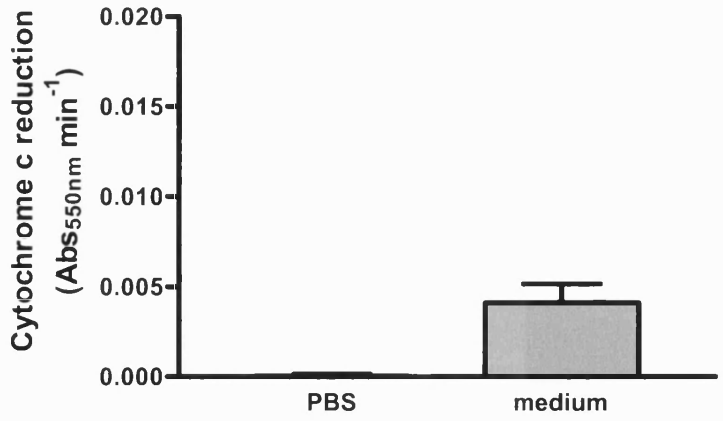

Figure 4.61 Rate of cytochrome *c* reduction by fibroblast growth medium.

Experiments were carried out in air using final concentrations of cytochrome *c* (50μM), and PBS or fibroblast growth medium (DMEM without phenol red, 10% FCS, 1% Penicillin and Streptomycin, 1% L-Glutamine) in a 3ml final volume at 37°C. The initial rate of change in absorbance was calculated from the raw absorbance data (Abs_{550nm} min^{-1}). The experiment was carried out on three separate occasions. Mean±SD. PBS n = 8, medium n = 12.

Allopurinol and SOD were also added to the assay in order to determine whether the reduction of cytochrome *c* by fibroblast growth medium was due to XO present in the FCS or by $O_2^{\bullet-}$ generation in the medium. Cytochrome *c* reduction by fibroblast growth medium is not inhibited by allopurinol or SOD (Figure 4.62), suggesting that the cytochrome *c* reduction is not due to the presence of XO or $O_2^{\bullet-}$ generation in fibroblast growth medium.

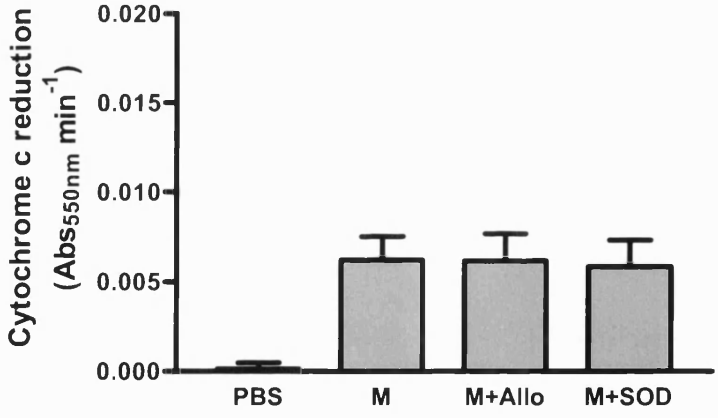

Figure 4.62 Reduction of cytochrome *c* by fibroblast growth medium.

Experiments were carried out using cytochrome *c* (50μM), allopurinol (100μM), SOD (70U ml^{-1}) diluted in fibroblast growth medium (DMEM 10% FCS, 1% PS, 1% LG) for a 3ml final volume at 37°C. Mean±SD PBS, Fibroblast growth medium (M) and M + allopurinol (Allo) n = 5, M+SOD n = 4.

The experiment in figure 4.63 was carried out to determine which of the fibroblast growth medium additions were responsible for the reduction of cytochrome *c*. This figure

shows that DMEM alone reduces cytochrome *c*, however, this rate is increased with the addition of penicillin/streptomycin and FCS. The addition of L-Glutamine to the DMEM does not appear to affect the rate of cytochrome *c* reduction.

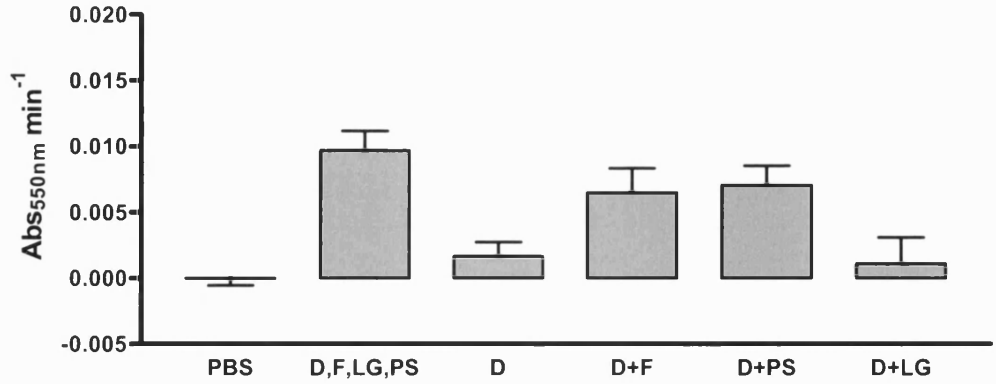

Figure 4.63 Reduction of cytochrome *c* by varying components of fibroblast culture medium.

Experiment was carried out using cytochrome *c* (50μM), DMEM without phenol red (D), 10% FCS (F), 1% Penicillin streptomycin (PS), 1% L-Glutamine (LG). Mean±SD. PBS n = 5. D, F, LG, PS n = 7. D n = 3. D+F and D+PS n = 4. D+LG n = 3.

A brief investigation was also carried out in which the fibroblast growth medium was sterile filtered as it would be before addition to cell culture to see if this filtering process had any effect on the reduction of cytochrome *c* (Figure 4.64). Figure 4.64 shows that there is no difference between sterile filtered and unfiltered medium in the rate of reduction of cytochrome *c*.

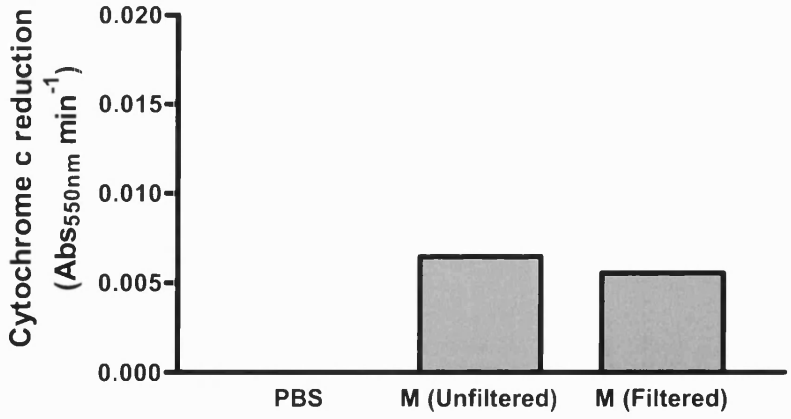

Figure 4.64 Reduction of cytochrome *c* by sterile filtered and unfiltered medium.

Experiments were carried out using cytochrome *c* (50μm), and fibroblast growth medium (M) (DMEM without phenol red, 10% FCS, 1% Penicillin and Streptomycin, 1% L-Glutamine) in a 3ml final volume. n = 1.

Experiments also show that DMEM with XO does not appear to reduce cytochrome *c* above the levels seen with DMEM alone (Figure 4.65). Suggesting that

substrates for XO are not present in DMEM; therefore XO can be diluted in DMEM before addition into the reaction mix.

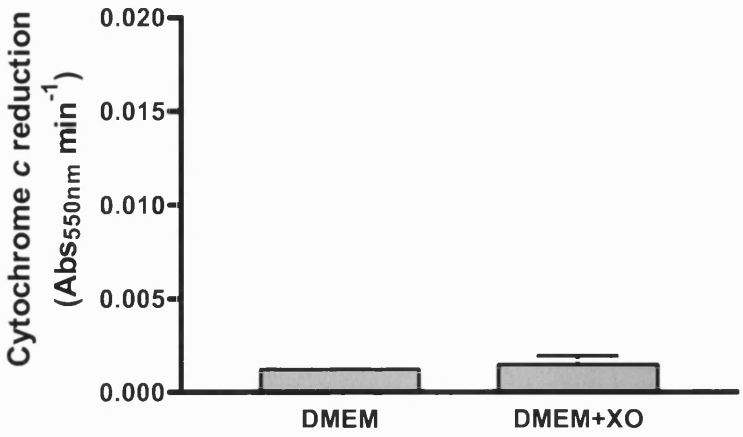

Figure 4.65 Reduction of cytochrome *c* by XO in DMEM.

Experiments were carried out using cytochrome *c* (50μM), and XO (1mU ml^{-1}) diluted DMEM (without phenol red) for a final volume of 3mls. Mean±SD. DMEM n = 1, DMEM + 1mU ml^{-1} XO, n = 3.

Figure 4.66 shows a comparison of the reduction of cytochrome *c* by XO and hypoxanthine in PBS and fibroblast growth medium. The rate of reduction of cytochrome *c* by XO and hypoxanthine is greater in PBS than in fibroblast growth medium (Figure 4.66). Furthermore, cytochrome *c* reduction in the media with hypoxanthine was found to be not significantly different compared with media alone. This suggests that there is no measurable XO activity in the FCS and is therefore used as a control in the subsequent experiments.

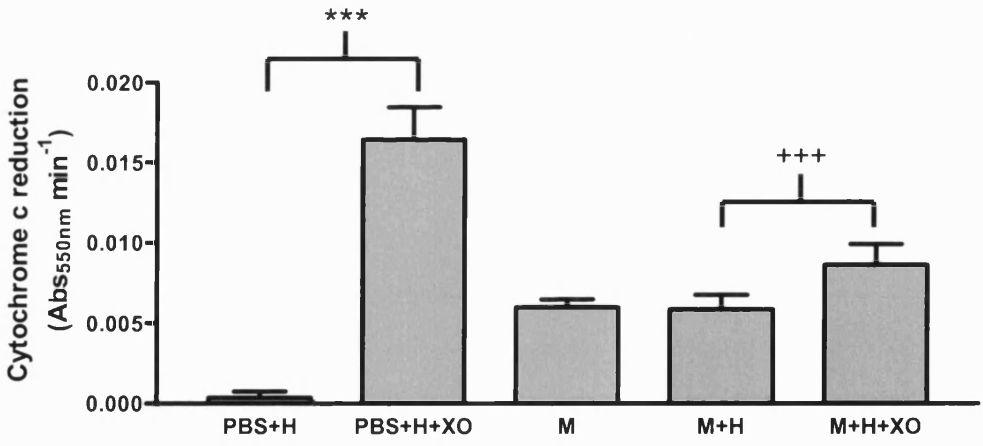

Figure 4.66 Reduction in XO activity in fibroblast growth medium.

Experiments were carried out using cytochrome (50μM), HEPES (20mM), XO (1mU ml^{-1}), Hypoxanthine (H) (1mM), diluted in PBS or fibroblast growth medium (DMEM without phenol red, 10% FCS, 1% Penicillin and Streptomycin, 1% L-Glutamine) (M) for a 3ml final volume at 37°C. Mean±SD. PBS+H n = 5, XO+PBS+H n = 8, MEDIA and MEDIA+H n = 6, XO+MEDIA+H n = 8. Statistical analysis was performed using a two-tailed unpaired t-test. *** P<0.001. PBS+H was used as a control for PBS+H+XO (*) and M was used as a control for M+H (NS). M+H was used as a control for M+H+XO (+)

Further assays to determine whether the FCS addition to the fibroblast culture medium was responsible for the reduced rate of cytochrome *c* reduction by XO observed in fibroblast culture medium compared with PBS. Figure 4.67 shows that decreasing the FCS concentration of the fibroblast growth medium has no affect on the rate of cytochrome *c* reduction when compared with the no enzyme media control. This result suggests that the reduced rate of cytochrome *c* reduction by XO in fibroblast growth medium is not due to $O_2^{\bullet-}$ scavengers, such as SOD, or XO inhibitors present in the FCS.

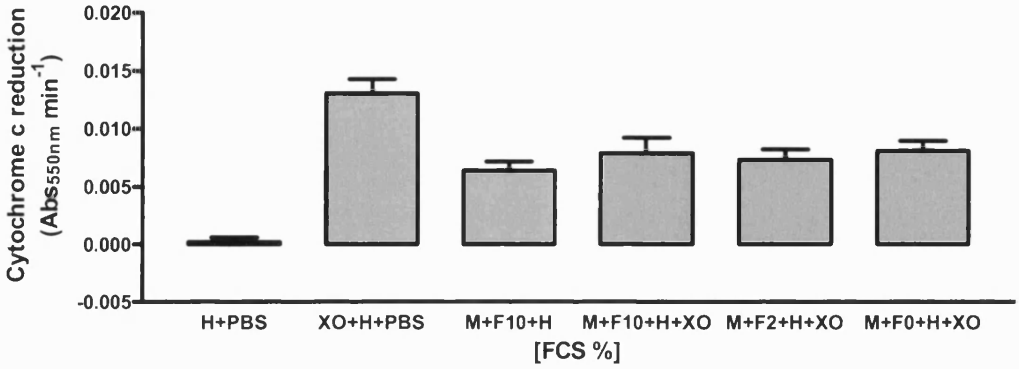

Figure 4.67 Initial rates of cytochrome *c* reduction by XO in fibroblast medium with varying FCS concentration.

Experiments were carried out using cytochrome (50μM), XO (1mU ml^{-1}), hypoxanthine (H) (1mM), HEPES (20mM) diluted in PBS or fibroblast growth medium with FCS at 0, 2, and 10% for a 3ml final volume at 37°C. Mean±SD. n = 6 apart from XO+H+PBS n = 5.

The SOD-inhibitable portion was used to determine $O_2^{\bullet-}$ generation by XO in fibroblast culture medium in air. Figure 4.70A and B show that compared with the hypoxanthine control, cytochrome *c* reduction is increased with increasing XO concentration at 0.5 and 1mU ml^{-1} XO. These rates are also SOD inhibitable which suggests that the rates are due to XO-generated $O_2^{\bullet-}$. Figure 4.70C) shows the SOD-inhibitable rate of $O_2^{\bullet-}$ generation at 0.5 and 1mU ml^{-1} XO in air in fibroblast growth medium. At a concentration of 0.5mU ml^{-1}, XO generated 0.056nmoles min^{-1} ml^{-1} $O_2^{\bullet-}$, and at 1mU ml^{-1} XO generated 0.158nmoles min^{-1} ml^{-1} $O_2^{\bullet-}$.

Figure 4.68 A)

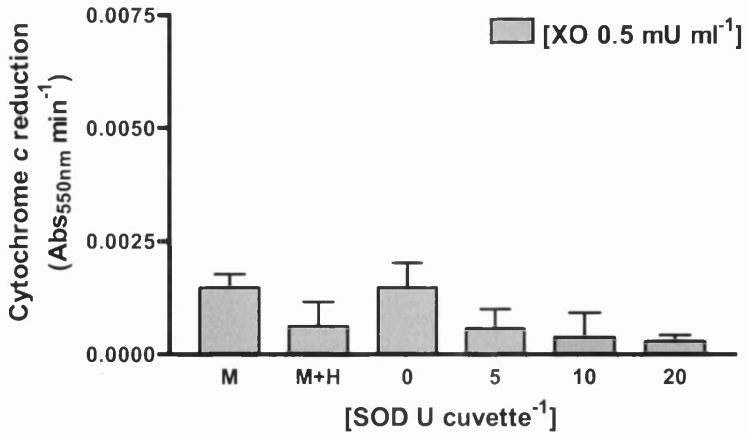

Figure 4.68 B)

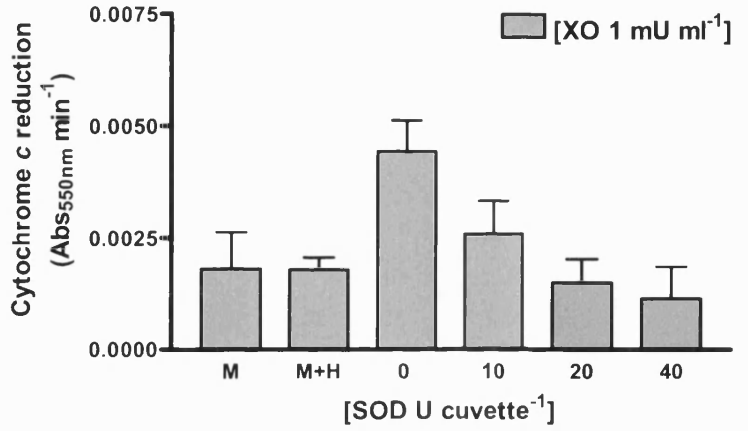

Figure 4.68 C)

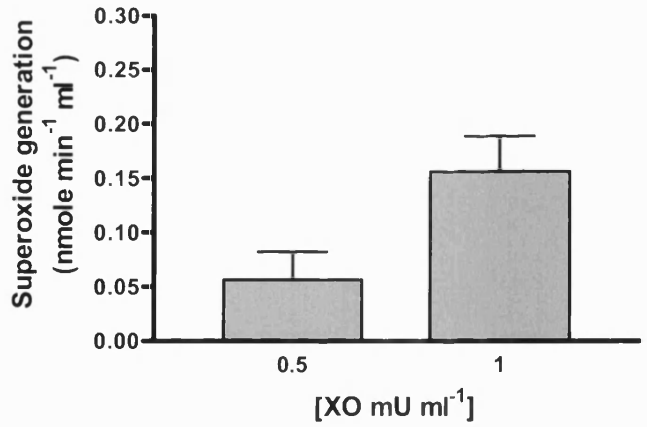

Figure 4.68 The SOD-inhibitable rates of superoxide generation by XO.

Experiments were carried out in air using cuvettes containing cytochrome (50μM), hypoxanthine (H) (1mM), HEPES (20mM) and XO diluted in fibroblast growth medium (M=DMEM without phenol red, Penicillin/Streptomycin, L-Glutamine, and 10% FCS) for a 3ml final volume at 37°C. Graph A shows the rate of cytochrome *c* reduction by 0.5mU ml^{-1} XO and inhibition with SOD (0, 5, 10, 20U $cuvette^{-1}$). Graph B shows the rate of cytochrome *c* reduction by 1mU ml^{-1} XO and inhibition with SOD (0, 10, 20, 40U $cuvette^{-1}$). Graph C shows the SOD inhibitable portion of the rate of superoxide generation with XO at (0.5 and 1mU ml^{-1}) Mean±SD. 0.5mU ml^{-1} XO: n = 3. 1mU ml^{-1} XO: M n = 6, M+H n = 2, 0 n = 4, 10 n = 5, 20 n = 5, 40 n = 5.

4.3.2.1.6 Superoxide generation by XO fibroblast culture medium in 1% oxygen

Experiments were carried out at 1% oxygen with varying concentrations of XO in fibroblast culture medium and cytochrome *c* reduction was followed for 3 hours. The graphs below show that fibroblast culture medium alone gradually reduces cytochrome *c* at 1% oxygen over 3 hours (Figure 4.69) addition of SOD (Figure 4.70) and catalase (Figure 4.71) to the culture medium does not affect the rate of reduction of the cytochrome *c* in medium alone suggesting that the reduction is not due to $O_2^{\bullet -}$ or H_2O_2 generation in the medium. Without the addition of inhibitors (Figure 4.69) there does not appear to be an increased rate of cytochrome *c* reduction in the presence of between 0-5mU ml^{-1} XO. There appears to be a slight rate of reduction in the presence of 50mU ml^{-1} XO which is absent in the presence of SOD (Figure 4.70). The rate of cytochrome *c* reduction at 50mU ml^{-1} is slightly increased in the presence of catalase (Figure 4.71) but this rate does not appear to be inhibited in the presence of both catalase and SOD (Figure 4.72). The rate of cytochrome *c* reduction at 0-50mU ml^{-1} XO in the absence or presence of SOD is not statistically significant when compared with the no enzyme control (figure 4.73). However, in the presence of catalase and with both catalase and SOD the reduction of cytochrome *c* at 50mU ml^{-1} XO is statistically significant when compared with the no enzyme control (Figure 4.73). However, overall the reduction of cytochrome *c* is low in 1% O_2 in the presence of 0-50mU ml^{-1} XO.

Figure 4.69-4.73

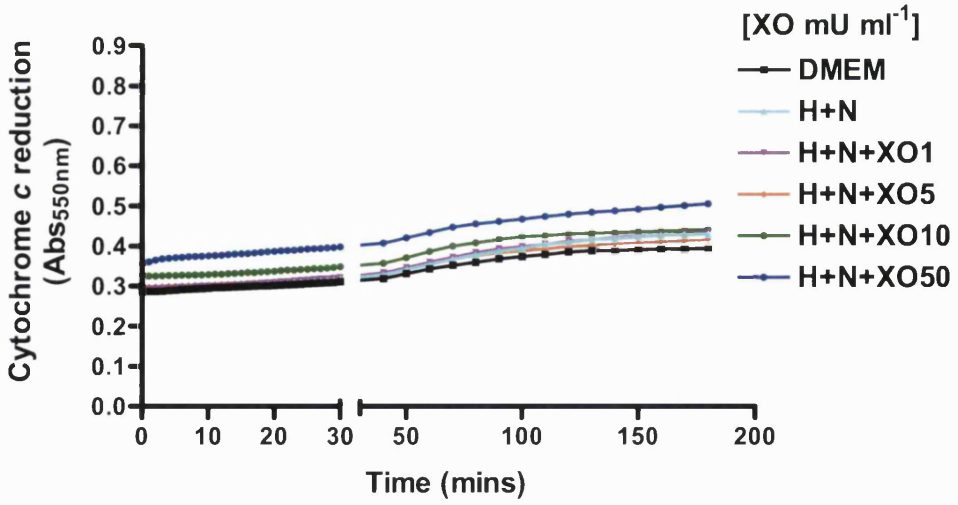

Figure 4.69 Timecourse of cytochrome *c* reduction in fibroblast medium by XO in 1% oxygen

DMEM without phenol red was placed in the hypoxia cabinet set at 1% oxygen. 5% FCS, 1% P/S, and 1% L-Glutamine was added the following morning. 20% more of each was added to account for dilution of XO and cytochrome *c* in PBS equilibrated overnight at 1% oxygen. Final concentrations of XO (0, 1, 5, 10, 50mU ml^{-1}), hypoxanthine (H) (1mM) and nitrite (N) (1mM) were used. Reduction of cytochrome *c* was followed at 550nm for 3 hours in a 96-well plate. This experiment was carried out on two separate occasions in quadruplicate. n = 8. Mean bars were removed for clarity.

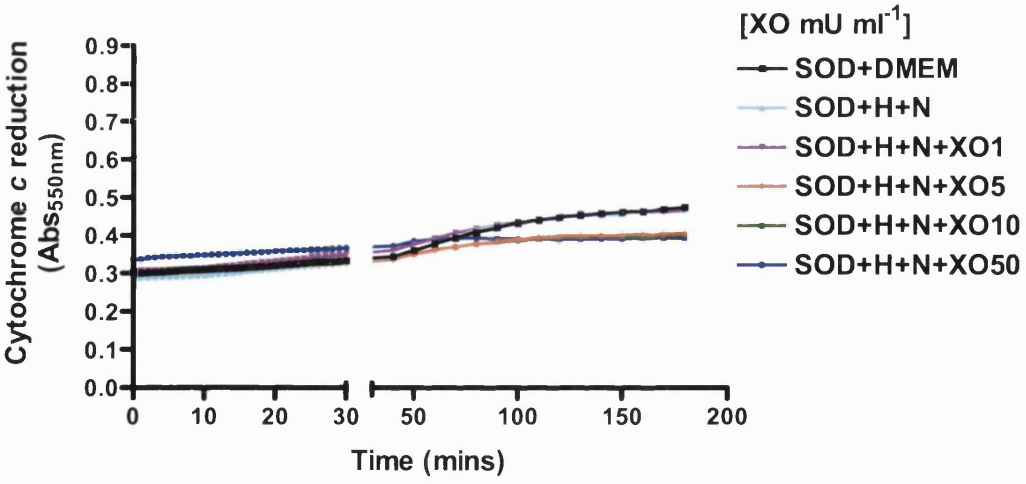

Figure 4.70 Timecourse of cytochrome *c* reduction in fibroblast medium by XO in 1% oxygen with SOD

DMEM without phenol red was placed in the hypoxia cabinet set at 1% oxygen. 5% FCS, 1% PS, and 1% L-Glutamine was added the following morning. 20% more of each was added to account for dilution of XO and cytochrome *c* in PBS equilibrated overnight at 1% oxygen. Final concentrations of SOD (50mU ml^{-1}), XO (0, 1, 5, 10, 50mU ml^{-1}), hypoxanthine (H) (1mM) and nitrite (N) (1mM) were used. Reduction of cytochrome *c* was followed at 550nm for 3 hours in a 96-well plate. This experiment was carried out on two separate occasions in quadruplicate. n = 8. Mean bars were removed for clarity.

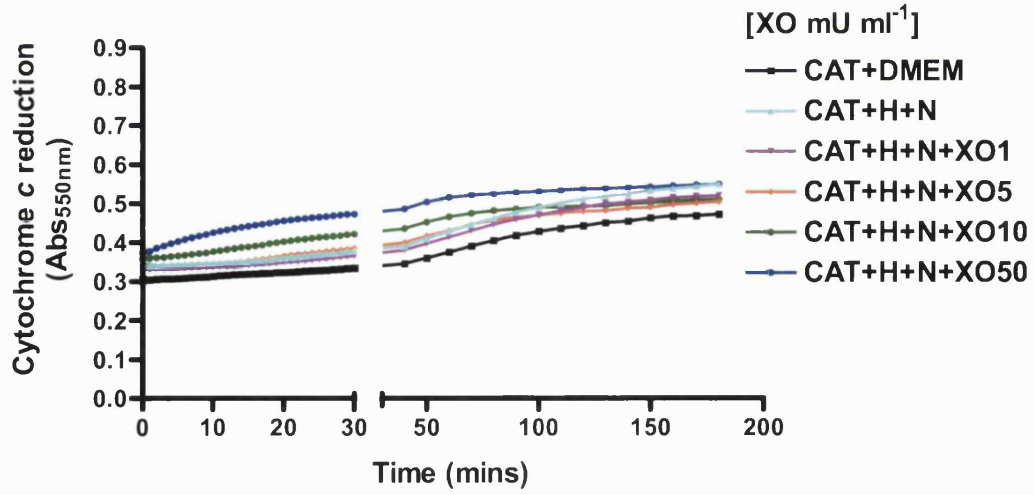

Figure 4.71 Timecourse of cytochrome *c* reduction in fibroblast medium by XO in 1% oxygen with catalase

DMEM without phenol red was placed in the hypoxia cabinet set at 1% oxygen. 5% FCS, 1% P/S, and 1% L-Glutamine was added the following morning. 20% more of each was added to account for dilution of XO and cytochrome *c* in PBS equilibrated overnight at 1% oxygen. Final concentrations of catalase (CAT) (250mU ml^{-1}), XO (0, 1, 5, 10, 50mU ml^{-1}), hypoxanthine (H) (1mM) and nitrite (N) (1mM) were used. Reduction of cytochrome *c* was followed at 550nm for 3 hours in a 96-well plate. This experiment was carried out on two separate occasions in quadruplicate. n = 8. Mean bars were removed for clarity.

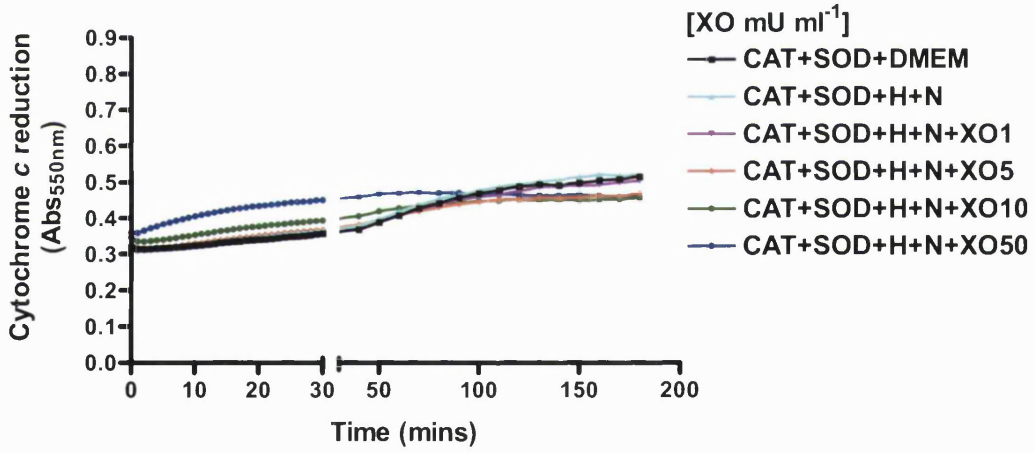

Figure 4.72 Timecourse of cytochrome *c* reduction in fibroblast medium by XO in 1% oxygen with catalase and SOD

DMEM without phenol red was placed in the hypoxia cabinet set at 1% oxygen. 5% FCS, 1% P/S, and 1% L-Glutamine was added the following morning. 20% more of each was added to account for dilution of XO and cytochrome *c* in PBS equilibrated overnight at 1 % oxygen. Final concentrations of SOD (50mU ml^{-1}), catalase (CAT) (250mU ml^{-1}), XO (0, 1, 5, 10, 50mU ml^{-1}), hypoxanthine (H) (1mM) and nitrite (N) (1mM) were used. Reduction of cytochrome *c* was followed at 550nm for 3 hours in a 96-well plate. This experiment was carried out on two separate occasions in quadruplicate. n=8. Mean bars were removed for clarity.

The rate of $O_2^{\bullet -}$ generation was also assessed and presented as bar graphs below (Figure 4.54).

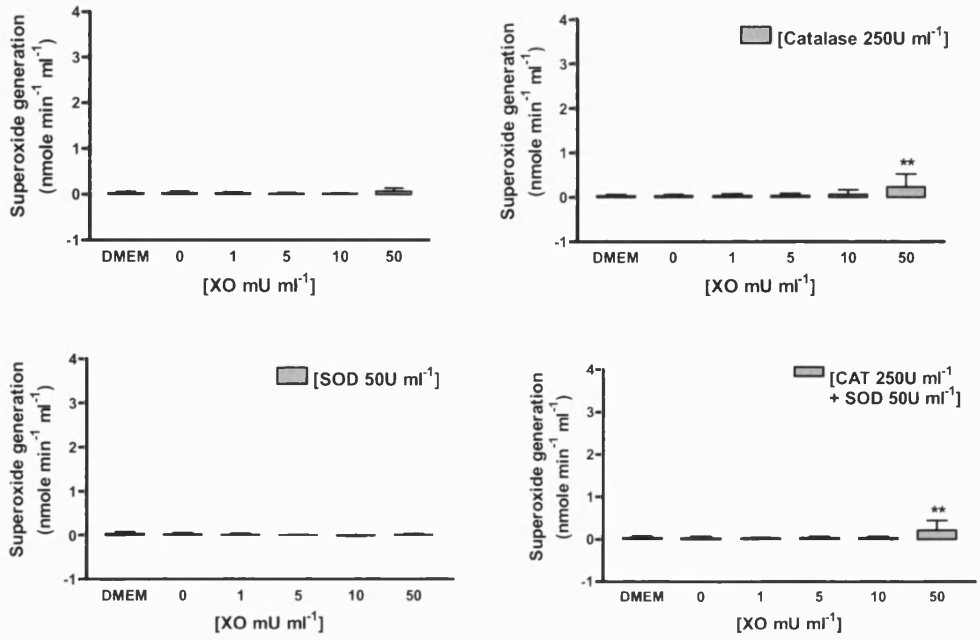

Figure 4.73 Initial rates of superoxide generation by XO in fibroblast medium at 1% oxygen with catalase and SOD.

DMEM without phenol red was placed in the hypoxia cabinet set at 1% oxygen. 5% FCS, 1% P/S, and 1% L-Glutamine was added the following morning. 20% more of each was added to account for dilution of XO and cytochrome *c* in PBS equilibrated overnight at 1% oxygen. Each assay was carried out with and without the addition of SOD (50mU ml^{-1}) and catalase (CAT) (250mU ml^{-1}). XO was used at (0, 1, 5, 10, 50mU ml^{-1}) with hypoxanthine (1mM) and nitrite (1mM). These graphs show the combined data from experiments carried out on two separate occasions (figure 4.91-4.95). n = 8. Statistical analysis using One-way ANOVA with Dunnett's post test using 0mU ml^{-1} XO as the control.

4.3.2.2 Oxidation of dihydrorhodamine for peroxynitrite generation by XO

4.3.2.2.1 Oxidation of dihydrorhodamine by SIN-1

The oxidation of dihydrorhodamine to rhodamine was used to measure the levels of $ONOO^-$ generated at varying concentrations of XO. Preliminary experiments were carried out using the $ONOO^-$ generator 3-morpholinosydononimine (SIN-1) to check that the assay was working. SIN-1 is a compound that releases $ONOO^-$, and is thought to generate equimolar amounts of $O_2^{\bullet-}$and $^{\bullet}NO$, which rapidly react to form $ONOO^-$. Assays were carried out in 3ml cuvettes. A comparison was made between a 2ml and a 3ml reaction volume in a 3ml cuvette to determine whether the absorbance values using a more economical 2ml reaction volume are the same as in a 3ml reaction volume. The absorbance values using either a 2ml or a 3ml reaction volume are identical therefore; the 2ml reaction volume is suitable for subsequent experiments (figure 4.74).

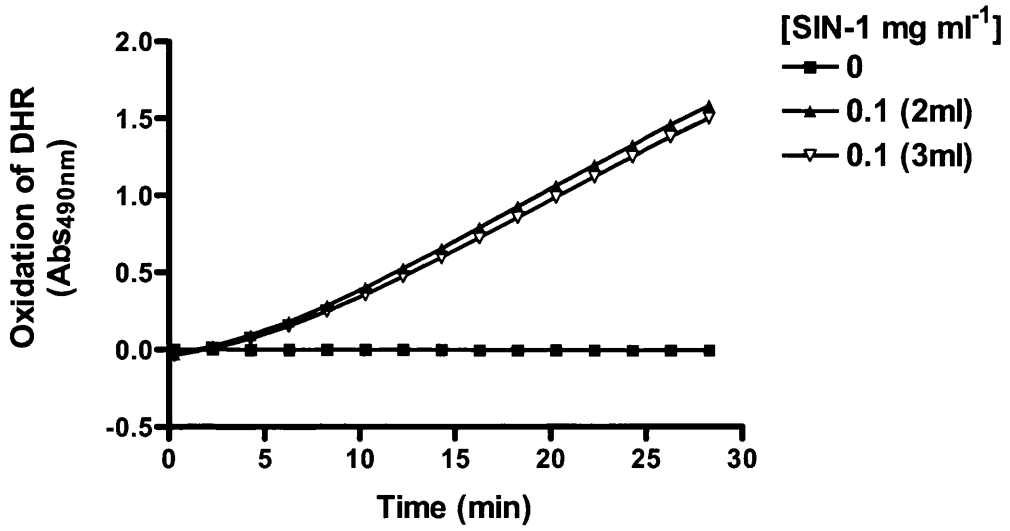

Figure 4.74 Oxidation of DHR using a 2ml or a 3ml reaction volume in a 3ml cuvette.

Experiment was carried out using a final concentration of SIN-1 at (0.1mg ml^{-1} or 5000μM), DHR (0.1mM), DTPA (0.1mM) in 2ml or a 3ml final volume in 3ml cuvettes at 37°C. Readings were taken every 30 sec however; only 2 min readings are shown on the graph for clarity. n = 1.

To reduce the assay volume further, and increase the sample number, a 96-well plate assay was also developed. However, the 96-well plate reader had a 490nm filter but not a 500nm filter. Therefore, a wavelength scan was carried out in a cuvette using the spectrophotometer (HITACHI) to assess whether 490nm would be an acceptable measuring wavelength (Figure 4.75). The absorbance peak of oxidized DHR is at 500nm (Figure 4.75 B) and 490nm falls on the shoulder of the peak. Therefore at this wavelength the absorbance is slightly reduced by an average of 23.2% when compared with 500nm. Therefore, it is possible to use the 490nm filter to follow the oxidation of DHR but the absorbance values will need to be increased by 23.2% to correct for this difference (Table 4.3).

Figure 4.75 A)

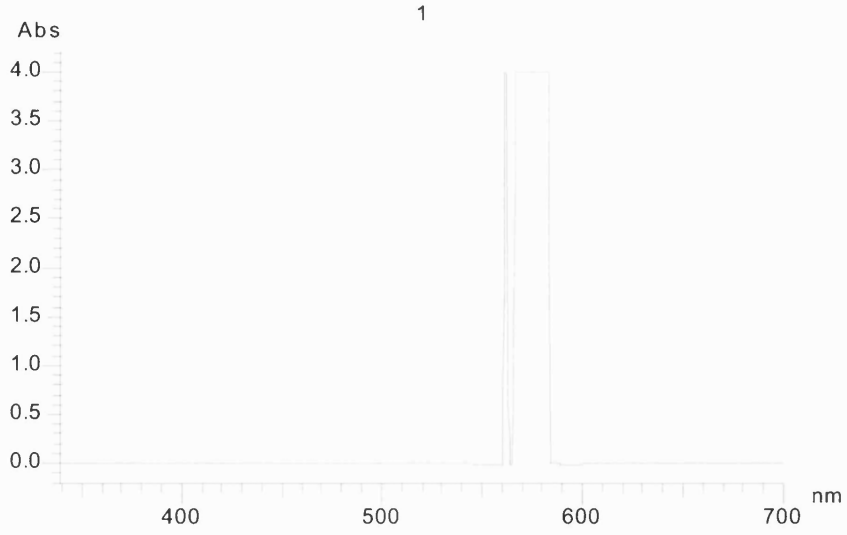

Figure 4.75 B)

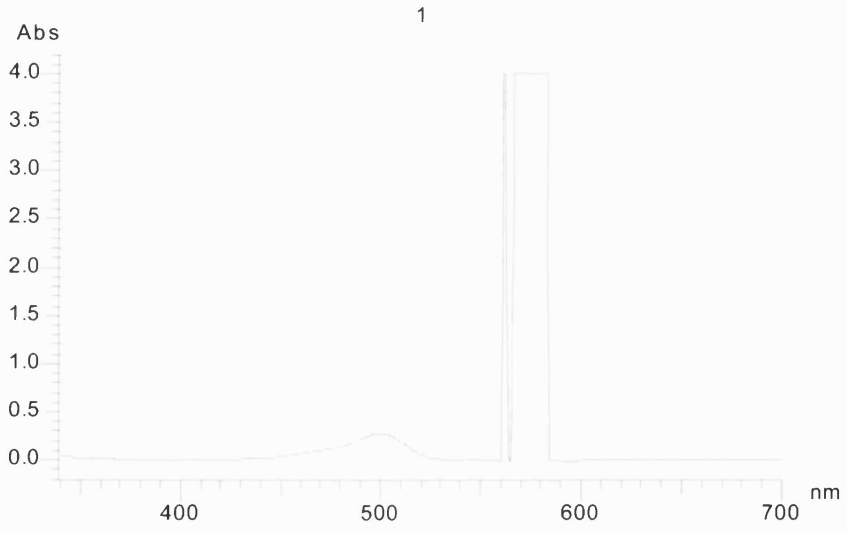

Figure 4.75 Wavelength scan of the oxidation of DHR.

Wavelength scans were carried out using final concentrations of DHR (0.1mM), DTPA (0.1mM) with and without SIN-1 (500μM) in a final volume of 2ml PBS at 37°C using the HITACHI spectrophotometer. Start wavelength 700nm finish wavelength 340nm scan speed 800nm per minute. Graph A shows a wavelength scan of unoxidised DHR: No SIN-1 (n = 1). Graph B shows an example of a wavelength scan of DHR oxidised by SIN-1 (n = 3).

	Abs 500 nm	Abs 490 nm	Reduction in abs at 490nm compared with 500nm (%)
1)Unoxidised DHR –No SIN-1	0.006	0.006	0
2) Oxidised DHR – SIN-1	0.085	0.065	23.5
3) Oxidised DHR – SIN-1	0.098	0.075	23.5
4) Oxidised DHR – SIN-1	0.280	0.217	22.5

Table 4.3Absorbance values at 500nm and 490nm and percentage change in absorbance

SIN-1 at a range of concentrations was added to a 96-well plate and the absorbance change at 490nm followed in a spectrophotometer. Figure 4.76 shows the absorbance over time for SIN-1 at a range of concentrations.

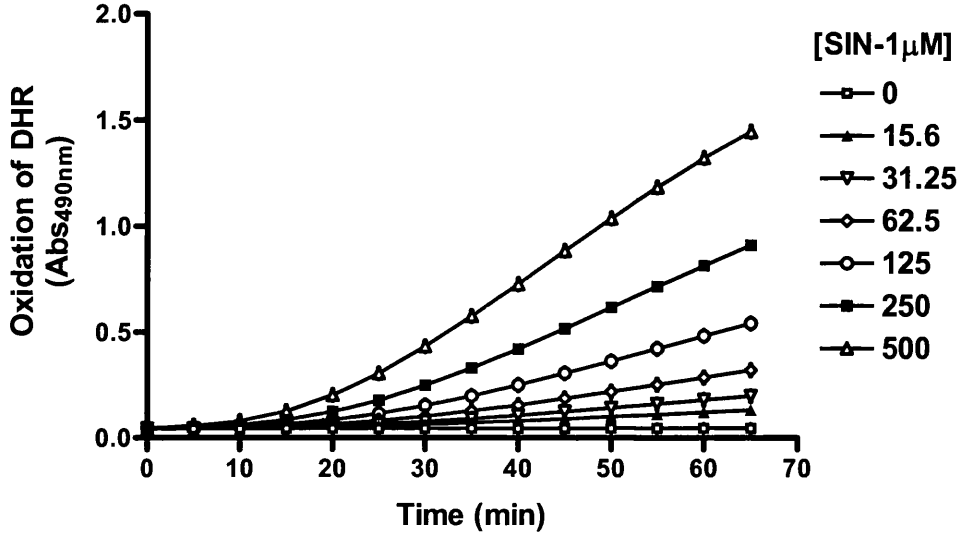

Figure 4.76 Oxidation of DHR at varying concentrations of SIN-1.

DHR (0.1mM), DTPA (0.1mM), SIN-1 (0, 15.6, 31.25, 62.5, 125, 250, 500μM) made up to a final volume of 200μl with PBS at 37°C. Absorbance readings were taken every minute for 70mins. The data for every 5 minute interval up to 65min are shown on this graph for clarity. Mean±SD. n = 3.

The dose dependent increase in absorbance overtime in the presence of SIN-1 follows sigmoidal kinetics in the highest concentration range (Figure 4.77). There is an initial lag phase in DHR oxidation to rhodamine followed by an increasing rate of change in absorbance until a plateau in reached. The fastest rate of change in absorbance was measured and the rate of generation of $ONOO^-$ calculated using the extinction coefficient of $75000M^{-1}$ cm^{-1} for the oxidation of DHR by $ONOO^-$ and a correction factor of 2.2 as the efficiency of oxidation is ~45 % (Crow, 1997) (Figure 4.77).

Figure 4.77 A)

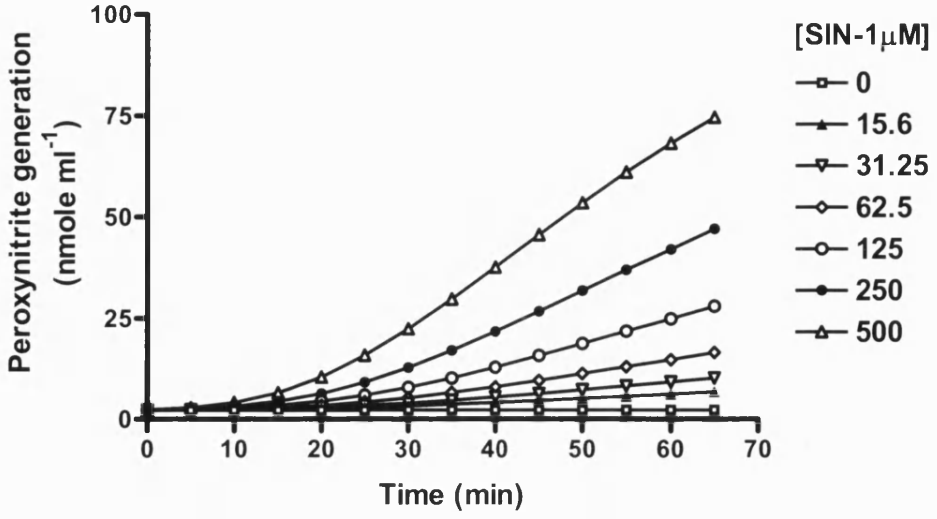

Figure 4.77 B)

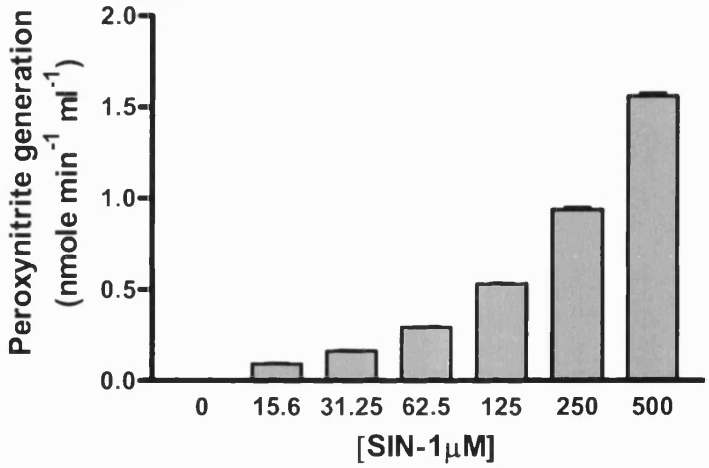

Figure 4.77 Peroxynitrite generation at varying concentrations of SIN-1.

Experiments were carried out using DHR (0.1mM), DTPA (0.1mM) and SIN-1 at (0, 15.6, 31.25, 62.5, 125, 250, 500μM) made up to a final volume of 200μl with PBS at 37°C. Graph A shows a timecourse of peroxynitrite generation. Absorbance readings were taken every 5 minutes for 70 mins and data was converted to peroxynitrite generation using the extinction coefficient. Graph B shows the initial rate of peroxynitrite generation (nmoles min^{-1} ml^{-1}) which was calculated using the data in figure 4.80B. Mean±SD. n = 3.

4.3.2.2.2 Oxidation of Dihydrorhodamine by XO

The DHR assay was repeated to measure $ONOO^-$ generation by XO and its substrates hypoxanthine and nitrite with and without the addition of DPI which inhibits $O_2^{\bullet-}$ production and mimics reduced oxygen conditions (Figure 4.78). Previous assays of bacterial killing by XOR carried out in our lab by Dr. Millar showed bacterial killing occurred at 50mU ml^{-1} XO, therefore this concentration was the starting point around

which the preliminary DHR assays are based. Figure 4.78 shows that XO or hypoxanthine alone do not oxidise DHR. However, oxidation of DHR occurs in the presence of XO and its substrates, hypoxanthine and nitrite. The oxidation of DHR occurs both with and without the addition of DPI, which inhibits $O_2^{\bullet-}$ generation. However, when DPI is included the rate is significantly increased compared with no DPI. Suggesting that $ONOO^-$ generation is increased when the reduction of oxygen to $O_2^{\bullet-}$ is inhibited at the FAD site as would also be the case in hypoxia. In the presence of DPI electrons are also used by XO to reduce nitrite at the molybdenum site to form $^{\bullet}NO$. Thus resulting in the simultaneous generation of $O_2^{\bullet-}$ and $^{\bullet}NO$ and ultimately $ONOO^-$.

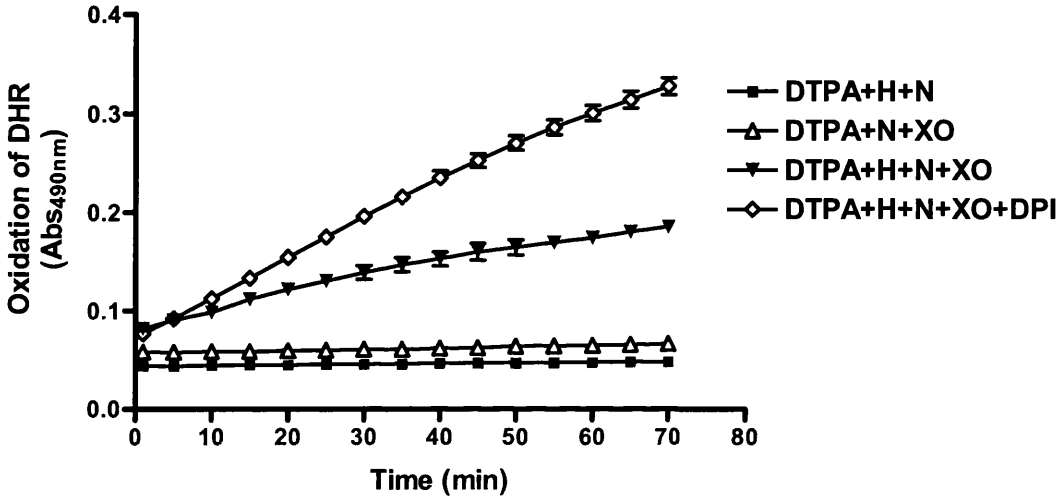

Figure 4.78 Timecourse of the oxidation of DHR by XO with DPI.

Experiment was carried out in air using final concentrations of DHR (0.1mM), DTPA (0.1mM), DPI (0.2mM), hypoxanthine (H) 1mM), nitrite (N) (1mM) and XO (50mU ml^{-1}) were used in a total volume of 200µl PBS at 37°C. Absorbance readings were taken every 5 minutes for 70 min. MEAN±SD. All n = 3, Except DTPA+H+N+XO n = 7. Mean±SD.

Peroxynitrite generation assays by XO were also carried out in cuvettes that could be sealed at a certain oxygen tension and stirred at 37°C. Further assays with XO and its substrates were carried out in the absence of DPI in air, with and without the iron chelator DTPA. Figure 4.79 shows that hypoxanthine, nitrite and XO oxidized DHR with and without DTPA (iron chelator). The rate of DHR oxidation appears to be slightly faster without DTPA particularly in the secondary rate which is observed after around 2 minutes.

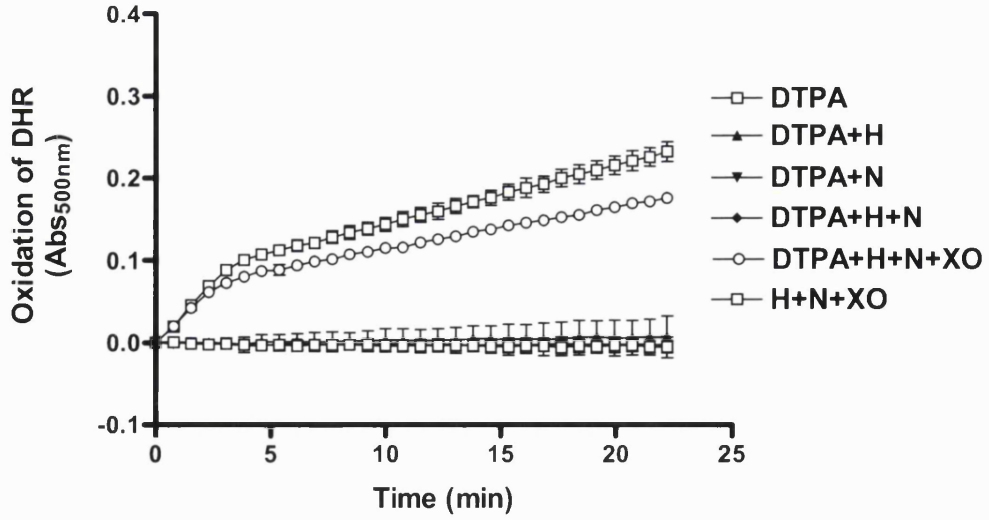

Figure 4.79 Oxidation of DHR by XO in air.

Experiment was carried out in air using final concentrations of XO (50mU ml^{-1}), DHR (0.1mM), DTPA (0.1mM), nitrite (N) (1mM), hypoxanthine (H) (1mM) were used in a 2ml final volume of PBS at 37°C. Readings were taken every 23 seconds for 22 minutes; however, an interval of 46 sec is shown the graph for clarity. n = 2. Mean±SD.

Preliminary assays were also carried out in hypoxia to see if there were any differences in the oxidation of DHR in air and 2% oxygen (figure 4.105). In air as previously shown, the rate of DHR oxidation by XO with hypoxanthine and nitrite is decreased in the presence of the iron chelator DTPA. In 2% oxygen however, the addition of DTPA does not have this effect (Figure 4.80). This figure also shows that at 2% oxygen there is a greater rate of DHR oxidation irrespective of the effect of hydroxyl radicals indicating increased generation of $ONOO^-$ in hypoxia.

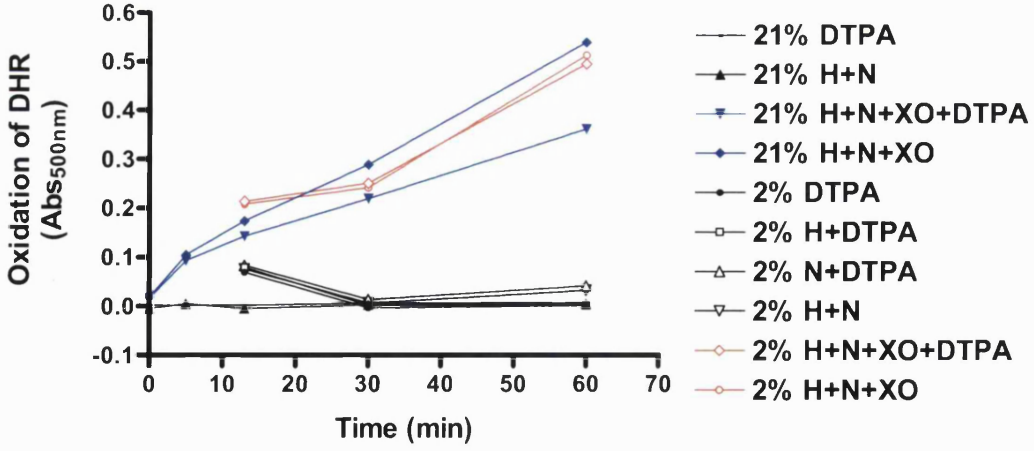

Figure 4.80 Oxidation of DHR in air and 2% Oxygen.

Experiments were carried out using final concentrations of XO (50mU ml^{-1}),) DHR (0.1mM, DTPA (0.1mM), nitrite (N) (1mM), hypoxanthine (H) (1mM) in a 2ml final volume of PBS in stirred and stoppered cuvettes at 37°C. The PBS used for the experiments was equilibrated either in air or alternatively

in the hypoxia cabinet overnight at 2%. The 2% cuvettes were also prepared and stoppered in the cabinet before removing for the relevant time intervals after which they were replaced with the lids removed in the cabinet. Cuvettes prepared in air are shown in red and cuvettes prepared in 2% oxygen are shown in blue. Readings were taken at various time points over a 60 minute time period. N = 1.

Further studies were carried out in air to see if the rate of DHR oxidation in air in the presence of XO with hypoxanthine and nitrite could be inhibited with allopurinol (figure 4.81). This figure shows that XO with hypoxanthine in the absence of nitrite oxidises DHR and this oxidation is increased when nitrite is included. This oxidation is inhibited by allopurinol suggesting that the oxidation of DHR is due to XO activity.

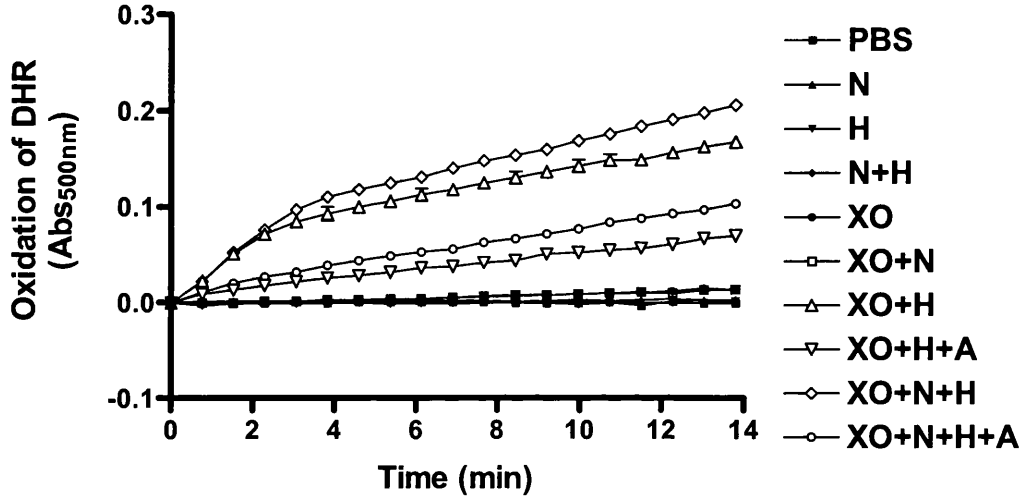

Figure 4.81 Oxidation of DHR in air.

Final concentrations of (50mU ml^{-1}) XO, DHR (0.1mM), nitrite (N) (1mM), hypoxanthine (H) (1mM) and allopurinol (A) (0.1mM) were used in a 2 ml final volume of PBS in stirred and stoppered cuvettes at 37 °C. Readings were taken every 30 seconds; however, every 60 second interval for 14 minutes is shown on the graph for clarity. All N = 1 except PBS, XO+H+PBS N = 2.

A further assay was carried out in air using XO at changing concentrations between 0 and 50mU ml^{-1} XO in the presence of hypoxanthine and nitrite (Figure 4.82A and B). Figure 4.82A shows that the substrates alone or XO alone do not oxidise DHR. XO in the presence of nitrite alone also does not oxidized DHR as the presence of electron donating substrate such as hypoxanthine is required. Hypoxanthine and XO are again shown to oxidise DHR and as this assay is carried out in the absence of DTPA it is likely that this rate is due to hydroxyl radical formation.

Figure 4.82B shows that hypoxanthine and nitrite XO in the presence of 50mU ml^{-1} XO shows an initial fast rate which lasts for 2.5 minutes and then continues to oxidise DHR at a reduced rate this effect did not occur at the lower enzyme concentrations that were tested. Decreasing concentrations of XO also showed a dose dependent decrease in DHR oxidation which no longer produced a measurable rate below 1mU ml^{-1} XO.

Figure 4.82 A)

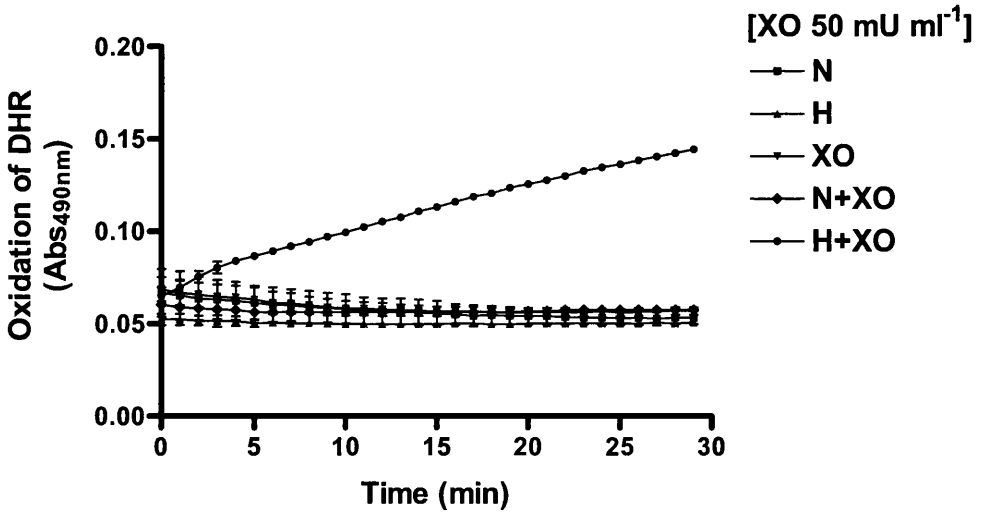

Figure 4.82 B)

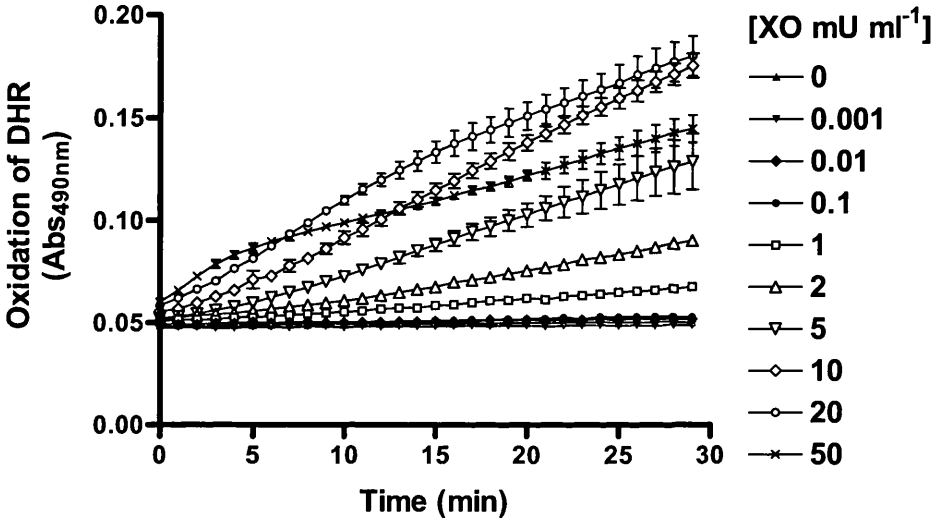

Figure 4.82 Oxidation of DHR in air.

Experiment was carried out in air graph A shows a timecourse of the oxidation of DHR by controls using final concentrations XO (50mU ml^{-1}), DHR (0.1mM), nitrite (N) (1mM), hypoxanthine (H) (1mM) in a 200µl final volume of PBS at 37°C. Graph B shows a timecourse of the oxidation of DHR by a range of XO concentrations. Final concentrations of XO at (0, 0.001, 0.01, 0.1, 1, 2, 5, 10, 20, 50mU ml^{-1}), DHR (0.1mM), nitrite (N) (1mM), hypoxanthine (H) (1mM) were diluted in a 200µl final volume of PBS at 37°C. Readings were taken every minute, for 30 minutes. Mean±SD. n = 3.

A brief experiment was carried out to determine the effect that urate, the end product of purine metabolism, had on the oxidation of DHR to ensure that urate did not oxidise DHR (Figure 4.83). This figure shows that uric acid does not oxidise DHR but shows a slight reduction of DHR over the 30 minute time period tested (Figure 4.83).

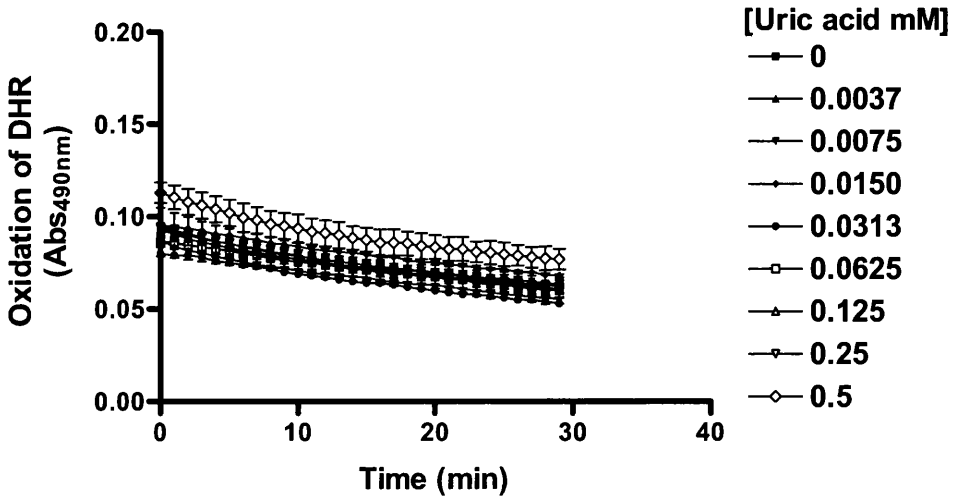

Figure 4.83 Oxidation of DHR by uric acid.

Experiment was carried out in air using a final concentration of uric acid at (0, 0.0037, 0.0075, 0.0150, 0.0313, 0.0625, 0.125, 0.25, 0.5mM), DHR (0.1mM) in a final volume of 200µl PBS in air at 37°C. Mean±SD. n = 3.

4.4 Discussion

4.4.1 Enzyme characterisation

The measurement of the protein content of XO was routinely measured for quality control between batches of the Biozyme enzyme. The results suggest that compared with the Bio-Rad protein assay (Figure 4.7, XO protein content 6.2mg ml^{-1}), the Bio-Rad *Dc* assay (Figure 4.8-4.9 XO protein content 10.49 and 10.81mg ml^{-1} respectively) was the most reliable method of protein measurement as it gave the closest values to the data sheets (~10.5mg ml^{-1} protein). The differences in the measurements by the two methods are likely to be due to varying specificities and/or sensitivity for amino acid residues. The pterin assay for the detection of XO and XDH activity (figure 4.10) showed that there was no XDH present in the Biozyme enzyme preparation. Studies have shown XO to have optimal $ONOO^-$ generation at lower oxygen concentrations (~7µM O_2) when compared with XDH (~180µM O_2) (Godber *et al*, 2000a). Therefore XO seems to be more effective as a $ONOO^-$ generator at the lower oxygen concentrations and therefore may be more effective as a dressing additive than XDH in a reduced oxygen environment such as that found within the chronic ulcer.

4.4.2 Development of methods for the measurement of XO activity in cell growth medium

4.4.2.1 Cytochrome *c* assay for superoxide generation by XO

The cytochrome *c* assay showed that in air, XO (8mU ml^{-1}) in the presence of xanthine produces a SOD-inhibitable rate of cytochrome *c* reduction. The addition of SOD dismutates $O_2^{\bullet-}$ to O_2 and H_2O_2 suggesting that the rate of cytochrome *c* reduction is due to $O_2^{\bullet-}$ generation by XO (Okado-Matsumoto and Fridovich, 2001). The rate of $O_2^{\bullet-}$ generation by XO (8mU ml^{-1}) was measured to be 4nmoles min^{-1} ml^{-1} (Figure 4.11). Furthermore, subsequent assays in 96-well plates, using lower concentrations of XO to conserve the stock, showed that 2mU ml^{-1} XO which produced 0.5nmoles min^{-1} ml^{-1} was inhibited by SOD at concentrations as low as 3.9U ml^{-1}, therefore these assays suggested that the concentration of SOD that was required to inhibit the enzyme could be reduced in order to conserve reagents in future experiments (figure 4.12 – 4.13).

As previously mentioned, assays were carried out in both cuvettes (3ml volume) and in 96-well plates (200µl volume) to try and conserve expensive reagents and increase the number of samples that could be assayed at one time. Preliminary assays, suggested that either of these methods were suitable for measuring cytochrome *c* reduction. However, comparisons of these two methods showed that there were differences between the rate of $O_2^{\bullet-}$ generation in the cuvette and the 96-well plate method. The results shown in figure (4.14) suggest that the rate of $O_2^{\bullet-}$ production is around 3 times faster in the cuvette than in the 96-well plate. As the difference between these two assays was considerable, the methods were repeated with reagents that were warmed in a water bath prior to the experiment to see if the difference in the rate of $O_2^{\bullet-}$ generation was due to temperature. An increased range of XO concentrations were also used to determine whether the two methods had comparable sensitivity at low XO concentrations. The results shown in figure 4.15-4.19 support the findings in the previous assays with the rates in the cuvette method being around twice as fast as in the 96-well plate method. Interestingly, however, the assays do appear to have comparable sensitivity at low enzyme concentrations suggesting that the difference is not due to the method of measurement. Assays were also carried out to compare the rate of $O_2^{\bullet-}$ generation both with and without a 15 minute shake mode at the beginning of the 96-well plate assay, and with and without stirring of the cuvette to determine whether these parameters influenced the rate of $O_2^{\bullet-}$ production (figure 4.20-4.21). Neither of these changes in the methodology affected the rate of $O_2^{\bullet-}$ generation to a great extent therefore it was decided that future experiments

would be carried out without shaking the 96-well plate prior to measurements and without stirring, in the cuvette to mimic the static cell culture conditions more closely. The expected $O_2^{\bullet-}$ generation rate was roughly calculated (Figure 4.22) and it appeared that the cuvette method was closer to the expected $O_2^{\bullet-}$ production rate therefore further developmental experiments were carried out using the cuvette method.

Cytochrome *c* assays were carried out in cuvettes to determine the rate of $O_2^{\bullet-}$ production at a range of XO concentrations that gave a proliferative response when applied to adult dermal fibroblasts (aHDF) according to Murrell *et al* (1990). Murrell's study used 1mM hypoxanthine and range of XO concentrations between 0 and 10mU ml^{-1} (enhanced proliferation was observed between 0.001 and 0.1mU ml^{-1}). Initial cytochrome *c* assays were therefore carried out using 1mM hypoxanthine and 1mU ml^{-1} XO, and initial rates of $O_2^{\bullet-}$ were measured to be 0.4nmole min^{-1} ml^{-1} (Figure 4.23). Superoxide dismutase inhibited this reaction confirming that $O_2^{\bullet-}$ is largely responsible (Figure 4.23). A higher concentration of SOD may be required for complete inhibition of the reduction of cytochrome *c*. Murrell's studies with aHDF also showed visible damage and detachment from the culture plate surface when cells were treated with 10mU ml^{-1} XO. Therefore, the $O_2^{\bullet-}$ generation by XO at 10mU ml^{-1} was also assessed (Figure 4.24). This figure shows that 10mU ml^{-1} XO produces around 5nmole min^{-1} ml^{-1} $O_2^{\bullet-}$, and that the reaction was also SOD-inhibitable confirming that the observed rate is largely due to $O_2^{\bullet-}$. Further $O_2^{\bullet-}$ measurements were carried out using an increased number of XO dilutions (0, 0.001, 0.01, 0.1, 1 and 10mU ml^{-1}). The rate of $O_2^{\bullet-}$ production was shown to increase with increasing concentrations of XO (Figure 4.25 and Table 4.2).

Experiments were also carried out to assess the effect of varying concentrations of hypoxanthine on $O_2^{\bullet-}$ generation by XO (1mU ml^{-1}). Figure 4.26 shows that the rate of $O_2^{\bullet-}$ generation increases with increasing hypoxanthine until around 5μM hypoxanthine. As the substrate concentration continues to increase up to 1mM hypoxanthine, and the enzyme becomes saturated, the rate of $O_2^{\bullet-}$ generation plateaus at a rate of 0.7nmole $O_2^{\bullet-}$ min^{-1} ml^{-1}. There does not appear to be any substrate inhibition at the highest concentration at 1mM hypoxanthine. Hypoxanthine at 1mM was used in Murrell's proliferation assays and was also used for the studies in this thesis. A high concentration of hypoxanthine is required to supply the enzyme with an excess of substrate, as it will not be replenished *in vitro* as it would physiologically *in vivo*.

As mentioned previously Murrell *et al*, (1990) used HEPES buffer in the culture medium for the proliferation study experiments, this methodology was repeated for some of the initial fibroblast studies carried out in this thesis. HEPES is a very commonly used biological buffer; however, previous studies have shown that HEPES has free radical-

scavenging properties. Therefore, cytochrome *c* assays were carried out to determine whether HEPES had any effect on $O_2^{\bullet-}$ generation by XO in air. The results suggest that HEPES does not significantly effect $O_2^{\bullet-}$ generation under these conditions (Figure 4.27). Furthermore, as enzymes can lose their activity over time, old and new batches of XO were routinely checked before addition to cell based assays, to ensure the consistency and reproducibility of experiments (figure 4.28).

Whilst carrying out the cuvette assays, it became clear that large quantities of reagents were required, and it was time-consuming to produce replicate experiments. Therefore, it became increasingly apparent that a 96-well plate method would be extremely advantageous. Further cytochrome *c* assays were carried out to compare the 96-well plate and the cuvette methodologies. It was finally found that the temperature at which the 96-well plate was actually carried out was lower than the temperature set. Therefore, the calibration of the plate reader temperature settings appeared to resolve the difference seen in the rate of $O_2^{\bullet-}$ generation in the cuvette and the 96-well plate (Figure 4.29-4.30). To achieve 37°C at the actual plate, the software needed to be set at 40°C. With these modifications, the cytochrome c assays for the detection of $O_2^{\bullet-}$ could also be carried out in 96-well plates. The 96-well plate methodology was also used to develop an assay to measure $O_2^{\bullet-}$ generation in hypoxia.

An initial 96-well plate assay is shown in figure 4.31, 10mU ml^{-1} XO was used with 1mM hypoxanthine to assess the activity of XO batches as mentioned previously prior to experiments with fibroblasts and bacteria (figure 4.31). Xanthine oxidoreductase at a concentration of 50mU ml^{-1} was also measured in figure 4.32 using hypoxanthine (1mM) and nitrite (1mM) as the substrates with 50mU ml^{-1} XO. Nitrite was also included in these assays as it will also be included in the cell based experiments to generate $^{\bullet}NO$, and also $ONOO^-$ through the simultaneous generation of $O_2^{\bullet-}$. Figure 4.32 shows that nitrite and hypoxanthine do not reduce cytochrome *c* either alone or in combination and cytochrome *c* is not reduced by nitrite and 50mU ml^{-1} XO. However, the reduction of cytochrome *c* by hypoxanthine and 50mU ml^{-1} XO is rapid both with and with out nitrite. An observation that was made when carrying out previous assays, although only at higher XO concentrations, was that cytochrome *c* was reduced and then rapidly re-oxidised to baseline levels (Figure 4.32). A repeat of this assay confirmed this finding (Figure 4.33). Therefore, at high XO concentrations of XO it is possible that this re-oxidation of the cytochrome *c*, underestimates the initial rate of $O_2^{\bullet-}$ generation, and it is also possible that this re-oxidation effect does not allow a true indication of the time course of $O_2^{\bullet-}$ generation by XO. To determine whether the reduction observed in figure 4.33 was due to $O_2^{\bullet-}$ generation, cytochrome *c* reduction by 50mU ml^{-1} XO was inhibited by varying

concentrations of SOD. Figure 4.34A) and B) showed that 50U ml^{-1} SOD completely inhibited XO-generated $O_2^{\bullet-}$ at 5nmoles min^{-1} ml^{-1} by dismutation of $O_2^{\bullet-}$ to H_2O_2 and oxygen confirming that the observed rate was due to $O_2^{\bullet-}$ generation. Additionally, XO-generated H_2O_2 was found to be responsible of the re-oxidisation of cytochrome *c* at 50mU ml^{-1} XO. Figure 4.35 showed that catalase completely prevented the re-oxidation of cytochrome *c* between 50 and 250U ml^{-1} catalase. Catalase converts H_2O_2 to H_2O and O_2 thus preventing it from re-oxidising cytochrome *c*.

The effect of the XO inhibitor allopurinol on the XO-generated $O_2^{\bullet-}$ was also assessed. Figure 4.36 clearly demonstrated inhibition of $O_2^{\bullet-}$ generation. However, even at high concentrations of allopurinol the assay was not inhibited to baseline levels. This is likely to be due to the fact that allopurinol is a suicide substrate of XO, which upon oxidation yields the product, alloxanthine or oxypurinol. The latter compound inactivates the enzyme by coordinating irreversibly to the reduced form of XO, at MO(IV) thus inhibiting the donation of further electrons by substrates at this site (Nakamura, 1991; Massey *et al*, 1970). However, electrons initially donated to XO by allopurinol can go on to generate $O_2^{\bullet-}$ until formation of oxypurinol inhibits the enzyme. Therefore this result suggests that oxypurinol would be a more suitable inhibitor for this assay.

In order to determine the levels of $O_2^{\bullet-}$ that human dermal fibroblasts and bacteria would be exposed to in culture. Cytochrome *c* assays were carried out over a 3 hour time period, and $O_2^{\bullet-}$ generation at varying concentrations of XO was assessed. Assays were also carried out in PBS, fibroblast growth medium and bacterial growth medium (LB) for comparison. Experiments were also carried out in hypoxia and in air to provide an idea of the range of $O_2^{\bullet-}$ that the fibroblasts and bacteria would be exposed to in culture. SOD was included in these assays to determine the portion of the cytochrome *c* reduction that is due to $O_2^{\bullet-}$. This is particularly important in the assays containing culture medium as there are likely to be components present that are able to reduce cytochrome *c*. Catalase was also used to prevent the re-oxidation of cytochrome *c* by XO-generated H_2O_2. Initial assays were carried out in PBS at 21% O_2 using 1, 10 and 50mU ml^{-1} XO (Figure 4.37-4.41). Figure 4.37A) and B) shows that in the absence of SOD and catalase XO at 50mU ml^{-1} with hypoxanthine (1mM) both in the presence and absence of nitrite (1mM) produces a rapid reduction of cytochrome *c* followed by re-oxidation, this effect has been shown in previous assay (figure 4.35) to be a result of H_2O_2 produced by XO along with $O_2^{\bullet-}$ at high enzyme concentrations. A slower re-oxidation effect was also observed at 10mU ml^{-1} XO. This re-oxidation effect did not occur at 1mU ml^{-1} XO, as $O_2^{\bullet-}$ and thus H_2O_2 generation is slower. Cytochrome *c* reduction progresses at a gradual rate at 1mU ml^{-1} XO. The addition of SOD showed that the rates observed in the previous assay were due to $O_2^{\bullet-}$ generation

by XO (Figure 4.38A and B). The addition of catalase in figure 4.39A and B was shown to prevent the re-oxidation of cytochrome *c* by removal of the H_2O_2, and to increase $O_2^{\bullet-}$ generation with a maximum generation of between 25 and 30nmoles ml^{-1} $O_2^{\bullet-}$ at 10 and 50mU ml^{-1} XO (Figure 4.39 B). Addition of both catalase and SOD to the assay (Figure 4.40) showed inhibition of the rates observed at 1 and 10mU ml^{-1} XO in figure 4.39. However, at 50mU ml^{-1} XO there was a slight rate of reduction observed. Interestingly, this rate was slightly faster in the absence of nitrite which could be due to $ONOO^-$ generation in the presence of nitrite which is known to re-oxidise cytochrome *c*. It is possible that rapid O_2 consumption by XO results in a hypoxic environment in the 96-well plate allowing $ONOO^-$ formation to occur in air. The rates may also occur at this enzyme concentration because the SOD added into this assay may not be able to completely scavenge all of the $O_2^{\bullet-}$ generated by XO at this concentration in the presence of catalase. It is also possible that the generation of O_2 from the breakdown of H_2O_2 also produces an increased level of $O_2^{\bullet-}$ generation, or that SOD is inactivated by these increased concentrations of ROS. The initial rate of $O_2^{\bullet-}$ generation at 21% oxygen in PBS was found to be around 5nmole min^{-1} ml^{-1} at 50mU ml^{-1} XO with hypoxanthine in the presence and absence of nitrite (Figure 4.41). Superoxide generation at 10mU ml^{-1} XO was found to be around 2.5nmole min^{-1} ml^{-1}, and with 1mU ml^{-1} XO around 0.1-0.3nmoles min^{-1} ml^{-1} (Figure 4.41).

The previous XO assays carried out in air (Figure 4.37-4.41), were repeated at 1% oxygen (Figure 4.42-4.45). In the absence of SOD and catalase figure 4.42 showed little cytochrome *c* reduction at 1% oxygen with only a suggestion of a rate at 50mU ml^{-1} XO. This suggests that in the limited oxygen that is available, XO can only produce low levels of $O_2^{\bullet-}$ at 50mU ml^{-1} XO. Addition of SOD, however, does not appear to have much effect on this rate (Figure 4.43). Interestingly, when catalase is added (figure 4.44), there is a significant increase in cytochrome *c* reduction in the presence of 50mU ml^{-1} XO and hypoxanthine both with and without nitrite, it is possible that these levels are artificially high due to oxygen used from the breakdown of H_2O_2 being used by XO to produce $O_2^{\bullet-}$ and H_2O_2. A further interesting point to note from this graph is that XO (50mUml^{-1}) in the presence of hypoxanthine without nitrite reduces cytochrome *c* to a greater extent that when nitrite is also included, which was also observed at 21% O_2 in the presence of catalase and SOD. This suggests that $O_2^{\bullet-}$ may be combining with $^{\bullet}NO$ to produce $ONOO^-$ which re-oxidises cytochrome *c*. Furthermore, in the presence of catalase and SOD (figure 4.45), the result is identical to that with catalase alone (Figure 4.44) suggesting that the rates observed in figure 4.44 are not due to $O_2^{\bullet-}$ generation. However, it could be that there is not enough SOD added to the reaction or that the SOD is inactivated over time by

XO-generated species. Studies have previously shown that H_2O_2 and $ONOO^-$ are capable of inactivating SOD and also catalase (Salo *et al*, 1988; Salo *et al*, 1990; MacMillan-Crow *et al*, 1998). However, analysis of the initial rates showed that in PBS at 1% O_2 low levels of $O_2^{\bullet-}$ generation were only detected at 50mU ml^{-1} XO at around 0.2nmoles min^{-1} ml^{-1}. Therefore, compared with experiments carried out in air (~21% oxygen), superoxide generation is dramatically decreased at 1% oxygen.

These experiments were also used to determine levels of $O_2^{\bullet-}$ generation in bacterial culture medium (LB) at 21% and 1% oxygen. In control experiments, without enzyme, at both oxygen concentrations, cytochrome *c* was reduced in the presence of LB and this reduction was unaffected by the addition of catalase or SOD suggesting that this reduction is not a result of H_2O_2 or $O_2^{\bullet-}$ (Figure 4.47 and 4.54). As LB is an undefined medium it is difficult to identify exactly what is responsible for the reduction of the cytochrome *c* however this background rate was taken into consideration when $O_2^{\bullet-}$ generation was determined. In air, XO was shown to reduce cytochrome *c* in LB without the addition of the substrates, suggesting that LB contains substrates that can be utilized by the enzyme (Figure 4.48). This rate was also SOD-inhibitable suggesting that $O_2^{\bullet-}$ generation by XO was responsible (Figure 4.48). In these assays in PBS the $O_2^{\bullet-}$ generation by XO at 10 and 50mU ml^{-1} was assessed with the addition of hypoxanthine (1mM) and nitrite (1mM). The reduction of cytochrome *c* in LB in the absence of catalase and SOD was similar to that shown previously in air at these enzyme concentrations, showing a rapid rate of cytochrome c reduction and then re-oxidation (Figure 4.49). Addition of SOD appeared to inhibit these rates suggesting that they were due to $O_2^{\bullet-}$ generation (Figure 4.50). Addition of catalase abolished the re-oxidation effect and 50mU ml^{-1} XO in the presence of hypoxanthine and nitrite appeared to produce an increased rate of cytochrome *c* reduction compared with hypoxanthine alone (Figure 4.51). It is possible that in the LB, XO is able to produce additional species to reduce cytochrome *c* to a greater extent when nitrite is also included. Alternatively, it may be that more hydrogen peroxide is formed in the absence of competition for electrons by nitrite resulting in re-oxidation to a greater extent in the absence of nitrite. Addition of SOD (Figure 4.52) largely inhibits these rates although not to control levels. This maybe due to the fact that XO in the presence of LB can produce other species reduce cytochrome *c*. Alternatively, it could be that an increased SOD concentration is required, or as previously discussed, that the activity of the SOD is inhibited by ROS or $ONOO^-$ generation.

At 1% O_2 in LB, XO reduced cytochrome *c* in the absence of any additional substrates, as shown previously in 21% O_2 in LB, however, the addition of SOD did not appear to inhibit this rate in the presence of absence of catalase (figure 4.55). Again, this

could be due to generation of species in LB by XO that are not SOD inhibitable, or inactivation of SOD by XO-generated species. At 1% O_2 (figure 4.56), a reduced rate of cytochrome *c* reduction was observed compared with at 21% O_2 (figure 4.49), and rates were only observed at 50mU ml^{-1} XO with hypoxanthine in the presence and absence of nitrite. These rates only showed a slight inhibition with the addition of SOD (Figure 4.57) and addition of catalase only slightly changed the profile of the graph by slightly reducing the re-oxidation effect (Figure 4.58). Addition of catalase and SOD did not inhibit the rate observed with catalase alone (Figure 4.59). Overall, these graphs suggest that $O_2^{\bullet-}$ generation is reduced in 1% oxygen as compared with in air. It is unclear whether the observed rates are due to $O_2^{\bullet-}$ although they were not SOD-inhibitable it is possible however, that the SOD is inactivated by XO-generated species.

Superoxide generation by XO was also measured in fibroblast growth medium. Initial assays in air showed that fibroblast growth medium alone reduced cytochrome *c* (Figure 4.61). Furthermore, this reduction was not found to be allopurinol or SOD inhibitable, suggesting that the rate was not due to $O_2^{\bullet-}$ generation by XO that could be present in the FCS, or by $O_2^{\bullet-}$ generation from other sources present in the fibroblast growth medium (Figure 4.62). These rates were subtracted in order to ascertain the levels of $O_2^{\bullet-}$ generation by XO in fibroblast growth medium. Analysis of the individual fibroblast growth medium components showed that DMEM (without phenol red), FCS and the penicillin streptomycin mixture reduced cytochrome *c* (Figure 4.63). L-Glutamine, did not reduce cytochrome *c* above levels seen with DMEM alone (Figure 4.63). Sterile filtering of the fibroblast growth medium, as would be done before the addition to cell culture, showed that the components of the fibroblast growth medium that were responsible for the cytochrome *c* reduction were not filtered out (Figure 4.64). Furthermore, the data sheet supplied with the DMEM (without phenol red) suggested that it did not contain any substrates for XO. However, Figure 4.65 confirmed that the DMEM did not contain substrates for $O_2^{\bullet-}$ generation by XO, therefore DMEM could be used to dilute the XO prior to assays using fibroblast growth medium.

Xanthine oxidase reduced cytochrome *c* considerably faster in PBS than in the presence of fibroblast growth medium (Figure 4.66). The lower rate with fibroblast growth medium could be due to the presence of antioxidants such as SOD in the FCS, or the reaction of $O_2^{\bullet-}$ with other components of the medium such as amino acids. However, figure 4.67 showed that a dilution and removal of FCS did not affect the rate of cytochrome *c* reduction in fibroblast growth medium. This suggests that FCS was not responsible for the reduced rate of cytochrome *c* reduction, and it is that more likely that the reduction of cytochrome *c* reduction is due to reaction of $O_2^{\bullet-}$ with amino acids present

in the DMEM. In support of this, emerging evidence in the literature suggests an important role for nutritional factors such as essential amino acids L-methionine and glycine in reducing oxidative stress (Erdmann *et al*, 2005).

In fibroblast growth medium at 1% O_2, $O_2^{\bullet-}$ -generation by XO was measured at 1, 5, 10 and 50mU ml^{-1}. In the absence of SOD and catalase 50mU ml^{-1} XO produced a slight rate of cytochrome *c* reduction, suggesting that low levels of $O_2^{\bullet-}$ are produced at high enzyme concentrations (Figure 4.69). However, the rate calculations did not show a statistical difference compared with the control (Figure 4.73). The addition of SOD (figure 4.70) appeared to inhibit the slight rate shown at 50mU ml^{-1} XO which suggests that the slight rate seen in the absence of SOD was due to $O_2^{\bullet-}$ generation. The rate of cytochrome *c* reduction was increased in the presence of catalase although this increase was not as marked as seen in previous assays, which is probably due to the fact that there is less H_2O_2 generation in low oxygen (Figure 4.71). Furthermore this increased rate was not inhibited by SOD which suggests that it is not entirely due to $O_2^{\bullet-}$ generation or that SOD has been inhibited by XO-generated species as previously discussed (Figure 4.72). It is unsurprising that there is such low $O_2^{\bullet-}$ detected in 1% oxygen as oxygen is required for $O_2^{\bullet-}$ generation and the $O_2^{\bullet-}$ that will be produced will rapidly react with $^{\bullet}NO$ to form $ONOO^-$. It is also possible that peroxynitrite generation slightly underestimates the $O_2^{\bullet-}$ generation by oxidation of the cytochrome *c*.

4.4.2.2 Oxidation of dihydrorhodamine for peroxynitrite generation by XO

Experiments were carried out to measure $ONOO^-$ by following the oxidation of dihydrorhodamine (DHR) to rhodamine. Initial experiments were carried out to develop the assay for measurements in a reduced volume in a cuvette (Figure 4.74), and a 96-well plate to conserve the expensive DHR and increase sample number (Figure 4.75 and Table 4.3). Assessment of the wavelength scans of DHR oxidized by SIN-1 also showed that the existing 490nm filter on the 96-well plate reader was suitable for $ONOO^-$ measurements avoiding the need to purchase a new and expensive 500nm filter. SIN-1 was used as a positive control for $ONOO^-$ generation and showed that the assay was detecting $ONOO^-$. Dihydrorhodamine was oxidised in a dose-dependent manner by increasing concentrations of SIN-1 (Figure 4.76-4.77).

The assay was then used to detect $ONOO^-$ generation by XO in air. In the presence of nitrite XO generates $^{\bullet}NO$ in increasing amounts as ambient O_2 is reduced, this situation provides the ideal conditions for generation of $ONOO^-$ which requires simultaneous generation of $^{\bullet}NO$ and $O_2^{\bullet-}$. Therefore, initial assays with XO in air were carried out using

diphenyliodonium chloride (DPI) which inhibits $O_2^{\bullet-}$ generation thereby simulating hypoxia and changing the competition for donated electrons in favour of nitrite, generating $^{\bullet}NO$ thus allowing for ideal $ONOO^-$ forming conditions. These studies showed that XO with hypoxanthine and nitrite where capable of DHR oxidation in the presence and absence of DPI, albeit to a lesser extent in the absence of DPI (figure 4.78). It is possible that the DHR oxidation by XO in the absence of DPI may also represent $ONOO^-$ generation, by virtue of the possibility that oxygen in the wells has been rapidly consumed by XO to generate $O_2^{\bullet-}$. The increased rate with the addition of DPI is clear evidence of $ONOO^-$ generation.

The previous assay carried out in air with hypoxanthine, nitrite, XO in the absence of DPI showed a slight rate of DHR oxidation. This assay was repeated in air with and without the iron chelator DTPA to determine how this addition affected the oxidation of DHR in the presence of XO and its substrates. Figure 4.79 clearly shows that the rate of oxidation in the absence of DTPA is faster. This can be explained by the fact that XO generates H_2O_2 which can combine with iron to produce hydroxyl radicals which are known to be detected by the DHR assay. Therefore this reaction is prevented in the presence of the iron chelator DTPA, resulting in a slower rate of DHR oxidation.

Figure 4.80 shows that in air, DHR oxidation in the presence of XO, hypoxanthine and nitrite is decreased in the presence of DTPA. This may be because, as previously discussed, DTPA prevents the formation of hydroxyl radicals which are known to oxidise DHR. In 2% oxygen however, DTPA does not appear to affect the rate of DHR oxidation. This may be due to the fact that in low oxygen availability less H_2O_2 is generated in favour of $^{\bullet}NO$ and $O_2^{\bullet-}$ for $ONOO^-$ generation resulting in a reduction in hydroxyl radical formation (Figure 4.80). This figure also suggests that there is increased generation of $ONOO^-$ in 2% oxygen.

Interestingly, figure 4.81 shows that XO and hypoxanthine without nitrite oxidises DHR. It is possible that this oxidation is due to hydroxyl radical formation as this assay was carried out in the absence of DTPA which prevents hydroxyl radical formation as previously discussed. This oxidation is increased with the addition of nitrite which suggests that $ONOO^-$ is contributing to the oxidation as shown by previous assays in the presence and absence of DTPA. This oxidation is also shown to be inhibited by allopurinol which confirms that XO is responsible for the oxidation of DHR. This figure also shows that allopurinol does not completely inhibit the oxidation of DHR, due in part, as mentioned previously, that allopurinol donates electrons to XO to produce oxypurinol before inactivating the molybdenum site of the enzyme. Also the allopurinol was used at a lower concentration than the hypoxanthine increasing the chances of hypoxanthine to be

used as a substrate due to the fact that the inhibition of XO by allopurinol is competitive. Oxypurinol may have been a better choice of inhibitor under these circumstances.

Figure 4.82A) shows that the substrates alone or XO alone do not oxidise DHR. XO in the presence of nitrite alone also does not oxidise DHR as the presence of electron donating substrate such as hypoxanthine is required for NO and $O_2^{\bullet-}$ generation for $ONOO^-$ generation by XO. As shown in assays previously discussed hypoxanthine and XO are shown to oxidise DHR and as figure 4.82 was carried out in the absence of DTPA it is likely that this rate is due to hydroxyl radical formation. Figure 4.82B) shows that hypoxanthine and nitrite in the presence of 50mU ml^{-1} XO produces an initial fast rate which lasts for 2.5 minutes and then continues to oxidise DHR at a reduced rate. It is possible that this effect is due to substrate depletion, inactivation of the enzyme by its products or excessive oxygen consumption by XO resulting in reduced $O_2^{\bullet-}$ and subsequent $ONOO^-$ generation. Furthermore, this effect was not evident at the lower XO concentrations that were tested.

The DHR provided a suggestion of $ONOO^-$ by XO, however due to time constraints, these assays were not developed any further. However, if time allowed further studies could be carried using another method to confirm these findings. For example hydroxylphenyl fluorescein (HPF) is a relatively new probe which can be used to detect peroxynitrite (Setsukinai *et al*, 2003). Although H_2O_2 was measured indirectly, in the cytochrome *c* assays, it would also be interesting to measure the H_2O_2 generated by XO in culture medium and variable oxygen.

4.4.3 Chapter summary

The results in this chapter highlight the inherent difficulties that are associated with the measurement of RONS, particularly in a cell culture environment where numerous reactions can take place and are challenging to unravel. Nevertheless, the findings of this chapter using pure enzyme confirm previous reports of superoxide generation by XO. Moreover, I have shown that this generation is reduced at low oxygen tension at a level similar to that of the chronic wound. The results in this chapter also highlight the ROS scavenging properties of cell culture medium and provide a useful caveat when using *in vitro* systems to model the complex environment of the chronic wound. These assays also identify the levels of superoxide that wound-related fibroblasts and bacterial cells would be exposed to *in vitro*. These assays also provide indirect evidence of H_2O_2 generation by XO. Furthermore, I have found evidence of $ONOO^-$ generation by XO at low oxygen tensions such as experienced in the chronic wound environment.

CHAPTER 5

5 Effects of XO-generated products on human dermal fibroblasts

5.1 Introduction

As previously dicussed XO is capable of generating a range of ROS, which have been reported to have proliferative effects on human endothelial cells and cultured fibroblastic cells, such as human dermal fibroblasts (Kim *et al*, 2001; Novogrodsky *et al*, 1982; Amstad *et al*, 1991; Han *et al*, 2003; Murrell *et al*, 1990). Studies have indicated that H_2O_2, $O_2^{\bullet-}$, and $^{\bullet}OH$ all stimulate human dermal fibroblast proliferation (Murrell *et al*, 1990). It is thought that ROS derived from both cellular and exogenous sources at physiological levels play a critical role as cell signalling "messengers". However, critical balances appear to exist in relation to cell proliferation on one hand and lipid peroxidation and cell death on the other. For example, H_2O_2 at 200μM has been shown to decrease fibroblast cell survival, whereas 10μM H_2O_2 activates the signal-regulated protein kinase pathway, which is required for cell survival. In the latter case, the initiation of signal transduction by H_2O_2 is mediated by metal-catalyzed free radical formation (Guyton *et al*, 1996).

This chapter aims to determine the effects of XO-generated species on human dermal fibroblasts at a range of oxygen concentrations to mimic the hypoxic chronic wound environment. It is hypothesised that XO has beneficial wound healing properties as, in addition to $O_2^{\bullet-}$ and H_2O_2 generation in air, XO can generate $^{\bullet}NO$ in the presence of nitrite in a range of hypoxic oxygen concentrations. Furthermore, the simultaneous generation of both $O_2^{\bullet-}$ and $^{\bullet}NO$ by XO results in $ONOO^-$ formation. As well as $O_2^{\bullet-}$ and H_2O_2, $^{\bullet}NO$ is also known to proliferate dermal fibroblasts (Dhaunsi and Ozand, 2004) whereas $ONOO^-$ is a powerful antimicrobial that can be damaging to cells. These studies investigate the potential proliferative effects of XO-generated species along with toxicity on human dermal fibroblasts at a range of oxygen tensions, in order to determine a concentration of XO which would provide maximum inhibitory power over bacterial growth in a chronic ulcer (chapter 6) with minimum cytotoxicity of dermal cells. Human dermal fibroblasts (HDF) were used in this study as my thesis is concerned with cutaneous ulcers, and fibroblasts are essential for tissue regeneration since adequate proliferation of these cells is essential for resolution of the wound healing process. The effects of XO on

the viability and proliferation of HDF was determined by assessment of metabolically active cells and DNA synthesis.

5.1.1 Chapter aims

The aim of this chapter is to determine the effect of varying concentrations of XO on the proliferation and viability of HDF in a range of oxygen tensions, to mimic the chronic ulcer environment. Dermal fibroblasts are vital for the healing process and successful wound closure. If XO is to prove useful in a wound setting it is important that it is effective against bacteria without having inhibitory effects on the healing process.

5.2 Materials and Methods

5.2.1 Cell culture

5.2.1.1 Origin of primary human dermal fibroblasts (HDF)

Primary neonatal human dermal fibroblasts (nHDF) were commercially supplied as a cryopreserved vial of $0.9x10^6$ cells per ampoule. The cells were derived from a newborn male. Suppliers assessed 90% viability and tested negative for bacteria, fungi, mycoplasma, HIV-1, hepatitis B and C (TCS CellWorks Ltd, Botolph Claydon, UK).

Normal adult human dermal fibroblasts (aHDF) were biopsied from uninjured skin of healthy individuals (N1, supplied by Royal Free Hospital, London and N2, N3, supplied by The Royal National Hospital for Rheumatic Diseases, Bath) and of a patient with a chronic venous leg ulcer (V1) that had been ongoing for at least 8 weeks (supplied by D.W. Thomas, Department of Oral Surgery, Medicine and Pathology, University of Wales College of Medicine, Cardiff). In all cases, fibroblasts were used between passage 2 and 12. Demographic information for the healthy individuals is unknown but the patient with the leg ulcer was an elderly female (age 65-70). The ulcer was uninfected and the patient had received no antibiotics for at least 6 weeks; there were no other systemic problems or mixed aetiology.

5.2.1.2 Maintenance, passage and subculture of dermal fibroblasts

5.2.1.2.1 Materials

DMEM (with and without phenol red see appendix 8.1), L-Glutamine 200mM, Penicillin/Streptomycin (10,000units ml^{-1} Penicillin and 10,000µg ml^{-1} Streptomycin), PBS (Gibco Life Tech, Paisley, Paisley, UK); Foetal calf serum (FCS) (GlobePharm Ltd,

UK); Accutase (TCS CellWorks Ltd, Botolph Claydon, UK); Trypsin EDTA x10 solution and cell dissociation solution (Sigma-Aldrich Co Ltd, Poole, UK).

5.2.1.2.2 Protocol

All procedures were carried out using aseptic technique in a laminar flow cabinet (Class II, Intermed M.D.H, M20229). Fibroblast growth medium was used for the isolation and serial culture of HDF (see appendix 8.1). Once confluence was achieved, used media was aspirated and discarded. Cells were rinsed in PBS to remove residual FCS. Trypsin/EDTA was added to the cells (5mls of 1X trypsin/EDTA, see Appendix 1, per 75cm^2 surface area) to allow dissociation. The flask was incubated at 37°C for 10 min, until there were visible signs of the cells rounding up and detaching into the medium. At this point fibroblast growth medium, containing FCS, was added to inactivate the trypsin and the cells dispersed by pipetting. The cell suspension was centrifuged (1,200rpm for 5 minutes), and the pellet resuspended in a 1ml volume of fresh medium. Accutase and cell dissociation solution were also initally compared with trypsin; however, trypsin was found to be the most suitable (see section 5.3.2.1). To determine a specific cell seeding density, a sample (40µl) of the cell suspension was removed for cell counting and assessment of viability (trypan blue exclusion assay), using a haemacytometer (See Section 1.4.2.1.7). The media was increased to the desired volume for seeding and cells incubated at 37°C in a humidified incubator with 5% CO_2 in 95% air.

5.2.1.3 Cryopreservation and revival of cells for cell stocks

Cells from almost confluent cultures of fibroblasts were cryopreserved by freezing in liquid nitrogen, to provide cell banks for continuity of experiments.

5.2.1.3.1 Materials

Cryo 1°C Freezing Container and 1ml NUNC Cryo-tubes (Fisher Scientific UK Ltd. Leicestershire, UK), Cell Freezing medium- DMSO, (Sigma-Aldrich Co Ltd, Poole, UK).

5.2.1.3.2 Protocol

Cells were detached (as for subculture) using trypsin/EDTA, and were resuspended at a density of 1x10^6 cells ml^{-1} in 2ml of cell freezing medium. 1ml of resuspended cells were added per cryovial. Cyrovials containing cells were then placed into a freezing container and left overnight at -70°C to gradually lower the temperature, prior to transfer to the liquid nitrogen store. To revive the cells, the vials were rapidly defrosted in a water

bath at 37°C. The suspension was then micro-pipetted into a tube and resuspended in a suitable volume of media for the required culture flask (5ml per 75 cm^2 surface area). Cells were incubated at 37°C in a 5% CO_2 and 95% air mixture. A minimum time of 16 hours was allowed for cell attachment and recovery before changing the media.

To determine the required number of culture flasks required for plating cells at a recommended seeding density of 2,500 viable cells per cm^{-2} (TCS Cellworks Ltd), the following calculations were carried out.

No. of cells available/2,500 = *cm^2 that can be plated*

cm^2 that can be plated/
effective growth area of flask = *no. of culture flasks that can be seeded*

5.2.1.4 Manually observed cell counts and assessment of viability using trypan blue

Trypan blue stain was used to test the permeability of the plasma membrane of the fibroblasts for an indication of the number of viable cells for seeding into the experimental assays.

5.2.1.4.1 Materials

Trypan Blue, (Sigma-Aldrich Co Ltd, Poole, UK) Haemocytometer, (Fisher Scientific UK Ltd. Leicestershire, UK)

5.2.1.4.2 Protocol

A 40µl volume was collected from cell suspensions after dissociation of a cell monolayer. The 40µl was added to 40µl of trypan blue (1:1 dilution), and left for 1-2 minutes. The trypan blue cell suspension (10µl) was pipetted into opposite chambers of an improved Neubauer haemocytometer. Approximately 10µl of the cell/trypan blue mixture was applied to fill the counting chamber and, blue (dead) and clear (viable) cells were counted from five of the nine 1mm^2 squares on the counting chamber (as indicated in Figure 5.1). The average number of cells per square was used in the calculation of the number of cells per ml of the starting cell suspension, as shown in (Equation 5.1).

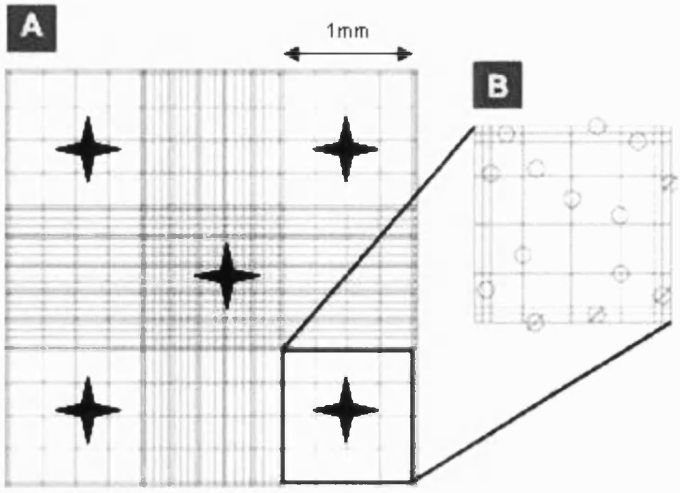

Figure 5.1 Improved Neubauer Haemocytometer for cell counting.

A One chamber of a haemacytometer slide under 10x objective and 10x ocular. The chamber is divided into 9 major squares cell counts were taken from the 5 highlighted squares (as indicated by black squares in A). **B** Detailed view of one of the 9 major squares. Only cells that overlap the top and left borders of squares should be counted to avoid overestimating the cell concentration. O: cells that should be counted; Ø: cells that should be ignored.

$$\text{Cells ml}^{-1} = \text{Mean cells per square x 2 x 10 000}$$

Equation 5.1Cell viability count

Following trypan blue-exclusion protocol cells viable cell counts could be calculated using this equation. The percentage of viable cells could be calculated after repeating the above calculation for trypan blue stained cells only. (x2: dilution factor, trypan blue dilution, x10 000: volume correction from volume of 1mm square under cover slip, 10^{-4}ml, to 1ml).

5.2.2 Characterisation of HDF

5.2.2.1 Immunocytochemistry

Prior to experimentation with HDF, they were characterized by analysis of a number of fibroblast specific proteins, namely the beta-subunit of prolyl-4-hydroxylase and disulphide-isomerase using immunocytochemisty.

5.2.2.1.1 Materials

Lab-tek chamber slide, 8-well on glass (Sigma-Aldrich Co Ltd, Poole, UK); Fibroblast Primary antibody (mouse anti-human monoclonal 5B5. Isotype: IgG1), negative control mouse IgG1, (DakoCytomation Ltd, Ely, UK); VECTA STAIN ABC Kit (alkaline phosphatase mouse IgG), (Vector Laboratories Ltd, Orton Southgate, Peterborough, UK); methanol, acetone, PBS (10X), Aquamount, (VWR International, Poole, UK); Fast Red, Mayer's haematoxylin, (Sigma-Aldrich Co Ltd, Poole, UK)

5.2.2.1.2 Protocol

HDF cells from a confluent T75 flask were resuspended in 2mls of fibroblast medium. The cell suspension (20µl) was added to each well of two 8-well chamber slides (~100,000 cells $well^{-1}$). Each slide was then topped up with 500µl of media per well. The cells were grown to confluence. The media was carefully aspirated, and each well was washed 3 times for 3 minutes each in PBS (1X). The cells where fixed in ice-cold methanol/acetone (1:1 v/v) for 3 mins. Each well was washed 3 times in PBS (1X) for 3 minutes each. Cells were incubated in blocking solution for 30 minutes. The slides were incubated overnight in a humidified chamber at 4°C using a 1:50 and 1:100 dilution of the fibroblast primary antibody solution. The antibody reacts with the beta-subunit of prolyl-4-hydroxylase and disulphide-isomerase, known to be essential for collagen synthesis and unique to fibroblasts. A negative control monoclonal primary antibody was used at a 1:200 dilution. The negative control was a monoclonal mouse IgG1 antibody to *aspergillus niger* glucose oxidase (neither present or inducible in mammalian tissues). A none antibody control was also included using blocking serum for the duration of the primary antibody incubation. The remainder of the protocol was carried out according to the Vecta stain ABC kit for secondary antibody application. Briefly, the slides were incubated for 5 minutes in 400µl alkaline phosphatase substrate solution (Fast Red; made up according to the manufacturers instructions) and stain development was followed using the microscope. When cells were sufficiently stained the slides were washed in tap water to terminate the reaction. Cells were counterstained for 1 minute using Mayer's haematoxylin. The nuclear staining was checked and the slides were washed in swirling tap water for 5 minutes. The slides were then mounted using Aquamount.

5.2.3 Effects of H_2O_2 and XO on the viability of HDF

5.2.3.1 Colourimetric methylthiazolyldiphenyl-tetrazolium bromide (MTT) reduction assay

Viability was assessed by using the colourimetric MTT assay. Yellow tetrazolium salt (MTT) is reduced in metabolically active cells by the mitochondrial enzyme succinyl dehydrogenase to form insoluble purple formazan crystals. These crystals are solublized by a detergent and the colour produced is quantified by spectrophotometry at 550nm. There is a linear relationship between cell number and absorbance, and the number of viable cells and absorbance. Therefore the assay can also be used for an indication of

proliferation. The protocol follows that of Mossman (1983) and Denizot and Lang (1986) with some modifications.

5.2.3.1.1 Materials

MTT, Dimethyl Sulfoxide (DMSO), (Sigma-Aldrich Co Ltd, Poole, UK), Tissue Culture Test Plates, 96-well Flat-bottomed plates, (Orange Scientific); DMEM (Without phenol red) (Gibco, Life Tech, Paisley, UK)

5.2.3.1.2 Protocol

Human dermal fibroblasts were seeded into plates (see individual figures for seeding densities) and incubated at 37°C in a 5% CO_2/95% air mixture, or in the oxygen controlled cabinet (see section 4.1.3) at 0-5% oxygen. After incubation the culture medium was removed by inverting the plate and blotting. Cells were treated with combinations of XO (0-100mU ml^{-1}) hypoxanthine (1mM) and nitrite (1mM). Cells were also treated with H_2O_2 (0-10,000μM) and basic fibroblast growth factor (bFGF, 0-50ng ml^{-1}) and plates were incubated for between 3 and 72 hours, after which time the media was removed by inverting and blotting. Cells were incubated at with 100μl of 0.5-1mg ml^{-1} MTT added to the relevant wells in fresh medium (excluding the first column to which 100μl of DPBS was added) and the plates incubated at 37°C generally for 3-4 hours. For experiments in low oxygen cells remained in the cabinet for 24 hours prior to the application of the test reagents, and during treatment with test reagents and MTT (see individual figure legends for the details of each experiment). A stock solution of MTT was dissolved in PBS at 5mg ml^{-1} and stored at -20°C wrapped in tin foil to keep dark. The MTT was filter-sterilized and the small amount of insoluble residue present in some batches was removed. Plates were then removed from the incubator and oxygen controlled cabinet and DMSO was added to all wells and mixed thoroughly to dissolve the purple formazan crystals. After a few minutes at room temperature to ensure that all the crystals had dissolved, the absorbances were read on a plate reader (Dynatech MR5000), using a test wavelength of 550nm. Absorbances were usually read within 10 minutes of adding the DMSO.

5.2.4 Effects of XO on the DNA synthesis and proliferation of HDF

5.2.4.1 Bromodeoxyuridine assay using chamber slides for cell counts

Traditionally, the measurement of cell proliferation has involved the use of [^{3}H]-thymidine to allow monitoring of DNA synthesis. However, the bromodeoxyuridine (BrdU) assay is based on the incorporation of the pyrimidine analogue 5-bromo-2'-deoxyuridine, instead of thymidine, into the DNA of proliferating cells. The BrdU assay has advantages over the [^{3}H]-thymidine assay in that it avoids the need for radioactive isotopes.

5.2.4.1.1 Materials

BrdU, polyoxyethylene-sorbitan monolaurate (Tween 20), (Sigma-Aldrich Co Ltd, Poole, UK); anti-bromodeoxyuridine antibody, (DakoCytomation Ltd, Ely, UK); phosphate buffered saline tablets, (Oxoid, Basingstoke, Hampshire, UK); ethanol, hydrochloric acid, (VWR International, Poole, UK); Vectastain Elite ABC peroxidase kit (Mouse IgG); 3,3'-diaminobenzidine (DAB) substrate kit for peroxidase, (Vector Laboratories Ltd, Petersborough, UK)

5.2.4.1.2 Protocol

Cells were grown to confluence in a T75 flask. Cells were then detached from the culture surface using 5mls of Trypsin and centrifuged for 5 minutes at 1,200 rpm. The pellet was resuspended in 1ml of fibroblast medium. Cells were counted manually using a haemocytometer and a viable cell count was taken. Cells were diluted and seeded onto 8-well slides (see individual figures for seeding densities). Cells were allowed to settle and attach for 24 hrs. The medium was carefully aspirated, control and test medium (500µl) added to each well and the cells incubated for 4 hrs. The control and test medium was carefully removed from each well and transferred into 1ml eppendorf tubes. Each well was carefully washed in 500µl of fibroblast medium and then aspirated. A stock solution of BrdU (1mM), dissolved in PBS and stored at 4°C, was diluted to 10µM and 400µl was added to each well. The slides were incubated at 4°C for between 18hrs (However, the BrdU incubation time varies for certain experiments, see individual figures). The next day, cells were washed in 500µl of PBS for 5 minutes and were fixed in 300µl 70% alcohol diluted in 0.5% PBS-Tween for 30 minutes. The alcohol was removed, and the cells were

hydrolysed in 300µl 4M HCL for 15 minutes to denature the DNA to the single stranded form. Each well was washed 3 times for 5 minutes in 300µl of 0.5% PBS-Tween. A 1:50 dilution of mouse IgG anti-BrdU primary antibody in 0.5% PBS-Tween 200µl was then added to each well. The slides were left overnight in a humidified chamber at 4°C. Each well was washed three times for 5 minutes in 0.5% PBS -Tween. The secondary, anti-mouse IgG biotinylated antibody and blocking serum were diluted 1:200 in 0.5% PBS-Tween according to the instructions in the Vectastain Elite ABC kit, and 300µl was added to each well before incubation at room temperature for 30 minutes. Wells were washed three times for 5 minutes in PBS (1X). Vectastain Elite ABC substrate reagent (Horse radish peroxidase (HRP)-avidin conjugate) was made up in 10mls PBS (1X) and 300µl added to each well for 30 minutes. Slides were washed three times for 5 minutes in PBS (1X). The wells of the chamber slides were removed and the slides incubated in DAB-reagent for 2 minutes using a DAB substrate kit for peroxidase (Figure 5.2). The nickel chloride component was also added to the slides enhancing the final colour of the stain (Brown to grey-black). The slides were rinsed in water and counterstained with Mayer's haematoxylin for 1 minute. Slides were mounted in Aquamount, and the cells counted under a NIKON inverted light microscope. Cells were counted using an eyepiece graticule at X20 magnification. Cell counts within the grid were taken in five random fields of view per well.

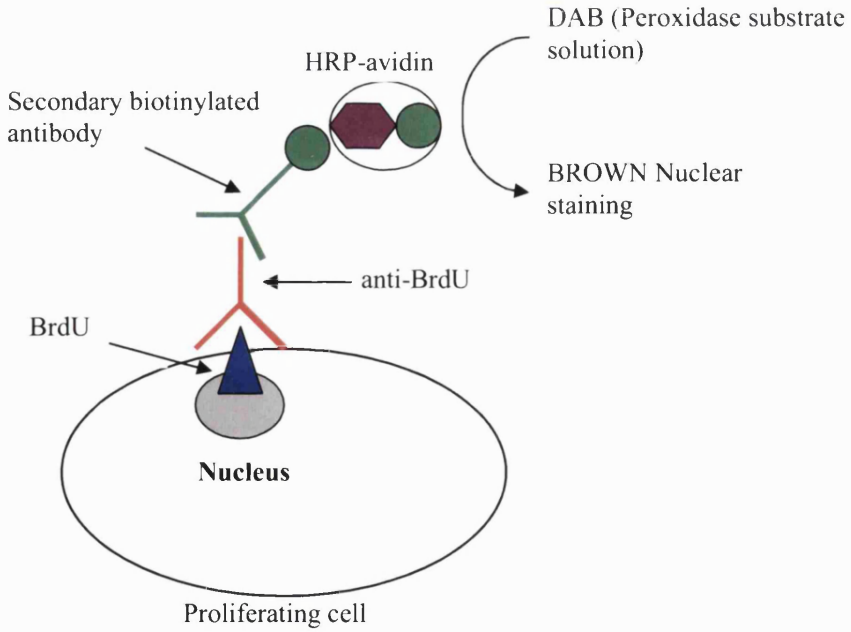

Figure 5.2 BrdU incorporation and visualisation.

5.2.4.2 Bromodeoxyuridine assay using an ELISA system in a range of oxygen tensions

The BrdU ELISA has major advantages over the cell counting method as it is faster, allows a larger number of samples to be processed simultaneously, reagents are supplied in a stable optimised form and the assay is at least as sensitive as the [^{3}H]-thymidine assay.

5.2.4.2.1 Materials

Cell Proliferation Biotrack ELISA System (Amersham Biosciences Ltd, Buckinghamshire, UK), Sulphuric acid (VWR International, Poole, UK). Mixed gases 0-5% oxygen, 5% CO_2 balanced nitrogen.

5.2.4.2.2 Protocol

Proliferation assays were performed using BrdU-incorporation assays (Amersham) based on the method by Gratzner (1982). Assays were performed according to manufacturer's instructions with some modifications. Adult dermal fibroblasts were seeded into 96-well plates and grown for 24 hours in a 5% CO_2 balanced air incubator. Fibroblasts to be treated at 21% O_2 remained in the incubator for a further 24 hours before treatment. Fibroblasts to be treated at 0, 1, 2 and 5% oxygen were transferred from the incubator into the oxygen controlled cabinet (see section 4.1.3) which was purged to the relevant gas mixture (0-5% oxygen, 5% CO_2 balanced nitrogen) and incubated for a further 24 hours. DMEM without phenol red was also placed into the cabinet in a vented tissue culture flask to equilibrate to the relevant pO_2. Fibroblasts were then treated for 72 hours with XO (0-50mU ml^{-1}), hypoxanthine (1mM), nitrite (1mM) and bFGF at (50ng ml^{-1}) diluted in fibroblast growth medium (DMEM without phenol red, 1% Penicillin/Streptomycin, 1% L-Glutamine, and 5% FCS) for a final volume of 200µl. BrdU labelling reagent (10µM) was then added to the cells in the incubator and oxygen controlled cabinet for four hours. After 4 hours the plates removed from the incubator and oxygen controlled cabinet. At room temperature, solutions supplied in the kit were used to fix the cells and denature the DNA for 30min, and block for 30 minutes. Fibroblasts were then incubated with 100µl peroxidase-labelled anti-brdU for 90 minutes. The wells were washed 3 times for 15minutes Then, 100µl 3,3'5,5'-tetramethylbenzidine (TMB) substrate was added to the wells until colour had developed (~15 mins). To terminate the reaction 25µl sulphuric acid (1M) was added to each well. The absorbance was then read on a plate reader at 450nm within 5 minutes.

5.2.5 Statistical analysis

Statistical analysis of data collected was performed using GraphPad Prism Version 4.00 (GraphPad Software Inc.). Statistical analysis performed using a one-way ANOVA statistical test and Dunnett's post test for analysis of variance between treatments.

5.3 Results

5.3.1 Characterisation of human dermal fibroblasts

5.3.1.1 Immunocytochemistry

Immunocytochemistry was carried out to confirm that the cells used in the following experiments were displaying positive fibroblastic characteristics and fibroblast markers. Figures 5.3 to 5.6 show typical growth characteristics, spindle shaped fibroblast morphology and positive staining for the beta-subunit of prolyl-4-hydroxylase which is essential for collagen biosynthesis and unique to fibroblasts. The fibroblast marker also detects disulphide isomerase which is identical to the beta-subunit of prolyl-4-hydroxylase. Primary antibody to aspergillus niger glucose oxidase which is neither found or induced in mammalian tissues was used as a negative primary antibody control. (Figure 5.7). A none primary antibody control was also included where no red-staining was observed (data not shown).

Figure 5.3-5.6

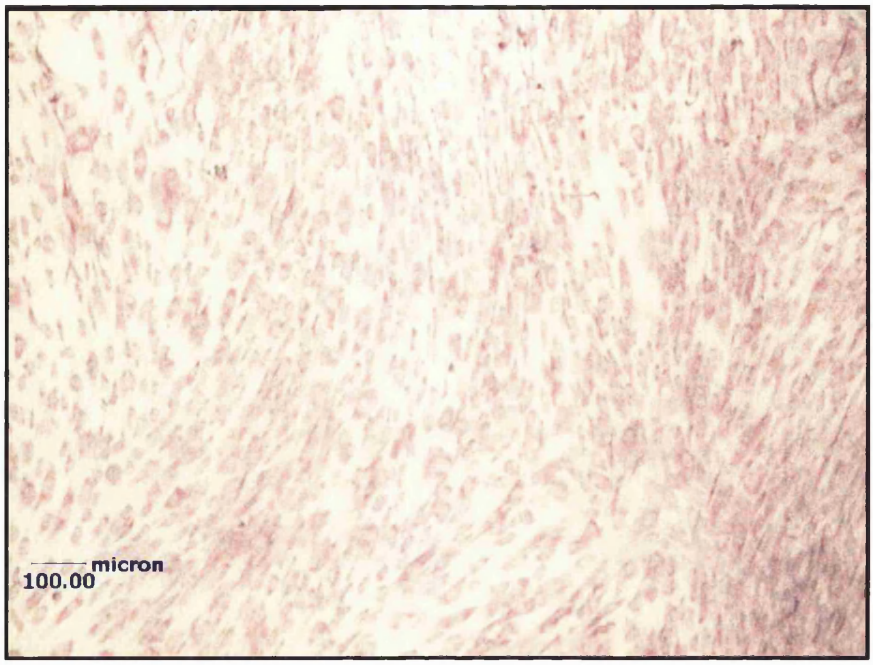

Figure 5.3 Neonatal human dermal fibroblasts stained with fibroblast marker

Immunocytochemistry of nHDF with mouse anti-human prolyl-4-hydroxylase antibody. Primary antibody dilution 1:100. Visualised using Vectastain ABC kit and fast red, and counterstained with Mayer's haematoxylin. Note. This image shows that there is greater than 80% staining showing a homogenous fibroblast culture. The swirling growth pattern is also characteristic of fibroblast growth in culture. (X5 magnification).

Figure 5.4 Neonatal human dermal fibroblasts stained with fibroblast marker

Immunocytochemistry of nHDF with mouse anti-human prolyl-4-hydroxylase antibody. Primary antibody dilution 1:50. Visualised using Vectastain ABC kit and fast red, and counterstained with Mayer's haematoxylin. Antibody reacts with β subunit of proly-4-hydroxylase and disulphide isomerase indicated by the red colour shown in the cytoplasm of the fibroblasts. The blue counterstain indicates nuclear staining. (X10 magnification).

Figure 5.5 Neonatal human dermal skin fibroblasts stained with fibroblast marker

Immunocytochemistry of nHDF with mouse anti-human prolyl-4-hydroxylase antibody. Primary antibody dilution 1:50. Visualised using Vectastain ABC kit and fast red, and counterstained with Mayer's haemotoxylin. Note. This image shows the typical fibroblast spindle shaped morphology. (X20 magnification).

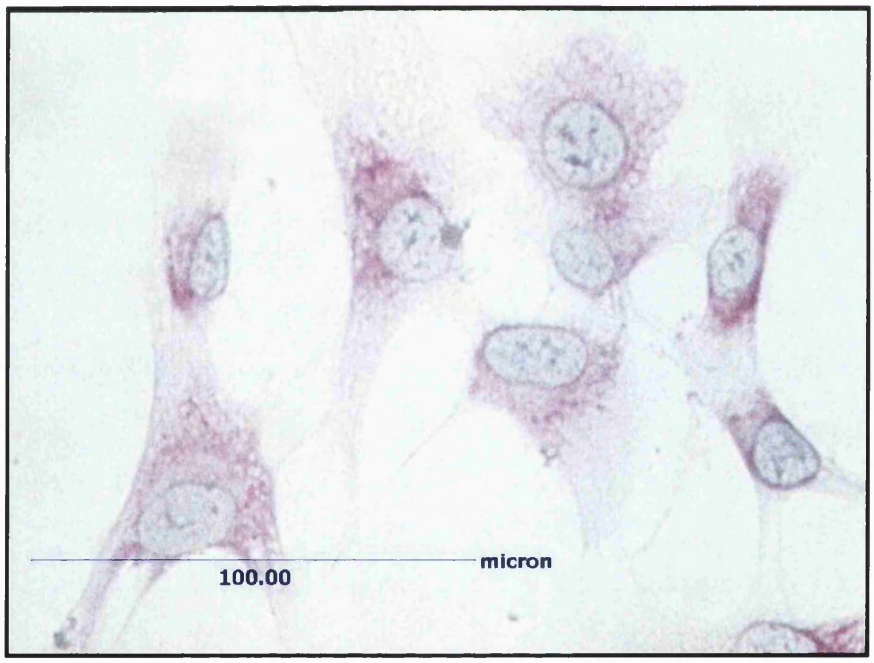

Figure 5.6 Neonatal human dermal skin fibroblasts stained with fibroblast marker

Immunocytochemistry of nHDF with mouse anti-human prolyl-4-hydroxylase antibody. Primary antibody dilution 1:50. Vectastain ABC kit and fast red, and counterstained with Mayer's haemotoxylin. Note. This close up clearly shows localization of the prolyl-4-hydroxylase in the cytoplasm of the cells, indicated by the red staining. (X40 magnification).

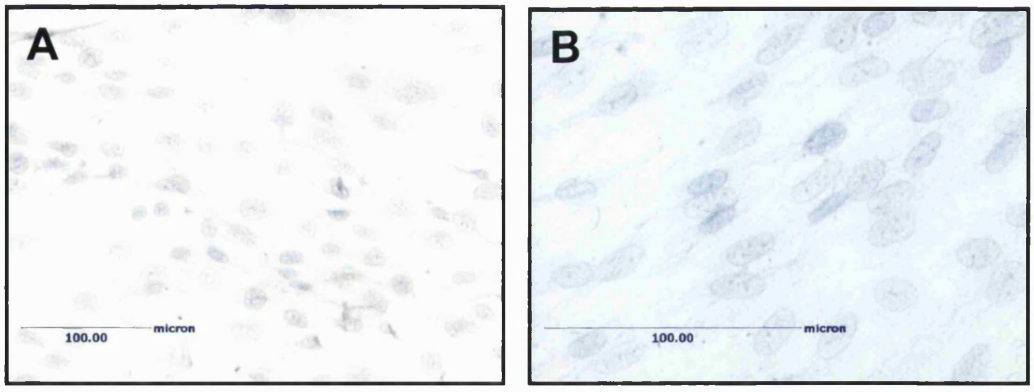

Figure 5.7 Negative antibody control.

A) X20 magnification. B) X40 magnification. Immunocytochemistry of nHDF with monoclonal mouse IgG1 antibody to aspergillus niger glucose oxidase. Primary antibody dilution 1:200. Visualised using VECTASTAIN ABC kit and fast red, and counterstained with Mayer's haemotoxylin. Note. There is no staining of the prolyl-4-hydroxyalse as indicated by the red stain in figure 5.2-5.5. However, a blue nuclear stain is clearly indicated by the Mayer's haematoxylin.

5.3.2 Effects of H_2O_2 and XO on the viability of human dermal fibroblasts

Metabolically active cells were assessed using the MTT reduction assay after exposure to varying concentrations of XO. An extensive range of XO concentrations were assayed in order to determine the concentration at which XO became cytotoxic to HDF. Murrell *et al* (1990) previously reported that concentrations of XO above 1mU ml^{-1} caused visible damage and detachment. The MTT assay can also detect changes in cell number and was also used as an indication as to whether XO enhanced the proliferation of HDF. Therefore dermal fibroblasts were exposed to a range of XO concentrations from 0-100mU ml^{-1}. Initial experiments were carried out using neonatal human dermal fibroblasts as they were already available as frozen stocks in the lab. These cells were useful for the development of assays, which were optimised for later use on adult HDF.

5.3.2.1 Dissociation of dermal fibroblast cultures for seeding

Cell dissociation solution was initially used to remove cells from the culture plastic for seeding of the dermal fibroblasts, and was chosen as it is a less harsh non-enzymatic method. However, there were problems with the initial MTT assays as it was difficult to derive an accurate cell count for seeding as the cells were not sufficiently dissociated and clumped together (Figure 5.8).

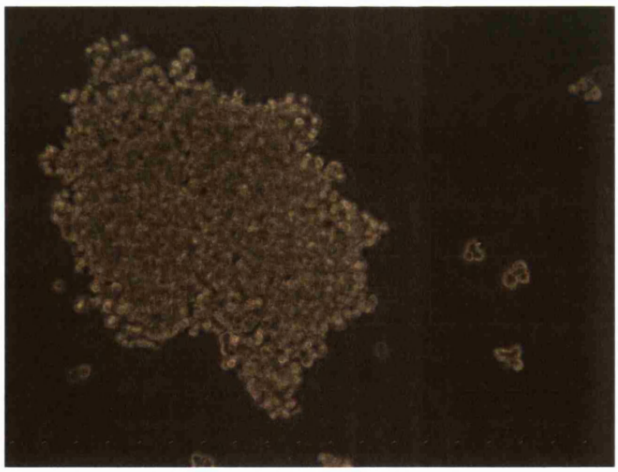

Figure 5.8 Clumps of cells after detachment from culture plastic using cell dissociation solution.

Note: Cells detached in sheets resulting in clumping, preventing accurate cell counts as observed under an inverted light microscope.

The alternative dissociation solutions Accutase and trypsin/EDTA that are commonly used in cell culture were also tried. Comparison of the methods showed that although cell dissociation solution is perhaps less harsh to the cells, the cells lifted from the plastic, only after around 45 mins, they also required gentle tapping, and they lifted off as sheets rather than individual cells. These sheets did not break up with vigorous pipetting and resulted in clumps of cells that were uncountable under the microscope. Accutase broke up the cell clumps and provided individual cells from which a cell count could be derived. However, the best results were found with trypsin/EDTA, as the cells needed only 10 minutes exposure and dissociated easily. Trypsin/EDTA proved to be the most successful at dissociating the cells for accurate cell counting and seeding and was therefore used for all future experimentation.

5.3.2.2 Effects of XO on the viability of nHDF in air

Prior to treatment of nHDF with XO, measurements were carried out to establish the sensitivity of the MTT assay at varying seeding densities. This was achieved by determining the relationship between the number of cells per cm^2 seeded into the well of a 96-well plate and the absorbance values at 550nm. Figure 5.9 shows that there is a linear relationship between the number of cells and the absorbance from $1x10^4$ up to around $5x10^4$ cells cm^{-2} with an Abs_{550nm} of around 2. This linear portion of the graph shows the seeding densities that are most sensitive for detecting changes in cell number. At cell numbers above between $5x10^4$ and $1x10^5$ the absorbance values begin to plateau and the assay loses its sensitivity.

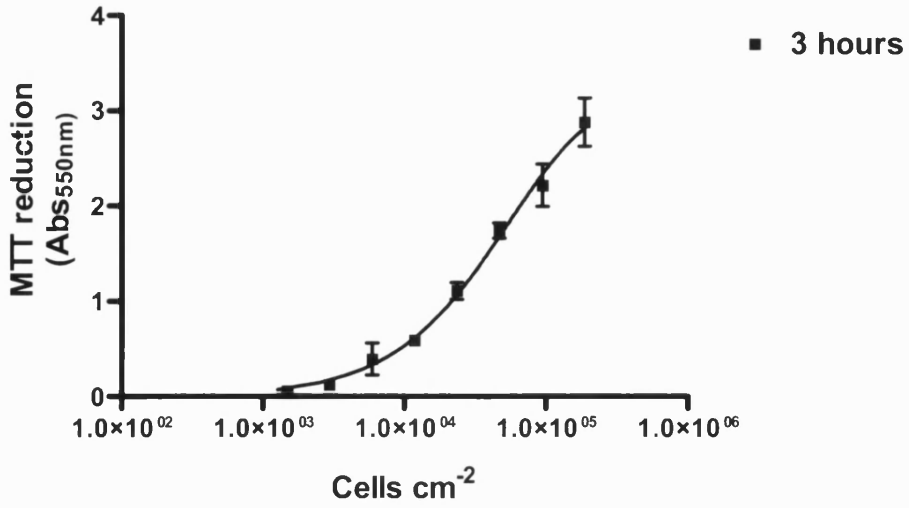

Figure 5.9 Cell number versus absorbance using the MTT assay

Neonatal human dermal fibroblasts were seeded into a 96-well plate at varying densities $1.5x10^3$, $3.0x10^3$, $6.0x10^3$, $1.2x10^4$, $2.4x10^4$, $4.8x10^4$, $9.6x10^4$, $1.9\ x10^5$ cells cm^{-2} in fibroblast growth medium (DMEM, 1% PS, 1% LG, 10% FCS) and cultured for 24 hours. MTT (1mg ml^{-1}) was added to DMEM without phenol red 1% PS, 1% LG, 10% FCS and 100µl added to the plate for 3 hours. Cells were solubilised with 100µl DMSO and the plate was read at 550nm. Mean±SD. n=3.

Neonatal human dermal fibroblasts were initially used to determine the effects of XO with hypoxanthine on the viability of skin fibroblasts. Figure 5.10 shows a significant decrease in MTT reduction at concentrations above 1mU ml^{-1} XO in the presence of 1mM hypoxanthine, suggesting a reduction in cell viability. Futhermore, cells in the presence of 1000U ml^{-1} XO without the addition of hypoxanthine did not reduce MTT. This result suggesting that there are substrates available in the medium that can be utilised by XO or that high concentrations of XO are cytotoxic.

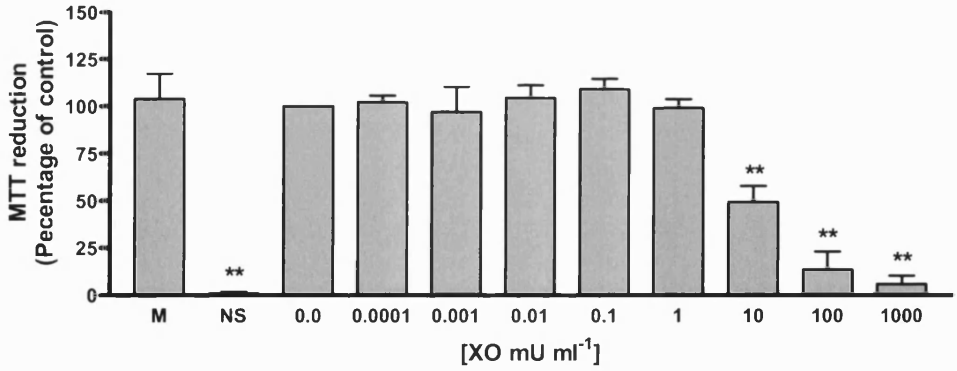

Figure 5.10 Viability of neonatal human dermal fibroblasts at varying XO concentrations.

Cells were seeded in 10% FCS, 1% PS, and 1% LG in phenol red free DMEM at 20,000 cells cm^{-2} and left for 24 hours to adhere to the 96-well plate. Cells were treated for 4 hours with a final concentration of XO at 0, 0.001, 0.1, 1, 10, 100 and 1000mU ml^{-1} XO and hypoxanthine (1mM) diluted in a final volume of 200µl DMEM without phenol red with 1% PS, 1% LG and HEPES (20mM). Cells were then incubated for 3 hours with MTT (1mg ml^{-1}). All incubations were carried out 37°C in 95% air/5% CO_2 incubator. No substrate (NS) wells contained 1000U ml^{-1} XO without hypoxanthine. Mean±SD. n=4. Results are displayed as a

percentage of the no enzyme control. Statistical analysis performed was One-way ANOVA with Dunnett's post test.

The experiment above was repeated using a more extensive range of XO concentrations Figure 5.11. This figure shows that XO concentrations between 1.562 and 6.25mU ml^{-1} XO appear to increase the reduction of MTT by nHDF and concentrations between 6.25mU ml^{-1} and 12.5mU ml^{-1} significantly reduce the viability of the fibroblasts.

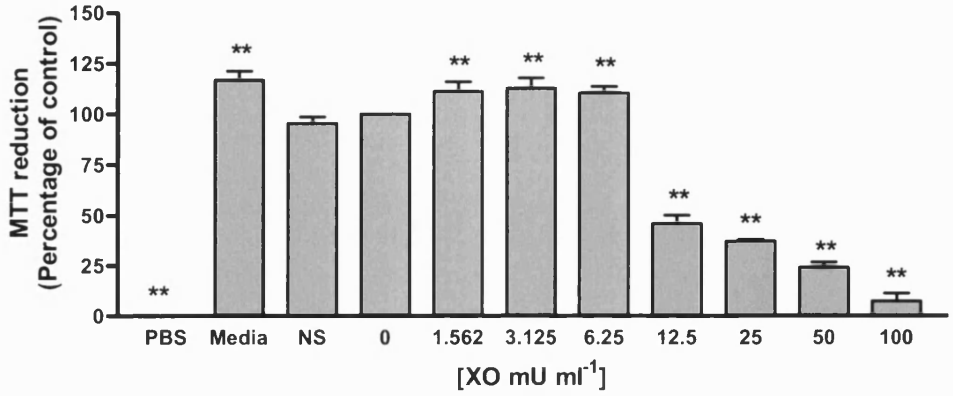

Figure 5.11Viability of neonatal human dermal fibroblasts at varying XO concentrations.

Cells were seeded in 10% FCS, 1% PS, and 1% LG in phenol red free DMEM at 25, 000 cells cm^{-2} and left for 24 hours to adhere to the 96-well plate. Cells were treated for 4 hours with a final concentration of XO at 0, 1.562, 3.125, 6.25, 12.5, 25, 50 and 100mU ml^{-1} XO and hypoxanthine (1mM) diluted in a final volume of 200µl DMEM without phenol red with 10% FCS, 1% PS, 1% LG and HEPES (20mM) buffer. Cells were then incubated for 3 hours with MTT (1mg ml^{-1}) or PBS as a control (See figure 5.9). All incubations were carried out 37°C in 95% air/5% CO_2 incubator. No substrate (NS) wells contained 100U ml^{-1} XO without hypoxanthine. Medium alone wells contained 200µl DMEM without phenol red with 10% FCS, 1% PS, 1% LG. Mean±SD. N=4. Results are displayed as a percentage of the no enzyme control. Statistical analysis performed was one-way ANOVA with Dunnett's post test.

The effects of varying concentrations XO on nHDF with increasing cell number was also assessed (Figure 5.12A and B). This figure shows that very low seeding densities such as 325 cells cm^{-2} are not sufficient to detect MTT reduction. As the seeding density increases to 10,000 cells cm^{-2} MTT reduction is detected and the assay is sensitive enough to show changes in absorbance at high concentrations of XO and at this seeding density there is a significant decrease in MTT reduction at concentrations of 6.25mU ml^{-1} XO and above. However, as the seeding density increases, to 20,000-25,000 cells cm^{-2} figure 5.12 does not show a significant decrease in MTT reduction until 12.5mU ml^{-1} XO.

Figure 5.12 A)

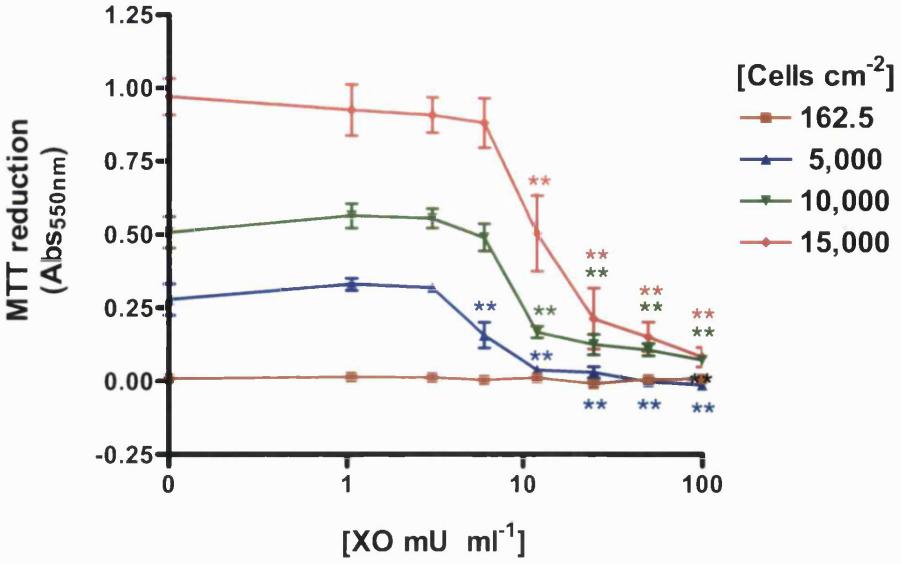

Figure 5.12 B)

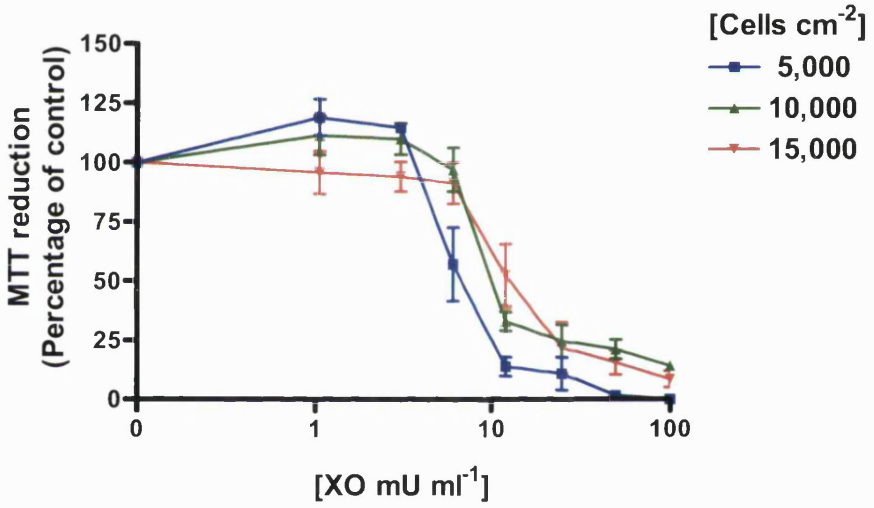

Figure 5.12 Effect of seeding density on the viability of nHDF exposed to XO.

Neonatal human dermal fibroblasts were seeded at 162.5, 5,000, 10,000 and 15,000 cells cm^{-2} and allowed to adhere to a 96-well plate for 24 hours. Cells were treated for 4 hours with a final concentration of XO at 0, 1.562, 3.125, 6.25, 12.5, 25, 50 and 100mU ml^{-1} XO and hypoxanthine (1mM) diluted in a final volume of 200µl DMEM without phenol red with 10% FCS, 1% PS, 1% LG and HEPES (20mM) buffer. Cells were then incubated for 3 hours with MTT (1mg ml^{-1}) or PBS as a control (See figure 5.10). All incubations were carried out 37°C in 95% air/5% CO_2 incubator. A) Absorbance values (Abs550nm) at changing XO concentrations. B) Data expressed as a percentage of the no enzyme control.

Assays were repeated to ensure that the assays in the presence of XO were reproducible. These assays showed similar results as in the preliminary assays; however it appeared that the effects of the enzyme on the viability of the cells was slightly reduced compared with previous assays. Cytochrome *c* assays showed no decrease in XO activity and therefore the slight decrease may be due to differences between FCS batches. Therefore, for all further experiments the FCS batch was kept constant. The controls in

Figure 5.13A) showed a slight reduction in viability in the presence of 100mU ml^{-1} XO without addition of hypoxanthine suggesting that substrates are present in the culture medium, most likely in the FCS. Figure 5.13B) showed a significant reduction in viability at 100mU ml^{-1} XO.

Figure 5.13A)

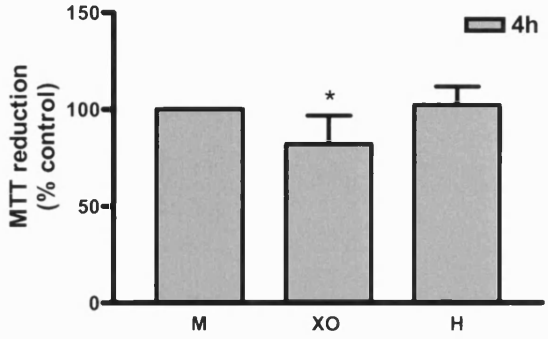

Figure 5.13B)

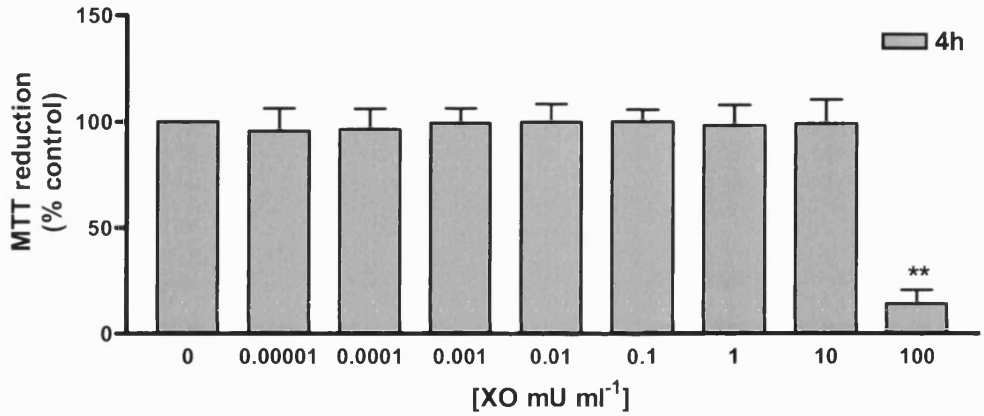

Figure 5.13 The effect of changing concentrations of XO on nHDF viability.

Neonatal human dermal fibroblasts were seeded at 9,600 cells per cm^{-2} and left to adhere for 24 hours. Cells were then treated for 4 hours with the test reagents diluted in fibroblast growth medium (DMEM, 1% LG, 1% PS and 10% FCS) and HEPES (20mM) in a final volume of 200µl. Graph A shows MTT reduction by cells treated with medium alone (M), XO (100mU ml^{-1}) and hypoxanthine (H) (1mM). Graph B shows MTT reduction by cells treated with final concentrations of hypoxanthine (1mM) and XO (0, 0.00001, 0.0001, 0.001, 0.01, 0.1, 1, 10, 100mU ml^{-1}). Experiments were carried out on 3 separate occasions in quadruplicate, therefore, n = 12. Mean±SD. Statistical analysis used was one-way ANOVA with dunnett's post test (*P<0.05 ** P<0.01).

Analysis of further XO concentrations showed that concentrations of 25mU ml^{-1} XO and above inhibited the growth of neonatal human dermal fibroblasts (Figure 5.14A and B).

Figure 5.14 A)

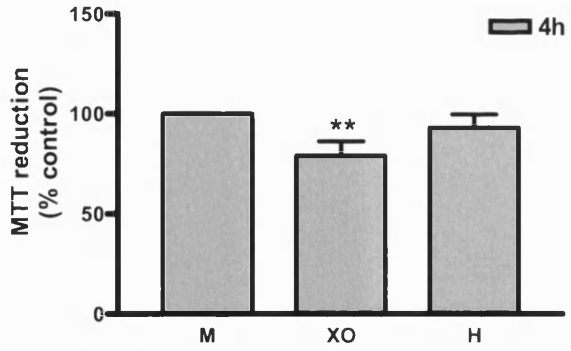

Figure 5.14B)

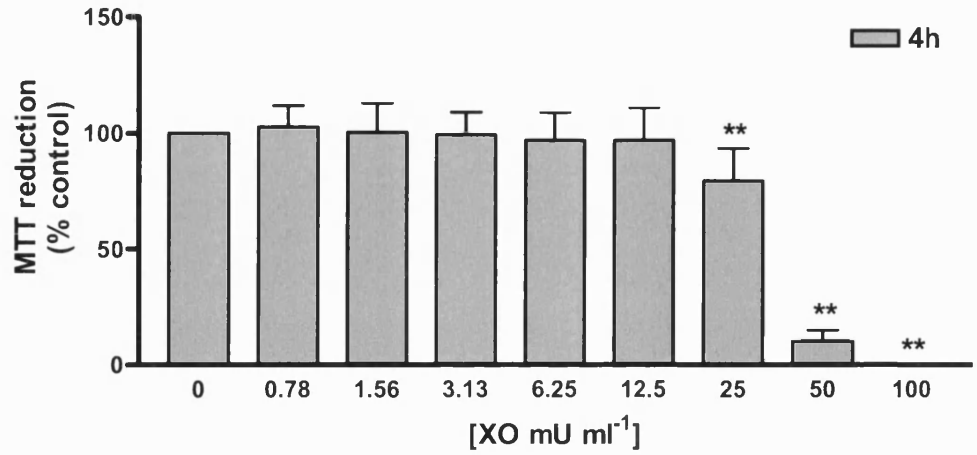

Figure 5.14 The effect of changing concentrations of XO on nHDF viability.

Neonatal human dermal fibroblasts were seeded at 9,600 cells cm^{-2} and left to adhere for 24 hours. Cells were then treated for 4 hours with the test reagents diluted in fibroblast growth medium (DMEM, 1% LG, 1% PS and 10% FCS) and HEPES (20mM) in a final volume of 200µl. Graph A shows MTT reduction by cells treated with medium alone (M), XO (100mU ml^{-1}) and hypoxanthine (H) (1mM). Graph B shows MTT reduction by cells treated with final concentrations of hypoxanthine (1mM) and XO (0, 0.78, 1.56, 3.13, 6.25, 12.5, 25, 50, 100mU ml^{-1}). Experiments were carried out on 3 separate occasions in quadruplicate, therefore, n=12. Mean ± SD. Statistical analysis used was one-way ANOVA with dunnett's post test (** $P<0.01$).

5.3.2.3 Effects of H_2O_2 on the viability and proliferation of nHDF

The MTT reduction assay is generally used for the detection of viable cells as shown in the previous graphs. However, it can also be used as a proliferation assay as the level of MTT reduction is directly related to cell number. As the previous assays did not show any significant increase in cell number in the concentration ranges described by Murrell *et al* (1990), the MTT assay was developed further as a possible method for the measurement of proliferation. The FCS concentration was also reduced to try to enhance the proliferative response to XO-generated species as the proliferation of the cells at 10% FCS may already be at optimal levels. Figure 5.15 shows the growth of nHDF at varying concentrations of FCS. After 24 hours at 0.1% FCS the cells show a reduced number of

viable cells compared with the start of the experiment, indicating that there is some cell death at this concentration after 24hours. At 1% FCS the number of viable cells does not appear to have increased suggesting that there is little proliferation occurring at 1% FCS after 24hours. At 5% FCS there is around half the number of viable cells compared with 10% FCS after 24 hours; this suggests that 5% FCS would be a suitable concentration for the proliferation assays as the cells are growing, but at a decreased rate.

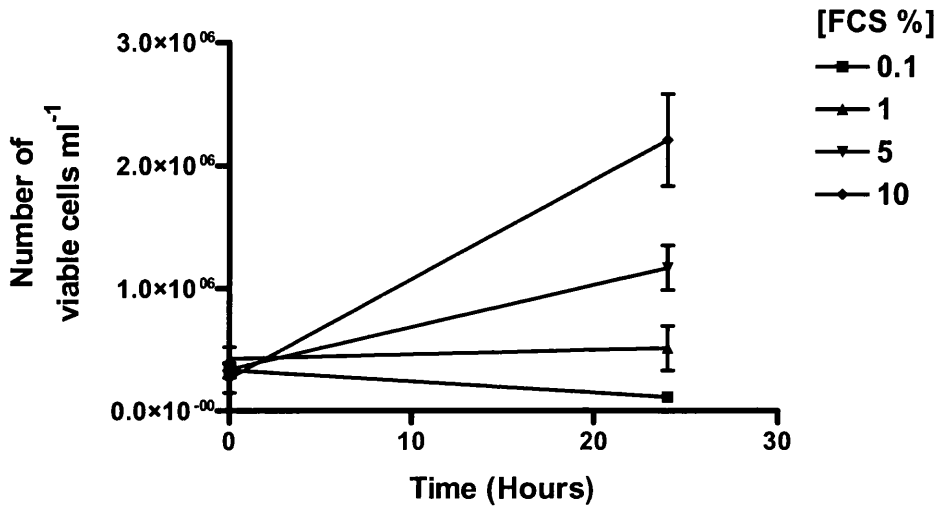

Figure 5.15 Growth of nHDF at varying concentrations of FCS

Neonatal human dermal fibroblasts were seeded into 12-well plates at 4,400 cells cm^{-2} and left to adhere for 24 hours in fibroblast growth medium (DMEM with 1% LG, 1% P/S and 10% FCS). Cells were then treated with test medium (DMEM with 1% PS, 1% LG, and FCS at 0.1, 1, 5 and 10%). At each time point cells were trypsinised and washed and resuspended in 200µl medium for cell counts. 20µl of cell suspension was mixed with 20µl of trypan blue and added to a haemocytometer for viable cell counts. Five individual counts were carried out per well. n=3. Mean±SD.

The previous trypan blue assay shown in figure 5.15 was repeated using the MTT assay and an increased number of FCS concentrations (Figure 5.16). After the first four hours there is little change in the absorbance suggesting that there is little change in the number of viable cells. However, at 24 hours the absorbance values increase suggesting an increased number of metabolically viable cells, with increasing FCS concentrations. After 28 hours, the absorbance values plateau at concentrations of 5% FCS and below, however, at 10% FCS there is a dramatic decrease in absorbance suggesting that there is a sharp drop in the number of viable cells, possible due to depletion of the nutrients of the culture medium by the high numbers of cells.

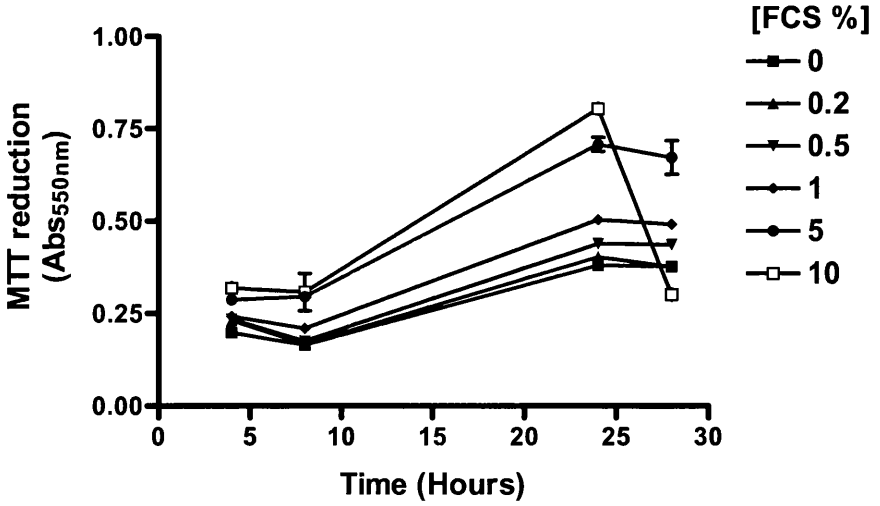

Figure 5.16 Growth of nHDF at varying concentrations of FCS

Cells were seeded at 9,678 cells per cm^{-2} into a 24-well plate and left to adhere for 24 hours in medium without phenol red 10% FCS, 1% LG, 1% PS. Cells were treated with varying levels of FCS 0-10% an individual plate was used for each time point 4h, 8h, 24h, 28h. A final concentration of 1mg ml^{-1} MTT was added to the plate 3 hours before the end of the incubation. The MTT was then aspirated from the wells and the plate was air dried and frozen at -20°C so that all plates could be analysed together. 100µl DMSO usually added to a 96-well plate (0.31 cm^2 growth area) therefore 616µl DMSO was added to the wells of the 24 well plate (1.91 cm^2 growth area).

Previous research carried out by Murrell *et al* (1990) suggested that XO mediated proliferation was predominantly due to H_2O_2 generation, and several other papers have shown that reactive oxygen species including H_2O_2 are capable of causing cell proliferation at low concentrations. Several assays were carried out to determine whether there is enhanced proliferation after exposure of nHDF to varying H_2O_2 concentrations. Figure 5.17 shows a significant increase in absorbance for the 10% FCS positive control suggesting an increase in viable cells. However, the cells treated with varying concentrations of H_2O_2 appear to be relatively unaffected by 0-50µM H_2O_2 (figure 5.17).

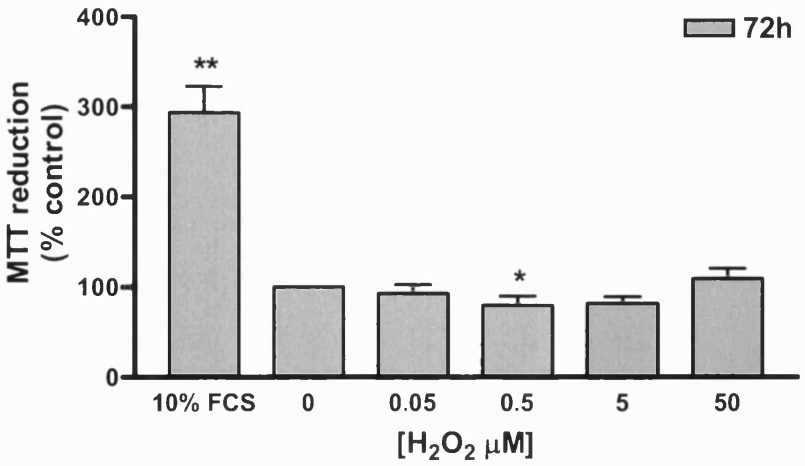

Figure 5.17 The effect of H_2O_2 on the viability of nHDF

Neonatal human dermal fibroblasts were seeded at 20,000 cells cm^{-2} and left to adhere for 24 hours. Cells were then treated for 72 hours with H_2O_2 (0, 0.05, 0.5, 5 and 50μM) diluted in test medium (DMEM with 0.2% FCS, 1% LG, 1% PS). Cells were also treated with 10% FCS as a positive control for proliferation. MTT (0.5 mg ml^{-1}) was added to the plates at for 3 hours. The assay was carried out in quadruplicate, except XO (50mU ml^{-1}) n=8. Mean±SD. Statistical analysis performed was one-way ANOVA with Dunnett's post test using 0μM H_2O_2 as the control (*P<0.05 ** P<0.01).

In Figure 5.18, the FCS concentration was increased to 2% and an increased range of H_2O_2 concentrations were used (0-500μM, Figure 5.18). This figure showed enhanced viability of nHDF between 3.906 and 31.25μM H_2O_2 and a decrease in viability at concentrations of 125μM H_2O_2 and above.

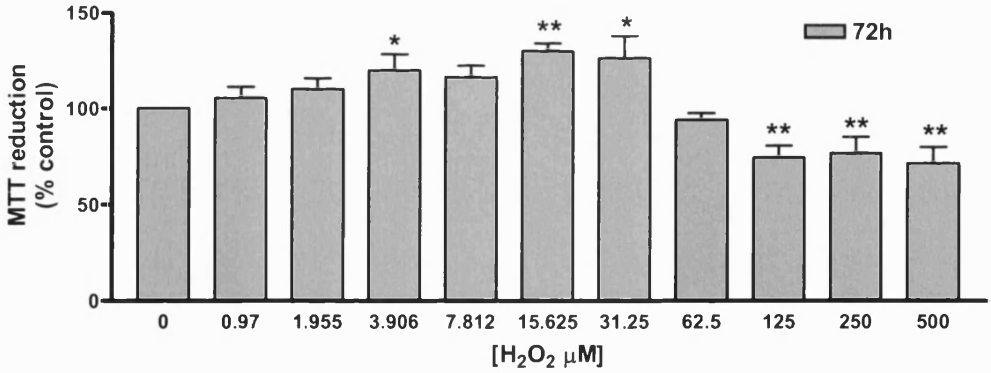

Figure 5.18 Treatment of nHDF with H_2O_2 for 72 hours

Neonatal human dermal fibroblasts were seeded at 8,000 cells cm^{-2} into a 96-well plates diluted in medium (DMEM without phenol red with FCS 2%, PS 1%, LG 1%) and allowed to adhere for 24 hours. Cells were treated for 72 hours with H_2O_2 (0, 0.97, 1.955, 3.906, 7.8, 15.6, 31.3, 62.5, 125, 250, 500μM) and HEPES (20mM), diluted in test medium (DMEM, FCS 2%, PS 1%, LG 1%). MTT (0.5mg ml^{-1}) was added to the plates at for 3 hours. n=4. Mean±SD. Statistical analysis performed was One-way ANOVA with Dunnett's post test using 0μM H_2O_2 as the control (*P<0.05 ** P<0.01).

The previous H_2O_2 assay (figure 5.18) was repeated again with further modifications to the protocol. The assay shown in figure 5.19 was carried out using an extended range of H_2O_2 concentrations (0-10,000μM) to show the full range of the effects

of H_2O_2 on the nHDF. The FCS concentration was also increased to 5% to try to maximise the proliferative response to H_2O_2 as an assay by Kim *et al,* (2001) showed an increase in viable cells and a suggestion of enhanced proliferation at between 0.01 and 10μM H_2O_2 and a significant dose dependent decrease in the number of viable cells at concentrations above 1000μM H_2O_2.

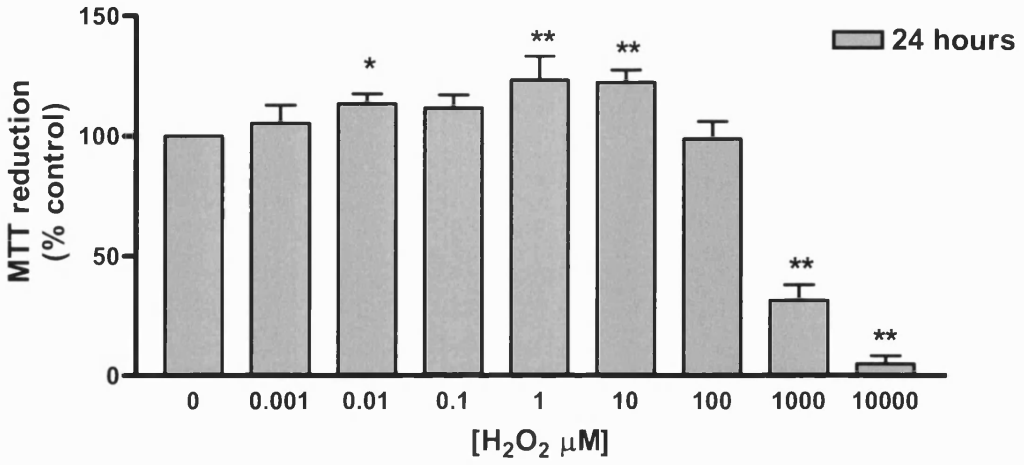

Figure 5.19 Treatment of nHDF with H_2O_2

Neonatal human dermal fibroblasts were seeded at 4,000 cells per cm^{-2} into a 24-well plate in medium (DMEM without phenol red with 1% LG, 1% PS and 5% FCS) and incubated for 48 hours. Fibroblasts were then treated with final concentrations of 0, 0.001, 0.01, 0.1, 1, 10, 100, 1000, and 10,000μM H_2O_2 and HEPES (20mM) diluted in medium (DMEM without phenol red with 1% PS, 1% LG and 5% FCS). After 24 hours MTT (0.5mg ml^{-1}) was added to the plates for 3 hours. 500μl DMSO was added to the wells to dissolve the cells and 100μl was transferred to a 96 well for absorbance readings at 550nm. n=4. Mean±SD. Statistical analysis performed was one-way ANOVA with Dunnett's post test using 0μM H_2O_2 as the control (*P<0.05 ** P<0.01).

Although Murrell *et al* (1990) carried out fibroblast proliferation studies in the presence of HEPES buffer; studies have shown that HEPES has radical scavenging activity. Therefore, assays were carried out to determine whether removal of the HEPES buffer affected the response of the dermal fibroblasts to changing concentrations of H_2O_2, and possibly enhanced the proliferative response. Experiments were carried out for 24, 48 and 72 hours with changing H_2O_2 concentrations with and without HEPES buffer (Figure 5.20A, B and C). Exposure to H_2O_2 for 24 hours with and without HEPES showed a slight decrease in viability in the absence of HEPES with increasing concentrations of H_2O_2; this decrease was not present in the presence of HEPES. This is probably due to scavenging of the H_2O_2 by HEPES. A study by Simpson *et al* (1988) implies that HEPES is capable of forming a complex with copper ions to breakdown H_2O_2 by the Fenton reaction.

Figure 5.20A)

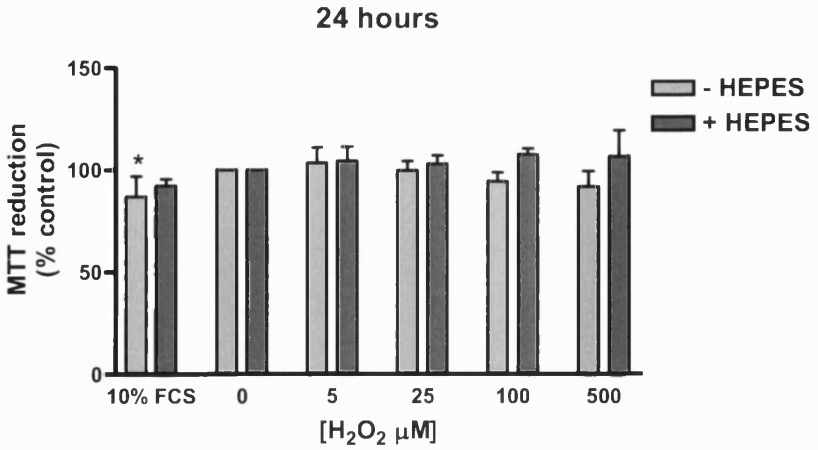

Figure 5.20B)

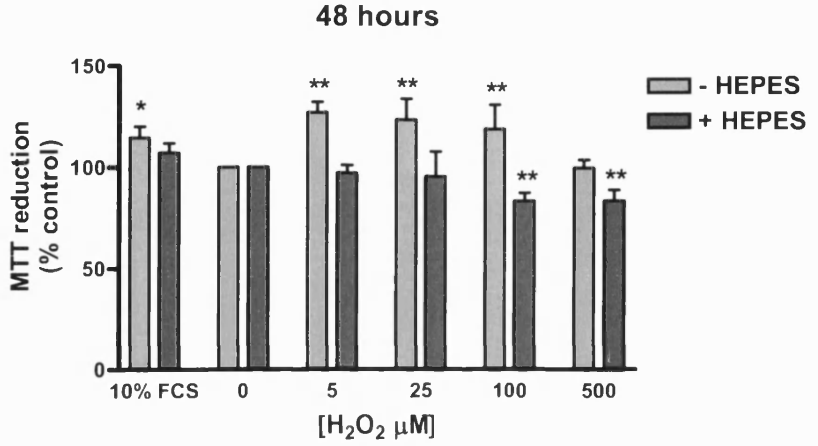

Figure 5.20C)

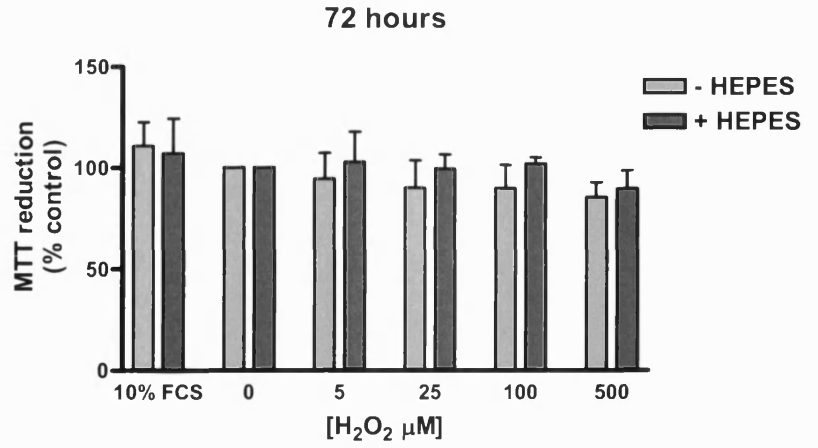

Figure 5.20 Treatment of cells with H_2O_2 with and without HEPES buffer for 24, 48 and 72 hours.

Neonatal human dermal fibroblasts were seeded in medium (DMEM with 5% FCS, 1% LG, 1% PS) with or without HEPES (20mM) at 523.56 cells per cm^{-2}. The medium was replaced with fresh after 3 days. The cells were treated 6 days after seeding with H_2O_2 (0, 5, 25, 100, 500μM) diluted in culture medium (5% FCS, 1% PS, 1% LG DMEM) with (+HEPES, 20mM) or without HEPES (-HEPES). Cells were then incubated for a further 24 (graph A), 48 (graph B) and 72 (graph C) hours. 10% FCS was also included as a positive control for proliferation. n=4. Mean±SD. Statistical analysis performed was one-way ANOVA with Dunnett's post test using 0μM H_2O_2 as the control (*P<0.05 ** P<0.01).

The exposure of nHDF to XO was repeated using 5% to determine whether the proliferative response was enhanced compared with assays previously carried out using 10% FCS. Figure 5.21 shows enhanced viability at 1mU ml^{-1} XO, indicating enhanced proliferation at this concentration of the enzyme. There also a reduction in the viability of nHDF at 20 and 50mU ml^{-1} XO.

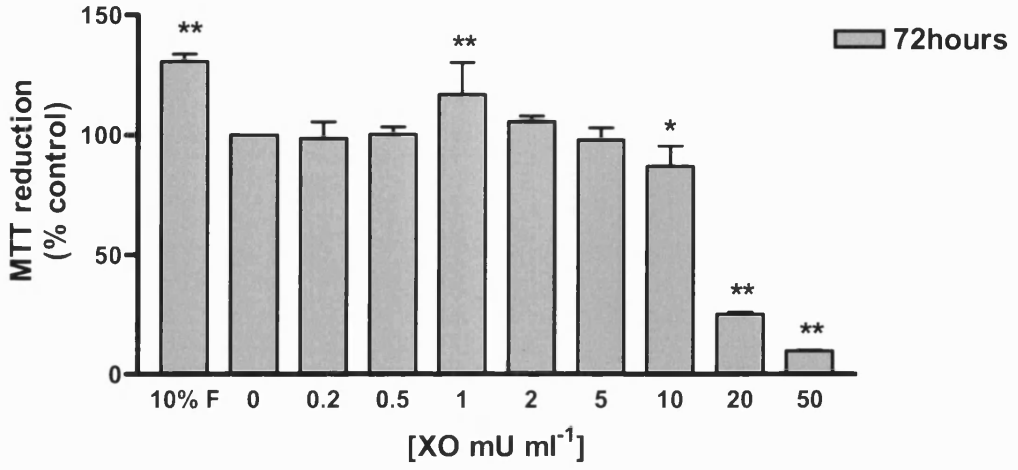

Figure 5.21 Treatment of nHDF with XO

Neonatal human dermal fibroblasts were seeded into 24-well plates at 2419 cells cm^{-2} and rested for 48 hours. Cells were then treated with XO (0, 0.2, 0.5, 1, 2, 5, 10, 20, 50mU ml^{-1}) and hypoxanthine (1mM) diluted in 5% FCS cells were incubated for 72 hours. 10% FCS (F) was also added as a positive control for proliferation. MTT was added for 3 hours. 500µl DMSO added per well 100µl transferred into a 96-well plate. n=4. Mean±SD. Statistical analysis performed was One-way ANOVA with Dunnett's post test using 0µM H_2O_2 as the control (*$P<0.05$ ** $P<0.01$).

Assays were also carried out using basic fibroblast growth factor (bFGF) to determine a suitable concentration to act as a positive control for fibroblast proliferation (Figure 5.22A-C). Figure 5.22A shows that after 24 hours, 25ng ml^{-1} bFGF and above significantly increases absorbance as compared to the control, suggesting an increase in viable cells. After 48 hours, figure 5.22B shows an increase in viable cells at the lower concentration of 5ng ml^{-1} bFGF and above. Figure 5.22C shows that after 72 hours the absorbance is significantly increased compared with the control at 10ng ml^{-1} bFGF and above. The 10% FCS positive control also shows an increase in viable cells after 72 hours. These assays suggest that 50ng ml^{-1} bFGF would be suitable as a positive control for future proliferation assays.

Figure 5.22A)

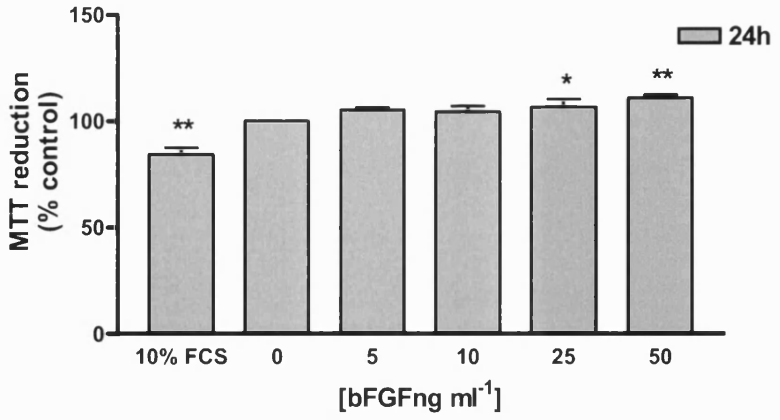

Figure 5.22B)

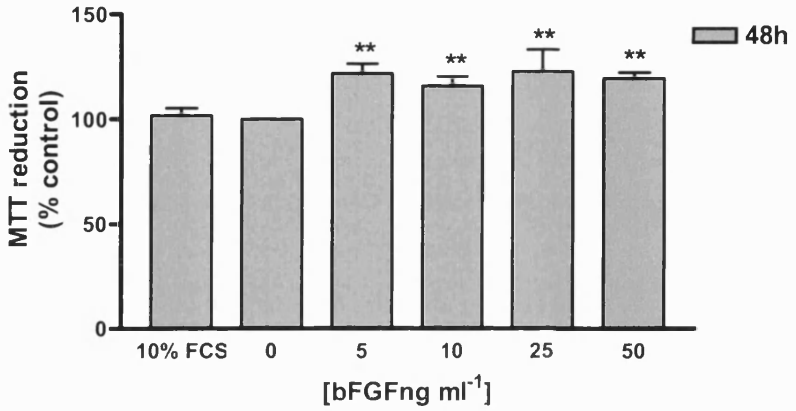

Figure 5.22C)

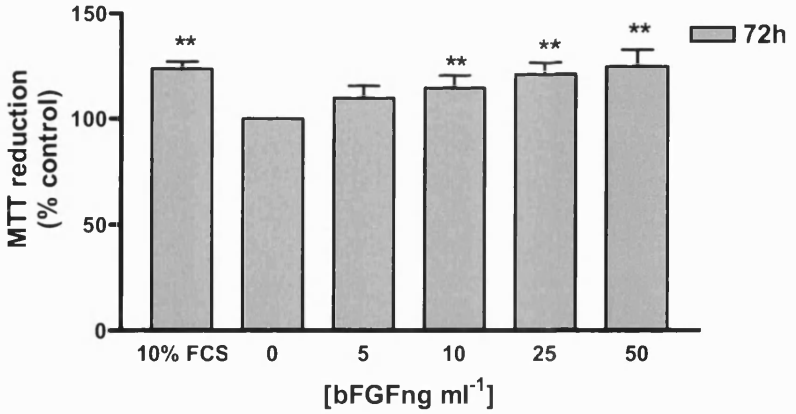

Figure 5.22 The effect of bFGF on nHDF

Neonatal human dermal fibroblasts were seeded into 24-well plates at 4839 cells cm^{-2} diluted in medium containing 5% FCS and rested for 48 hours before treatments with 10% FCS and bFGF (0, 5, 10, 25 and 50ng ml^{-1}) for 24, 48 and 72 hours. MTT (0.5mg ml^{-1}) was added for 3 hours. n =4. Mean±SD. Statistical analysis performed was One-way ANOVA with Dunnett's post test.

5.3.2.4 Effects of XO on the viability of human dermal fibroblasts in a range of oxygen tensions

Assays in different oxygen concentrations were carried using adult human dermal fibroblasts (aHDF) as the majority of chronic ulcers occur in adult patients. Furthermore, neonatal fibroblasts are known to have enhanced proliferative capabilities as compared with adult fibroblasts (Schneider and Mitsui, 1976). Assays were repeated to determine the sensitivity of the MTT assay on aHDF at varying cell densities and after varying lengths of exposure to 0.5mg ml^{-1} MTT (Figure 5.23). This figure shows that 3226 cells cm^{-2} and above, is the optimal suitable seeding density to detect changes in cell number and between 3 or 4 hours exposure to MTT. There is a slight decrease in sensitivity when using a 2 hour incubation with MTT whereas the sensitivity when using a 3 and 4 hour incubation with MTT are comparable.

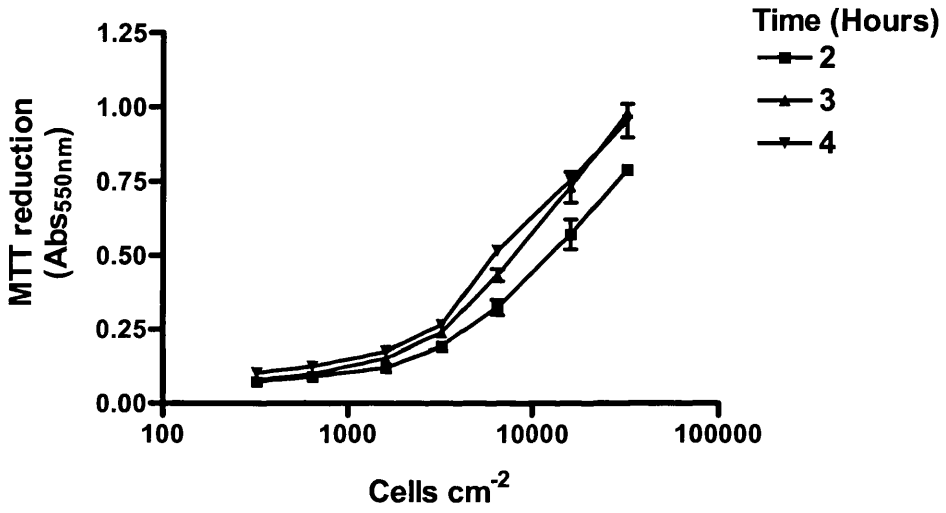

Figure 5.23 Sensitivity and kinetics of the MTT assay at 21% Oxygen.

Adult human dermal fibroblasts (N1) were diluted in 5% FCS DMEM without phenol red, 1% LG, 1% PS and seeded into a 96-well plate at 323, 645, 1613, 3226, 6452, 16129, 32258 cells cm^{-2}. The cells were incubated for 48h in a 5% CO_2 95% air incubator. MTT was then added and the cells reincubated for an additional 2h, 3h and 4h.

MTT assays were initially carried out to determine the effects of a range of XO concentrations between 0 and 50mU ml^{-1} XO on aHDF at 0% oxygen. These data however, were excluded from the data at 1, 2, 5 and 10% oxygen as the cell seeding was increased for these assays. Figure 5.24A shows that at 0% oxygen, there was no statistical difference between the medium alone control, and wells including substrates or XO alone. Addition of bFGF did not show any increase in absorbance suggesting that there is no increase in viable cells or measurable proliferative response. The data taken at 24 hours at 0% oxygen (figure 5.24B) suggest that there is little effect of XO on aHDF.

Figure 5.24A)

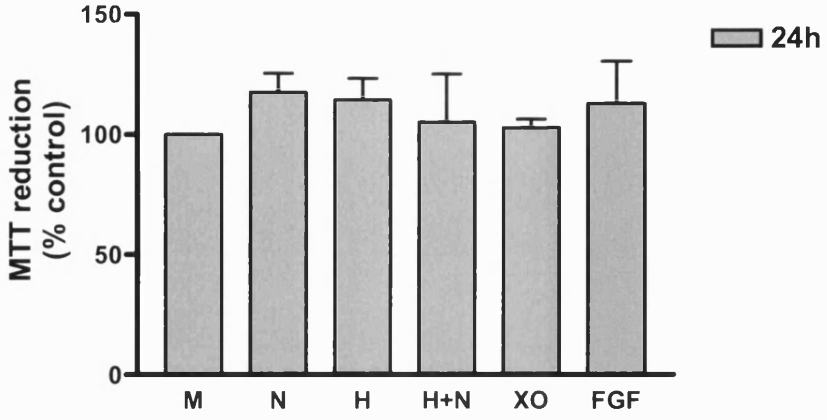

Figure 5.24B)

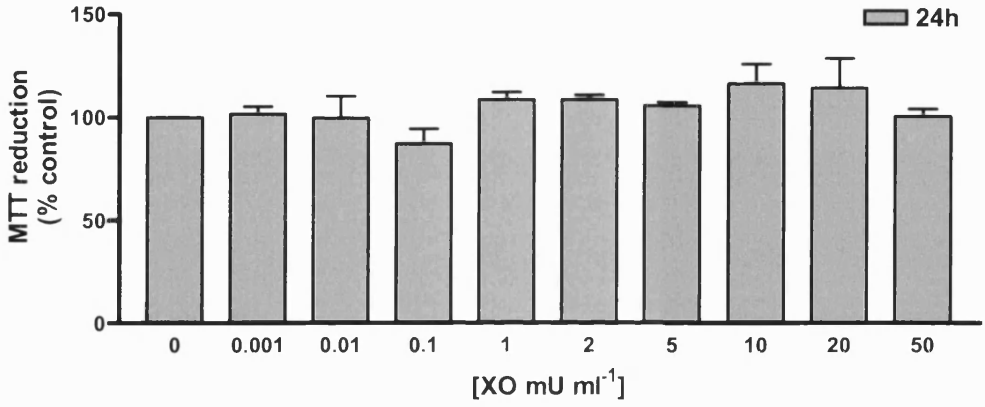

Figure 5.24 Treatment of aHDF with XO at 0% oxygen.

Adult human dermal fibroblasts (N1) were seeded at 1129 cells cm^{-2} into a 96-well plate and allowed to adhere to the plate for 48 hours. Cells were treated for 24 hours. Graph A shows the controls and they include fibroblast growth medium alone (M=DMEM, 1% P/S, 1% L-Glutamine and 5% FCS) and medium plus nitrite (N, 1mM), hypoxanthine (H, 1mM), hypoxanthine and nitrite (H+N, 1mM+1mM), XO (50mU ml^{-1}) and bFGF (10ng ml^{-1}). Graph B shows cells treated with final concentrations of XO at 0, 0, 0.001, 0.01, 0.1, 1, 2, 5, 10, 20, 50mU ml^{-1} with nitrite (1mM) and hypoxanthine (1mM). The background that was observed in wells containing no cells was substracted, and the data were expressed as a percentage of the control. Statistical analysis using one-way ANOVA with dunnett's post test showed no statistical significance on either graph when compared with controls. n = 3. Mean±SD.

Figure 5.25 shows that in air (21% O_2) there is a significant reduction in cell viability at 5, 10 and 50mU ml^{-1} with only after 3 hours of exposure to XO. However, at oxygen concentrations below 21% the cells appear to be unaffected by XO. At 1% oxygen there is even a suggestion of increased viability at 50mU ml^{-1} XO (Figure 5.25). The V1 fibroblasts, which are normal fibroblasts from a patient with a chronic wound (figure 5.26), also show a significant reduction in viability at 10 and 50mU ml^{-1} XO at 21% oxygen. These results also mirror the previous results in figure 5.25 which showed that below 21% oxygen, the fibroblasts were unaffected by XO at 0-50mUml^{-1}.

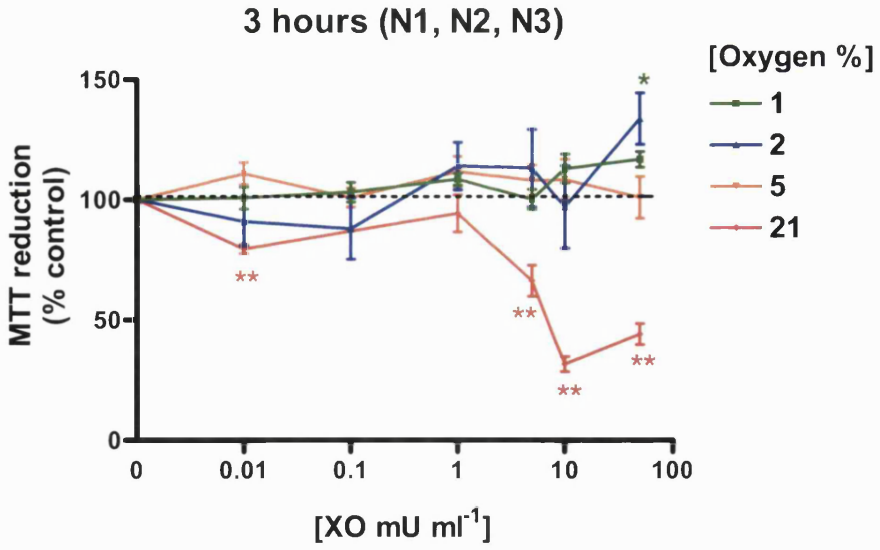

Figure 5.25 Treatment of aHDF with XO for 3 hours in 1, 2, 5, and 21% O_2

Cells were seeded at around 3,500 cells cm^{-2} and allowed to adhere for 48 hours cells were then exposed to hypoxanthine (1mM), nitrite (1mM) and XO (0, 0.01, 0.1, 1, 5, 10, 50mU ml^{-1}) diluted in medium (DMEM without phenol red, 5% FCS, 1% LG, 1% PS) for 3 hours. Results are shown as SEM. Statistical analysis one-way ANOVA and Dunnett's post test for multiple comparisons. 21% n =6, 5% n =12, 2% n =8, 1% n =6.

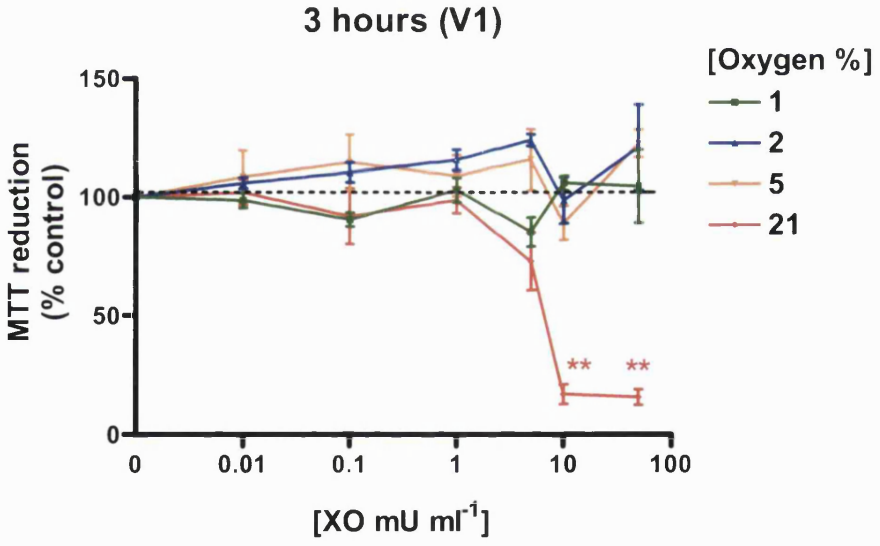

Figure 5.26 Treatment of aHDF with XO for 3 hours in 1, 2, 5, and 21% O_2

Cells were seeded at around 3,500 cells cm^{-2} and allowed to adhere for 48 hours cells were then exposed to hypoxanthine (1mM), nitrite (1mM) and XO (0, 0.01, 0.1, 1, 5, 10, 50mU ml^{-1}) diluted in medium (DMEM without phenol red, 5% FCS, 1% LG, 1% PS) for 3 hours. Results are shown as SEM. Statistical analysis one-way ANOVA and Dunnett's post test. n =4.

After a 24h exposure of normal aHDF to XO in 21% oxygen (Figure 5.27), there is a significant reduction in cell viability at 5, 10 and 50mU ml^{-1} XO (Figure 5.27). However, as the oxygen concentration decreases, the viability of the fibroblasts does not appear to be effected even at high enzyme concentrations. Interestingly, this figure also

shows a significant increase in viability at 1% oxygen at 10 and 50mU ml^{-1} XO (Figure 5.27). Similar results are also observed in figure 5.28 with fibroblasts from a chronic wound patient (V1). This figure shows a significant reduction in absorbance, and therefore viability, at 21% oxygen, whereas, with decreasing oxygen concentrations there appears to be increased viability at high XO concentrations (5-50mU ml^{-1} XO).

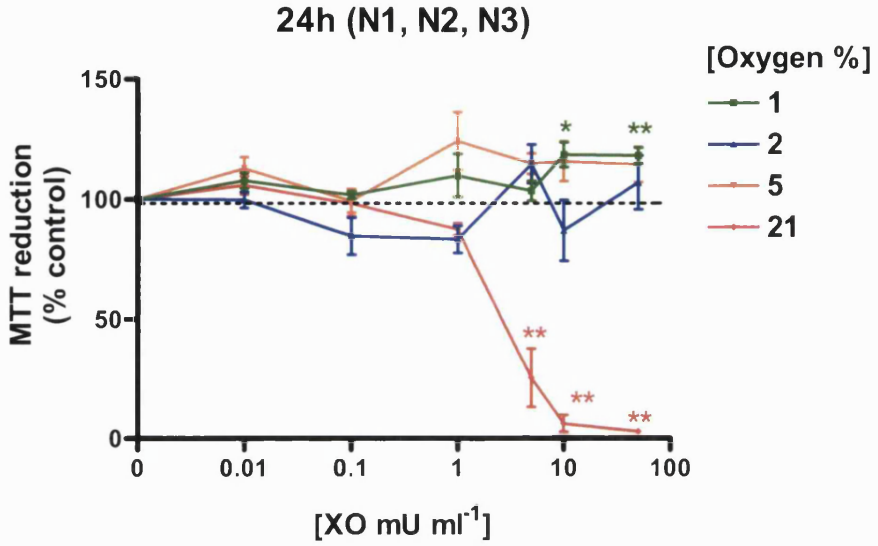

Figure 5.27 Treatment of aHDF with XO for 24 hours in 1, 2, 5, and 21% O_2

Cells seeded at around 3,500 cells cm^{-2} and allowed to adhere for 48 hours cells were then exposed to hypoxanthine (1mM), nitrite (1mM) and XO (0, 0.01, 0.1, 1, 5, 10, 50mU ml^{-1}) diluted in medium (DMEM without phenol red, 5% FCS, 1% LG, 1% P/S) for 24 hours. Results are shown as SEM. Statistical analysis performed was one-way ANOVA with Dunnett's post test for multiple comparisons. At 21% oxygen n=6, 5% n=12, 2% n=12, 1% n=6.

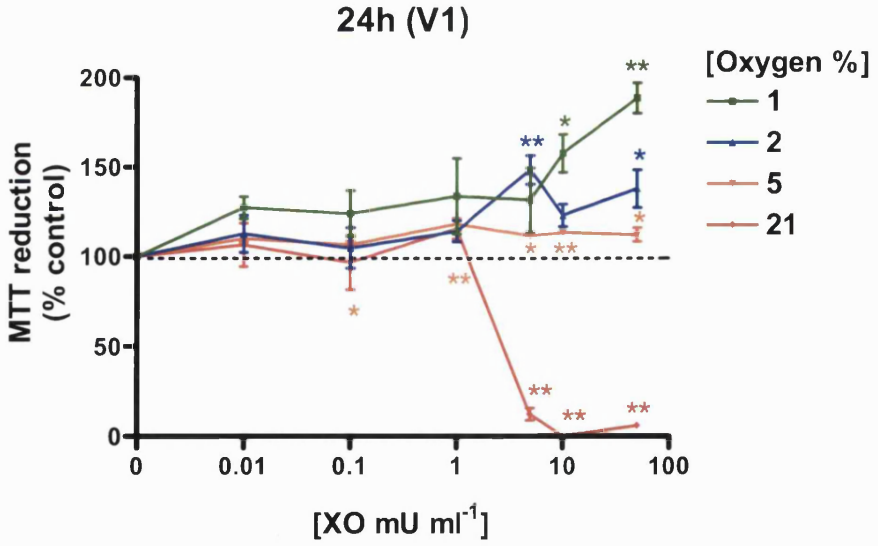

Figure 5.28 Treatment of aHDF with XO for 24 hours in 1, 2, 5, and 21% O_2.

Cells seeded at around 3,500 cells cm^{-2} and allowed to adhere for 48 hours cells were then exposed to hypoxanthine (1mM), nitrite (1mM) and XO (0, 0.01, 0.1, 1, 5, 10, 50mU ml^{-1}) diluted in medium (DMEM without phenol red, 5% FCS, 1% LG, 1% P/S) for 24 hours. Results are shown as SEM. Statistical analysis performed was one-way ANOVA with Dunnett's post test. At all oxygen concentrations n =4.

Fibroblasts from a separate experiment were seeded at a low density and treated with XO for 24 hours. Figure 5.29 also shows pictures of fibroblasts taken after exposure to 0-50mU ml^{-1} XO for 24 hours at 21% O_2. At high XO concentrations greater than 5mU ml^{-1} XO there is an increase in the roundness of the fibroblasts and visible damage and detachment from the culture surface, suggesting that excessive toxicity has damaged these cells beyond repair, having an appearance similar to that described for apoptotic cells. These cells also appear condensed but relatively intact, and the cytoplasm appears to have a granular appearance which may be due to the presence of enlarged vacuoles in the cytoplasm which are also features of apoptosis. These observations correspond with the assays shown in figure (5.27-5.28) which show that the fibroblasts do not reduce MTT suggesting that the cells are dead. However, figure 5.29 does not show any obvious visual signs of cell death at 5mU ml^{-1} XO, whereas, the MTT assay suggests that the metabolic viability of fibroblasts exposed to these concentrations of XO in hyperoxia (21% O_2) is significantly reduced.

The viability of the aHDF was also assessed after 72 hours exposure to XO at range of oxygen concentrations (Figure 5.30). In hyperoxia (21% oxygen) there is a significant decrease in MTT reduction at 5mU ml^{-1} XO and no MTT reduction was observed at 10-50mU ml^{-1} XO indicating an absence of any viable fibroblasts. As the oxygen concentration decreases, at 5% oxygen (normoxia) there is around a 20% reduction in viability at 10mU ml^{-1} XO, and a complete absence of MTT reduction at 50mU ml^{-1} XO. At 2% oxygen there is a significant increase in viability at 5mU ml^{-1} XO, and at 1% around a 25% decrease in viability at 50mU ml^{-1} XO. These findings were again similar to assays also carried out using V1 fibroblasts. However, at 2% oxygen the V1 fibroblasts show a significant increase in viability at 50mU ml^{-1} XO (Figure 5.31).

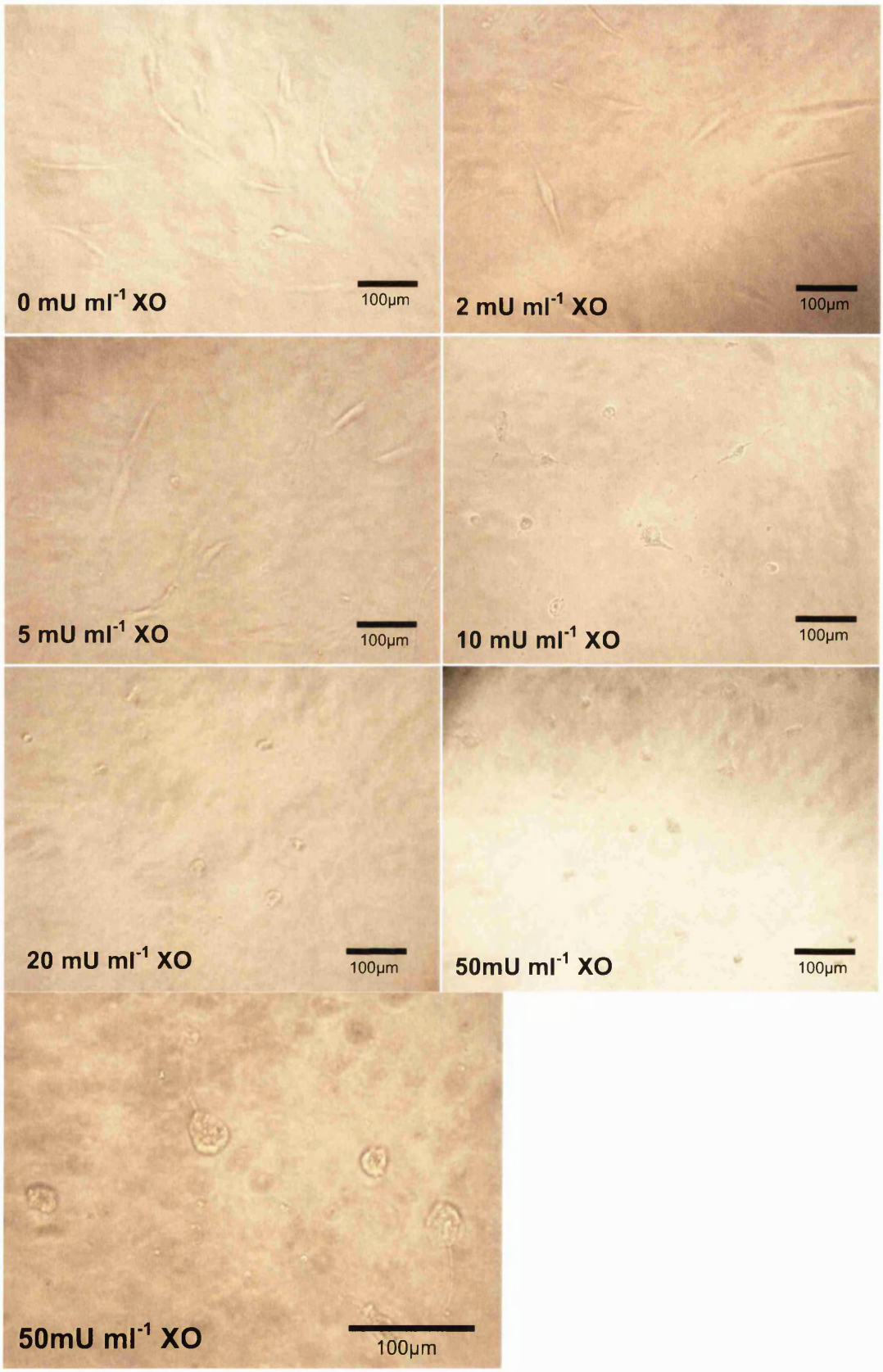

Figure 5.29 Treatment of aHDF with XO for 24 hours at 21% O_2

Fibroblasts (N1) were seeded at 1129 cells cm^{-2} and treated with hypoxanthine (1mM), nitrite (1mM), XO (0-50mU ml^{-1}). Cells were then visualised using the inverted microscope and pictures were taken using a digital camera.

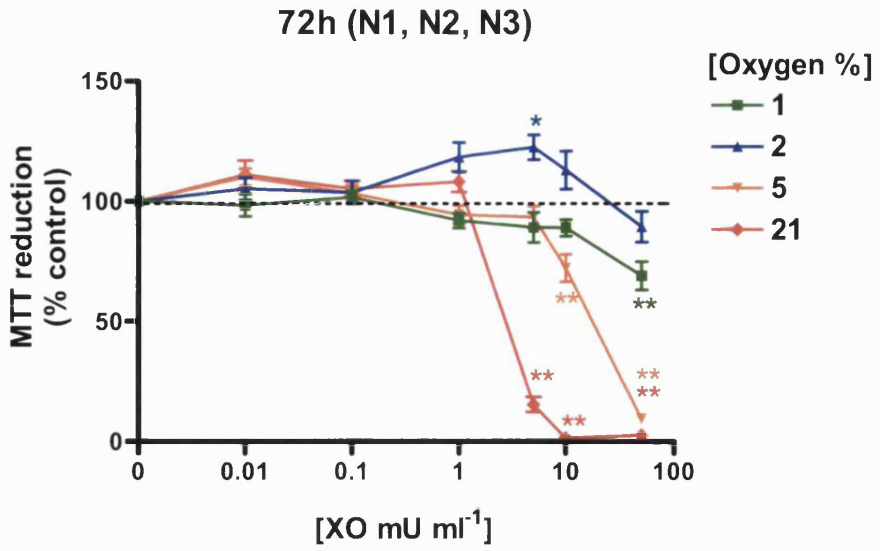

Figure 5.30 Treatment of aHDF with XO for 72 hours in 1, 2, 5, and 21% O_2

Adult human dermal fibroblasts (N1, N2 and N3) were seeded at around 3,500 cells cm^{-2} and allowed to adhere for 48 hours. Cells were then exposed to hypoxanthine (1mM), nitrite (1mM) and XO (0, 0.01, 0.1, 1, 5, 10, 50mU ml^{-1}) diluted in medium (DMEM without phenol red, 5% FCS, 1% LG, 1% PS) for 72 hours. bFGF (50ng ml^{-1}) was also added to the plates a positive control for proliferation and showed enhanced proliferation compared to the 0mU ml^{-1} XO control at 1 and 2% oxygen (data not shown). Results are shown as SEM. Statistical analysis performed was One-way ANOVA with Dunnett's post test. 12% n=10, 5% n=12, 2% n=12, 1% n=10.

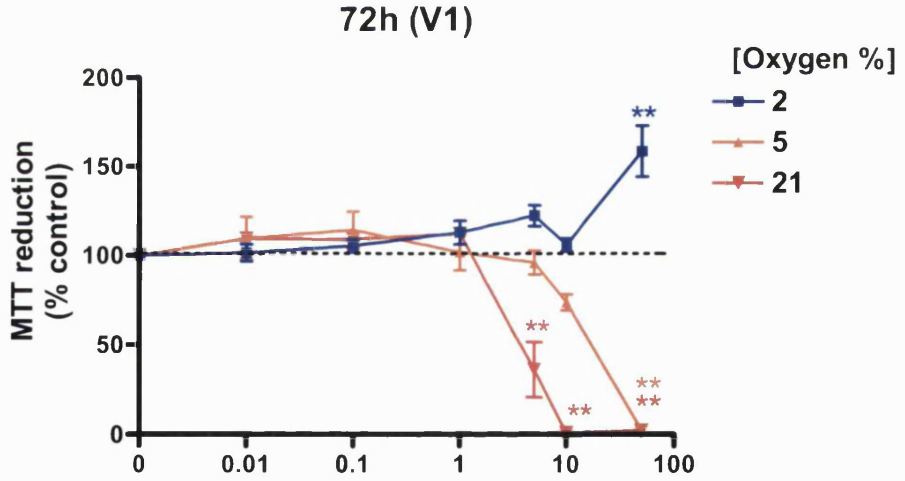

Figure 5.31 Treatment of aHDF with XO for 72 hours in 1, 2, 5, and 21% O_2

Cells seeded at around 3,500 cells cm^{-2} and allowed to adhere for 48 hours cells were then exposed to hypoxanthine (1mM), nitrite (1mM) and XO (0, 0.01, 0.1, 1, 5, 10, 50mU ml^{-1}) diluted in medium (DMEM without phenol red, 5% FCS, 1% LG, 1% PS) for 72 hours. bFGF (50ng ml^{-1}) was also added to the plates a positive control for proliferation. Results are shown as SEM. Statistical analysis performed was one-way ANOVA with Dunnett's post test. n=4.

5.3.3 Effects of XO on the DNA synthesis and proliferation of HDF

BrdU incorporation assays were used to assess the proliferation of HDF after exposure to varying concentrations of XO and hypoxanthine. Murrell *et al* (1990) previously showed enhanced proliferation of HDF using a [^{3}H]-thymidine incorporation assay. However, the immunological BrdU method used in this thesis has advantages over methods using [^{3}H]-thymidine in that it avoids radioactive material and the proportion of cells labelled by the two methods is the same (Oku, *et al* 1987).

5.3.3.1 Bromodeoxyuridine assay using chamber slides for cell counts

Neonatal human dermal fibroblasts were used to develop the initial BrdU assays. Fibroblasts were seeded into chamber slides so that the number of proliferating cells could be counted under the microscope. In the first set of experiments, cells were seeded at 10,000 cells cm^{-2} into 8-well chamber slides and incubated for 24 hours. Cells were then incubated for 4 hours with hypoxanthine (1mM) and XO (0-0.01mU ml^{-1}) and then with BrdU for 18 hours. The results indicate that after 18 hours, the majority of cells have doubled and incorporated BrdU into their nuclei and are positively labelled (figure 5.32-5.35). Furthermore, the fibroblasts clearly show several stages of cell division (Figure 5.33). However, a small percentage of negatively labelled cells are present on the slides (Figure 5.34-5.35) it is possible, that these cells are dead.

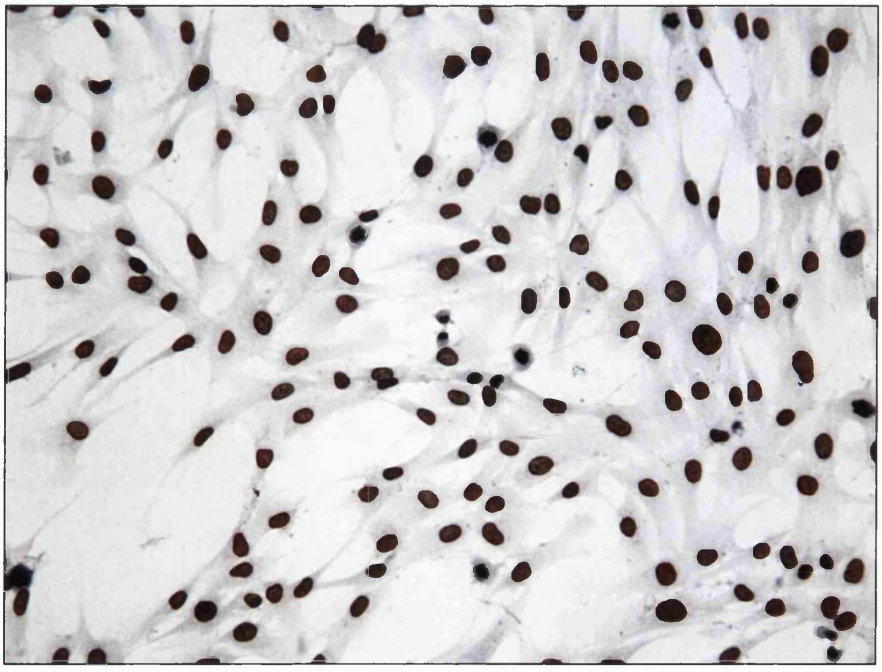

Figure 5.32 BrdU labelled nHDF (Substrate only control).

Cells were seeded at 10,000 cells cm^{-2} and incubated for 24 hours in fibroblast medium (Appendix I) Cells were then incubated for a further 4 hours in fibroblast medium incuding hypoxanthine (1mM) and HEPES (20mM) (Substrate only control). The cells were incubated with BrdU (10μM) for 18 hours and the assay was completed as described in the methods in section 5.2.4.1.2. Note. This image shows that the vast majority of cells are positively stained for incorporation of bromodeoxyuridine into the nucleus. (X20 magnification)

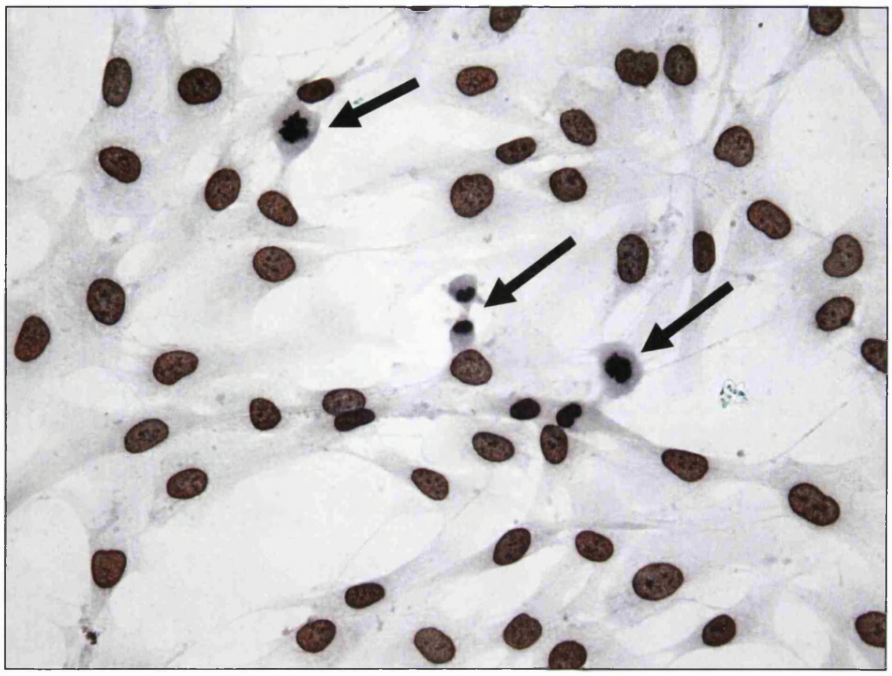

Figure 5.33 BrdU labelled nHDF (Substrate only Control).

Cells were seeded at 10,000 cells cm^{-2} and incubated for 24 hours in fibroblast medium (Appendix I) Cells were then incubated for a further 4 hours in fibroblast medium incuding hypoxanthine (1mM) and HEPES (20mM) (Substrate only control). The cells were incubated with BrdU (10μM) for 18 hours and the assay was completed as described in the methods in section 5.2.4.1.2. Note. This image is a magnified image of Figure 5.32 and shows several stages of proliferation (X40 magnification).

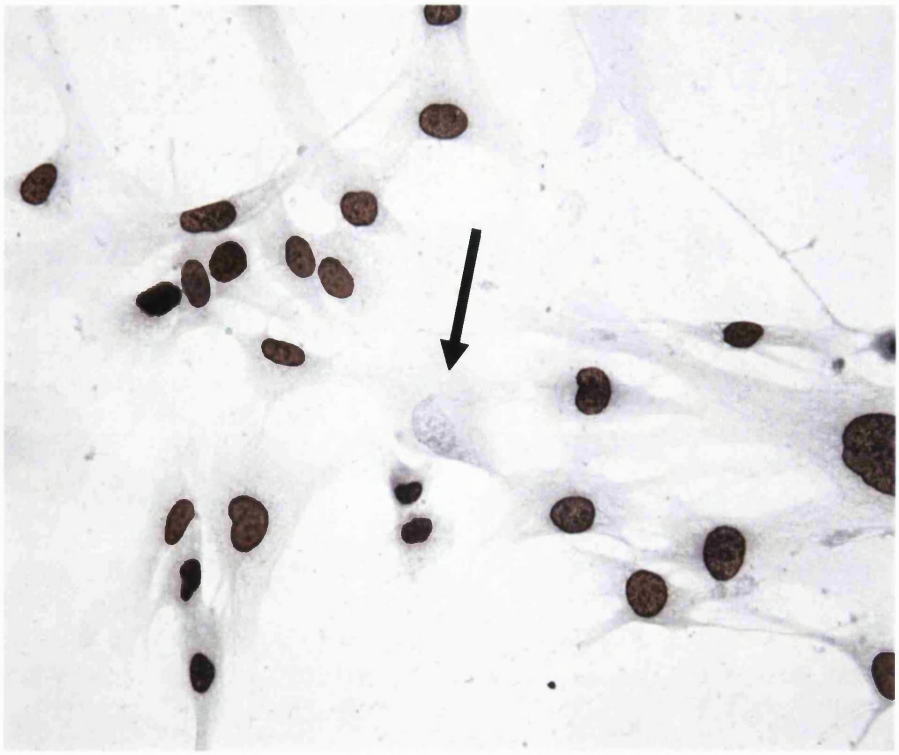

Figure 5.34 BrdU labelled nHDF (Substrate only Control).

Cells were seeded at 10,000 cells cm^{-2} and incubated for 24 hours in fibroblast medium (Appendix I) Cells were then incubated for a further 4 hours in fibroblast medium incuding hypoxanthine (1mM) and HEPES (20mM) (Substrate only control). The cells were incubated with BrdU (10μM) for 18 hours and the assay was completed as described in the methods in section 5.2.4.1.2. Note. This image shows a single cell that is negatively stained for BrdU incorporation (See arrow). Brown nucleus = BrdU positive cell. Blue nucleus = negatively stained cell counterstained with Mayer's haematoxylin. (X40 magnification).

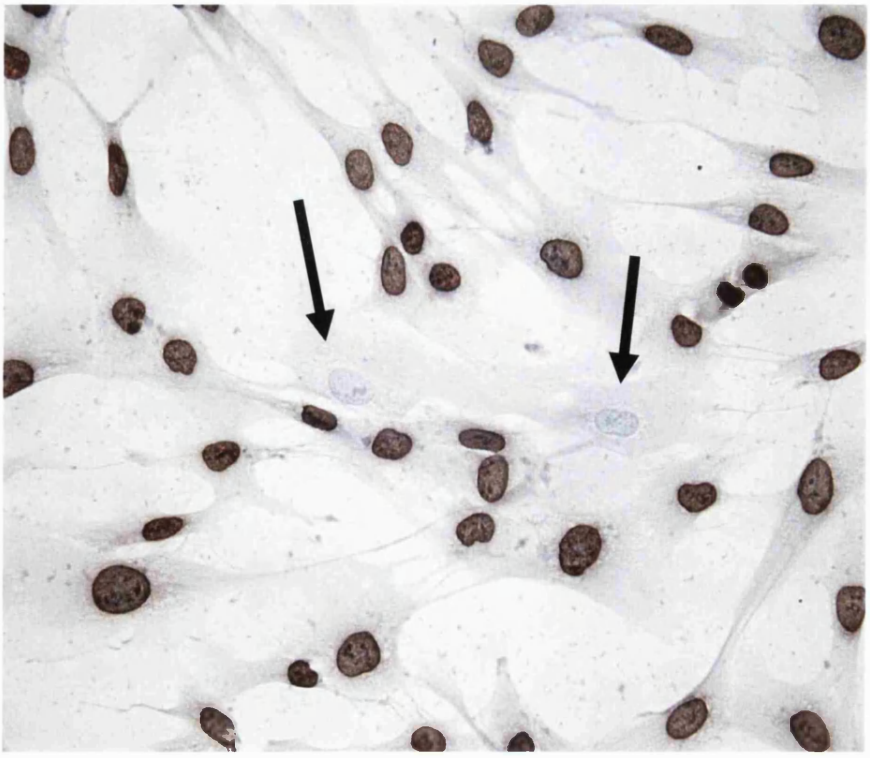

Figure 5.35 BrdU labelled nHDF treated with XO (0.001mU ml^{-1}).

Cells were seeded at 10,000 cells cm^{-2} and incubated for 24 hours in fibroblast medium (Appendix I) Cells were then incubated for a further 4 hours in fibroblast medium incuding hypoxanthine (1mM) and HEPES (20mM) and 0.001mU ml^{-1} XO. The cells were incubated with BrdU (10μM) for 18 hours and the assay was completed as described in the methods in section 5.2.4.1.2. Note. This image shows a couple of cells that are negatively stained for BrdU incorporation (See arrows). However the cells are predominantly positively labeled for BrdU incorporation. Brown nucleus = BrdU positive cell. Blue nucleus = negatively stained cell counterstained with Mayer's haematoxylin. (X40 magnification).

A total cell count of the proliferating cells shown in Figure 5.32-5.35 was carried out for each of the test treatments (Figure 5.36). These results suggest that there is a significantly increased number of proliferating cells in the 0.001mU ml^{-1} XO treated wells compared to the control. However, this increase is not significant in the wells treated with 0.01mU ml^{-1} XO. However, this experiment is preliminary, and would therefore need to be repeated.

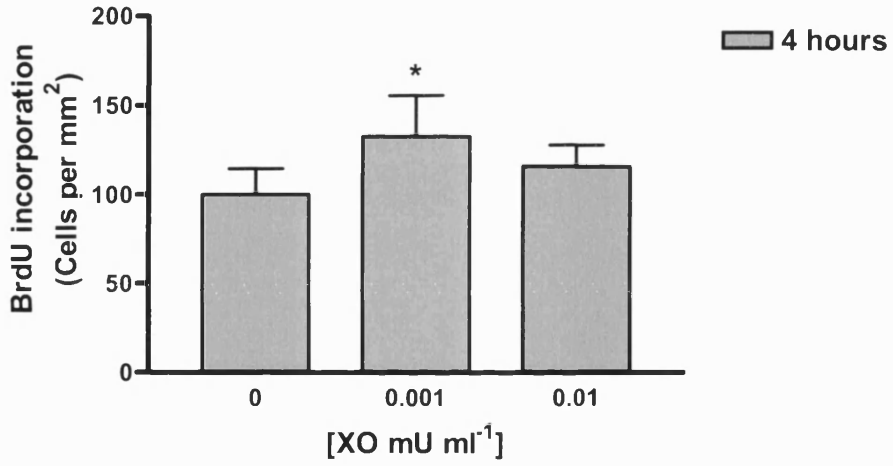

Figure 5.36Count of BrdU positive cells after treatment with XO.

The assay was carried out using BrdU (10μM), XO (0.001 and 0.01mU ml^{-1}), hypoxanthine (1mM) and HEPES (20mM). Values are expressed as mean ± SD each treatment was carried out in quadruplicate on one occasion. Statistical analysis performed was One way ANOVA with Dunnett's post test for multiple comparisons, 0.001mU ml^{-1} XO $P<0.05$ **. Cell counts were taken from five fields of view ($1mm^{-2}$) of each of the test wells.

A second set of experiments were carried out in order to assess whether a reduction in the BrdU incubation time to 4 hours would result in a more countable number of BrdU positive cells which could be expressed as the percentage of proliferating cells. In these experiments the BrdU was added to the test medium for 4 hours. The results clearly show an even distribution of both BrdU positive cells and negatively labelled cells counterstained with Mayer's haematoxylin (Figure 5.37-5.39). Therefore, a 4 hour incubation with BrdU, was determined as most suitable for a countable percentage of

BrdU positive cells so that enhanced DNA synthesis between wells may be more easily identified.

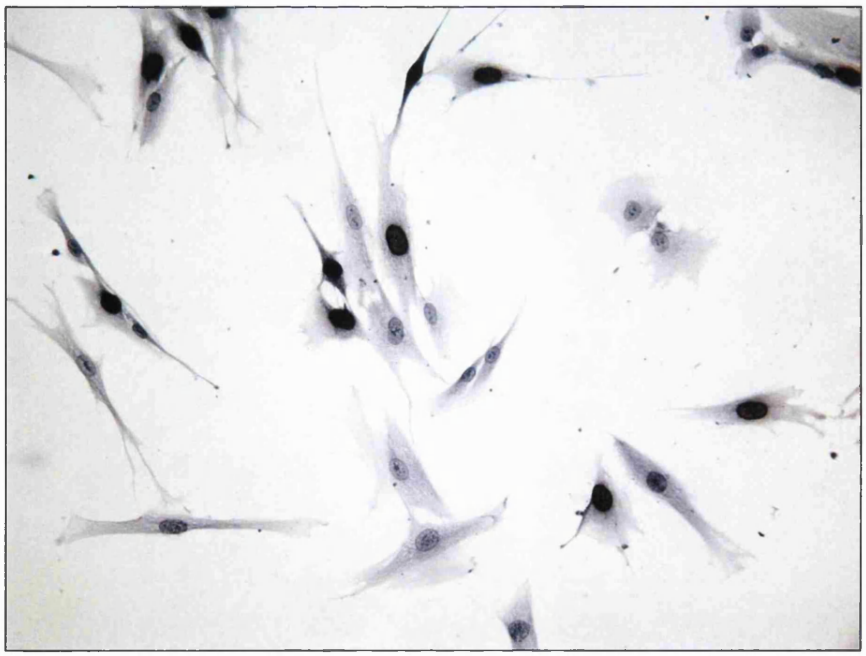

Figure 5.37 BrdU labelled nHDF with (4 hour BrdU incubation).

Cells seeded at 5,000 cells cm^{-2} and incubated for 24 hours in fibroblast medium. Cells were then incubated with BrdU (10μM) for 4 hours. The assay was completed as described in the methods in section 5.2.4.1.2. Note. This image shows around 50% of the cells to be either positively or negatively stained for BrdU incorporation. Brown nucleus= BrdU positive cell. Blue nucleus= negatively stained cell counterstained with Mayer's haematoxylin. (X20 magnification).

Figure 5.38 BrdU labelled nHDF with (4 hour incubation).

Cells seeded at 5,000 cells cm^{-2} and incubated for 24 hours in fibroblast medium. Cells were then incubated with BrdU (10μM) for 4 hours. The assay was completed as described in the methods in section 5.2.4.1.2.

Note. This image indicates both positive and negative nuclear staining. Brown nucleus = BrdU positive cell. Blue nucleus = negatively stained cell counterstained with Mayer's haematoxylin. (X40 magnification).

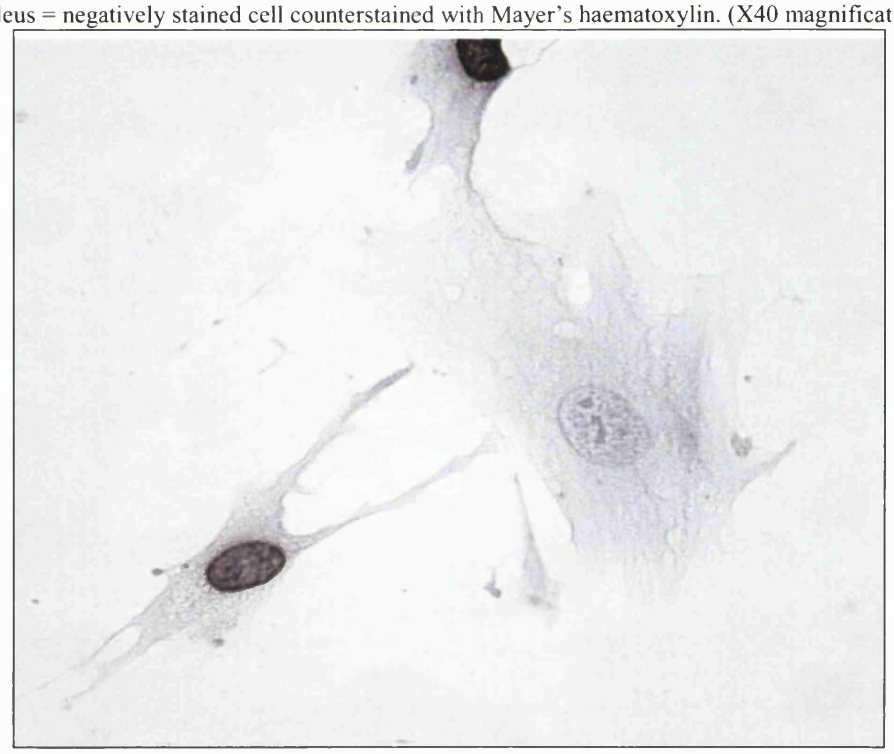

Figure 5.39 BrdU labelled nHDF (4 hour incubation).

Cells seeded at 5,000 cells cm^{-2} and incubated for 24 hours in fibroblast medium. Cells were then incubated with BrdU (10μM) for 4 hours. The assay was completed as described in the methods in section 5.2.4.1.2. Note. This image indicates both positive and negative nuclear staining. Brown nucleus = BrdU positive cell. Blue nucleus = negatively stained cell counterstained with Mayer's haematoxylin. (X40 magnification).

Figure 5.40 and 5.41 shows the growth of nHDF and the resulting BrdU incorporation over a 32 hour time period. Figure 5.40 shows that all cells have proliferated by 24h as all show positive labelling with BrdU. Negatively labelled cells are present in the monolayer between 0 and 8 hours, with around 50% labelling with BrdU after 4 hours (Figure 5.40). Therefore, this experiment confirms that a 4 hour incubation time with BrdU would be suitable for assessment of the percentage of proliferating cells at varying XO treatments as compared to a control.

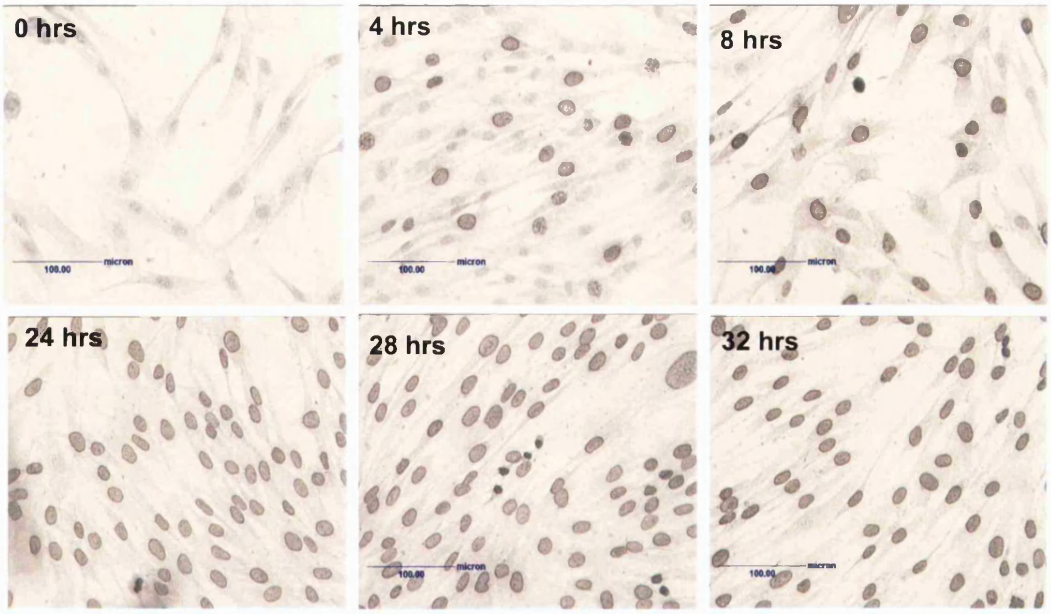

Figure 5.40 BrdU incorporation for the assessment of nHDF growth.

Four-well chamber slides were seeded at 8824 cells cm^{-2} and left to adhere for 24 hours in fibroblast growth medium (DMEM with PS 1%, LG 1% and FCS 10%). BrdU (10μM) was then added to each well in fresh fibroblast growth medium and after 0, 4, 8, 24, 28 and 32 hours the BrdU was removed from the wells and rinsed with PBS. Cells with then fixed and the anti-BrdU antibodies added as described in the methods.

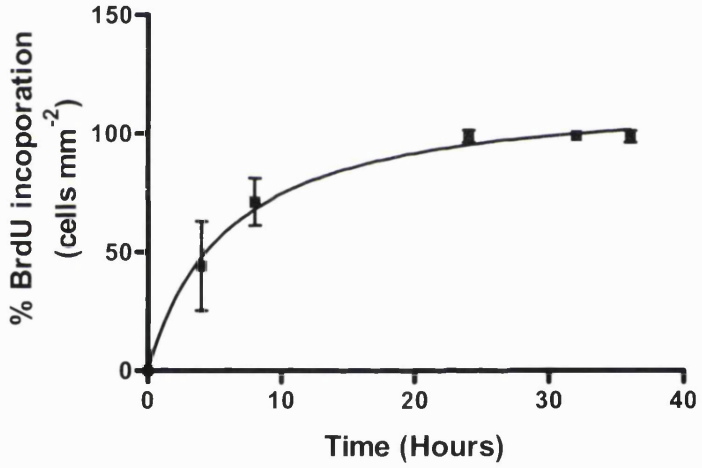

Figure 5.41 Growth curve of the BrdU incorporation of nHDF over 32 hours.

A graph of the data from figure 5.40 expressed as the percentage of BrdU positive cells mm^{-2}. Counts were repeated four times per well. n=4. Mean±SD.

Although assessment of BrdU incorporation by cell counting appears to work in principle it became clear that only a limited number of samples could assayed at one time and cell counts proved extremely time consuming. Therefore, it was decided that a 96-well ELISA method would be a more suitable option for the continuation of these experiments.

5.3.3.2 Bromodeoxyuridine assay using an ELISA system in a range of oxygen tensions

BrdU ELISA assays were performed according to the manufacturer's instructions with some modifications (see methods section 5.2.4.2). These assays were carried out at the same time as the MTT assays shown in Figure 5.24-5.31 at range of oxygen tensions. The BrdU ELISA was developed using aHDF seeded into 96-well plates using a 5% FCS test medium as shown in section 5.3.2.4.

Before exposure of cells to XO preliminary experiments were carried out to determine the sensitivity of the BrdU ELISA, and a suitable seeding density and duration of exposure to BrdU for the proliferation assays (Figure 5.42-5.43). Figure 5.42 was carried out in air (~21% O_2) and shows that around 1000 cells cm^{-2} is a suitable seeding density for the proliferation assays as it is in the lower end of the linear region of the graph. A 4 hour BrdU incorporation incubation time was chosen for assessment of DNA synthesis for comparisons with the MTT assays, Murrell *et al* (1990) also used a 4 hour incubation time for [^{3}H] thymidine incorporation assays. This experiment was repeated in 0% oxygen (figure 5.43) using the oxygen controlled cabinet and showed a reduced level of BrdU incorporation suggesting that DNA synthesis is slower as the oxygen levels decrease.

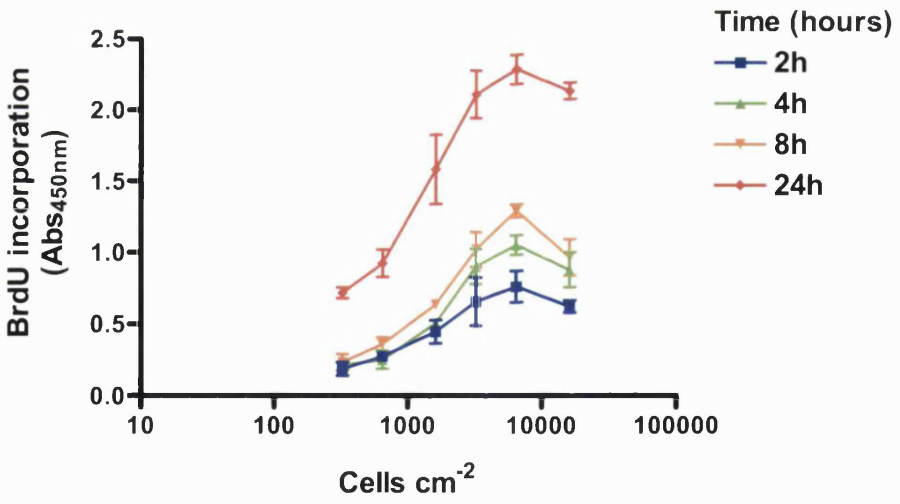

Figure 5.42 Sensitivity and kinetics of the cell proliferation ELISA in 21% oxygen.

Adult human dermal fibroblasts were seeded at 323, 645, 1610, 3230, 6450, 16,130, 32,260 cells cm^{-2} in fibroblast medium (DMEM without phenol red with 5% FCS, 1% LG, 1% PS) and cultured in a 5% CO_2 95% air incubator for 48 hours. After this time cells were incubated with BrdU (10μM) for 2 (Blue line), 4 (Green line), 8 (Orange line), and 24 hours (Red line). n=3.

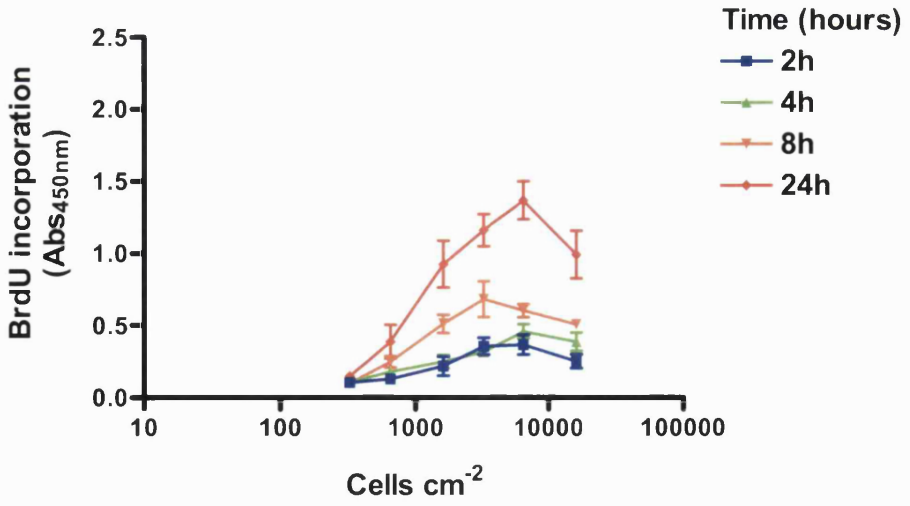

Figure 5.43 Sensitivity and kinetics of the cell proliferation ELISA in 0% oxygen.

Adult human dermal fibroblasts were seeded at 323, 645, 1610, 3230, 6450, 16,130 cells cm^{-2} in fibroblast medium (5% FCS DMEM without phenol red, 1% LG, 1% PS) and cultured for 24h in a 5% CO_2 95% air incubator and a further 24h in the controlled oxygen cabinet purged with 5% CO_2, balanced nitrogen. After this time cells were incubated with BrdU (10μM) for 2 (Blue line), 4 (Green line), 8 (Orange line), and 24 hours (Red line). n=3.

BrdU assays were initially carried out to determine the effects of a range of XO concentrations between 0 and 50mU ml^{-1} XO on adult human dermal fibroblasts at 0% oxygen. This data however, was excluded from the data analysis at 1, 2, 5 and 10% oxygen as the cell seeding was increased for these assays. Figure 5.44 shows that at 0% oxygen, there was no statistical significance between cells treated with XO and the control which did not contain XO. Addition of bFGF did not show any increase in absorbance compared with the control (data not shown). These results suggested that there was little cell growth at 0% oxygen. However, a small amount of BrdU incorporation occurred, and (figure 5.44) suggests that XO has a slight effect on aHDF at 0% oxygen after 24 hours.

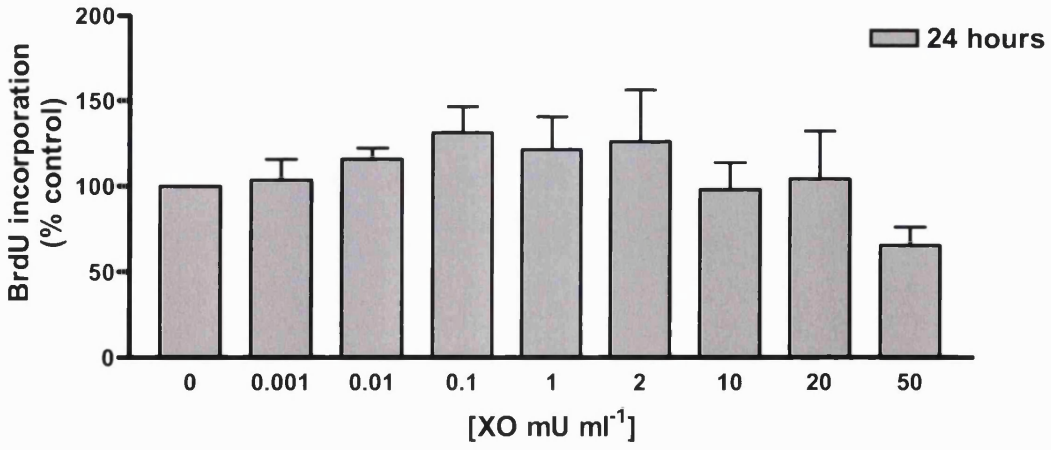

Figure 5.44Treatment of aHDF with XO in 0% oxygen.

Adult human dermal fibroblasts (N1) were seeded at 1129 cells cm^{-2} at passage 6 into a 96-well plate and allowed to adhere to the plate for 48 hours in a 5% CO_2 95% air incubator at 37°C. Cells were then

transferred into the oxygen controlled cabinet purged with 5% CO_2 balanced nitrogen and incubated for 24 hours. Cells were then treated inside the cabinet and incubated for a further 24 hours. This figure shows cells treated with final concentrations of XO at 0, 0, 0.001, 0.01, 0.1, 1, 2, 5, 10, 20, 50mU ml^{-1} with nitrite (1mM) and hypoxanthine (1mM) diluted in fibroblast medium (DMEM without phenol red, 5% FCS, 1% PS, 1% LG). The background that was observed in wells containing no cells was subtracted, and the data were expressed as a percentage of the control. Statistical analysis using one-way ANOVA with Dunnett's post test showed no statistical significance on either graph when compared with controls. n =3. Mean±SD.

Adult human dermal fibroblasts were then exposed to XO from 0 to 50mU ml^{-1} at 1, 2, 5 and 21% oxygen for 72 hours at an increased seeding density (Figure 5.44 and 5.45). A 72 hour time point was chosen as previous MTT assays indicated increased proliferation at 72 hours. Basic fibroblast growth factor (50ng ml^{-1}) was also included as a positive control for enhanced DNA synthesis and proliferation, as shown in previous assays using nHDF (Figure 5.22C). After 72 hours of exposure of normal aHDF to bFGF in 0-21% O_2 there is a significant increase in DNA synthesis compared with the controls. This increase was similar at each oxygen concentration, with a suggestion of increased proliferation with increasing oxygen (Figure 5.45A). Figure 5.45B shows that after 72 hours of exposure of normal aHDF to XO at 21% oxygen (hyperoxia) there is a significant reduction in BrdU incorporation and DNA synthesis at 5, 10 and 50mU ml^{-1} XO. However, at 21% oxygen there is also a significant increase in proliferation at 0.1mU ml^{-1} XO. At 5% oxygen (normoxia) the DNA synthesis is significantly reduced at 50mU ml^{-1} XO. At 1 and 2% oxygen, the fibroblasts appear to be unaffected by XO and although it is not statistically significant this graph also suggests an increase in DNA synthesis at high XO concentrations (Figure 5.45B).

The results from assays carried out on aHDF from the skin of a chronic wound patient (V1) showed some differences compared with those shown in normal aHDF (figure 5.45). Incubation of V1 fibroblasts with bFGF showed enhanced DNA synthesis after 72 hours, although interestingly the proliferative response was significantly enhanced at 2% O_2 as compared with at 5 and 21% O_2 (Figure 5.46A). Incubation of V1 fibroblasts with XO at 21% oxygen (hyperoxia, figure 5.46B) show a significant dose dependent decrease in DNA synthesis at concentrations above 1mU ml^{-1} XO, suggesting that these fibroblasts may be more sensitive to the effects of XO than the normal aHDF. Nevertheless, there is only around a 20% decrease in BrdU incorporation at 1mU ml^{-1}, whereas, at 50mU ml^{-1} XO there is complete inhibition of BrdU incorporation suggesting that cell proliferation has been ablated, or the cells are dead. In 5% oxygen (normoxia) XO slightly inhibits BrdU incorporation at 50mU ml^{-1}. Interestingly however, at 5% there is a significant increase in BrdU incorporation at 5 and 10mU ml^{-1} XO suggesting that there is enhanced proliferation at these concentrations of XO. At 2% oxygen, BrdU incorporation and DNA synthesis appear to be comparable to the control at low XO concentrations.

However, at 5mU ml^{-1} XO and above, there is a significant increase in BrdU incorporation and enhanced DNA synthesis.

Figure 5.45 A)

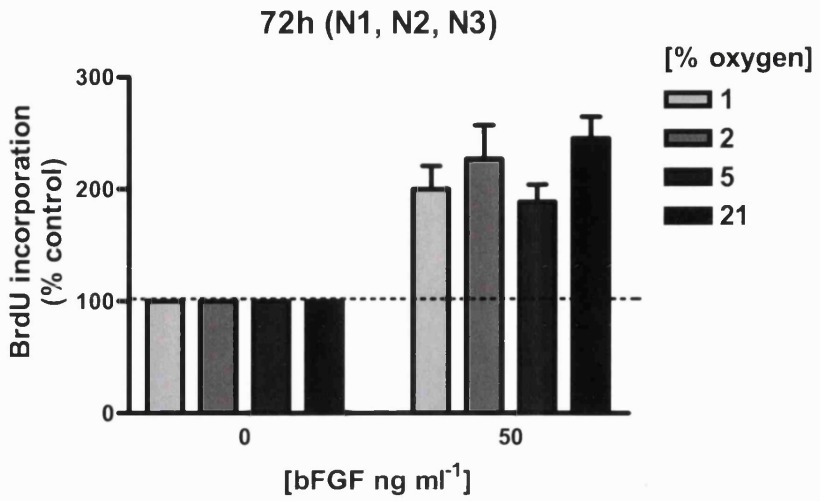

Figure 5.45 B)

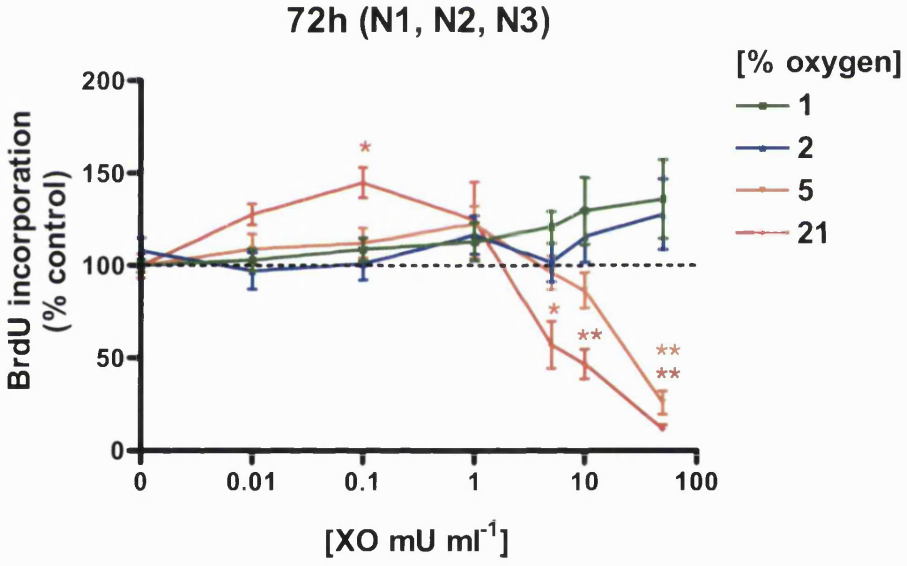

Figure 5.45 Treatment of aHDF with XO for 72 hours in 1, 2 5 and 21% oxygen.

Adult human dermal fibroblasts were seeded at around 3500 cells cm^{-2} and incubated for 24 hours in a 5% CO_2 balanced air incubator. The cells that were treated at 21% (air) remained in the incubator for a further 24 hours before treatment. Cells that were treated in 1, 2 and 5% oxygen were transferred into the oxygen controlled cabinet (which was purged 5% CO_2 and the relevant oxygen concentration) and allowed to equilibrate for 24h before treatment. Cells were then treated for 72 hours. Graph A shows BrdU incorporation by aHDF after 72 hours exposure to bFGF (50ng ml^{-1}) at 2, 5 and 21% oxygen these experiments were carried out at the same time as exposure to XO at the same oxygen concentration and the data is shown as a percentage of the control (0mU ml^{-1} XO). Mean±SEM. Graph B shows brdU incorporation by aHDF after 72 hours exposure to hypoxanthine (1mM) and nitrite (1mM) and XO (0, 0.01, 0.1, 1, 5, 10 and 50mU ml^{-1} XO) diluted in fibroblast medium containing (DMEM with out phenol red, 5% FCS, 1% LG, 1% PS). Mean±SEM. 1% n=8, 2% n=11, 5% n=9, 21% n=10. Statistical analysis performed was One way ANOVA with Dunnett's post test (*P<0.05).

Figure 5.46 A)

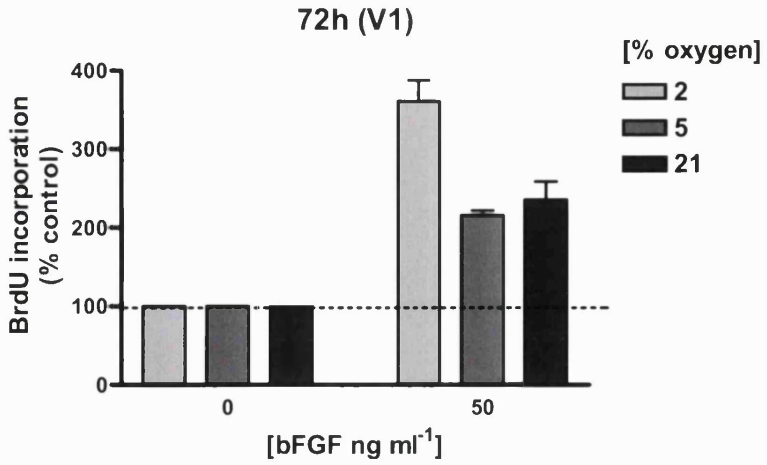

Figure 5.46 B)

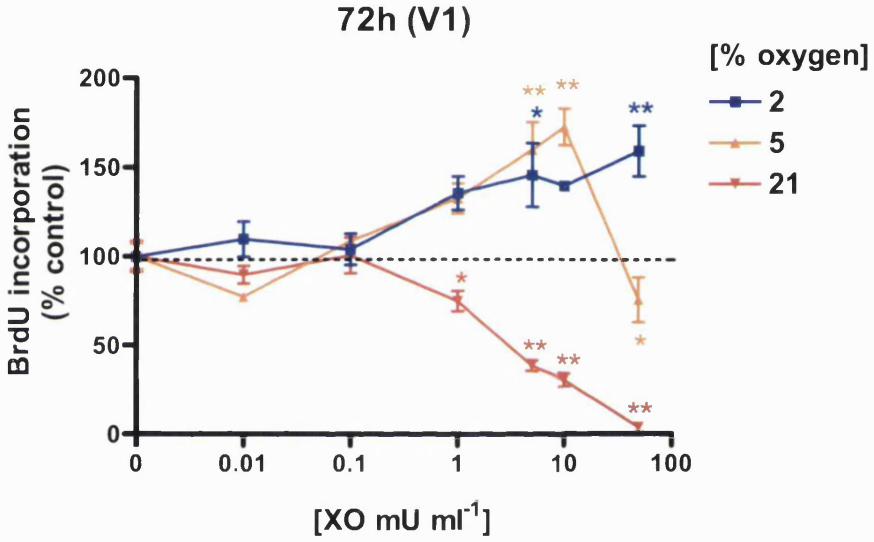

Figure 5.46 Treatment of aHDF with XO for 72 hours in 2, 5 and 21% oxygen.

Adult human dermal fibroblasts were seeded at around 3500 cells cm^{-2} and incubated for 24 hours in a 5% CO_2 balanced air incubator. The cells that were treated at 21% (air) remained in the incubator for a further 24 hours before treatment. Cells that were treated in 2 and 5% oxygen were transferred to the anaerobic cabinet which was purged 5% CO_2 and the relevant oxygen concentration for the experiment and incubated for 24h before treatment. Cells were then treated for 72 hours. Graph A shows BrdU incorporation by aHDF after 72 hours exposure to bFGF (50ng ml^{-1}) at 2, 5 and 21% oxygen these experiments were carried out at the same time as exposure to XO at the same oxygen concentration and the data is shown as a percentage of the control (0mU ml^{-1} XO). Mean±SEM. Graph B shows brdU incorporation by aHDF after 72 hours exposure to hypoxanthine (1mM) and nitrite (1mM) and XO (0, 0.01, 0.1, 1, 5, 10 and 50mU ml^{-1} XO) diluted in fibroblast medium containing (DMEM with out phenol red, 5% FCS, 1% LG, 1% PS). Mean±SEM. 2% n=4, 5% n=3, 21% n=4. Statistical analysis performed was one way ANOVA with Dunnett's post test (*P<0.05).

5.4 Discussion

Reactive oxygen species have been implicated in both the proliferation and cytoxicity of mammalian cells. More specifically, XO has also been shown to produce a

proliferative response in fibroblasts including aHDF (Preeta and Nair, 2000; Kim *et al*, 2001; Murrell *et al*, 1990). I have confirmed this using aHDF and further shown a similar effect in nHDF. Furthermore, I have investigated the effects of XO on nHDF, which are used in commercially available skin grafts, and on aHDF in a range of oxygen tensions to mimic the chronic wound environment.

5.4.1 Characterisation of human dermal fibroblasts

Visualisation of human dermal fibroblast morphological features and positive staining for prolyl-4-hydroxylase, confirmed that all fibroblasts used in the study belong to a homogenous population of spindle-shaped fibroblastic cells. Figures 5.2-5.7 provide an example of the typical staining observed. Prolyl-4-hydroxylase catalyses the hydroxylation of proline in –X-Pro-Gly- sequences in collagens and related proteins. This co-translational and post-translational modification plays a central role in the synthesis of all collagens, as 4-hydroxyproline residues are essential for the folding of the newly synthesized collagen polypeptide chains into triple-helical molecules.

5.4.2 Effects of XO on the viability of human dermal fibroblasts

Experiments to determine the effect of XO on HDF using the MTT assay were initially carried out using nHDF. During the development of this assay, problems were found with dissociation of the fibroblast monolayer and difficulty in obtaining accurate cell counts for seeding into experimental assays due to cell clumping (figure 5.8). Cells were initially dissociated using cell dissociation solution, a non-enzymatic method of removal as it was thought that this method would be less harsh to the cells. Accutase and trypsin/EDTA were also assessed and trypsin/EDTA was finally used in all future experimentation as it successfully broke down the ECM between cells allowing for accurate cell counts for seeding. The relationship between cell seeding numbers per cm^2 and the absorbance values achieved after exposure to MTT for 3 hour was assessed and showed that between 10,000 and 50,000 cells cm^{-2} was most suitable for assessing changes in cell number in the XO treatments assays (figure 5.9).

Neonatal human dermal fibroblasts were treated with XO using a range of concentrations from 0-100mU ml^{-1}, that were the concentrations previously used by Murrell *et al* (1990). Treatment of the cells at these concentrations showed a significant dose dependent decrease in the absorbance at concentrations of XO above 1mU ml^{-1} as compared with the control (Figure 5.10). This suggests that the reductive metabolism and therefore, viability of the fibroblasts is significantly reduced at 10, 100 and 1000mU ml^{-1}

XO; it is likely that the fibroblast's antioxidant systems are unable to cope with the $O_2^{\bullet-}$ and H_2O_2 that is generated at these concentrations (chapter 4). Neonatal human dermal fibroblasts exposed to lower concentrations of XO in the range of 0-1mU ml^{-1} showed no significant difference in viability in comparison with the control. These findings were identical to those reported by Murrell *et al* (1990) using adult fibroblasts who observed cell death at concentrations above 1mU ml^{-1} XO.

The effects of XO on nHDF at concentrations above 1mU ml^{-1} XO was examined more extensively. Figure 5.11 showed that the viability of cells between 1.5- and 6.25mU ml^{-1} was slightly increased compared with the control, suggesting a possible increase in viability or cell number, which could be a result of the generation of low levels of ROS by XO. Although others have described the proliferative effect of XO on fibroblasts, this is the first study showing the enhanced proliferation of neonatal human dermal fibroblasts. Furthermore, as expected, and in agreement with Murrell *et al* (1990), at high concentrations of XO (12.5-100mU ml^{-1}) there was a significant reduction in cell viability (i.e cell death), which also supports the data shown in (Figure 5.10).

The effect of a range of XO concentrations was assessed at varying seeding densities (Figure 5.12). These assays showed that at a seeding density of 10,000-15,000 cells cm^{-2}, fibroblasts were slightly less sensitive to the effects of XO than cells seeded at 5,000 cells cm^{-2}. Seeding densities at 5,000 and above showed a reduction in viability at 12.5mU ml^{-1} XO, but at 5,000 cells cm^{-2} there was also a reduction in viability at 6.25mU ml^{-1} XO. This is probably due to the scavenging systems of the increased number of cells being able to more effectively scavenge XO-generated ROS.

Preliminary experiments of the treatment of fibroblasts with XO were later repeated for reproducibility with a new batch of FCS. These experiments (Figure 5.13) showed that the viability of nHDF was significantly impaired at 100mU ml^{-1} XO as previously shown in figure 5.10. However, at 10mU ml^{-1} XO cell viability was comparable to the control (figure 5.13), whereas in figure 5.10 cell viability at this concentration was decreased by around 50%. Therefore the killing effects of the XO when using the new batch of FCS were not quite as effective as when using the previous batch, and tests on the enzyme ensured that the activity had not decreased. Studies carried out on human dermal fibroblasts have previously reported a cytoprotective function for FCS (Hidalgo and Dominguez, 1998). Serum is high in growth and survival factors, and protects fibroblasts from possible toxic effects. FCS also contains growth factors which favour cell migration (Bartold and Raben, 1996) and protective factors against oxidative damage which provokes lipid peroxidation in cell membranes. Repeats of these assays carried out using a more extensive range of XO (Figure 5.14) confirmed that there was a

slight decrease in the cytotoxic effects of XO which only showed around an 80% decrease in viability at 25mU ml^{-1} XO compared with the previous assay shown in figure (figure 5.11) which showed a 50% reduction in viability at 12.5mU ml^{-1} XO. These results clearly indicate that the levels of cytoprotective factors in the new batch of FCS were greater than in the initial batch. Due to these changes in the sensitivity of fibroblasts to XO, the new batch of FCS was kept constant for all further experimentation.

Several studies have reported the proliferative effects XO and inhibitor studies by Murrell *et al* (1990) showed that both $O_2^{\bullet-}$ and H_2O_2 were responsible with H_2O_2 being more potent. Direct application of low concentrations of H_2O_2 has also been shown to enhance the proliferation of a range of mammalian cells including human endothelial cells and human dermal fibroblasts (Luczak *et al*, 2004; Murrell *et al*, 1990). As previously mentioned, the MTT assay has also been used for an indication of enhanced proliferation however cells need to be incubated for extended periods of time so that changes in cell number can be detected. Therefore, the MTT assay was used to assess the enhanced proliferation of human dermal fibroblasts. Preliminary assays were carried out using H_2O_2 as a positive control for oxidant-derived proliferation. The experiments to examine the effects of varying concentrations of FCS that were done on the growth of nHDF also had the purpose of optimising the FCS level to achieve the best H_2O_2-induced proliferation assessment. The growth of nHDF was shown to dose dependently decrease with decreasing concentrations of FCS in figures 5.15 and 5.16 by two different methods. Fig 5.15 was made using data from a trypan blue viable cell count method using a microscope and manual counting. Although this is a very accurate and informative method, it is also very labour intensive and includes wash steps that might cause the loss of some cells. This could result in significant underestimation of cell number particularly when the total cell number is low. The method used for all other viable cell counts in this was the MTT assay. This does not actually measure individual cells but can estimate cell number by the amount of formazan crystals that form inside viable cells. It is a very efficient method as the count estimation can be made using a 96-well plate reader allowing for multiple experiments to be performed at once.

Initial assays to assess the proliferative effects of H_2O_2 showed that very low concentrations of FCS did not allow for the resolution of any differences in proliferation. Much better results were obtained when the FCS was increased ten fold to 2%. This was still a relatively low concentration but enough to allow cells to proliferate at a measurable rate without providing an inhibitory amount of substances such as catalase (Korhonen *et al*, 1983). The FCS concentration was also increased in a further assay to 5% (Figure 5.19) and H_2O_2 was also added at between 0 and 10,000μM, this assay showed a

significant increase in the number of viable cells at 0.01, 1 and 10μM H_2O_2 and a decrease in the number of viable cells at concentrations above 1000μM H_2O_2. These results concur with the study of Kim *et al* (2001) who was examining the proliferative effect of H_2O_2 on Chinese hamster lung fibroblastic (V79) cells. The study also used 5% FCS that gave them a positive proliferative response to 50μM H_2O_2. Figure 5.19 shows that in this study a pro proliferative response was achieved at much lower concentrations of H_2O_2. There are many possible reasons for this including the possibility that the different FCS has an effect, as was found here between two different batches, but the most likely reason is that the V79 cell type was either less sensitive to H_2O_2 or that they contained intrinsic protection against reactive oxygen species.

All previous assays were carried out in the presence of HEPES to try to replicate the proliferation studies carried out by Murrell *et al* (1990). However, as HEPES is reported to have radical scavenging activity, H_2O_2 assays were carried out in the presence and absence of HEPES (Figure 5.20A-B). Figure 5.20B showed that, after 48 hours exposure to H_2O_2, there was a significant increase in the number of viable cells at 5, 25 and 100μM H_2O_2 in the absence of HEPES, whereas, in the presence of HEPES there was a significant decrease in the number of viable cells at 100 and 500μM H_2O_2. This may be because HEPES is known to contribute to the breakdown of H_2O_2 and the formation of hydroxyl radicals which cause damage to cellular DNA via the fenton reaction. This implies that the proliferative response to H_2O_2 may be enhanced in the absence of HEPES buffer and therefore it was removed for future assays. A further assay carried out with varying concentrations of XO in the absence of HEPES showed an increase in viability at 1mU ml^{-1} XO and a decrease in viability at 10, 20 and 50mU ml^{-1} XO after 72 hours exposure (Figure 5.21), which also supported the findings shown by Murrell *et al* (1990).

The effects of varying concentrations of bFGF on nHDF were tested in the proliferation assays for use as a positive control. Increasing concentrations of bFGF showed increased viability at 24, 48 and 72 hours (Figure 5.22). Basic fibroblast growth factor gave the best response at 50ng ml^{-1} at 24, 48 and 72 hours exposure. Before adult fibroblasts were exposed to XO, a sensitivity assay was carried out to ascertain the optimal duration of incubation with MTT and the most suitable seeding densities for detection of changes in cell number (figure 5.23). This figure showed that a 3 or 4 hour incubation period was similarly sensitive for the detection of changes in cell number; however, a 4 hour incubation with MTT was chosen for maximum sensitivity. This figure also showed that a minimum seeding density of around 3-4000 cells per cm^{-2} would be suitable for detecting changes in cell number.

Unfortunately, due to an error in seeding, the experimental assays for the treatment of aHDF with XO at 0% oxygen had low cell numbers. These results were therefore kept separate from other fibroblast assays Figure 5.24. This figure did not show any significant changes in cell viability between 0 and 50mU ml^{-1} XO at 0% oxygen indicating that, in the absence of oxygen, XO, even at high concentration, is unable to produce species that affect the viability of adult dermal fibroblasts. This is unsurprising as, the complete absence of oxygen XO cannot generate $O_2^{\bullet-}$ or H_2O_2 and consequently $ONOO^-$ and hydroxyl radical formation is not possible.

The results shown in section 5.3.2.4 that examines the effects of XO on the viability of human dermal fibroblasts in a range of oxygen tensions, demonstrate that in conditions likely to be prevailing in a chronic wound, the enzyme does not have an adverse effect. The eventual aim of this work is to develop a dressing that can be applied to chronic wounds containing XO. For this to be a viable proposal the enzyme while exposed to the tissue, must not have deleterious effects on the patients own tissue for the duration of the dressing application (up to 24 hours). On the contrary it is hoped that the pro-proliferative effect of XO products will be a beneficial aid to the healing process. The results of varying the levels of enzyme on aHDF at different oxygen tensions clearly confirm that there is no toxic effect of the enzyme under a range of conditions that might be expected in the ulcer. The most relevant oxygen tensions to the chronic wound are 1-2%, at these levels it can be seen that, not only are the cells viable, but they are actually showing an increase in number (figure 5.28). This effect is likely to be due to the generation of low levels of ROS that would have a proliferative effect in a similar way to the hydrogen peroxide effects shown earlier in the chapter 5 (figure 5.19 for example). The data also indicate that the cells are tolerant to the highest concentrations of enzyme used (50mU ml^{-1}). This is at the upper end of the range of enzyme concentrations that would be considered for a dressing and is a concentration that has antimicrobial capability, as will be seen in chapter 6. The only significant adverse effects were seen with prolonged exposures (72 hours) of high enzyme concentration under hyperoxic conditions (21%), these experiments were only done for completeness as the conditions are well outside the range of any envisaged *in vivo* situation.

Figure 5.29 also shows pictures of fibroblasts taken after exposure to 0-50mU ml^{-1} XO for 24 hours at 21% O_2. At high XO concentrations greater than 5mU ml^{-1} XO there is an increase in the roundness of the fibroblasts and visible damage and detachment from the culture surface, suggesting that excessive toxicity has damaged these cells beyond repair, resulting in apoptosis. These cells also appear condensed but relatively intact, and the cytoplasm appears to have a granular appearance which may be due to the presence of

enlarged vacuoles in the cytoplasm which are features of apoptosis. These observations correspond with the assays shown in figure (5.27-5.28) which show that the fibroblasts do not reduce MTT suggesting that the cells are dead. However, figure 5.29 does not show and obvious visual signs of cell death at 5mU ml^{-1} XO, whereas, the MTT assay suggests that the metabolic viability of fibroblasts exposed to these concentrations of XO in hyperoxia (21% O_2) is significantly reduced.

Normal aHDF were also exposed to XO in varying oxygen concentrations for 72 hours (Figure 5.30). At 1% oxygen fibroblasts showed a significant decrease in viability at 50mU ml^{-1} XO, however, it was only around a 25% decrease in viability. At 2% oxygen a slight increase in viability is observed at 5mU ml^{-1} XO again suggesting that XO at low oxygen concentrations could be increasing cell numbers. At 5% oxygen (normoxia) there is around a 20% decrease in cell viability at 10mU ml^{-1} and 50mU ml^{-1} appears to be toxic to the cells as there is no MTT reduction. Xanthine oxidase at 5, 10 and 50mU ml^{-1} is also toxic to fibroblasts as shown after 24 hours exposure. This result was similar for the fibroblasts derived from chronic ulcer patients (Figure 5.31). With increased viability observed at 2% oxygen at 50mU ml^{-1} XO, and decreased viability and toxicity observed at 50mU ml^{-1} XO in normoxia (5% oxygen) and at 5, 10 and 50mU ml^{-1} XO in hyperoxia (21% oxygen).

5.4.3 Effects of XO on the proliferation of HDF

As with the MTT assay (section 5.3.2), a number of experiments were carried out to determine the optimum cell number and incubation period required for accurate assessment of proliferation (Figure 5.32-5.41). Finally, it was decided that a 96-well BrdU ELISA would provide a fast and sensitive method of assaying multiple samples, and would also be easier to transfer in and out of the oxygen controlled cabinet for experiments in reduced oxygen.

The BrdU ELISA assays in varying oxygen tensions were carried out at the same time as the MTT assays shown in section 5.2.3.4. Initial sensitivity assays showed that a concentration of 1000 cells cm^{-2} and an incubation of 4 hours with BrdU, as used by Murrell *et al* (1990), would be sufficient for the assessment of DNA synthesis (Figure 5.42-5.43). At 0% oxygen the level of BrdU incorporation was considerably reduced but this was expected as it is likely that there would be little or no proliferation at this oxygen concentration. It is also possible that the pO_2 inside the cabinet was not absolute zero oxygen as very low levels of oxygen may be contained in the nitrogen and CO_2 cylinders and possibly also introduced through the sleeves.

Adult HDF were treated with bFGF as a positive control for proliferation (Figure 5.45A). A significant proliferative response was observed at 1, 2, 5 and 21% oxygen confirming that the assay was working well and effectively detected proliferative responses. When the same control was run on dermal fibroblasts from the skin of a chronic wound patient (V1), there appeared to be a clear increase in proliferation at 2% oxygen over the higher oxygen levels (Figure 5.46A) This increase in proliferation might suggest that these cells are better conditioned and adapted to hypoxia as they are from a patient with a vascular ulcer. Similar adaptations to hypoxia have been suggested in skin fibroblasts in studies by Panchenko *et al* (2000). These cells also appear to prefer lower oxygen levels in the XO-stimulated proliferation assays. Comparing graphs 5.45B and 5.46B it can be seen that the V1 cells show very poor growth at 21% oxygen and particularly robust proliferation at 2% oxygen compared to normal fibroblasts. This is a strikingly good result in support of the hypothesis that XO will provide valuable pro-healing effects in chronic wound beds where the oxygen tension will be predominantly in the region of 2% (Falanga *et al*, 1992b).

5.4.4 Chapter summary

This chapter confirms previous reports that XO can enhance the growth of aHDF which are essential for wound healing using standard culture conditions in air. Furthermore, I have observed similar proliferative effects of XO on nHDF, which are used in commercially available skin grafts. This chapter also shows that the viability and proliferation of aHDF, including patients with chronic wounds, were not adversely affected when exposed to XO in low oxygen tensions relavent to the chronic wound. Furthermore, these results do in fact appear to show some evidence of enhanced proliferation at high enzyme concentration in low oxygen. The XO concentrations investigated in this study provide a range with which to test the sensitivity of bacteria for a potential antimicrobial role without having an inhibitory effect on the wound healing process.

CHAPTER 6

6 Effects of XO-generated products on bacteria relevant to the chronic wound

6.1 Introduction

As discussed previously (Chapter 2), poor vascular supply and systemic factors mean that the tissues of individuals prone to chronic ulcers are at an increased risk of bacterial invasion (Falanga, 1993a). Chronic ulcers are characteristically hypoxic, and can support a diverse microbial flora including aerobic, facultative anaerobes and anaerobic bacteria. There is no single unifying theory as to the aetiology of chronic ulcers and it is likely to be multifactorial, however, it is a universally supported view that bacteria can contribute to non-healing. A wide range of bacteria have been isolated from a variety of chronic wounds, although cultural analyses have documented that *staphylococci, streptococci, enterococci* and facultative gram-negative bacilli are the bacterial groups frequently recovered from chronic ulcers (Hansson *et al*, 1995).

6.1.1 Facultative anaerobes and chronic wound infection

The facultative anaerobes that have been investigated for the purposes of his thesis are strains that are known to have been isolated from infected ulcers and are *Staphylococcus aureus* (*S. aureus*), *Streptococcus faecalis* (*S. faecalis*), *Proteus mirabilis* (*P. mirabilis*), *Escherichia coli* (*E. coli*) and *Pseudomonas aeruginosa* (*P. aeruginosa*) (Bowler and Davies, 1999; Abdulrazak *et al*, 2005; Howell-Jones *et al*, 2005) and are therefore covered in more detail in section 6.1.2.1.

6.1.1.1 Gram positive bacteria *S. aureus* and *S. faecalis*

Gram-positive *S. aureus* are part of the normal flora present on the skin surfaces and mucosal and nasal membranes of most healthy humans, and also represents a large spectrum of bacteria that are important pathogens in chronic wound infections. *S. aureus* is an immobile coccus which forms grape-like clusters and is grouped with the *Bacillus* species. It is also a facultative anaerobe, allowing it to grow in a range of oxygen tensions. *S. aureus* can cause a range of infections from mild, such as skin infections and food poisoning, to life-threatening, such as pneumonia, sepsis, osteomyelitis, and infectious

endocarditis. *S. aureus* is one of the major causes of community-acquired and hospital-acquired infections, causing high morbidity and mortality in the UK and throughout the world. It produces numerous toxins including superantigens that cause unique disease entities such as toxic-shock syndrome and staphylococcal scarlet fever, and has acquired resistance to practically all antibiotics. *S. aureus* has been considered a serious bacterial pathogen since the organism developed a resistance to penicillin in the 1950s. In 1961 it developed resistance to meticillin, invalidating almost all antibiotics including the most potent β-lactams. Since the 1970s, meticillin-resistant *S. aureus* (MRSA) has become the main cause of nosocomial infection worldwide. The proportion of MRSA has risen worldwide during the last two decades, with increasing epidemics in UK hospitals (Ayliffe, 1997). The therapeutic glycopeptide vancomycin was the only antimicrobial agent effective against MRSA, but there has since been the emergence of vancomycin resistance in enterococci in 1988 (Nicas *et al*, 1989), in coagulase-negative staphylococci in 1987 (Schwalbe *et al,* 1987) and in MRSA with reduced vancomycin susceptibility in 1996 (Hiramatsu *et al,* 1997), therefore there has been speculation that the incidence of vancomycin-resistant *S. aureus* (VRSA) will increase. The spread of antimicrobial-resistant nosocomial pathogens such as MRSA and VRSA is secondary to both over- and misuse of antimicrobials and incomplete compliance with recommended infection control precautions. We are now exposed to the threat of MRSA without having developed any antibiotics with greater activity than vancomycin. Epidemic and endemic infections in healthcare facilities are now emerging around the globe as the cause of severe infection in the community. All this is compounded by very limited pharmaceutical research and development on new antimicrobial agents. There is, therefore, an urgent need to revitalise the pipeline of new antimicrobial agents to effectively meet this challenge. According to Armstrong and Lipsky (2004) Gram-positive cocci particularly *S. aureus*, are the most important pathogens in diabetic foot infections, where peripheral vascular (i.e. arterial) insufficiency and the increasing prevalence of antibiotic resistance are primary barriers to successfully managing these infections. The *Streptococcus faecalis* is a gram-positive facultative anaerobe. It belongs to the genus streptococcus and is arranged as cocci in chains. It causes many of the same problems as other members of the intestinal flora, including opportunistic urinary tract infections and wound infections. Little is known about its pathogenesis.

6.1.1.2 Gram-negative bacteria *P. mirabilis, P. aeruginosa and E.coli*

P. mirabilis is a facultative anaerobic, Gram-negative rod-shaped bacterium. It belongs to the *Enterobacteriaceae* family and is a highly motile swarmer bacterium and

does not form regular colonies. Instead, *Proteus* forms what are known as "swarming colonies" when plated on non-inhibitory media. *P. mirabilis* are often found as free living organisms in soil and water but they also cause urinary tract infections, wound infections, septicaemia and pneumonias, mostly in hospitalised patients. Most strains of *P. mirabilis* are sensitive to ampicillin and cephalosporins. *E. coli* is also a Gram-negative facultative anaerobe, it has a rod-shaped morphology and belongs to the family *Enterobacteriaceae* and are characterised by their ability to produce potent enterotoxins. *Pseudomonas aeruginosa* is also a Gram-negative, aerobic rod belonging to the bacterial family *Pseudomonadaceae.* These bacteria are common inhabitants of soil and water, but are also the epitome of an opportunistic pathogen in humans. A major factor in its prominence as a pathogen is its intrinsic resistance to antibiotics and disinfectants. The bacterium almost never infects uncompromised tissues, yet there is hardly any tissue that it cannot infect if the tissue defenses are compromised in some manner. *P. aeruginosa* contaminates surgical wounds, abscesses and burns and can cause urinary tract infections, respiratory system infections, dermatitis, soft tissue infections, bacteremia, bone and joint infections, gastrointestinal infections and a variety of systemic infections. *P. aeruginosa* is primarily a nosocomial pathogen and occurs in about 20-30% of all ulcers (Halbert *et al*, 1992; Hansson *et al*, 1995). Previous studies have shown that around 50% of all chronic ulcer-derived *P. aeruginosa* isolates express elastase. From the clinical point of view, this finding could perhaps underlie the observation that not all chronic ulcers deteriorate during *P. aeruginosa* infection, a finding that has caused some debate as to whether this pathogen causes wound delay or not. Studies have since shown the production of a highly conserved metalloproteinase, elastase, by ulcer derived strains of *P. aeruginosa* which degrades wound fluid and human skin proteins during infection *ex vivo*. Furthermore, elastase producing *P. aeruginosa* degraded various antiproteinases, complement C3, kininogens (KIN), fibroblast proteins and the proteoglycan decorin, and inhibited fibroblast growth (Schmidtchen *et al*, 2003).

The complete sequence of the *P. aeruginosa* strain PAO1 that has been used in this study has been elucidated, and is known to have a large bacterial genome at 6.3 million base pairs (Stover *et al*, 2000). The sequence provides insights into the basis of the versatility and intrinsic drug resistance. Consistent with its larger genome size and environmental adaptability, *P. aeruginosa* contains a high proportion of regulatory genes for a bacterial genome and a large number of genes involved in the catabolism, transport and efflux of organic compounds as well as four potential chemotaxis systems. The size and complexity of the genome also reflects an evolutionary adaptation permitting it to

thrive in diverse environments and resist the effects of a variety of antimicrobial substances.

6.1.2 XOR and bacterial killing

Previous work has demonstrated the ability of XOR to mediate cell death in both *Escherichia coli* and *Salmonella enteritides* (Stevens *et al*, 2000). Furthermore, the expression of this enzyme in mammalian milk combined with its bactericidal properties, have suggested a role in the reduction of infective bacteria in the neonatal gut. The ability of breast milk-derived XOR to limit the growth of both *Escherichia coli* and *salmonella enteritides* has been successfully demonstrated *in vitro*. Recent results have also demonstrated bactericidal properties of XOR *in vitro* in calves highlighting the importance of maternal milk in the treatment of neonatal infections. Previous work has also suggested an antibacterial role in the digestive tract for XOR, which is present in intestinal epithelial cells (Godber, 2000a). This case was based on the enzyme's capacity to generate $^{\bullet}NO$. It was supported by the literature reports that nitrite levels in the immediate vicinity of enteric bacteria could achieve millimolar concentrations and that XOR has affinity for acid polysaccharides such as occur in bacterial capsules. Similar and even stronger arguments apply to XOR-derived $ONOO^-$ generation across a very wide range of oxygen tensions, encompassing all situations likely to be encountered physiologically. The following experiments were designed to assess the effect of chemically generated oxidants and XOR on the growth and viability of bacteria relevant to the chronic wound with a view to developing a novel anti-bacterial dressing. It is in these ischaemic wounds that XOR could be most beneficial as peripheral vascular insufficiency, impaired healing and increased antibiotic resistance are the main problems in these types of wound.

6.1.3 Bacterial survival and antioxidant mechanisms

White blood cells produce H_2O_2 to kill bacteria. In both cases catalase prevents the H_2O_2 from harming the cell itself. Prokaryotes, organisms like bacteria that lack a nuclear membrane, also lack membrane bound organelles such as peroxisomes, where catalase is contained in animal cells. Antioxidant enzymes like catalase and SOD are located in the periplasmic space which is the space between the inner and outer membranes of the cell wall. There are numerous enzymes located here that would be toxic if they were found inside the cell. The catalase found here can act on toxic molecules that are transported to the periplasm or the enzyme can be released outside the bacterial wall where it can act on

toxic molecules in the environment. Catalase that is released by the bacteria plays a role in protecting the bacteria from being destroyed by white blood cells during an infection.

The presence of oxygen radical detoxification systems in bacteria is well documented (Fee, 1991; Nunoshiba, 1996). *E. coli* possess a SOD-like enzyme which generates H_2O_2. This species is then detoxified by a catalase-like enzyme to oxygen and water (McCormick *et al*, 1998). The importance of SOD in the defence of bacteria against $O_2^{\bullet-}$ generation was assessed by Gort and Imlay (1998). They controlled the expression of cytoplasmic SOD within the *E. coli* to show the relative amounts of $O_2^{\bullet-}$ generation that were required to cause enzyme inactivation, growth deficiencies and DNA damage. These studies showed a graded response to the loss of SOD in the cells. At small reductions in SOD activity, a substantial reduction in the activity of labile dehydratases was seen. A greater than four-fold increase sensitised cells to DNA damage.

Schwartz *et al* (1983), however, showed the cytotoxicity of neutrophils to bacteria and suggested that even though the bacteria contained the protective antioxidant enzymes, under the conditions within the phagosome, the flux of $O_2^{\bullet-}$ and H_2O_2 generated was sufficient to overwhelm the cells antioxidant mechanisms. Other enzymes have been associated with antioxidant mechanisms. Lundberg *et al* (1999) suggested that Glucose-6-phosphate dehydrogenase is required in *S typhimurium* resistance to reactive oxygen species. The DNA repair enzyme formamidopyrimidine-DNA glycosylase was also essential to antioxidant defence from *E. coli* treated with high levels of H_2O_2 (Alhama *et al*, 1998).

The individual cytotoxicity of $^{\bullet}NO$ and $O_2^{\bullet-}$ relies on the susceptibility of the target organism to the stress derived from these free radical species. Nunoshiba *et al* (1992 and 1995) have shown that $^{\bullet}NO$ signals *E. coli* through the same transcription factors as $O_2^{\bullet-}$, and the genes induced by $^{\bullet}NO$ are those essential for the protection against oxidative damage. Also in *Salmonella typhimurium* Crawford and Goldberg (1998) have shown that a flavohaem protein regulates gene expression on stimulation by $^{\bullet}NO$. It has also been confirmed in *E. coli* that a flavohaem affords protection from $^{\bullet}NO$. Specifically, the haem serves a dioxygenase function that produces mainly nitrate. These studies identify enzymes with reactions that were thought to occur only by chemical means. It was also emphasised that the reactions of $^{\bullet}NO$ with haemoglobins were evolutionary conserved and have been adapted for cell-specific functions (Hausladen *et al*, 1998).

It is clear then that bacteria and viruses can be susceptible to free radical attack but also have some relevant antioxidant enzymes to survive particular stresses. XO has been shown previously to generate $O_2^{\bullet-}$ and $^{\bullet}NO$. XO-derived $O_2^{\bullet-}$ and H_2O_2 have been implicated in antiviral activity by causing apoptosis in the infected cells (Skulachev,

1998), in association with duodenal ulcers and *Helicobacter pylori* infections (Ben-Hamida *et al*, 1998) and *in vitro* susceptibility of *Mycobacterium leprae* to oxygen-mediated damage (Dhople, 1996). However the effectiveness of either $O_2^{\bullet -}$ or $^{\bullet}NO$ alone has been questioned in the light of their possible reaction products.

6.1.4 Chapter aim

This chapter deals with the susceptibility of bacteria relevant to the chronic wound to a range of reactive species generated either enzymatically or by chemical means. It also aims to investigate changes in the growth and viability of bacteria treated with XOR in situations where the oxygen tension is variable as in the chronic wound. The ability of XOR generated species to reduce the number of infectious bacteria will provide justification for the addition of this enzyme into an ulcer dressing or for incorporation into a tissue engineered dermal graft.

6.2 Principles, methods and materials

6.2.1 Culture of bacterial strains

6.2.1.1 Materials

Agar No. 1, Tryptone-Soya Broth (TSB) (Oxoid Limited. Hampshire, UK); Luria-Bertani Broth, Glycerol (Sigma Aldrich Company Ltd. Dorset, UK); Petri dishes (Fisher Scientific UK Ltd. Leicestershire, UK).

A range of severe disease, chronic wound and abscess *S. aureus* isolates were obtained from Dr Enright (University of Bath).

Table 6.1

Isolate	Site	Details
Mu 3 171	Pus from a surgical wound	Moderate vancomycin resistance (VRSA). (Hiramatsu *et al*, 1997).
Mu 50	Isolated from pus of a Japanese baby with a surgical wound infection that did not respond to vancomycin in 1997	Derivative of Mu3. Moderate vancomycin hetero-resistance (hVRSA) (Kuroda *et al*, 2001).
117 (138)	Isolated from a septicaemia patent	Penicillin, ciproflaxin, trimethoprin resistant and meticillin susceptible *S. aureus* (MSSA). (Oxford hospital collection).
N315	Pharyngeal smear of a Japanese patient isolated in 1982	Prototype* of meticillin resistant *S. aureus* (MRSA) (Kuroda *et al*, 2001). * Prototypic in the sense that it was the first MRSA isolate to have the resistance determinant mecA sequenced.

Table 6.1 Severe disease *S. aureus* isolates.

S. aureus strains used also came from the Oxford strain collection (from Enright *et al*, 2000) and were isolates from pus drains and abscess sites: 197, 357, 13, 283 were community-acquired and 301 and 307 were hospital-acquired. Bacterial isolates were selected from prospectively selected patients with invasive *S. aureus* disease identified in the Oxford region in 1997 or 1998. Invasive *S. aureus* disease was defined as the isolation of the organism from a normally sterile site in a patient with clinical signs and symptoms consistent with *S. aureus* infection. Isolates from patients with deep local infections associated with prosthetic material were excluded, as were isolates from patients with septicemia in which *S. aureus* was isolated from only one blood culture bottle (of at least two inoculated). Patients were assigned to one of two groups on the basis of clinical details: those with community-acquired disease and those with hospital-acquired disease. Community-acquired disease was defined as an illness consistent with invasive *S. aureus* disease that required admission to hospital and that resulted in the isolation of *S. aureus* from a specimen taken from a normally sterile site within 24 hours of admission. In addition, patients hospitalised for any reason within the preceding 6 months were excluded from this category.

Other bacterial species that are known to have been isolated from chronic wounds, and were used in the present study are *Pseudomonas aeruginosa* (*P. aeruginosa*) PAO1 *Escherichica coli* (*E. coli*) MC4100, *Proteus mirabilis* (*P. mirabilis*) DV429, *Streptococcus faecalis* (*S. faecalis*) 775, *Staphylococcus aureus* (*S. aureus*) NCTC

(National collection of Type Cultures) 6571 all strains were obtained from University of Bath (Dr. Wood).

6.2.1.2 Protocol

S. aureus disease isolates were cultured on nutrient Tryptone-Soya Agar (TSA) at 37°C by streaking out using a sterile plastic loop from frozen stock cultures. Manipulation of the bacteria was carried out in a laminar flow cabinet (class II) to prevent contamination of the cultures and provide some protection for the user. Colony formation occurred with overnight incubation. Single colonies were inoculated into 6mls of Tryptone-Soya Broth (TSB) and grown overnight in air before each experiment. Alternatively TSB was directly inoculated from stocks and grown overnight in air. Cells were cultured at 37°C in glass bijous with shaking at 200 revolutions min^{-1}. A control tube was also set up which contained TSB alone.

The long-term storage of bacterial stocks of *P. aeruginosa, E. coli, P. mirabilis, S. faecalis* and *S. aureus* was achieved by dilution of bacteria in Luria-Bertani Broth (LB) with 20% glycerol and freezing at -70°C. Using a flamed loop, bacteria from the long-term storage stock were streaked-out onto an agar plate (see section 8.2.2 in the appendix for agar plate preparation) and incubated at 37°C until colonies were formed. Once colonies had formed plates were stored at 4°C for up to two weeks. When required single colonies were used to inoculate baffled flasks containing 20mls LB and cultures were incubated overnight at 37°C in air with continuous agitation at 100 revolutions min^{-1}.

6.2.2 Chemically generated oxidants, XO and reduced Oxygen on bacterial growth

The rate of cell growth after treatment with H_2O_2 and $ONOO^-$ and XO was assessed by utilising the change in absorbance over time of bacteria in nutrient broth. The effect of reduced or low oxygen concentration on bacterial growth rate was also measured to characterise this parameter during further experiments that required manipulation of the oxygen environment. The bacteria used in this study are facultative anaerobes being able to utilise a range of electron donors, other than oxygen in its absence.

6.2.2.1 Peroxynitrite generation

6.2.2.1.1 Materials

Sodium nitrite, hydrogen peroxide, sodium hydroxide, manganese dioxide (Sigma Aldrich Company Ltd. Dorset, UK), hydrochloric acid (BDH Laboratory supplies, Poole, UK) 0.22μm syringe filter (Fisher Scientific UK Ltd. Leicestershire, UK).

6.2.2.1.2 Protocol

Peroxynitrite was generated using a quenched flow reaction apparatus as described by Reed *et al* (1974). An aqueous solution of 10ml sodium nitrite (0.6M) was rapidly mixed with 10ml of hydrochloric acid (HCL, 0.6M) and hydrogen peroxide (H_2O_2, 0.7M) this was achieved using Y-shaped tubing and two plastic syringes to plunge the solutions together. The combined solutions were immediately quenched with 20ml sodium hydroxide (NaOH, 3M). All reaction solutions were kept on ice. This method leads to some residual nitrite and H_2O_2 contamination. The H_2O_2 was removed by reacting solutions of chemically formed $ONOO^-$ with 4g manganese dioxide (MnO_2) for 4-5 minutes followed by filtration through 0.22μm filter (Haenen *et al*, 1997). The concentration of the resulting solution containing $ONOO^-$ was calculated by measuring the absorbance (Hitachi, U-2010) at 302nm of a 1 in 10 and a 1 in 100 dilution in 1M NaOH and using equation 6.1. Stock solutions were stable for several weeks at -20°C (Crow, 1997). However, stock $ONOO^-$ was generated weekly and was not used after 7 days of synthesis. Also $ONOO^-$ was allowed to decompose ($dONOO^-$) at room temperature for 3 days to be used as the control for the residual nitrite/nitrate and NaOH (Bauer *et al*, 1992; Pfeiffer *et al*, 1997). Sufficient buffering and dilution in PBS reduced the effect of the residual NaOH further.

$A = \varepsilon cl$ (ε = Extinction coefficient of $ONOO^- = 1670 M^{-1} cm^{-1}$ Hughes and Nicklin 1968)

If $A_{302nm} = 2.3$ (1 in 10 dilution)

$2.3 = 1670 \times c \times l$

Therefore, $2.3 / 1670 = c$

Therefore $c = 1.38 \times 10^{-3} \times 10$ (dilution factor) $= 0.0138$ M $= 13.8$mM

Equation 6.1. Calculation of the concentration of peroxynitrite using the Beer-Lambert equation.

A=absorbance, ε = extinction coefficient (Molar absorbtivity with units of $M^{-1} cm^{-1}$), c = concentration of the compound in solution expressed in M, l = Pathlength of the sample (Pathlength of cuvette in which sample is contained in cm. The pathlength of the cuvette is 1 cm).

In order to try and improve the yield of $ONOO^-$ from 13.8mM (See equation 2.) The apparatus for the $ONOO^-$ generation was improved based on that described by Koppenol *et al* (1996) who used a vacuum pump to draw the sodium nitrite and HCL, H_2O_2 into Y-shaped tubing where they were eventually reacted together along a 4cm stretch of tubing at a rate of 30ml min^{-1}. The combined solutions were then drawn along, and quenched in a collection tube containing 1.5M NaOH. For this method the solutions remained the same apart from the NaOH quenching solution that was reduced to a concentration of 1.5M. The rest of the procedure was as stated previously. The yield for the improved method was 74mM $ONOO^-$.

6.2.2.2 The effect of H_2O_2 and $ONOO^-$ and XO on bacterial growth

6.2.2.2.1 Materials

Allopurinol, hypoxanthine, hydrogen peroxide, sodium hydroxide, disposable polystyrene cuvettes, (Sigma Aldrich Company Ltd. Dorset, UK), hydrochloric acid (BDH Laboratory supplies, Poole, UK), XO (Biozyme Laboratories. Gwent, UK).

6.2.2.2.2 Protocol

Assays were carried out in cuvettes in 2 or 3 ml volumes and followed at 600nm at 37°C (Hitachi, U-2010). Alternatively, the assay was automated using a 96-well plate reader (Dynex Technologies, MRX TC II), a 595nm filter and clear bottomed sterile 96-well plates. The plate reader was temperature controlled at 37°C and the plates were left *in situ* during the experiments. For the XO assays, reagents were sterile filtered through a 0.22μm syringe filter and diluted in LB giving final concentrations of 1mM hypoxanthine, 1mM allopurinol and 0.5, 1, 5, 10 and 50mU ml^{-1} XO. For the H_2O_2 concentrations between 0-100mM were used and $ONOO^-$ was diluted between 0-0.5mM (see experiments for specific concentrations). A final volume of 200μl was used for these experiments. A program of measurement steps was written for the spectrophotometer to follow, including multiple readings and incubation times of 15 minutes between each measurement for a duration of 4-6 hours. This technique allowed for large throughput experiments to be carried out in triplicate or quadruplicate with little intervention once the assay was running. This assay was used to assess the effect of treatments on the growth of a range of bacteria. By calculating the mean generation time (See section 6.2.2.3) in the absence and presence of a range of concentrations of oxidants it was possible to determine the growth rate relative to an untreated control.

6.2.2.3 The effect of reduced oxygen on bacterial growth

6.2.2.3.1 Materials

2% O_2 and 5% CO_2 balanced nitrogen (BOC Gases. Guildford, UK), disposable polystyrene cuvettes, magnetic stirrers (Sigma Aldrich Company Ltd. Dorset, UK), parafilm (Fischer Scientific UK Ltd. Leicestershire, UK).

6.2.2.3.2 Protocol

E. coli and S. aureus were cultured overnight as stated previously and then added to 2mls of LB in 3ml cuvettes which were either saturated with room air or equilibrated to 2% O_2, 5% CO_2 balanced nitrogen overnight in the miniMACS Anaerobic Workstation (Don Whitley Scientific Ltd). For experiments in 2% O_2 the overnight cultures were diluted inside the Anaerobic Workstation, the cuvettes were covered with parafilm and removed from the Workstation at hourly intervals for measurements. All cuvettes were incubated at 37°C whilst being stirred with sterile magnetic stirrers and the absorbance at 600nm was measured at hourly intervals to compare the growth rates.

6.2.2.4 Mean growth rate constant and generation time

For the bacterial growth experiments, the mean growth rate constant and generation time for the cell population was calculated. The mean growth rate constant and generation time may be calculated from the following equation (Equation 6.2) using data from the exponential growth phase of cell division.

$$k = n/t$$
$$= (\log N_t - \log N_0) / 0.301t$$

If the population doubles $t = g$, therefore $Nt = 2N_0$, which can be substituted into the above equation:

$$k = (\log(2N_0) - \log N_0) / 0.301g$$
$$= (\log 2 + \log N_0 - \log N_0) / 0.301g$$
$$k = 1/g$$

The mean generation time is the reciprocal of the mean growth rate constant (k):

$$g = 1/k$$

Equation 6.2. Calulation of the Mean Growth Rate Constant and Generation Time of a Bacterial Cell Culture.

Where g = mean generation time; k = mean growth rate constant; n = number of generations in time t; N_0 = the initial population number; N_t = the population at time t; t = time (Prescott *et al*, 1996).

Absorbance values were used to determine the region of the growth curve for which the growth was logarithmic. This was evaluated by plotting the absorbance data on a logarithmic (log_{10}) scale. The growth rate constant was determined by replotting the data over the linear time period and converting the absorbance data into log2 values (divide by 0.301). A straight line was plotted through the points of the growth slope to give the mean growth rate constant as a function of time (e.g log_2A_{600} min). The inverse of this slope shows how many minutes it takes for the culture to increase its density by log_2A_{600} absorbance units. Since it is log_2, a change of 1 absorbance unit means that the culture absorbance has doubled (mean generation time).

6.2.3 Effect of H_2O_2 and XO on bacterial viability in air

6.2.3.1 Assessment of viability using disk inhibition assays

The sensitivity of strains to H_2O_2 and XO-generated species were determined using a disk inhibition assay (Ballion *et al*, 1999 and Elvers *et al*, 2004) in which the zone of killing is measured.

6.2.3.1.1 Materials

Whatman filter paper disks, (3M, 6mm Diameter) (Fisher Scientific, UK Ltd. Leicestershire, UK), sodium nitrite, Hypoxanthine, H_2O_2 (Sigma Aldrich Company Ltd. Dorset, UK), XO (Biozyme Laboratoritories. Gwent, UK).

6.2.3.1.2 Protocol

S. aureus were grown overnight in air in LB at 37°C. Agar plates were also prepared prior to experiments as described in the appendix (section 8.2.2). Culture samples were adjusted to an Abs_{600} of 0.45 and 2.5ml samples of the diluted culture were added to 50ml of soft agar (0.4%, see appendix 8.2 for recipe) for a final abs_{600nm} of 0.021. Sterile filtered 1mM hypoxanthine and 1mM nitrite were included in the 50ml final volume of soft agar for certain experiments. All additions were made to the melted agar which was maintained at 45°C in a waterbath. The soft LB agar overlay (4mls) was subsequently poured onto over-dried LB plates (see appendix 8.2 for preparation). Samples (25µl) of H_2O_2 in PBS or XO with or without its substrates were added to sterile filter paper disks and transferred to the soft agar surface using flame sterilised forceps.

The zone of killing (no growth visible) was measured after incubating the disks for 24 hours at 37°C.

6.2.4 Effect of XO on bacterial viability in variable oxygen

6.2.4.1 Assessment of viable cells by colony counts

The number of viable cells of control and XO treated bacteria were assessed at a range of oxygen tensions by counting of the number of colony forming units (CFU) on agar. Assessments of viability were carried out using the Miles-Mizra count technique. This technique counts the viable population and involves the preparation of a dilution series of the test culture, and the division of an agar plate into an appropriate number of sectors. A pipette is then used to place drops of the diluted suspension onto each sector. Sectors which receive a dilution with a high concentration of cells will show overlapping growth. At lower concentration the number of colonies will be able to be counted. This method depends on the use of several replicate tests.

6.2.4.1.1 Materials

LB (Sigma Aldrich Company Ltd. Dorset, UK), Agar No. 1 (Oxoid Limited. Hampshire, UK), Petri dishes (Fisher Scientific UK Ltd. Leicestershire, UK), 96-well plates, Sodium nitrite, Hypoxanthine (Sigma Aldrich Company Ltd. Dorset, UK), XO (Biozyme Laboratoritories. Gwent, UK).

6.2.4.1.2 Protocol

Bacteria from overnight cultures were inoculated into 96-well plates in air using sterile technique in the presence of a Bunsen flame and then placed in a 37°C incubator. Alternatively, the plates were inoculated in the hypoxia cabinet which was set up prior to the experiment as described in section (4.2.5). For the XO treatment studies the plates were treated with XO 0, 10 and 50mU ml^{-1}, 1mM hypoxanthine and 1mM nitrite. Plates were removed from the incubator or the hypoxia cabinet at hourly or 3 hourly intervals and 20µl samples were taken from test wells and repeatedly diluted in 180µl of LB (10-fold dilutions). For each sample, four or three 10-fold dilutions were plated onto agar plates (see appendix 8.2 for plate preparation) for a countable number of cells and 20µl of each dilution was added to the plate in triplicate (Figure 6.1). The inoculated plates were incubated at 37°C overnight. Each batch of incubated cells also had a non-inoculated plate that had undergone the air drying procedure to show the level of background contamination. Two agar plates were required per test condition for the hypoxia

experiments for an n = number of four. 64 plates were used at each oxygen concentration (4 test conditions x 4 strains of bacteria x 2 time points).

The number of viable cells ml^{-1} were determined as follows:

Average viable count per 20µl drop x dilution factor x 50 = $CFUml^{-1}$ of original sample.

Figure 6.1

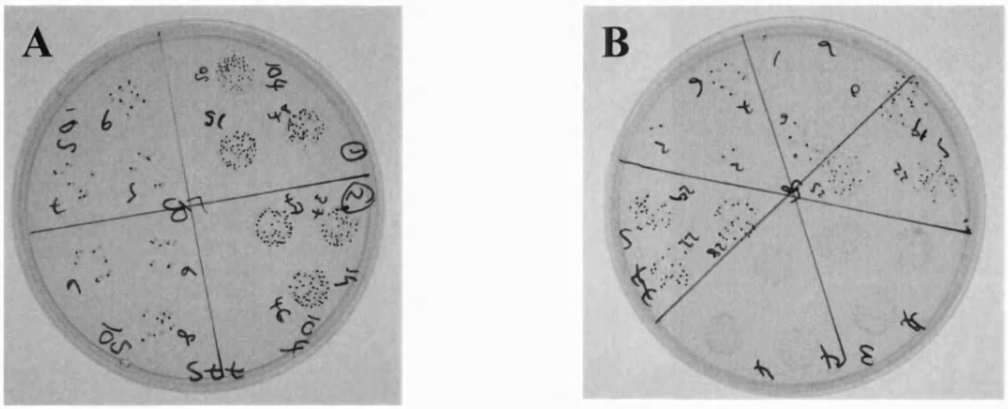

Figure 6.1 Agar plate layout for colony counts.

(A) Agar plates were initially divided into four quadrants to culture four 10-fold dilutions of a sample taken from one well of the 96-well plate. (B) However, later experiments which required a higher n number showed that the plates could be divided into six segments allowing for two lots of three 10-fold dilutions of 2 different samples therefore halving the number of plates required.

6.2.5 Statistical analysis

Statistical analysis of data collected was performed using GraphPad Prism Version 4.00 (GraphPad Software Inc.). Statistical analysis performed was, a one-way ANOVA statistical test with Dunnett's post test for analysis of variance between treatments.

6.3 Results

6.3.1 Effect of H_2O_2 and $ONOO^-$ on the growth of *S. aureus* disease Isolates

6.3.1.1 Growth curves of *S. aureus* strains

Initial assays were carried out to assess the growth of the *S. aureus* disease isolates (Mu 3, Mu 50, 117, N317) in 96-well plates at varying dilutions of the bacterial culture. The overnight cultures were diluted 1 in 10 ($1x10^{-1}$) and 1 in 20 ($5x10^{-2}$), the cultures were then serially diluted 1 in 10 giving 22 different dilutions. The results which are shown below, demonstrate that clear sigmoidal growth curves (shown below in red) were only achieved at a $1x10^{-1}$ and $5x10^{-2}$ dilution of the overnight culture, therefore these dilutions were used for future treatment experiments (figure 6.2-6.5).

Figure 6.2-6.5

A) B)

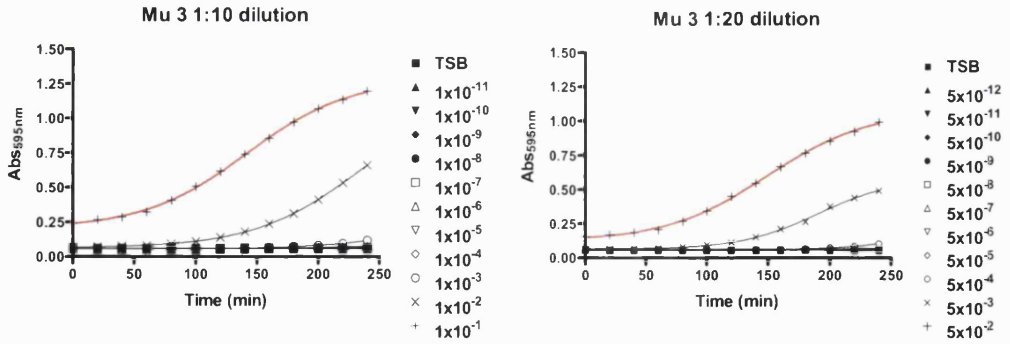

Figure 6.2 Growth curves of *S. aureus* (Isolate Mu 3) at varying concentrations.

Dilutions of overnight cultures of *S. aureus* began at A): 1:10 dilution ($1x10^{-1}$) as indicated by the red line and B): a 1:20 dilution ($5x10^{-2}$) as indicated by the red line. Further log dilutions made across a 96-well plate in TSB for a 200µl final volume per well. The changes in absorbance readings over time indicated growth and were recorded at 595nm at 20 min intervals over a 4 hour time period. n = 1.

A) B)

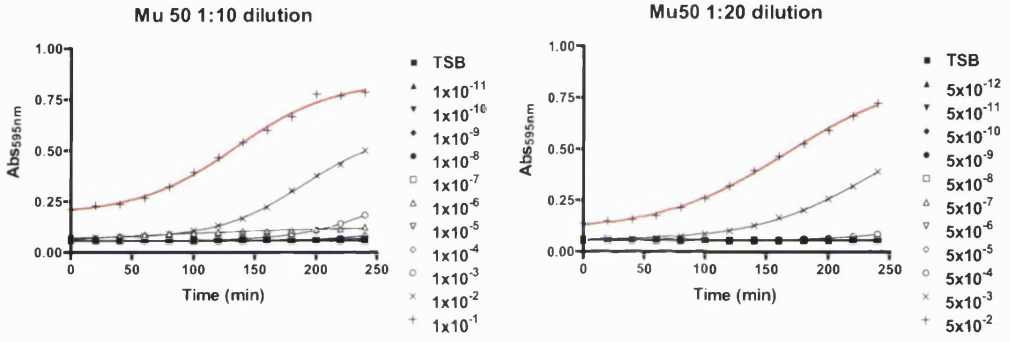

Figure 6.3Growth curves of *S. aureus* (Isolate Mu 50) at varying concentrations.

Dilutions of overnight cultures of *S. aureus* began at A): 1:10 dilution ($1x10^{-1}$) as indicated by the red line and B): a 1:20 dilution ($5x10^{-2}$) as indicated by the red line. Further log dilutions made across a 96-well plate in TSB for a 200µl final volume per well. The changes in absorbance readings over time indicated growth and were recorded at 595nm at 20 min intervals over a 4 hour time period. n = 1.

A) B)

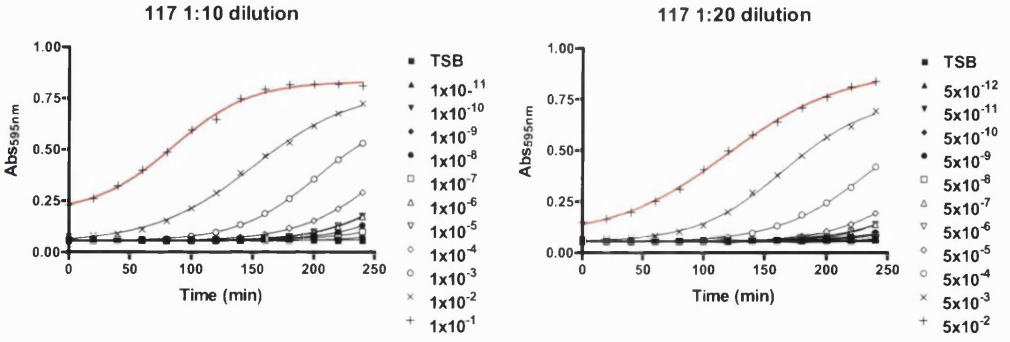

Figure 6.4 Growth curves of *S. aureus* (Isolate 117) at varying concentrations.

Dilutions of overnight cultures of *S. aureus* began at A): 1:10 dilution ($1x10^{-1}$) as indicated by the red line and B): a 1:20 dilution ($5x10^{-2}$) as indicated by the red line. Further log dilutions made across a 96-well plate in TSB for a 200µl final volume per well. The changes in absorbance readings over time indicated growth and were recorded at 595nm at 20 min intervals over a 4 hour time period. n = 1.

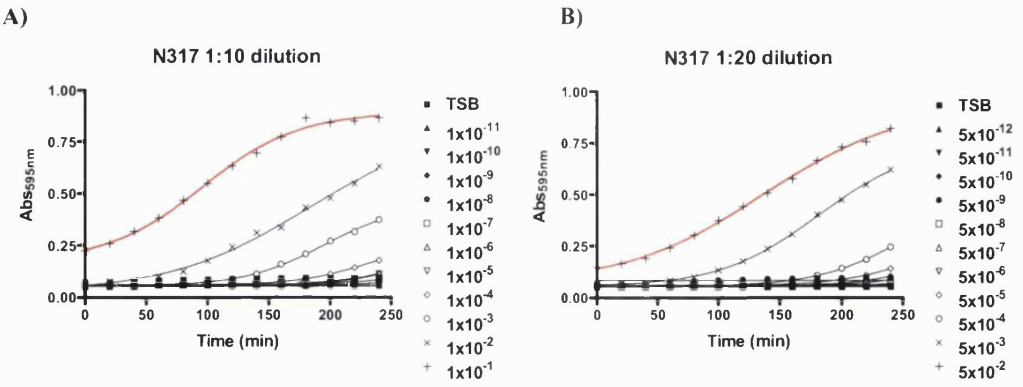

Figure 6.5 Growth curves of *S. aureus* (Isolate N317) at varying concentrations.

Dilutions of overnight cultures of *S. aureus* began at A): 1:10 dilution ($1x10^{-1}$) as indicated by the red line and B): a 1:20 dilution ($5x10^{-2}$) as indicated by the red line. Further log dilutions made across a 96-well plate in TSB for a 200µl final volume per well. The changes in absorbance readings over time indicated growth and were recorded at 595nm at 20 min intervals over a 4 hour time period. n = 1.

The growth rates (Table 6.2) and doubling times (Table 6.3) at a $1x10^{-1}$ and $5x10^{-2}$ dilution of the start culture were calculated and show that the growth rates are faster and doubling time shorter at $5x10^{-2}$ dilution of the start culture compared with a $1x10^{-1}$ dilution. The growth rates and doubling times of the four strains are similar; however, Mu 3 has the fastest growth rate and shortest doubling time.

Table 6.2

Dilution of start culture	**Mu 3 (171)**	**Mu 50**	**117 (138)**	**N317**
$1x10^{-1}$	0.0156	0.0136	0.0150	0.0132
$5x10^{-2}$	0.0186	0.0147	0.0173	0.0161

Table 6.2 Rate of bacterial growth (log2 A595nm min^{-1}) of four *S. aureus* strains.

Growth rates at a $1x10^{-1}$ and a $5x10^{-2}$ dilution of the start culture were calculated from the raw data in figure 6.2-6.5. n = 1.

Table 6.3

Dilution of start culture	**Mu 3 (171)**	**Mu 50**	**117 (138)**	**N317**
$1x10^{-1}$	64.23	73.53	66.58	75.64
$5x10^{-2}$	53.68	68.03	57.74	62.31

Table 6.3 Doubling times of bacterial growth (minutes) of four *S. aureus* strains.

Doubling times at a $1x10^{-1}$ and a $5x10^{-2}$ dilution of the start culture were calculated from the raw data in figure 6.2-6.5. n = 1.

6.3.1.2 Effects of H_2O_2 on the growth of *S. aureus* strains

The growth of *S. aureus* strains Mu 3 (171), Mu 50, 117 (138) and N317 was followed after the treatment of both a $1x10^{-1}$ and a $5x10^{-2}$ dilution of the start culture with H_2O_2 (Figure 6.6-6.9). At a $5x10^{-2}$ dilution of the culture 100mM H_2O_2 slowed bacterial

growth to a greater extent than when bacteria are treated at a $1x10^{-1}$ dilution as shown in the growth curves in figure 6.6-6.9 (shown in red) and in the growth rates (figure 6.10). H_2O_2 has a significant effect on the growth of *S. aureus* at 100mM 117, Mu 50 and N315 were most sensitive at this concentration, whereas Mu 3 was the least sensitive (figure 6.10). At 10mM H_2O_2 the only strain to show a significant reduction in the growth rate when compared with the control was 117 (figure 6.10).

Figure 6.6-6.9

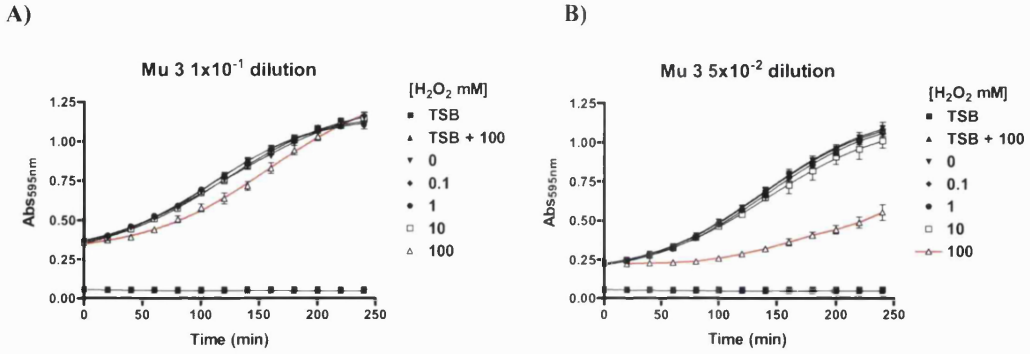

Figure 6.6 Growth Curves of *S. aureus* (Isolate Mu 3) Treated with H_2O_2

Experiments were carried out in air at a $1x10^{-1}$ (A) and $5x10^{-2}$ (B) dilution of the overnight culture. Bacteria were treated with H_2O_2 at 0, 0.1, 1, 10 and 100mM. The effects of 100mM H_2O_2 are indicated by the red line. Absorbance readings were taken at 595nm at 20min intervals for 4 hours at 37°C. Mean±SD. n = 4.

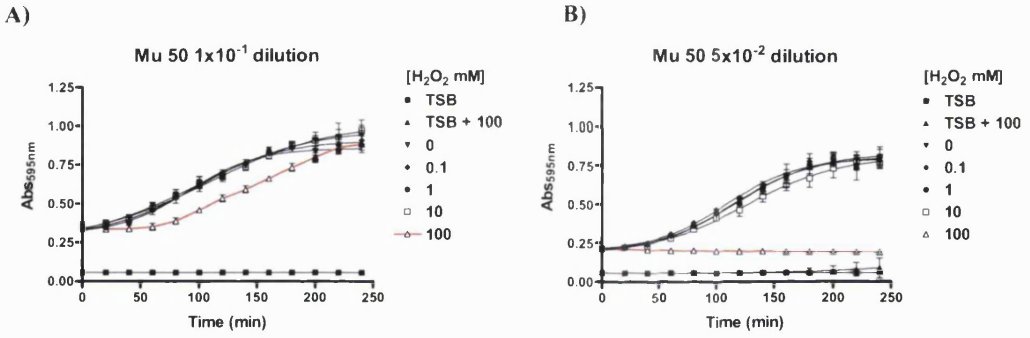

Figure 6.7 Growth curves of *S. aureus* (Isolate Mu 50) Treated with H_2O_2

Experiments were carried out in air at a $1x10^{-1}$ (A) and $5x10^{-2}$ (B) dilution of the overnight culture. Bacteria were treated with H_2O_2 at 0, 0.1, 1, 10 and 100mM. The effects of 100mM H_2O_2 are indicated by the red line. Absorbance readings were taken at 595nm at 20min intervals for 4 hours at 37°C. Mean±SD. n = 4.

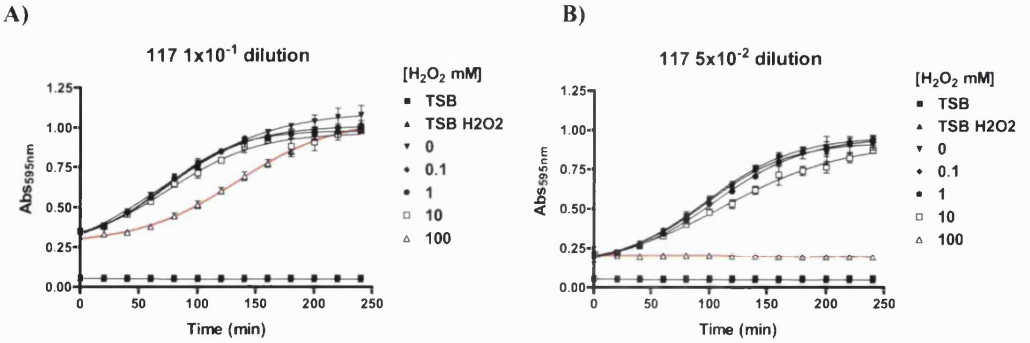

Figure 6.8 Growth curves of *S. aureus* (Isolate 117) Treated with H_2O_2

Experiments were carried out in air at a $1x10^{-1}$ (A) and $5x10^{-2}$ (B) dilution of the overnight culture. Bacteria were treated with H_2O_2 at 0, 0.1, 1, 10 and 100mM. The effects of 100mM H_2O_2 are indicated by the red line. Absorbance readings were taken at 595nm at 20min intervals for 4 hours at 37°C. Mean±SD. n = 4.

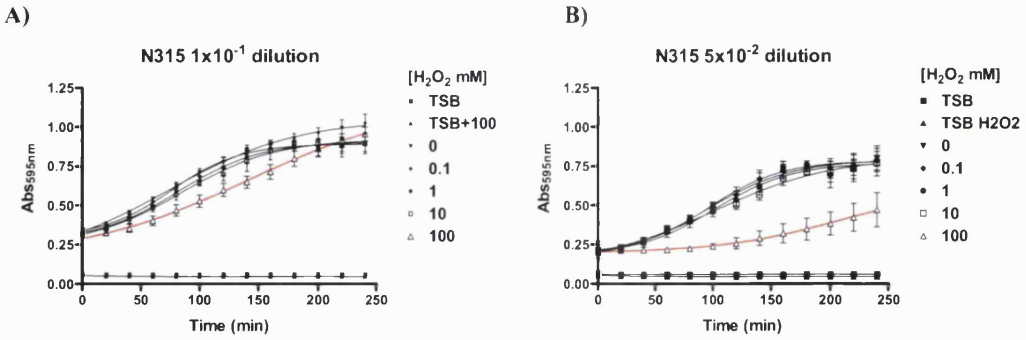

Figure 6.9 Growth curves of *S. aureus* (Isolate N315) treated with H_2O_2.

Experiments were carried out in air at a $1x10^{-1}$ (A) and $5x10^{-2}$ (B) dilution of the overnight culture. Bacteria were treated with H_2O_2 at 0, 0.1, 1, 10 and 100mM. The effects of 100mM H_2O_2 are indicated by the red line. Absorbance readings were taken at 595nm at 20min intervals for 4 hours at 37°C. Mean±SD. n = 4.

Figure 6.10

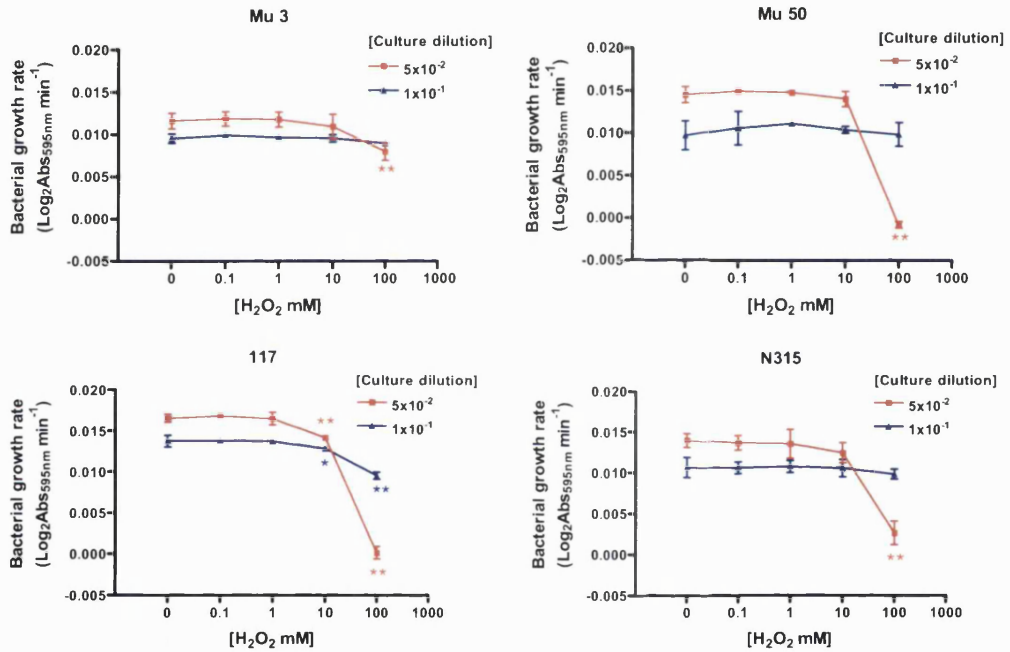

Figure 6.10 Maximal growth rates of *S. aureus* Isolates treated with H_2O_2.

Experiments were carried out in air at a $1x10^{-1}$ (as shown in red) and $5x10^{-2}$ (as shown in blue) dilution of the overnight culture of strains Mu3, Mu50, N317, 117. Bacteria were treated with H_2O_2 at 0.1, 1, 10 and 100mM at 37°C. Rates were calculated from the log phase of growth using the growth curves in figure 6.6-6.9. Mean±SD. n = 4. The statistical analysis used was One-way ANOVA with Dunnett's post test.

A range of isolates from pus drains and abscess sites that were hospital or community acquired were also tested for sensitivity to H_2O_2. The effect of H_2O_2 on isolate 13, 357, 197, 283, 301 and 307 was assessed using a $5x10^{-2}$ and a $2.5x10^{-2}$ dilution of the start culture (Figure 6.11-6.16). The starting concentrations of the bacterial culture were based on the results in section 6.3.1.2 showing that the lower concentration showed

greater sensitivity to H_2O_2. The results show that at a $2.5x10^{-2}$ dilution of the start culture, 10 and 100mM H_2O_2 completely inhibits the growth of the *S. aureus* isolates. However, at a $5x10^{-2}$ dilution of the start culture only 100mM H_2O_2 is effective (Figure 6.17). The effect of the H_2O_2 on all the strains appears to be comparable at these concentrations (Figure 6.17).

Figure 6.11-6.16

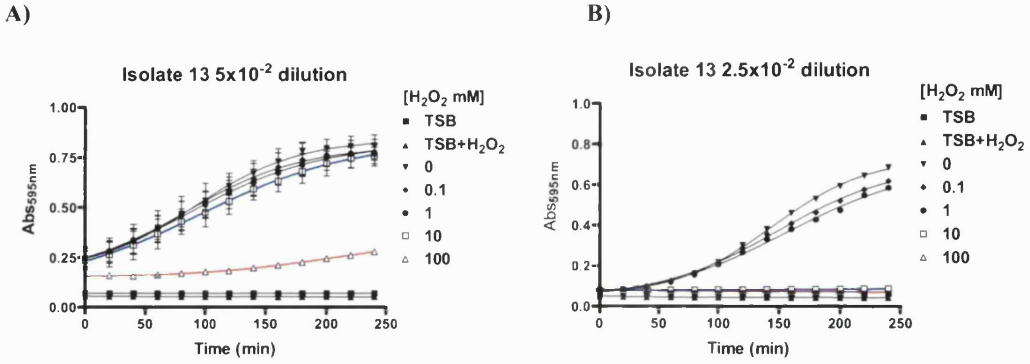

Figure 6.11 Growth curves of *S. aureus* (Isolate 13) treated with H_2O_2.

Experiments were carried out in air using a $5x10^{-2}$ (A) and a $2.5x10^{-2}$ (B) dilution of the overnight culture. Bacteria were treated with H_2O_2 at 0, 0.1, 1, 10 and 100 mM. The effects of 100mM H_2O_2 are indicated by the red line and 10mM H_2O_2 by the blue line. Absorbance readings were taken at 595 nm at 20 min intervals for 4 hours at 37°C. Mean ± SD. $5x10^{-2}$: n = 4 (Except 100mM n =1). $2.5x10^{-2}$: n = 1

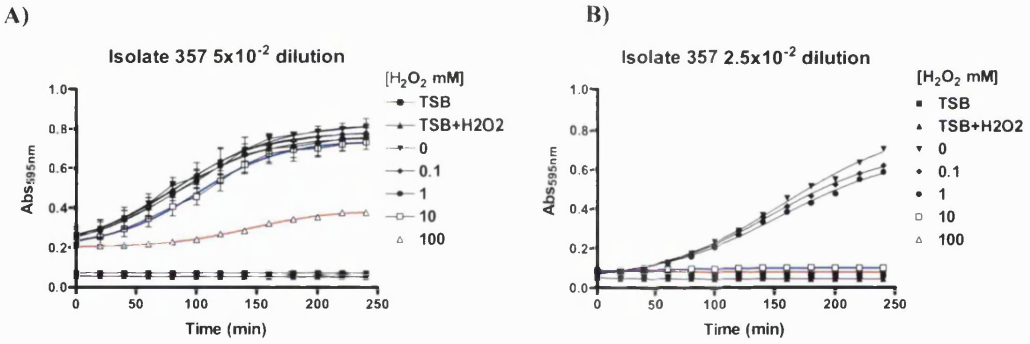

Figure 6.12 Growth curves of *S. aureus* (Isolate 357) treated with H_2O_2.

Experiments were carried out in air using a $5x10^{-2}$ (A) and a $2.5x10^{-2}$ (B) dilution of the overnight culture. Bacteria were treated with H_2O_2 at 0, 0.1, 1, 10 and 100 mM. The effects of 100mM H_2O_2 are indicated by the red line and 10mM H_2O_2 by the blue line. Absorbance readings were taken at 595 nm at 20 min intervals for 4 hours at 37°C. Mean ± SD. $5x10^{-2}$: n = 4 (Except 100mM n = 1). $2.5x10^{-2}$: n = 1.

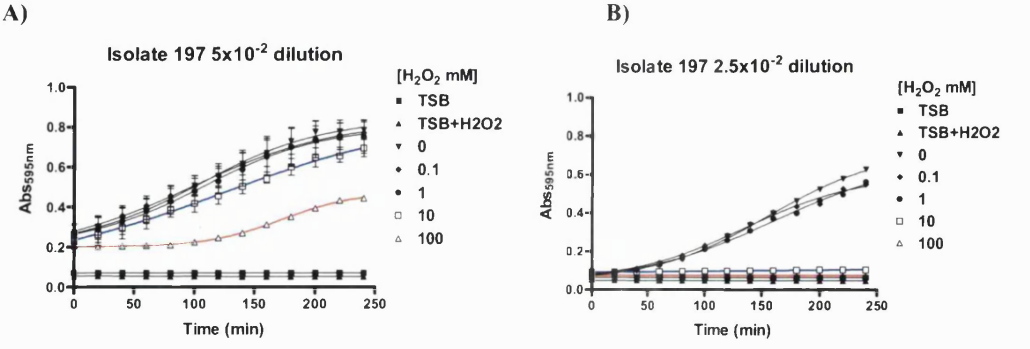

Figure 6.13 Growth curves of *S. aureus* (Isolate 197) treated with H_2O_2.

Experiments were carried out in air using a $5x10^{-2}$ (A) and a $2.5x10^{-2}$ (B) dilution of the overnight culture. Bacteria were treated with H_2O_2 at 0, 0.1, 1, 10 and 100 mM. The effects of 100mM H_2O_2 are indicated by the red line and 10mM H_2O_2 by the blue line. Absorbance readings were taken at 595 nm at 20 min intervals for 4 hours at 37°C. Mean ± SD. $5x10^{-2}$: n = 4 (Except 100mM n = 1). $2.5x10^{-2}$: n = 1.

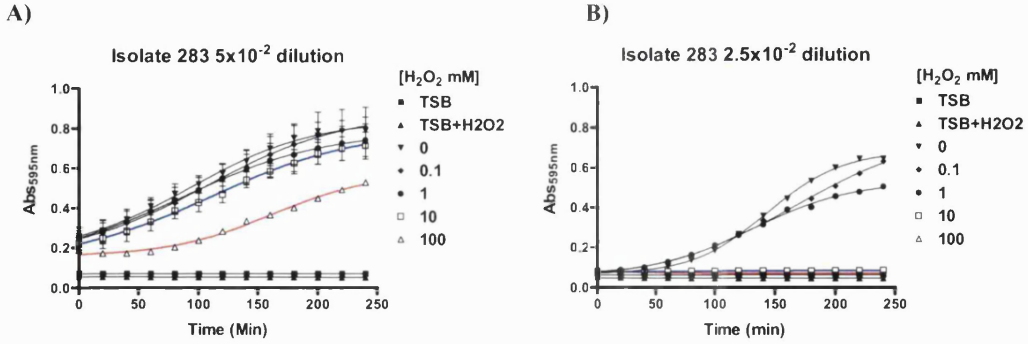

Figure 6.14 Growth curves of *S. aureus* (Isolate 283) treated with H_2O_2.

Experiments were carried out in air using a $5x10^{-2}$ (A) and a $2.5x10^{-2}$ (B) dilution of the overnight culture. Bacteria were treated with H_2O_2 at 0, 0.1, 1, 10 and 100 mM. The effects of 100mM H_2O_2 are indicated by the red line and 10mM H_2O_2 by the blue line. Absorbance readings were taken at 595 nm at 20 min intervals for 4 hours at 37°C. Mean ± SD. $5x10^{-2}$: n = 4 (Except 100mM n = 1). $2.5x10^{-2}$: n = 1.

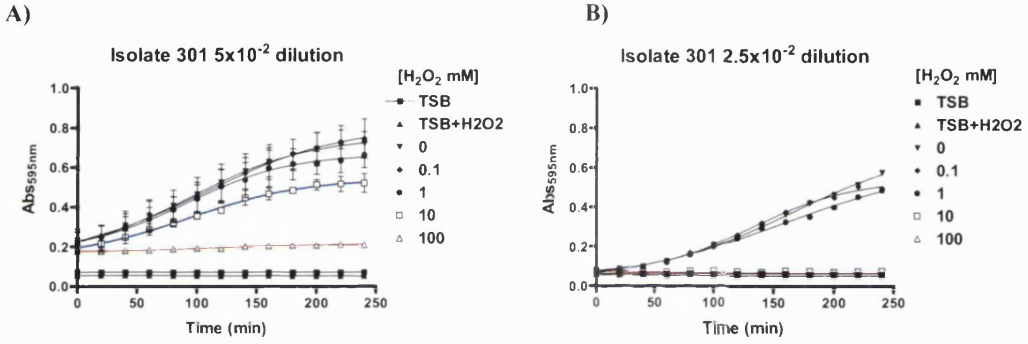

Figure 6.15 Growth curves of *S. aureus* (Isolate 301) treated with H_2O_2.

Experiments were carried out in air using a $5x10^{-2}$ (A) and a $2.5x10^{-2}$ (B) dilution of the overnight culture. Bacteria were treated with H_2O_2 at 0, 0.1, 1, 10 and 100 mM. The effects of 100mM H_2O_2 are indicated by the red line and 10mM H_2O_2 by the blue line. Absorbance readings were taken at 595 nm at 20 min intervals for 4 hours at 37°C. Mean ± SD. $5x10^{-2}$: n = 4 (Except 100mM n = 1). $2.5x10^{-2}$: n = 1.

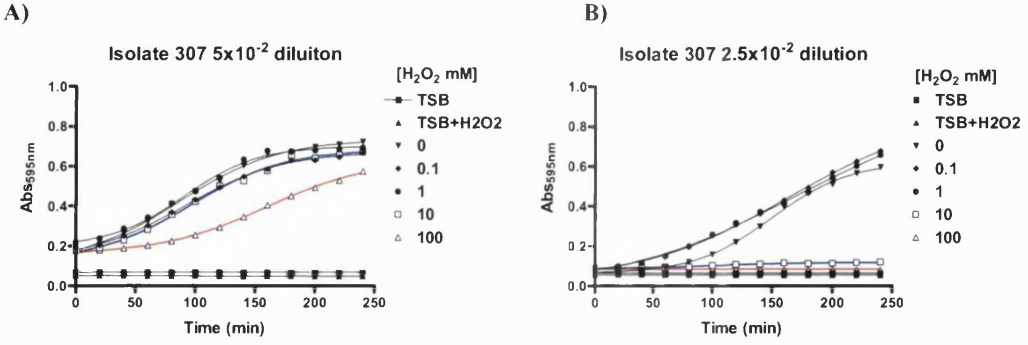

Figure 6.16 Growth curves of *S. aureus* (Isolate 13) treated with H_2O_2.

Experiments were carried out in air using a $5x10^{-2}$ (A) and a $2.5x10^{-2}$ (B) dilution of the overnight culture. Bacteria were treated with H_2O_2 at 0, 0.1, 1, 10 and 100 mM. The effects of 100mM H_2O_2 are indicated by the red line and 10mM H_2O_2 by the blue line. Absorbance readings were taken at 595 nm at 20 min intervals for 4 hours at 37°C. Isolate 307 $5x10^{-2}$ n = 1 and $2.5x10^{-2}$ n = 1.

Figure 6.17

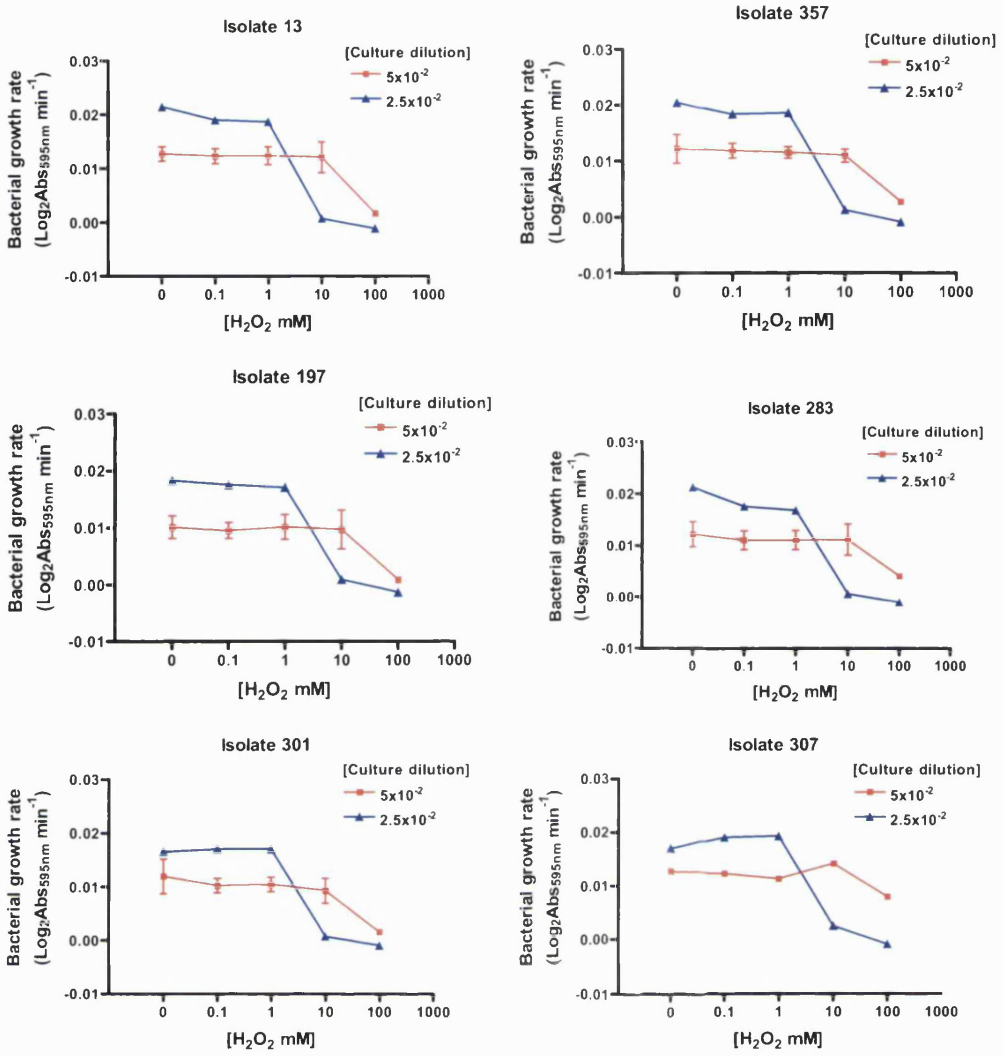

Figure 6.17 Growth rates of *S. aureus* strains after treatment with H_2O_2

Experiments were carried out at a $5x10^{-2}$ (as shown in red) and $2.5x10^{-2}$ (as shown in blue) dilution of the overnight cultures of isolate 13, 357, 197, 301 and 307. Bacteria were treated with H_2O_2 at 0, 0.1, 1, 10 and 100mM. (See figure 6.5 for the examples of growth curves). Mean±SD. Isolate 13, 357, 197, 283, 301 : $5x10^{-2}$ n = 4 Except 100mM n = 1. $2.5x10^{-2}$ n = 1. Isolate 301 $5x10^{-2}$ n = 1 and $2.5x10^{-2}$ n = 1. Statistical analysis was not performed as the number for some of the conditions was too small.

6.3.1.3 Effects of $ONOO^-$ on the growth of *S. aureus* strains

Peroxynitrite was generated on the lab bench as in section 6.2.2.1. A method by Reed *et al* (1974) was initially used however this produced a low yield of 13.5mM. In an attempt to improve the yield modifications of the methodology and equipment were experimented with based around the method described by Koppenol *et al* (1996) eventually resulting in an improved yield up to 74mM $ONOO^-$. Initial experiments to examine the efficacy of a range of $ONOO^-$ concentrations to kill bacteria were performed. These experiments indicated that a concentration of 0.5mM was sufficient to kill bacteria but the effect was lost on further dilution to 0.1mM. These preliminary experiments could

not be expanded upon or reproduced because of a laboratory safety audit of procedural risk assessments. This resulted in a change in laboratory safety policy that prohibited the use of pathogenic strains of bacteria such as the *S. aureus* disease isolates that were being used in this study.

As it became impossible to use these bacteria for any further experiments, it was decided to move directly onto the XO treatment experiments. Furthermore, because of the change in safety policy with regard to *S. aureus* disease strains it was impossible to use these strains for the experiments in variable oxygen which would involve the use of multiple plates on the lab bench. Therefore, four laboratory strain facultative bacteria that are known to be relevant to the chronic wound and could be used on the lab bench, and could be easily accessed on a daily basis were supplied by Dr. Pauline Wood for future experiments.

6.3.2 Effect of H_2O_2 and XO on the growth of bacterial species relevant to the chronic wound

6.3.2.1 Growth curves of *S. faecalis, E. coli, S. aureus, P. aeruginosa*

The facultative anaerobes *S. faecalis, E. coli, S. aureus, P. aeruginosa* supplied by Dr. Pauline Wood were used to check that the bacteria followed normal sigmoidal growth in 96-well plates in air. Varying concentrations of the bacterial overnight cultures were used and growth was followed over 6 hours. The growth of *S. aureus, E. coli* and *S. faecalis* follow sigmoidal growth characteristics with a lag phase log phase and stationary phase of growth. *P. aeruginosa,* however, shows a reduced growth rate and extended lag phase compared with the other bacteria (Figure 6.18).

Figure 6.18

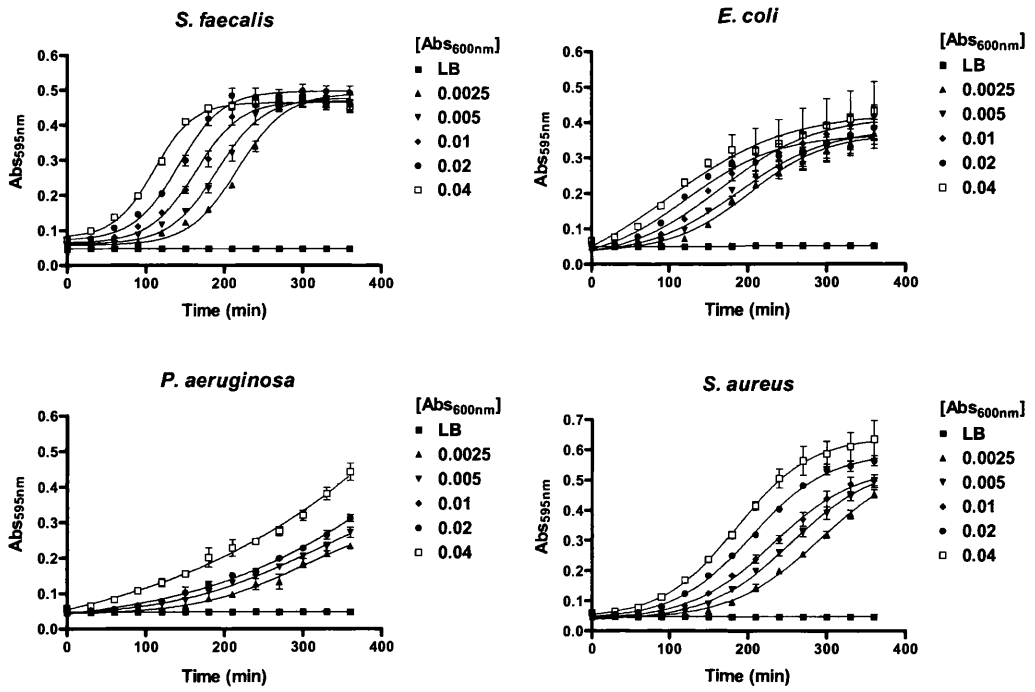

Figure 6.18 Growth curves of four facultative anaerobes with varying cell concentration.

Overnight cultures were diluted in cuvettes to an A_{600nm} of 0.08 and doubling dilutions of the strains were carried out in 5ml bijous. 100µl of each dilution was added to the wells of a 96-well plate along with 100µl of LB for final concentrations of 0.0025, 0.005, 0.01, 0.02, 0.04 Abs_{600nm} in a 200µl total volume. The plate was read at 37°C every 30mins for 6 hours. Mean ± SD. n = 4.

6.3.2.2 Correlation of absorbance versus viable cell counts.

Experiments were carried out to determine the relationship between the growth curve absorbance readings taken in a 96-well plate and the corresponding number of viable cells ml^{-1} for *S. aureus*, *P. mirabilis*, *S. faecalis and E. coli* (Figure 6.19-6.21). *P. mirabilis*, was included in these studies as a substitute for *P. aeruginosa.* However, *P. aeruginosa* was included in some of the later XO studies in air. The results in figure 6.19 follow a similar profile until around four hours, after this time the absorbance values begin to plateau suggesting that the cells have reached stationary phase. This effect however, is not mirrored in several of the cell counts which continue to rise after 4 hours. The *E. coli* appear to show a reduction in viability at 6 hours. The results in figure 6.20 and show that for *staphylococcus aureus* and *proteus mirabilis* there appears to be a linear relationship until the stationary phase is reached (*Staphylococcus aureus* ~0.4 abs_{595nm}, *Proteus mirabilis DV429* ~0.5 abs_{595nm}) where the number of viable cells appear to continue to increase and the absorbance plateaus. There is a linear relationship between abs 595 nm and cells ml^{-1} for the first 4 hours of growth for all of the strains (Figure 6.21).

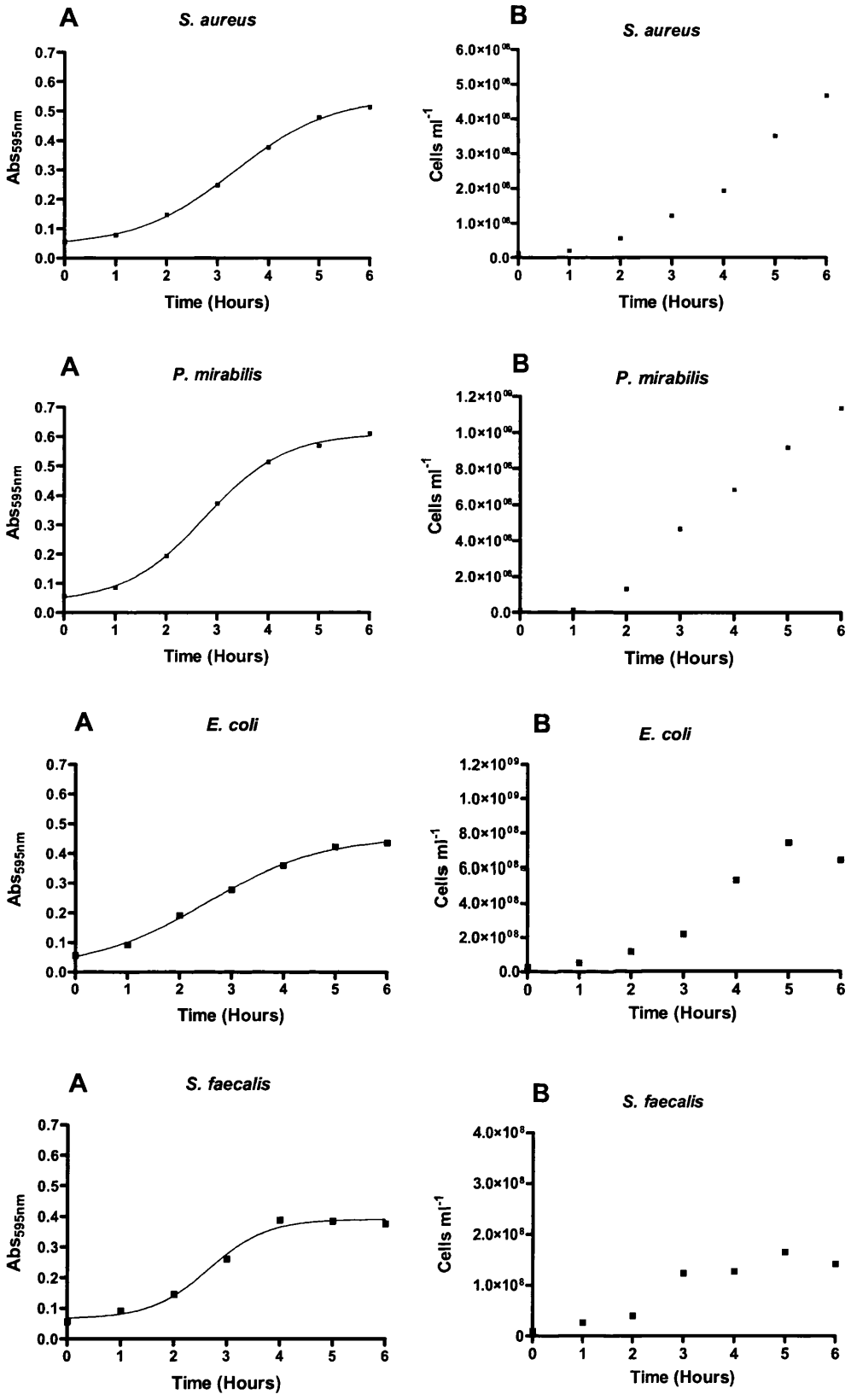

Figure6.19 Correlation of Abs_{595nm} versus cells ml^{-1} of *S. aureus*, *P. mirabilis*, *S. faecalis*, *E. coli*

Overnight cultures of *S. aureus*, *P. mirabilis*, *S. faecalis*, *E. coli* were each diluted to 0.02 Abs_{600nm} in LB and 200µl added to 6 wells of a 96-well plate. Cultures were grown at 37°C in air for 6 hours. (A) Absorbance at 595 nm was taken at hourly intervals and, (B) Viable counts (Cells ml^{-1}) determined simultaneously for colony counts at hourly intervals. This was achieved by removal of 20µl of sample and diluted using the Miles-Mizra technique for a countable number of colonies on agar n = 1.

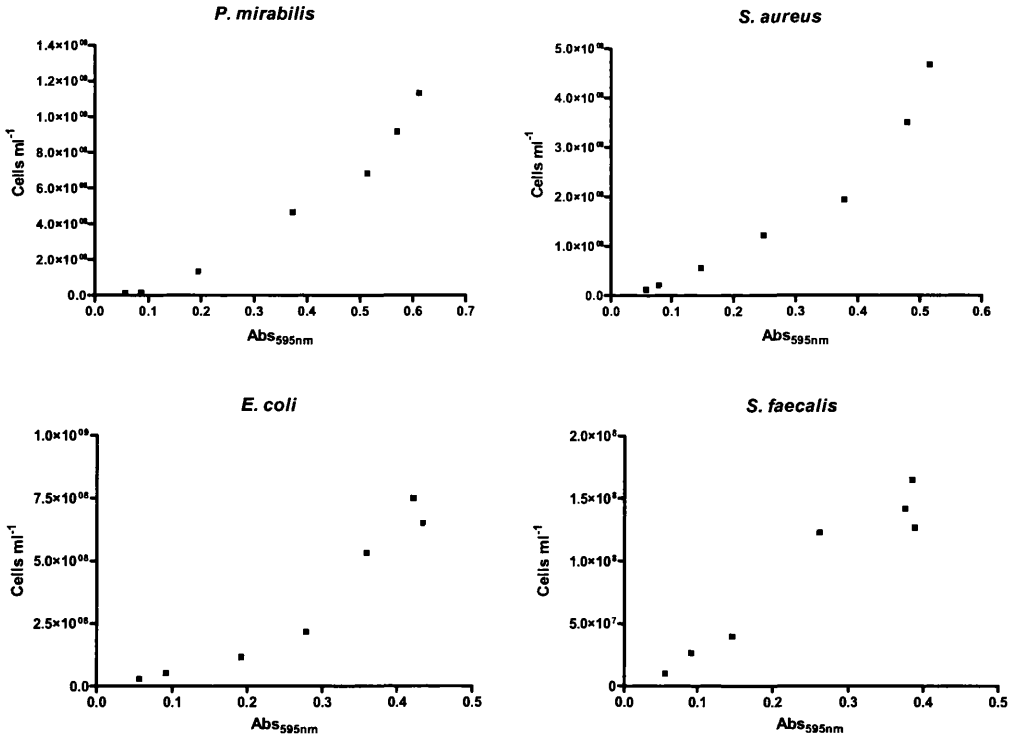

Figure 6.20 Correlation of absorbance against viable count.

Using the raw data in figure 6.27 the cells ml^{-1} were plotted against Abs_{595nm} to determine if there is a linear relationship. There appears to be a linear relationship in the first few hours of growth (See figure 6.29).

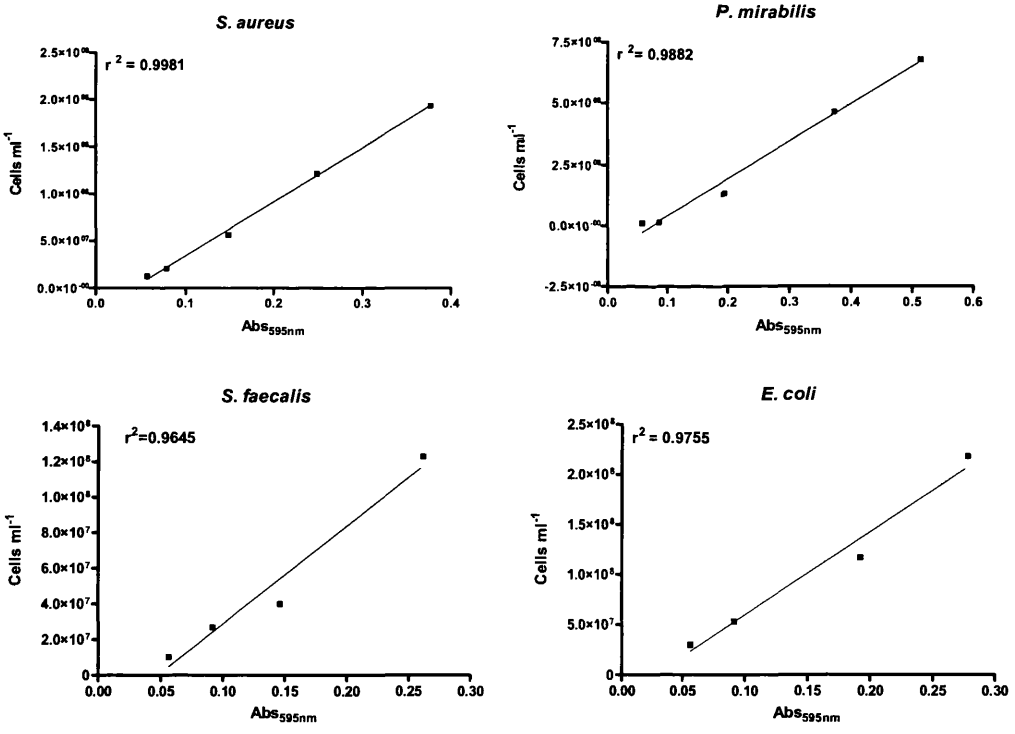

Figure 6.21 Linear relationship between abs_{595nm} and cells ml^{-1} before stationary phase is reached.

There is a linear relationship in the first 4-5 hours of growth as indicated by the r^2 values on the graphs above.

6.3.2.3 Treatment of *S. aureus* and *S. faecalis* with H_2O_2

The effect of a range of concentrations of H_2O_2 on the growth of *S. aureus* (Figure 6.22) and *S. faecalis* (Figure 6.23) was assessed. Hydrogen peroxide at 2mM slowed the growth of *S. aureus* with complete inhibition of growth at 5mM H_2O_2 and above. Hydrogen peroxide at 1 and 2mM slowed the growth of *S. faecalis* with complete inhibition at 5mM H_2O_2.

Figure 6.22A)

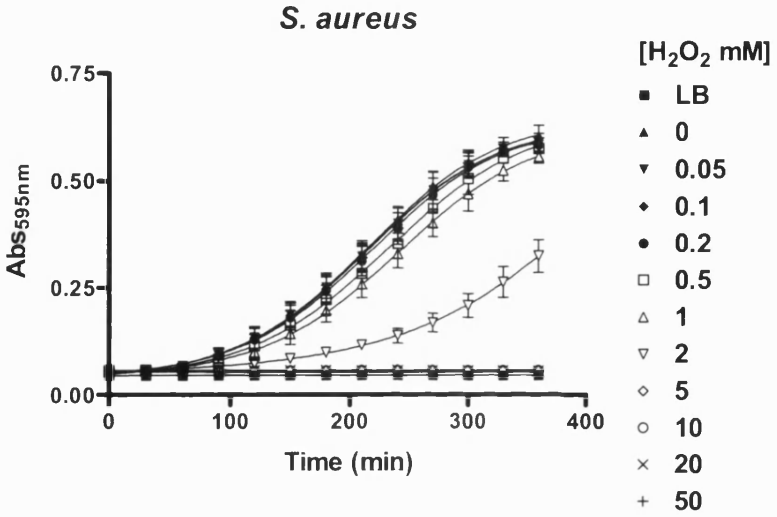

Figure 6.22B)

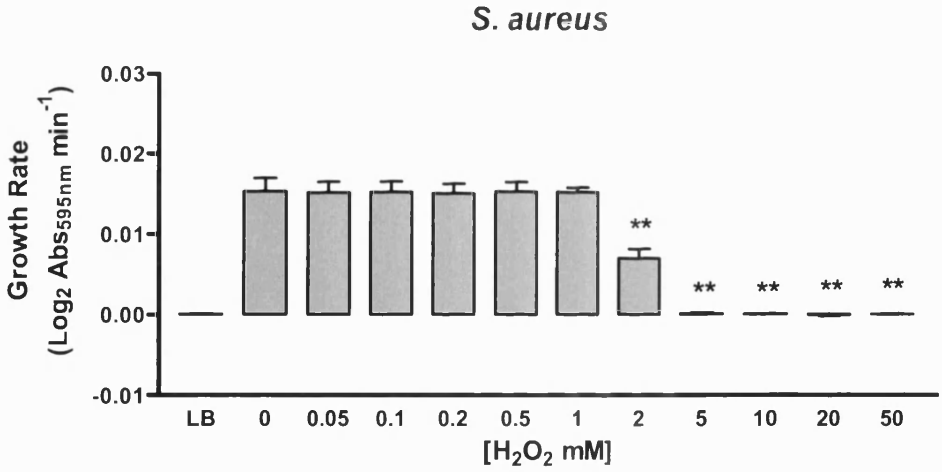

Figure 6.22 Treatment of *S. aureus* with H_2O_2

Experiments were carried out in air in a 96-well plate. The overnight culture was diluted to 0.04 Abs_{600nm} and 100µl added to the plate. Bacteria were then treated with 100µl H_2O_2 diluted in LB for final concentrations of 0, 0.05, 0.1, 0.2, 0.5, 1, 2, 5, 10, 20 and 50mM and a 200µl final volume. The plate was maintained at 37°C and absorbance readings were taken at 595nm at 30min intervals over 6 hours. Graph A shows growth curves of *S. aureus* at varying concentrations of H_2O_2. Graph B shows maximal growth rates of *S. aureus*. The effect of H_2O_2 added on the growth rate which was calculated from the log phase A_{595nm} readings over time. Data was then analysed using One-Way ANOVA with Dunnett's post test using 0mM H_2O_2 as a control. Results are from two experiments performed in quadruplicate, therefore n = 8. Mean±SD.

Figure 6.23A)

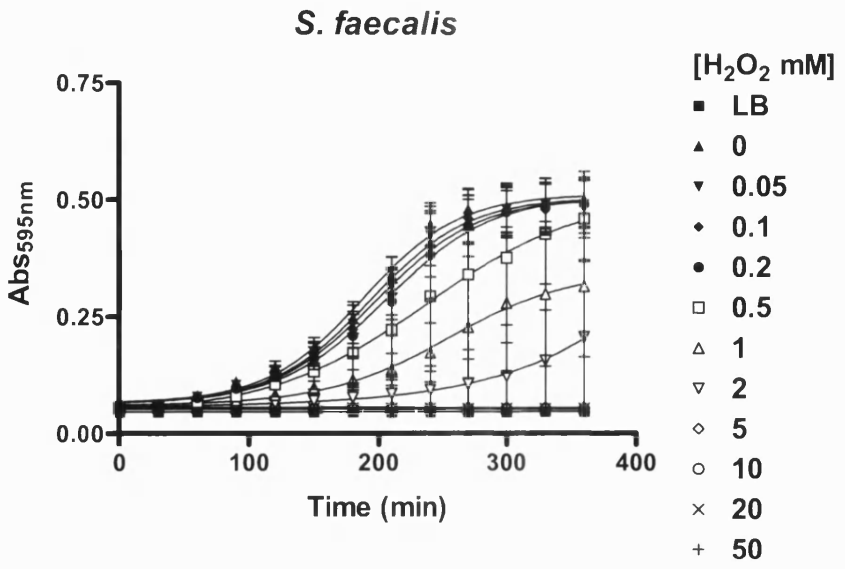

Figure 6.23B)

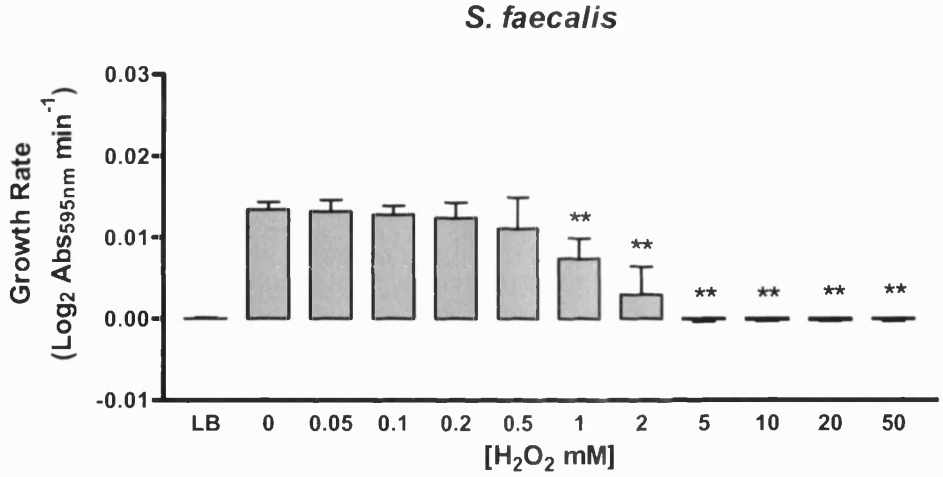

Figure 6.23 Treatment of *S. faecalis* with H_2O_2.

Experiments were carried out in air in a 96-well plate. The overnight culture was diluted to 0.04 Abs_{600nm} and 100µl added to the plate. Bacteria were then treated with 100µl H_2O_2 diluted in LB for final concentrations of 0, 0.05, 0.1, 0.2, 0.5, 1, 2, 5, 10, 20 and 50mM and a 200µl final volume. The plate was maintained at 37°C and absorbance readings were taken at 595nm at 30min intervals over 6 hours. Graph A shows growth curves of *S. faecalis* at varying concentrations of H_2O_2. Graph B shows maximal growth rates of *S. faecalis*. The effect of H_2O_2 added on the growth rate which was calculated from log phase A_{595nm} readings over time. Data was then analysed using One-Way ANOVA with Dunnett's post test using 0mM H_2O_2 as a control. Results are from two experiments performed in quadruplicate, therefore n = 8. Mean±SD.

6.3.2.4 Treatment of *S. faecalis* with SIN-1

A brief study was carried out to assess the effects of the peroxynitrite generator SIN-1 on the growth of *S. faecalis*. Prior to this study, $ONOO^-$ generation by SIN-1 was measured in PBS and LB to provide information on the activity of the SIN-1 stock in PBS as compared with in LB. Experiments were also carried out in the presence of iron

chelator DTPA which prevents iron mediated hydroxyl radical formation which can oxidase DHR. The comparison between PBS and LB without DTPA shows that the rate of DHR oxidation is considerably slower in the LB suggesting a decrease in $ONOO^-$ generation. DHR oxidation by SIN-1 in PBS in the presence of DTPA is marginally decreased. This is also the case in the LB although the reduction in DHR oxidation is far more evident in this case (Figure 6.24). Figure 6.25 shows the inhibition of the growth of *S. faecalis* at 500 and 1000μM SIN-1.

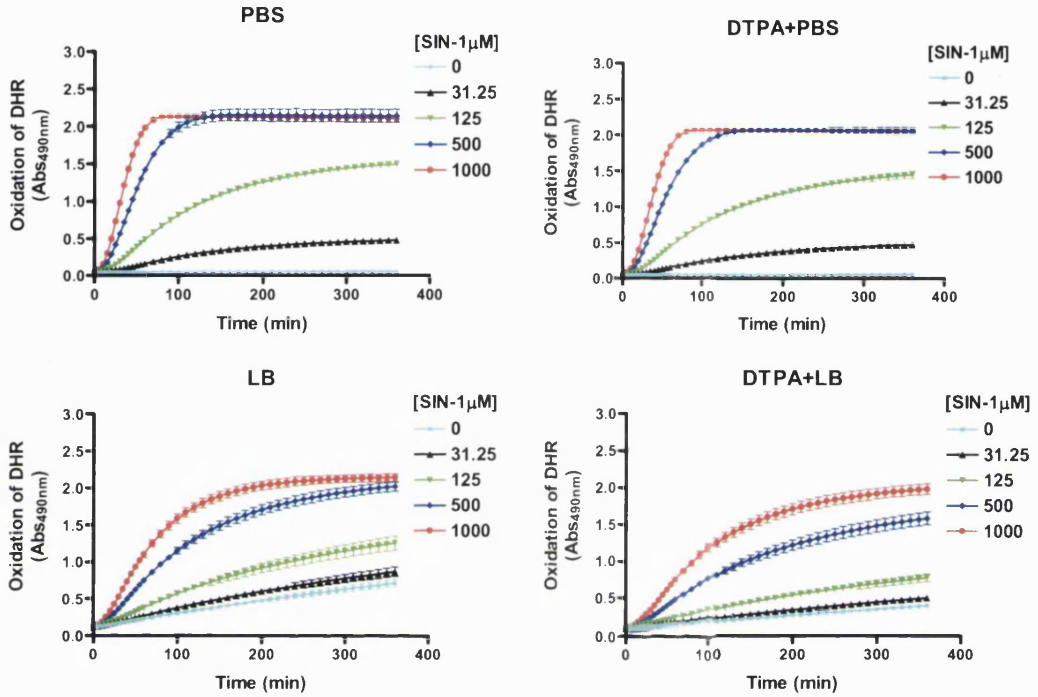

Figure 6.24 Oxidation of DHR with SIN-1 in PBS and LB with and without DTPA.

Experiments were carried out in air in a 96-well plate using DHR (0.1mM) and SIN-1 (0, 31.25, 125, 500 and 1000μM) diluted in both LB and PBS with and without the addition of DTPA (0.1mM). Absorbance readings were taken at 490nm over a 6 hour time period at 37°C (See section 4.2.2.2 for methodology). Mean±SD. n = 4.

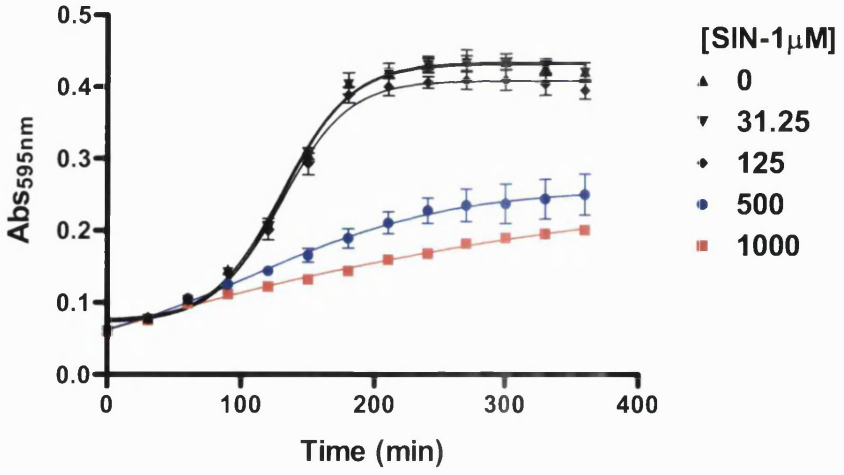

Figure 6.25 Treatment of *S. faecalis* with $ONOO^-$

Overnight cultures of *S. faecalis* were diluted to 0.04 Abs_{600nm} in cuvettes with LB and 100µl added to a 96-well plate. SIN-1 (0, 31.25, 125, 500 and 1000µM) was diluted in LB and 100µl added to the plate for a 200µl final concentration. The plate was incubated at 37°C and readings were taken at 595nm every 30 minutes over 6 hours. This figure shows a growth curve of *S. faecalis* treated with SIN-1. Inhibition of growth is shown in blue (500µM) and red (1000µM). n = 4. Mean ± SD.

6.3.2.5 Treatment of *E. coli* with XO in air (cuvette method)

Initial experiments to assess the effects of XO on bacteria relevant to the chronic wound were carried out in cuvettes using *E. coli*. Figure 6.26A and B suggests that XO does not affect the growth of *E. coli* in stirred cuvettes at 1 and 5mU ml^{-1} XO. However, there does appear to be a slight slowing of growth at 50mU ml^{-1} XO (Figure 6.24A and B). Subsequent assays were performed in 96-well plates to increase the number of samples that could be assayed and the number of replicates.

Figure 6.26A)

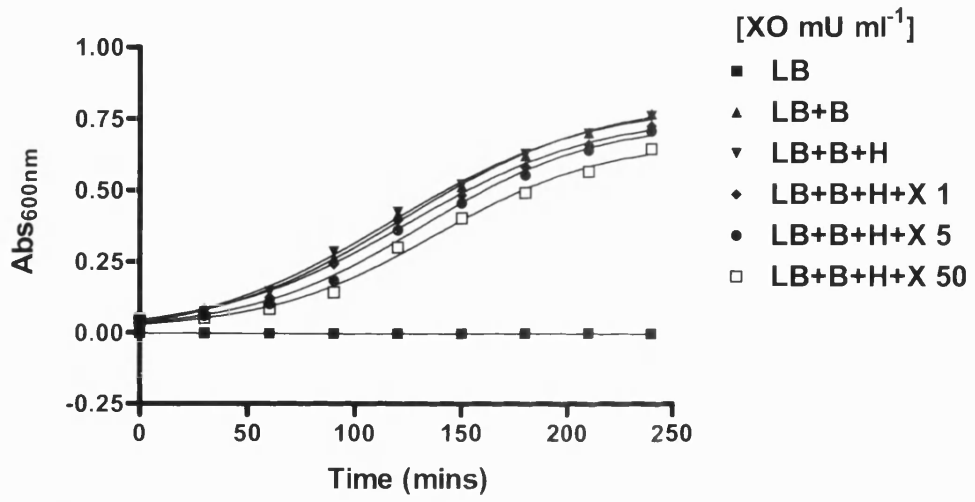

Figure 6.26 B)

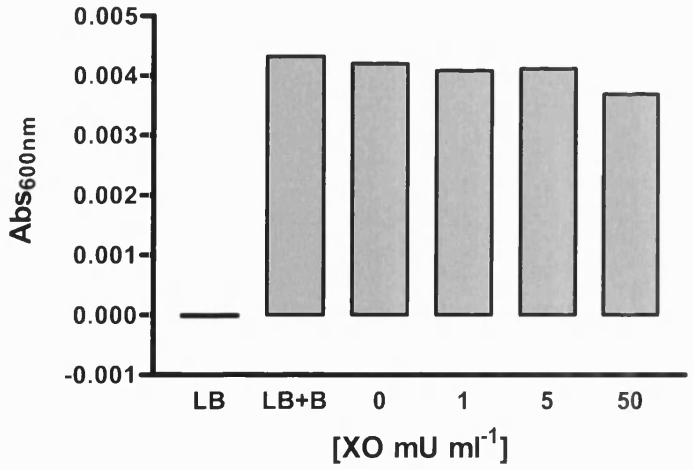

Figure 6.26 Growth curves of *E. coli* treated with XO in air.

Experiments were carried out in air at 37°C in stirred cuvettes. The overnight culture was diluted in LB to 0.04 Abs_{600nm} the *E. coli* bacteria (B) were then treated with 0, 1, 5, 50 mU ml^{-1} XO and 1mM hypoxanthine (H) diluted in LB for a final volume of 2mls. Absorbance readings were taken at 600nm at 30min intervals

over 4 hours. Graph A shows growth curves of *E. coli* treated with hypoxanthine and XO. Graph B shows maximal growth rates (log phase) of *E. coli* treated with XO. n = 1.

6.3.2.6 Treatment of bacterial species with XO in air (96-well plate method)

The effect of a range of concentrations of XO in air on the growth of *S. aureus, S. faecalis, E. coli, P. aeruginosa, P. mirabilis* were assessed in 96-well plates (Figure 6.27-6.36). For each bacterial species there are two figures, the first shows the relevant controls for the experiment and the second figure shows the treatment of the bacterial species with hypoxanthine and a range of XO concentrations (0-50mU ml^{-1}). The treatment of *S. aureus* (Figure 6.27A and B controls) shows that 1mM hypoxanthine and allopurinol alone do not affect the growth of *S. aureus*. However, XO (50 mU ml^{-1}) appears to slow the growth of *S. aureus* both with and without the addition of hypoxanthine which suggests that substrates for XO are present in the LB. Addition of allopurinol reverses this effect confirming that the slowing of growth is due to XO. Treatment of the bacteria with a range of XO concentrations and hypoxanthine (figure 6.28A and B) shows that 10mU ml^{-1} XO significantly slows the growth of *S. aureus*, and 50mU ml^{-1} XO completely inhibits the growth of *S. aureus*. Allopurinol completely reverses this inhibition of growth (Figure 6.28 A and B).

Figure 6.27A)

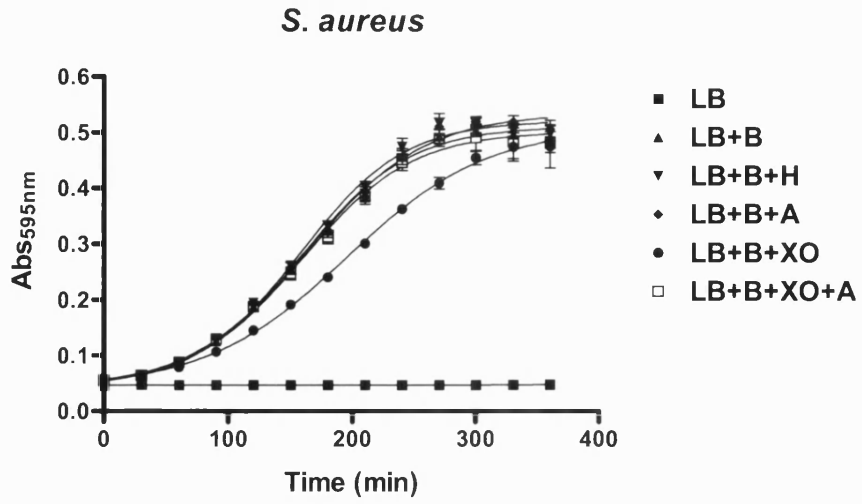

Figure 6.27B)

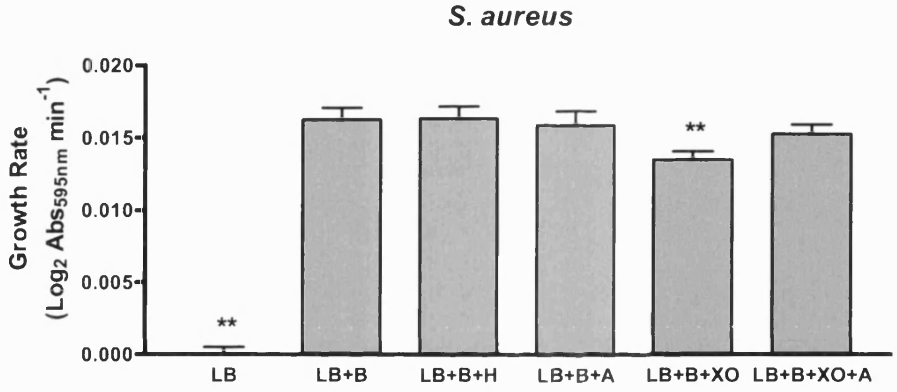

Figure 6.27 Treatment of *S. aureus* with XO in air (Controls).

Overnight cultures of *S.aureus* were diluted to 0.04 Abs_{600nm} in cuvettes and 100µl added to a 96-well plate. Bacteria (B) were then treated with combinations of 1mM hypoxanthine (H), 50 mU ml^{-1} XO and 1mM allopurinol (A) diluted in LB for a final volume per well of 200µl. The plate was incubated at 37°C and readings were taken at 595nm every 30 minutes over 6 hours. A) Growth curves of *S. aureus* treated with varying combinations of hypoxanthine, XO and allopurinol. B) Maximal growth (log phase) of *S. aureus* treated with varying combinations of hypoxanthine, XO and allopurinol. Statistical analysis was performed using One-way ANOVA with Dunnett's post test and LB+B as the control. ** =P<0.01. Data is from two experiments carried out on two separate occasions in quadruplicate, therefore n = 8. Mean±SD.

Figure 6.28A)

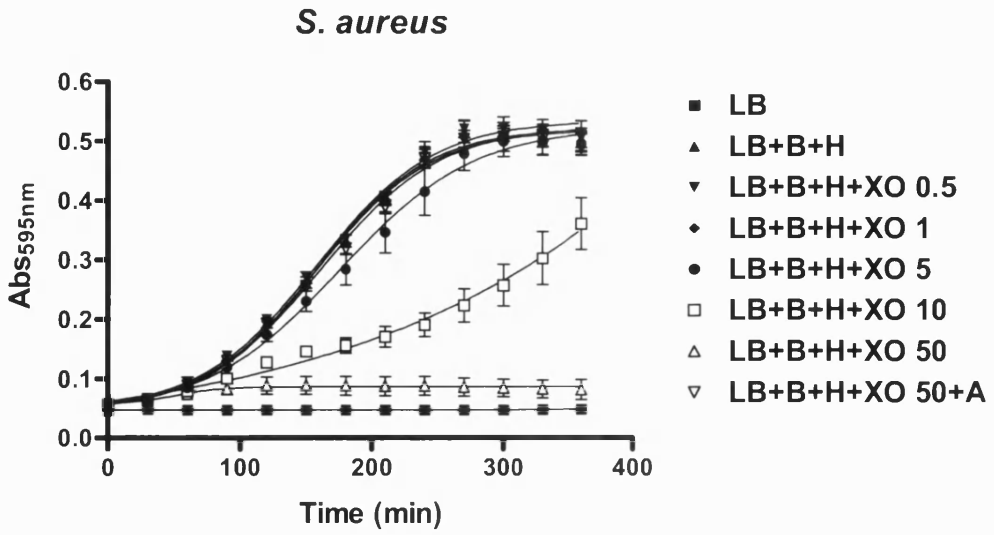

Figure 6.28B)

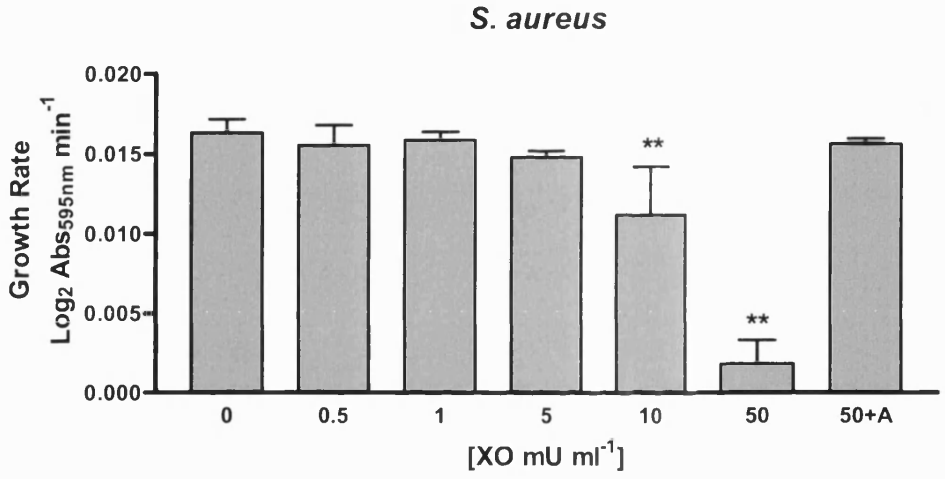

Figure 6.28 Treatment of *S. aureus* with XO in air.

Overnight cultures of *S. aureus* were diluted to 0.04 Abs_{600nm} in cuvettes and 100µl added to a 96-well plate. Bacteria (B) were then treated with 1mM hypoxanthine (H), 0, 0.5, 1, 5, 10 and 50 mU ml^{-1} XO and 1mM allopurinol (A) diluted in LB for a final volume per well of 200µl. The plate was incubated at 37°C and readings were taken at 595nm every 30 minutes over 6 hours. A) Growth curves of *S. aureus* treated with varying concentrations of XO and allopurinol. B) Maximal growth (log phase) of *S. aureus* treated with hypoxanthine, XO and allopurinol. Statistical analysis used was One-way ANOVA with Dunnett's post test using 0mU ml^{-1} XO as the control. ** =$P<0.01$. Data is from two experiments carried out on two separate occasions in quadruplicate, therefore n = 8. Mean ± SD.

For *S. faecalis* the controls shown in Figure 6.29A and B suggest that 1mM hypoxanthine and allopurinol alone do not affect the growth of *S. faecalis*. Furthermore, in this case XO (50 mU ml^{-1}) in LB without the addition of hypoxanthine does not slow the growth of *S. faecalis* which maybe because the *S. aureus* is more sensitive to XO generated species than *S. faecalis*. Treatment of *S. faecalis* with a range of XO concentrations in the presence of hypoxanthine (Figure 6.30A and B) shows that 10 and

50mU ml^{-1} XO in the presence of hypoxanthine significantly slows the growth of *S. faecalis*, however, at 50 mU ml^{-1} XO does not completely inhibit growth as found for *S. aureus* (Figure 6.28). This inhibition growth is completely reversed in the presence of allopurinol (Figure 6.30 A and B).

Figure 6.29A)

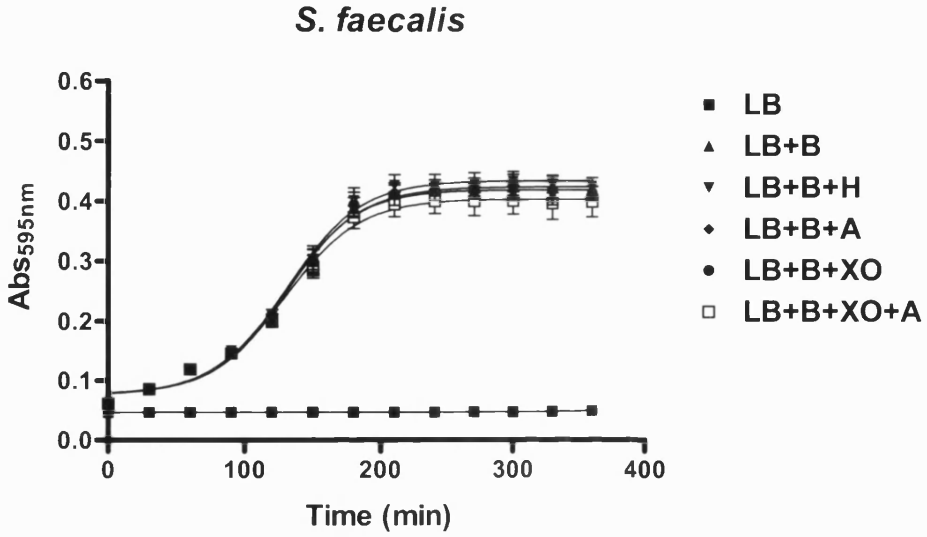

Figure 6.29B)

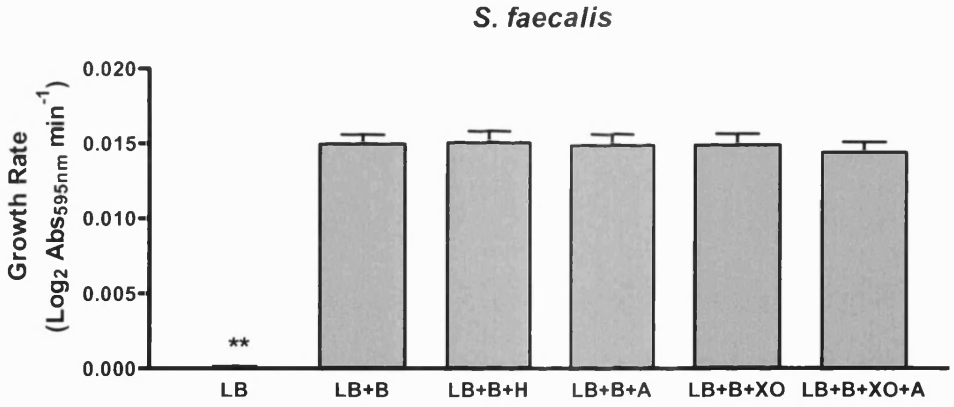

Figure 6.29Treatment of *S. faecalis* with XO in air (Controls).

Overnight cultures of *S. faecalis* were diluted to 0.04 Abs_{600nm} in cuvettes and 100µl added to a 96-well plate. Bacteria (B) were then treated with combinations of 1mM hypoxanthine (H), 50 mU ml^{-1} XO and 1mM allopurinol (A) diluted in LB for a final volume per well of 200µl. The plate was incubated at 37°C and readings were taken at 595nm every 30 minutes over 6 hours. A) Growth curves of *S. faecalis* treated with varying combinations of hypoxanthine, XO and allopurinol. B) Maximal growth (log phase) of *S. faecalis* treated with varying combinations of hypoxanthine, XO and allopurinol. Statistical analysis was performed using One-way ANOVA with Dunnett's post test and LB+B as the control. ** =P<0.01. Data is from two experiments carried out on two separate occasions in quadruplicate, therefore n = 8. Mean±SD.

Figure 6.30A)

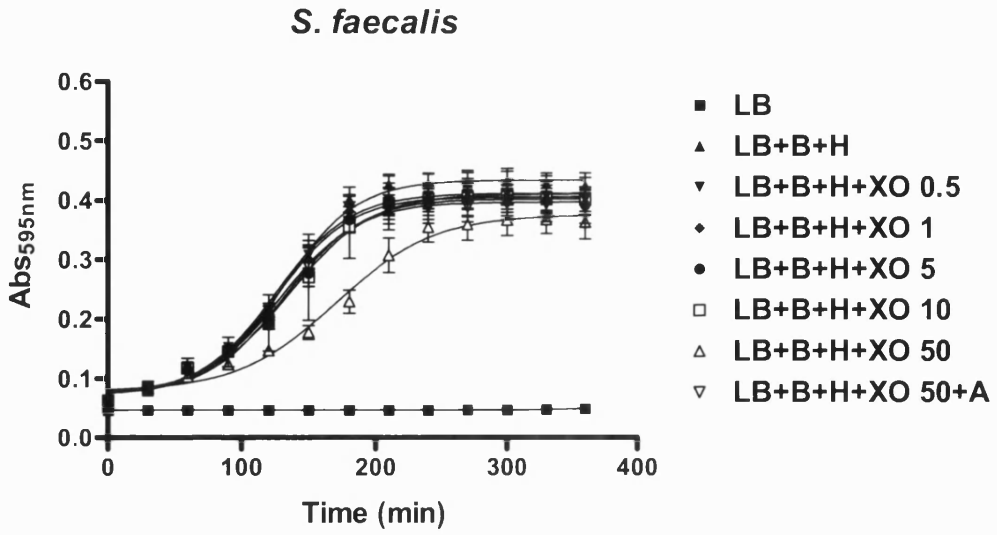

Figure 6.30B)

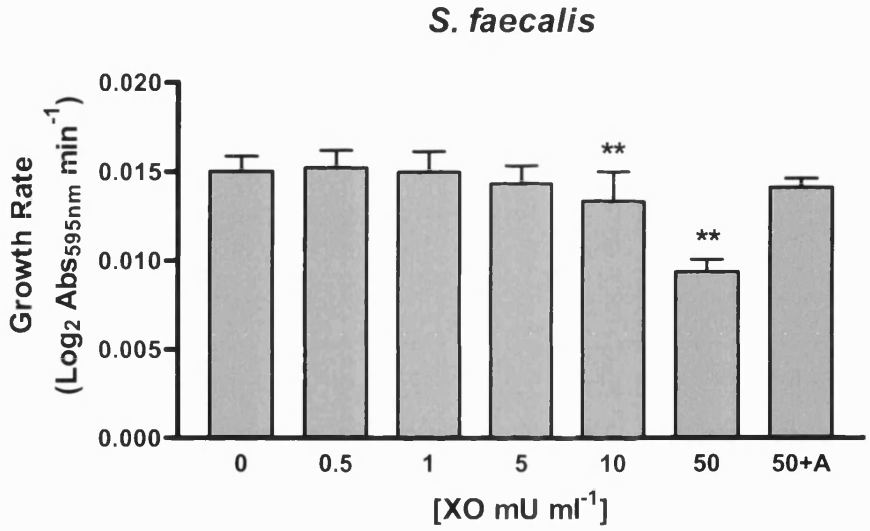

Figure 6.30 Treatment of *S. faecalis* with XO in air.

Overnight cultures of *S .faecalis* were diluted to 0.04 Abs_{600nm} in cuvettes and 100µl added to a 96-well plate. Bacteria (B) were then treated with 1mM hypoxanthine (H), 0, 0.5, 1, 5, 10 and 50mU ml^{-1} XO and 1mM allopurinol (A) diluted in LB for a final volume per well of 200µl. The plate was incubated at 37°C and readings were taken at 595nm every 30 minutes over 6 hours. A) Growth curves of *S. faecalis* treated with varying concentrations of XO and allopurinol. B) Maximal growth (log phase) of *S. faecalis* treated with hypoxanthine, XO and allopurinol. Statistical analysis was performed using One-way ANOVA with Dunnett's post test and 0mU ml^{-1} XO as the control. ** =P<0.01. Data are from two experiments carried out on two separate occasions in quadruplicate, therefore n = 8. Mean ± SD.

Treatment with *E. coli* (Figure 6.31A and B controls) shows that 1mM hypoxanthine and allopurinol alone do not affect the growth of *E. coli*, and as for *S. faecalis*, XO (50 mU ml^{-1}) in LB without the addition of hypoxanthine also does not slow the growth of *E. coli*. Treatment with XO (Figure 6.32A and B) shows that 5, 10 and 50mU ml^{-1} XO in the presence of hypoxanthine significantly slows the growth of *E. coli*

(Figure 6.32A and B). The inhibition of the growth of *E. coli* was reversed in the presence of XO inhibitor, allopurinol (Figure 6.32A and B).

Figure 6.31A)

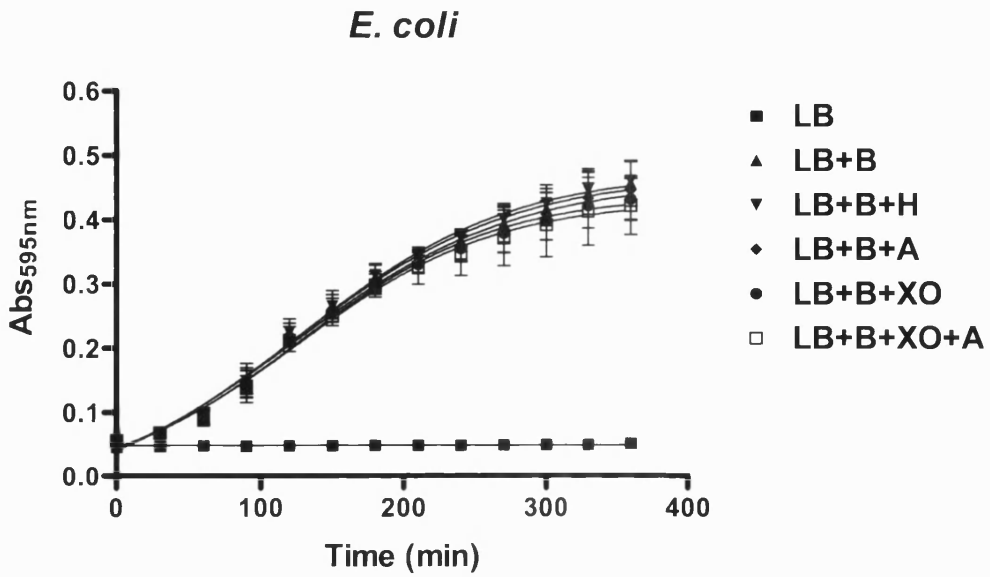

Figure 6.31 B)

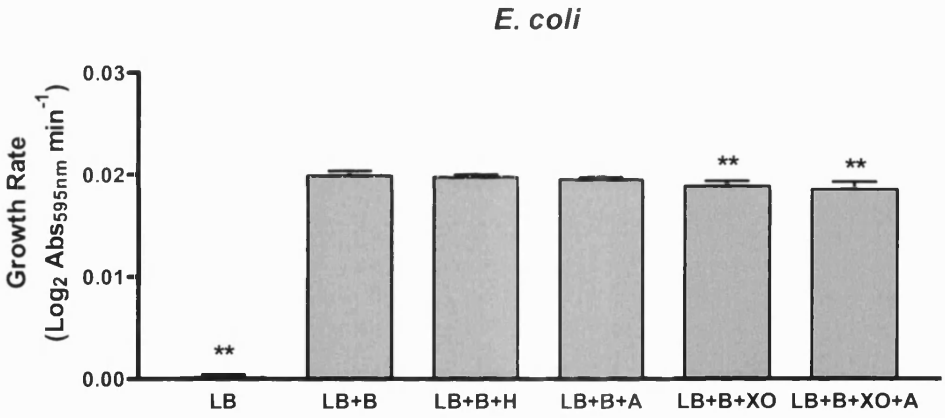

Figure 6.31Treatment of *E. coli* with XO in air (Controls).

Overnight cultures of *E. coli* were diluted to 0.04 Abs_{600nm} in cuvettes and 100µl added to a 96-well plate. Bacteria (B) were then treated with combinations of 1mM hypoxanthine (H), 50mU ml^{-1} XO and 1mM allopurinol (A) diluted in LB for a final volume per well of 200µl. The plate was incubated at 37°C and readings were taken at 595nm every 30 minutes over 6 hours. A) Growth curves of *E. coli* treated with varying combinations of hypoxanthine, XO and allopurinol. B) Maximal growth (log phase) of *E. coli* treated with varying combinations of hypoxanthine, XO and allopurinol. Statistical analysis was performed using One-way ANOVA with Dunnett's post test and LB+B as the control. ** =P<0.01. Data is from two experiments carried out on two separate occasions in quadruplicate, therefore n = 8. Mean±SD.

Figure 6.32A)

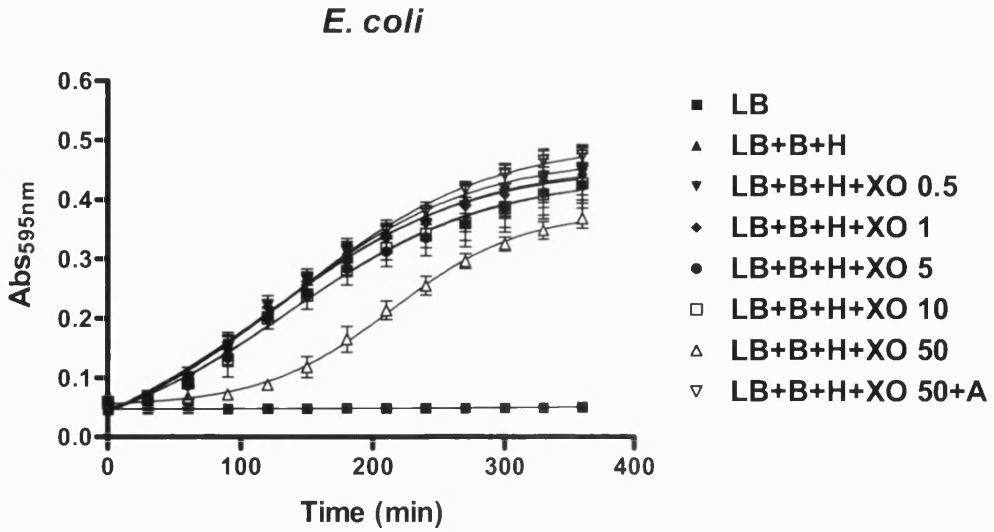

Figure 6.32B)

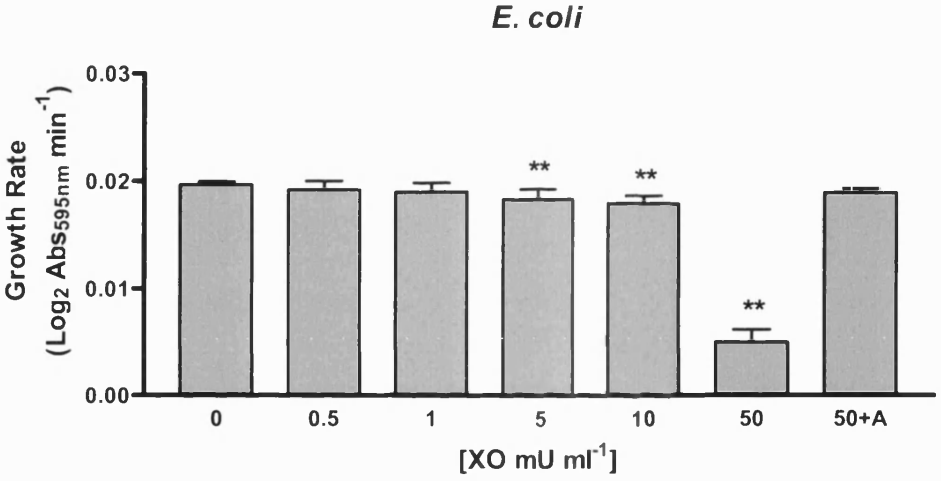

Figure 6.32 Treatment of *E. coli* with XO in air.

Overnight cultures of *E. coli* were diluted to 0.04 Abs_{600nm} in cuvettes and 100µl added to a 96-well plate. Bacteria (B) were then treated with 1mM hypoxanthine (H), 0, 0.5, 1, 5, 10 and 50mU ml^{-1} XO and 1mM allopurinol (A) diluted in LB for a final volume per well of 200µl. The plate was incubated at 37°C and readings were taken at 595nm every 30 minutes over 6 hours. A) Growth curves of *E. coli* treated with varying concentrations of XO and allopurinol. B) Maximal growth (log phase) of *E. coli* treated with hypoxanthine, XO and allopurinol. Statistical analysis was performed using One-way ANOVA with Dunnett's post test and 0mU ml^{-1} XO as the control. ** =P<0.01. Data is from two experiments carried out on two separate occasions in quadruplicate, therefore n = 8. Mean ± SD.

As shown previously, the growth curve for *P. aeruginosa* in air shows an extended lag phase and a reduced growth rate compared with the other bacteria (Figure 6.33A and 6.34A). The controls for the XO experiment again shows that the growth of *P. aeruginosa* is unaffected by 1mM hypoxanthine. However, the results suggest that allopurinol and XO (50 mU ml^{-1}) significantly reduces the growth rate of *P. aeruginosa* (Figure 6.33A and B). Treatment of *P.aeruginosa* with XO (Figure 6.34A and B) shows that 5, 10 and 50mU ml^{-1} XO in the presence of hypoxanthine significantly slows the growth of *P. aeruginosa*

(Figure 6.34). The inhibition of the growth of *E. coli* by XO is reversed in the presence of, XO inhibitor, allopurinol (Figure 6.34 A and B).

Figure 6.33A)

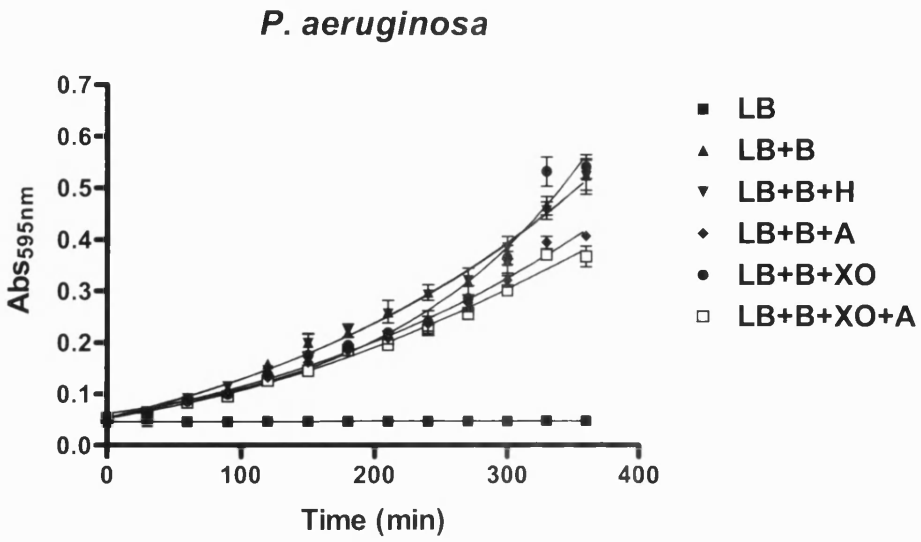

Figure 6.33B)

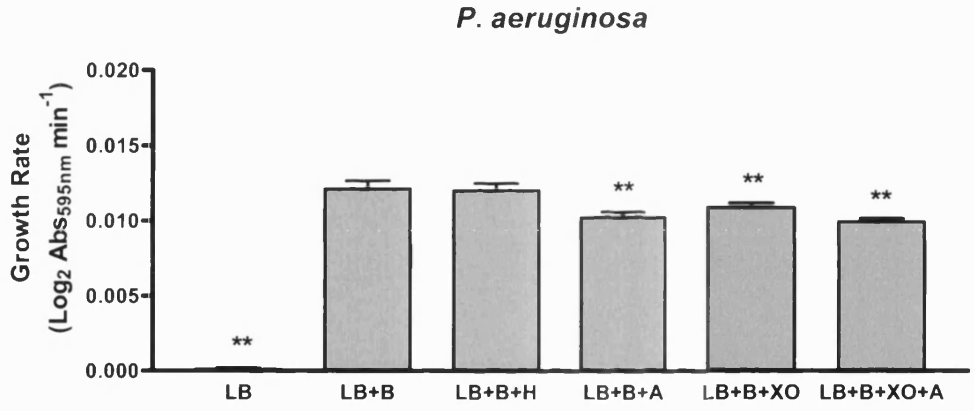

Figure 6.33 Treatment of *P. aeruginosa* with XO in air (Controls).

Overnight cultures of *P. aeruginosa* were diluted to 0.04 Abs_{600nm} in cuvettes and 100µl added to a 96-well plate. Bacteria (B) were then treated with combinations of 1mM hypoxanthine (H), 50mU ml^{-1} XO and 1mM allopurinol (A) diluted in LB for a final volume per well of 200µl. The plate was incubated at 37°C and readings were taken at 595nm every 30 minutes over 6 hours. A) Growth curves of *P. aeruginosa* treated with varying combinations of hypoxanthine, XO and allopurinol. B) Maximal growth (log phase) of *P. aeruginosa* treated with varying combinations of hypoxanthine, XO and allopurinol. Statistical analysis was performed using One-way ANOVA with Dunnett's post test and LB+B as the control. ** =$P<0.01$. Data is from an experiment carried out in quadruplicate, therefore n = 4. Mean±SD.

Figure 6.34A)

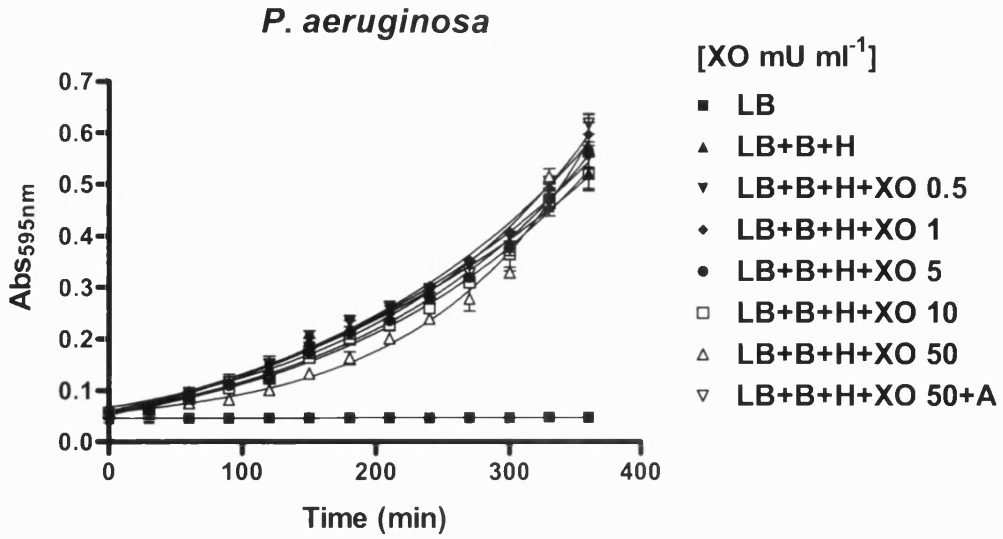

Figure 6.34B)

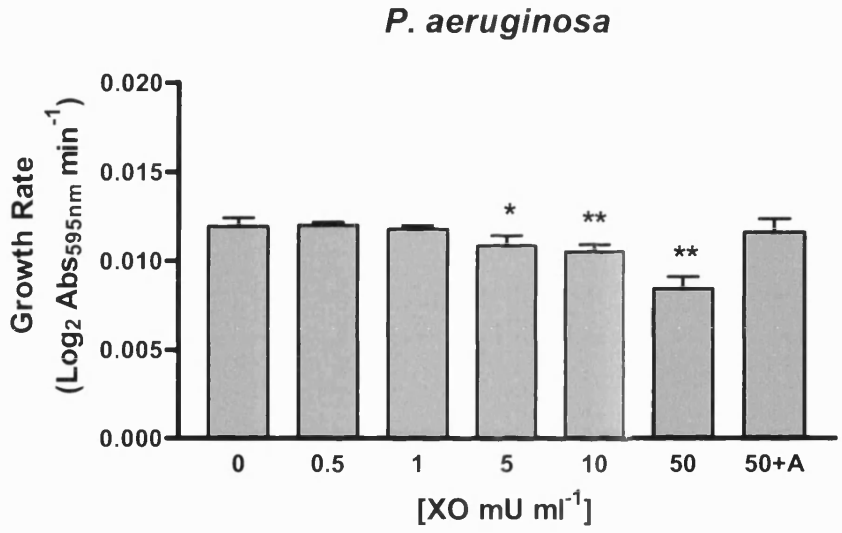

Figure 6.34 Treatment of *P. aeruginosa* with XO in air.

Overnight cultures of *P. aeruginosa* were diluted to 0.04 Abs_{600nm} in cuvettes and 100µl added to a 96-well plate. Bacteria (B) were then treated with 1mM hypoxanthine (H), 0, 0.5, 1, 5, 10 and 50mU ml^{-1} XO and 1mM allopurinol (A) diluted in LB for a final volume per well of 200µl. The plate was incubated at 37°C and readings were taken at 595nm every 30 minutes over 6 hours. A) Growth curves of *P. aeruginosa* treated with varying concentrations of XO and allopurinol. B) Maximal growth (log phase) of *P. aeruginosa* treated with hypoxanthine, XO and allopurinol. Statistical analysis was performed using One-way ANOVA with Dunnett's post test and XO 0mU ml^{-1} as the control. * = $P<0.05$, ** = $P<0.01$. Data is from an experiment carried out in quadruplicate, therefore n = 4. Mean ± SD.

The control experiments for *P. mirabilis* (Figure 6.35A and B) show that hypoxanthine (1mM), allopurinol (1mM), and XO (50 mU ml^{-1}) added to the bacterial culture individually do not affect the growth of *P. mirabilis*. Figure 6.36A and B shows that 50mU ml^{-1} XO in the presence of hypoxanthine significantly slows the growth of *P. mirabilis*. However, the growth rate of *P. mirabilis* is also inhibited in the presence of XO inhibitor, allopurinol (Figure 6.36B).

Figure 6.35A)

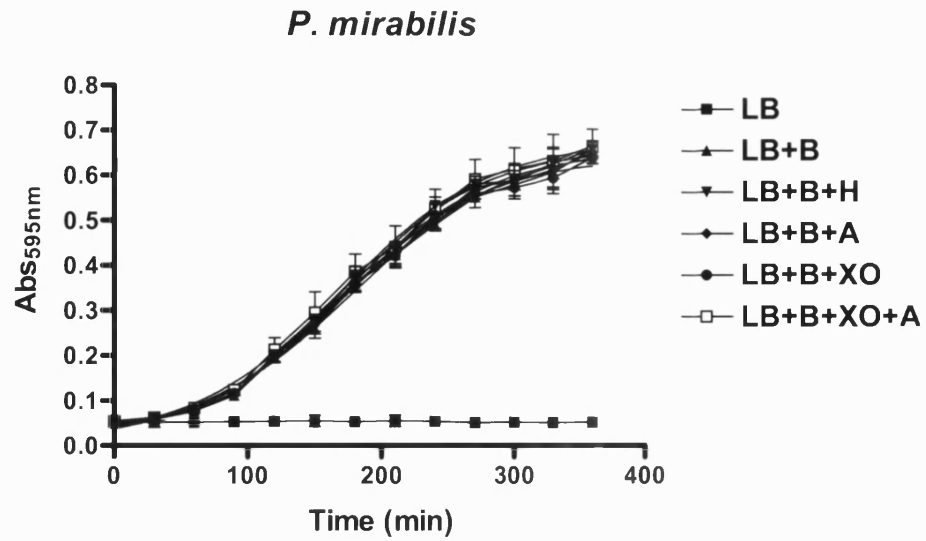

Figure 6.35B)

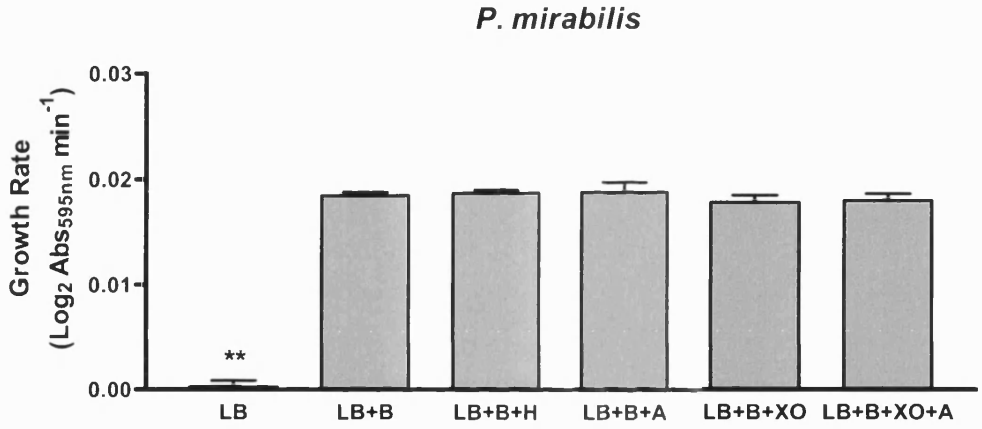

Figure 6.35 Treatment of *P. mirabilis* with XO in air (Controls).

Overnight cultures of *P. mirabilis* were diluted to 0.04 Abs_{600nm} in cuvettes and 100µl added to a 96-well plate. Bacteria (B) were then treated with combinations of 1mM hypoxanthine (H), 50mU ml^{-1} XO and 1mM allopurinol (A) diluted in LB for a final volume per well of 200µl. The plate was incubated at 37°C and readings were taken at 595nm every 30 minutes over 6 hours. A) Growth curves of *P. mirabilis* treated with varying combinations of hypoxanthine, XO and allopurinol. B) Maximal growth (log phase) of *P. mirabilis* treated with varying combinations of hypoxanthine, XO and allopurinol. Statistical analysis was performed using One-way ANOVA with Dunnett's post test and LB+B as the control. ** =P<0.01. Data is from an experiment carried out in quadruplicate, therefore n = 4. Mean±SD.

Figure 6.36A)

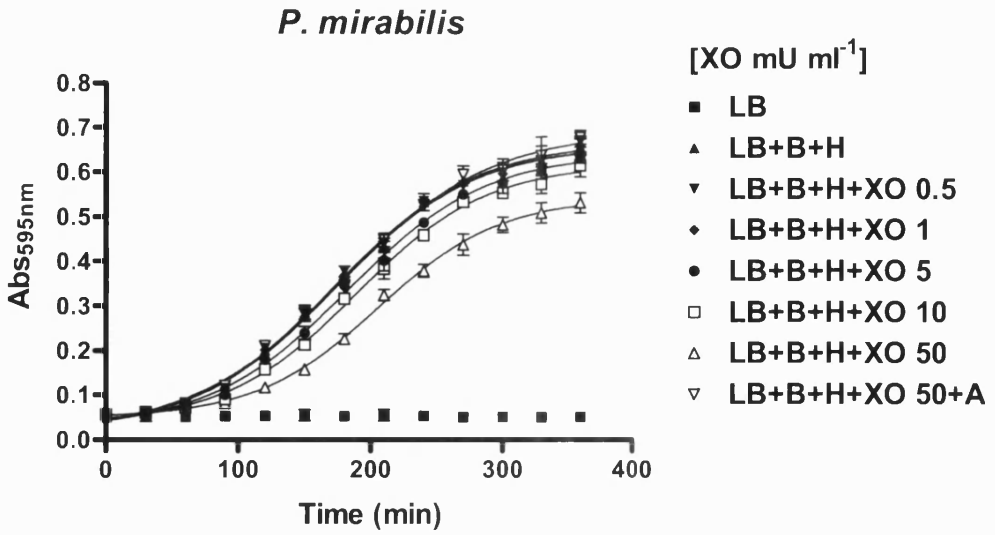

Figure 6.36B)

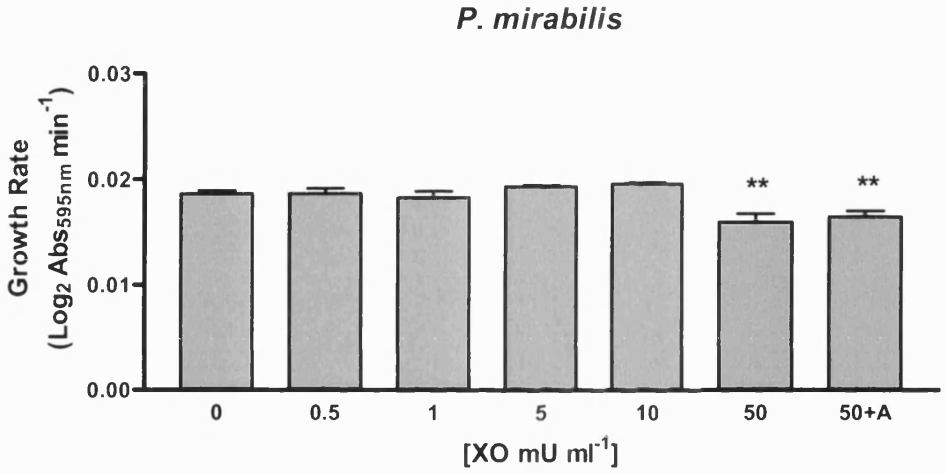

Figure 6.36. Treatment of *P. mirabilis* with XO in air.

Overnight cultures of *P. mirabilis* were diluted to 0.04 Abs_{600nm} in cuvettes and 100µl added to a 96-well plate. Bacteria (B) were then treated with 1mM hypoxanthine (H), 0, 0.5, 1, 5, 10 and 50mU ml^{-1} XO and 1mM allopurinol (A) diluted in LB for a final volume per well of 200µl. The plate was incubated at 37°C and readings were taken at 595nm every 30 minutes over 6 hours. A) Growth curves of *P. mirabilis* treated with varying concentrations of XO and allopurinol. B) Maximal growth (log phase) of *P. mirabilis* treated with hypoxanthine, XO and allopurinol. Statistical analysis was performed using One-way ANOVA with Dunnett's post test and 0mU ml^{-1} XO as the control. ** =P<0.01. Data is from an experiment carried out in quadruplicate, therefore n = 4. Mean ± SD.

6.3.3 Effects of H_2O_2 and XO on the viability of bacteria in air

The effects of varying treatments on bacteria have previously been assessed by following growth by measurements of absorbance over time. However, although this method gives an idea of the effects of varying treatments on growth, it is unable to determine the viable cells in the culture. Therefore this section aims to develop a method for the measurement of viability in a range of oxygen tensions.

6.3.3.1 Disk inhibition assays

6.3.3.1.1 Treatment of *S. aureus* with H_2O_2

Resistance to the oxidative stress inducer H_2O_2 was assessed as a positive control to check that the disk inhibition assay was working. The agar plates shown in Figure 6.37 show clear inhibition of the growth of *S. aureus* as demonstrated by the zones formed around the filter paper disks. The assays show that zones are formed at a 1 in 100 dilution (88mM) and above of the H_2O_2 stock. The diameters of the zones that were formed are recorded in table 6.4.

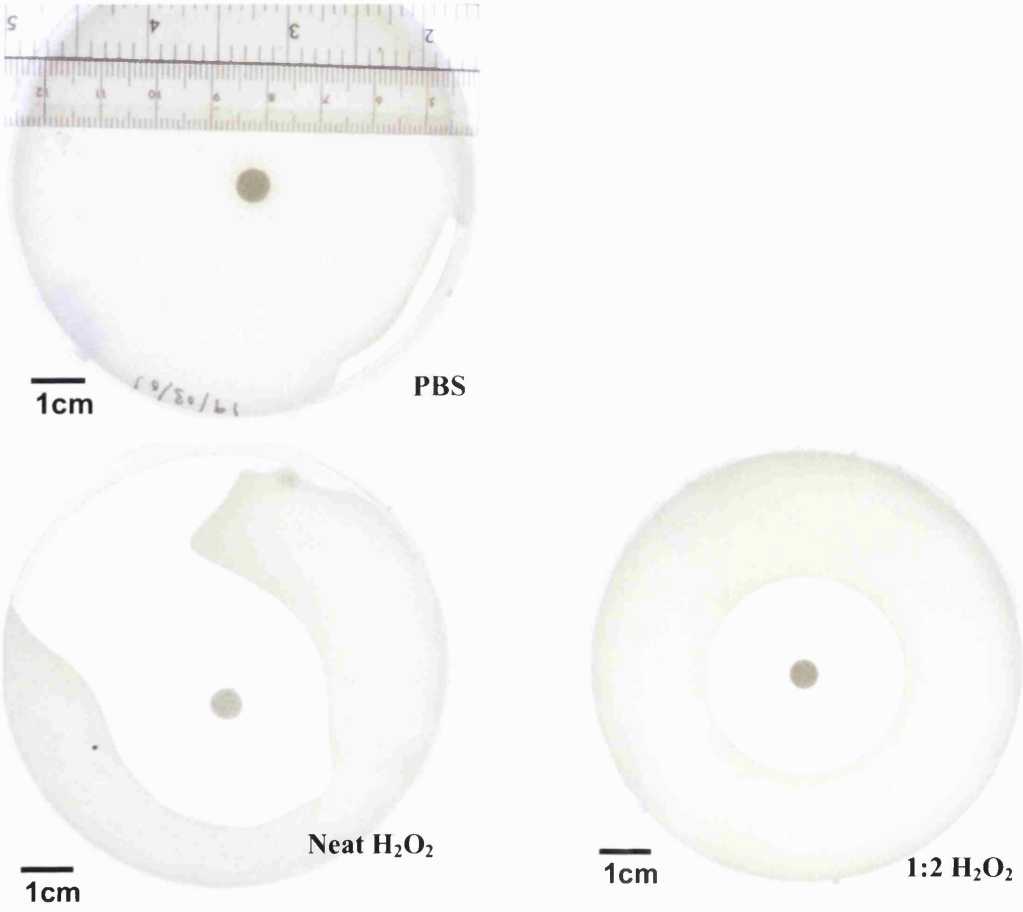

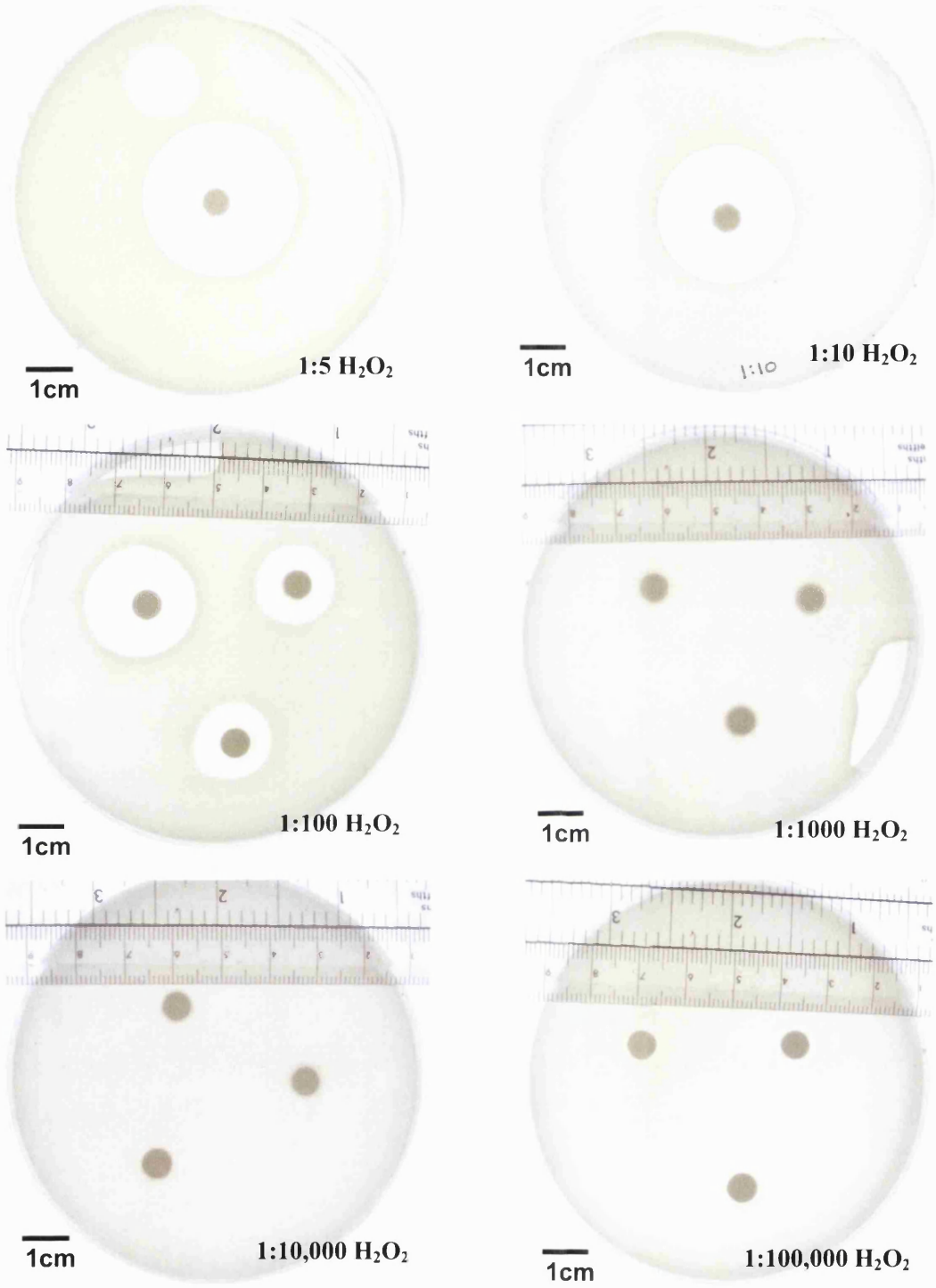

Figure 6.37 Inhibition of the growth of *S. aureus* using H_2O_2.

Overnight *S. aureus* cultures were added to soft agar (0.4%) for a final concentration of 0.02 abs_{600nm} (~$1.3x10^{-7}$ cells ml^{-1}) and 4mls added to an over-dried LB plate. The soft agar was allowed to set and samples of H_2O_2 (20µl) diluted in PBS were added to sterile filter paper disks and carefully laid onto the surface of the agar using flamed forceps. The Zone of killing was measured (no growth visible) was measured in millimeters (mm) after incubating the plates for 24 hours at 37°C.

H_2O_2 dilution in PBS	Initial H_2O_2 (mM) concentration on disk	Mean diameter of disk inhibition zone (mm)* for *S. aureus*
PBS	0	0
1:100,000	0.088	0
1:10,000	0.88	0
1:1000	8.8	0
1:100	88	14, 15, 22
1:10	880	30, 29
1:5	1760	33
1:2	4400	38
Neat	8800	Zone too large for accurate measurement

Table 6.4 Sensitivity of *S. aureus* to H_20_2.

*Values are expressed as a mean diameter of the zone of killing.

6.3.3.1.2 Treatment of *S. aureus* with XO

Based on the H_2O_2 assay diffusion zone assays, experiments were set up to assess the effect of XO on the viability of *S. aureus*. The agar plates shown in figure 6.38 show that faint zones of inhibition can be seen around the disks containing XO when compared with a PBS alone control. However, the zones are considerably smaller than those seen with the H_2O_2 and as a result quantitative measurements are not possible. The inhibition zones are also not obvious when the XO is boiled, suggesting that the zones seen with the XO are not a result of preservatives in the enzyme stock.

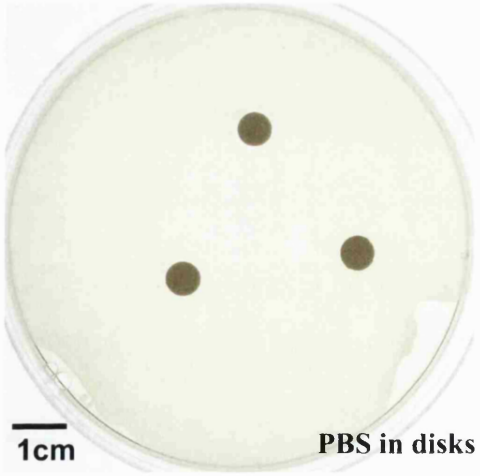

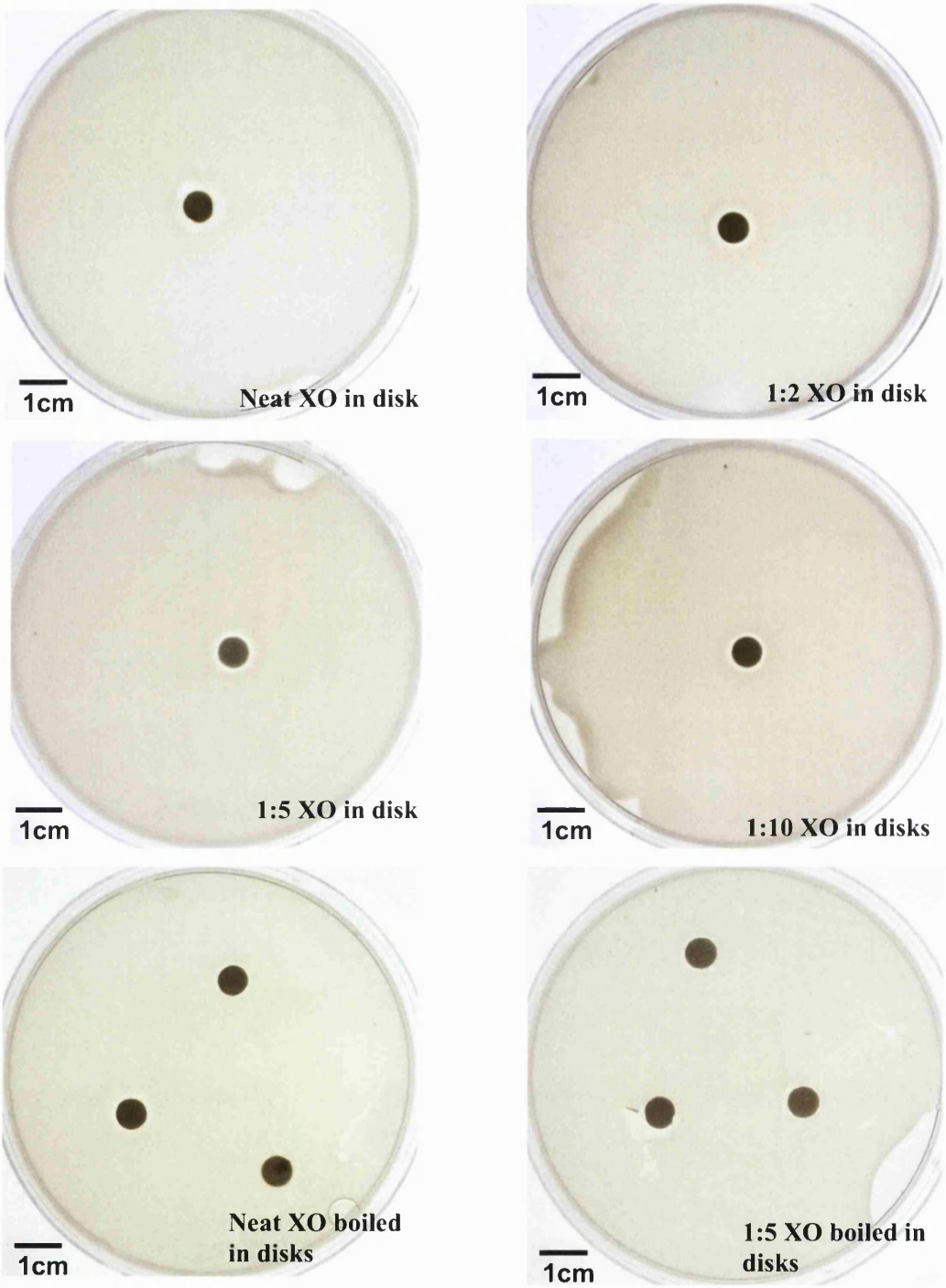

Figure 6.38 Treatment of *S. aureus* with XO in air

Overnight *S. aureus* cultures were added to soft agar (0.4%) for a final concentration of 0.02 Abs_{600nm} (~$1.3x10^{-7}$ cells ml^{-1}) with nitrite (1mM) and hypoxanthine (1mM), 4mls was then added to an over-dried LB plate. Samples of XO were prepared by diluting the stock 1:10 (1,061mU ml^{-1}), 1:5 (2,122mU ml^{-1}), 1:2 (5,305mU ml^{-1}) and Neat (10,610mU ml^{-1}) in PBS. The soft agar was allowed to set and XO dilutions (20µl) were added to sterile filter paper disks and carefully laid onto the surface of the agar using flamed forceps. The boiled XO samples were prepared by boiling at 60°C for 5 minutes. The plates were then incubated for 24 hours at 37°C.

Diffusion zone assays were again set up with bacteria alone added to the soft agar layer without substrates. The disks were dipped into a reaction mixture containg both the XO and substrates before addition to the test plates (Figure 6.39). It was thought that this method may overcome problems with diffusion of the substrate in the soft agar layer. However, figure 6.39 does show any obvious clearance zones, this may be beause the reaction was over rapidly before any reactive species could diffuse from the disk.

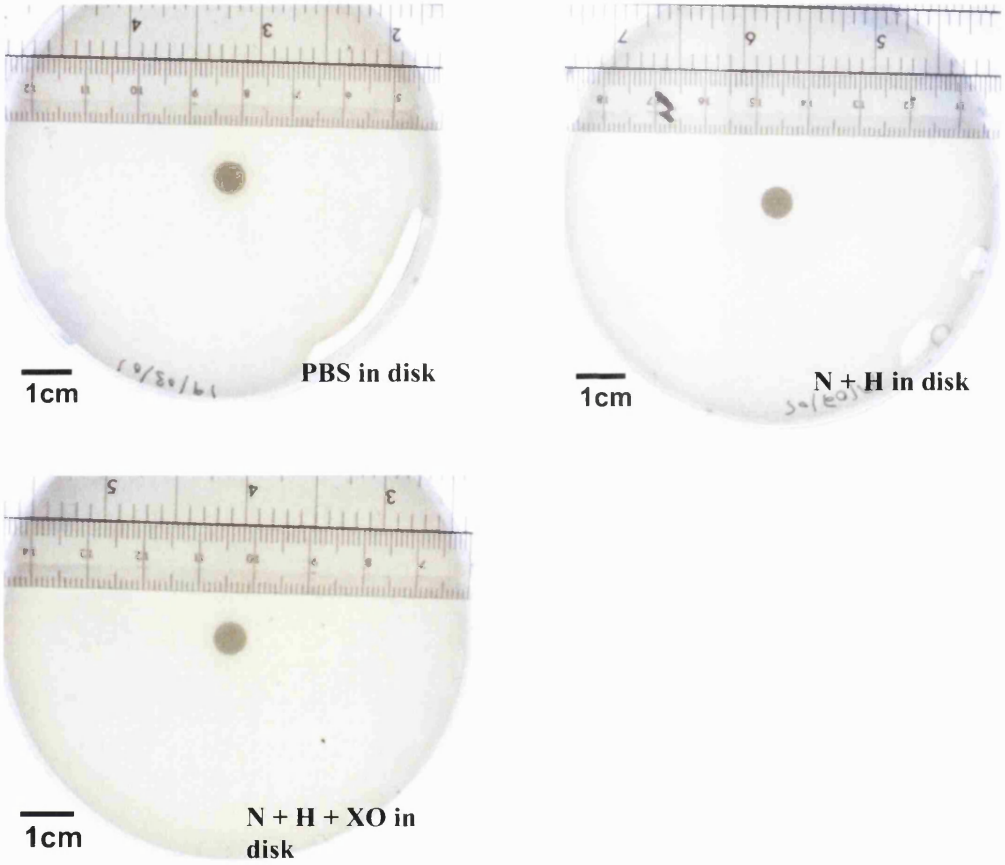

Figure 6.39 Treatment of *S. aureus* with XO in air

Overnight *S. aureus* cultures were added to soft agar (0.4%) for a final concentration of 0.02 Abs_{600nm} (~$1.3x10^{-7}$ cells ml^{-1}) and 4mls added to an over-dried LB plate. The soft agar was allowed to set and a 2ml reaction was prepared containing final concentrations of 1mM hypoxanthine (H), nitrite (N) and XO 1061mU ml^{-1} diluted in PBS. The sterile filter paper disks were rapidly dipped into the reaction and carefully laid onto the surface of the agar using flamed forceps. The plates were then incubated for 24 hours at 37°C.

6.3.4 Effects of XO on the viability of bacteria in varying oxygen concentrations

6.3.4.1 Growth of *E. coli* and *S. aureus* in air (21%) and 2% oxygen.

The bacteria used in this study are facultative anaerobes, meaning that they are able to utilise a range of electron donors other than oxygen in its absence, and thus grow in

a range of oxygen tensions. The effect of low oxygen concentration on bacterial growth was measured in order to characterise this parameter prior to the experiments in reduced oxygen (Figure 6.40).

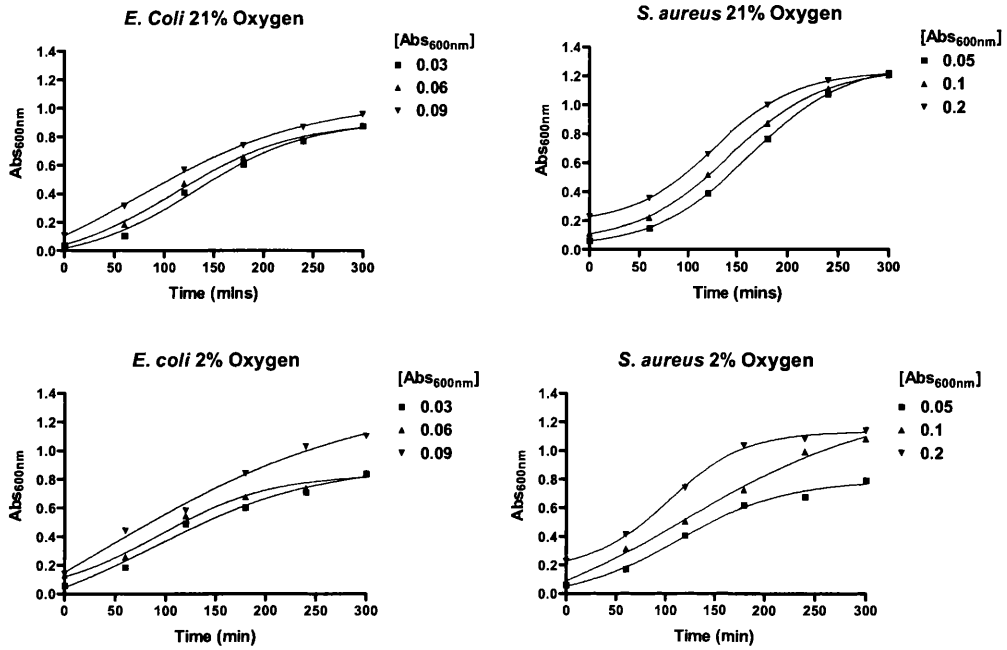

Figure 6.40 Growth curves of *E. coli* and *S. aureus* in 21 % and 2 % oxygen.

Overnight cultures of *S. aureus* and *E. coli* were diluted in 2mls LB in cuvettes with sterile magnetic stirrers. The spectrophotometer was blanked with LB alone, and the change in absorbance at 600nm of LB and bacteria was recorded at 37°C over 5 hours. For experiments in 2% oxygen overnight cultures were diluted in the hypoxia cabinet in LB that was equilibrated in the hypoxia cabinet overnight. The cuvettes were covered with parafilm and removed from the hypoxia cabinet at hourly intervals and replaced after the absorbance readings were taken at 600nm. n = 1.

6.3.4.2 Treatment of bacteria with XO in variable oxygen for 1 and 3 hours

Experiments in variable oxygen were carried out using the controlled oxygen cabinet set at 0, 1, 2, 5 and 21% oxygen to try and mimic the environment of the chronic ulcer (0-2%) normal tissue (2-5%) and hyperoxia (21%). XO was used at 10 and 50mU ml^{-1} to treat the bacteria which were concentrations previously shown to reduce the growth rate of bacteria in air (21%) in the presence of hypoxanthine. For the assays shown below nitrite was also included as a XO substrate for the production of $^{\bullet}NO$ in hypoxia. Each of the bacterial species (*S. aureus, S. faecalis, P. mirabilis* and *E. coli*) were treated with hypoxanthine (1mM) and nitrite (1mM) for 1 and 3 hours to determine whether these substrates alone decreased the viability of the bacteria when compared with LB, figure 6.41-6.44A showed that was not the case.

The bacterial species were then treated with hypoxanthine and nitrite and 10 and 50mU ml^{-1} XO for 1 and 3 hours. After an hour exposure, *S. aureus* showed a reduction in

the number of viable cells inhibition of growth at 0, 1 and 2% O_2 at 50mU ml^{-1} XO. However, there also appears to be a slight increase in viable cells compared with the control at 1 and 5% O_2 at 10mU ml^{-1} (Figure 6.41B). After a 3 hour exposure to 50mU ml^{-1} XO, *S. aureus* showed a significant decrease in the number of viable cells at 0, 1 and 2% oxygen (~50% reduction), there was also a decrease in the number of viable cells at 5% oxygen (~25% reduction) and at 21% oxygen (~50% reduction). After a 3hour exposure at 10mU ml^{-1} *S. aureus* showed a reduction in the number of viable cells at 0% and 21% oxygen, however, there was also an increase in the number of viable cells at 2% oxygen as shown after an hour's exposure to 10mU ml^{-1} XO in low oxygen (Figure 6.41B).

After 1 hour *S. faecalis* showed a reduction in the number of viable cells at 1, 2 and 5% O_2 at 10mU ml^{-1} XO and at 1% O_2 with 50mU ml^{-1} XO (Figure 6.42B). After 3 hours XO showed a reduction in viability at 50mU ml^{-1} XO at 1% O_2 and a slight increase in the number of viable cells at 10mU ml^{-1} XO at 2% and 21% O_2. The decrease in viable cells was not as great as shown previously with *S. aureus* (Figure 6.42B).

P. mirabilis showed a reduction in viability at 5 and 21% O_2 with 10mU ml^{-1}, and at 1, 5 and 21% O_2 with 50mU ml^{-1}, after 1 hour's exposure (Figure 6.43B). After 3 hours there was a reduction in viable cells at 2% O_2 (~25%) and at 21% O_2 (~70%) with 10mU ml^{-1} XO. At 50mU ml^{-1} XO there was a reduction in the viable cells at 0% (~25%), 1% (~40%) and 2% O_2 (~50%). There was also a decrease in viability at 5% oxygen (~40%) and at 21% O_2 (~65%) reduction (Figure 6.43B).

E. coli did not show as much growth inhibition at low oxygen tensions as shown with the previous bacteria. After 1 hour there was a slight reduction in viable cells only at 50mU ml^{-1} XO at 5% O_2 and 21% O_2 (Figure 6.44B). After 3 hours exposure of *E. coli* to XO there appeared to be a significant increase in viable cells at 2% oxygen at both 10 and 50mU ml^{-1} XO and a decrease in the number of viable cells at 10 and 50mU ml^{-1} (Figure 6.44B).

These data suggests that *S. aureus, S. faecalis* and *P. mirabilis* are sensitive to the effects of XO in low oxygen concentrations between 0-2% O_2. *S. aureus* and *P. mirabilis* appear to be the most sensitive to XO-generated species.

Figure 6.41 A)

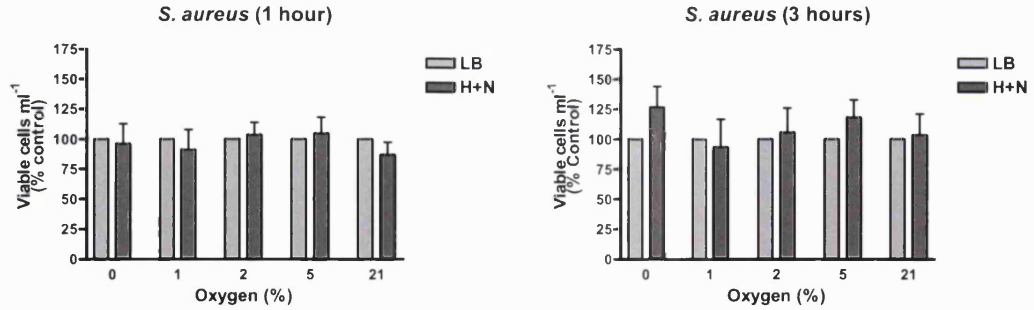

Figure 6.41 B)

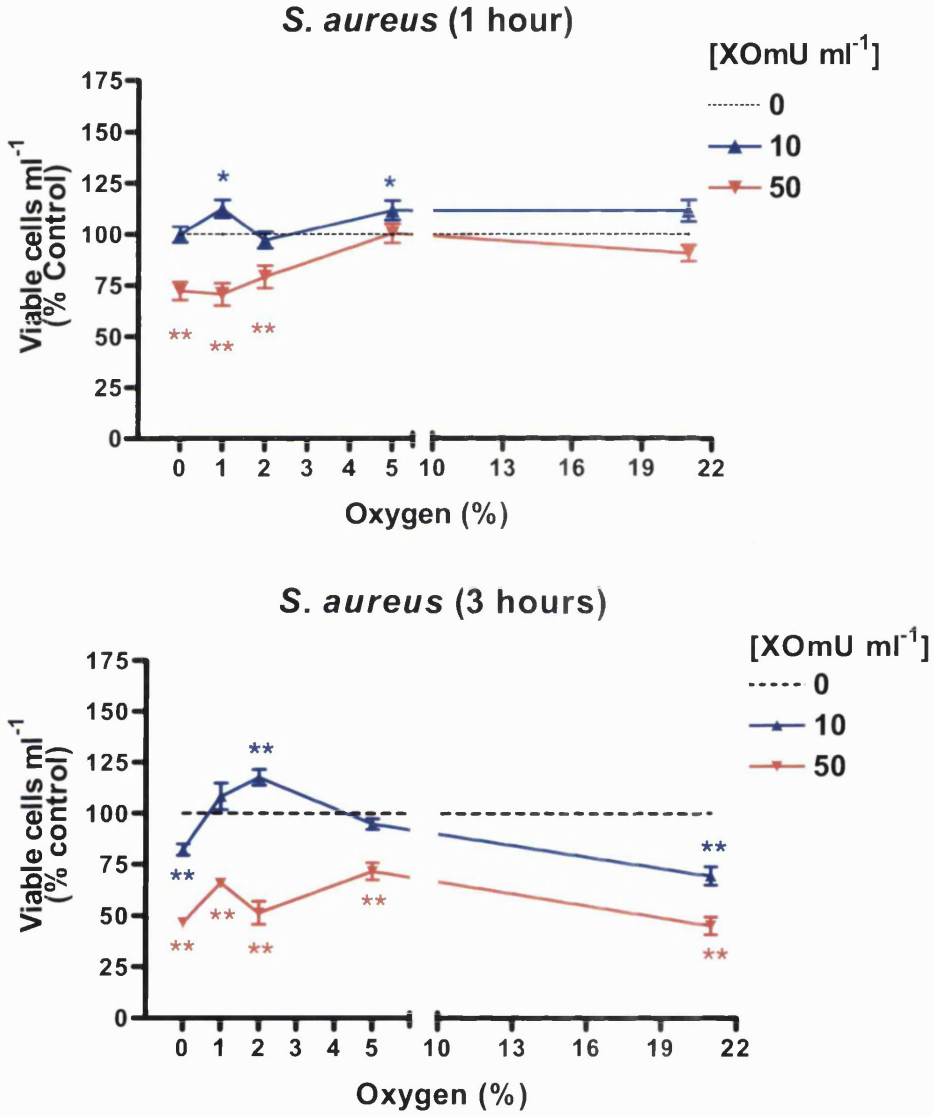

Figure 6.41 Treatment of *S. aureus* with XO in variable oxygen.

96-well plates were inoculated with an overnight bacterial culture diluted to at Abs_{600nm}. A) Controls: Bacteria were treated with hypoxanthine (1mM) and nitrite (1mM) for 1 hour at 0, 1, 2, 5 and 21% oxygen. The numbers of viable cells were assessed by colony counts and the data is presented as a percentage of the control (untreated bacteria). B) Bacteria were treated with 10 and 50mU ml^{-1} XO for 1 hour in the presence of hypoxanthine (1mM) and nitrite (1mM) at 0, 1, 2, 5 and 21% oxygen. The numbers of viable cells were assessed by colony counts and the data is presented as a percentage of the control (0mU ml^{-1}, cells treated with hypoxanthine (1mM) and nitrite (1mM) alone). n = 4. Mean ± SEM Statistical analysis was performed using one way analysis of variance (ANOVA) and Dunnett's post test using 0mU ml^{-1} as the control.

Figure 6.42 A)

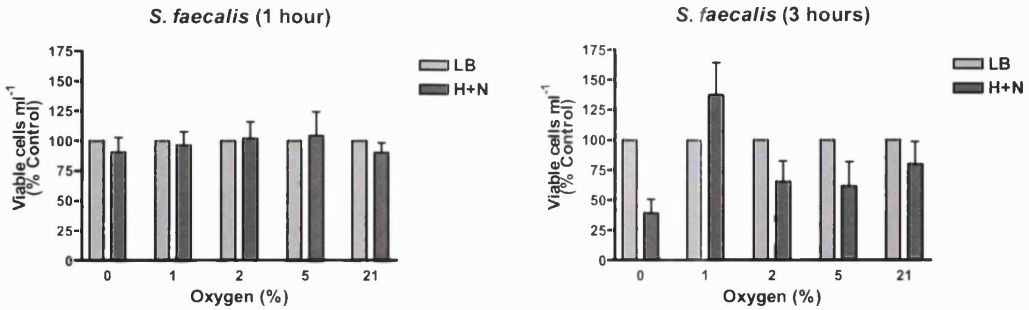

Figure 6.42 B)

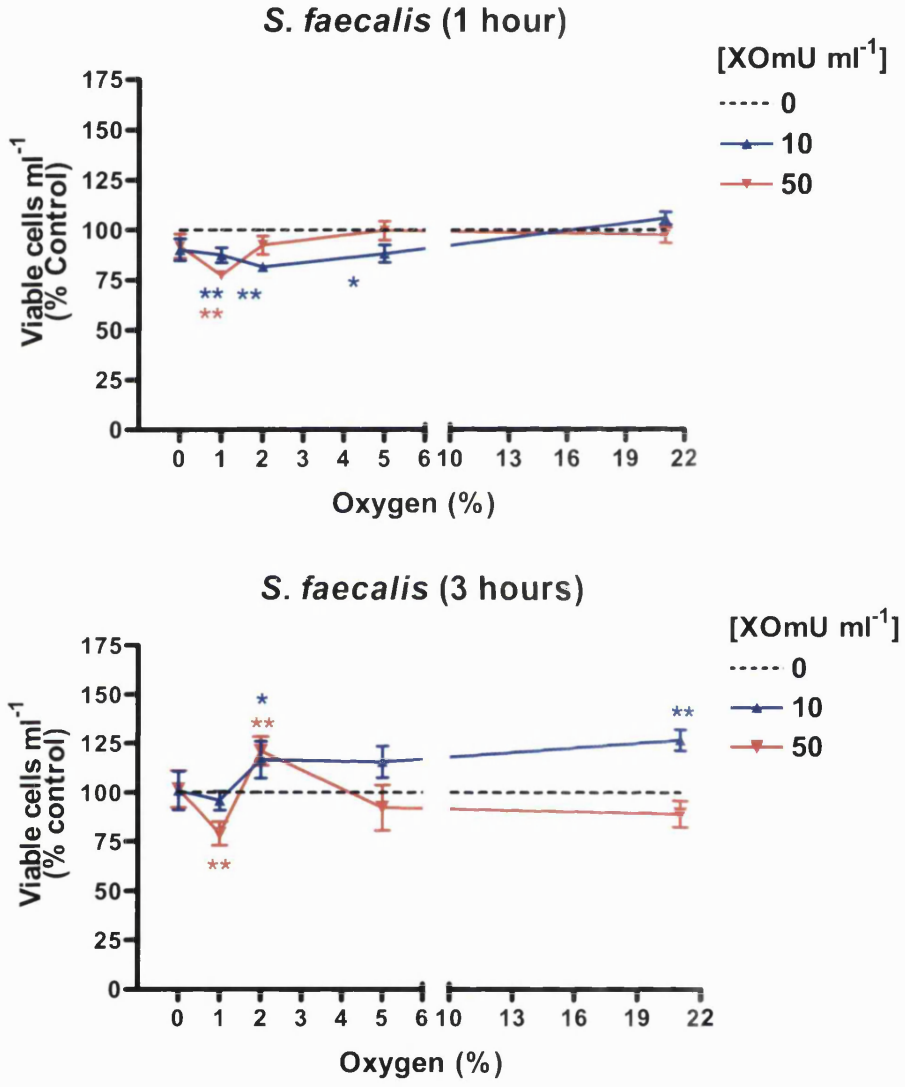

Figure 6.42Treatment of *S. faecalis* with XO in variable oxygen.

96-well plates were inoculated with an overnight bacterial culture diluted to at Abs_{600nm}. A) Controls: Bacteria were treated with 1mM hypoxanthine and 1mM nitrite for 1 hour at 0, 1, 2, 5 and 21% oxygen. The numbers of viable cells were assessed by colony counts and the data is presented as a percentage of the control (untreated bacteria). B) Bacteria were treated with 10 and 50mU ml^{-1} XO for 1 hour in the presence of 1mM hypoxanthine and 1mM nitrite at 0, 1, 2, 5 and 21% oxygen. The numbers of viable cells were assessed by colony counts and the data is presented as a percentage of the control (0 mU ml^{-1}- Cells treated with 1mM hypoxanthine and 1mM nitrite alone). n = 4. Mean ± SEM. Statistical analysis was performed using one way analysis of variance (ANOVA) and Dunnett's post test using 0mU ml^{-1} as the control.

Figure 6.43 A)

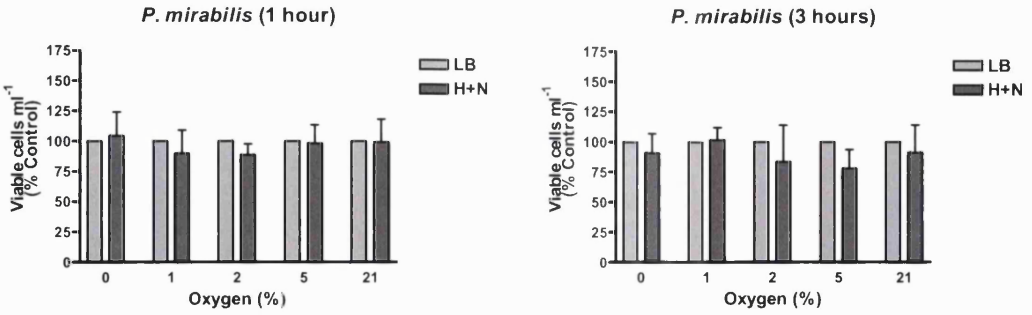

Figure 6.43 B)

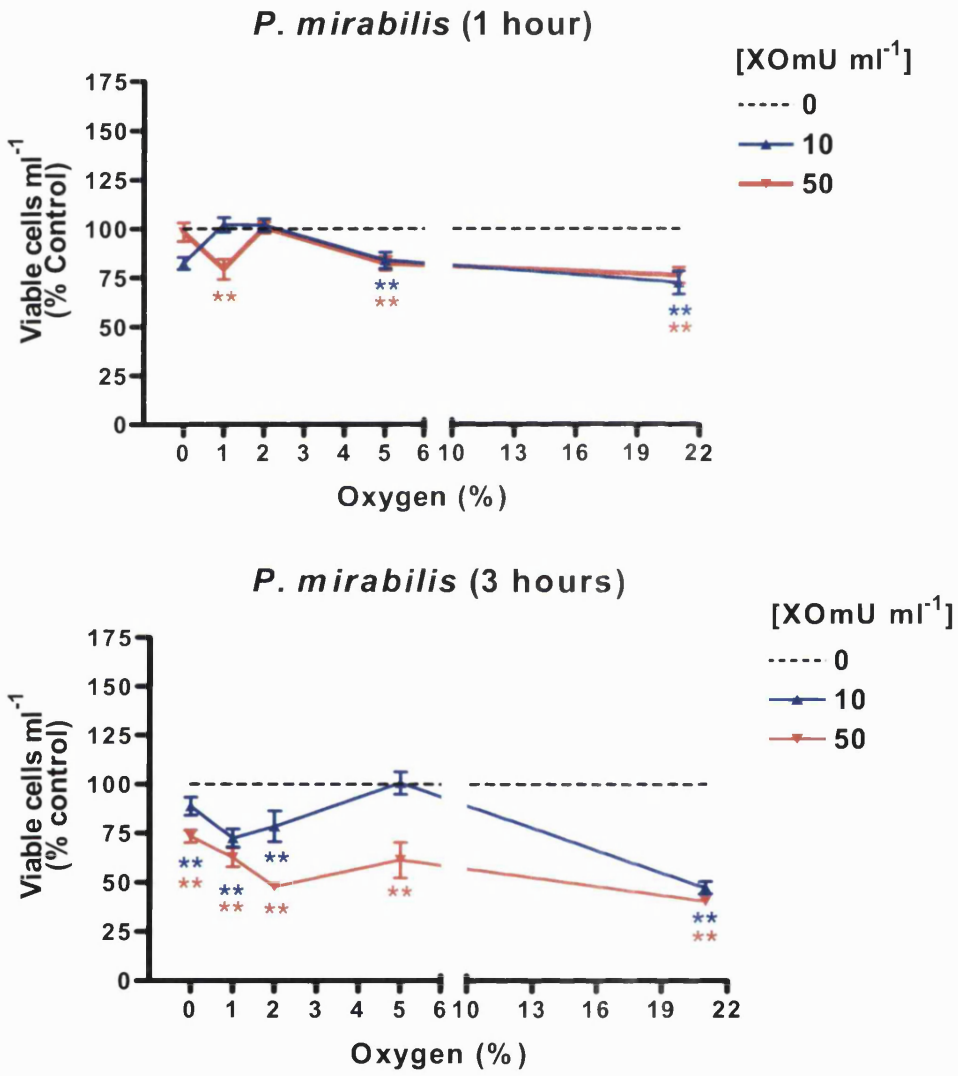

Figure 6.43Treatment of *P. mirabilis* with XO in variable oxygen.

96-well plates were inoculated with an overnight bacterial culture diluted to at Abs_{600nm}. A) Controls: Bacteria were treated with hypoxanthine (1mM) and nitrite (1mM) for 1 hour at 0, 1, 2, 5 and 21% oxygen. The numbers of viable cells were assessed by colony counts and the data is presented as a percentage of the control (untreated bacteria). B) Bacteria were treated with 10 and 50mU ml^{-1} XO for 1 hour in the presence of hypoxanthine (1mM) and nitrite (1mM) at 0, 1, 2, 5 and 21% oxygen. The numbers of viable cells were assessed by colony counts and the data is presented as a percentage of the control (0mU ml^{-1}, cells treated with hypoxanthine (1mM) and nitrite (1mM) alone). n = 4. Mean ± SEM. Statistical analysis was performed using one way analysis of variance (ANOVA) and Dunnett's post test using 0mU ml^{-1} as the control.

Figure 6.44 A)

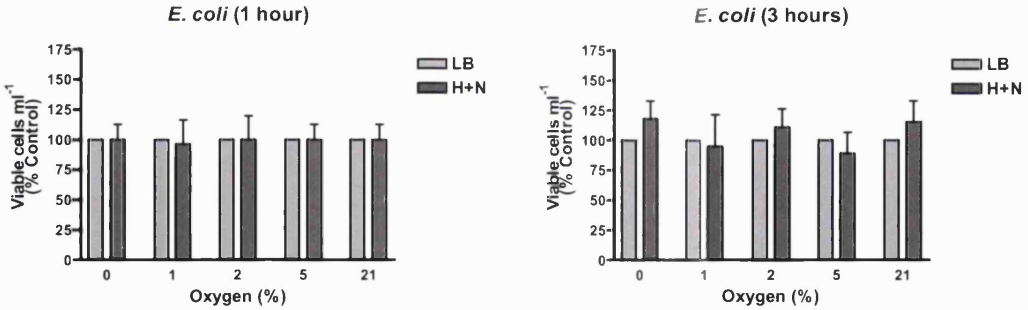

Figure 6.44 B)

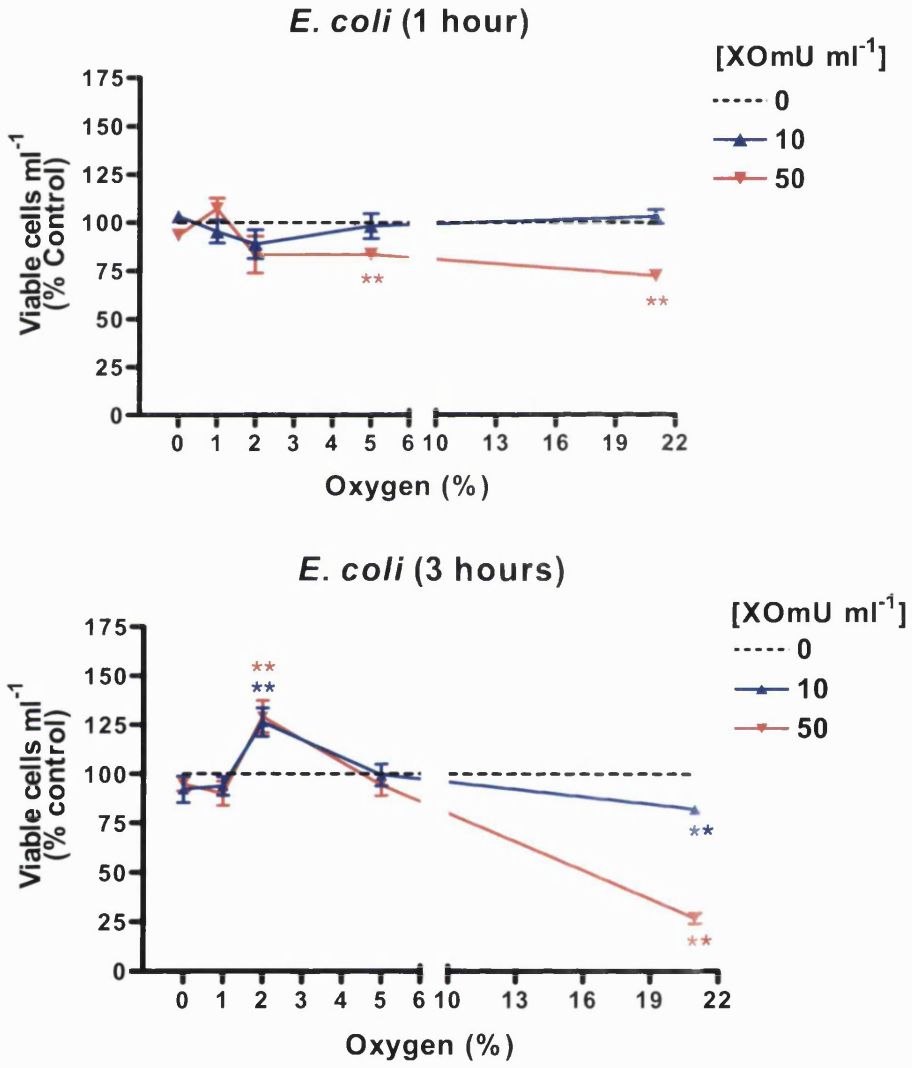

Figure 6.44 Treatment of *E. coli* with XO in variable oxygen.

96-well plates were inoculated with an overnight bacterial culture diluted to at Abs_{600nm}. A) Controls: Bacteria were treated with hypoxanthine (1mM) and nitrite (1mM) for 1 hour at 0, 1, 2, 5 and 21% oxygen. The numbers of viable cells were assessed by colony counts and the data is presented as a percentage of the control (untreated bacteria). B) Bacteria were treated with 10 and 50mU ml^{-1} XO for 1 hour in the presence of hypoxanthine (1mM) and nitrite (1mM) at 0, 1, 2, 5 and 21% oxygen. The numbers of viable cells were assessed by colony counts and the data is presented as a percentage of the control (0mU ml^{-1}, cells treated with hypoxanthine (1mM) and nitrite (1mM) alone). n = 4. Mean ± SEM Statistical analysis was performed using one way analysis of variance (ANOVA) and Dunnett's post test using 0mU ml^{-1} as the control.

6.4 Discussion

6.4.1 The effect of H_2O_2 and $ONOO^-$ on the growth of *S. aureus* disease isolates

XOR-generated RONS such as H_2O_2 and $ONOO^-$ have been shown in previous studies to have antibacterial properties (Stevens *et al*, 2000). Hydrogen peroxide is known to have strong oxidising properties and has been used as an antiseptic and anti-bacterial agent for many years, with strong solutions of H_2O_2 has historically being used clinically to disinfect wounds. However, a 3% solution is often recommended to cleanse wounds, as high concentrations can be damaging to the tissues.

Initial assays in this chapter were carried out to determine the effectiveness of H_2O_2 in reducing the growth of *S. aureus* isolates from chronic disease tissues. These isolates include MRSA and VRSA strains which are known to contaminate chronic leg ulcers. These experiments were to highlight the potential benefits of including a H_2O_2-generating enzyme in a wound dressing. Growth curves for *S. aureus* isolates (Mu 3, Mu 50, 117 and N317) were produced at two concentrations of the overnight culture (Figure 6.2-6.5). Further analysis of these growth rates showed that the growth was faster (Table 6.2) and the doubling time reduced (Table 6.3) when culture medium was inoculated with fewer bacteria (figure 6.2-6.5). This may be due to the higher bacterial concentration in the test well depleting available nutrients and oxygen more quickly giving suboptimal growth rates. The growth of all of these isolates were broadly similar, however interestingly, isolate Mu 3 (VRSA) had the fastest growth rate and shortest doubling time (Table 6.2 and 6.3).

Treatment of these strains with H_2O_2 showed that higher concentrations of the overnight culture were less sensitive to the effects of H_2O_2 (Figure 6.6-6.9). At the higher concentration of the overnight culture ($1x10^{-1}$ dilution), 10mM and 100mM H_2O_2 only significantly slowed the growth rate of one of the four isolates (177), whereas the lower concentration of the overnight culture (dilution $5x10^{-2}$) allowed H_2O_2 to be more effective at significantly reducing the growth rate of all isolates (Figure 6.10). The reasons for the differences in the reduced sensitivity of the bacterial cultures higher concentrations of the overnight culture might simply be due to the number of *Staphylococci*, which are known to be vigorous catalase-producers. Isolate Mu 3, which is a VRSA appears to be the least sensitive to the effects of H_2O_2 and isolate 117 which is neither meticillin nor vancomycin

resistant appears to be most sensitive to H_2O_2. This finding is interesting as the bacterial strains with antibiotic resistance appear to be less sensitive to the effects of H_2O_2. This result suggests that the bacteria have not only developed antibiotic resistance but may also have enhanced their defences against oxidative stress to make them better adapted to survive in the wound environment. It was also interesting to note that, particularly at the higher concentration of the overnight culture ($1x10^{-1}$), growth had obviously been slowed at 100mM H_2O_2, although the bacterial numbers were able to eventually climb to reach control values (Figure 6.6-6.10) This effect could be due to the selection of a resistant bacterial population or more likely, that the bacterial catalase has removed the H_2O_2 effect by breaking it down into H_2O and oxygen and the remaining viable bacteria are able to grow and repair the damage to reach a similar absorbance value to the control. The bacteria may also up-regulate catalase in the later stages of growth.

A range of isolates from pus drains and abscess sites that were hospital or community acquired (13, 357, 197, 283, 301 and 307) were also tested for sensitivity to H_2O_2 in the same way as before but a dilution of $5x10^{-2}$ and a $2.5x10^{-2}$ of the start culture was used (Figure 6.11-6.16). These experiments produced results that were comparable to the previous experiments on the *S. aureus* isolates discussed above. The sensitivity of these strains to H_2O_2 was also very similar to that found in the previous experiments. At a higher concentration ($5x10^{-2}$ dilution) of the start culture 100mM H_2O_2 clearly reduced the growth rate of all *S. aureus* strains. However, at a lower concentration ($2.5x10^{-2}$ dilution) of the overnight culture both 10mM and 100mM H_2O_2 reduced the growth of the *S. aureus* isolates (Figure 6.17).

As described in section 3.2.5 XO can lead to the production of the potent antimicrobial $ONOO^-$. Experiments were therefore designed to examine the effects of $ONOO^-$ on the *S. aureus* isolates. Peroxynitrite was generated on the lab bench as in section 6.2.2.1 and several problems were encountered with this procedure in terms of generating a reasonable yield with which to treat the bacteria. It is possible to purchase authentic $ONOO^-$, but it is expensive and does not withstand long-term storage so it is more cost effective if it can be generated on the lab bench. A method by Reed *et al* (1974) was initially used which produced a low yield of 13.5mM. Modifications of the methodology and equipment were experimented with in an attempt to improve the yield based around the method described by Koppenol *et al* (1996) eventually resulting in an improved yield up to 74mM $ONOO^-$. Initial experiments to examine the efficacy of a range of $ONOO^-$ concentrations to kill bacteria were performed. These experiments indicated that a concentration of 0.5mM was sufficient to kill bacteria but the effect was lost on further dilution to 0.1mM. These preliminary experiments could not be expanded

upon or reproduced because of a laboratory safety audit of procedural risk assessments. This resulted in a change in laboratory safety policy that prohibited the use of pathogenic strains of bacteria such as the *S. aureus* disease isolates that were being used in this study.

6.4.2 Effect of H_2O_2, SIN-1 and XO on the growth of bacterial species relevant to the chronic wound

Further investigations into the growth of bacteria were carried out after exposure to H_2O_2, and SIN-1 (a peroxynitrite generator) to assess their antimicrobial effects, and also XO itself. Four species of bacteria that are commonly isolated from infected chronic wounds (Table 2.1) were supplied by Dr. Pauline Wood, *S. faecalis*, *E. coli*, and *S. aureus* and *P. mirabilis*. Investigations into the growth of these bacterial species showed normal sigmoidal growth in a 96-well plate in air for *S. faecalis*, *E. coli*, and *S. aureus*. *Pseudomonas aeruginosa* (PAO1) however, showed a reduced growth rate and an extended lag phase when compared with the other species of bacteria (figure 6.18). This observation was confirmed in a study by Sabra *et al* (2002) who also showed that *P. aeruginosa* (PAO1) prefers microaerobic conditions (i.e. dissolved oxygen tension value around 1% of air saturation) for growth and for the formation of some of its virulence factors such as elastase. This study also showed that PAO1 can create these growth conditions by strongly reducing the transfer rate of oxygen from the gas into the liquid phase, causing oxygen-limited or microaerophilic conditions in the culture after a short period of cultivation, even at high aeration rates with pure oxygen. It is thought that PAO1 can generate this microaerophilic growth environment by at least two mechanisms: (i) blockage of the transfer of oxygen and (ii) formation of a polysaccharide capsule on the cell surface which may act as a physical barrier to prevent diffusion of oxygen into the cells.

More extensive investigations into the growth of these bacterial strains also involved viable cell counts at hourly intervals over 6 hours of growth to determine the relationship between the absorbance values and the number of viable cells ml^{-1} (Figure 6.19-6.21). *P. mirabilis* was included in these studies as a substitute for *P. aeruginosa*. These studies showed that the profile of absorbance values in a 96-well plate versus colony counts for the corresponding number of cells were very similar until around 4 hours when the absorbance values plateau as the culture reached stationary phase and the cell number appears to continue to rise (Figure 6.19-6.20). This result is a common observation in bacterial cultures and is likely to be due to physiological changes in the cells as they reach stationary phase. Furthermore, absorbance values at this stage of

growth may not give an accurate indication of what is actually happening in the culture in terms of cell number. However, there is a linear relationship between absorbance and cell number for the first four hours of growth (figure 6.21).

Treatment of Gram positive *S. aureus* and *S. faecalis* with H_2O_2 showed that both were more sensitive to the effects of H_2O_2 than previously found with the *S. aureus* disease isolates. However, this effect maybe due to the H_2O_2 stock losing its activity because it is known to decompose over time, the stock was not tested routinely over time so it was not possible to compare experiments that were carried out on separate occasions. However, the experiments in figure (6.22-6.23) show that H_2O_2 does have an antibacterial or bacteriostatic effect on these bacteria. There was a slightly reduced level of sensitivity to the effects of H_2O_2 of *S. aureus* compared with *S. faecalis* significant inhibition of growth occurred at 2mM H_2O_2 and complete inhibition at 5mM H_2O_2. The bacterium *S. faecalis* showed significant inhibition at 1mM H_2O_2 and complete inhibition at 5mM H_2O_2. The sensitivity of bacteria to H_2O_2 is known to vary (Schaeffer *et al*, 1980) and may be affected by the growth phase of the organism, the culture medium and the temperature (Amin and Olson, 1968; Campbell and Dimmick, 1966; Yoshpe-Purer and Henis, 1976). However, this slight difference in sensitivity is probably due to the fact that *Staphylococci* are vigorous catalase producers whereas *Streptococci* or *enterococci* are catalase negative or only weakly positive. The bacterium *S. aureus* also has a peptidoglycan protective layer, which is 80nm thick (Jawetz *et al*, 1984), studies have suggested the thicker this peptidoglycan layer; the more resilient the bacteria are to surface-active antimicrobial agents.

A brief study was carried out to assess the effects of the peroxynitrite generator SIN-1 on the growth of *S. faecalis*. Prior to this study, peroxynitrite generation by SIN-1 was measured in PBS and LB to provide information on the activity of the SIN-1 stock both in PBS and in bacteria culture medium (LB). The DHR oxidation is considerably slower in LB compared with PBS suggesting a decrease in $ONOO^-$ generation in LB. These findings are likely to be due to the rapid reaction of $ONOO^-$ with proteins and other components present in the culture medium. These experiments were also repeated in the presence of iron chelator DTPA which prevents iron mediated hydroxyl radical formation which can also oxidise DHR. Peroxynitrite generation by SIN-1 in PBS and the presence of DTPA appears to be marginally decreased; however, as this is expected as there should be little iron or other metal ions present in the PBS to catalyse hydroxyl radical formation (Figure 6.24). The oxidation of DHR in LB was considerably decreased in the presence of DTPA, this is probably a result of hydroxyl radical formation catalysed by the fenton reaction using iron present in the LB (Figure 6.24). Treatment of *S. faecalis* with SIN-1

showed that growth was in inhibited at 500 and 1000μM SIN-1 (Figure 6.25). Time constraints meant that these experiments were not carried out on all of the strains; however, this would be an interesting study for further experimentation. However, this brief assay indicates that peroxynitrite is capable of inhibiting the growth of bacteria relevant to the chronic wound.

It has long been known that XO can generate ROS in air such as H_2O_2 and $O_2^{\bullet-}$. Therefore these species have conferred an antimicrobial role to the enzyme for an equally long time. Therefore it was interesting to assess whether XO in air in the presence of hypoxanthine was effective against bacterial species known to be found in chronic ulcers. An initial experiment carried out in cuvettes showed a slight inhibition of growth at 50mU ml^{-1} XO in the presence of hypoxanthine (Figure 6.26). Further experimentation was carried out in 96-well plates to confirm this finding (Figure 6.27-6.36). Control experiments carried out with each bacterial species initially confirmed that neither hypoxanthine nor allopurinol added to the bacterial cultures alone inhibited growth of the bacterial species, meaning that any alterations in the culture growth rates were due to XO activity and the generation of ROS (Figure 6.27, 6.29, 6.31, 6.33 and 6.35). In some cases the XO added to the culture medium without hypoxanthine showed some inhibition of growth suggesting that there may be endogenous substrate that can be utilised by the enzyme in the culture medium This inhibition was also inhibited by allopurinol which confirms that the reduction in growth rate was due to XO (Figure 6.27, 6.29, 6.31, 6.33 and 6.35). Using a range of XO concentrations in the presence of hypoxanthine (1mM) it was discovered that XO has antibacterial properties and significantly reduced the growth rates of all the bacterial strains (Figure 6.28, 6.30, 6.32, 6.34, and 6.36). The bacterial species *P. aeruginosa* and *E. coli* appeared to be the most sensitive to the effects of XO with a reduction in growth rate at 5, 10 and 50mU ml^{-1}. The growth rate of *S. faecalis* and *S. aureus* were inhibited at 10 and 50mU ml^{-1} and *P. mirabilis* was the least sensitive to the effects of XO with a reduction in growth rate only occurring at 50mU ml^{-1} XO. The effects of 50mU ml^{-1} XO were inhibited by allopurinol, supporting the role of XO as the antibacterial agent. The implications of XO's antibacterial activity are discussed in more detail in the main discussion chapter. It was also interesting to note that by the end of the culture incubation time, as found previously using H_2O_2, all cultures reached approximately the same Abs_{595nm} value (Figure 6.28, 6.30, 6.32, 6.34, and 6.36). This could be due to the selection of a resistant bacterial population, removal of ROS by antioxidant systems allowing growth to resume or more likely, that the substrate becomes exhausted and remaining viable cells continue growing. The differences in sensitivity to XO of the bacterial species may be explained by varying catalase activity which can

counteract the damaging effects of the H_2O_2 generation. In 1972, Taylor and Achanzar demonstrated differences in the catalase activity of a variety of gram-negative organisms. Catalase production is high in *Proteus* spp, whereas *Escherichia* spp. and *Pseudomonas* spp. have little activity. Gram-positive *Staphylococcus* spp. also produce catalase whereas *Streptococcus* spp. do not (Schaeffer *et al*, 1980).

6.4.3 Effect of H_2O_2 and XO on the viability of bacterial species relevant to the chronic wound

Disk inhibition assays clearly showed that H_2O_2 inhibited the growth of *S. aureus* producing clear zones on the agar. The *S. aureus* showed clear zones of inhibition at 88mM but not at 8.8mM H_2O_2. These assays do not appear to be as sensitive as the previous growth assays which showed complete inhibition of *S. aureus* growth at 5mM H_2O_2. This difference in sensitivity is probably due to the fact that in the zone inhibition assays the H_2O_2 needs to diffuse through soft agar in order to kill the bacteria, whereas in the previous assays the H_2O_2 was diffusing through liquid culture medium. However, these assays did show that the assay was working (Figure 6.37 and Table 6.4).

When XO substrates hypoxanthine and nitrite were included in the soft agar layer with the *S. aureus*, and XO in the disks only small faint inhibition zones were formed even with the concentrated stock. However, the zones were likely to be due to the activity of the XO as boiling the enzyme before addition to the disks appeared to abolish the slight zone effect as seen with the concentrated enzyme. The apparent insensitivity of the *S. aureus* to XO may be due to a reduced rate of ROS production by XO as a result of the slow diffusion of substrates in the soft agar (Figure 6.38). A second assay was set up in which the substrates and enzyme were all added into the filter paper disk. This assay did not show any inhibition zones at all this may be because the substrate is rapidly used by the XO in the disk before it diffuses into the agar (Figure 6.39).

6.4.4 Effect of XO on the viability of bacteria relevant to the chronic wound in variable oxygen

Bacteria were also exposed to XO in the presence of hypoxanthine (1mM) and nitrite (1mM) at a range of oxygen tensions. Bacteria were exposed to XO and in the linear phase of growth (1 and 3 hours) assessment of the number of viable cells were assessed by colony counts (Figure 6.41-44). All bacterial strains apart from *E. coli* showed a reduction in the number of viable cells at a range of hypoxic oxygen concentrations relevant to the chronic ulcer both at 10 and 50mU ml^{-1} XO. However, the inhibitory

effects were generally enhanced in the presence of 50mU ml^{-1} XO. Interestingly, it was the organisms with high cellular catalase activity (*Staphylococcus aureus* and *Proteus mirabilis*) that were more sensitive to the effects of XO in hypoxia (Schaeffer *et al*, 1980), which perhaps suggests that the toxic species are not H_2O_2. These results provide further evidence of an anti-bacterial role for XO. However, there also appeared to be a slight increase in the numbers of viable cells in some cases in low oxygen or at low concentrations of XO. In this case low levels of XO-generated species may act to induce genes or up-regulate antioxidant enzymes such as SOD leading to an increase in growth above control levels. For example, in bacteria it has been shown that the OxyR protein which functions as a transcriptional regulator of H_2O_2-inducible genes is directly activated by oxidation and the *E. coli* SoxR transcription factor is known to be sensitive to oxidation by $O_2^{\bullet-}$ (Thannickal and Fanburg, 2000; Farr and Kogoma, 1991).

6.4.5 Chapter summary

The results shown in this chapter suggest that the antimicrobial properties of XO could be beneficial in the chronic wound setting, and that 50mU ml^{-1} XO may provide the most effective antimicrobial activity. However, the levels of bacterial killing are perhaps slightly disappointing for some of the bacterial species. It is possible that addition of XO in the log phase of growth and using different combinations of substrates (see general discussion) may enhance the antimicrobial effects. *In vivo*, anaerobic bacteria also form a major source of infection and it is possible that these might be more susceptible to oxidative killing. It may also be possible that bacteria used, being long term maintained laboratory cultures may behave differently to naturally acquired bacterial infections in wounds.

CHAPTER 7

7 General Discussion-A potential role for XO in the healing of chronic wounds

The studies in this thesis were designed to evaluate a potential new approach to addressing a major problem in current healthcare particularly in elderly populations. Chronic ulcers cost the NHS over £1 billion per annum mainly because current treatment regimes are inadequate in most cases. Effective treatment of such lesions requires a combination of factors to work in unison to result in healing. Tissue regeneration must be induced at the same time as inhibiting bacterial infection. The hypoxic nature of the beds of chronic ulcers is not conducive for the natural healing process to be effective in affected patients, but yet provides an ideal environment for bacterial infection. Xanthine oxidase is an enzyme that has properties that could potentially exploit the hypoxic environment to induce tissue regeneration and kill bacteria. The experiments performed in this study were aimed at substantiating the hypothesis that XOR incorporated into a form of dressing would provide an efficacious combination of actions. The experimental section of this thesis confines itself to three aspects of the role of XOR in relation to the chronic wound. The first aimed to characterise the properties of the enzyme in relation to relevant environments at same time as refining the measuring methods employed. The second role investigated was the pro-proliferative activity of the enzyme at levels that were not toxic to dermal fibroblasts. The final role investigated was that of an anti-infective agent for common wound-related bacteria.

In the literature and anecdotally, a wide range of evidence exists to support a role for XO-generated species in wound healing, and also more specifically of interest in this thesis a role in proliferation and bacterial killing. Probably the best anecdotal evidence that supports the hypothesis comes from a traditional Nepalese treatment for wounds which consists of a dressing (poultice) soaked in Yaks' milk directly applied to the lesion. Yaks' milk is particularly rich in protein and fat, and is likely to have high levels of XOR, but this has not been confirmed here. The proliferation studies were based on literature provided by Murrell *et al*, (1990) who previous reported increased proliferation of adult human dermal fibroblasts for exposure to XO. Numerous studies also describe the proliferation of a wide range of mammalian cells as a response to XO-generated products and RONS. Furthermore XO is known to be present in high concentrations in the

components of milk such as whey, and also in colostrum (the first breastmilk from pregnant mothers), which are sold as health food supplements and are reported to have beneficial effects on wound healing (Rayner *et al*, 2000). Studies have generally attributed the beneficial effects to the presence of certain growth factors in conjunction with the high protein content, much of which is XOR.

The bactericidal properties of XOR in the presence of the substrate hypoxanthine have long been known (Green and Pauli, 1943). The defensive properties of XOR have also been demonstrated in mice infected with *Salmonella typhimurium* (Umezawa *et al*, 1997) where the generation of not just $O_2^{\bullet -}$ but also $ONOO^-$ were proposed to be antibacterial. Also, XO-derived ROS are important for phagocytic killing in macrophages (Takao *et al*, 1996; Potoka *et al*, 1998). Anecdotally a common and effective treatment for the bacterial conjunctivitis in babies is expressed breast milk. As previously stated human breastmilk is particularly rich in XOR (Stevens *et al*, 2000), it is here that the enzyme displays perhaps its most important physiological role. In the presence of nitrite, the ability of XOR to generate $ONOO^-$ (reviewed in the introductory chapters), a powerful bactericidal agent (Brunelli *et al*, 1995), have lead researchers to speculate that the high quantities of XOR in milk may act to sterilise the gut. Indeed the generation of $^{\bullet}NO$ by human milk XOR is greatest in the first 5 weeks postpartum, where protection of the neonatal gut would be most beneficial (Stevens *et al*, 2000). Although nitrite concentrations in the gut are not particularly high, the source of substrate for $ONOO^-$ generation by XOR may actually be derived from bacterial pathogens themselves (DeMoss and Hsu, 1991). It is thought that XOR may attach to bacterial pathogens via GAG-like structures on the bacterial surface (Roberts, 1996) and therefore catalyse the generation of RONS in the bacterial microenvironment where nitrite is secreted and concentrations are adequate. Therefore the bacteria may initiate their own destruction.

Investigations into the hypothesis that the pro-proliferative and antimicrobial properties of XOR may be beneficial in the healing of chronic ulcers began with measurements of XO-generated species at XO concentrations in a range that included concentrations that were previously found to be proliferative to human dermal fibroblasts (Murrell *et al*, 1990). Assays for the measurement of XO-generated species were optimised in Chapter 4 (first experimental chapter). Xanthine oxidase (Biozyme) was characterised for protein content and was not found to contain any of the dehydrogenase form of the enzyme (Pterin assay). Superoxide generation by XO (Cytochrome *c* assay) was measured in a variety of environments including in fibroblast culture medium, bacterial culture medium, and at 21% and 1% oxygen. Superoxide generation by XO was found to be dramatically reduced at 1% oxygen, as compared with 21% oxygen, with little

or no $O_2^{\bullet-}$ being detected. Superoxide generation by XO was also found to be decreased in both fibroblast culture medium and bacterial culture medium as compared with in PBS which was particularly noticeable at 21% oxygen. Superoxide generation by XO at variable enzyme and substrate concentrations was also assessed. Peroxynitrite generation by XO (DHR assay) was also assessed and results suggested that $ONOO^-$ generation was increased in low oxygen concentrations.

In Chapter 5 the effects of XO on HDF which are directly related to the wound-healing process were investigated. Wounds produced in the dermis are healed by mechanisms of epithelialisation, contraction and matrix deposition. It is in this phase that synthesis and collagen accumulation, proteoglycans and binding proteins are produced. In the wound healing process, dermal fibroblasts are the main cell type involved in matrix production (Moulin, 1995; Deigelmann, 1997) and were chosen for this study since they are the primary matrix-producing cells, even though the more complex process of wound healing cannot be correlated simply with fibroblasts proliferation. Furthermore, *in vitro* assessment of human fibroblast cytotoxicity has previously been used as a useful method for characterising cell toxicity mechanisms of topically-applied antiseptics. XO-generated species are known to vary in changing oxygen concentrations and low levels of these species are known to have proliferative whereas high levels of these species are known to have toxic effects. Therefore human dermal fibroblasts were exposed to varying levels of XO in an attempt to determine the level of enzyme at which proliferation is enhanced but which is not cytotoxic. More importantly these fibroblasts were exposed to a range of hypoxic oxygen concentrations to simulate conditions encountered within the chronic wound. Experiments of cell viability (MTT) and proliferation (BrdU) using a range of dermal fibroblasts showed, that at in hyperoxia (21% O_2), XO decreased cell viability and DNA synthesis at high concentrations of XO (5-50mU ml^{-1}), however there were also indications of proliferation at low XO (0.1-1mU ml^{-1}) as suggested in the literature. As the oxygen concentrations decreased, it was noted that the toxic effects of the XO, even at high concentrations also decreased. In fact, there were even suggestions of enhanced proliferation at high XO concentrations in low oxygen tensions that are known to prevail in the chronic wound. This effect may be due to XO acting to provide low levels of RONS in low oxygen to enhance proliferation. However, for this effect to occur high levels of XO are required which possibly suggests that the high XO concentration provides a burst of ROS with the low levels of available oxygen to enhance proliferation. These results suggest that in the low oxygen environment of the chronic wound the toxic effects on HDF are limited and high concentrations of XO may even serve to enhance proliferation of human dermal fibroblasts in the wound bed.

The third experimental chapter (chapter 6) investigated the anti-bacterial role of XO on bacterial species relevant to chronic wounds. Bacterial viability was assessed by growth curves, diffusion zone assays and viable colony counts. At 21% oxygen 5, 10 and 50mU ml^{-1} XO was found to slow the growth of bacteria relevant to the chronic wound. Colony counts of bacteria exposed to varying oxygen concentrations at 10 and 50mU ml^{-1} XO showed differential effects on bacteria relevant to the chronic wound. However, there were suggestions that XO was capable of affecting the bacterial cell numbers significantly in hyperoxia and hypoxia after 3 hours exposure. Equivalent concentrations were also shown to be toxic to human dermal fibroblasts after 3 hours but only at 21% oxygen (hyperoxia). However, whilst the findings shown in this thesis support an antibacterial role for XO, the effects of XO-generated species in low oxygen on bacteria relevant to the chronic wound was not as obvious as expected. This suggests that further work may be needed to enhance the sensitivity of the assays used to assess the antimicrobial effects of the enzyme in low oxygen. It may be that the effects of the enzyme would be enhanced *in vivo* as there would be a continuous supply a substrate, for the *in vitro* assays shown in this thesis the substrate was only added at the start of the assay. It is possible that a future experiment could be designed with multiple substrate additions to the plate to prevent depletion, however, using the oxygen controlled cabinet it would increase the risk of affecting the pO_2 inside the cabinet during the experiment. Therefore, for the assays in this thesis, entry into the cabinet was kept at a minimum. Furthermore, research carried out in our lab (Hewinson, 2005) showed that inflammatory mediators such as thrombin appeared to upregulate XO activity after a short incubation (mins) prior to enzyme activity assays. These studies also showed that although thrombin increased XO electron-donating substrate turnover a statistically significant increase in the generation of $O_2^{\bullet -}$ by XO was not observed, however the presence of thrombin enhanced XO's antibacterial properties which could be due to increase H_2O_2 generation. Furthermore, analysis of the XO amino-acid sequence and crystal structure revealed an accessible thrombin cleavage sequence homologous to that found in the fibrinogen Aα chain. Theses results suggest that thrombin could cleave XO, a process that could potentially alter enzyme conformation and therefore activity. It is therefore, possible that in the chronic wound setting the activity of XO may be enhanced by inflammatory factors present in the chronic wound. It is also difficult to compare the results from the *in vitro* assays to what would actually occur *in vivo*, as XO uses oxygen as it a substrate so at high XO concentrations the XO may rapidly use oxygen present in the culture dish whereas *in vitro* there may be a more gradual supply of oxygen from blood vessels distant from the wound bed.

The limited effects of XO on the chronic wound bacteria could be also to do with the eventual urate generation by XO and its reported $ONOO^-$ scavenging ability. Hypoxanthine was routinely used in these experiments, and the oxidation of hypoxanthine by XO is known produce xanthine as its product. However, oxidation of xanthine by XO will also produce urate. If an alternative substrate such as NADH were used then urate generation would be avoided. However, for the purposes of this study hypoxanthine was used throughout in order to draw a comparison between the fibroblast proliferation studies and bacterial killing. Furthermore, in the chronic wound XO is likely to encounter a range of substrates including both NADH and hypoxanthine which may act as electron donors. Although the levels of substrate that would be present in chronic wounds is unknown, based on levels of hypoxanthine detected in disease states after periods of chronic ischaemia it is highly likely that XO would have sufficient substrate present in the wound without the exogenous addition of an pharmaceutically acceptable substrate.

Furthermore, facultative anaerobes (as used in these studies) tend to produce antioxidants to combat the negative effects of ROS. For example, the *Staphylococci sp* used here are vigorous catalase-producers. Anaerobic bacteria (as commonly found in a chronic wound) are more susceptible to the effects of XO, as oxygen and its metabolites are toxic to them and they have lower or undetectable levels of antioxidants like SOD and catalase.

It is also difficult to compare the effects of XO on HDF and bacteria as they are both grown in different culture media, which contain various components which act to scavenge XO-generated products. Furthermore, these are complex culture media which are designed to meet all of the cells nutritional requirements and are for optimal growth. In the chronic wound environment the growth characteristics of the fibroblasts and bacteria would be very different.

The data presented in this thesis suggest that the addition of XO, above physiological levels that may be encountered in normal tissues (2mU ml^{-1}), may have beneficial effects when incorporated into a wound dressing or dermal graft for application to a chronic wound (Figure 7.1). Although adequate levels of the purine degradation product hypoxanthine would be available for XOR activity in the chronic wound, XO can also use a variety of other electron donors, potentially enhancing the generating capacity of the enzyme, since only the effects hypoxanthine were tested in this thesis. A pharmaceutically acceptable electron donor system could also be used to supplement substrate levels already present in the wound. It is possible that XO may be incorporated into a dressing in a dried form which activates upon wetting by exudates from the wound bed. Alternatively, XO could be incorporated into a collagen gel matrix graft along with fibroblasts to cover the wound, and promote healing by enhancing the proliferation of

fibroblasts and killing bacteria. XO could be derived from a variety of sources; it can be cheaply derived from dairy waste products such as buttermilk and whey, both of which contain very high levels of the active enzyme. XO could also be cheaply produced large amounts in bioreactors using *Aspergillus niger* which is a filamentous fungi expression system developed as host for the production of secreted proteins. This source would avoid any potential concern over the transfer of bovine pathogens. *A. niger* was first used commercially as host for the production of the mammalian protein bovine chymosin in the manufacture of cheese.

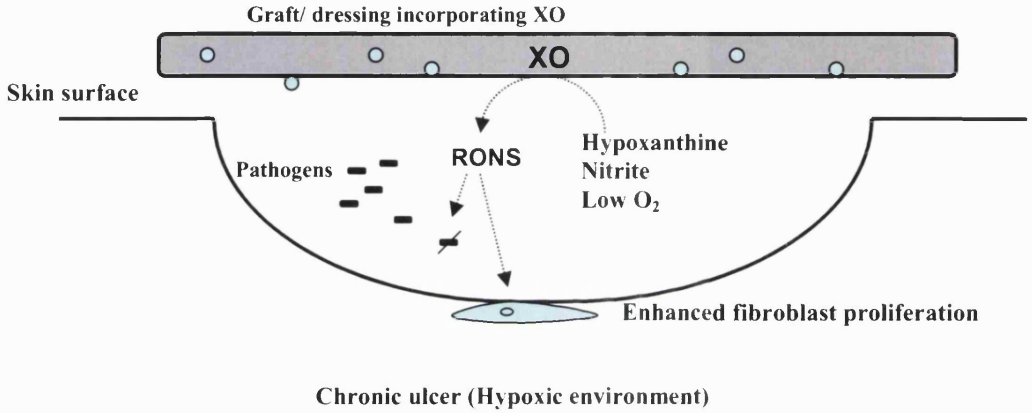

Figure 7.1 The Proposed model of XO-Release from a dermal graft or dressing for enhanced healing in a chronic ulcer

Prolonged hypoxia and ischaemia causes the breakdown of the skin, resulting chronic ulcer formation. Pathogens are able to enter the wound and the hypoxic environment encourages the growth of a range of facultative and anaerobic bacteria. XO is known to be capable of producing a range of RONS in hypoxia. Therefore, incorporation of XO into a dermal graft or dressing has the potential to resolve wound healing by increasing the proliferation of HDF (Chapter 5) and killing bacteria (Chapter 6).

Interestingly, the usage of honey as a wound dressing in ancient and traditional medicine has recently been re-discovered, and is in fairly widespread use as a topical antibacterial agent for the treatment of wounds, burns and skin ulcers, there being many reports of its effectiveness (Molan *et al*, 2001). Much of the effectiveness of honey as a dressing appears to be due to its antimicrobial properties. The major antibacterial activity has been found to be due to H_2O_2 produced enzymatically in the honey (Bang *et al*, 2003). The glucose oxidase enzyme is secreted from the hypopharyngeal gland of the bee into the nectar to assist in the formation of honey from the nectar. As the healing process will not occur unless infection is cleared from a lesion: swabbing of wounds dressed with honey has shown that the infecting bacteria are rapidly cleared. Therefore, in this respect honey is superior to the expensive modern hydrocolloid wound dressings as a moist dressing. This is because, although tissue re-growth in the healing process is enhanced by a moist environment, and deformity is prevented if the re-growth is not forced down by a dry scab

forming on the surface, moist conditions favour the growth of infecting bacteria. Antibiotics are ineffective in this situation, and antiseptics cause tissue damage, so slow the healing process. It is possible that XO could work on a similar principle to honey which has already been shown to be effective in wound healing as a dressing. However, XO has the added advantage of being able to produce a range of RONS in a range of hypoxic oxygen concentrations.

In summary the data presented in this thesis suggest that, under conditions that simulate the low oxygen tension of the chronic wound, XO-generated species are capable of the proliferation of HDF whilst also showing some inhibition of bacteria that are relevant to the chronic wound.

7.1 Future work

The studies presented in this thesis provide a sound basis on which to develop an XO-based treatment for chronic wounds. Nevertheless, further studies could be undertaken to extensively characterise the system. These could include the exposure of human umbilical vein endothelial cells (HUVECs) to XO and assessment of angiogenesis by tubule formation assays and *in vivo* wounding studies. Wound healing could be assessed by dermal fibroblast migration, using the monolayer scratch-wound model assay. Experiments may be conducted to assess the sensitivity of keratinocytes to XO-generated products. It would also be relevant to carry out further studies using fibroblasts derived from the bed of a chronic wound; however these cells are difficult to culture. Further research could also be carried out to elucidate the signalling mechanisms in fibroblasts using specific inhibitors (eg MAP kinase inhibitors), and gene expression by gene arrays, matrix production, MMP production and growth factor production. The effects of XO on co-cultures of wound-relevant cells such as endothelial cells, smooth muscle cells and keratinocytes may also be studied. The chronic wound environment could also be simulated more effectively using a bioreactor system flow system to carefully monitor the behaviour of the cells, and allow for regular addition of substrates, for example, or removal of medium for analysis.

In addition, it would be interesting to repeat the bacterial assays to determine the effects of XO on bacteria with different electron donating substrates such as NADH. More extensive studies of the effects of XO on biofilms and anaerobic bacteria that have been isolated from chronic wounds would also provide more information on the antibacterial effects that XO may have in a chronic wound setting.

The experiments carried out in this thesis provide preliminary fundamental data on the action of XO on wound relevant cells in low oxygen to simulate conditions which may be encountered within the chronic wound. However, in order for XO to be beneficial in this setting this research should be extended to determine how XO could be incorporated into a dressing or a dermal graft to allow efficient delivery to the ulcer bed. It may be that XO could be incorporated into a hydrogel dressing, or a collagen gel within which fibroblasts are also incorporated. Furthermore, it is important to understand that the chronic wound represents a complex environment, and whilst every effort was made in these *in vitro* studies to mimic certain aspects of this environment, it is important that the effects of this enzyme are also studied in animal wounding experiments, and in models of delayed healing.

The results presented here are encouraging, and since XO is a constitutive protein in humans and has not shown any adverse effects of being applied directly to skin, it is possible that it could be trialled on human chronic ulcers sooner than expected.

8 Appendix

8.1 Fibroblast culture

8.1.1 Fibroblast growth Medium

To 500ml Dulbecco's Modified Eagle's medium (DMEM), was added 50ml of foetal calf serum (FCS). To this 5ml of the antibiotics penicillin and streptomycin and L-Glutamine were added at a final concentration of 100U ml^{-1} Penicillin (Stock 10,000U ml^{-1}), 100µg ml^{-1} streptomycin (Stock 10,000µg ml^{-1}) and 2mM L-Glutamine (stock 200mM L-Glutamine). This was used for the isolation and serial culture of human dermal fibroblasts. DMEM with and without phenol red was used (See table 8 for ingredients).

Component	31885 (With Phenol Red) 1 X Liquid mg/ L	11880 (Without Phenol Red) 1 X Liquid mg/ L
INORGANIC SALTS:		
$CaCl_2 . 2H_2O$	264.00	264.00
$Fe(NO_3) . 9H_2O$	0.10	0.10
KCl	400.00	400.00
$MgSO_4 \cdot 7H_2O$	200.00	200.00
NaCl	6400.00	6400.00
$NaHCO_3$	3700.00	3700.00
$NaH_2PO_4 \cdot 2 H_2O$	141.00	141.00
OTHER COMPONENTS:		
D-Glucose	1000.0	1000.0
Phenol Red	15.0	-
Sodium Pyruvate	110.00	110.00
AMINO ACIDS:		
L-Arginine · HCl	84.00	84.00
L-Cystine	48.00	48.00
L-Glutamine	580.00	-
Glycine	30.00	30.00
L-Histidine HCl · H_2O	42.00	42.00
L-Isoleucine	105.00	105.00
L-Leucine	105.00	105.00
L-Lysine · HCl	146.00	146.00
L-Methionine	30.00	30.00
L-Phenylalanine	66.00	66.00
L-Serine	42.00	42.00
L-Theonine	95.00	95.00
L-Tryptophan	16.00	16.00
L-Tyrosine	72.00	72.00
L-Valine	94.00	94.00
VITAMINS:		
D-Ca pantothenate	4.00	4.00
Choline Chloride	4.00	4.00
Folic Acid	4.00	4.00
i-Inositol	7.20	7.20
Nicotinamide	4.00	4.00
Pyridoxine HCl	4.00	4.00
Riboflavin	0.40	0.40
Thiamine HCl	4.00	4.00

Table 8.1Dulbecco's Modified Eagle's Medium with and without the addition of phenol Red

8.1.2 Trypsin/EDTA

For detaching cells from growth substrates, a pre-mixed X 10 concentrate (50g/L porcine trypsin and 20g/L EDTA), was diluted to 1X in PBS, and stored in 50ml aliquots containing (0.025g trypsin and 0.01g EDTA) at -20°C. 5mls of the 1X stock was used to dissociate cells

8.2 Bacterial Growth medium

8.2.1 Luria Broth (LB)

500ml milliQ water was added to 12.5g LB (L3522, Sigma). This solution was sterilised by autoclaving for 30mins at 121°C.

8.2.2 LB agar plates

Agar plates were set up by first dissolving 12.5g LB and 6g agar (12.5%) (LP0011 Oxoid Ltd, Basingstoke, Hampshire, England) in 500ml of MilliQ water. This solution was then sterilised by autoclaving for 30 minutes at 121°C, cooled to ~50°C then poured into sterile plastic Petri dishes. On cooling the agar solidified to form a gel that was covered with the Petri dish lid and the plates kept at 4°C until use, which was typically within one week. Prior to use, the agar plates required air drying to remove condensation that formed within the Petri dishes during storage. This was achieved by inverting each plate and removing the lid in a warm room (37°C). The plates were allowed to dry until all signs of condensation had been removed which was typically within 35 minutes. The plates were then recovered with their lids and stored at room temperature before use which was within 6 hours of air drying.

8.2.3 Soft agar overlay (0.4%)

0.2g Agar 1.25g LB 50mls milliQ water

9 References

Abdulrazak, A., Bitar, Z. I., Al Shamali, A. A., & Mobasher, L. A. (2005). Bacteriological study of diabetic foot infections. *J. Diabetes Complications.* 19, 138-141.

Adachi, T., Fukushima, T., Usami, Y., & Hirano, K. (1993). Binding of human xanthine oxidase to sulphated glycosaminoglycans on the endothelial-cell surface. *Biochem. J.* 289 (Pt 2), 523-527.

Ademiluyi, S. A., Rotimi, V. O., Coker, A. O., Banjo, T. O., & Akinyanju, O. (1988). The anaerobic and aerobic bacterial flora of leg ulcers in patients with sickle-cell disease. *J. Infect.* 17, 115-120.

Agren, M.S. (1999a). Matrix metalloproteinases (MMPs) are required for re-epithelialization of cutaneous wounds. *Arch. Dermatol. Res.* 291, 583-590.

Agren, M. S., Steenfos, H. H., Dabelsteen, S., Hansen, J.B., & Dabelsteen, E. (1999b). Proliferation and mitogenic response to PDGF-BB of fibroblasts isolated from chronic venous leg ulcers is ulcer-age dependent. *J. Invest. Dermatol.* 112, 463-469.

Agren, M.S., Eaglstein, W.H., Ferguson, M.W., Harding, K.G., Moore, K., Saarialho-Kere, U.K., & Schultz, G.S. (2000). Causes and effects of the chronic inflammation in venous leg ulcers. *Acta Derm. Venereol. Suppl (Stockh)* 210, 3-17.

Akaike, T., Sato, K., Ijiri, S., Miyamoto, Y., Kohno, M., Ando, M., & Maeda, H. (1992). Bactericidal activity of alkyl peroxyl radicals generated by heme-iron-catalyzed decomposition of organic peroxides. *Arch. Biochem. Biophys.* 294, 55-63.

Alhama, J., Ruiz-Laguna, J., Rodriguez-Ariza, A., Toribio, F., Lopez-Barea, J., & Pueyo, C. (1998). Formation of 8-oxoguanine in cellular DNA of Escherichia coli strains defective in different antioxidant defences. *Mutagenesis.* 13, 589-594.

Allen, D.B., Maguire, J.J., Mahdavian, M., Wicke, C., Marcocci, L., Scheuenstuhl, H., Chang, M., Le, A.X., Hopf, H.W. & Hunt, T.K. (1997) Wound hypoxia and acidosis limit neutrophil bacterial killing mechanisms. *Arch. Surg.* 132, 991-6.

Amin, V. M. & Olson, N. F. (1968). Influence of catalase activity on resistance of coagulase-positive staphylococci to hydrogen peroxide. *Appl. Microbiol.* 16, 267-270.

Amstad, P., Peskin, A., Shah, G., Mirault, M. E., Moret, R., Zbinden, I., & Cerutti, P. (1991). The balance between Cu, Zn-superoxide dismutase and catalase affects the sensitivity of mouse epidermal cells to oxidative stress. *Biochemistry.* 30, 9305-9313.

Antezana, M., Sullivan, S., Usui, M., Gibran, N., Spenny, M., Larsen, J., Ansel, J., Bunnett, N., & Olerud, J. (2002). Neutral endopeptidase activity is increased in the skin of subjects with diabetic ulcers. *J. Invest. Dermatol.* 119, 1400-1404.

Armstrong, D. G. & Lipsky, B. A. (2004). Advances in the treatment of diabetic foot infections. *Diabetes Technol. Ther.* 6, 167-177.

Ashcroft, G.S., Herrick, S.E., Tarnuzzer, R.W., Horan, M.A., Schultz, G.S., & Ferguson, M.J. (1997). Age-related differences in the temporal and spatial regulation of matrix metalloproteinases MMPs in normal skin and acute cutaneous wounds of healthy humans. *Cell Tissue Res.* 290, 581-591.

Ayliffe, G. A. (1997). The progressive intercontinental spread of methicillin-resistant *Staphylococcus aureus*. *Clin. Infect. Dis.* 24 Suppl 1, S74-S79.

Azzi, A., Montecucco, C., & Richter, C. (1975). The use of acetylated ferricytochrome c for the detection of superoxide radicals produced in biological membranes. *Biochem. Biophys. Res. Commun.* 65, 597-603.

Backhouse, C. M., Blair, S. D., Savage, A. P., Walton, J., & McCollum, C. N. 1987. Controlled trial of occlusive dressings in healing chronic venous ulcers. *Br. J. Surg.* 74, 626-627.

Badiavas, E.V., Abedi, M., Butmarc, J., Falanga, V., & Quesenberry, P. (2003) Participation of bone marrow derived cells in cutaneous wound healing. *J. Cell Physiol.* 196, 245-50.

Bae, Y. S., Kang, S. W., Seo, M. S., Baines, I. C., Tekle, E., Chock, P. B., & Rhee, S. G. (1997). Epidermal growth factor (EGF)-induced generation of hydrogen peroxide. Role in EGF receptor-mediated tyrosine phosphorylation. *J Biol. Chem.* 272, 217-221.

Baichwal, V. R. & Baeuerle, P. A. (1997). Activate NF-kappa B or die? *Curr. Biol.* 7, R94-R96.

Baillon, M. L., A. H. Van Vilet, J. M. Ketley, C. Constantinidou, & C. W. Penn. (1999). An iron-regulated alkyl hydroperoxide reductase (AhpC) confers aerotolerence and oxidative stress resistance to the microaerophillic pathogen *Campylobacter jejuni J. Bacteriol.* 181, 4798-4804.

Baker, S. R., Stacey, M. C., Jopp-McKay, A. G., Hoskin, S. E., & Thompson, P. J. (1991). Epidemiology of chronic venous ulcers. *Br. J. Surg.* 78, 864-867.

Ball, E. G. (1939) Xanthine oxidase: Purification and properties. *J. Biol. Chem.* 128, 51-67.

Bang, L. M., Buntting, C., & Molan, P. (2003). The effect of dilution on the rate of hydrogen peroxide production in honey and its implications for wound healing. *J. Altern. Complement. Med.* 9, 267-273.

Barbul, A., Fishel, R. S., Shimazu, S., Wasserkrug, H. I., Yoshimura, N. N., Tao, R. C., & Efron, G., (1985). Intravenous hyperalimentation with high arginine levels improves wound healing and immune function. *J. Surg. Res.* 38, 328-334.

Barbul, A., Lazarou, S. A., Efron, D. T., Wasserkrug, H. I., & Efron, G. (1990). Arginine enhances wound healing and lymphocyte immune responses in humans. *Surgery.* 108, 331-337.

Barrick, B., Campbell, E.J., & Owen, C.A. (1999). Leukocyte proteinases in wound healing: roles in physiologic and pathologic processes. *Wound Repair Regen. 7*, 410-422.

Bartold, P. M. & Raben, A. (1996). Growth factor modulation of fibroblasts in simulated wound healing. *J Periodontal Res.* 31, 205-216.

Bauer, M. L., Beckman, J. S., Bridges, R. J., Fuller, C. M., & Matalon, S. (1992). Peroxynitrite inhibits sodium uptake in rat colonic membrane vesicles. *Biochim. Biophys. Acta.* 1104, 87-94.

Bauer, J. A., Rao, W., & Smith, D.J. (1998). Evaluation of linear polyethyleneimine/nitric oxide adduct on wound repair: therapy versus toxicity. *Wound. Repair Regen.* 6, 569-577.

Bautista, A. P. & Spitzer, J. J. (1994). Inhibition of nitric oxide formation *in vivo* enhances superoxide release by the perfused liver. *Am. J Physiol.* 266, G783-G788

Beckman, J. S., Parks, D. A., Pearson, J. D., Marshall, P. A., & Freeman, B. A. (1989). A sensitive fluorometric assay for measuring xanthine dehydrogenase and oxidase in tissues. *Free Radical Biology and Medicine.* 6, 607-615.

Beckman, J. S., Beckman, T. W., Chen, J., Marshall, P. A., & Freeman, B. A. (1990). Apparent hydroxyl radical production by peroxynitrite: implications for endothelial injury from nitric oxide and superoxide. *Proc. Natl Acad. Sci.USA.* 87, 1620-1624.

Beckman, J. S. & Koppenol, W. H. (1996). Nitric oxide, superoxide, and peroxynitrite: the good, the bad, and ugly. *Am. J. Physiol.* 271, C1424-C1437.

Ben-Hamida, A., Man, W. K., McNeil, N., & Spencer, J. (1998). Histamine, xanthine oxidase generated oxygen-derived free radicals and Helicobacter pylori in gastroduodenal inflammation and ulceration. *Inflamm. Res.* 47, 193-199.

Bendy, R. H., Jr. & Landman, M. E. (1964). A survey of infections in a community hospital. *J. Med. Soc. N. J.* 61, 454-457.

Benjamin, N., O'Driscoll, F., Dougall, H., Duncan, C., Smith, L., Golden, M., & McKenzie, H. (1994). Stomach NO synthesis. *Nature.* 368, 502.

Boulton, A.J., Bowker, J.H., Gadia, M., Lemerman, R., Caswell, K., and Skyler, J.S. (1986). Use of plaster casts in the management of diabetic neuropathic foot ulcers. *Diabetes Care.* 9, 149-152.

Bowdy, B. D., Marple, S. L., Pauly, T. H., Coonrod, J. D., & Gillespie, M. N. (1990). Oxygen radical-dependent bacterial killing and pulmonary hypertension in piglets infected with group B *streptococci. Am. Rev. Respir. Dis.* 141, 648-653.

Bowler, I. C. & Storr, J. A. (1998). Costs of endemic MRSA. *J. Hosp. Infect.* 40, 159.

Bowler, P.G., Davies, B.J., (1999). The microbiology of infected and noninfected leg ulcers. *Int. J. of Dermatol.* 38, 573-578.

Boykin, J. V., Jr. (2000). The nitric oxide connection: hyperbaric oxygen therapy, becaplermin, and diabetic ulcer management. *Adv. Skin Wound. Care.* 13, 169-174.

Bray, R., Pettersson, R., & Ehrenberg, A. (1961). The chemistry of xanthine oxidase.` Anaerobic reduction of xanthine oxidase studied by electron spin resonance and magnetic susceptibility. *Biochem. J.* 81, 178.

Bray, R. C., Barber, M. J., Dalton, H., Lowe, D. J., & Coughlan, M. P. (1975). Iron-sulphur systems in some isolated multi-component oxidative enzymes. *Biochem. Soc. Trans.* 3, 479-482.

Brogi, E., Wu, T., Namiki, A., & Isner, J. M. (1994). Indirect angiogenic cytokines upregulate VEGF and bFGF gene expression in vascular smooth muscle cells, whereas hypoxia upregulates VEGF expression only. *Circulation.* 90, 649-652.

Brook, I. (1987). Synergistic aerobic and anaerobic infections. *Clin. Ther.* 10 Suppl A, 19-35.

Brook, I. (1988). Enhancement of growth of aerobic, anaerobic, and facultative bacteria in mixed infections with anaerobic and facultative gram-positive cocci. *J Surg. Res.* 45, 222-227.

Brunelli, L., Crow, J. P., & Beckman, J. S. (1995). The comparative toxicity of nitric oxide and peroxynitrite to Escherichia coli. *Arch. Biochem. Biophys.* 316, 327-334.

Bucalo, B., Eaglestein, W. H., & Falanga, V. (1993) Inhibition of cell proliferation by chronic wound fluid. *Wound Repair Regen.* 1, 181-186.

Bullen, E. C., Longaker, M. T., Updike, D. L., Benton, R., Ladin, D., Hou, Z., & Howard, E. W. (1995). Tissue inhibitor of metalloproteinases-1 is decreased and activated gelatinases are increased in chronic wounds. *J. Invest. Dermatol.* 104, 236-240.

Burdon, R. H. (1995). Superoxide and hydrogen peroxide in relation to mammalian cell proliferation. *Free Radic. Biol. Med.* 18, 775-794.

Butler, A.R. & Rhodes, P. (1997). Chemistry, analysis, and biological roles of S-nitrosothiols. *Anal. Biochem.* 249, 1-9.

Buxser, S. E., Sawada, G., & Raub, T. J. (1999). Analytical and numerical techniques for evaluation of free radical damage in cultured cells using imaging cytometry and fluorescent indicators. *Methods. Enzymol.* 300, 256-275.

Byers, P. H., Holbrook, K. A., Barsh, G. S., Smith, L. T., & Bornstein,P. (1981). Altered secretion of type III procollagen in a form of type IV Ehlers-Danlos syndrome. Biochemical studies in cultured fibroblasts. *Lab. Invest* 44, 336-341.

Byers, P. H. (1989). Inherited disorders of collagen gene structure and expression. *Am. J. Med. Genet.* 34, 72-80.

Byun, J., Henderson, J. P., Mueller, D. M., & Heinecke, J. W., (1999). 8-Nitro-2'-deoxyguanosine, a specific marker of oxidation by reactive nitrogen species, is generated by the myeloperoxidase-hydrogen peroxide-nitrite system of activated human phagocytes. *Biochemistry* 38, 2590-600.

Campbell, J. E. & Dimmick, R. L. (1966). Effect of 3 percent hydrogen peroxide on the viability of Serratia marcescens. *J. Bacteriol.* 91, 925-929.

Carr, R. W., Delaney, C. A., Westerman, R. A., & Roberts, R. G. (1993). Denervation impairs cutaneous microvascular function and blister healing in the rat hindlimb. *Neuroreport* 4, 467-470.

Claudy, A. L., Mirshahi, M., Soria, C., & Soria, J. (1991). Detection of undegraded fibrin and tumor necrosis factor-alpha in venous leg ulcers. *J. Am. Acad. Dermatol.* 25, 623-627.

Colin, D., Loyant, R., Abraham, P., & Saumet, L. J. (1996). Changes in sacral transcutaneous oxygen tension in evaluation of different mattresses in the prevention of pressure ulcers. *Adv. Wound Care.* 9, 25-28.

Cook, H., Davies, K. J., Harding, K. G., & Thomas, D. W. (2000). Defective extracellular matrix reorganization by chronic wound fibroblasts is associated with alterations in TIMP-1, TIMP-2, and MMP-2 activity. *J. Invest. Dermatol.* 115, 225-233.

Colsky, A. S., Kirsner, R. S., & Kerdel, F. A. (1998). Analysis of antibiotic susceptibilities of skin wound flora in hospitalized dermatology patients. The crisis of antibiotic resistance has come to the surface. *Arch. Dermatol.* 134, 1006-1009.

Cornwall, J. V., Dore, C. J., & Lewis, J. D. (1986). Leg ulcers: epidemiology and aetiology. *Br. J Surg.* 73, 693-696.

Corran, H. S., Dewan, J. G., Gordon, A. H., & Green, D. E. (1939). Xanthine oxidase and milk flavoprotein: With an Addendum by J. St L. Philpot. *Biochem. J.* 33, 1694-1708.

Cosgrove, S. E., Sakoulas, G., Perencevich, E. N., Schwaber, M. J., Karchmer, A. W., & Carmeli, Y. (2003). Comparison of mortality associated with methicillin-resistant and methicillin-susceptible Staphylococcus aureus bacteremia: a meta-analysis. *Clin. Infect. Dis.* 36, 53-59.

Crawford, M. J. & Goldberg, D. E. (1998). Regulation of the Salmonella typhimurium flavohemoglobin gene. A new pathway for bacterial gene expression in response to nitric oxide. *J Biol. Chem.* 273, 34028-34032.

Crow, J. P. 1997. Dichlorodihydrofluorescein and dihydrorhodamine 123 are sensitive indicators of peroxynitrite in vitro: implications for intracellular measurement of reactive nitrogen and oxygen species. Nitric.Oxide. 1, 145-157.

Cullen, B., Silcock, D., Brown, L. J., Gosiewska, A., & Geesin, J.C. (1997). The differential regulation and secretion of proteinases from fetal and neonatal fibroblasts by growth factors. *Int. J. Biochem. Cell. Biol.* 29, 241-250.

Curran, R. D., Billiar, T. R., Stuehr, D. J., Hofmann, K., & Simmons, R. L. (1989). Hepatocytes produce nitrogen oxides from L-arginine in response to inflammatory products of Kupffer cells. *J. Exp. Med.* 170, 1769-1774.

Daltrey, D. C., Rhodes, B., & Chattwood, J. G. (1981). Investigation into the microbial flora of healing and non-healing decubitus ulcers. *J. Clin.Pathol.* 34, 701-705.

Danielsen, L., Westh, H., Balselv, E., Rosdahl, V. T., & Doring, G. (1996). Pseudomonas aeruginosa exotoxin A antibodies in rapidly deteriorating chronic leg ulcers. *Lancet.* 347, 265

D'Arcangelo, D., Facchiano, F., Barlucchi, L. M., Melillo, G., Illi, B., Testolin, L., Gaetano, C., and Capogrossi, M. C. (2000). Acidosis inhibits endothelial cell apoptosis and function and induces basic fibroblast growth factor and vascular endothelial growth factor expression. *Circ. Res.* 86, 312-318.

Davidson, B. C., Giangregorio, A., Girao, L. A. F. (1993) The influence of c18 fatty-acids on the growth of fibroblasts of different degrees of transformation in culture. *Anticancer Res.* 13, 795-800.

DeCarlo, A. A., Grenett, H. E., & Harber, G. J. (1998) Induction of matrix metalloproteinases and a collagen-degrading phenotype in fibroblasts and epithelial cells by secreted *Porphyromonas gingivalis* proteinase. *J. Periodontal Res.* 33, 409-420.

DeMoss, J. A. & Hsu, P. Y. (1991). NarK enhances nitrate uptake and nitrite excretion in Escherichia coli. *J. Bacteriol.* 173, 3303-3310.

Deng, X., Xiao, L., Lang, W., Gao, F., Ruvolo, P., & May, W. S., Jr. (2001). Novel role for JNK as a stress-activated Bcl2 kinase. *J. Biol.Chem.* 276, 23681-23688.

Denizot, F. & Lang, R. (1986). Rapid colorimetric assay for cell growth and survival. Modifications to the tetrazolium dye procedure giving improved sensitivity and reliability. *J Immunol. Methods.* 89, 271-277.

Devary, Y., Gottlieb, R. A., Smeal, T., & Karin, M. (1992). The mammalian ultraviolet response is triggered by activation of Src tyrosine kinases. *Cell* 71, 1081-1091.

Dhaunsi, G. S. & Ozand, P. T. (2004). Nitric oxide promotes mitogen-induced DNA synthesis in human dermal fibroblasts through cGMP. *Clin. Exp. Pharmacol. Physiol.* 31, 46-49.

Dhople, A. M. (1996). *In vitro* susceptibility of Mycobacterium leprae to oxygen-mediated damage. *Microbios.* 85, 35-44.

Diegelmann, R. F. (1997). Cellular and biochemical aspects of normal and abnormal wound healing: an overview. *J. Urol.* 157, 298-302.

Dissemond, J., Goos, M., & Wagner, S. N. (2002). The role of oxidative stress in the pathogenesis and therapy of chronic wounds. *Hautarzt* 53, 718-723.

Dissemond, J., Witthoff, M., Brauns, T.C., Haberer, D., & Goos, M. (2003). pH values in chronic wounds. Evaluation during modern wound therapy. *Hautarzt* 54, 959-965.

Drath, D. B. & Karnovsky, M. L. (1975). Superoxide production by phagocytic leukocytes. *J. Exp. Med.* 141, 257-262.

Droge, W. (2002). Free radicals in the physiological control of cell function. *Physiol Rev.* 82, 47-95.

Dykhuizen, R. S., Frazer, R., Duncan, C., Smith, C. C., Golden, M., Benjamin, N., & Leifert, C. (1996). Antimicrobial effect of acidified nitrite on gut pathogens: importance of dietary nitrate in host defense. *Antimicrob. Agents Chemother.* 40, 1422-1425.

Eldad, A., Burt, A., & Clarke, J.A. (1987) Cultured epithelium as a skin substitute. *Burns.* 13, 173-180.

Elvers, K. T., Wu, G., Gilberthorpe, N. J., Poole, R. K., & Park, S. F., (2004). Role of an Inducible Single-Domain Hemoglobin in Mediating Resistance to Nitric Oxide and Nitrosative Stress in Campylobacter jejuni and Campylobacter coli. *J. Bacteriol.* 186, 5332-5341.

Enright, M. C., Day, N. P., Davies, C. E., Peacock, S. J., & Spratt, B. G. (2000). Multilocus sequence typing for characterization of methicillin-resistant and methicillin-susceptible clones of Staphylococcus aureus. *J. Clin. Microbiol.* 38, 1008-1015.

Erdmann, K., Grosser, N., & Schroder, H. (2005). L-methionine reduces oxidant stress in endothelial cells: role of heme oxygenase-1, ferritin, and nitric oxide. *AAPS.* J 7, E195-E200.

Eriksson, G., Eklund, A. E., & Kallings, L. O. (1984). The clinical significance of bacterial growth in venous leg ulcers. *Scand. J. Infect. Dis.* 16, 175-180.

Evans, T., Carpenter, A., Kinderman, H., & Cohen, J. (1993). Evidence of increased nitric oxide production in patients with the sepsis syndrome. *Circ.Shock* 41, 77-81.

Fagrell, B. (1982). Microcirculatory disturbances - the final cause for venous leg ulcers? *Vasa* 11, 101-103.

Falanga, V., Moosa, H. H., Nemeth, A. J., Alstadt, S. P., & Eaglstein, W. H. (1987). Dermal pericapillary fibrin in venous disease and venous ulceration. *Arch. Dermatol.* 123, 620-623.

Falanga, V., Qian, S. W., Danielpour, D., Katz, M. H., Roberts, A. B., & Sporn, M. B. (1991a). Hypoxia upregulates the synthesis of TGF-beta 1 by human dermal fibroblasts. *J. Invest. Dermatol.* 97, 634-637.

Falanga, V., McKenzie, A., & Eaglstein, W. H. (1991b). Heterogeneity in oxygen diffusion around venous ulcers. *J. Dermatol. Surg. Oncol.* 17, 336-339.

Falanga, V., Eaglstein, W. H., Bucalo, B., Katz, M. H., Harris, B., & Carson, P. (1992a). Topical use of human recombinant epidermal growth factor (h-EGF) in venous ulcers. *J. Dermatol. Surg. Oncol.* 18, 604-606.

Falanga, V., Kirsner, R., Katz, M. H., Gould, E., Eaglstein, W. H., & McFalls, S. (1992b). Pericapillary fibrin cuffs in venous ulceration. Persistence with treatment and during ulcer healing. *J. Dermatol. Surg. Oncol.* 18, 409-414.

Falanga, V. (1993a). Venous ulceration. *J. Dermatol. Surg. Oncol.* 19, 764-771.

Falanga, V. (1993b). Growth factors and wound healing. *J. Dermatol. Surg. Oncol.* 19, 711-714.

Falanga, V. (1993c). Chronic wounds: pathophysiologic and experimental considerations. *J. Invest Dermatol.* 100, 721-725.

Falanga, V., Martin, T. A., Takagi, H., Kirsner, R. S., Helfman, T., Pardes, J., & Ochoa, M. S. (1993). Low oxygen tension increases mRNA levels of alpha 1 (I) procollagen in human dermal fibroblasts. *J. Cell Physiol* 157, 408-412.

Falanga, V. & Eaglstein, W. H. (1993). The "trap" hypothesis of venous ulceration. *Lancet* 341, 1006-1008.

Falanga, V. & Kirsner, R .S. (1993). Low oxygen stimulates proliferation of fibroblasts seeded as single cells. *J. Cell Physiol.* 154, 506-510.

Falanga, V., Grinnell, F., Gilchrest, B., Maddox, Y. T., & Moshell, A. (1994). Workshop on the pathogenesis of chronic wounds. *J. Invest. Dermatol.* 102, 125-127.

Falanga, V., Grinnell, F., Gilchrest, B., Maddox, Y. T., & Moshell, A., (1995). Experimental approaches to chronic wounds. *Wound Rep. Reg.* 3, 132-140.

Falanga, V., Margolis, D., Alvarez, O., Auletta, M., Maggiacomo, F., & Altman, M., (1998) Rapid healing of venous ulcers and lack of clinical rejection with an allogenic cultured human skin equivalent. *Arch. Dermatol.* 134, 293-300.

Farr, S. B., & T. Kogoma. (1991). Oxidative stress responses in *Escherichia coli* and Salmonella typhimurium. *Microbiol. Rev.* 55, 561-585.

Fee, J. A. (1991). Regulation of sod genes in Escherichia coli: relevance to superoxide dismutase function. *Mol. Microbiol.* 5, 2599-2610.

Fletcher, A., Cullum, N., & Sheldon, T. A. (1997). A systematic review of compression treatment for venous leg ulcers. *BMJ.* 316, 576-580.

Flynn, J. (2003). Povidone-iodine as a topical antiseptic for treating and preventing wound infection: a literature review. *Br. J. Nurs.* 8 suppl6, S36-S42.

Frank, S., Stallmeyer, B., Kampfer, H., Kolb, N., & Pfeilschifter, J. (1999). Nitric oxide triggers enhanced induction of vascular endothelial growth factor expression in cultured keratinocytes (HaCaT) and during cutaneous wound repair. *FASEB J.* 13, 2002-2014.

Fray, M.J., Dickinson, R.P., Huggins, J.P., & Occleston, N.L. (2003). A potent, selective inhibitor of matrix metalloproteinase-3 for the topical treatment of chronic dermal ulcers. *J. Med. Chem.* 46, 3514-3525.

Fridovich, I., & Handler, P. (1962). Xanthine oxidase: V. Differential inhibition of the reduction of various electron acceptors. *J. Biol. Chem.* 237, 916-921.

Gardner, P. R., Costantino, G., Szabo, C., & Salzman, A. L. (1997). Nitric oxide sensitivity of the aconitases. *J. Biol.Chem.* 272, 25071-25076.

Garthwaite, J., Charles, S. L., & Chess-Williams, R. (1988). Endothelium-derived relaxing factor release on activation of NMDA receptors suggests role as intercellular messenger in the brain. *Nature.* 336, 385-388.

Gawkrodger, D, J (1992). Dermatology. Churchill livingstone

Gentzkow, G. D., Iwasaki, S. D., Hershon, K. S., Mengel, M., Prendergast, J. J., & Ricotta, J. J. (1996). Use of Dermagraft, a cultured human dermis, to treat diabetic foot ulcers. *Diabetes Care.* 19, 350-354.

Gilchrist, B. & Reed, C. (1989). The bacteriology of chronic venous ulcers treated with occlusive hydrocolloid dressings. *Br. J. Dermatol.* 121, 337-344.

Gilliland, E. L., Nathwani, N., Dore, C. J., & Lewis, J. D. (1988). Bacterial colonisation of leg ulcers and its effect on the success rate of skin grafting. *Ann. R. Coll. Surg. Engl.* 70, 105-108.

Godber, B. L., Doel, J. J., Durgan, J., Eisenthal, R., & Harrison, R. (2000a). A new route to peroxynitrite: a role for xanthine oxidoreductase. *FEBS Letters.* 475, 93-96.

Godber, B. L., Doel, J. J., Sapkota, G. P., Blake, D. R., Stevens, C. R., Eisenthal, R., & Harrison, R. (2000b). Reduction of nitrite to nitric oxide catalyzed by xanthine oxidoreductase. *J. Biol. Chem.* 275, 7757-7763.

Gold, H. S. & Moellering, R. C., Jr. (1996). Antimicrobial-drug resistance. *N. Engl. J. Med.* 335, 1445-1453.

Gordillo, G. M. & Sen, C. K. (2003). Revisiting the essential role of oxygen in wound healing. *Am. J. Surg.* 186, 259-263.

Gort, A. S. & Imlay, J. A. (1998). Balance between endogenous superoxide stress and antioxidant defenses. *J. Bacteriol.* 180, 1402-1410.

Gossrau, R. F., Frederiks, W. M., & Van Noorden, C. J. (1990) Histochemistry of reactive oxygen species (ROS)-generating oxidases in cutaneous and mucous epithelia of laboratory rodents with special reference to xanthine oxidase. *Histochemistry.* 94, 539-544.

Gough, A., Clapperton, M., Rolando, N., Foster, A. V. M., Philpott-Howard, J., & Edmonds, M. E. (1997). Randomised placebo-controlled trial of granulocyte-colony stimulating factor in diabetic foot infection. *Lancet.* 350, 833-859.

Gould, L.J., Yager, D. R., Cohen, I. K., & Diagelmann, R. F. (1997). *In vitro* analysis of fetal fibroblast collagenotytic activity. *Wound. Rep. Reg.* 5, 151-158.

Gratzner, H. G. (1982). Monoclonal antibody to 5-bromo- and 5-iododeoxyuridine: A new reagent for detection of DNA replication. *Science.* 218, 474-475.

Green, D.E., & Pauli, R. (1943). The antibacterial action of the xanthine oxidase system. *Proceedings of the Society for Experimental Biology and Medicine.* 54, 148-150.

Green, L. C., Ruiz, d. L., Wagner, D. A., Rand, W., Istfan, N., Young, V. R., & Tannenbaum, S. R. (1981). Nitrate biosynthesis in man. *Proc.Natl.Acad.Sci.U.S.A.* 78, 7764-7768.

Grinnell, F. (1984). Fibronectin and wound healing. *J. Cell. Biochem.* 26, 107-116.

Grinnell, F., Ho, C. H., & Wysocki, A. (1992). Degradation of fibronectin and vitronectin in chronic wound fluid: analysis by cell blotting, immunoblotting, and cell adhesion assays. *J. Invest Dermatol.* 98, 410-416.

Grinnell, F. (1994). Fibroblasts, myofibroblasts, and wound contraction. *J. Cell Biol.* 124, 401-404.

Grinnell, F., & Zhu, M., (1996). Fibronectin degradation in chronic wounds depends on the relative levels of elastase, α_1-proteinase inhibitor, and α_2-macroglobulin. *J. Invest. Dermatol.* 106, 335-341.

Guest, M., Smith, J. J., Sira, M. S., Madden, P., Greenhalgh, R. M., & Davies, A. H. (1999). Venous ulcer healing by four-layer compression bandaging is not influenced by the pattern of venous incompetence. *Br. J Surg.* 86, 1437-1440.

Guyton, K. Z., Liu, Y., Gorospe, M., Xu, Q., & Holbrook, N. J. (1996). Activation of mitogen-activated protein kinase by H2O2. Role in cell survival following oxidant injury. *J Biol. Chem.* 271, 4138-4142.

Haenen, G., Paquay, J.B., Korlhouwer, R.E., & Bast, A. (1997) Peroxynitrite scavenging by flavonoids. *Biochem. Biophys. Res. commun.* 236, 591-593

Haining, J.L., & Legan, J.S. (1967). Fluorometric assay for xanthine oxidase. *Analytical Biochemistry.* 21, 337-343.

Halbert, A. R., Stacey, M. C., Rohr, J. B., & Jopp-McKay, A. (1992). The effect of bacterial colonization on venous ulcer healing. *Australas. J Dermatol.* 33, 75-80.

Halliwell, B. & Whiteman, M. (2004). Measuring reactive species and oxidative damage *In vivo* and in cell culture: how should you do it and what do the results mean? *Br. J Pharmacol.* 142, 231-255.

Hampton, M. B., Kettle, A. J., & Winterbourn, C. C. (1998). Inside the neutrophil phagosome: oxidants, myeloperoxidase, and bacterial killing. *Blood* 92, 3007-3017.

Han, M. J., Kim, B. Y., Yoon, S. O., & Chung, A. S. (2003). Cell proliferation induced by reactive oxygen species is mediated via mitogen-activated protein kinase in Chinese hamster lung fibroblast (V79) cells. *Mol. Cells* 15, 94-101.

Han, Y., Tuan, T., Wu, H., Hughes, M., and Garner, W.L (2000). TNF-α stimulates activation of pro-MMP2 in human skin through NF-κB mediated induction of MT1-MMP. *Journal of Cell Science.* 114, 131-139.

Hancock, J.T. (1999). Nitric oxide, hydrogen peroxide, and carbon monoxide. In *Cell Signalling.* pp 167-184. Addison Wesley Longman Limited, England, UK.

Hancock, J. T., Salisbury, V., Ovejero-Boglione, M. C., Cherry, R., Hoare, C., Eisenthal, R., & Harrison, R. (2002). Antimicrobial properties of milk: dependence on presence of xanthine oxidase and nitrite. *Antimicrob. Agents Chemother.* 46, 3308-3310.

Hansson, C., Hoborn, J., Moller, A., & Swanbeck, G. (1995). The microbial flora in venous leg ulcers without clinical signs of infection. Repeated culture using a validated standardised microbiological technique. *Acta Derm. Venereol.* 75, 24-30.

Harding, K. G., Morris, H. L., & Patel, G. K. (2002). Science, medicine and the future: healing chronic wounds. *BMJ* 324, 160-163.

Harrington, C., Zagari, M. J., Corea, J., & Klitenic, J. (2000). A cost analysis of diabetic lower-extremity ulcers. *Diabetes Care* 23, 1333-1338.

Harrison, R. (2002) Structure and function of xanthine oxidoreductase: Where are we now? *Free Radical Biology and Medicine.* 33, 774-797.

Harrison, J. W. & Svec, T. A. (1998). The beginning of the end of the antibiotic era? Part I. The problem: abuse of the "miracle drugs". *Quintessence. Int.* 29, 151-162.

Harrison-Balestra, C., Eaglstein, W. H., Falabela, A. F., & Kirsner, R. S. (2002). Recombinant human platelet-derived growth factor for refractory nondiabetic ulcers: a retrospective series. *Dermatol. Surg.* 28, 755-759.

Hasan, A., Murata, H., Falabella, A., Ochoa, S., Zhou, L., Badiavas, E., and Falanga, V. (1997). Dermal fibroblasts from venous ulcers are unresponsive to the action of transforming growth factor-beta 1. *J. Dermatol. Sci.* 16, 59-66.

Hausladen, A., Gow, A. J., & Stamler, J. S. (1998). Nitrosative stress: metabolic pathway involving the flavohemoglobin. *Proc. Natl. Acad. Sci. USA* 95, 14100-14105.

Hawkey, P. M. (1998). The origins and molecular basis of antibiotic resistance. *BMJ* 317, 657-660.

Hayflick L, Moorhead PS. (1961) The serial cultivation of human diploid cell strains. *Exp. Cell Res.* 25, 585-621.

He, Z., Ong, C.H., Halper, J., & Bateman, A. (2003). Progranulin is a mediator of the wound response. *Nat. Med.* 9, 225-229.

Heck, D. E., Laskin, D. L., Gardner, C. R., & Laskin, J. D. (1992). Epidermal growth factor suppresses nitric oxide and hydrogen peroxide production by keratinocytes. Potential role for nitric oxide in the regulation of wound healing. *J. Biol. Chem.* 267, 21277-21280.

Heiden, M., Seitz, R., & Egbring, R. (1996). The role of inflammatory cells and their proteases in extravascular fibrinolysis. *Semin. Thromb. Hemost.* 22, 497-501.

Helfman, T. & Falanga,V. (1993). Gene expression in low oxygen tension. *Am. J. Med. Sci.* 306, 37-41.

Henke, P. K., Bergamini, T. M., Watson, A. L., Brittian, K. R., Powell, D. W., & Peyton, J. C. (1998). Bacterial products primarily mediate fibroblast inhibition in biomaterial infection. *J. Surg. Res.* 74, 17-22.

Herouy, Y., May, A. E., Pornschlegel, G., Stetter, C., Grenz, H., Preissner, K. T., Schopf, E., Norgauer, J., & Vanscheidt, W. (1998). Lipodermatosclerosis is characterized by elevated expression and activation of matrix metalloproteinases: implications for venous ulcer formation. *J Invest. Dermatol* 111, 822-827.

Herrick, S.E., Ashcroft, G., Ireland, G., Horan, M., McCollum,C., & Ferguson,M. (1997). Up-regulation of elastase in acute wounds of healthy aged humans and chronic venous leg ulcers are associated with matrix degradation. *Lab. Invest.* 77, 281-288.

Herrick, S.E., Ireland, G.W., Simon, D., McCollum, C.N., & Ferguson, M.W. (1996). Venous ulcer fibroblasts compared with normal fibroblasts show differences in collagen but not fibronectin production under both normal and hypoxic conditions. *J. Invest Dermatol.* 106, 187-193.

Hewinson, J. (2005) Vascular endothelial release of xanthine oxidoreductase. *Doctoral Dissertation. University of Bath,* UK.

Hibbs, J. B., Jr., Taintor, R. R., & Vavrin, Z. (1987). Macrophage cytotoxicity: role for L-arginine deiminase and imino nitrogen oxidation to nitrite. *Science* 235, 473-476.

Hidalgo, E. & Dominguez, C. (1998). Study of cytotoxicity mechanisms of silver nitrate in human dermal fibroblasts. *Toxicol. Lett.* 98, 169-179.

Higley, H.R., Ksander, G.A., Gerhardt, C.O., and Falanga, V. (1995). Extravasation of macromolecules and possible trapping of transforming growth factor-β in venous ulceration. *British J. Dermatol.* 132, 79-85.

Hille, R. (1996). The mononuclear molybdenum enzymes. *Chem Rev 96*, 2757-816.

Hiramatsu, K., Hanaki, H., Ino, T., Yabuta, K., Oguri, T., & Tenover, F. C. (1997). Methicillin-resistant Staphylococcus aureus clinical strain with reduced vancomycin susceptibility. *J Antimicrob. Chemother.* 40, 135-136.

Holt, D., Kirk, S.J., Regan, M.C., Hurson, M., Lindblad, W.J., and Barbul, A. (1992) Effect of age on wound healing in healthy humans. *Surgery.* 112, 293-298.

Hooper, D. C., Bagasra, O., Marini, J. C., Zborek, A., Ohnishi, S. T., Kean, R., Champion, J. M., Sarker, A. B., Bobroski, L., Farber, J. L., Akaike, T., Maeda, H., & Koprowski, H. (1997). Prevention of experimental allergic encephalomyelitis by targeting nitric oxide and peroxynitrite: implications for the treatment of multiple sclerosis. *Proc. Natl. Acad. Sci. U.S.A.* 94, 2528-2533.

Horobin, A.J., Shakesheff, K.M., Woodrow, S., Robinson, C., and Pritchard, D.I. (2003). Maggots and wound healing: an investigation of the effects of secretions from Lucilia sericata larvae upon interactions between human dermal fibroblasts and extracellular matrix components. *Br. J. Dermatol.* 148, 923-933.

Houston, M., Estevez, A., Chumley, P., Aslan, M., Marklund, S., Parks, D. A., & Freeman, B. A. (1999). Binding of xanthine oxidase to vascular endothelium. Kinetic characterization and oxidative impairment of nitric oxide-dependent signaling. *J. Biol. Chem.* 274, 4985-4994.

Howard, E.W., Bullen, E.C., and Banda, M.J. (1991). Preferential inhibition of 72- and 92-kDa gelatinases by tissue inhibitor of metalloproteinase-2. *J. Biol. Chem.* 266, 13070-13075.

Howell-Jones, R. S., Wilson, M. J., Hill, K. E., Howard, A. J., Price, P. E., & Thomas, D. W. (2005). A review of the microbiology, antibiotic usage and resistance in chronic skin wounds. *J Antimicrob.Chemother.* 55, 143-149.

Huie, R.E., & Padmaja, S. (1993). The reaction of NO with superoxide. *Free Radical Research Communications.* 18, 195-199.

Hughes, M., and Nicklin, H.G., (1968) The chemistry of pernitrites. Part I. Kinetics of decomposition of pernitrous acid. *J. chem. Soc.* A, 450-452.

Inoue, H., Hisamatsu, K., Ando, K., Ajisaka, R., & Kumagai, N. (2002). Determination of nitrotyrosine and related compounds in biological specimens by competitive enzyme immunoassay. *Nitric. Oxide.* 7, 11-17.

Iocono, J.A, Krummel, T.M., Keefer, K.A., Allison, G.M., Paul, H. (1998) Repeated additions of hyaluronan alters granulation tissue deposition in sponge implants in mice. *Wound Repair Regen.* 6, 442-8.

Irani, K., Xia, Y., Zweier, J. L., Sollott, S. J., Der, C. J., Fearon, E. R., Sundaresan, M., Finkel, T., & Goldschmidt-Clermont, P. J. (1997). Mitogenic signaling mediated by oxidants in Ras-transformed fibroblasts. *Science* 275, 1649-1652.

Ischiropoulos, H., Zhu, L., & Beckman, J. S. (1992). Peroxynitrite formation from macrophage-derived nitric oxide. *Arch. Biochem. Biophys.* 298, 446-451.

Jawetz, E., Melnick, J.L., & Adelberg, E.A. (1984). Review of Medical Microbiology (Lange Medical Publishing, Los Altos, CA)

Jeng, H.L., Chan, C.P., Ho, Y.S. (1999). Effects of butyrate and propionate on the adhesion, growth, cell cycle kinetics, and protein synthesis of cultured human gingival fibroblasts. *J Peridontol.* 70, 1435-1442.

Jones, C. E., Crowell, J. W., & Smith, E. E. (1968). Significance of increased blood uric acid following extensive hemorrhage. *Am. J. Physiol* 214, 1374-1377.

Kamata, H. & Hirata, H. (1999). Redox regulation of cellular signalling. *Cell Signal.* 11, 1-14.

Kan, C., Abe, M., Yamanaka, M., & Ishikawa, O. (2003). Hypoxia-induced increase of matrix metalloproteinase-1 synthesis is not restored by reoxygenation in a three-dimensional culture of human dermal fibroblasts. *J. Dermatol. Sci.* 32, 75-82.

Kannel, W.B. (1985). Lipids, diabetes, and coronary heart disease: insights from the Framingham *Study. Am. Heart J.* 110, 1100-1107.

Karnovsky, M. L., Lazdins, J., Drath, D., & Harper, A. (1975). Biochemical characteristics of activated macrophages. *Ann. N. Y. Acad. Sci.* 256, 266-274

Katz, M. H., Alvarez, A. F., Kirsner, R. S., Eaglstein, W. H., & Falanga, V. (1991). Human wound fluid from acute wounds stimulates fibroblast and endothelial cell growth. *J Am. Acad. Dermatol* 25, 1054-1058.

Kayyali, U. S., Donaldson, C., Huang, H., Abdelnour, R., & Hassoun, P. M. (2001). Phosphorylation of xanthine dehydrogenase/oxidase in hypoxia. *J Biol. Chem.* 276, 14359-14365.

Keefer, L. K., Flippen-Anderson, J. L., George, C., Shanklin, A. P., Dunams, T. M., Christodoulou, D., Saavedra, J. E., Sagan, E. S., & Bohle, D. S. (2001). Chemistry of the diazeniumdiolates. I. Structural and spectral characteristics of the [N(O)NO]- functional group. *Nitric. Oxide.* 5, 377-394.

Keen, H. & Jarrett, R.J. (1979). The WHO multinational study of vascular disease in diabetes: 2. Macrovascular disease prevalence. *Diabetes Care* 2, 187-195.

Khorramizadeh, M. R., Tredget, E. E., Telasky, C., Shen, Q., & Ghahary, A. (1999). Aging differentially modulates the expression of collagen and collagenase in dermal fibroblasts. *Mol. Cell Biochem.* 194, 99-108.

Kilcullen, J.K., Ly, Q.P., Chang, T.H. (1998) Nonviable *Staphylococcus aureus* and its peptidoglycan stimulate macrophage recruitment angiogenesis, fibroplasias, and collagen accumulation in wounded rats. *Wound Rep. Regen.* 6, 149-156.

Kim, B. Y., Han, M. J., & Chung, A. S. (2001). Effects of reactive oxygen species on proliferation of Chinese hamster lung fibroblast (V79) cells. *Free Radic. Biol. Med.* 30, 686-698.

Kingston, D. & Seal, D. V. (1990). Current hypotheses on synergistic microbial gangrene. *Br. J Surg.* 77, 260-264.

Kisker, C., Schindelin, H., and Rees, D.C. (1997) Molybdenum-cofactor-containing enzymes: structure and mechanism. *Annu. Rev. Biochem.* 66, 233-267.

Kitahama, A., Elliott, L.F., Kerstein, M.D., and Menendez, C.V. (1982). Leg ulcer. Conservative management or surgical treatment? *JAMA* 247, 197-199.

Kontiainen, S. & Rinne, E. (1988). Bacteria in decubitus ulcers. *Infection* 16, 305.

Kooy, N. W., Royall, J. A., Ischiropoulos, H., & Beckman, J. S. (1994). Peroxynitrite-mediated oxidation of dihydrorhodamine 123. *Free Radic.Biol.Med.* 16, 149-156.

Koppenol, W. H., Kissner, R., & Beckman, J. S. (1996). Syntheses of peroxynitrite: to go with the flow or on solid grounds? *Methods Enzymol.* 269, 296-302.

Korhonen, H. J. & Reiter, B. 1983. Production of H2O2 by bovine blood and milk polymorphonuclear leucocytes. Acta Microbiol.Pol. 32, 53-64.

Kourembanas, S., Marsden, P.A., McQuillan, L.P., and Faller, D.V. (1991). Hypoxia induces endothelin gene expression and secretion in cultured human endothelium. *J. Clin. Invest.* 88, 1054-1057.

Krischel, V., Bruch-Gerharz, D., Suschek, C., Kroncke, K.D., Ruzicka, T., and Kolb-Bachofen, V. (1998). Biphasic effect of exogenous nitric oxide on proliferation and differentiation in skin derived keratinocytes but not fibroblasts. *J. Invest. Dermatol.* 111, 286-291.

Krishnaswami, S., Ly, Q. P., Rothman, V. L., & Tuszynski, G. P. (2002). Thrombospondin-1 promotes proliferative healing through stabilization of PDGF. *J Surg. Res.* 107, 124-130.

Kuroda, M., Ohta, T., Uchiyama, I., Baba, T., Yuzawa, H., Kobayashi, I., Cui, L., Oguchi, A., Aoki, K., Nagai, Y., Lian, J., Ito, T., Kanamori, M., Matsumaru, H., Maruyama, A., Murakami, H., Hosoyama, A., Mizutani-Ui, Y., Takahashi, N. K., Sawano, T., Inoue, R., Kaito, C., Sekimizu, K., Hirakawa, H., Kuhara, S., Goto, S., Yabuzaki, J., Kanehisa, M., Yamashita, A., Oshima, K., Furuya, K., Yoshino, C., Shiba, T., Hattori, M., Ogasawara, N., Hayashi, H., & Hiramatsu, K. (2001). Whole genome sequencing of meticillin-resistant Staphylococcus aureus. *Lancet* 357, 1225-1240.

Kyriakis, J. M. & Avruch, J. (2001). Mammalian mitogen-activated protein kinase signal transduction pathways activated by stress and inflammation. *Physiol. Rev.* 81, 807-869.

Landmesser, U., Dikalov, S., Price, S. R., McCann, L., Fukai, T., Holland, S. M., Mitch, W. E., & Harrison, D. G. (2003). Oxidation of tetrahydrobiopterin leads to uncoupling of endothelial cell nitric oxide synthase in hypertension. *J Clin. Invest.* 111, 1201-1209.

Langer, R. and Vacanti, J.P. (1993). Tissue engineering. *Science* 260, 920-926.

Larjava, H., Vitto, V., Eerola, E. (1987). Inhibition of gingival fibroblast growth by *Bacteroides gingivalis.* Infect. Immun. 55, 201-205.

Laskey, R. A., Fairman, M. P., & Blow, J. J. (1989). S phase of the cell cycle. *Science.* 246, 609-614.

LeBel, C. P., Ischiropoulos, H., & Bondy, S. C. (1992). Evaluation of the probe 2',7'-dichlorofluorescin as an indicator of reactive oxygen species formation and oxidative stress. *Chem. Res. Toxicol.* 5, 227-231.

Lee,P.C., Salyapongse,A.N., Bragdon,G.A., Shears,L.L., Watkins,S.C., Edington,H.D., and Billiar,T.R. (1999). Impaired wound healing and angiogenesis in eNOS-deficient mice. *Am. J. Physiol* 277, 1600-1608.

LeGrand,E.K. (1998). Preclinical promise of becaplermin (rhPDGF-BB) in wound healing. *Am. J. Surg.* 176, 48S-54S.

Lenski, R. E. (1997). The cost of antibiotic resistance--from the perspective of a bacterium. *Ciba Found.Symp.* 207, 131-140.

LeRoy, E. C., Trojanowska, M. I., & Smith, E. A. (1990). Cytokines and human fibrosis. *Eur.Cytokine Netw.* 1, 215-219.

Letzelter, C., Croute, F., Pianezzi, B., Roques, C., Soleilhavoup, J. P. (1998). Supernatant cytotoxicity and proteolytic activity of selected oral bacteria against human gingival fibroblasts *in vitro. Arch. Oral Biol.* 43, 15-23

Levin, B. R., Lipsitch, M., Perrot, V., Schrag, S., Antia, R., Simonsen, L., Walker, N. M., & Stewart, F. M. (1997). The population genetics of antibiotic resistance. *Clin.Infect.Dis.* 24 Suppl 1, S9-16.

Levy, S. (1994). Balancing the drug resistance equation. *Trends Microbiol* 2, 341-43.

Li, H., Samouilov, A., Liu, X., & Zweier, J. L. (2003). Characterization of the magnitude and kinetics of xanthine oxidase-catalyzed nitrate reduction: evaluation of its role in nitrite and nitric oxide generation in anoxic tissues. *Biochemistry* 42, 1150-1159.

Lindan, O., Greenway, R. M., & Piazza, J. M. (1965). Pressure distribution on the surface of the human body. 1. Evaluation in lying and sitting positions using a ''bed of springs and nails''. *Arch. Phys. Med. Rehabil.* 46, 378-385.

Liu, X., Lin, W. M., Yan, X. H., Chen, X. H., Hoidal, J. R., & Xu, P. (2003). Improved method for measurement of human plasma xanthine oxidoreductase activity. *J. Chromatogr. B Analyt. Technol. Biomed. Life Sci.* 785, 101-114.

Long, R., Light, B., & Talbot, J. A. (1999). Mycobacteriocidal action of exogenous nitric oxide. *Antimicrob. Agents Chemother.* 43, 403-405.

Louie, J.T., Bartlett, J.G., Tally, F.P. (1976) Aerobic and anaerobic bacteria in diabetic foot ulcers. *Ann. Intern. Med.* 85, 461-463.

Lowe, D. J., Lynden-Bell, R. M., & Bray, R. C. (1972). Spin-spin interaction between molybdenum and one of the iron-sulphur systems of xanthine oxidase and its relevance to the enzymic mechanism. *Biochem. J* 130, 239-249.

Lowry, O.H., Bessey, O.A., & Crawford, E.J. (1949). Pterine Oxidase. *Journal of Biological Chemistry*. 180, 399-410.

Luczak, K., Balcerczyk, A., Soszynski, M., & Bartosz, G. (2004). Low concentration of oxidant and nitric oxide donors stimulate proliferation of human endothelial cells *in vitro*. *Cell Biol.Int.* 28, 483-486.

Lum, H. & Roebuck, K. A. (2001). Oxidant stress and endothelial cell dysfunction. *Am.J Physiol Cell Physiol* 280, C719-C741.

Lundberg, B. E., Wolf, R. E., Jr., Dinauer, M. C., Xu, Y., & Fang, F. C. (1999). Glucose 6-phosphate dehydrogenase is required for Salmonella typhimurium virulence and resistance to reactive oxygen and nitrogen intermediates. *Infect.Immun.* 67, 436-438.

MacMillan-Crow, L. A., Crow, J. P., & Thompson, J. A. (1998). Peroxynitrite-mediated inactivation of manganese superoxide dismutase involves nitration and oxidation of critical tyrosine residues. *Biochemistry* 37, 1613-1622.

Madsen, S. M., Westh, H., Danielsen, L., & Rosdahl, V. T. (1996). Bacterial colonization and healing of venous leg ulcers. *APMIS 1*04, 895-899.

Maragos, C.M., Morley, D., Wink, D.A., Dunams, T.M., Saavedra, J.E., Hoffman, A., Bove, A.A., Isaac, L., Hrabie, J.A., and Keefer, L.K. (1991). Complexes of .NO with nucleophiles as agents for the controlled biological release of nitric oxide. *Vasorelaxant effects. J. Med. Chem. 34*, 3242-3247.

Marletta, M. A., Hurshman, A. R., & Rusche, K. M. (1998). Catalysis by nitric oxide synthase. *Curr.Opin.Chem.Biol.* 2, 656-663.

Marinkovich, M.P., Keene, D.R., Rimberg, C.S., and Burgeson, R.E. (1993). Cellular origin of the dermal-epidermal basement membrane. *Dev. Dyn. 197*, 255-267.

Markley, H.G., Faillace, L.A., & Mezey, E. (1973). Xanthine oxidase activity in rat brain. *Biochimica et Biophysica Acta.* 309, 23-31.

Martin, T. A., Hilton, J., Jiang, W. G., & Harding, K. (2003). Effect of human fibroblast-derived dermis on expansion of tissue from venous leg ulcers. *Wound. Repair Regen.* 11, 292-296.

Massey, V. (1959). The microestimation of succinate and the extinction coefficient of cytochrome c. *Biochim. Biophys. Acta* 34, 255-256.

Massey, V., Komai, H., Palmer, G., & Elion, G. B. (1970). On the mechanism of inactivation of xanthine oxidase by allopurinol and other pyrazolo[3,4-d]pyrimidines. *J. Biol. Chem.* 245, 2837-2844.

Mast, B A. & Schultz, G S. (1996) Interactions of cytokines, growth factors, and proteases in acute and chronic wounds. *Wound. Repair Regen.* 4, 411-420.

Masters, K.S., Leibovich, S.J., Belem, P., West, J.L., & Poole-Warren, L.A. (2002). Effects of nitric oxide releasing poly(vinyl alcohol) hydrogel dressings on dermal wound healing in diabetic mice. *Wound. Repair Regen.* 10, 286-294.

Mauch, C. & Kreig, T. (1990). Fibroblast-matrix interactions and their role in the pathogenesis of fibrosis. *Rheum. Dis. Clin. North Am.* 16, 93-107.

McCord, J.M., & Fridovich, I., (1968) The reduction of cytochrome c by milk Xanthine Oxidase. *The Journal of Biological Chemistry.* 243, 5753-5760.

McCord, J.M., & Fridovich, I. (1969). Superoxide dismutase an enzymic function for erythrocuprein (hemocuprein). *The Journal of Biological Chemistry.* 244, 6049-6055.

McCord, J.M. (1985). Oxygen-derived free radicals in postischemic tissue injury. *N. Engl. J. Med.* 312, 159-163.

McCormick, M. L., Buettner, G. R., & Britigan, B. E. (1998). Endogenous superoxide dismutase levels regulate iron-dependent hydroxyl radical formation in Escherichia coli exposed to hydrogen peroxide. *J. Bacteriol.* 180, 622-625.

McKelvey, T. G., Hollwarth, M. E., Granger, D. N., Engerson, T. D., Landler, U., & Jones, H. P. (1988). Mechanisms of conversion of xanthine dehydrogenase to xanthine oxidase in ischemic rat liver and kidney. *Am. J. Physiol.* 254, G753-G760.

Mendez, M.V., Stanley, A., Park, H.Y., Shon, K., and Philips, T. (1998). Fibroblasts cultured from venous ulcers display cellular characteristics of senescence. *J.Vasc. Surg.* 28, 876-883.

Menon, G.K. (2002). New insights into skin structure: scratching the surface. Adv. Drug Deliv. Rev. 54, S3-17.

Millar, T. M., Stevens, C. R., & Blake, D. R. (1997). Xanthine oxidase can generate nitric oxide from nitrate in ischaemia. *Biochem. Soc. Trans.* 25, 528S.

Millar, T.M., Stevens, C.R., Benjamin, N., Eisenthal, R., Harrison, R., and Blake, D.R. (1998). Xanthine oxidoreductase catalyses the reduction of nitrates and nitrite to nitric oxide under hypoxic conditions. *FEBS Letters.* 427, 225-228.

Millar, T.M. (1999). Novel aspects of the function and activity of xanthine oxidase. *Doctoral Dissertation.* University of Bath, UK.

Millar, T. M., Kanczler, J. M., Bodamyali, T., Blake, D. R., & Stevens, C. R. (2002). Xanthine oxidase is a peroxynitrite synthase: newly identified roles for a very old enzyme. *Redox.Rep.* 7, 65-70.

Millar, T. M. (2004). Peroxynitrite formation from the simultaneous reduction of nitrite and oxygen by xanthine oxidase. *FEBS Lett.* 562, 129-133.

Miller, E.J., Harris, E.D., Jr., Chung, E., Finch, J.E., Jr., McCroskery, P.A., and Butler, W.T. (1976). Cleavage of Type II and III collagens with mammalian collagenase: site of cleavage and primary structure at the NH2-terminal portion of the smaller fragment released from both collagens. *Biochemistry* 15, 787-792.

Miller, R. A. & Britigan, B. E. (1997). Role of oxidants in microbial pathophysiology. *Clin. Microbiol. Rev.* 10, 1-18.

Moellering, R. C., Jr. (1995). Past, present, and future of antimicrobial agents. *Am.J Med.* 99, 11S-18S.

Molan, P. C. (2001). Potential of honey in the treatment of wounds and burns. *Am. J. Clin. Dermatol.* 2, 13-19.

Moosa, H. H., Falanga, V., Steed, D. L., Makaroun, M. S., Peitzman, A. B., Eaglstein, W. H., and Webster, M. W. (1987). Oxygen diffusion in chronic venous ulceration. *J. Cardiovasc. Surg.* (Torino) 28, 464-467.

Morel, F., Doussiere, J., & Vignais, P. V. (1991). The superoxide-generating oxidase of phagocytic cells. Physiological, molecular and pathological aspects. *Eur. J Biochem.* 201, 523-546.

Morrell, C. J., Walters, S. J., Dixon, S., Collins, K. A., Brereton, L. M., Peters, J., & Brooker, C. G. (1998). Cost effectiveness of community leg ulcer clinics: randomised controlled trial. *BMJ* 316, 1487-1491.

Mossman, T. (1983). Rapid colrimetric assay for cellular growth and survival: application to proliferation and cytotoxicity assays. *J. Immunol. Methods* 65, 55-63.

Most, R.S. and Sinnock, P. (1983). The epidemiology of lower extremity amputations in diabetic individuals. *Diabetes Care* 6, 87-91.

Motohashi, N. & Saito, Y. (2002). Induction of SOS response in Salmonella typhimurium TA4107/pSK1002 by peroxynitrite-generating agent, N-morpholino sydnonimine. *Mutat. Res.* 502, 11-18.

Moulin, V. (1995). Growth factors in skin wound healing. *Eur. J Cell Biol.* 68, 1-7.

Mulder, G.D. and Vande Berg, J.S. (2002). Cellular senescence and matrix metalloproteinase activity in chronic wounds. Relevance to debridement and new technologies. *J. Am. Podiatr. Med. Assoc.* 92, 34-37.

Murphy, G., McAlpine, C.G., Poll, C.T., and Reynolds, J.J. (1985). Purification and characterization of a bone metalloproteinase that degrades gelatin and types IV and V collagen. *Biochim. Biophys. Acta* 831, 49-58.

Murrell, G.A., Francis, M.J., and Bromley, L. (1990). Modulation of fibroblast proliferation by oxygen free radicals. *Biochem. J.* 265, 659-665.

Murray, B. E. (1994). Can antibiotic resistance be controlled? *N.Engl.J Med.* 330, 1229-1230.

Nakamura, M. (1991). Allopurinol-insensitive oxygen radical formation by milk xanthine oxidase systems. *J Biochem.(Tokyo)* 110, 450-456.

Nelzen, O., Bergqvist, D., & Lindhagen, A. (1994). Venous and non-venous leg ulcers: clinical history and appearance in a population study. *Br.J Surg.* 81, 182-187.

Nelzen, O., Bergqvist, D., & Lindhagen, A. (1997). Long-term prognosis for patients with chronic leg ulcers: a prospective cohort study. *Eur. J Vasc. Endovasc. Surg.* 13, 500-508.

Nicas, T. I., Wu, C. Y., Hobbs, J. N., Jr., Preston, D. A., & Allen, N. E. (1989). Characterization of vancomycin resistance in Enterococcus faecium and Enterococcus faecalis. *Antimicrob. Agents Chemother.* 33, 1121-1124.

Nicco, C., Laurent, A., Chereau, C., Weill, B., & Batteux, F. (2005). Differential modulation of normal and tumor cell proliferation by reactive oxygen species. *Biomed. Pharmacother.* 59, 169-174.

Niinikoski, J., Hunt, T.K., and Dunphy, J.E. (1972). Oxygen supply in healing tissue. *Am. J. Surg.* 123, 247-252.

Novogrodsky, A., Ravid, A., Rubin, A. L., & Stenzel, K. H. (1982). Hydroxyl radical scavengers inhibit lymphocyte mitogenesis. *Proc. Natl. Acad. Sci.U.S.A* 79, 1171-1174.

Nunoshiba, T., Hidalgo, E., Amabile Cuevas, C. F., & Demple, B. (1992). Two-stage control of an oxidative stress regulon: the Escherichia coli SoxR protein triggers redox-inducible expression of the soxS regulatory gene. *J Bacteriol.* 174, 6054-6060.

Nunoshiba, T., DeRojas-Walker, T., Tannenbaum, S. R., & Demple, B. (1995). Roles of nitric oxide in inducible resistance of Escherichia coli to activated murine macrophages. *Infect.Immun.* 63, 794-798.

Nunoshiba, T. (1996). Two-stage gene regulation of the superoxide stress response soxRS system in Escherichia coli. *Crit Rev.Eukaryot.Gene Expr.* 6, 377-389.

O'Kane, S., and Ferguson, M.W.J. (1997). Transforming growth factor βs and wound healing. Int *J. Biochem. Cell Biol.* 29, 63-78.

Okado-Matsumoto, A. & Fridovich, I. (2001). Assay of superoxide dismutase: cautions relevant to the use of cytochrome c, a sulfonated tetrazolium, and cyanide. *Anal.Biochem.* 298, 337-342.

Oku, T., Takigawa, M., & Yamada, M. (1987). Cell proliferation kinetics of cultured human keratinocytes and fibroblasts measured using a monoclonal antibody. *Br. J Dermatol* 116, 673-679.

Ollendorf, D. A., Kotsanos, J. G., Wishner, W. J., Friedman, M., Cooper, T., Bittoni, M., & Oster, G. (1998). Potential economic benefits of lower-extremity amputation prevention strategies in diabetes. *Diabetes Care* 21, 1240-1245.

Olofsson, B., Ljunghall, K., Nordin-Bjorklund, K., Sorensen, S., & Leppert, J. (1996). [Two therapeutic models in venous leg ulcers are compared: better results with optimized compression]. *Lakartidningen* 93, 4752-4754.

Onimaru,M., Yonemitsu,Y., Tanii,M., Nakagawa,K., Masaki,I., Okano,S., Ishibashi,H., Shirasuna,K., Hasegawa,M., and Sueishi,K. (2002). Fibroblast growth factor-2 gene transfer can stimulate hepatocyte growth factor expression irrespective of hypoxia-mediated downregulation in ischemic limbs. *Circ. Res.* 91, 923-930.

Pabst, M. J., Hedegaard, H. B., & Johnston, R. B., Jr. (1982). Cultured human monocytes require exposure to bacterial products to maintain an optimal oxygen radical response. *J Immunol.* 128, 123-128.

Palmer, G., Bray,R.C., and Beinert,H. (1964). Direct studies on the electron transfer sequence in xanthine oxidase by electron paramagnetic resonance spectroscopy. Techniques and description of spectra. *J. Biol. Chem.* 239, 2667.

Palmer, R. M., Ferrige, A. G., & Moncada, S. (1987). Nitric oxide release accounts for the biological activity of endothelium-derived relaxing factor. *Nature* 327, 524-526.

Palolahti, M., Lauharanta, J., Stephens, R.W., Kuusela, P., & Vaheri, A. (1993). Proteolytic activity in leg ulcer exudate. *Exp. Dermatol.* 2, 29-37.

Panchenko, M. V., Farber, H. W., & Korn, J. H. (2000). Induction of heme oxygenase-1 by hypoxia and free radicals in human dermal fibroblasts. *Am. J. Physiol. Cell. Physiol.* 278, C92-C101.

Pani, G., Colavitti, R., Bedogni, B., Anzevino, R., Borrello, S., & Galeotti, T. (2000). A redox signaling mechanism for density-dependent inhibition of cell growth. *J Biol.Chem.* 275, 38891-38899.

Pardee, A. B. (1989). G1 events and regulation of cell proliferation. *Science* 246, 603-608.

Parks, D. A. & Granger, D. N. (1986). Xanthine oxidase: biochemistry, distribution and physiology. *Acta Physiol Scand. Suppl* 548, 87-99.

Parks, D. A. & Granger, D. N. (1988). Ischemia-reperfusion injury: a radical view. *Hepatology* 8, 680-682.

Parks, D. A., Williams, T. K., & Beckman, J. S. (1988). Conversion of xanthine dehydrogenase to oxidase in ischemic rat intestine: a reevaluation. *Am. J. Physiol* 254, G768-G774.

Pearce, L. L., Kanai, A. J., Birder, L. A., Pitt, B. R., & Peterson, J. (2002). The catabolic fate of nitric oxide: the nitric oxide oxidase and peroxynitrite reductase activities of cytochrome oxidase. *J Biol.Chem.* 277, 13556-13562.

Pecoraro, R.E., Ahroni, J.H., Boyko, E.J., & Stensel, V.L. (1991a). Chronology and determinants of tissue repair in diabetic lower-extremity ulcers. *Diabetes* 40, 1305-1313.

Pecoraro, R.E. (1991b). The nonhealing diabetic ulcer--a major cause for limb loss. *Prog. Clin. Biol. Res.* 365, 27-43.

Peschen, M., Grenz, H., Brand-Saberi, B., Bunaes, M., Simon, J.C., Schopf, E., & Vanscheidt. (1998a). Increased expression of platelet-derived growth factor receptor-α and -β and vascular endothelial growth factor in the skin of patients with chronic venous insufficiency. *Arch. Dermatol. Res.* 290, 291-297.

Peschen,M., Grenz,H., Grothe,C., Schoepf,E., & Vanscheidt,W. (1998b). Patterns of epidermal growth factor and transforming growth factor-β_3 expression in the skin with chronic venous insufficiency. *Eur. J. Dermatol.* 8, 334-338.

Pfeiffer, S., Gorren, A. C., Schmidt, K., Werner, E. R., Hansert, B., Bohle, D. S., & Mayer, B. (1997). Metabolic fate of peroxynitrite in aqueous solution. Reaction with nitric oxide and pH-dependent decomposition to nitrite and oxygen in a 2:1 stoichiometry. *J. Biol.Chem.* 272, 3465-3470.

Picard-Ami, L.A., Jr., MacKay, A., & Kerrigan, C.L. (1991). Pathophysiology of ischemic skin flaps: differences in xanthine oxidase levels among rats, pigs, and humans. *Plast. Reconstr. Surg.* 87, 750-755.

Pitaru, S., Soldinger, M., & Madgar, D. (1987) Bacterial endotoxin inhibits migration, attachment and orientation of human gingival fibroblasts *in vitro* and delays collagen gel contraction. 66, 1449-1455.

Porras, A.G., Olson, J.S., & Palmer, G. (1981). The reaction of reduced xanthine oxidase with oxygen. Kinetics of peroxide and superoxide formation. *Journal of Biological Chemistry.* 256, 9096-9103.

Potoka, D. A., Takao, S., Owaki, T., Bulkley, G. B., & Klein, A. S. (1998). Endothelial cells potentiate oxidant-mediated Kupffer cell phagocytic killing. *Free Radic.Biol.Med.* 24, 1217-1227.

Preeta, R. & Nair, R. R. (2000). Superoxide anions mediate proliferative response in cardiac fibroblasts. *Indian J. Med. Res.* 111, 127-132.

Radi, R., Peluffo, G., Alvarez, M. N., Naviliat, M., & Cayota, A. (2001). Unravelling peroxynitrite formation in biological systems. *Free Radic.Biol. Med.* 30, 463-488.

Ramsey, S.D., Newton, K., Blough, D., McCulloch, D.K., Sandhu, N., Reiber, G.E., & Wagner,E.H. (1999). Incidence, outcomes, and cost of foot ulcers in patients with diabetes. *Diabetes Care* 22, 382-387.

Rao, C. N., Ladin, D. A., Liu, Y. Y., Chilukuri, K., Hou, Z. Z., & Woodley, D. T. (1995). Alpha 1-antitrypsin is degraded and non-functional in chronic wounds but intact and functional in acute wounds: the inhibitor protects fibronectin from degradation by chronic wound fluid enzymes. *J. Invest. Dermatol.* 105, 572-578.

Rayner, T. E., Cowin, A. J., Robertson, J. G., Cooter, R. D., Harries, R. C., Regester, G. O., Smithers, G. W., Goddard, C., & Belford, D. A. (2000). Mitogenic whey extract stimulates wound repair activity *in vitro* and promotes healing of rat incisional wounds. *Am.J Physiol Regul.Integr.Comp Physiol* 278, R1651-R1660.

Reed, J., Ho, H.H., and Jolly, W.L. (1974) Chemical synthesis with a quenched flow reactor. Hydroxytrihydroborate and Peroxynitrite. *J. Am. Chem. Soc.* 96: 1248-49.

Rees, R., Smith,D., Li,T.D., Cashmer,B., Garner,W., Punch,J., and Smith,D.J., Jr. (1994). The role of xanthine oxidase and xanthine dehydrogenase in skin ischemia. *J. Surg. Res. 56*, 162-167.

Reenstra, W.R., Yaar, M., Gilchrest, B.A. (1993) Effect of donor age on epidermal growth factor processing in man. *Exp. Cell. Res.* 209(1):118-22.

Reenstra, W. R., Yaar, M., & Gilchrest, B. A. (1996). Aging affects epidermal growth factor receptor phosphorylation and traffic kinetics. *Exp.Cell Res.* 227, 252-255.

Reenstra, W. R., Orlow, D., & Bursa, J. A., (2004) Increased expression of growth factor receptors in response to hyperbaric oxygen (HBO) is nitric oxide (NO)-dependant. *Academic. Emerg. Medicine.* 11 (5), 517-518.

Reuler, J. B., and Cooney, T. G. (1981). The pressure sore: pathophysiology and principle of management. *Ann Intern. Med.* 94, 661-666.

Richert, D., & Westerfeld, W. W. (1954). The relationship of iron to xanthine oxidase. *J Biol Chem.* 209, 179.

Rittenberg, T., & Ehrlich, H. P. (1992) Free fatty acids and dialysed serum alterations of fibroblast populated collagen lattice contraction. *Tissue Cell.* 24, 243-251.

Roberts, I. S. (1996). The biochemistry and genetics of capsular polysaccharide production in bacteria. *Annu. Rev. Microbiol.* 50, 285-315.

Robbins, R. A. & Grisham, M. B. (1997). Nitric oxide. *Int. J Biochem.Cell Biol.* 29, 857-860.

Robinson, M. J. & Cobb, M. H. (1997). Mitogen-activated protein kinase pathways. *Curr. Opin. Cell Biol.* 9, 180-186.

Robson, M. C., Phillips, L. G., Lawrence, W. T., Bishop, J. B., Youngerman, J. S., & Hayward, P. G. (1992). The safety and effect of topically applied recombinant basic fibroblast growth factor on healing of chronic pressure sores. *Ann. Surg.* 216, 401-408.

Robson, M.C. (1997). Wound infection. A failure of wound healing caused by an imbalance of bacteria. *Surg. Clin. North Am.* 77, 637-650.

Roeckl-Wiedmann, I., Bennett, M., & Kranke, P. (2005) Systematic review of hyperbaric oxygen in the management of chronic wounds. *Br. J. Surg.* 92(1):24-32.

Romero, N., Denicola, A., Souza, J. M., & Radi, R. (1999). Diffusion of peroxynitrite in the presence of carbon dioxide. *Arch. Biochem. Biophys.* 368, 23-30.

Rotstein, O. D., Pruett, T. L., & Simmons, R. L. (1985a). Mechanisms of microbial synergy in polymicrobial surgical infections. *Rev. Infect. Dis.* 7, 151-170.

Rotstein, O. D., Pruett, T. L., & Simmons, R. L. (1985b). Lethal microbial synergism in intra-abdominal infections. Escherichia coli and Bacteroides fragilis. *Arch.Surg.* 120, 146-151.

Royall, J. A. & Ischiropoulos, H. (1993). Evaluation of 2',7'-dichlorofluorescin and dihydrorhodamine 123 as fluorescent probes for intracellular H2O2 in cultured endothelial cells. *Arch.Biochem.Biophys.* 302, 348-355.

Rubbo, H., Radi, R., Trujillo, M., Telleri, R., Kalyanaraman, B., Barnes, S., Kirk, M., & Freeman, B. A. (1994). Nitric oxide regulation of superoxide and peroxynitrite-dependent lipid peroxidation. Formation of novel nitrogen-containing oxidized lipid derivatives. *J Biol.Chem.* 269, 26066-26075.

Ruckley, C. V. (1997). Socioeconomic impact of chronic venous insufficiency and leg ulcers. *Angiology* 48, 67-69.

Sabra, W., Kim, E. J., & Zeng, A. P. (2002). Physiological responses of Pseudomonas aeruginosa PAO1 to oxidative stress in controlled microaerobic and aerobic cultures. *Microbiology* 148, 3195-3202.

Salo, D. C., Lin, S. W., Pacifici, R. E., & Davies, K. J. (1988). Superoxide dismutase is preferentially degraded by a proteolytic system from red blood cells following oxidative modification by hydrogen peroxide. *Free Radic.Biol.Med.* 5, 335-339.

Salo, D. C., Pacifici, R. E., Lin, S. W., Giulivi, C., & Davies, K. J. (1990). Superoxide dismutase undergoes proteolysis and fragmentation following oxidative modification and inactivation. *J Biol.Chem.* 265, 11919-11927.

Sanders, S.A., Eisenthal, R., & Harrison, R., (1997). NADH oxidase activity of human xanthine oxidoreductase Generation of superoxide anion. *Eur. J. Biochem.* 245, 541-548.

Saran, M. & Bors, W. (1990). Radical reactions *In vivo*--an overview. *Radiat.Environ.Biophys.* 29, 249-262.

Saran, M., Beck-Speier, I., Fellerhoff, B., & Bauer, G. (1999). Phagocytic killing of microorganisms by radical processes: consequences of the reaction of hydroxyl radicals with chloride yielding chlorine atoms. *Free Radic. Biol. Med.* 26, 482-490.

Schaeffer, A. J., Jones, J. M., & Amundsen, S. K. (1980). Bacterial effect of hydrogen peroxide on urinary tract pathogens. *Appl. Environ. Microbiol.* 40, 337-340.

Schaffer, M. R., Tantry, U., Gross, S. S., Wasserburg, H. L., & Barbul, A. (1996). Nitric oxide regulates wound healing. *J. Surg. Res.* 63, 237-240.

Schaffer, M. R., Efron, P. A., Thornton, F. J., Klingel, K., Gross, S. S., & Barbul, A. (1997a). Nitric oxide, an autocrine regulator of wound fibroblast synthetic function. *J. Immunol.* 158, 2375-2381.

Schaffer, M. R., Tantry, U., Efron, P. A., Ahrendt, G. M., Thornton, F. J., & Barbul, A. (1997b). Diabetes-impaired healing and reduced wound nitric oxide synthesis: a possible pathophysiologic correlation. *Surgery* 121, 513-519.

Schmidt, H. H., Seifert, R., & Bohme, E. (1989). Formation and release of nitric oxide from human neutrophils and HL-60 cells induced by a chemotactic peptide, platelet activating factor and leukotriene B4. *FEBS Lett.* 244, 357-360.

Schmidtchen, A., Frick, I. M., Andersson, E., Tapper, H., & Bjorck, L. (2002). Proteinases of common pathogenic bacteria degrade and inactivate the antibacterial peptide LL-37. *Mol.Microbiol.* 46, 157-168.

Schmidtchen, A., Holst, E., Tapper, H., & Bjorck, L. (2003). Elastase-producing Pseudomonas aeruginosa degrade plasma proteins and extracellular products of human skin and fibroblasts, and inhibit fibroblast growth. *Microb. Pathog.* 34, 47-55.

Schneider, E. L. & Mitsui, Y. (1976). The relationship between *in vitro* cellular aging and *in vivo* human age. *Proc. Natl. Acad. Sci.U.S.A* 73, 3584-3588.

Schardinger, F. (1902). Z. Unters. *Nahr. Genussm. 5*, 1113-1121.

Schrag, S. J., Perrot, V., & Levin, B. R. (1997). Adaptation to the fitness costs of antibiotic resistance in Escherichia coli. *Proc. Biol. Sci.* 264, 1287-1291.

Schraibman, I. G. (1990). The significance of beta-haemolytic streptococci in chronic leg ulcers. *Ann. R.Coll. Surg. Engl.* 72, 123-124.

Schultz, G. S., Sibbald, R. G., Falangam V., Ayello, E. A., Dowsett, C., Harding, K., Romanelli, M., Stacey, M. C., Teot, L., & Vanscheidt, W. (2003) Wound bed preparation: a systematic approach to wound management. *Wound Repair Regen.* 11 Suppl 1:S1-S28.

Schwalbe, R. S., Stapleton, J. T., & Gilligan, P. H. (1987). Emergence of vancomycin resistance in coagulase-negative staphylococci. *N. Engl. J. Med.* 316, 927-931.

Schwartz, C. E., Krall, J., Norton, L., McKay, K., Kay, D., & Lynch, R. E. (1983). Catalase and superoxide dismutase in Escherichia coli. *J Biol.Chem.* 258, 6277-6281.

Schwentker, A., Vodovotz, Y., Weller, R., & Billar, T. R. (2002). Nitric oxide and wound repair: role of cytokines? *Nitric Oxide.* 7, 1-10.

Seifter, E., Rettura, G., Barbul, A., & Levenson, S.M. (1978). Arginine: an essential amino acid for injured rats. *Surgery.* 84, 224-30.

Setsukinai, K., Urano, Y., Kakinuma, K., Majima, H. J., & Nagano, T. (2003). Development of novel fluorescence probes that can reliably detect reactive oxygen species and distinguish specific species. *J Biol. Chem.* 278, 3170-3175.

Shi, Y., Patel, S., Niculescu, R., Chung, W., Desrochers, P., & Zalewski, A. (1999). Role of matrix metalloproteinases and their tissue inhibitors in the regulation of coronary cell migration. *Arterioscler. Thromb. Vasc. Biol.* 19, 1150-1155.

Shi, H.P., Efron, D.T., Most, D., Tantry, U. S., & Barbul, A. (2000). Supplemental dietary arginine enhances wound healing in normal but not inducible nitric oxide synthase knockout mice. *Surgery* 128, 374-378.

Shi, H. P., Most, D., Efron, D., Witte, M. B., Barbul, A., (2003). Supplemental L-arginine enhances wound healing in diabetic rats. *Wound Rep. Reg.* 11, 198-203.

Simpson, J. A., Cheeseman, K. H., Smith, S. E., & Dean, R. T. (1988). Free-radical generation by copper ions and hydrogen peroxide. Stimulation by Hepes buffer. *Biochem. J* 254, 519-523.

Skinner, K. A., White, C. R., Patel, R., Tan, S., Barnes, S., Kirk, M., Darley-Usmar, V., & Parks, D. A. (1998). Nitrosation of uric acid by peroxynitrite. Formation of a vasoactive nitric oxide donor. *J Biol. Chem.* 273, 24491-24497.

Skulachev, V. P. (1998). Possible role of reactive oxygen species in antiviral defense. *Biochemistry (Mosc.)* 63, 1438-1440.

Smith, A. D., Morris, V. C., & Levander, O. A. (2001). Rapid determination of glutathione peroxidase and thioredoxin reductase activities using a 96-well microplate format: comparison to standard cuvette-based assays. *Int. J Vitam. Nutr. Res.* 71, 87-92.

Sorensen, O. E., Follin, P., Johnsen, A. H., Calafat, J., Tjabringa, G. S., Hiemstra, P. S., & Borregaard, N. (2001). Human cathelicidin, hCAP-18, is processed to the antimicrobial peptide LL-37 by extracellular cleavage with proteinase 3. *Blood.* 97, 3951-3959.

Spenny, M. L., Muangman, P., Sullivan, S. R., Bunnett, N. W., Ansel, J. C., Olerud, J. E., & Gibran, N.S. (2002). Neutral endopeptidase inhibition in diabetic wound repair. *Wound. Repair Regen.* 10, 295-301.

Spratt, B. G. (1996). Antibiotic resistance: counting the cost. *Curr.Biol.* 6, 1219-1221.

Squadrito, G. L., Cueto, R., Splenser, A. E., Valavanidis, A., Zhang, H., Uppu, R. M., & Pryor, W. A. (2000). Reaction of uric acid with peroxynitrite and implications for the mechanism of neuroprotection by uric acid. *Arch. Biochem. Biophys.* 376, 333-337.

Stacey, M. C., Burnand, K. G., Mahmoud-Alexandroni, M., Gaffney, P. J., & Bhogal, B. S. (1993). Tissue and urokinase plasminogen activators in the environs of venous and ischaemic leg ulcers. *Br. J. Surg.* 80, 596-599.

Stallmeyer, B., Kampfer, H., Kolb, N., Pfeilschifter, J., & Frank, S. (1999). The function of nitric oxide in wound repair: inhibition of inducible nitric oxide-synthase severely impairs wound reepithelialization. *J. Invest. Dermatol.* 113, 1090-1098.

Stanley, A. C., Park, H. Y., Phillips, T. J., Russakovsky, V., & Menzoian, J. O. (1997). Reduced growth of dermal fibroblasts from chronic venous ulcers can be stimulated with growth factors. *J. Vasc. Surg.* 26, 994-999.

Stephens, P., Cook, H., Hilton, J., Jones, C. J., Haughton, M. F., Wyllie, F. S., Skinner, J. W., Harding, K. G., Kipling, D., and Thomas, D. W. (2003a). An analysis of replicative senescence in dermal fibroblasts derived from chronic leg wounds predicts that telomerase therapy would fail to reverse their disease-specific cellular and proteolytic phenotype. *Exp. Cell Res.* 283, 22-35.

Stephens, P., Wall, I. B., Wilson, M. J., Hill, K. E., Davies, C. E., Hill, C. M., Harding, K. G., & Thomas, D. W. (2003b). Anaerobic cocci populating the deep tissues of chronic wounds impair cellular wound healing responses *in vitro*. *British. J. Dermatol.* 148, 456-466.

Stevanin, T. M., Ioannidis, N., Mills, C. E., Kim, S. O., Hughes, M. N., & Poole, R. K. (2000). Flavohemoglobin Hmp affords inducible protection for Escherichia coli respiration, catalyzed by cytochromes bo' or bd, from nitric oxide. *J. Biol. Chem.* 275, 35868-35875

Stevens, C. R., Millar, T. M., Clinch, J. G., Kanczler, J. M., Bodamyali, T., & Blake, D. R. (2000). Antibacterial properties of xanthine oxidase in human milk. *Lancet.* 356, 829-830.

Stover, C. K., Pham, X. Q., Erwin, A. L., Mizoguchi, S. D., Warrener, P., Hickey, M. J., Brinkman, F. S., Hufnagle, W. O., Kowalik, D. J., Lagrou, M., Garber, R. L., Goltry, L., Tolentino, E., Westbrock-Wadman, S., Yuan, Y., Brody, L. L., Coulter, S. N., Folger, K. R., Kas, A., Larbig, K., Lim, R., Smith, K., Spencer, D., Wong, G. K., Wu, Z., Paulsen, I. T., Reizer, J., Saier, M. H., Hancock, R. E., Lory, S., & Olson, M. V. (2000). Complete genome sequence of Pseudomonas aeruginosa PA01, an opportunistic pathogen. *Nature.* 406, 959-964.

Sundaresan, M., Yu, Z. X., Ferrans, V. J., Irani, K., & Finkel, T. (1995). Requirement for generation of H2O2 for platelet-derived growth factor signal transduction. *Science.* 270, 296-299

Szabo, C., Zingarelli, B., O'Connor, M., Salzman, A. L. (1996). DNA strand breakage, activation of poly (ADP-ribose) synthetase, and cellular energy depletion are involved in the cytotoxicity of

macrophages and smooth muscle cells exposed to peroxynitrite. *Proc. Natl. Acad. Sci. USA* 93: 1753-8.

Takeyama, N., Shoji, Y., Ohashi, K., & Tanaka, T. (1996). Role of reactive oxygen intermediates in lipopolysaccharide-mediated hepatic injury in the rat. *J. Surg. Res.* 60, 258-262.

Tallman, P., Muscare, E., Carson, P., Eaglstein, W. H., & Falanga, V. (1997). Initial rate of healing predicts complete healing of venous ulcers. *Arch. Dermatol.* 133, 1231-1234.

Takao, S., Smith, E. H., Wang, D., Chan, C. K., Bulkley, G. B., & Klein, A. S. (1996). Role of reactive oxygen metabolites in murine peritoneal macrophage phagocytosis and phagocytic killing. *Am.J Physiol.* 271, C1278-C1284.

Takeuchi, T., Nakaya, Y., Kato, N., Watanabe, K., & Morimoto, K. (1999). Induction of oxidative DNA damage in anaerobes. *FEBS Lett.* 450, 178-180.

Taub, P. J., Silver, L., & Wienberg, H. (2000) Plastic surgical perspectives on vascular endothelial growth factor as gene therapy for angiogenesis. *Plast. Reconstruct. Surg.* 105, 1034-1042.

Taylor, W. I. & Achanzar, D. (1972). Catalase test as an aid to the identification of Enterobacteriaceae. *Appl. Microbiol.* 24, 58-61.

Tentolouris, N., Jude, E. B., Smirnof, I., Knowles, E. A., & Boulton, A. J. (1999). Methicillin-resistant Staphylococcus aureus: an increasing problem in a diabetic foot clinic. *Diabet. Med.* 16, 767-771.

Thannickal, V. J. & Fanburg, B. L. (2000). Reactive oxygen species in cell signaling. *Am. J Physiol Lung Cell Mol. Physiol* 279, L1005-L1028.

Thomas, D. R., Goode, P. S., Tarquine, P. H., & Allman, R. M. (1996). Hospital-acquired pressure ulcers and risk of death. *J. Am. Geriatr.Soc.* 44, 1435-1440.

Thomson, L., Trujillo, M., Telleri, R., & Radi, R. (1995). Kinetics of cytochrome c2+ oxidation by peroxynitrite: implications for superoxide measurements in nitric oxide-producing biological systems. *Arch. Biochem. Biophys.* 319, 491-497.

Thornton, F. J., Schaffer, M. R., Witte, M. B., Moldawer, L. L., MacKay, S. L., Abouhamze, A., Tannahill, C. L., & Barbul, A. (1998). Enhanced collagen accumulation following direct transfection of the inducible nitric oxide synthase gene in cutaneous wounds. *Biochem. Biophys. Res. Commun.* 246, 654-659.

Timpl, R. (1989). Structure and biological activity of basement membrane proteins. *Eur. J. Biochem.* 180, 487-502.

Tomasek, J. J., Halliday, N. L., Updike, D. L., Ahern-Moore, J. S., Vu, T. K., Liu, R. W., & Howard, E. W. (1997). Gelatinase A activation is regulated by the organization of the polymerized actin cytoskeleton. *J. Biol. Chem.* 272, 7482-7487.

Torres, J., Sharpe, M. A., Rosquist, A., Cooper, C. E., & Wilson, M. T. (2000). Cytochrome c oxidase rapidly metabolises nitric oxide to nitrite. *FEBS Lett.* 475, 263-266.

Trengove, N. J., Stacey, M. C., McGechie, D. F., & Mata, S. (1996). Qualitative bacteriology and leg ulcer healing. *J Wound.Care* 5, 277-280.

Tubaro, E., Lotti, B., Santiangeli, C., & Cavallo, G. (1980). Xanthine oxidase: an enzyme playing a role in the killing mechanism of polymorphonuclear leucocytes. *Biochem. Pharmacol.* 29, 3018-3020.

Uitto, J. & Prockop, D. J. (1974). Synthesis and secretion of under-hydroxylated procollagen at various temperatures by cells subject to temporary anoxia. *Biochem. Biophys. Res. Commun.* 60, 414-423.

Umezawa, K., Akaike, T., Fujii, S., Suga, M., Setoguchi, K., Ozawa, A., & Maeda, H. (1997). Induction of nitric oxide synthesis and xanthine oxidase and their roles in the antimicrobial mechanism against Salmonella typhimurium infection in mice. *Infect. Immun.* 65, 2932-2940.

Vaalamo, M., Weckroth, M., Puolakkainen, P., Kere, J., Saarinen, P., Lauharanta, J., & Saarialho-Kere, U. K. (1996). Patterns of matrix metalloproteinase and TIMP-1 expression in chronic and normally healing human cutaneous wounds. *Br. J. Dermatol.* 135, 52-59.

Vande Berg, J. S., Rudolph, R., Hollan, C., & Haywood-Reid, P. L. (1998). Fibroblast senescence in pressure ulcers. *Wound. Repair. Regen.* 6, 38-49.

Veves, A., Falanga, V., Armstrong, D.G., & Sabolinski, M. L. (2001). Graft skin, a human skin equivalent is effective in the management of non infected neuropathic diabetic foot ulcers. *Diabetes Care.* 24, 290-295.

Wagner, S., Hussain, M. Z., Hunt, T. K., Bacic, B., & Becker, H. D. (2004). Stimulation of fibroblast proliferation by lactate-mediated oxidants. *Wound. Repair Regen.* 12, 368-373.

Wall, I. B., Davies, C. E., Hill, K. E., Wilson, M. J., Stephens, P., Harding, K. G., and Thomas, D. W. (2002). Potential role of anaerobic cocci in impaired human wound healing. *Wound. Repair. Regen.* 10, 346-353.

Wall, S. J., Bevan, D., Thomas, D. W., Harding, K. G., Edwards, D. R., & Murphy, G. (2002). Differential expression of matrix metalloproteinases during impaired wound healing of the diabetes mouse. *J. Invest. Dermatol.* 119, 91-98.

Wall, S. J., Sampson, M. J., Levell, N., & Murphy,G. (2003). Elevated matrix metalloproteinase-2 and -3 production from human diabetic dermal fibroblasts. *Br. J. Dermatol.* 149, 13-16.

Wang, J., Van Praagh, A., Hamilton, E., Wang, Q., Zou, B., Muranjan, M., Murphy, N. B., & Black, S. J. (2002). Serum xanthine oxidase: origin, regulation, and contribution to control of trypanosome parasitemia. *Antioxid. Redox. Signal.* 4, 161-178.

Weckroth, M., Vaheri, A., Lauharanta, J., Sorsa, T., & Konttinen, Y. T. (1996). Matrix metalloproteinases, gelatinase and collagenase, in chronic leg ulcers. *J. Invest. Dermatol.* 106, 1119-1124.

Weitzberg, E. & Lundberg, J. O. (1998). Nonenzymatic nitric oxide production in humans. *Nitric. Oxide.* 2, 1-7.

Werner, S., Breeden, M., Hubner, G., Greenhalgh, D. G., & Longaker, M. T. (1994a). Induction of keratinocyte growth factor expression is reduced and delayed during wound healing in the genetically diabetic mouse. *J. Invest. Dermatol.* 103, 469-473.

West, J. (1990) Respiratory Physiology, 4th edition., Williams and Wilkins, Baltimore, MD.

Wetzler, C., Kampfer, H., Pfeilschifter, J., & Frank, S. (2000). Keratinocyte-derived chemotactic cytokines: expressional modulation by nitric oxide *in vitro* and during cutaneous wound repair *in vivo*. *Biochem. Biophys. Res. Commun.* 274, 689-696.

Weyl, A., Vanscheidt, W., Weiss, J. M., Peschen, M., Schopf, E., & Simon, J. (1996). Expression of the adhesion molecules ICAM-1, VCAM-1, and E-selectin and their ligands VLA-4 and LFA-1 in chronic venous leg ulcers. *J. Am. Acad. Dermatol.* 34, 418-423.

White, P., Thomas, D.W., Fong, S., Stelnicki, E., Meijlink, F., Largman, C., & Stephens, P. (2003). Deletion of the homeobox gene PRX-2 affects fetal but not adult fibroblast wound healing responses. *J. Invest. Dermatol.* 120, 135-144.

Wink, D. A., Hanbauer, I., Laval, F., Cook, J. A., Krishna, M. C., & Mitchell, J. B. (1994). Nitric oxide protects against the cytotoxic effects of reactive oxygen species. *Ann. N. Y. Acad. Sci.* 738, 265-278.

Winter, G. D. (1962). Formation of a scab and the rate of epithelialisation of superficial wounds in the skin of young domestic pig. *Nature.* 193, 293-294.

Witte, M. B., Thornton, F. J., Efron, D. T., & Barbul, A. (2000). Enhancement of fibroblast collagen synthesis by nitric oxide. *Nitric. Oxide.* 4, 572-582.

Woessner, J. F., & Nagase, H., (2000) Matrix Metalloproteinases and TIMPs. *Oxford Universtiy Press.*

Wysocki, A. B. & Grinnell, F. (1990). Fibronectin profiles in normal and chronic wound fluid. *Lab Invest.* 63, 825-831.

Wysocki, A.B., Staiano-Coico, L., & Grinnell, F. (1993). Wound fluid from chronic leg ulcers contains elevated levels of metalloproteinases MMP-2 and MMP-9. *J. Invest. Dermatol.* 101, 64-68.

Xanthoudakis, S., Miao, G., Wang, F., Pan, Y. C., & Curran, T. (1992). Redox activation of Fos-Jun DNA binding activity is mediated by a DNA repair enzyme. *EMBO J* 11, 3323-3335.

Xiong, M., Elson, G., Legarda, D., & Leibovich, S. J. (1998). Production of vascular endothelial growth factor by murine macrophages: regulation by hypoxia, lactate, and the inducible nitric oxide synthase pathway. *Am. J. Pathol.* 153, 587-598.

Yager, D. R., Zhang, L. Y., Liang, H. X., Diegelmann, R. F., & Cohen, I. K. (1996). Wound fluids from human pressure ulcers contain elevated matrix metalloproteinase levels and activity compared to surgical wound fluids. *J. Invest Dermatol.* 107, 743-748.

Yager, D. R., Chen, S. M., Ward, S. I., & Olutoye, O. O. (1997). Ability of chronic wound fluids to degrade pepide growth factors is associated with increased levels of elastase activity and diminished levels of proteinase inhibitors. *Wound. Repair. Regen.* 5, 23-32.

Yamasaki, K., Edington, H.D., McClosky, C., Tzeng, E., Lizonova, A., Kovesdi, I., Steed, D.L., & Billiar, T.R. (1998). Reversal of impaired wound repair in iNOS-deficient mice by topical adenoviral-mediated iNOS gene transfer. *J. Clin. Invest* 101, 967-971.

Yoshpe-Purer, Y. & Henis, Y. (1976). Factors affecting catalase level and sensitivity to hydrogen peroxide in Escherichia coli. *Appl. Environ. Microbiol.* 32, 465-469.

Zhu, L., Gunn, C., & Beckman, J. S. (1992). Bactericidal activity of peroxynitrite. *Arch. Biochem. Biophys.* 298, 452-457.